THE MINERALOGY OF THE TOKOMARU SILT LOAM AND THE OCCURRENCE OF CRISTOBALITE AND TRIDYMITE IN SELECTED NORTH ISLAND SOILS

A thesis presented in partial fulfilment of
the requirements for the degree of
Doctor of Philosophy in Soil Science
at Massey University

ROBERT CLELAND WALLACE

1987

ABSTRACT

The origin of cristobalite has been investigated in a selection of soils from North Island. These include Tokomaru silt loam in the Manawatu, and Hamilton clay loam, Naike clay and Te Kowhai silt loam in the Hamilton basin. The occurrence of cristobalite, in conjunction with associated sand and silt mineralogy, has been used to interpret both the provenance of soil parent materials and aspects of soil genesis.

Cristobalite isolated from the soils is α-cristobalite (opal-C) and is invariably accompanied by tridymite (tridymite-M structure). SEM data suggest that rather than discrete phases, cristobalite and tridymite usually occur intergrown with each other. Together they constitute up to 15% of the soils examined and usually occur in higher concentrations in upper soil horizons. Oxygen isotope abundances for cristobalite and tridymite range from 7.5-8.4 $^{o}/_{oo}$ and are independent of grain size and relative proportions of cristobalite and tridymite. These data, together with the highly ordered crystal structure and subhedral morphologies of grains, indicate that cristobalite and tridymite formed at high temperature. Both are shown to occur in a number of the rhyolitic tephras from the Taupo Volcanic Zone (e.g. Aokautere and Okareka ashes) and leucocratic lavas from the Egmont centre. Cristobalite and tridymite in the soils therefore probably originated from volcanic sources.

Various forms of amorphous silica were also identified in the soils of the Hamilton basin. In upper soil horizons, microfossils and phytoliths dominate but at depth the Naike clay and Hamilton clay loam contain two inorganic forms of amorphous silica. These comprise microspheres similar to those described in precious opal. Oxygen isotope data (26.6-26.9 $^{\text{o}}/_{\text{oo}}$) are consistent with their being of low temperature origin.

In the Tokomaru silt loam, although the mineralogy is dominantly quartzofeldspathic, variations in sand mineralogy and sand chemistry identify tephric additions at specific depths in the loess. Microprobe data on pyroxenes, amphiboles, glasses and titanomagnetites at these depths and in reference tephras from the Egmont centre and the Taupo Volcanic Zone demonstrate that it is possible to identify the sources of the tephras in the soil and so place some time constraints on the age of the loess:

0-50 cm	Mixed rhyolitic and andesitic tephras from the Egmont centre and the Taupo Volcanic Zone. These have accumulated during the last 11 ka.
1.1-1.2 m	Rhyolitic ash, tentatively correlated with the Rerewhakaaitu Ash (14.7 ka B.P.) from the Okataina centre.
1.2-1.3 m	Andesitic tephra from the Egmont centre.
c. 1.6 m	Andesitic tephra from the Egmont centre.
c. 2.0 m	Andesitic tephra from the Egmont centre.
2.21-2.34 m	Aokautere Ash (20 ka B.P.) from the Taupo centre.

The distribution of phytolith types in this soil demonstrate a change at c. 50 cm depth which is interpreted as resulting from post-glacial afforestation. This is inferred to have occurred at 11-12 ka B.P.

Quartz accumulation rates demonstrate that there are markedly increased rates of loess accumulation from 14.7 ka to 12 ka, after which time there was a dramatic reduction. The loess that accumulated between these dates may not be so directly related to cold climate conditions as to an increased supply of suitable material from local sources.

ACKNOWLEDGEMENTS

During the course of this research project I have received support and encouragement from many people and I would like to express my gratitude to the following for this assistance.

Dr. V.E. Neall, my principal supervisor, for his enthusiasm, patience and wise counsel when I drifted into areas with which I was unfamiliar and who allowed new and interesting avenues of inquiry to be freely pursued.

To the "Quaternary team" in the Department of Soil Science, Drs. R.B. Stewart (latterly also as co-supervisor) and A.S. Palmer, and Messrs C.G. Vucetich and B.V. Alloway for helpful discussion during the course of the project.

Members of the Department of Soil Science, particularly Drs. J.A. Pollok, M. A. Turner, A.N. Macgregor and J.H. Kirkman encouraged and assisted me in resolving minor problems or in learning new techniques.

To Drs. C.M. Lees, J.P. Skipworth, R.N. Patel and Mr. A.G. Robertson for initial assistance with the inquiry into phytoliths.

Drs. H.S. Gibbs and D.J. Lowe, Waikato University provided informative assistance and guidance when collecting the soils from the Hamilton Basin.

Messrs D.H. Hopcroft and R. Bennet, Applied Biochemistry Division, D.S.I.R. and Dr. J.D. Collen, Victoria University, are thanked for supplying their technical skills and assistance in producing the electron micrographs.

Dr. P. Blattner and Miss C. Houston, Geological Survey, introduced me to oxygen isotope analysis techniques and supplied the oxygen isotope data.

Mr. K. Palmer, Victoria University, assisted with the XRF analyses and facilitated ready access to the electron microprobe.

Dr. C.W. Childs undertook some preliminary mossbauer studies and, together with Dr. J.D.G. Milne, made unpublished chemical data available.

To the "production team", particularly Glenys, Martin Eggels and Anne Rouse for giving of their time and expertise so freely.

Finally to my main support team (Glenys, Kerry, Heather and Cleland) for encouragement, support and patience during all phases of the project. For sharing the "highs" with me and helping me through the "lows" - Thank you.

TABLE OF CONTENTS

CHAPTER 1

CHAPTER 2

CHAPTER 3 The Distribution and Origin of Cristobalite and Tridymite in some New Zealand Soils

Discussion:

CHAPTER 4 Sand and Silt Mineralogy and Geochemistry of the Tokomaru Silt Loam

Introduction:

Discussion:

CHAPTER 5

Summary and Conclusions:

LIST OF FIGURES

Figure **Page**

Figure **Page**

Figure **Page**

LIST OF TABLES

TABLE Page

CHAPTER ONE

INTRODUCTION

During weathering silica is released to the soil solution and while much of this is lost from the soil (e.g. Stevens and Vucetich 1984) the occurrences of 'silica' cements in duripans, silans and "silcretes" indicates that some silica, probably as amorphous coatings, remains in the soil. Investigation of the transformation of amorphous silica to cristobalite (in deep sea sediments, and precious opal) has demonstrated that cristobalite could form from amorphous opal under temperatures and pressures similar to those in the pedosphere. It has been suggested (e.g. see M^{c}Keague and Cline 1963; Lowe 1986) that cristobalite in soils is pedogenic. The present study was undertaken to carry out a detailed investigation of the mineralogy of selected North Island soils, using oxygen isotope analysis and optical techniques to determine the validity of the pedogenic origin hypothesis for cristobalite in soils.

Application of thermodynamic principles to isotopic systems predicts that temperature and initial $^{18}O/^{16}O$ ratio of a system are the major factors determining the fractionation of ^{18}O and ^{16}O between a hydrous fluid or melt and phases crystallising from such a system (Urey 1947). The amount of ^{18}O and ^{16}O entering a mineral structure during formation is dependent on molecular vibrations which are in turn proportional to the mass of the atoms involved. Increased thermal energy at higher temperatures minimises the effect of mass difference, and the fractionation factor is therefore lowered. The temperature dependent nature of the fractionation has been used to establish marine palaeotemperature scales. These methods use the fractionation of ^{18}O and ^{16}O between calcareous or siliceous organisms and sea water (see Urey *et al.* 1951; Epstein *et al.* 1953; Emiliani 1966; Shackleton and Opdyke 1973) and this technique is now commonly used in palaeoenvironmental studies. Investigation of oxygen isotopes in silicate systems (e.g. Taylor and Epstein 1962; Garlick and Epstein 1967; Savin and Epstein 1970) demonstrated that there was considerable isotopic fractionation between mineral/mineral and mineral/melt pairs and that these were shown to vary systematically with inferred temperature of formation (Clayton and Epstein 1958; Engel *et al.* 1958). Subsequent calibration of the fractionations between specific mineral pairs has led to their use as geothermometers (e.g. O'Neil and Epstein 1966; O'Neil and Taylor 1967; Epstein and Taylor 1967; Bottinga and Javoy 1973; Blattner and Bird 1974). The isotopic composition of a mineral is therefore a function of temperature and the composition of the system from which the mineral forms. While in many instances the isotopic composition of the system is poorly known, in general low $\delta^{18}O$ fractionation indicates high temperature of formation and high fractionation values indicate low temperatures of formation.

As part of developing improved techniques for soil sand mineralogical identification an investigation of the Tokomaru silt loam was undertaken (Wallace and Neall 1984) and thin section techniques suitable for investigating the internal morphologies of grains developed. With these techniques it is now possible to identify phases within pumiceous fragments and to differentiate lithic grains of sedimentary origin from those of igneous origin. During this developmental stage minor amounts of cristobalite were identified in the Tokomaru silt loam, so a detailed investigation of this profile was also undertaken.

AIMS

The primary aims of the present investigation were:

(1) To determine the occurrence, distribution and origin of cristobalite and associated phases in North Island soils using oxygen isotopes as a principal tool.

(2) To identify the nature and distribution of silica phases other than quartz and cristobalite in the soils.

(3) To tabulate the principal mineral constituents of the sand and silt fractions of the Tokomaru silt loam and to quantify the tephra input.

(4) To identify the source(s) of the tephric additions to the Tokomaru silt loam.

(5) To interpret the pedogenesis of the soils studied.

CHAPTER TWO

METHODS AND TECHNIQUES

SAMPLE PREPARATION

This investigation was concerned with detailed studies of selected soils to ascertain the provenance of their soil stratigraphic units. A continuous channel sampling method was used. Sampling involved excavating a channel up to 15 cm deep and covering a 10 cm vertical interval (or to horizon boundaries where they were convenient or sharp). Samples were taken to a depth of one metre in the Hamilton silty clay, Naike clay and Te Kowhai silt loam and to 2.5 m in the Tokomaru silt loam. Where there were prominent vertical joints these were avoided to minimise contamination from illuvial materials. The samples were air dried, gently crushed to pass through a 2 mm sieve and subdivided using a Jones splitter into approximately 100g samples. Large samples were obtained because it was anticipated that most of the work would be done on the coarser fractions and these were relatively minor constituents in all the soils.

The soil samples were treated with NaOAc-HOAc(pH 5), H_2O_2 and sodium citrate-sodium bicarbonate-sodium dithionite (CBD) to remove carbonates, organic matter and cementing materials respectively (Jackson 1956). They were then fractionated into various sizes by sieving (>63 µm), sedimentation (63-20 µm) and centrifugation (20-5 µm, 5-2 µm, <2 µm) after Jackson (1956).

PREPARATION FOR MINERALOGICAL ANALYSIS

The soils have a low mafic content so concentration of this fraction was achieved using either a Franz Isodynamic Magnetic Separator to separate magnetic and non-magnetic fractions or

bromoform (specific gravity of 2.8) to produce a heavy and light fraction. Preliminary investigation of the coarser fractions involved optical investigation of grain mounts for each particular size fraction. Volume percentages of the various phases were determined using a ribbon point count method (Galehouse 1969) with between 500 and 1000 points (depending on the required accuracy, Pettijohn *et al.* 1972) being counted. Duplicates of some fractions indicated that the various trends are significant. For detailed investigations thin sections and polished thin sections of the various light and heavy, magnetic and non magnetic fractions were prepared (Wallace *et al.* 1985). The categories of mineral frequency are: abundant, 50-30%; very common, 29-10%; common, 9-5%; scarce, 4-1% and rare <1%.
The mineral categories are briefly described in Appendix 3.

ISOLATION OF CRISTOBALITE

To carry out the oxygen isotope investigation of cristobalite it was necessary to obtain a pure concentrate and a method using chemical dissolution and density separation was employed. Chapman *et al.* (1969) describe a method involving a fusion with sodium pyrosulphate ($Na_2S_2O_7$) followed by treatment with fluorosilicic acid (H_2SiF_6) to determine the amount of quartz in a soil quantitatively. Henderson *et al.* (1972) modified this technique by substituting an HCl/NaOH cycle for the sodium pyrosulphate treatment because fusion with $Na_2S_2O_7$ tends to enrich the ^{18}O content of cristobalite (Henderson *et al.* 1971). Subsequent work (Pisciotto 1978) however, has shown that the pyrosulphate step minimally depletes the ^{18}O ($<1\ ^{o}/_{oo}$). This apparent contradiction was not investigated during the present study and the method of Henderson *et al.* (1972) has been used here with minor modifications. Most previous workers used highly weathered material or relatively pure samples (mainly geological and not pedological) which were free of volcanic glass. The glass present in the soils of this study caused problems as it is of a variable density and is relatively unreactive to the HCl/NaOH/H_2SiF_6 (ABFS) treatment. Rather than subject the sample to excessive ABSF treatments to remove the glass, and therefore perhaps preferentially remove low temperature cristobalite, an extra density separation (SG c. 2.25 Mg m^{-3}) was used.

Initial work showed that the cristobalite in the coarse fractions of the soils studied occurs as cristobalite aggregated with clay or as intergrowths (e.g. with feldspar). It was therefore necessary that, after the initial cleaning of the sample and division into size fractions, the samples be given a 24 hour ABSF treatment to remove most of the impurities and any coatings or intergrowths associated with the cristobalite. The samples were then mixed with polyvinylpyrrolidone (PVP) using the ultrasonic probe for dispersion, transferred to test tubes containing the tetrabromoethane nitrobenzene solution (SG 2.38) with an eye dropper and centrifuged for the prescribed time. This step was repeated until X-ray diffraction (XRD) indicated that quartz was absent. Most of the light fraction contains significant amounts of biogenic silica and glass so rather than subject the cristobalite to repeated ABFS treatments to remove the biogenic material a second density separation (SG c. 2.25 Mg m^{-3}) was undertaken. This concentrate was given a final ABFS treatment, treated overnight with boric acid (Sridhar *et al.* 1975) and given an XRD and scanning electron microscope (SEM) purity check.

The amount of cristobalite was determined by quantitative XRD techniques. After ABFS treatment to remove the feldspars and ferromagnesian minerals, cristobalite, quartz and glass remained. A method intergrating the area under the peaks was used to determine the amount of cristobalite and quartz and these were corrected to account for the ABFS-soluble fraction and the amount of glass.

ISOLATION OF QUARTZ

While the quartz content of the coarser fractions was determined by optical methods this was not appropriate for the finer fractions and dissolution techniques were employed. The samples were given repeated HCl/H_2SiF_6 treatments (Henderson *et al.* 1972) until XRD showed that only quartz remained. Samples were repeatedly washed, then dried and weighed. Where there was significant cristobalite in a sample the amount of quartz was determined, together with the cristobalite by the XRD techniques described above.

ISOLATION OF PHYTOLITHS

In an attempt to investigate the vegetative history of the Tokomaru silt loam, opal phytoliths were separated from various depths in the soil, and for comparison, from tree species and two peats.

Separation of Phytoliths from the Soil: The technique for isolation of phytoliths from the soil is similar to that of Rovner (1971). The process was modified to account for lower yields at depth and to split off the coarse fraction (mainly coarse organic matter) and fine fractions (Jackson 1956) to reduce the bulk. The procedure is as follows:

(1) Acidify 60 grams of soil with HOAc and treat overnight with H_2O_2 to remove most fine organic matter, then disperse ultrasonically.

(2) Wash into test tubes through a 250 µm sieve (to remove the coarse fraction, commonly dominated by organic matter) and centrifuge, discarding the <5 µm fraction.

(3) Add dilute HCl to the test tubes and heat in a water bath, avoiding excessive heat, to remove remaining cementing materials.

(4) Repeatedly wash, ultrasonically disperse and spin down until the supernatant is clear.

(5) If required for ease of handling, split the sample into required grain size fractions by adjusting the centrifuging time and speed (Jackson 1956), then dry.

(6) A suitable mixture of nitrobenzene and tetrabromoethane to give a density of 2.3 is used to separate off the light (phytolith-bearing) fraction (Rovner 1971). Remove the light fraction and repeat density separation on the sample until the yield is negligible. Wash the light fraction repeatedly with acetone, dry, weigh and mount.

Separation of Phytoliths from Vegetation: Early investigators commonly used high temperature oxidation to concentrate the phytoliths in vegetation (Beavers and Stephen 1958; Lanning *et al.* 1958; Twiss *et al.* 1969) but this method produced distorted or fused material that had frequently been transformed to cristobalite (Jones and Handreck 1967). Jones and Milne (1963) used a nitric/perchloric acid digestion mixture at relatively low temperatures and preserved the phytolith outlines more faithfully. This method, as refined by Rovner (1971) was used to prepare material for the current study. In many cases the acid digest produced a waxy cake so the samples were finally heated in acetone to remove the wax.

ELECTRON MICROPROBE ANALYSES

Although the sand mineralogy preserves a record of volcanic additions to the mainly quartzofeldspathic Tokomaru silt loam (Wallace and Neall 1982), the Aokautere Ash is the only macroscopic indicator of tephric additions. Thus bulk sampling methods (e.g. Kohn 1970) are inappropriate for determining the chemistries of the volcanic additions. The fully automated JEOL JXA733 superprobe at Victoria University was used to determine the mineral chemistries and so help elucidate the origins of the volcanic materials. After separation of the required grain size fraction, polished thin sections (Wallace *et al.* 1985) were prepared and the minerals analysed for the major elements using 15 Kv, 12 nano-amps and a focussed beam counting for three ten second periods (Watanabe *et al.* 1981). The analysis of glasses, particularly alkali loss, is a problem with a microprobe (Wallace 1974; Froggatt 1983). To analyse glasses the beam current was lowered to 8 nano-amps, beam diameter increased to 10 µm and a fresh area of glass chosen for each of the 10 second counts.

X-RAY FLUORESCENCE ANALYSES

Major element chemistry was determined by using the fused disc method (see Roser 1983), after the samples had been ground in a tungsten carbide mill. Loss on ignition is determined by the weight loss on heating to 1000°C. Trace elements were analysed on borate-backed pressed pellets (Roser 1983).

INFRA-RED ANALYSIS

For infrared analyses one milligram of sample was ground with 170 milligrams of KBr and pressed under vacuum into a glass disc. After overnight drying at 55°C the sample was analysed in a Pye Unicam Sp3-300 infrared spectrophotometer.

PHOSPHORUS ANALYSIS

As well as being determined by XRF methods the phosphorus content of the Tokomaru silt loam was determined colorimetrically after ignition at 550°C and 16 hours of end over end shaking in 1N H_2SO_4 (Walker and Adams 1958).

CARBON ANALYSIS

Carbon was determined with a LECO induction furnace using the standard LECO method. The carbon is converted to CO_2 which is then adsorbed onto ascarite (NaOH + asbestos) which is weighed.

OXYGEN ISOTOPE ANALYSIS

The oxygen isotope analyses were carried out on a NAA 6-60 RMS, 15 cm radius, 60° sector double collecting mass spectrometer at the Institute of Nuclear Sciences. Oxygen is liberated by reaction with BrF_5 at high temperature (Clayton and Mayeda 1963) and then using a Toepler pump (Blattner and Bird 1974) is converted to CO_2 which is the feed stock to the mass spectrometer. The data is reported as parts per thousand, $^{o}/_{oo}$, relative to standard mean ocean water (SMOW of Craig 1961).

CHAPTER THREE

THE DISTRIBUTION AND ORIGIN OF CRISTOBALITE AND TRIDYMITE IN SOME NEW ZEALAND SOILS

INTRODUCTION

Cristobalite, tridymite and quartz, together with opaline silica are the silica phases of significance in soils (Wilding *et al.* 1977). One of the initial aims of the present project was to both investigate the source(s) of cristobalite in selected New Zealand soils and to determine its significance in soil genesis. Preliminary tests showed, however, that cristobalite is intimately associated with tridymite in the soil so the project was expanded to include studies of tridymite as well.

In siliceous deep sea sediments biogenic silica (also referred to as amorphous silica or opaline silica) is transformed during diagenesis to cristobalite-tridymite phases (Wise and Hsu 1971; Hein 1981; Iijima and Tada 1981). Opaline silica in soils is thus a potential precursor of cristobalite and/or tridymite so forms of opaline silica in soils are therefore also included in this review.

NOMENCLATURE

Cristobalite forms either during diagenesis (here referred to as the low temperature pathway) or under conditions such as those associated with igneous processes (here referred to as the high temperature pathway).

(a) Low Temperature Pathway: Studies of the "low temperature" pathway (e.g. Florke 1955; Jones *et al.* 1963) showed that there were two broad groupings of "opaline silica":

Type-1: specimens that gave x-ray patterns indicative of a well- ordered crystal structure, Type-2: samples that were almost amorphous, giving only a few diffuse x-ray bands (see Fig. 3.1).

Florke (1955) also showed that there were some tridymite reflections in x-ray scans of "opaline silica". A comprehensive examination of gem opal and α-cristobalite by Jones *et al.* (1963, 1964) showed that the opal structure could vary from highly crystalline (α-cristobalite) to x-ray amorphous (opal). They produced x-ray diffraction (XRD) traces that showed opals corresponding to type-2 had only a broad peak at 4.1Å while type-1 opals showed XRD patterns with sharper and more numerous peaks corresponding to α-cristobalite. Electron microscope scans of fracture surfaces of opals indicated a distinct difference in surface morphology between the two types of opal (Jones *et al.* 1964). Type-1 opaline silica had a fine grained featureless surface while the surface of type-2 opaline silica comprised closely packed silica spheres (individual spheres were 1500-3500Å in diameter and uniform for a specific sample, see also Jones *et al.* 1964; Wenk *et al.* 1976; Klein and Hurlbut 1985).

Jones and Segnit (1971) subdivided the low temperature silica phases into three groups based on XRD patterns:

(1) Opal-C: considered to be the equivalent of α-cristobalite. It is recognised that minor tridymite may be present as tridymite subdomains in a dominantly cristobalite structure. Opal-C is identified by having at least a full range of XRD peaks (4.05, 3.14, 2.85, 2.48, 2.12, 2.02, 1.93, 1.87Å - see also Brown 1980; Carpenter and Wennemer 1985),

(2) Opal-CT: having only two peaks present, 4.1Å and 2.48Å. These peaks are broad reflecting various degrees of structural disorder. There is often considerable interstratified tridymite, and

(3) Opal-A: which includes varieties of hydrous silica with a broad diffuse XRD band at *c.* 4.1Å. Most precious opals occur in this group.

In experiments in which opal-A was heated Jones and Segnit (1971) showed that, with time and temperature, the 4.1Å cristobalite peak developed out of the broad opal-A band. This confirmed earlier

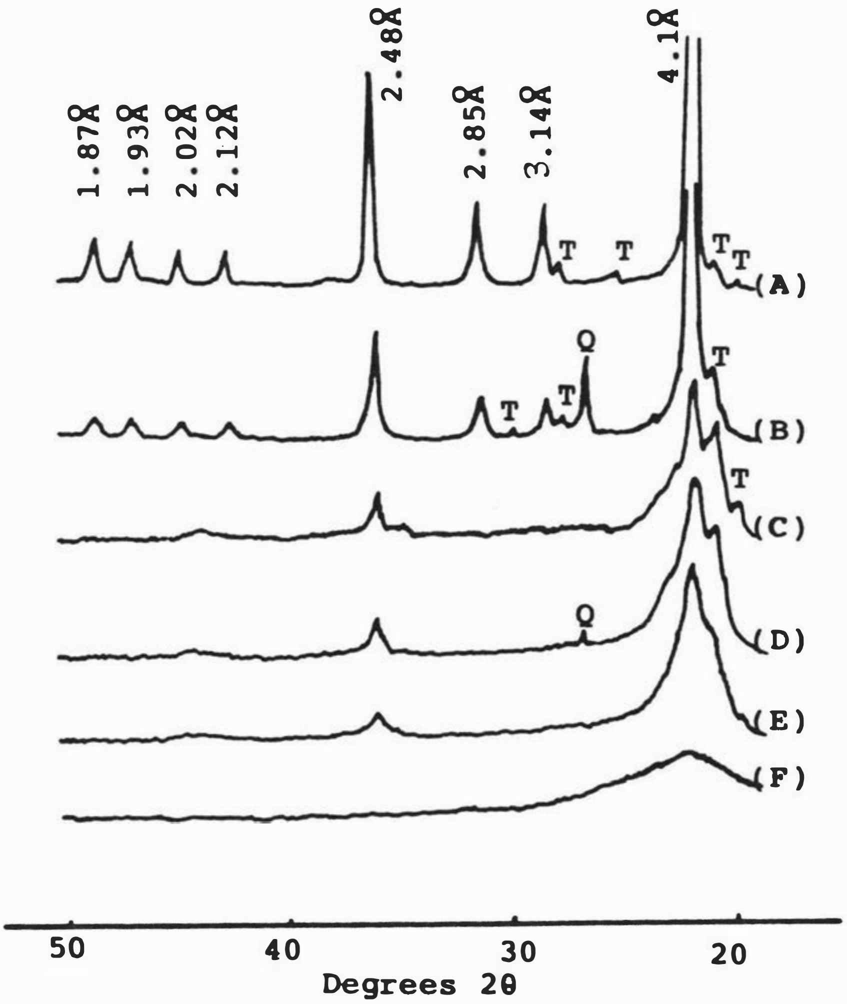

Figure 3.1: Diffraction traces of forms of silica. A is alpha-cristobalite; B is opal-C; C, D and E are opal-CT; F is opal-A. Adapted from Jones and Segnit (1971). Q is quartz. T is tridymite.

data from Florke (1955) and Frondel (1962) from which they concluded that the sequence opal-A --- opal-CT --- opal-C was a continuum. On heating, the tridymite disorder diminishes but tridymite may still be present in opal-C, suggesting that the tridymite domains are large enough to resist thermal conversion to cristobalite.

From the above studies it is concluded that during early diagenesis there is a relatively low temperature discontinuous transition from poorly crystalline hydrous silica to cristobalite and that, based on XRD characteristics, this can be divided into three forms: Opal-A (highly disordered, near amorphous), opal-CT (disordered cristobalite with tridymite subdomains) and opal-C (ordered α-cristobalite). The considerable structural disorder of opal-CT, manifest as tridymite stacking, can persist through the transition to opal-C.

(b) High Temperature Pathway: Opal-C is usually referred to as α-cristobalite when it forms in high temperature environments. Studies involving reactions of α-cristobalite show that it has a similar structure to opal-C (e.g. Brown 1980; Carpenter and Wennemer 1985) and also highlight the complexity of the relationship between cristobalite and tridymite (Hill and Roy 1958a, 1958b; Sato 1963a, 1963b, 1963c; Roy and Roy 1964; Rockett and Foster 1967; Tada and Iijima 1983; Carpenter and Wennemer 1985). In a detailed study of synthetic tridymite, Hill and Roy (1958a, 1958b) identified metastable (tridymite-M) and stable (tridymite-S) varieties, each of which had its characteristic x-ray pattern and therefore structure. Sato (1963a, 1963b, 1963c) further developed the nomenclature of these structural states and introduced a third form, tridymite-MS. Sato identified the various forms of tridymite according to the degree of development of minor peaks and the presence or absence of doublet peaks.

Tridymite-S	Doublet peaks at 3.85, 3.0, 2.5, 2.3Å and only a very weak peak at 3.25Å.
Tridymite-M	No doublets but a strong 3.25Å peak.
Tridymite-MS	Doublet peaks at 3.85, 3.0, 2.5, 2.3Å and a strong peak at 3.25Å.

The complex nature of the tridymite structure makes XRD identification of tridymite difficult, not just because there is considerable variability in the presence or absence of peaks but because the major peaks (4.33, 4.10 and 3.83Å) show a considerable range of relative intensities (see Hill and Roy 1958b; Sato 1963a, 1963c; Roy and Roy 1964; Rockett and Foster 1967; Carpenter and Wennemer 1985). It was also shown that these tridymites might be interstratified with cristobalite.

The terminology used in the present report is based on the criteria established by Jones and Segnit (1971) and Sato (1963a, 1963c). The term opal/cristobalite is used to denote the whole group opal-A, opal-CT and opal-C.

STRUCTURE

Cristobalite and tridymite are tectosilicates comprising a three dimensional framework of SiO_4 tetrahedra although the precise nature of the structure is not well understood. The tetrahedra combine in relatively regular 6-sided rings with the apical oxygen of the tetrahedra pointing alternately up and down. Kihara (1978, 1980) reports that in some tridymite the rings are deformed into "D" shapes. The rings form sheets which are stacked perpendicular to the (111) axis in cristobalite and the (0001) axis in tridymite. In tridymite the basal oxygens are positioned directly above those in the underlying sheets while in cristobalite the SiO_4 tetrahedra in each additional sheet are rotated by 60°. To make up a unit cell the sheets of SiO_4 tetrahedra are stratified in an ABC-ABC-ABC sequence (see Deer *et al.* 1967) in cristobalite (*i.e.* 3 sheets repeated) and AB-AB-AB pattern in tridymite (a 2 sheet repeat sequence). Commonly tridymite domains and cristobalite domains occur within the one unit, *i.e.* mineral grains often contain interstratified sequences of tridymite and cristobalite.

A comprehensive examination of the transformation of opal to cristobalite (Jones *et al.* 1963, 1964) showed that there was a continuous variation from amorphous opal to poorly ordered cristobalite with tridymite domains (opal-CT) and finally α-cristobalite (opal-C). Similarly tridymites have been shown to contain cristobalite (opal-C) domains (Hill and Roy 1958a, 1958b; Roy and Roy 1964; Carpenter and Wennemer 1985).

The structural relationship between the SiO_4 tetrahedra in cristobalite and tridymite produces a comparatively open, low density structure with relatively large channels or openings (1.7Å in cristobalite and 1.3Å in tridymite, Holmquist 1961) in which foreign ions might be trapped (*e.g.* Na, K, Li, Al). It may be that these ions are necessary to stabilise the structure under surface conditions. Tridymite can only be synthesised in the presence of mineralisers and some authors (e.g. Florke 1955; Holmquist 1961) have suggested that tridymite may not be a polymorph of silica but rather a binary system with alkali oxides. Mason (1966) suggests tridymite may be isomorphous with feldspathoids. Hill and Roy (1958b) and Rockett and Foster (1967) however, argue that tridymite is a polymorph of silica.

A distinct morphology of opal-CT was described from deep sea sediments and coastal plain sediments of the eastern United States (Rex 1969; Calvert 1971a, 1971b; Weaver and Wise 1972; Wise and Hsu 1971). This consisted of small, spherulitic rosettes 3-10 µm in diameter and comprising thin, radiating blades between 300-500Å thick. The term lepisphere was proposed by Wise and Kelts (1972) for opal-CT with this morphology (see also Oehler 1973; Wilson *et al.* 1974; Jones and Segnit 1975; Florke *et al.* 1975, 1976).

Opal-A is amorphous to x-rays so investigations of its structure have been largely by direct observation with the electron microscope rather than by XRD. Studies of silica in the form of petrified wood (e.g. Segnit *et al.* 1970; Stein 1982; Scurfield and Segnit 1984; Senkayi *et al.* 1985) have identified microspheres, spherulites and more structureless varieties of silica which have invaded woody material, often faithfully reproducing the cellular structure. Australian studies of precious opal (mineralogically opal-A) have shown that it is composed of uniformly sized microspheres (1500-3500Å diameter) arranged in a cubic or hexagonal packing pattern (Jones *et al.* 1964, 1966; Darragh *et al.* 1966; Sanders 1968; Jones and Segnit

1969; Wenk *et al.* 1976; Klein and Hurlbut 1985). These microspheres themselves comprise smaller particles *c.*300-400Å in diameter (Darragh *et al.* 1966; Jones *et al.* 1966). It is diffraction of white light by planes of the microspheres that is thought to produce the iridescence seen in opals (Sanders 1968; Darragh *et al.* 1966).

THERMAL STABILITY

Based on energy considerations quartz should be more stable than cristobalite and tridymite under surface conditions. These three phases however, are related to each other by slow transformations that involve reconstruction of the Si-O bond, requiring considerable energy to convert from one polymorph to another. This, together with the stabilising influence of traces of chemical impurities, allows cristobalite and tridymite to exist metastably under surface conditions. Within each polymorph type there is a series of high and low temperature structures (*i.e.* α and β forms, Fig. 3.2) that involve displacive transitions (lattice re-orientation) without breaking bonds. Because this occurs spontaneously within a specific temperature range the lowest temperature form should be stable under surface conditions. There is, however, some evidence that β-cristobalite may persist under low temperatures in special circumstances. Greig (1932) and Sosman (1932) have described this phenomenon where β-cristobalite is enclosed in glass and suggest that the rigidity of the glass which "sets" above the cristobalite inversion temperature inhibits the re-orientation of the crystal during inversion.

The inception of the Deep Sea Drilling Projects (DSDP) created an impetus for researching the relationship between biogenic silica (opaline silica), cristobalite-tridymite and quartz. It has been shown that with increasing depth of burial, biogenic silica (opal-A) in siliceous sediments is replaced by opal-CT which may in turn be replaced by quartz. In siliceous deposits the neoformation of cristobalite is thought to be a step in a sequence from biogenic opal

HIGH TEMPERATURE PATHWAY

Heating cycle

$\alpha\text{-quartz} \xrightarrow{575^{o}C} \beta\text{-quartz} \xrightarrow{870^{o}C} \beta_2\text{-tridymite} \xrightarrow{1470^{o}C} \beta\text{-cristobalite} \xrightarrow{1625^{o}C} \text{melt}$

$\alpha\text{-quartz} \xrightarrow{575^{o}C} \beta\text{-quartz} \xrightarrow{1050^{o}C} \text{cristobalite}$ #

Cooling cycle

$\alpha\text{-quartz} \xleftarrow{575^{o}C} \beta\text{-quartz}$

$\alpha\text{-tridymite} \xleftarrow{117^{o}C} \beta_1\text{-tridymite} \xleftarrow{163^{o}C} \beta_2\text{-tridymite}$

$\alpha\text{-cristobalite} \xleftarrow{\text{variable } 198^{o}C - 277^{o}C} \beta\text{-cristobalite}$

Reaction proposed by Florke (1956) in the absence of mineralisers.

LOW TEMPERATURE PATHWAY

$\text{opaline silica} \xrightarrow{*} \text{cristobalite/tridymite} \xrightarrow{+} \text{quartz}$

$\text{opal-A} \xrightarrow{*} \text{opal-CT} \xrightarrow{*} \text{quartz}$

* occurs in 5-10 ma at 40-50^{o}C or 30-40 ma at 20-30^{o}C

\+ occurs at approximately 70-85^{o}C and the time constraint is unknown except that cristobalite-tridymite is not found in rocks older than the Cretaceous.

Figure 3.2: Summary of the thermal transitions of some silica phases.

to cristobalite (with or without tridymite) i.e. equivalent to opal-CT, then quartz during diagenesis (Iijima and Tada 1981; Hein *et al.* 1978). These workers (see also Isaacs 1982; Murata and Nakata 1974; Kastner *et al.* 1977; Keller and Isaacs 1985) have shown that the reaction is partially dependent on host rock composition in that it occurs at lower temperatures in the purer diatomites compared with siliceous/argillaceous mixtures. Isaacs (1982) also showed that the presence of carbonate did not dictate whether the reaction proceeded but Kastner *et al.* (1977) have shown that although carbonate was not required directly, it was important in that it increased the alkalinity of the water and so stimulated the reaction. Other factors influencing the reaction rate include pore water chemistry [Kastner *et al.* (1977) demonstrated that Mg and possibly Al, Fe and Mn hydroxides assisted nucleation] and surface area (Hein *et al.* 1978), but the primary factors are time and temperature (Jones and Segnit 1971; Mizutani 1977; Iijima and Tada 1981).

The transformation of opal-A to opal-CT is a dissolution/precipitation reaction (Murata and Nakata 1974; Stein and Kirkpatrick 1976). Heydemann (1964), Florke *et al.* (1975) and Jeans (1978) have suggested that another phase (the so called silica-X) was a transitional phase between opal-A and opal-CT and Hein *et al.* (1978) recognised an intermediate phase, opal-A$'$, which was composed of thin blades 20-27Å thick which they suggested was a proto opal-CT. Estimates of the temperature of the opal-A to opal-CT transition include 35-50°C (Hein *et al.* 1978), 40-50°C (Aoyagi and Kazama 1980), 38-54°C (Pisciotto 1981) and 44-48°C (Keller and Isaacs 1985). Hein *et al.* (1978) suggested that while the transition occurred in 5-10 ma at 40-50°C along continental and island arc margins (where sedimentation rates were higher and there was increased diagenesis) it took 30-40 ma at 20-30°C in open oceans with low sedimentation rates (Fig. 3.2).

The nature of the opal-CT to quartz transition is more enigmatic. There are few sections where the transition is exposed, either through lack of suitable lithologies or from marine cores not reaching deep enough. Opinions are divided as to whether the transformation is due to solution/precipitation or solid/solid inversion (Ernst and Calvert 1969; Heath and Moberly 1971; Greenwood

1973; Murata and Larsen 1975; Stein and Kirkpatrick 1976). Aoyagi and Kazama (1980) suggested that the transition occurred at 70°C; Pisciotto (1981) suggested 55-110°C and Keller and Isaacs (1985) suggested 70-85°C, depending on the composition of the enclosing sediments.

Precious opal (opal-A) comprises amorphous silica microspheres *c.* 1500-3500Å in diameter. This form of opaline silica is thought to develop by dehydration of silica gels (Jones *et al.* 1966; Darragh *et al.* 1966). Detailed observation of the microspheres has shown that they consist of smaller particles (*c.* 300-400Å diameter) and Darragh *et al.* (1966) suggest that they are produced by evaporation from silica-bearing waters under near surface conditions. Under relatively static conditions these particles settle as loose flocs to produce a thin gel. With additional aggregation and desiccation they develop into the 1500-3500Å microspheres seen in precious opal.

ISOTOPES

The development of techniques to isolate opal/cristobalite (Henderson *et al.* 1972) have now made it possible to determine the oxygen isotopic composition of these phases.

Henderson *et al.* (1971, 1972) determined that there was a broad correlation of $\delta^{18}O$ with temperature of formation similar to that for quartz. High $\delta^{18}O$ values are found for poorly crystalline opal-A (including diatoms) and low $\delta^{18}O$ values for opal-C from hydrothermal deposits. Oxygen isotope relations between diagenetic silica minerals (Murata *et al.* 1977) indicated decreasing $\delta^{18}O$ ($37.4^{o}/_{oo}$ to $23.8^{o}/_{oo}$) with increasing crystallinity and they determined that opal-CT formed at approximately 48°C while "microquartz" formed at about 79°C. These temperatures are in good agreement with those determined by Hein *et al.* (1978) and Aoyagi and Kazana (1980). In a study of opal/cristobalite from hydrothermal springs in Japan, Jackson *et al.* (1977) showed, using the electron microscope, that those phases from low temperature springs (high $\delta^{18}O$) were "spheroidal and spongey" compared with those formed at higher temperatures (low $\delta^{18}O$) which formed irregular plates or prisms.

Cristobalite in a podzol from Northland, New Zealand was concluded to be of hydrothermal or volcanic origin (Henderson *et al.* 1972) while in a recent investigation cristobalite in Ando soils from Japan, Indonesia and Guadalupe and a podzol from Japan was shown to be inherited from a primary volcanic source (Mizota *et al.* 1987).

These data (Table 3.1) indicate that opal-C (α-cristobalite) from a high temperature environment can clearly be differentiated from opal-CT or opal-A from low temperature diagenetic environments similar to conditions prevailing in soils.

OCCURRENCE

Geological Environments

(1) In sedimentary environments opal/cristobalite has been identified in a wide range of rock types such as bentonite (Brindley 1957; Guven and Grim 1972; Henderson *et al.* 1971); shales (Davis 1970); claystones (Reynolds 1970; Weaver and Wise 1974); interbedded argillite/porcellanite sequences (Aoyagi and Kazama 1980; Iijima and Tada 1981; Murata and Nakata 1974; Pisciotto 1981; Isaacs 1982) and greensand/chalk sequences (Jeans 1978). In all of these examples none of the rocks are older than Upper Cretaceous. These authors describe some or all of the sequence:

biogenic silica --- opal-A --- opal-CT --- quartz.

With the initiation of DSDP (e.g. JOIDES 1967) there has been considerable work undertaken on silica in deep ocean sediments (see Hein 1981). In North Atlantic deep sea sediments Calvert (1971a, 1971b) identified opal-CT and found that while siliceous deposits older than the Cretaceous were cherts (i.e. quartzitic) all younger deposits were porcellanites (containing opal-CT). Since this initial work opal/cristobalite has been shown to be extensive in ocean sediments (e.g. South Atlantic, Wise and Hsu 1971; Antarctic and Mid-Pacific, Weaver and Wise 1972; North Pacific, Hein *et al.* 1978).

Table 3.1: Summary of oxygen isotope data for cristobalite.

Environment	Mineral type	$\delta^{18}O$	No.	Ref.
Diatoms	(opal-A)	36.2, 37.4		*1
Diatoms	(opal-CT ?)	34.0		*2
Miocene diatoms	(opal-A ?)	32.2		*3
Porcellanite	(opal-CT)	27.9-33.8	(10)	*1
Porcellanite	(opal-CT)	30.2-32.1	(6)	*4
Porcellanite	(opal-CT)	35.7,35.9	(2)	*8
Bentonite	(opal-CT)	25.5-29.9	(4)	*2
Soils	low cristobalite (opal-C)	8.3-9.1	(3)	*3
Soils	opal-C and/or tridymte	5.3-11.0	(4)	*7
Hydrothermal	low cristobalite	8.8, 9.3		*2
Terrestrial volcanics	opal-C + tridymite(?)	6.8-11.4	(4)	*2,7
Lunar volcanics	?	7.2		*6
Quartz in cherts associated with porcellanites		24.5-27.1	(13)	*4
		23.8 ± 0.3		*1
		28 - 36	(10)	*8

* 1-Murata et al. (1977); 2 - Henderson et al. (1971); 3 - Henderson et al. (1972); 4 - Pisciotto (1981); 5 - Jackson et al. (1977); 6 - Taylor and Epstein (1970); 7 - Mizota et al. (1987); 8 - Hein and Yeh (1981).

Various forms of silica (opal-A, opal-CT and tridymite) also form as precious to semi-precious opal and wood opal, usually in terrestrial deposits. Here the minerals form lepispheres, microspheres and massive varieties that fill joints and cavities or form pseudomorphs after woody tissue (Mitchell 1967; Buurman 1972; Mitchell and Tufts 1973; Stein 1982; Scurfield and Segnit 1984; Senkayi *et al.* 1985).

Opal-A is also precipitated in South Australian lakes (Skinner 1963; Peterson and von der Borch 1965) in association with magnesite and dolomite under extremely alkaline conditions (pH up to 10.2).

(2) As well as forming in a diagenetic environment, cristobalite is also reported from environments with demonstrably higher temperatures, e.g:

Zones of hydrothermal alteration (Tokuda 1960; Jackson *et al.* 1977; Murray *et al.* 1977; Sarna-Wojcicki *et al.* 1981; Hampton and Bailey 1985),

Lavas e.g. lunar basalts (Appleman *et al.* 1971; Champness *et al.* 1971; Christie *et al.* 1971; Keil and Prinz 1971; Klein *et al.* 1971; Sippel *et al.* 1971), Japanese lavas (Kuno 1933),

Ignimbrites (Mahood *et al.* 1985),

Volcanic mudflows (Mullineaux and Crandell 1962, see also Verhoogen 1937), and

Tephras - in Indonesia (Hardjosoesastro 1956), Nevada (Moncure *et al.* 1981), Japan (Mizota and Aomine 1975; Yamada and Shoji 1977), Chile (Wada and Kakuto 1984) and in the 1980 eruptions from Mount St. Helens (Fruchter *et al.* 1980; Dethier *et al.* 1981; Gage *et al.* 1981; Kuntz *et al.* 1981; Lofgrens 1981; Bernard and Guern 1986).

This type of cristobalite is equivalent to opal-C.

Tridymite, which often occurs with cristobalite, is commonly associated with zones of hydrothermal alteration (Frondel 1962) and silicic volcanics such as rhyolites, obsidian, trachyte, dacite and andesites (Frondel 1962; Klein and Hurlbut 1985). Fruchter *et al.* (1980) and Dethier *et al.* (1981) report tridymite in ash from the 1980 eruption of Mount St. Helens. Tridymite is also described from stony meteorites (Klein and Hurlbut 1985) and lunar lavas (Appleman *et al.* 1971; Keil and Prinz 1971). It forms in cavities and vesicles, apparently during the latter stages of magmatic activity and Rogers (1928) considered it to be pneumatolytic. Trace amounts of tridymite have often been described in the fine microlitic mesostasis which crystallises last as a lava cools (Frondel 1962; Appleman et *al*. 1971; Keil and Prinz 1971).

(3) In New Zealand, cristobalite has been described from (1) the devitrified matrix of the Whakamaru Ignimbrite (Ewart 1965, 1971), (2) dacites from the Taupo Volcanic Zone (Cole 1979; Worthington 1985), (3) hydrothermal deposits e.g. Northland (Murray *et al.* 1977; Harvey 1980), and (4) pumice xenoliths thermally metamorphosed by the 1886 Tarawera basalt (identified during the present study). This type of cristobalite is similar to opal-C.

In geological environments opal-A and opal-CT occur in rock types that are associated with the low temperature pathway while opal-C and tridymite occur in rock types associated with the high temperature pathway.

Pedological Environments

(1) Opal/cristobalite is common in soils developed in parent materials associated with volcanism, e.g. in Indonesia (Hardjosoesastro 1956; Sjarif and Gilkes 1986), Japan (Mizota and Aomine 1975; Mizota *et al.* 1987), South America (Cortez and Franzmeier 1972), Israel (Yaalon 1962) and New Zealand (e.g. Swindale and Jackson

1960; Lowe 1987). The very sharp nature of the XRD peaks, together with the coarse nature of the cristobalite (it occurs in clay to sand size grains), led Mizota and Aomine (1975) to conclude that it was of primary volcanic origin (see also Wilding *et al*. 1977). Recently determined oxygen isotope ratios of cristobalite/tridymite from some Japanese soils supports this conclusion (Mizota *et al*. 1987).

(2) In New Zealand soils cristobalite is scarce and tridymite has only rarely been identified. Fieldes and Williamson (1955) refer to cristobalite in the Okaihau gravelly clay, but the first significant report on cristobalite in the pedosphere was by Swindale and Jackson (1960) who described opal/cristobalite from the silt fractions of soils with a rhyolitic provenance. It is not possible to determine the crystallinity of this opal/cristobalite from their data but they do refer to some as being of the "stuffed" structure (Buerger 1954), indicating that some may have been opal-CT or opal-C plus tridymite. Oxygen isotope analysis of the opal/cristobalite (Henderson *et al*. 1972) indicated that it was of a relatively high temperature origin, *i.e.* hydrothermal or volcanic. Reconnaissance soil mineralogical studies (Fieldes and Weatherhead 1968; New Zealand Soil Bureau 1968; Claridge and Weatherhead 1978) indicated that cristobalite could be up to 9% of the silts in some New Zealand soils. More detailed recent investigations (e.g. M^{c}Queen 1975; Davoren 1976; Jessen 1977; Bruce 1978; Hogg 1979; Lowe 1981, 1986; Shepherd 1984) report significant cristobalite in the volcanic ash soils of the Hamilton Basin, particularly the brown granular loams. Benny (1982) identified cristobalite and tridymite in a study of the Okareka Ash and overlying tephric loess in the vicinity of Lake Rotorua (see also Birrell and Pullar 1973), and Stewart (1982) reports minor amounts of cristobalite in soils developed on basalts in Northland. These occurrences appear to correlate closely with siliceous tephric material.

Tridymite, where identified, (New Zealand Soil Bureau 1968; Claridge and Weatherhead 1978) is also associated with soils developed from tephric materials.

(3) Opal-A occurs in both biogenic and inorganic forms in soils (Wilding *et al*. 1977). Biogenic opal is minor though ubiquitous in most soils either as plant phytoliths (Bartoli and Guillet 1977; Beavers and Stephen 1958; Jones and Beavers 1964; also see chapter 4) or from aquatic environments (sponge spicules, diatoms and radiolaria). Laminar opaline silica (Parfitt 1975; Shoji and Saigusa 1978; Shoji *et al*. 1986) is another form of opaline silica which is commonly associated with humic horizons and soils rich in volcaniclastic materials. Inorganic silica serves as a cement in some indurated soil horizons (duripans) in areas of Mediterranean and arid climate.

The occurrence of biogenic silica as phytoliths or microfossils is relatively common in New Zealand soils (New Zealand Soil Bureau 1968; see chapter 4). This is due to (1) the nature of the rocks that are the soil parent materials - many contain radiolaria, sponge remains and diatoms, (2) the ubiquitous plant cover prior to relatively recent human settlement and (3) the relatively stable nature of biogenic opal (Bartoli and Wilding 1980). Laminar opaline silica has also been reported in New Zealand soils (Fieldes and Furkert 1966; Henmi and Parfitt 1980; see also Lowe 1987).

PRESENT INVESTIGATION

Cristobalite in soils has been postulated as being either inherited or pedogenic (see Hardjosoesastro 1956; Henderson *et al*. 1971; Lowe 1981, 1986; Mitchell (1975); Wada 1980; Wilding and Drees 1974; Wilding *et al*. 1977). In a study of soils in the Waikato region where cristobalite is relatively common in some soils with poor drainage, Lowe (1981, 1987) suggested that cristobalite was authigenic. He suggested that cristobalite formed in soils where drainage was poor because the soil solution became enriched in Si. This Si precipitated to form hydrogels which crystallised as cristobalite during dry periods. If this pathway is correct then any cristobalite so formed should have a high $\delta^{18}O$ commensurate with its low temperature of formation and poor crystallinity (*i.e.* opal-CT).

To characterise the form of cristobalite present in these soils four soil types were chosen for detailed analysis. Three are from the Hamilton basin (Hamilton clay loam, Naike clay and Te Kowhai silt loam) and have formed from volcaniclastic parent materials while the fourth (Waiareka clay) is formed from mixed loess-calcareous basaltic tuff near Oamaru (Fig. 3.3). The profiles were continuously channel sampled over 10 cm intervals down to a depth of one metre. After particle size analysis cristobalite and tridymite in various fractions were separated. During this process concentrates of a very low density fraction (opal-A) and a heavy fraction (opaques, ferromagnesian silicates and zircons) were produced.

During initial x-ray investigation the cristobalite in the soil was shown to be closely associated with tridymite and to be of a well-ordered variety (opal-C). It was therefore deduced that the cristobalite was probably of a high temperature origin and introduced into the soil along with the volcaniclastic materials. Accordingly representatives of possible volcanic sources were processed to isolate cristobalite. Tephras sampled included (1) the Rotoma Ash, Rotoehu Ash, Okareka Ash (from which cristobalite and tridymite had been previously reported, Benny 1982), and the Rotomahana Mud, all from the Okataina Volcanic Centre, and (2) the Aokautere Ash, Waimihia Lapilli and Taupo Pumice from the Taupo Volcanic Centre. Andesitic lavas and tephra from Mt. Egmont were also processed to isolate cristobalite. Two extra soils were processed: (1) the Tokomaru silt loam, the detailed mineralogy of which is presented in chapter 4, and (2) a profile through peaty beds at Onaero near the edge of the Mt. Egmont ring plain in northeastern Taranaki.

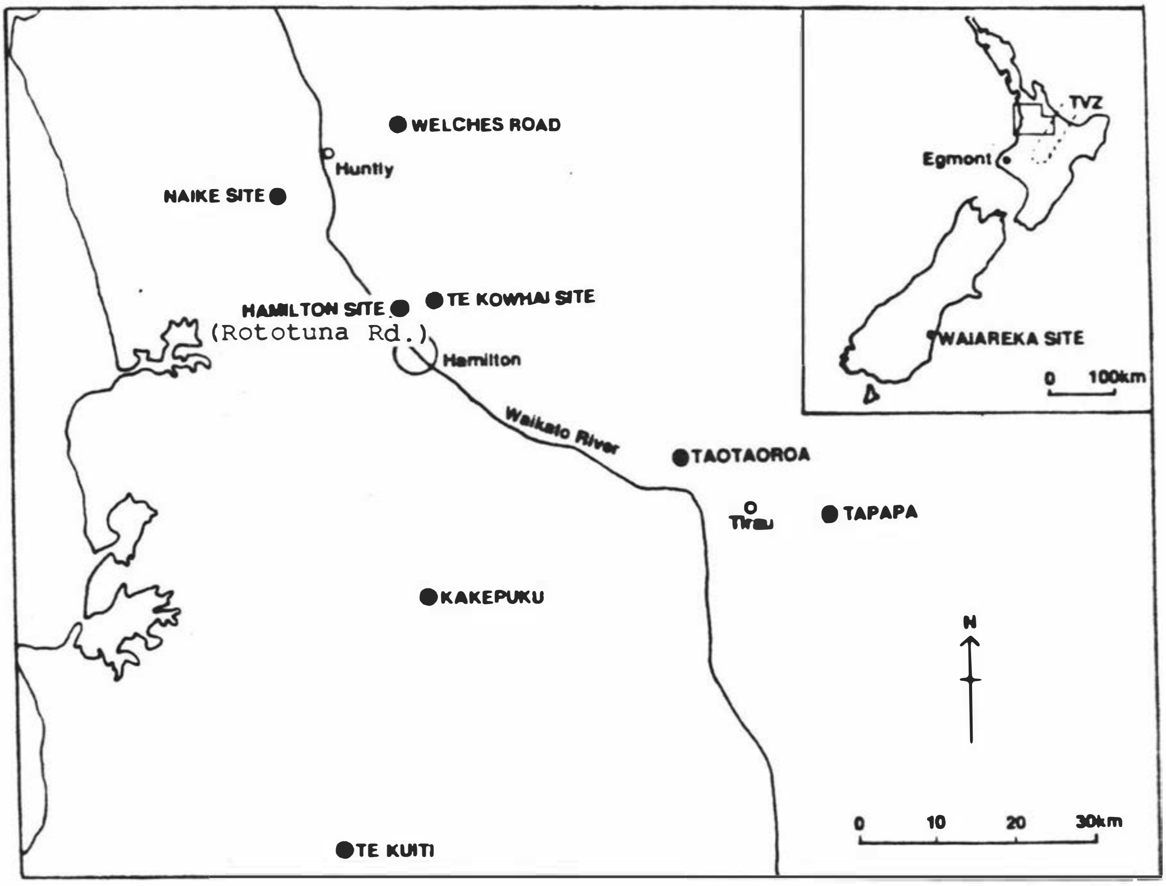

Figure 3.3: Location map of part of the Hamilton basin showing the sites mentioned in the text. TVZ in the insert is Taupo Volcanic Zone.

Soil description

(1) The Hamilton clay loam is a brown granular loam (New Zealand Soil Bureau, 1968). The sampling site (Rototuna Road; S14/102830[1]) was on a flat terrace tread at an altitude of 50 m. Annual rainfall is 1200 mm. A detailed soil description is given in Lowe (1981).

The soil profile can be divided into two units. The underlying clay-rich unit (here referred to as the lower unit) is part of the Hamilton Ash Group (Ward 1967; Pain 1975; Shepherd 1984) while the overlying sandier unit (upper unit) is a composite unit of loess, and andesitic and rhyolitic tephric accretions (M^{c}Craw 1967; Pullar 1967; Vucetich and Pullar 1969).

The Hamilton Ash Group comprises clay-rich, highly weathered tephra, which mantle the low ridges and isolated hillocks that are erosion remnants of Lower-Middle Pleistocene sediments. It contains numerous palaeosols (Shepherd 1984) and is the result of continuous accretion of numerous rhyolitic and andesitic tephra that have been reworked and rapidly weathered (Ward 1967; Stevens and Vucetich 1984; 1985). The ash is now dominated by clay minerals but there are small amounts of residual sand-sized grains, mainly quartz, magnetite, ilmenite and zircon (Shepherd 1984). At Rototuna Road the clays are predominately halloysite with less allophane (Lowe 1981) but near Te Kuiti they are dominantly allophane (Stevens and Vucetich 1984; 1985). A minimum age for the ash is *c*.70 ka (Gibbs 1980). In a detailed study of the Hamilton Ash Group at Welches Road where it is c. 3.8 m thick, Shepherd (1984) identified numerous palaeosols and eight members (H_1 - H_8). Member H_2, a prominent pale horizon at the base of the Group, is the Ohinewai Tephra Formation (Vucetich *et al*. 1978). Mairoa Ash (68 cm thick) overlies the Hamilton Ash Group. At Rototuna Road the top of the Hamilton Ash Group (*i*.e. the top of the lower unit) is correlated with the H_5 or H_6 member (Lowe 1981).

The upper unit is much less weathered and contains more weatherable minerals (e.*g*. glass, feldspars, ferromagnesian silicates) and less clays compared with the lower unit (Lowe 1981; Shepherd 1984;

---

[1] Grid references are based on the metric 1:50 000 series (NZMS 260).

Stevens and Vucetich 1984; 1985; Joe 1986). Based on mineralogical evidence, Lowe (1981) identified the Rotoehu, Aokautere, Okareka and Tuhua tephras in the upper unit. These do not form discrete bands because they have been mixed. The presence of the Rotoehu Ash indicates that there have been tephra additions to the upper unit for at least the last *c.* 42 ka.

Cristobalite has been frequently reported from the Hamilton clay loam. New Zealand Soil Bureau (1968), Lowe (1981) and Joe (1986) report up to *c.* 30% cristobalite in the clays from the upper unit while Lowe (1981), Shepherd (1984) and Joe (1986) report up to *c.* 15% cristobalite in the sands or silts. Generally, larger amounts of cristobalite have been reported from the upper unit compared with the lower unit.

(2) The Naike clay is a brown granular loam. The sampling site (S14/934975) was on an 11° slope of a hill spur at an altitude of 100 m. Annual rainfall is 1240 mm. The parent material is the Hamilton Ash Group and details of the soil site are given by New Zealand Soil Bureau (1968) and Anon (1981). These reports indicate that there is a marked change in properties at *c.* 20 cm. Above 20 cm there is an increased sand content and these sands comprise more weatherable minerals (feldspars and Fe-Mg silicates) compared with deeper horizons where quartz, magnetite, ilmenite and muscovite are more common. The clay content of the top 20 cm is lower and contains more vermiculite, kaolinite and allophane (with halloysite) compared with deeper levels where the clay content is higher (>88%) and is totally dominated by halloysite. The total element chemistry (e.g. Mn, K, Si, Al, Zn, Rb, Y and Ba) and soil solution chemistry (*e.g.* K, Na, Al) also demonstrate a marked change at *c.* 20 cm depth (Anon 1981).

New Zealand Soil Bureau (1968) and Anon (1981) both record minor cristobalite in the clay fraction of the top of the profile while the New Zealand Soil Bureau (1968) record a trace of tridymite in the sand fraction of the C horizon.

(3) The Te Kowhai silt loam is a gleyed yellow-brown pumice soil on a flat, poorly drained site (S14/120819), adjacent to a sand quarry. Altitude is 30 m and the site receives 1270 mm annual rainfall. The soil has formed in a swale of an old channel on a gently undulating plain developed in the Hinuera Formation.

The Hinuera Formation (Schofield 1965; Hume *et al.* 1975) is a low angle fan of volcanogenic alluvium that was deposited by the braided river system of the Waikato River during several phases of fan building (M^{c}Craw 1967; Hume *et al.* 1975). It is composed of gravelly sands and silts which are reworked rhyolitic volcanic debris (mainly pumiceous) from the central North Island. It also contains localised peats. The youngest phase of fan building (Hinuera-2) has been dated at 20 - 15 ka (Hume *et al.* 1975; M^{c}Glone *et al.* 1978; Green and Lowe 1985) and the final phase of alluvial sedimentation in the region of the gravel pit ceased approximately 15.5 ka ago (Green and Lowe 1985; Lowe 1987).

Details of the soil at the sand quarry are given by Anon (1981) while M^{c}Queen (1975) presented a detailed study of the Horotiu-Te Kowhai soil complex. The Horotiu silt loam is a yellow-brown loam with a clay fraction dominated by allophane, and forms on well drained sites in pumiceous alluvium (Hinuera Formation). It forms a soil complex with the Te Kowhai silt loam, a gley soil with a clay fraction dominated by halloysite and found in poorly drained sites on the Hinuera Formation (M^{c}Queen 1975; Joe 1986).

The mineralogy of the Te Kowhai silt loam is dominated by glass (Joe 1986). Cristobalite is common (up to 5% of the clay and 15% of the sand fractions). Quartz and feldspar are relatively constant components of the sand fraction (*c.* 20%) except below one metre depth where there is a marked increase with a concomitant decrease in glass content (Joe 1986). Heavy minerals are rare in the sands except for the top 20-30 cm where there is a significant rise in this fraction (mainly orthopyroxene, magnetite and hornblende).

(4) The Waiareka clay is a brown granular clay (New Zealand Soil Bureau 1968). The sampling site (J41/419602) was on a bench at an altitude of *c.* 30 m. Annual rainfall is 600 mm.

This soil has developed on the Eocene Waiareka Volcanic Formation (Gage 1957; Suggate *et al.* 1978). In the region of the railway cutting this comprises calcareous basaltic tuffs. The clay fraction is dominated by montmorillonite and the sand fraction is mainly quartz, feldspar, cristobalite and epidote group minerals (New Zealand Soil Bureau 1968). There is a change in the components of the sand fraction at *c.* 55 cm with chlorite abundant, and many of the scarcer phases absent, below this depth. Similarly, the soil chemistry (Fe, P, Na, K and Ca) indicates that there is a significant change at 55 cm. This change is taken to reflect the transition to the relatively unweathered Waiareka Volcanic Formation.

RESULTS

GRAIN SIZE DISTRIBUTION

Although different grain size divisions were used in previous work on the soils of the present study (New Zealand Soil Bureau 1968; Lowe 1981; Anon. 1981), published results are in good agreement with those of the present investigation.

The Hamilton soil is a silty clay (Fig. 3.4) with horizons above 50 cm being coarser than those in lower horizons. The top 30 cm has a uniform and sandier texture while between 30 and *c.* 60 cm there is a transition to clay-rich lower horizons.

The Ap horizon of the Naike soil has a coarser texture than the 2Bt1 horizon (30-80 cm depth) which has a very high clay content (Fig. 3.5). Below 80 cm is a 3Bt2 horizon in which the sand content is similar to the Ap horizon. The Bw horizon (20-30 cm depth) is transitional between the sandy Ap and clay-rich 2Bt1 horizons. The coarse nature of the 3Bt2 horizon is mainly due to authigenic halloysite nodules whereas the coarse A horizon is due to coarse grained primary minerals.

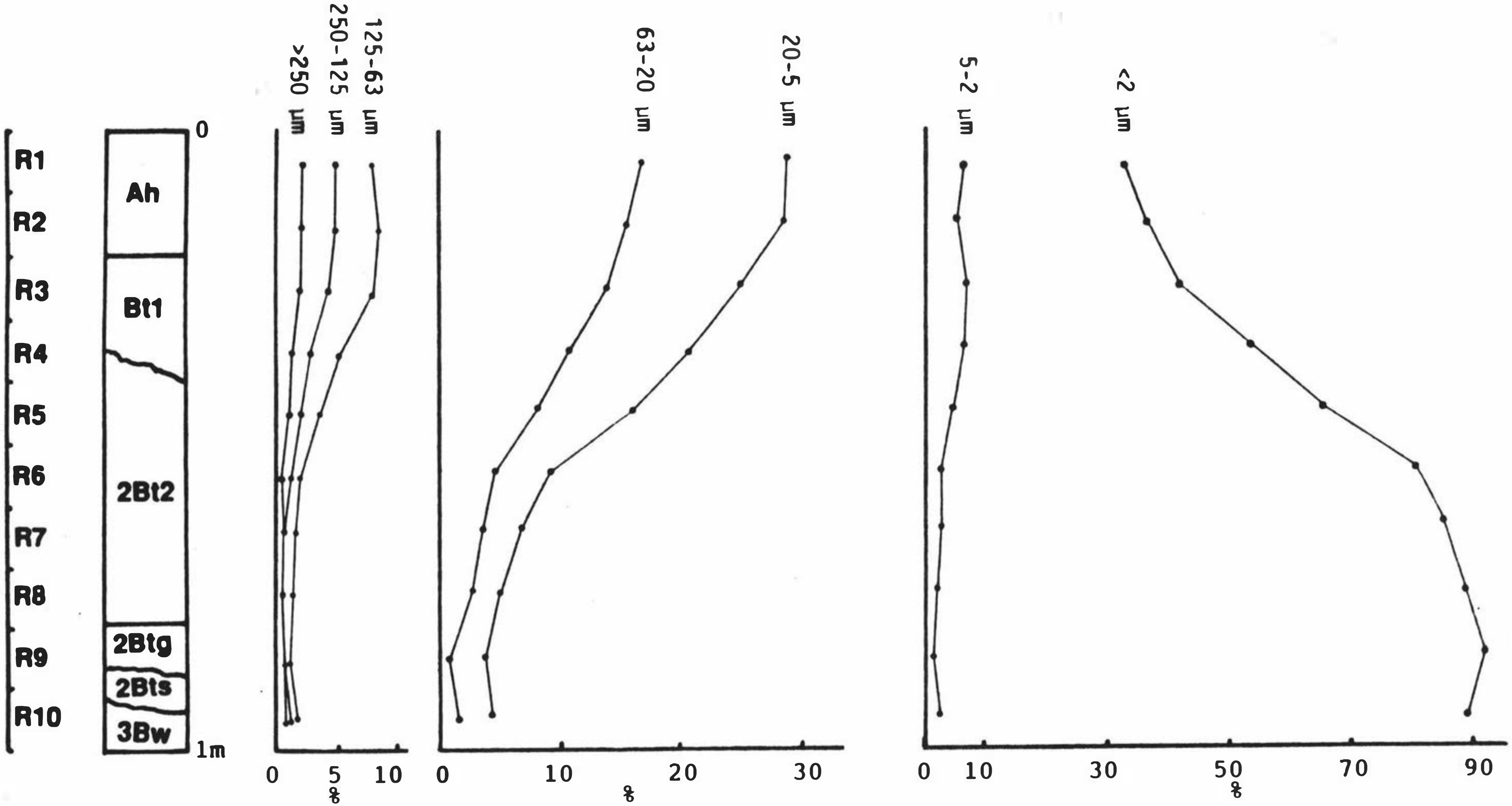

Figure 3.4: Variations in the grain size distribution for various size fractions of the Hamilton clay loam.

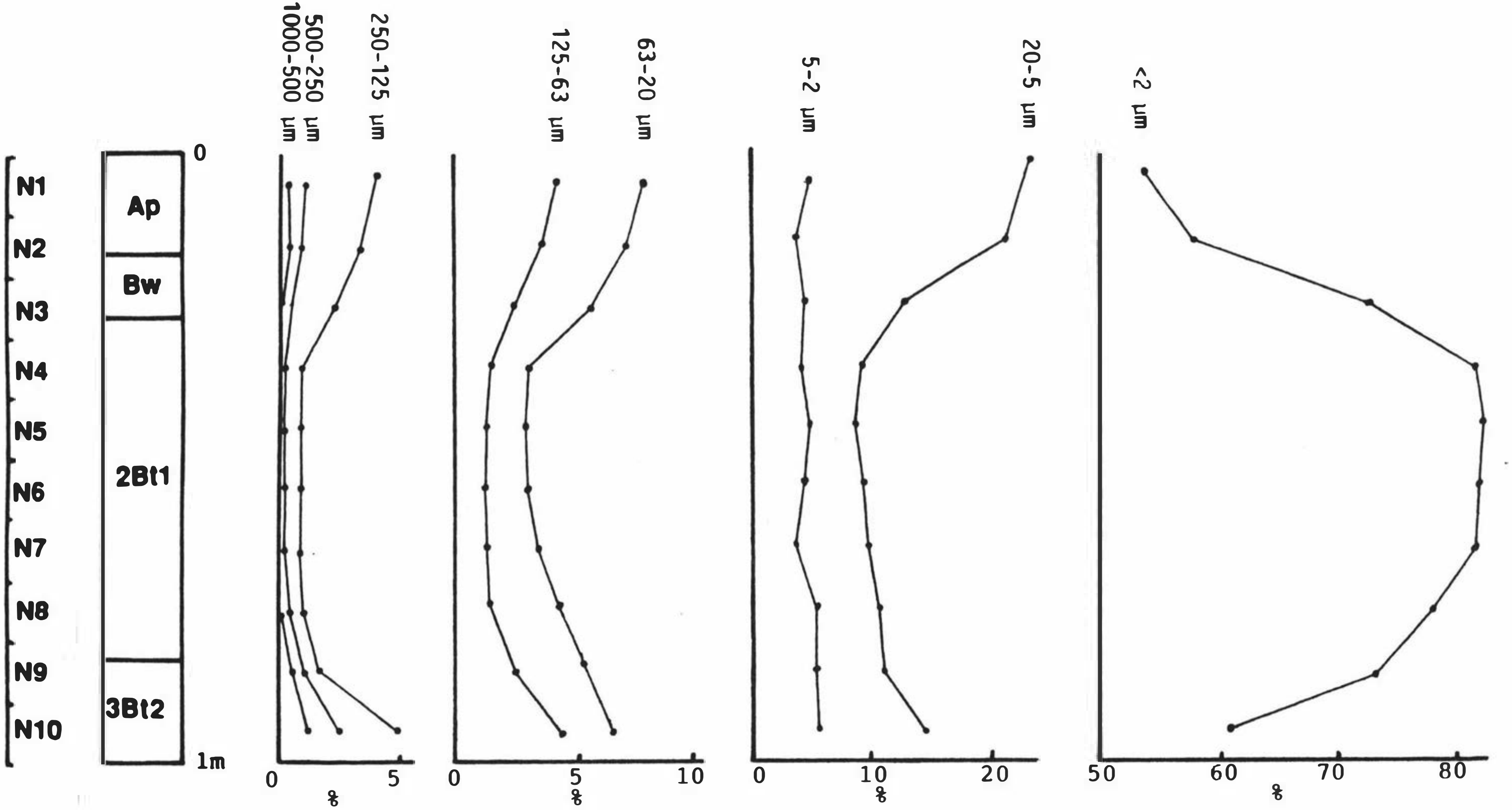

Figure 3.5: Variations in the grain size distribution for various size fractions of the Naike clay.

The Te Kowhai soil has a variable texture as would be expected from an alluvial parent material (Fig. 3.6). It is stratified and there is an increase in the very fine sand and coarse silt towards the base of the profile. The medium and fine silt fractions increase towards the top of the profile.

Particle size parameters show the Waiareka soil to be a silty clay. The upper 30 cm (A and B horizons) are uniform in texture while the BC horizon (30-40 cm depth) is transitional to the C horizon. Towards the base there is an increasing abundance of blocks of the Waiareka Volcanic Formation (up to 10 cm in diameter). These blocks have coatings of clays, presumably translocated down joints in the welded tuffaceous parent material.

Cristobalite was not identified in this soil profile. During the XRD scans however, quartz was observed to be abundant in the top 30 cm but absent below 40 cm. Quartz has not been previously identified in the Waiareka Volcanic Formation and its presence in the soil is interpreted as resulting from aerosolic additions to the profile. Although such additions could be derived from volcanic sources as a component of airfall tephra (e.g. Stewart 1982; Stewart *et al.* 1984; 1986) there is no apparent volcanic source of an appropriate age or composition in the region. The quartz therefore probably results from loess additions to the profile.

Due to the absence of cristobalite this soil is not considered further.

GRAIN MORPHOLOGY

An electron microscope study showed that there were a variety of morphologies in the cristobalite concentrates. The dominant form (Fig. 3.7) is of blocky material with euhedral pits. This type of grain often has striations on its surface (Fig. 3.7). Various forms of residual cristobalite and tridymite (Figs. 3.8, 3.9) are interpreted as remnants of mesostasis intergrowths from which silicates and glass have been removed. A morphology which comprises clusters of striated euhedral crystals occurs in pumiceous xenoliths in the 1886 Tarawera Basalt (Fig. 3.10). Also rare are forms that are apparently composed of florets of very thin blades (Fig. 3.11) which are similar to lepispheres.

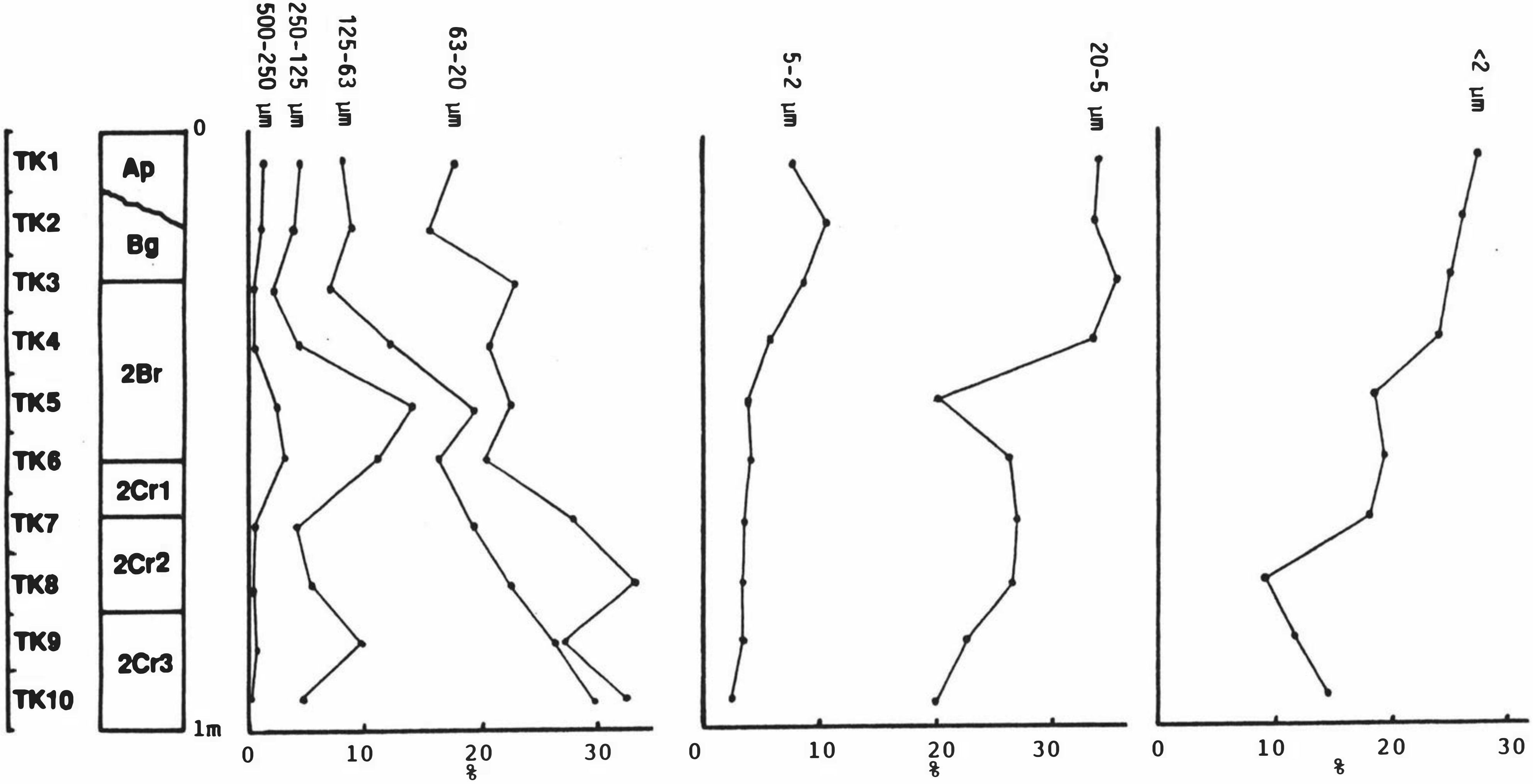

Figure 3.6: Variations in the grain size distribution for various size fractions of the Te Kowhai silt loam.

A

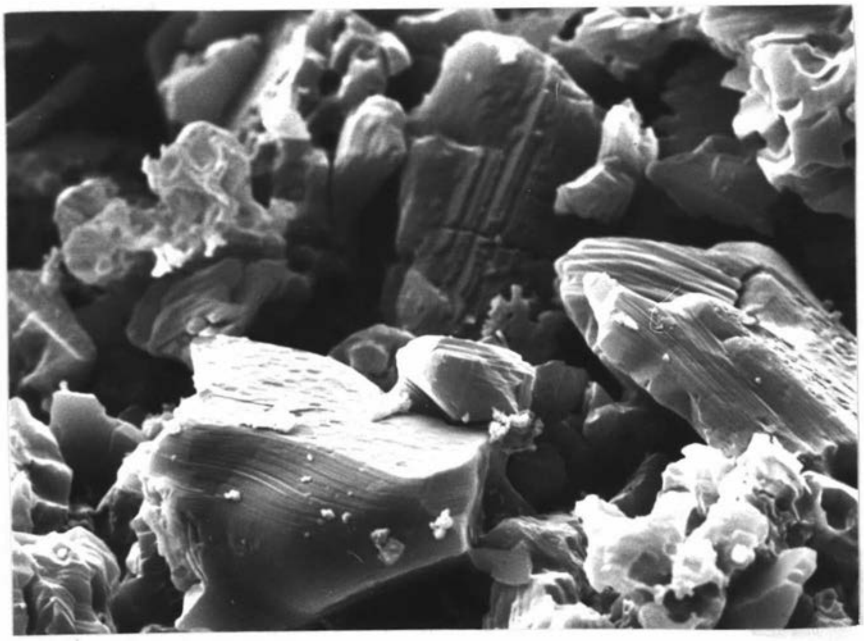

B

Figure 3.7 : (A) Typical blocky cristobalite with euhedral pits and surface striations. (B) Surface striations enhanced by acid treatment. Scale bar represents 10 microns.

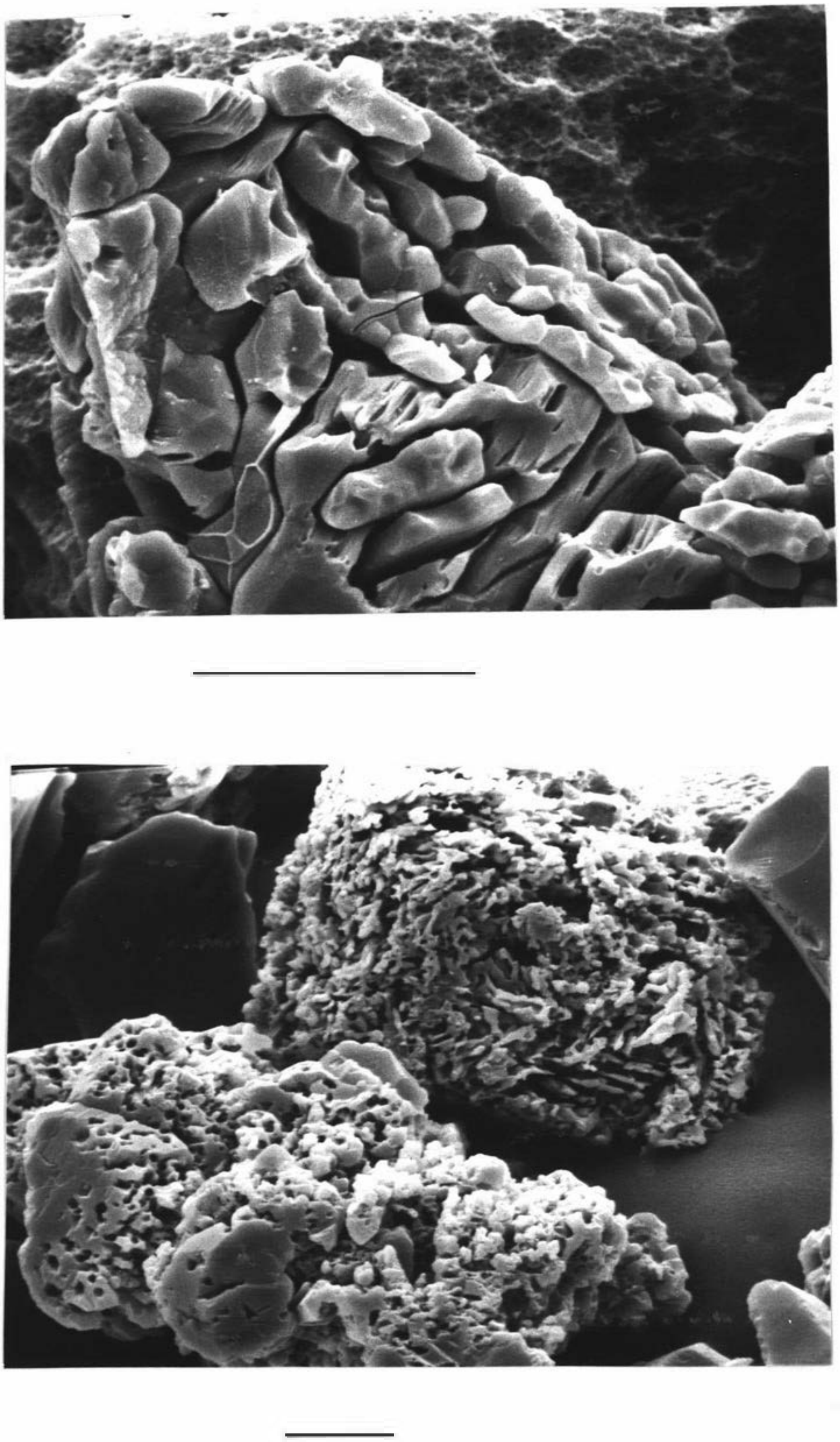

Figure 3.8 : Less common forms of cristobalite.
Remnants of mesostasis type intergrowths.
Scale bar represents 10 microns.

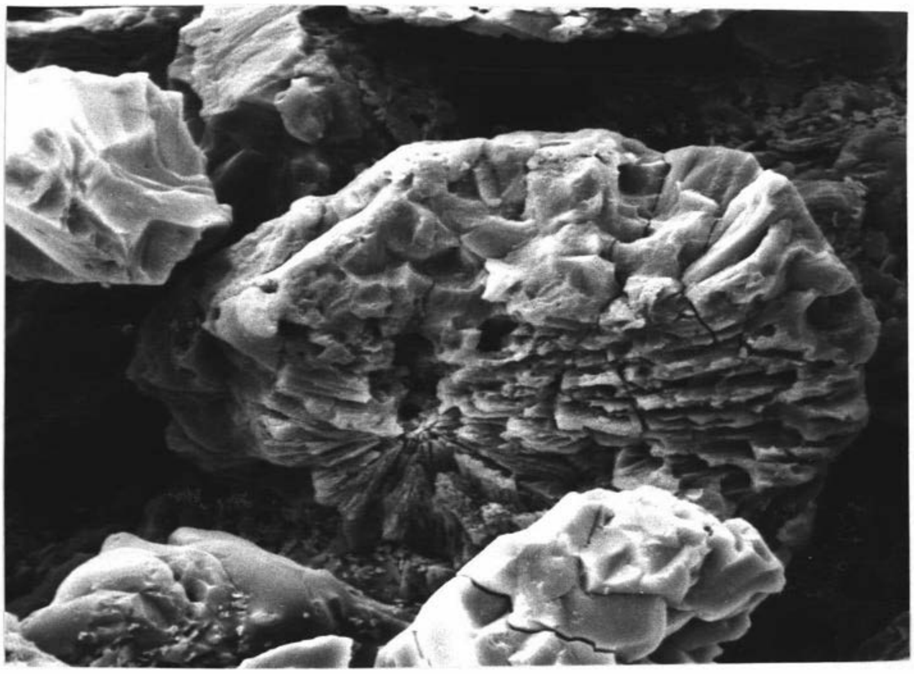

A

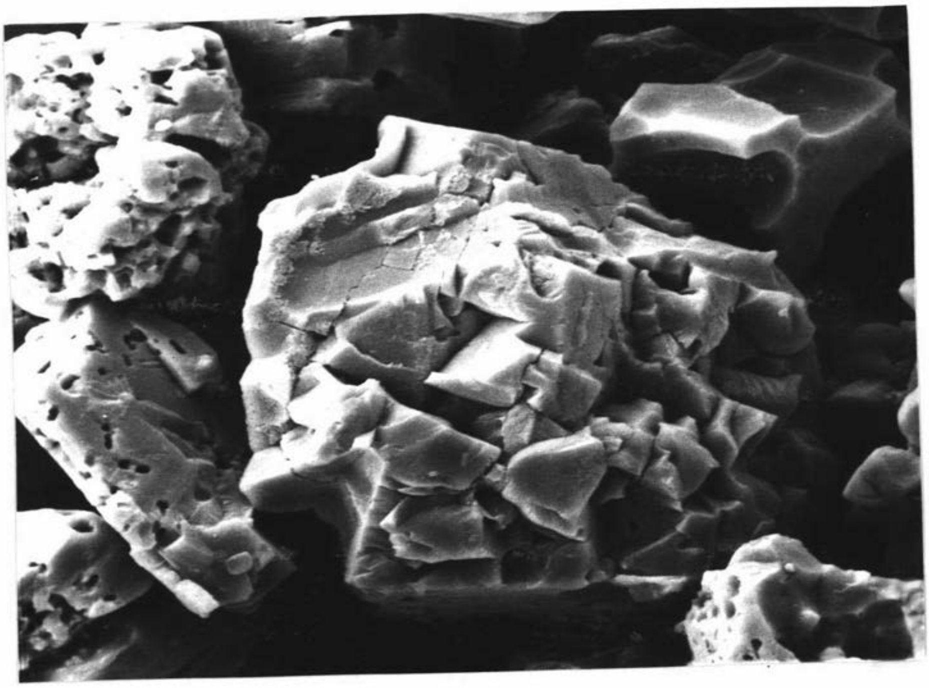

B

Figure 3.9: (A) Cristobalite remnants from a spherulitic intergrowth. (B) Cristobalite which is thought to represent material crystallised from an interstitial liquid phase. Scale bar represents 30 microns.

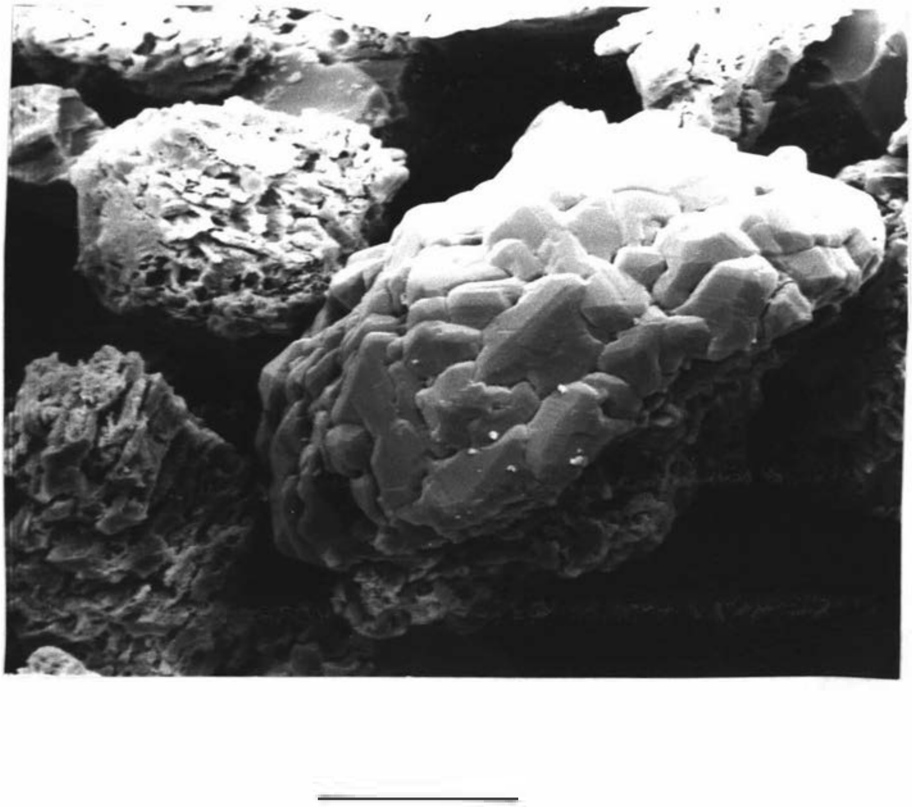

Figure 3.10: Striated cristobalite from pumiceous xenoliths in Tarawera basalt. Scale bar represents 30 microns.

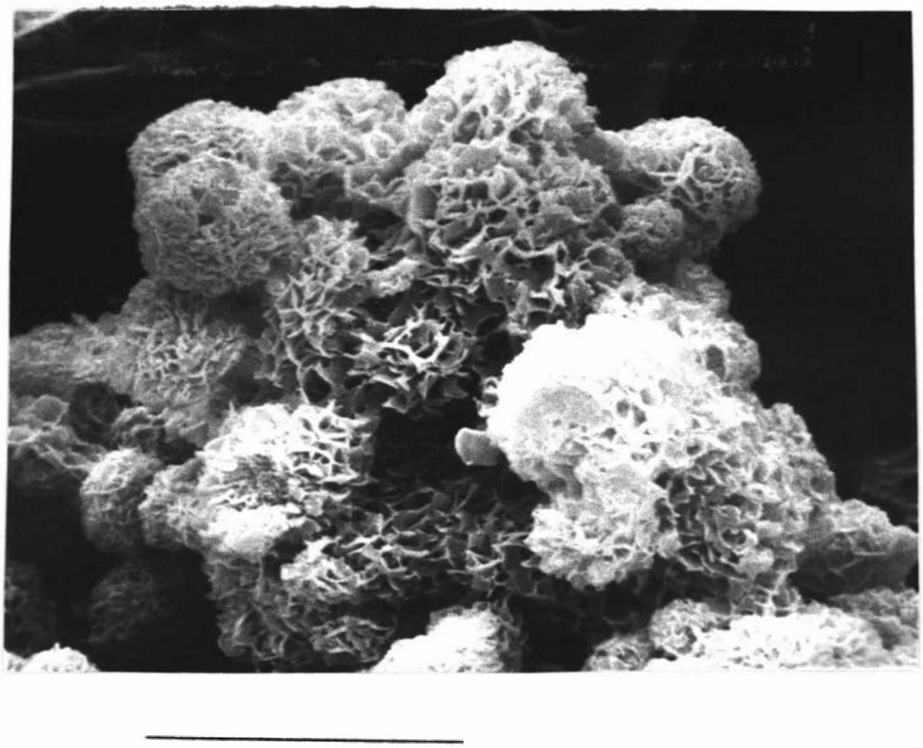

Figure 3.11: An unusual form of cristobalite which is similar to lepispheres. Scale bar represents 10 microns.

The XRD traces of most samples contain tridymite peaks but it is not possible to determine if the tridymite is discrete. Grains with wedge-shaped twins similar to those described for tridymite have been observed optically in some samples and it is thought that the hexagonal grains illustrated in figure 3.12 may be tridymite. This phase appears to be uncommon. Frondel (1962; see also Wilson *et al.* 1974) reports that "high-tridymite", which has hexagonal symmetry, is found as thin plates with hexagonal outlines but Jones and Segnit (1975) and Florke *et al.* (1976) also describe opal-CT with a platy hexagonal morphology. Based on this electron microscope study the evidence for discrete tridymite is equivocal.

During sample preparation a low density fraction (<2.25 Mg m^{-3}) was separated. This included volcanic glass shards, phytoliths, diatoms, sponge debris and two distinct forms of what has been interpreted as opal-A (Fig. 3.13). One of these distinct forms occurs in the Hamilton soil while the other is from the Naike soil. Although their distributions were not systematically studied some general observations can be made.

The opal-A from the Hamilton soil is composed of rounded equidimensional to prismatic, or platy forms (Fig. 3.14). In grain mounts these forms are concentrically zoned (up to 5 zones per grain) and SEM investigation shows that the outer shells of some grains are cracked and appear to have "exfoliated" from the grain core. This exfoliation phenomenon only occurs with the samples prepared for the electron microscope and is thought to be due to ultra-desiccation under high vacuum during sample preparation. Although the outer surfaces of the grains are reasonably smooth, close examination of the surface revealed by the "exfoliation" indicates that it comprises equidimensional particles c. 1600Å in diameter. This form is referred to as concentric opal-A and occurs in samples R6, R9 and R10 but not in R1, R2 or R3, i.e. it occurs in the lower unit of the Hamilton soil.

The opal-A from the Naike soil is composed of irregular subangular to subrounded grains which contain a high density of micron-sized inclusions. These give the grains a dusty appearance, so this form is

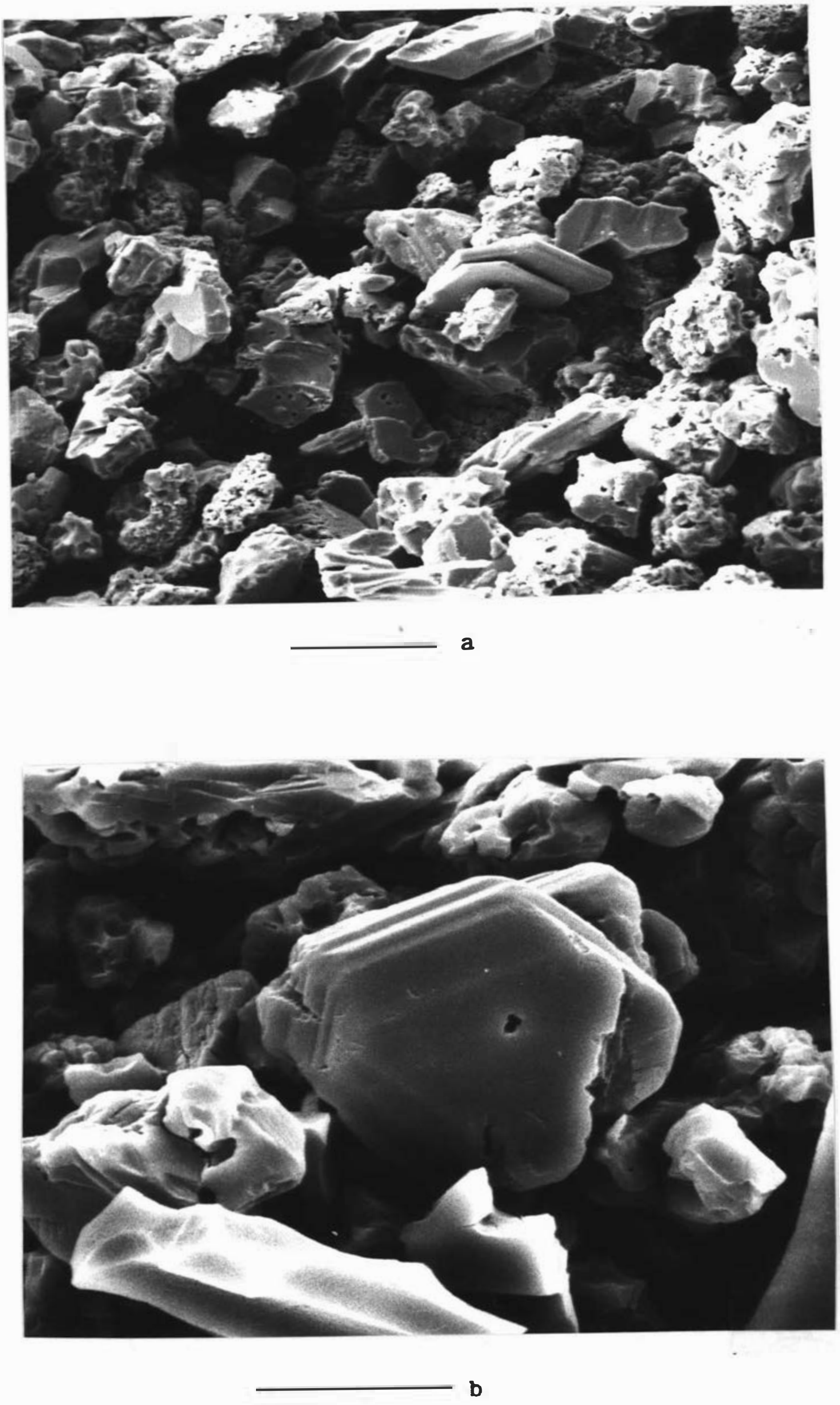

Figure 3.12: Tridymite or cristobalite in the form of hexagonal plates. Scales are 50 microns (a) and 10 microns (b).

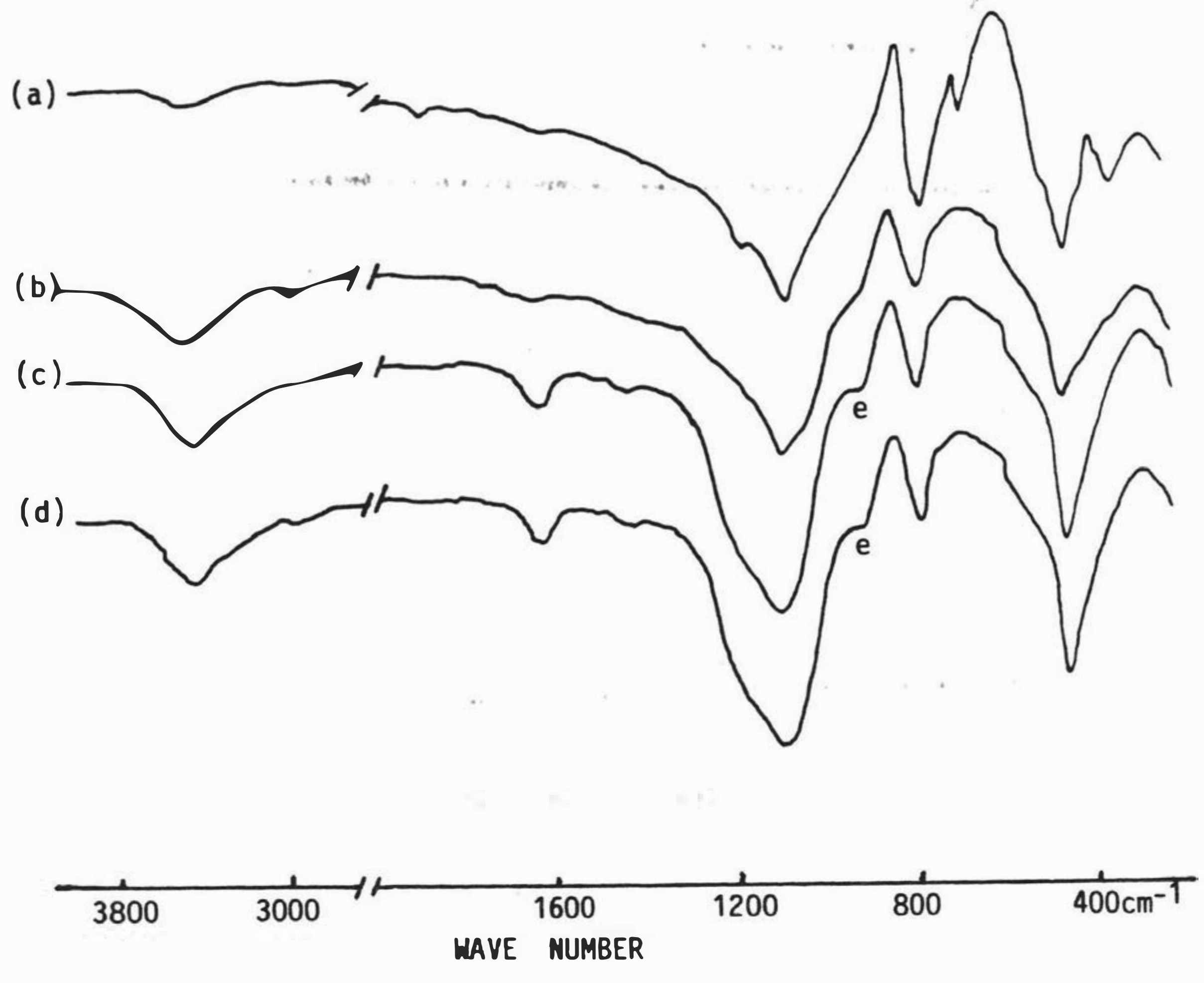

Figure 3.13: Infra-red spectra of some silica phases from the soils studied. (a) Quartz. (b) Phytoliths. (c) Concentric opal-A. (d) Dusty opal-A. (e) Wave number 960 cm^{-1} is referred to in the text.

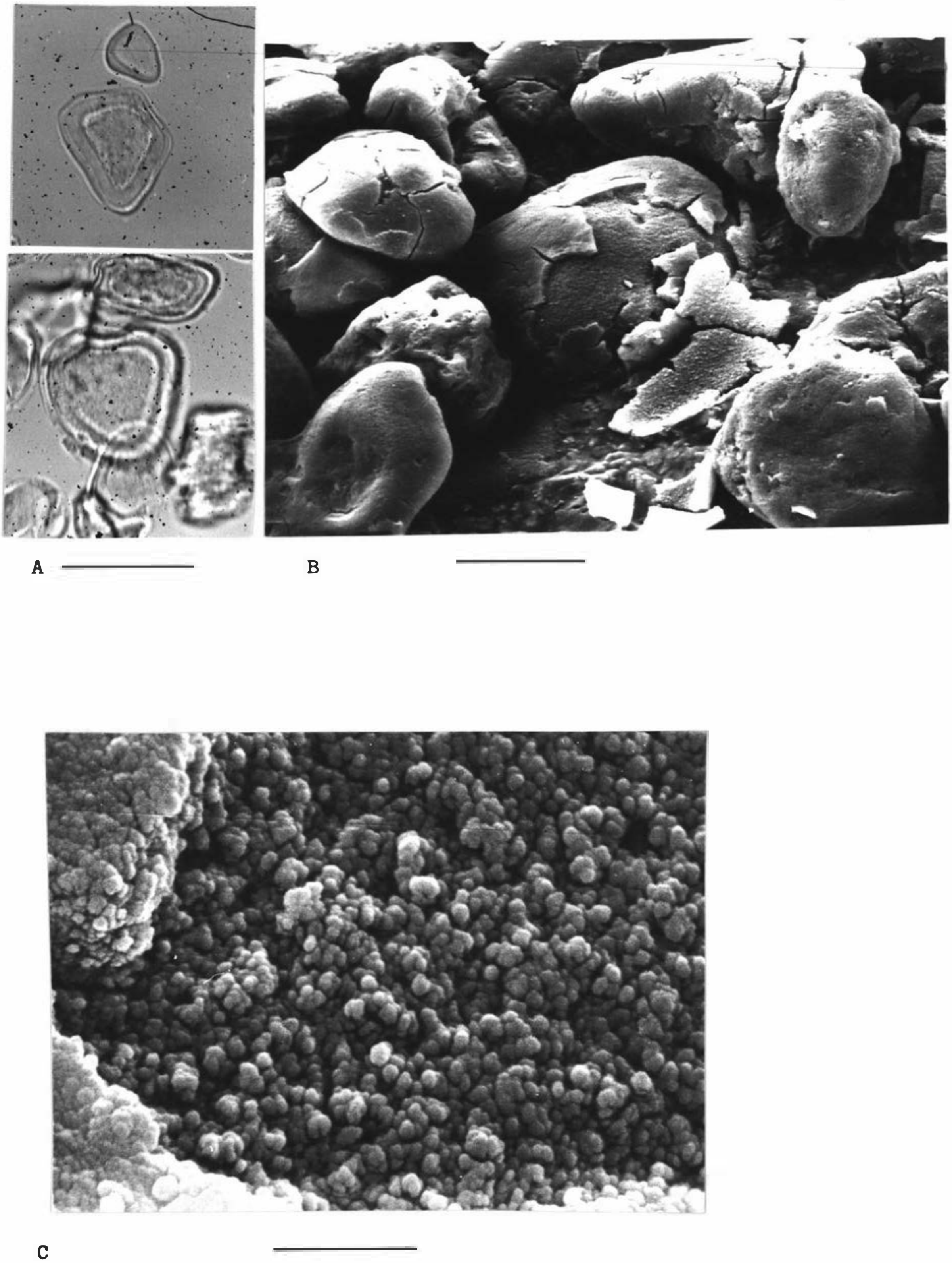

Figure 3.14: Morphology of the concentric opal-A.
(A) Optical zoning (transmitted light, scale is 40 microns).
(B) SEM image showing exfoliation (scale is 20 microns).
(C) High magnification SEM (scale is 1 micron).

referred to as dusty opal-A. In rare cases the inclusions are anisotropic and appear to represent minerals incorporated in the grains during growth. The inclusions invariably have a higher refractive index than their host. Electron microscope study indicates that this form has a very porous surface (Fig. 3.15). The dusty opal-A occurs in samples N8 and N10 but not in the top 20 cm of the Naike soil.

OPAL-C AND TRIDYMITE-M NOMENCLATURE

Identification of the low density silica polymorphs based on x-ray diffraction is complicated because (1) cristobalite and tridymite may occur as both intergrown or discrete phases, (2) the I_{100} peaks for tridymite and cristobalite overlap, and (3) the relative intensities of peaks in the same phase are variable depending on the structural state. Further, β-cristobalite which has an XRD pattern similar to α-tridymite (Brown 1980) may occur at surface temperatures and pressures (Greig 1932; Sosman 1932). These problems may be compounded in soils due to mixing. To facilitate better identification and discrimination between cristobalite and tridymite, selected samples were given an additional density separation (S.G. of 2.3 gm cm^{-3}) to separate cristobalite and tridymite. Although the resultant concentrates were not monomineralic the one with the lower density shows enhanced tridymite XRD peaks while the other shows enhanced cristobalite peaks (Fig. 3.16). Based on this x-ray data, electron microscopy and optical data, it is concluded that at least some of the tridymite reflections are due to discrete tridymite.

The multiplicity of cristobalite peaks in the concentrate heavier than 2.3 Mg m^{-3} (Fig. 3.16) indicates that the phase present is opal-C (i.e. α-cristobalite). Tridymite peaks also occur and this tridymite may either be present as discrete grains or as subdomains in cristobalite. In the tridymite concentrate the absence of doublet reflections at 3.85Å, 3.00Å and 2.50Å and a relatively strong reflection at 3.25Å indicate that the tridymite phase is tridymite-M.

β-cristobalite is also a possible component in the soil but the absence from the diffractograms of major reflections at 2.53, 1.64 and 1.46Å (Brown 1980) suggests that it is not common in these soils.

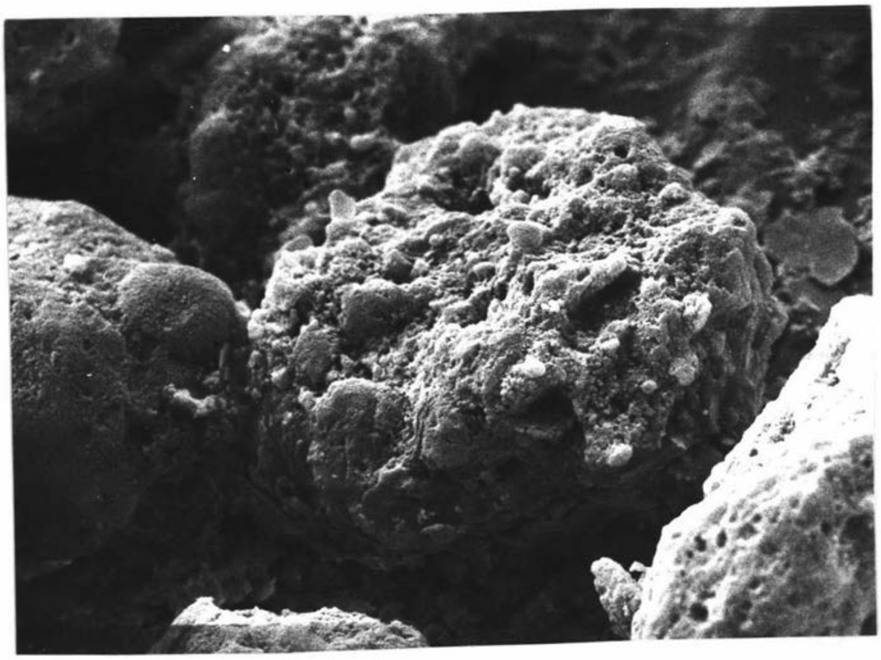

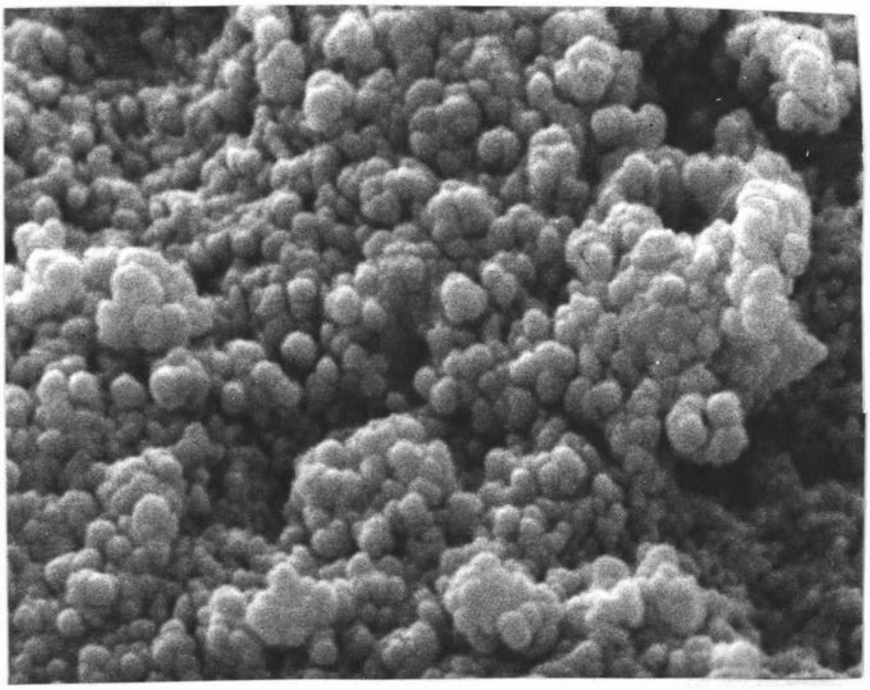

Figure 3.15: Morphology of the dusty opal-A showing the rough nature of the surface (A) and the microspheres within the grains (B). Scales bars are 20 microns for (A) and 1 micron for (B).

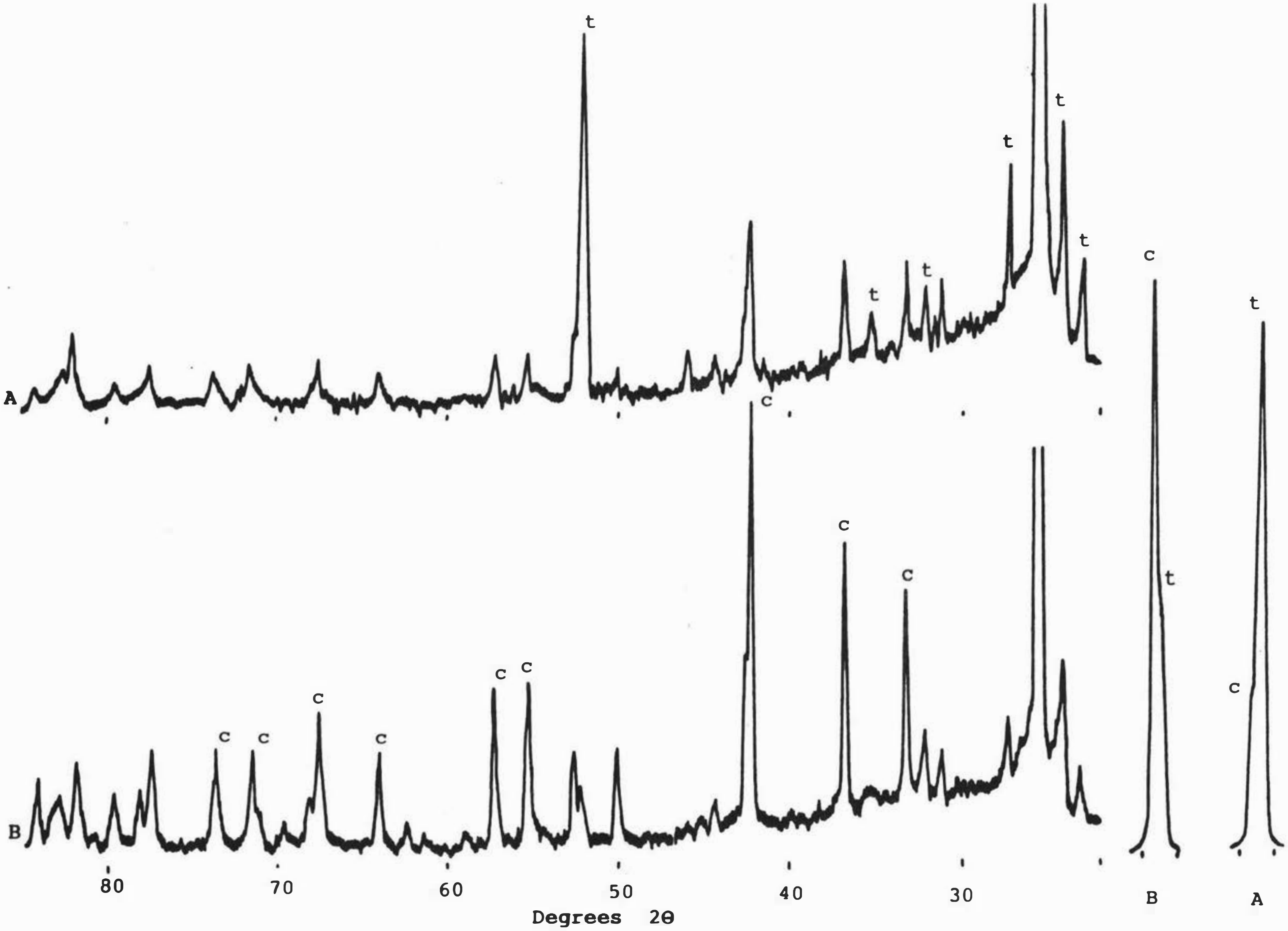

Figure 3.16: XRD patterns of concentrates of tridymite (A) and cristobalite (B) after repeated density separations at 2.3 Mg m^{-3}. The detail of the I_{100} reflections between 25° and 26° 2θ is also shown. Diagnostic reflections are marked, c for cristobalite and t for tridymite.

Furthermore, optical investigation indicates that the concentrates are dominated by grains which are weakly anisotropic, thus precluding β-cristobalite (cubic) as a dominant phase. High cristobalite (i.e. β-cristobalite) has recently been reported from soils (Mizota *et al.* 1987) but the d-spacings of the reflections they have indexed, together with close examination of their diffractograms, suggest that this phase is probably tridymite (reflections at 4.3, 4.1, 3.82, 2.97 and 2.48Å). Although the relative intensities of the reflections of their β-cristobalite do not fit tridymite as documented by Brown (1980), neither do they fit the relative intensities of β-cristobalite. Hill and Roy (1958a), Roy and Roy (1964) and Tada and Iijima (1983) show that the relativity of peak intensity is quite variable. The β-cristobalite identified by Mizota *et al.* (1987) is therefore probably tridymite.

In the standardised XRD traces (Fig. 3.17) the cristobalite type is identified using the 3.14Å and 2.85Å reflections. If they are present the phase is identified as opal-C whereas if they are absent opal-CT is indicated. The tridymite phase present is tridymite-M and this has been identified using the form and presence of the reflections at 3.85, 3.25 and 3.00Å. The relative proportions of opal-C and tridymite-M are difficult to determine because the I_{100} peaks (c. 4.05Å and 4.11Å respectively) overlap considerably. This ratio may be meaningless because each phase may occur as subdomains in the other, but as an approximate measure of the maximum concentration of these two phases the height above background of their I_{100} peaks (or the level of a shoulder peak if one is very dominant) is taken as a measure of the amount present.

CRYSTALLINITY OF CRISTOBALITE AND TRIDYMITE IN THE SOILS

To investigate possible variations in the types of cristobalite and tridymite present, plagioclase and mafic minerals were removed from the samples by the ABFS treatment (chapter 2). The final concentrates were dominated by quartz, cristobalite and or tridymite with additional minor phases which were resistant to the pre-treatment (e.g. zircon, rutile, anatase). XRD analyses of these concentrates, standardised so that the traces are comparable, were prepared from a selected grain size for each profile.

Cristobalite has been reported from the sand fractions of the soils being studied (e.g. Shepherd 1984; Joe 1986) but in the present study, after ABFS treatment, cristobalite and tridymite were found to be rare in the very fine sands and absent in the coarser fractions. During washing after the ABFS treatment, fines (< c. 20 µm) were released by the sands and subsequent investigation of this material revealed that it was dominated by opal-C and tridymite. The sand fractions of the soil contain abundant pumice grains and volcanogenic lithic fragments and it is here suggested that the cristobalite and tridymite in this fraction occurs either as fine crystals attached to, or trapped in pumice, or as components in lithics. Much of the cristobalite reported from the sand fractions of the soils probably has a similar origin.

Opal-C and tridymite-M are common in the silt and clay fractions.

(A) Coarse Silt: In the Hamilton soil (Fig. 3.17a) the top 40 cm are dominated by tridymite-M with only minor opal-C. Below 40 cm the reflections are more uniform and indicate that opal-C and tridymite-M are present in approximately equal amounts. The XRD patterns for the Naike soil (Fig. 3.17b) demonstrate that there is an approximately uniform distribution of opal-C and tridymite-M down the profile. In the Te Kowhai soil the XRD pattern of the minor peaks reflect the distribution of relatively uniform amounts of opal-C and tridymite-M down the profile (Fig. 3.17c).

(B) Medium Silt: In the Hamilton soil there are well developed peaks for opal-C in all samples except the bottom two where the 3.14, 2.85 and 4.48Å reflections are greatly reduced. This is attributed to the much lower cristobalite and tridymite contents of sample R10. Like opal-C, tridymite-M appears to be uniformly distributed down the profile except for the two basal samples where the 3.85, 3.25 and 3.0Å reflections are greatly reduced. Expanding the scan range to higher angles for these two samples produces a significant reflection at 2.04Å, i.e. consistent with tridymite. In the Naike soil opal-C and tridymite-M are comparatively uniformly distributed down the profile (Fig. 3.17e) although in sample N8 they are both much reduced. The medium silt fraction of the Te Kowhai soil also has uniformly distributed opal-C or tridymite-M (Fig. 3.17f).

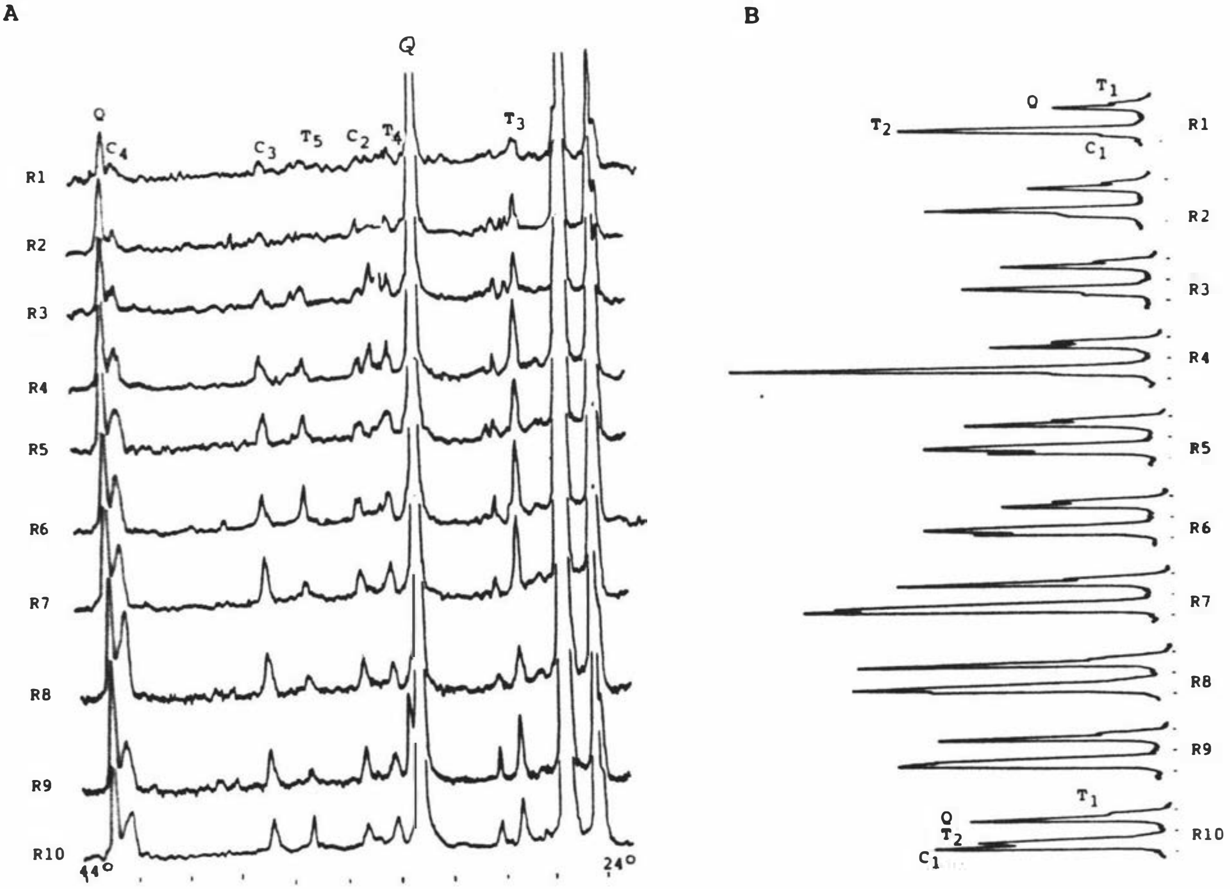

Figure 3.17a: Hamilton coarse silt fraction.

Figure 3.17: Forms of the XRD patterns between 24° and 44° 2θ for opal-C, tridymite-M and quartz in the silt fractions of the Hamilton, Naike and Te Kowhai soils. Q designates quartz reflections. C_1, C_2, C_3, C_4 are the 4.05, 3.14, 2.85 and 2.48Å reflections of opal-C. T_1, T_2, T_3, T_4 and T_5 refer to the 4.33, 4.11, 3.85, 3.25 and 3.0Å reflections of tridymite. (A) shows the smaller reflections, (B) shows the detail of the reflections between 24° and 26° 2θ. These are repeated for each sample down the profiles.

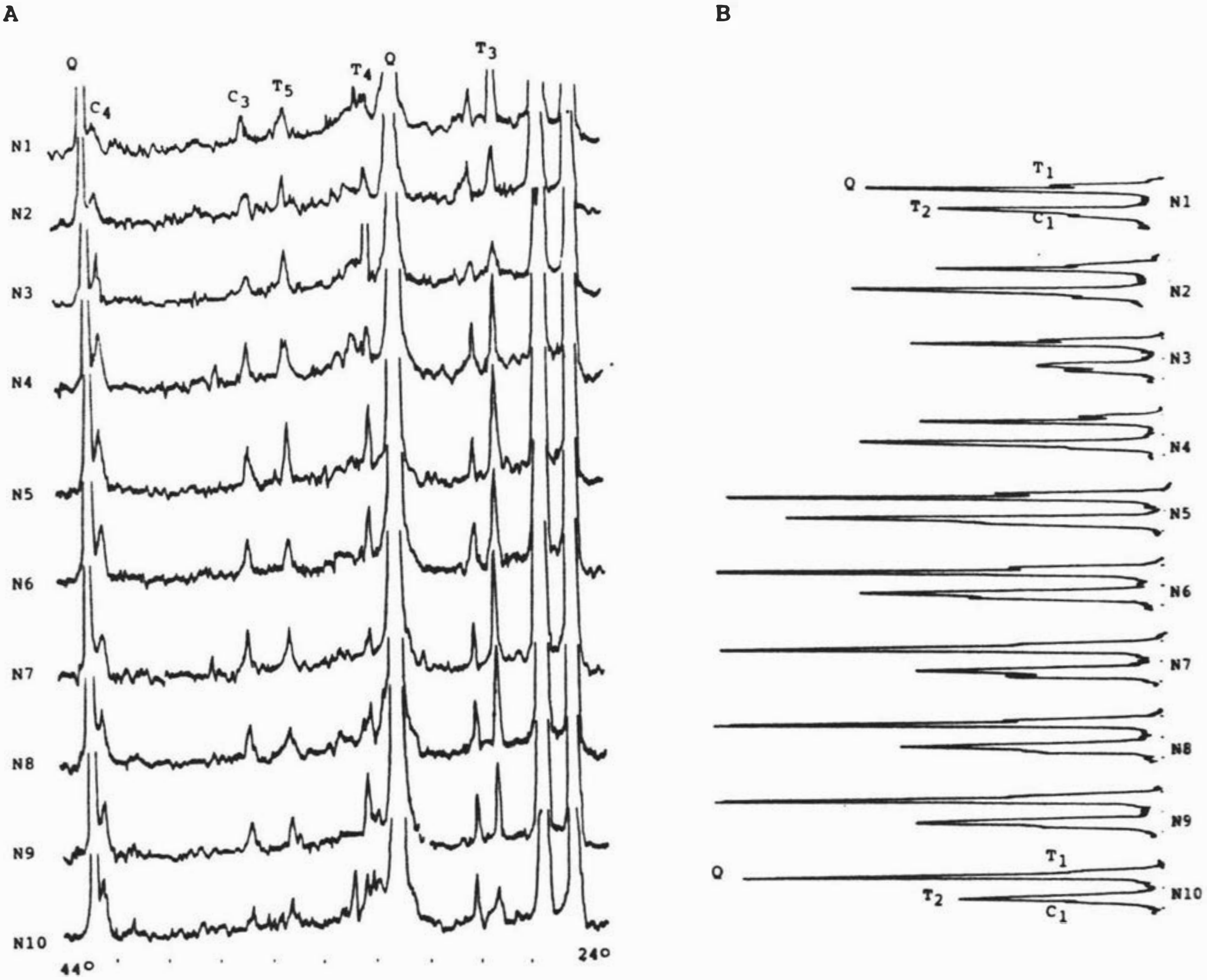

Figure 3.17b: Naike coarse silt fraction.

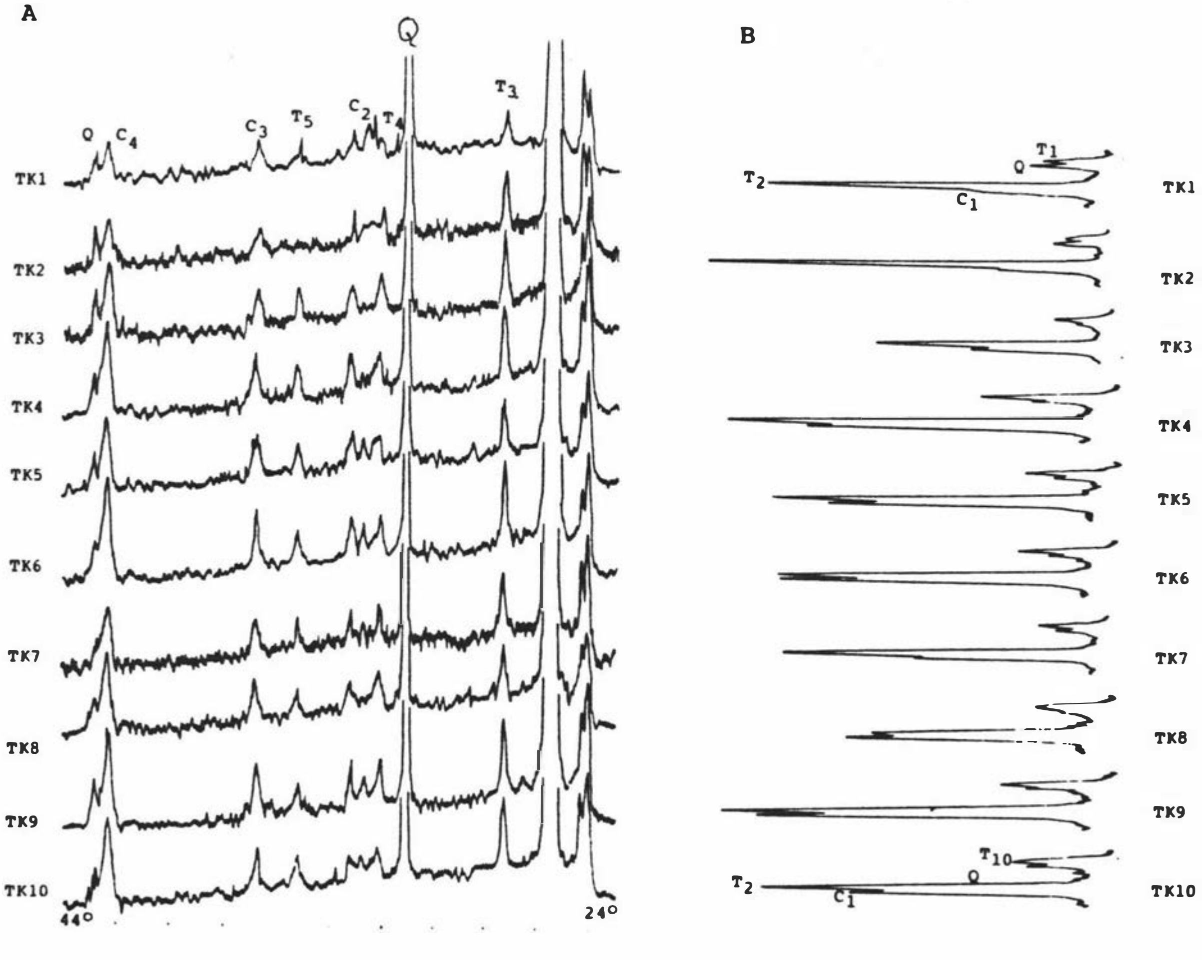

Figure 3.17c: Te Kowhai coarse silt fraction.

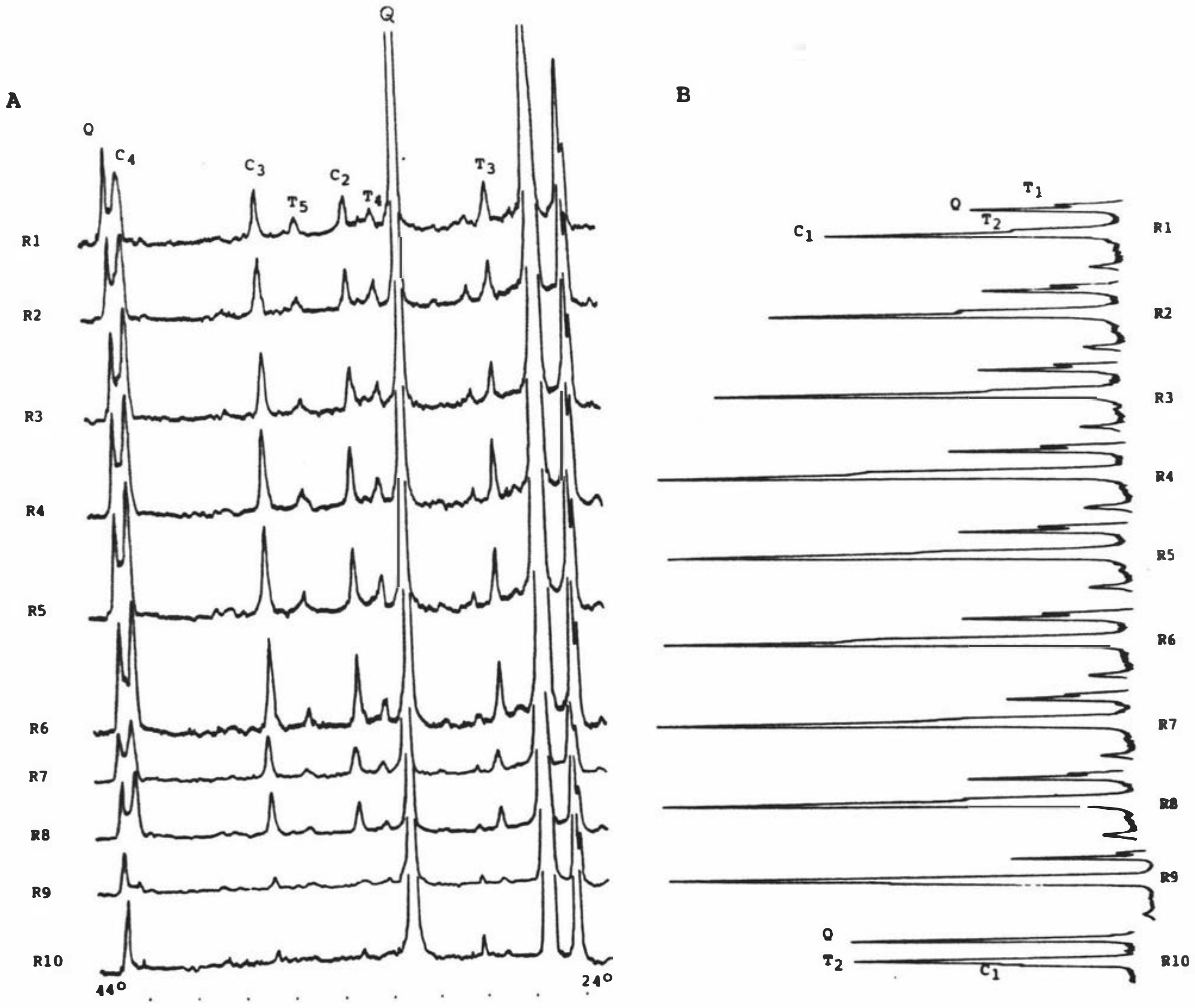

Figure 3.17d: Hamilton medium silt fraction.

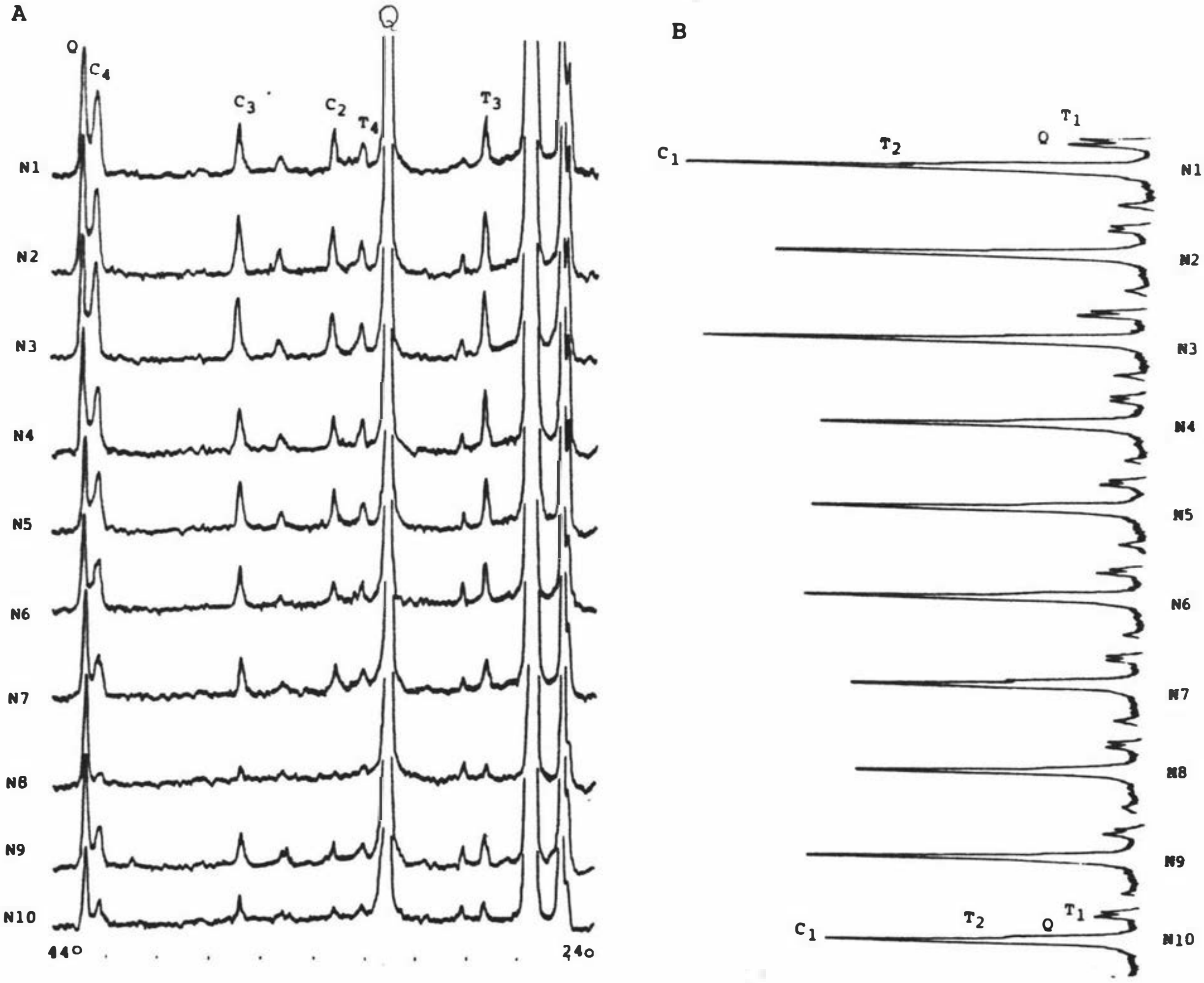

Figure 3.17e: Naike medium silt fraction.

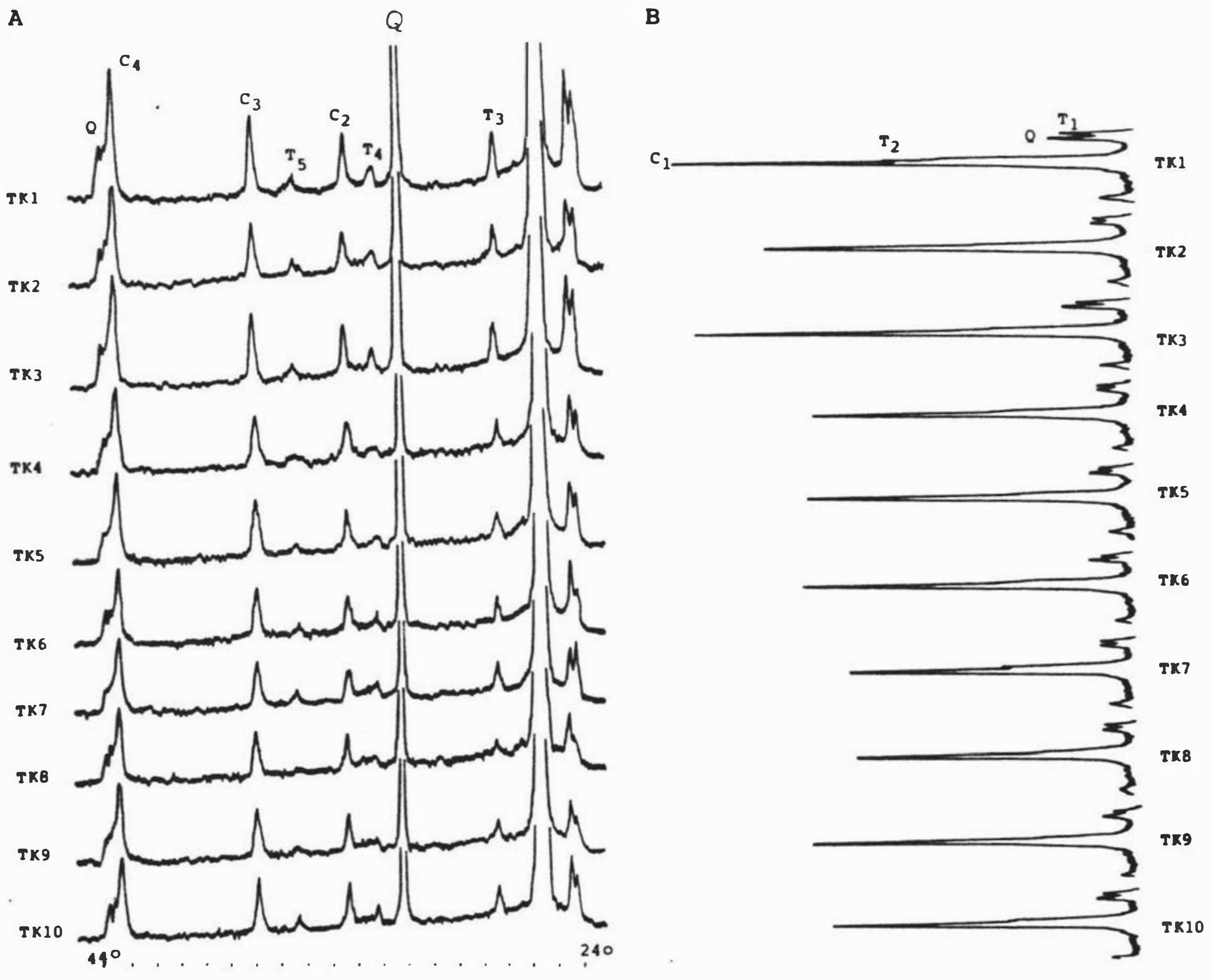

Figure 3.17f: Te Kowhai medium silt fraction.

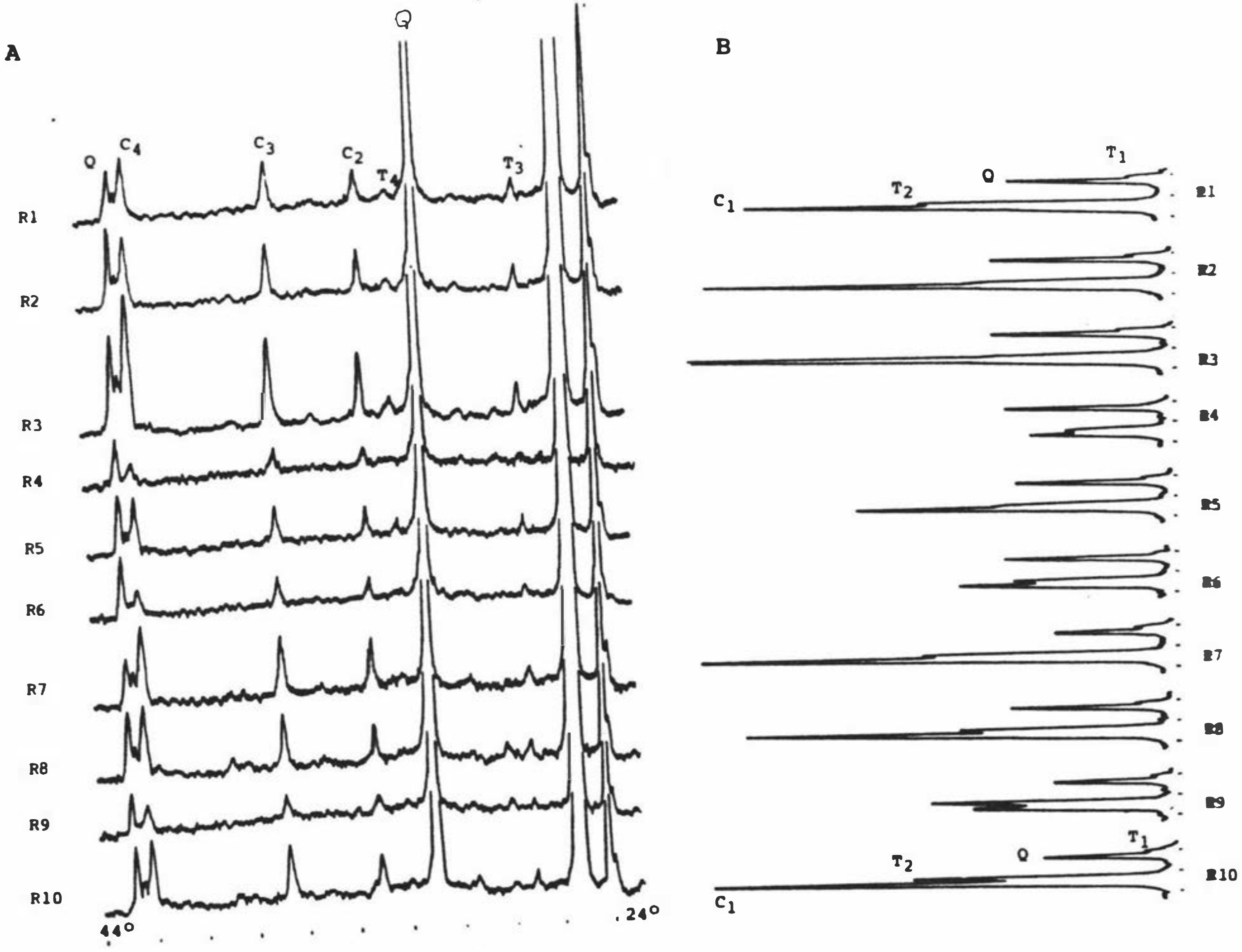

Figure 3.17g: Hamilton fine silt fraction.

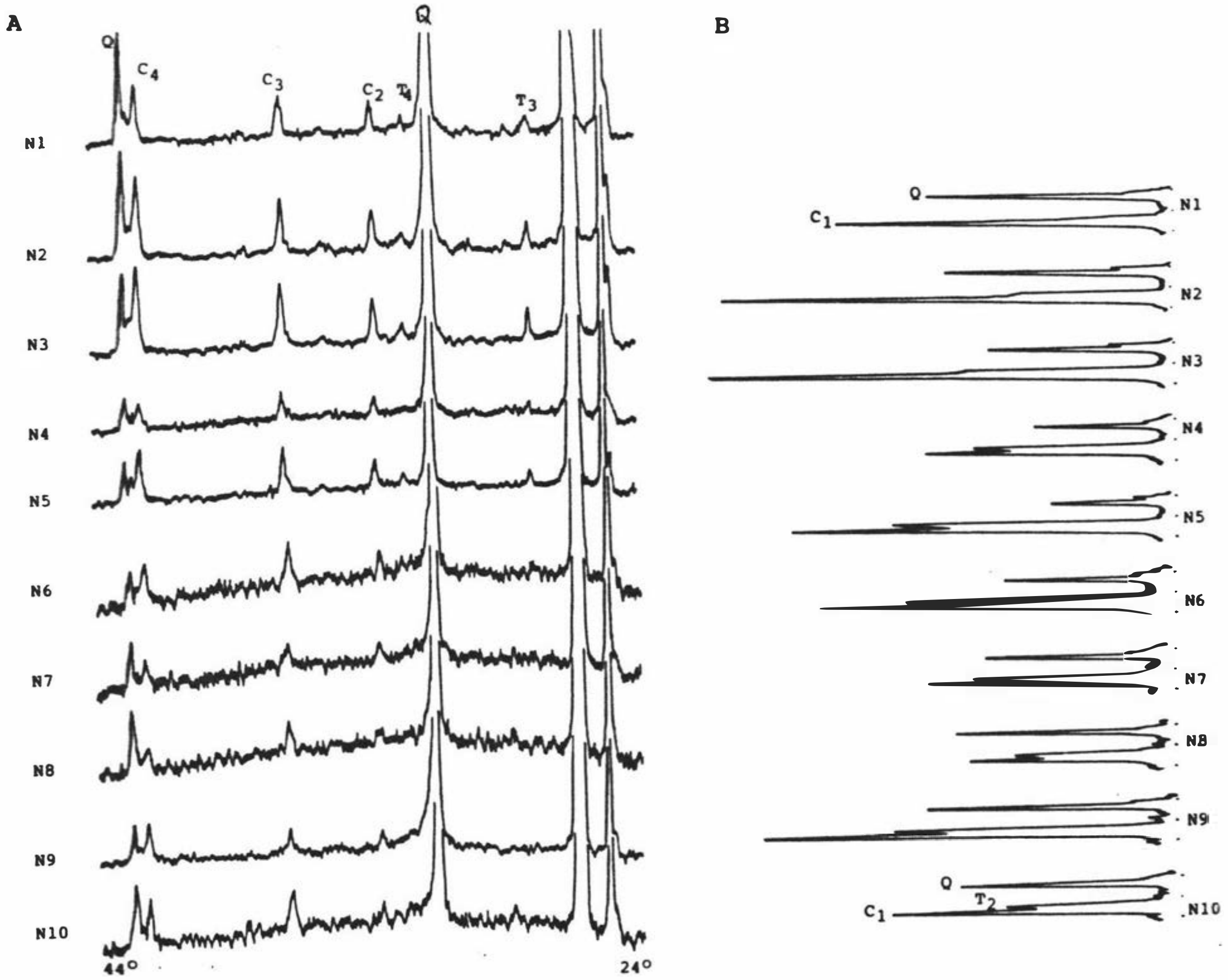

Figure 3.17h: Naike fine silt fraction.

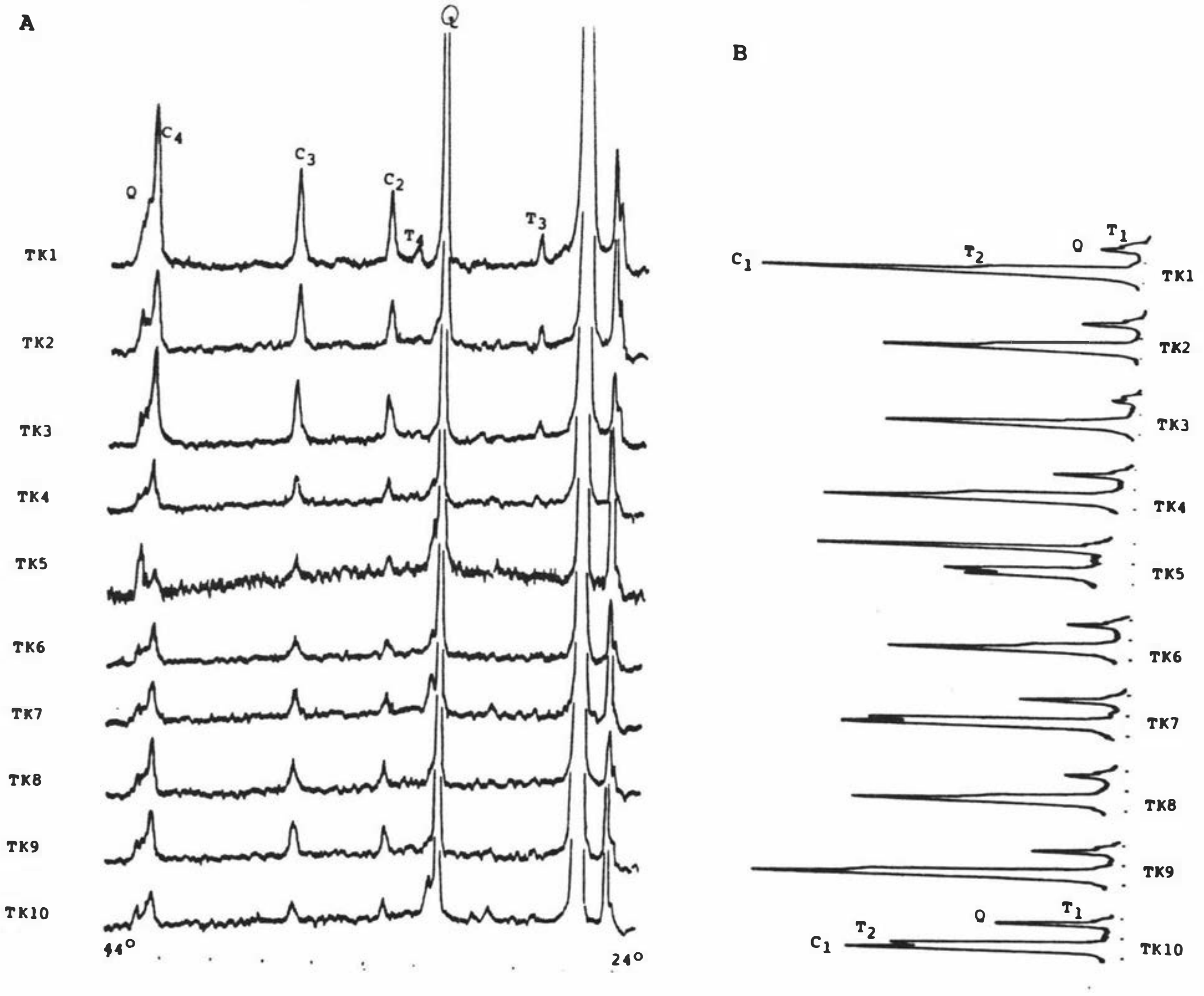

Figure 3.17i: Te Kowhai fine silt fraction.

(C) Fine Silt: In the fine silt the tridymite-M 3.00Å and 3.25Å reflections are absent while the 3.85Å peak is quite variable. Plots of the I_{100} reflection (Fig. 3.17) indicate that tridymite is apparently still a major component so the above changes in the XRD patterns may reflect a change in the form of tridymite. Electron microscopy shows, however, that most of the grains have a similar morphology (they are not composed of two forms, cristobalite and tridymite), so the tridymite with reduced reflections may result because tridymite now no longer occurs as a discrete phase but as tridymite subdomains in cristobalite.

In the Hamilton soil opal-C occurs apparently uniformly distributed throughout the profile although there is a zone between 30 and 60 cm deep where the 2.48, 2.85 and 3.14Å peaks are smaller. Tridymite is represented by reflections at 4.33, 4.11 and 3.85Å. In the Naike soil there is a general tendency for reduced 2.48, 2.85 and 3.14Å opal-C peak size with increasing depth. Furthermore below 30 cm the 3.85Å tridymite-M peak is very weak or absent. This reduction in spectra intensity is thought to represent very low opal-C and tridymite-M content. The XRD patterns for the Te Kowhai soil demonstrate that all samples are opal-C and that there is a decline in the size of the opal-C peaks with depth. Between 40 and 50 cm deep there are smaller peaks compared with adjacent samples. Tridymite is represented by the 4.11 and 4.33Å reflections but the 3.85Å reflection is only strong in the top 30 cm.

(D) Clay Size Fraction: There is no consistent evidence for tridymite in this size fraction. This absence may be due to either a grain size phenomenon i.e. tridymite does not occur in the clay size fraction in these samples, or tridymite subdomains in cristobalite may no longer occur. If it is due to a lack of tridymite subdomains then it may be because at <2 μm cristobalite crystals can absorb any strain in the lattice (perhaps produced during the β to α transition) whereas in larger grains the strain is relieved via tridymite subdomains.

In the Hamilton soil (Fig. 3.18) opal-C is the dominant silica polymorph. Towards the base of the profile the diffractogram peaks become less well defined due to the low concentrations of the silica

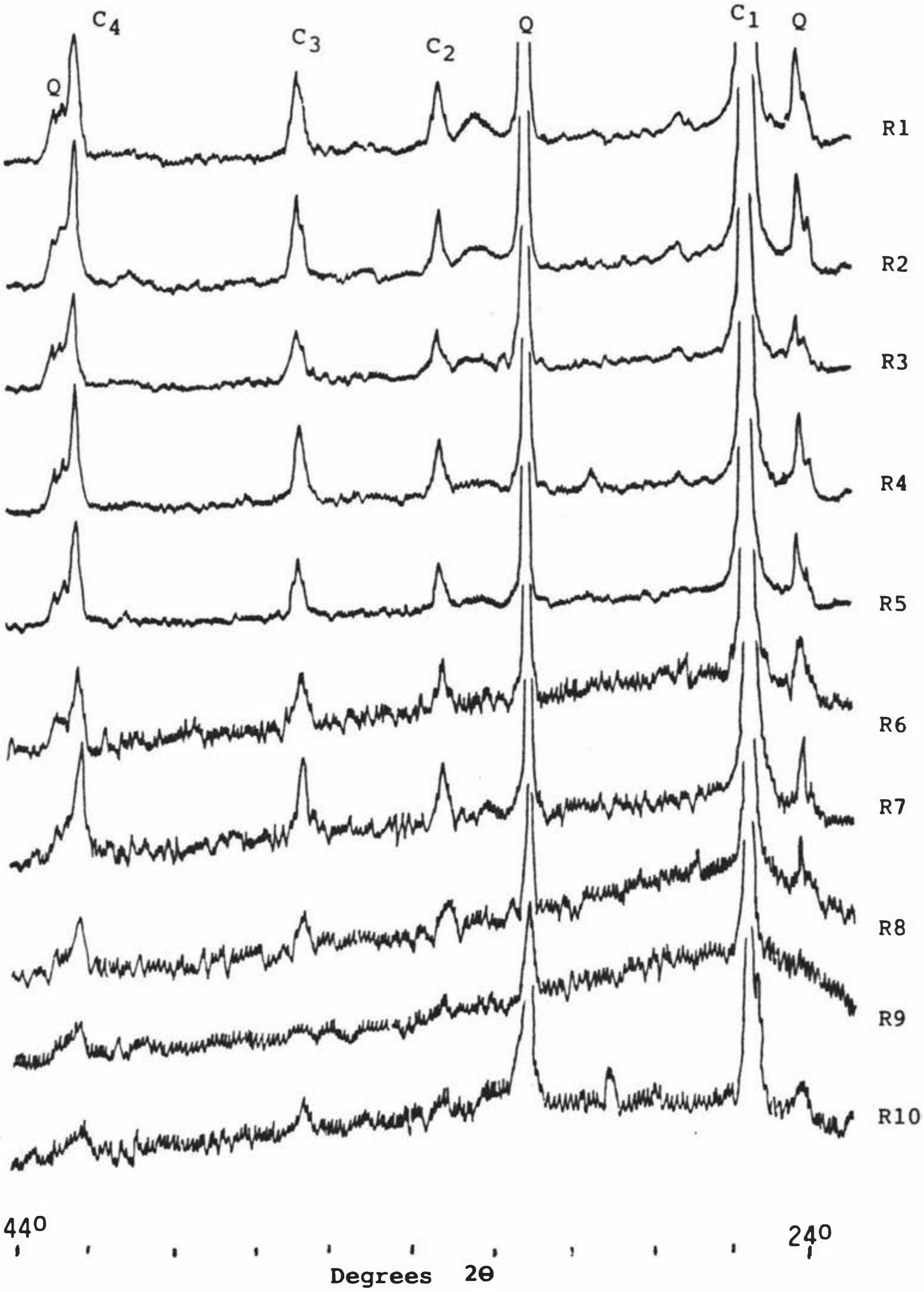

Figure 3.18: Forms of the XRD patterns of the clay fractions in the Hamilton soil. NB there is a change in range by a factor of 2 between R5 and R6. Symbols as for figure 3.17.

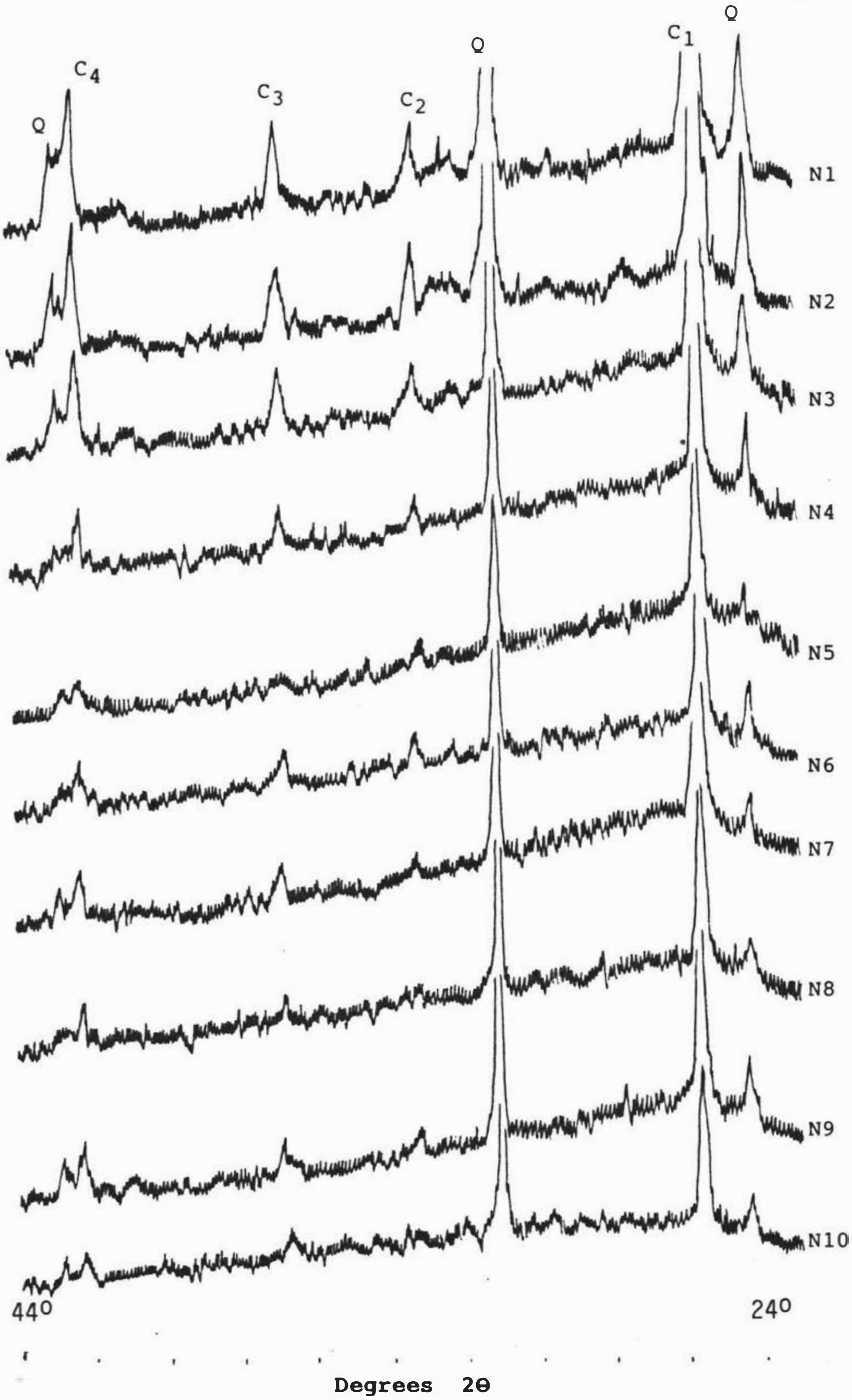

Figure 3.19: Forms of the XRD patterns of the clay fractions in the Naike soil. Symbols as for figure 3.17.

polymorphs. In samples R9-10 the 2.85Å and 3.14Å peaks are minimal indicating that they could comprise opal-CT. The diminution of the opal-C peaks could, however, also be a function of low opal-C content rather than crystallinity (opal-CT); note that definition of quartz spectra is also reduced towards the base. In the Naike soil indisputable opal-C is common above 30 cm. Below 30 cm the diffraction peaks are less diagnostic of opal-C with the size of the 2.85Å and 3.14Å peaks being highly variable. As in the case of the Hamilton soil the very small size or absence of the 2.85Å and 3.14Å peaks (e.g. sample N5 and N8) may reflect a very low opal-C content (see the following section) rather than the appearance of opal-CT. The top three samples of the Te Kowhai soil have strong opal-C spectra (Fig. 3.20) while below 30 cm the spectra of opal-C are less well defined. In two samples (TK9 and TK10) the opal-C reflections are very weak or absent and this is attributed to very low concentrations of opal-C; note the concomitant reduction in the size of the quartz spectra towards the base.

DISTRIBUTION OF CRISTOBALITE AND TRIDYMITE IN THE SOILS:

It is not possible to indisputably determine if the tridymite-M and opal-C identified in the XRD scans are discrete grains, intergrowths of two phases, or mixtures. Therefore where they occur together their distribution down a profile has been plotted both as discrete opal-C and tridymite-M and as the sum opal-C + tridymite-M.

(a) Hamilton clay loam: In the coarse silt, opal-C content increases with depth to a value of c. 14% of this fraction at 60 to 70 cm depth after which there is a decline. When plotted as a proportion of the total sample however, opal-C is relatively constant down to 70 cm but there is a significant reduction below 70 cm (Fig. 3.21). This difference in trends between the two measures is because there are marked variations in the percentage of the coarse silt fraction down the profile. This demonstrates that trends within subsamples which are themselves only minor components of the total sample should be interpreted cautiously. Tridymite-M, which generally exceeds opal-C, is more variable with higher concentrations in the Ah and Bt1 horizons (2.5% in sample R1 and 2% in R4) and less than 0.5% below 50 cm.

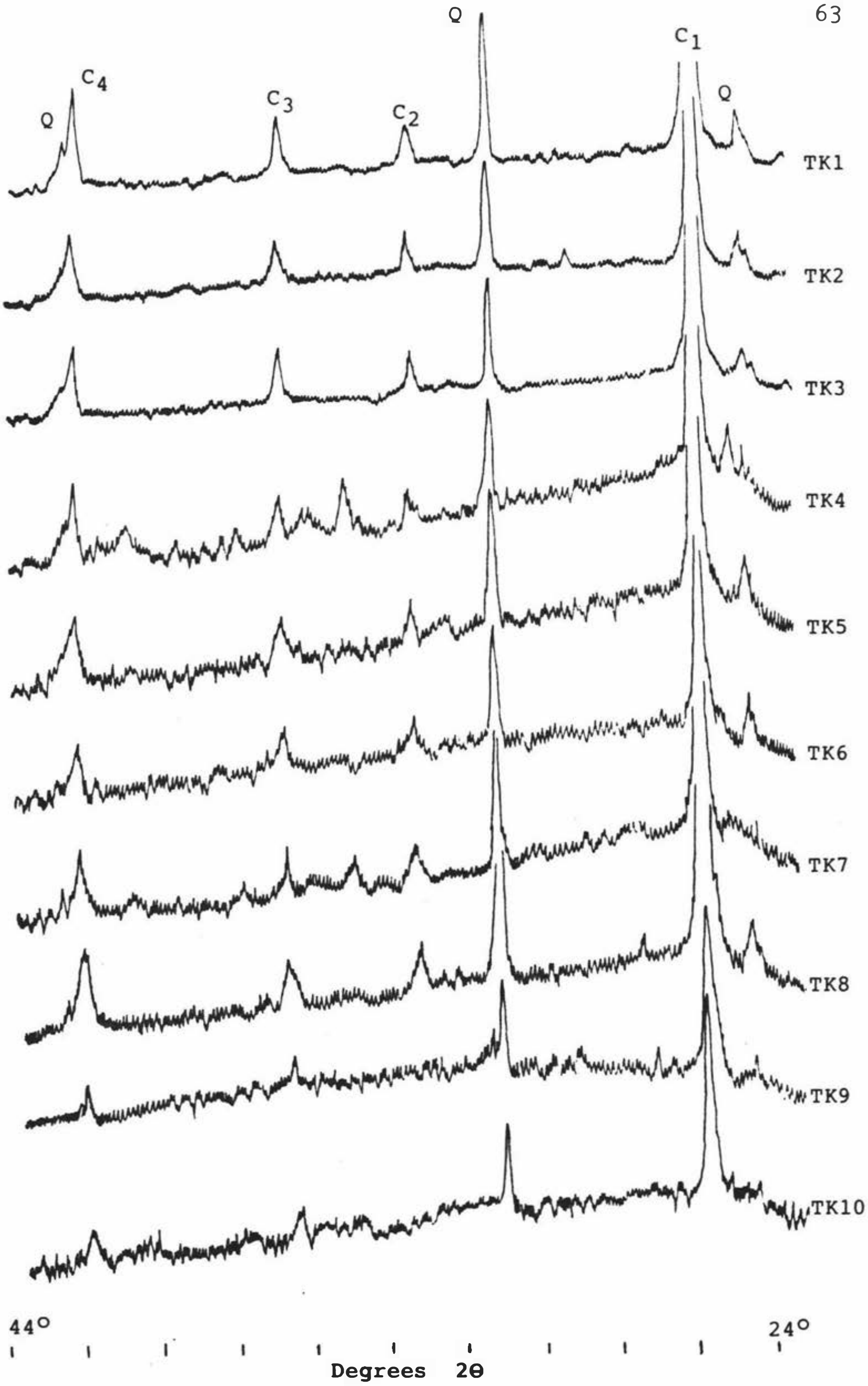

Figure 3.20: Forms of the XRD patterns of the clay fractions in the Te Kowhai soil. N.B. there is a change in range by a factor of 2 between TK3 and TK4. Symbols as for figure 3.17.

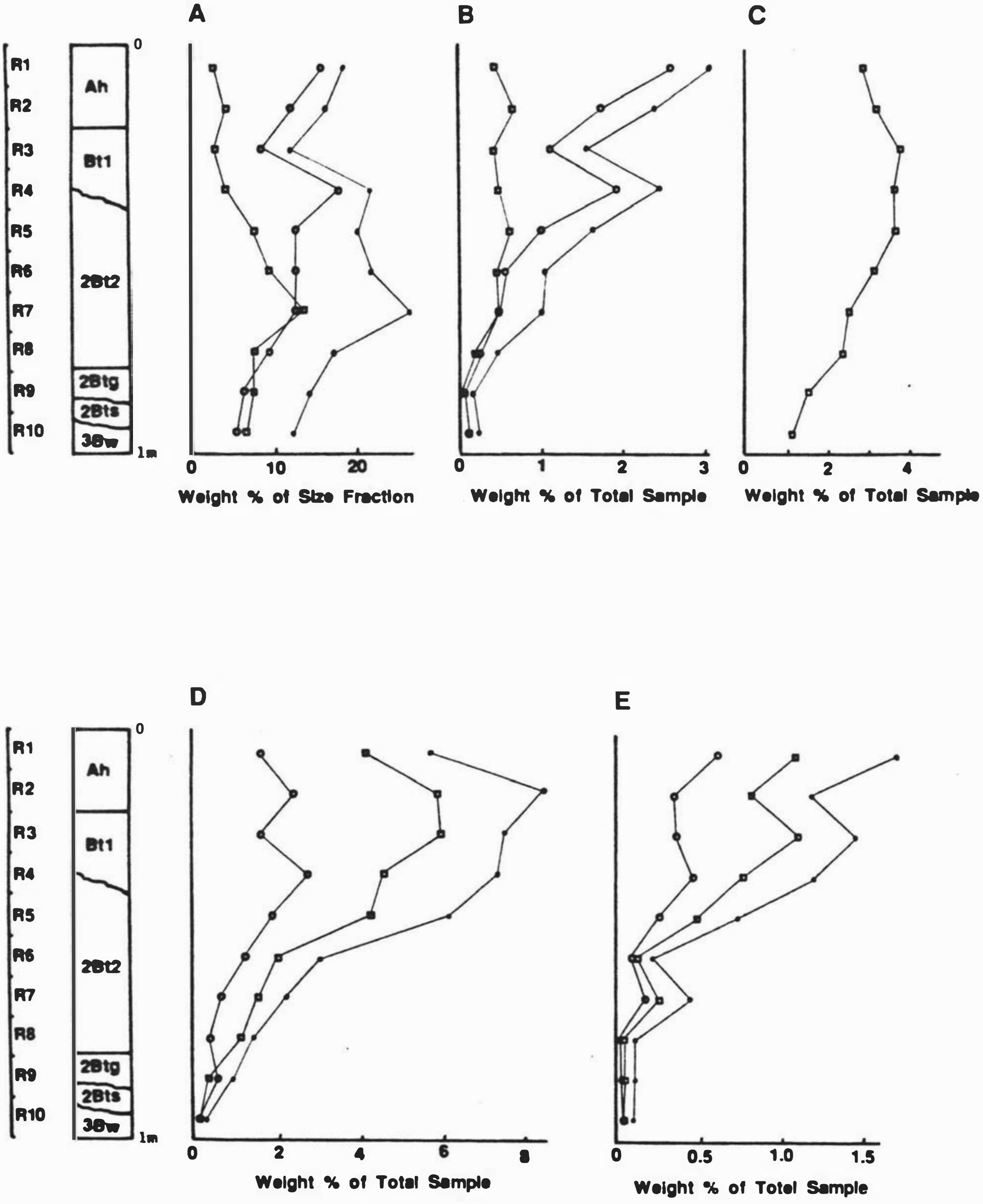

Figure 3.21: Hamilton soil - Abundance of cristobalite (□), tridymite (o) and sum of tridymite + cristobalite (·) in the coarse silt as a proportion of the size fraction (A) and total sample (B). Also shown are the distributions in the medium (D) and fine silts (E), and clay fraction (C).

In the medium silt fraction (Fig. 3.21) opal-C now dominates. Both opal-C and tridymite-M are reduced below 50 cm, particularly at the base of the profile.

The fine silts show general trends of decreasing opal-C and tridymite content with depth. Tridymite is reduced from 0.5% of the total sample at R4 to 0.1% at R6 while opal-C decreases from 0.75% to 0.1% in the same interval. There are maxima in the tridymite-M content as a percentage of total sample at samples R1 and R4 while opal-C shows local maxima at samples R1 and R3 (Fig. 3.21).

In the clay fraction tridymite is only a trace constituent. Opal-C has values of 3-3.5% of total sample in the upper horizons but declines to 1% in sample R10. The trends for "cristobalite" distribution as a percentage of the clay fraction are very similar to those published by Joe (1986).

Data on the distribution of opal-C and tridymite-M in the Hamilton soil demonstrate the following trends:

(1) there are consistently higher values of tridymite-M in sample R1 and R4 throughout the silt fractions,
(2) there are increased or high values of opal-C as a percentage of total sample at 20-30 cm depth,
(3) there is a marked reduction in both opal-C and tridymite-M in the silt fractions at about 50 cm,
(4) the proportion of tridymite-M reduces with reducing grain size.

(b) Naike Clay: In this soil opal-C tends to dominate over tridymite-M in the medium and fine silts while tridymite-M dominates the coarse silt but is rare or absent in the clay size fraction (Fig. 3.22). Opal-C and tridymite-M are more abundant in the top 20-30 cm.

In the coarse and medium silts tridymite-M as a percentage of total sample has a maximum value at 10-20 cm depth while in the fine silts tridymite-M is slightly higher in the top 30 cm. Opal-C in the coarse and fine silts has higher and uniform values in the top 30 cm compared with lower levels. In the medium silt there is a maximum value at 10-20 cm and the values are very low below 30 cm.

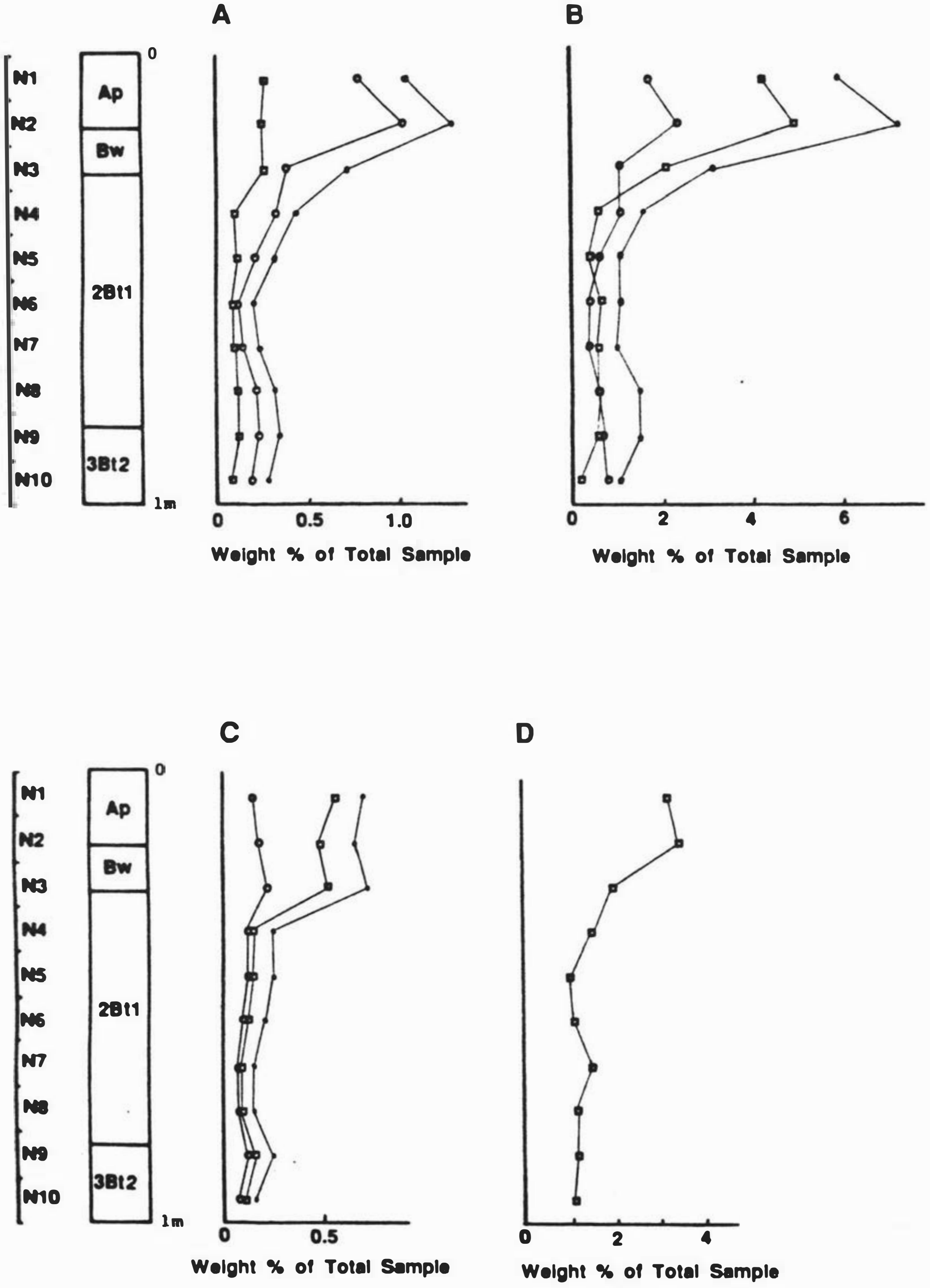

Figure 3.22: Naike soil - Abundance of cristobalite (□), tridymite (o) and the sum of cristobalite + tridymite (·) in the coarse silt (A), medium silt (B) fine silt (C) and clays (D).

In the clay-size fraction opal-C content is low below 40 cm (c. 0.1% of total sample) then rises to values of c. 3% in the Ah horizon. As a proportion of the clay fraction opal-C reaches c. 7% in the top 20 cm which is higher that the 3% described from the A horizon by Anon. (1981).

(c) Te Kowhai Silt Loam: In the coarse silt of the Te Kowhai soil (Fig. 3.23) tridymite-M as a percentage of total sample has a uniform distribution (2.2-2.8%) except for a higher value in sample TK7 (4%). The opal-C concentration is stratified with low total values (<1%) in the top 20 cm and higher values (c. 2%) below 20 cm. An exception is sample TK8 where opal-C content increases to 3.8% of the total sample. In the medium silts the top 30 cm (particularly the 10-30 cm interval) has a higher opal-C content (c. 6% of total sample) while a zone at 70-90 cm also has higher opal-C content (2.5%) compared with the zone between 30 and 60 cm (1.5%). Tridymite-M concentration is stratified, ranging from higher values in the top 30 cm to lower values below 40 cm. In the fine silt fractions both opal-C and tridymite-M are higher in the top 30-40 cm.

The opal-C distribution in the clay-size fraction increases to 2% of the total sample in the top 20 cm. The value in the top 20 cm is 7% of the clays. This is similar to data of Joe (1986) who reports 5% "cristobalite" in the clays from the topsoil and Anon. (1981) who reports 6% "cristobalite" in the clay fraction of the top 18 cm. Both Anon. (1981) and Joe (1986) show that the cristobalite content of the clay fraction decreases with depth.

(d) Tokomaru silt loam: In the fine silt fraction of this soil opal-C occurs in two zones (Table 3.2). At the level of the Aokautere Ash (sample 3) opal-C forms 4% of the fine silt while in the top 4 samples the fine and medium silts contain c. 1.1% and c. 0.8% opal-C respectively. In both fractions sample T21 contains traces of cristobalite while it was not detected in the zone below T21 until sample T4. Although the low opal-C content in the top 4 samples means any trends are equivocal it does appear that samples T22 and T24 are regions where there is slightly more opal-C.

(e) Onaero: Only the <32 μm fraction from the Onaero profile was processed to concentrate cristobalite. Opal-C is a relatively constant proportion of this fraction (c. 2-3%, Table 3.2) but in two samples

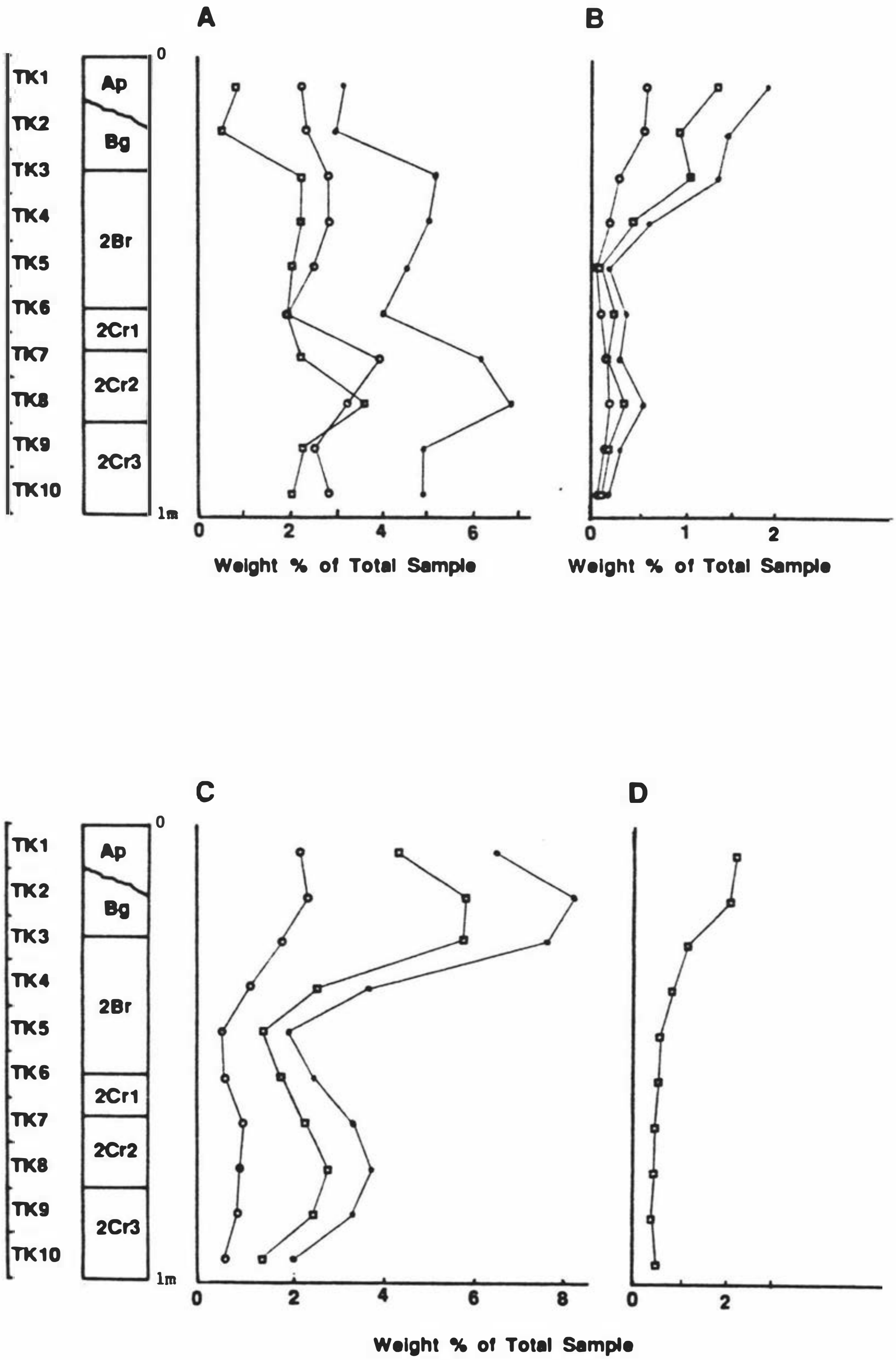

Figure 3.23: Te Kowhai soil - Abundance of cristobalite (□), tridymite (o) and the sum of cristobalite + tridymite (•) in the coarse silt (A), medium silt (C) fine silt (B) and clays (D).

Table 3.2: Cristobalite content in the Tokomaru soil and the soil at the Onaero site.

Onaero site

Sample	Depth(m)	% cristobalite⁺
BVA3	0.2-0.3	1.6
BVA4	0.3-0.4	2.6
BVA5	0.4-0.5	2.0
BVA6	0.5-0.6	2.0
BVA7	0.6-0.7	2.2
BVA8	0.7-0.8	1.8
BVA9	0.8-0.9	2.4
BVA10	0.9-1.0	3.0
BVA11	1.0-1.1	2.6
BVA12	1.1-1.2	2.7
BVA13	1.2-1.3	2.5
BVA14	1.3-1.4	4.0
BVA15	1.4-1.5	4.0

+ in the <32 micron fraction.

Tokomaru soil (% cristobalite)

Sample	fine silt	medium silt
T3	4.0	4.1
T4	3.8	3.2
T21	trace	trace
T22	1.1	0.8
T23	0.5	0.4
T24	1.1	0.8
T25	1.0	0.7

(BVA14 and BVA15) there is a significant increase to 4%. Sample 15 contains the Aokautere Ash. Based on small peaks at 4.11Å and 3.85Å traces of tridymite have been tentatively identified in sample 13.

Only the 5-2 µm fraction of the Egmont loam was processed and it produced a weak cristobalite pattern (Fig. 3.24).

ISOTOPES

Theoretically the $\delta^{18}O$ content of cristobalite in soils should readily identify the environment in which cristobalite and or tridymite formed. Reliably pure concentrates are required for analysis and there are significant practical problems in concentrating cristobalite from soils. These include (1) the occurrence of cristobalite and tridymite in the finest grain sizes, (2) the ubiquitous presence of some form of opaline silica, and (3) the abundance of pumiceous shards of variable density. Most of the pumiceous material is derived from the Taupo Volcanic Zone and fortunately the $\delta^{18}O$ values for this glass (6.35-7.6 $^{o}/_{oo}$, Taylor *et al.* 1986) are similar to cristobalite determined in this study so minor glass contamination is thought inconsequential. An extra step in the preparation procedure was introduced to separate the opaline silica but this required repeated density separations (S.G. 2.0 Mg m^{-3}) to achieve a satisfactory separation. It was therefore only practical to prepare a limited number of reliably pure concentrates.

The results (Table 3.3) emphasise the bimodal nature of the data. Data from opal-C and tridymite-M mixtures cluster between 7.5 and 8.0 $^{o}/_{oo}$ irrespective of grain size or relative proportions of opal-C and tridymite-M.

The various forms of amorphous silica (opal-A) have values that range from 26.6 to 30.1 $^{o}/_{oo}$. Data from phytoliths in the Hamilton soil (30.1 $^{o}/_{oo}$) and living vegetation (27.5 $^{o}/_{oo}$ for phytoliths from beech wood) are lower than the value of 37.2 $^{o}/_{oo}$ reported by Jackson *et al.* (1971). However they are still consistent with equilibration at normal surface temperatures. Similarly the slightly higher $\delta^{18}O$ values for the concentric and dusty opal-A from the bases of the Naike (26.9 $^{o}/_{oo}$) and Hamilton (26.6 $^{o}/_{oo}$) soils are consistent with a low temperature paragenesis.

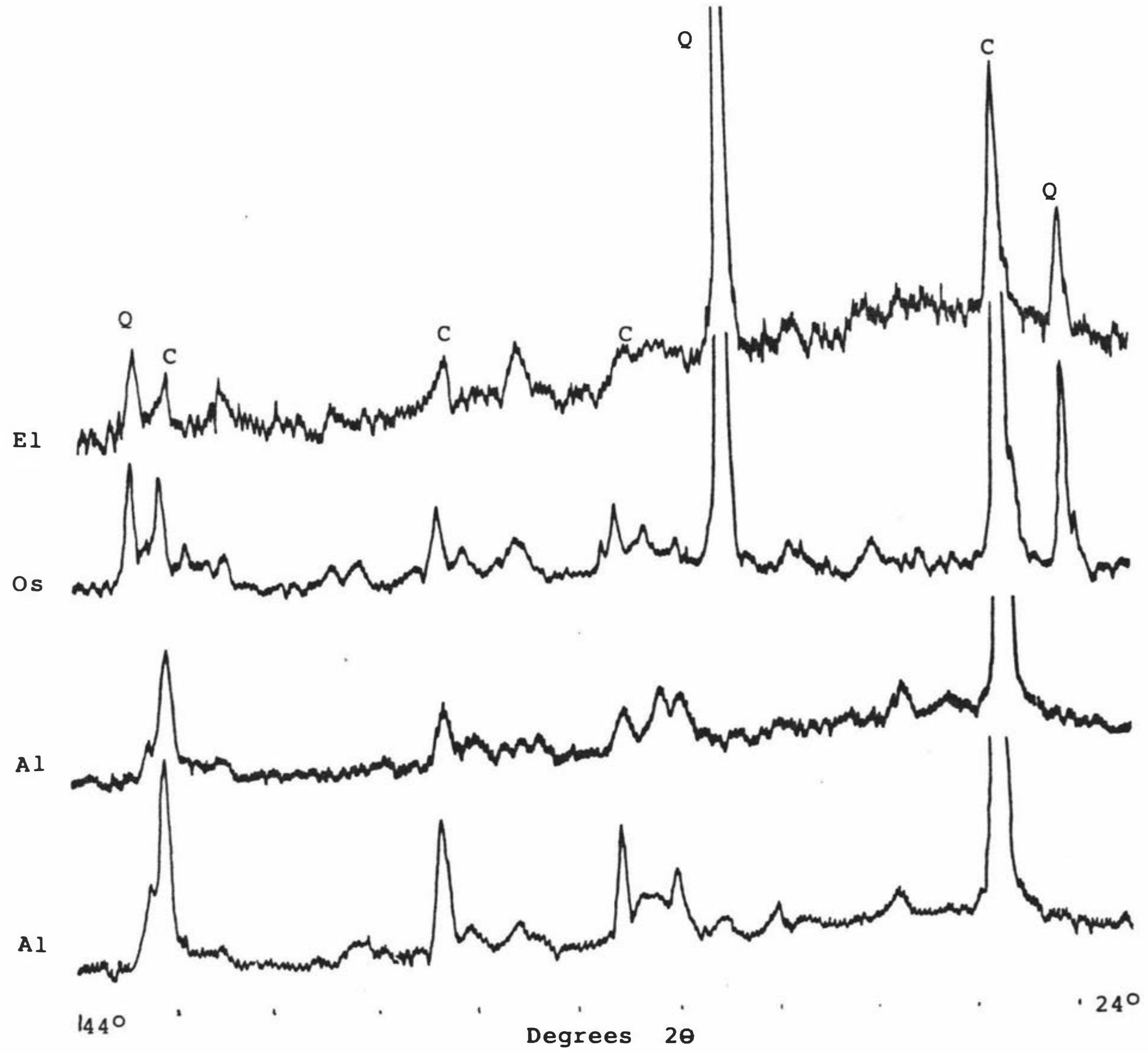

Figure 3.24: Typical XRD spectra of silica phases in Egmont loam (El), Onaero section (Os), and two andesitic lavas (Al). Symbols are quartz (Q), cristobalite (C).

Table 3.3: Oxygen isotope values from silica phases in soils from the Hamilton region.

SAMPLE	SIZE FRACTION	MINERAL	$\delta^{18}O$
R1	coarse silt(h+)	cristobalite	7.76
R1	coarse silt(l+)	tridymite	7.55
R4	coarse silt	cristobalite	7.51
R4	medium silt	cristobalite	7.62
R9	coarse silt	cristobalite	7.53
R9	medium silt	cristobalite	7.55
R10	coarse silt	cristobalite	8.18
R10	medium silt	cristobalite	8.02
N2	medium silt	cristobalite	7.22
N4	coarse silt	cristobalite	8.74
TK5	medium silt	cristobalite	8.40
R1	coarse silt	phytoliths	30.1
Vegetation		beech	27.5*1
R10	coarse silt	concentric opal-A	26.6*2
N10	coarse silt	dusty opal-A	26.9*3

* Low yields 1 = 70%, 2 = 88%, 3 = 63%
\+ h = higher density fraction, l = lower density fraction

Analyst C. Houston.

IGNEOUS SOURCES OF CRISTOBALITE AND TRIDYMITE

(a) Taranaki: In addition to soils from Taranaki, some andesitic lavas from Mt Egmont were also processed to identify any silica polymorphs present. The lavas were separated into two groups, (1) melanocratic varieties which usually had a dark glassy matrix, and (2) leucocratic varieties with mafic and plagioclase phenocrysts in a tectosilicate-rich microlitic groundmass. The melanocratic lavas did not yield any cristobalite or tridymite but opal-C did occur in the leucocratic lavas (Fig. 3.24).

(b) Taupo Volcanic Centre: Based on a precursory investigation it was determined that while there was no significant cristobalite or tridymite in the Taupo or Waimihia tephras sampled it was in the Aokautere Ash. Henderson *et al.* (1971) did not detect cristobalite in the Aokautere Ash and it is here suggested that this was due to the relatively narrow grain size limits within which cristobalite appears to occur in tephric materials. XRD of the 5-2 μm fraction of material collected during a detailed sampling of the Aokautere Ash type section yielded significant cristobalite and tridymite spectra (Fig. 3.25). These exhibit strong c. 4.1Å cristobalite and tridymite reflections but the rest of the spectra are poor. Other tridymite reflections were not observed and the 3.14Å opal-C refection is missing. A sample of the Aokautere Ash from the West Coast of the South Island (Mew *et al.* 1986) was also processed. The spectrum from this sample also contains reflections from both cristobalite and tridymite.

(c) Okataina Volcanic Centre: It was known from Benny (1982) that there was both cristobalite and tridymite in the Okareka Ash and the overlying loess, so samples from two of Benny's sites (Loop Road and Ngongataha) were investigated. The spectra from these samples (Fig. 3.26) confirm Benny's investigation and demonstrate that opal-C and tridymite-M are common constituents of the ash and loess. It is worthy of note that the loesses appear to be richer in cristobalite and especially tridymite compared with the ashes, e.g. at Ngongataha the 3.85Å tridymite-M peak from the loess sample is significantly larger than that in the ash. At Loop Road this effect is less marked. The grain size used in the XRD analyses differs between ash and loess

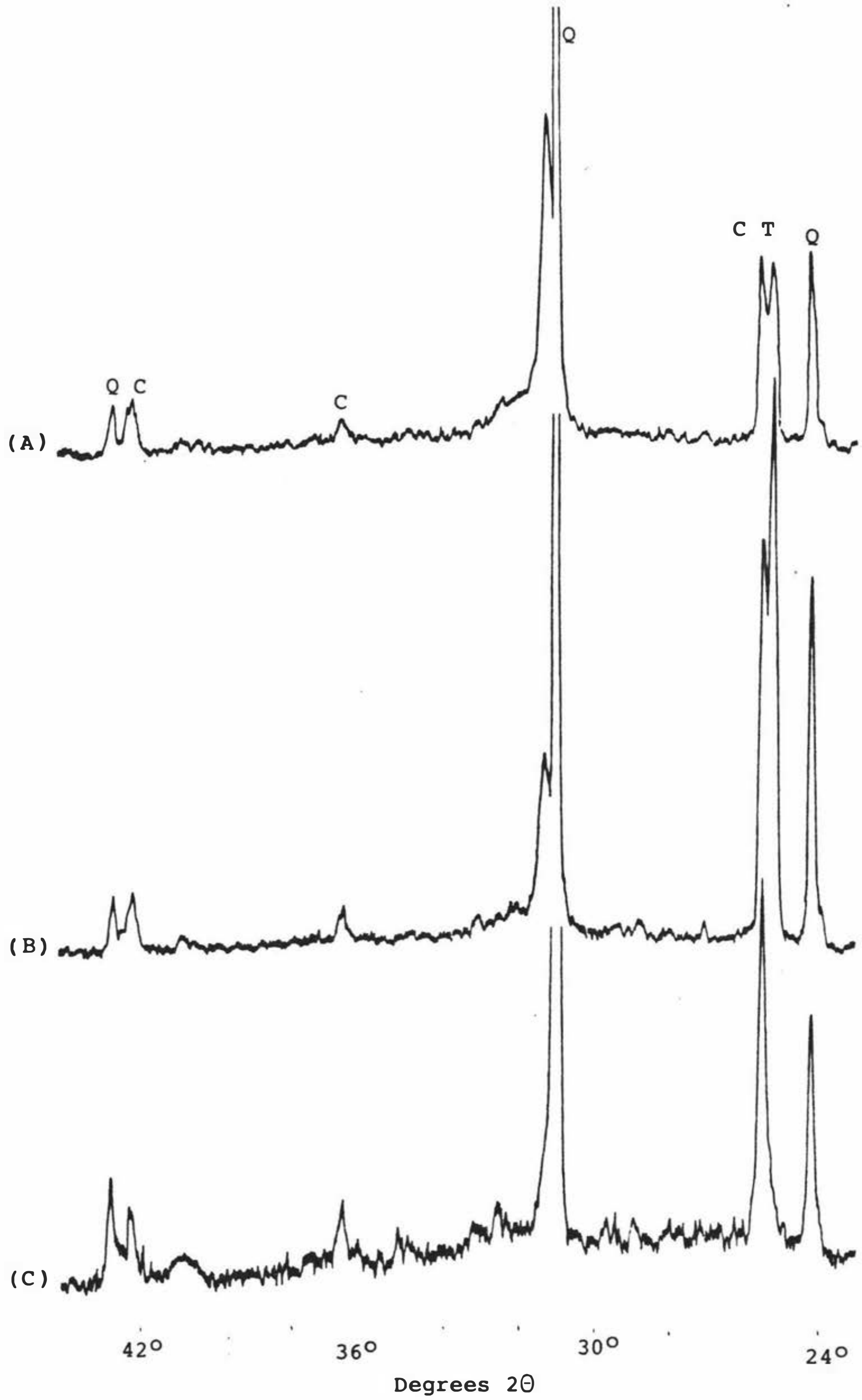

Figure 3.25: XRD spectra of silica phases in the Aokautere Ash at the type section. Samples are from the coarse base of the graded unit (A), the middle of the graded unit (B), and the overlying fine ash (C). Reflections are cristobalite (C), tridymite (T) and quartz (Q).

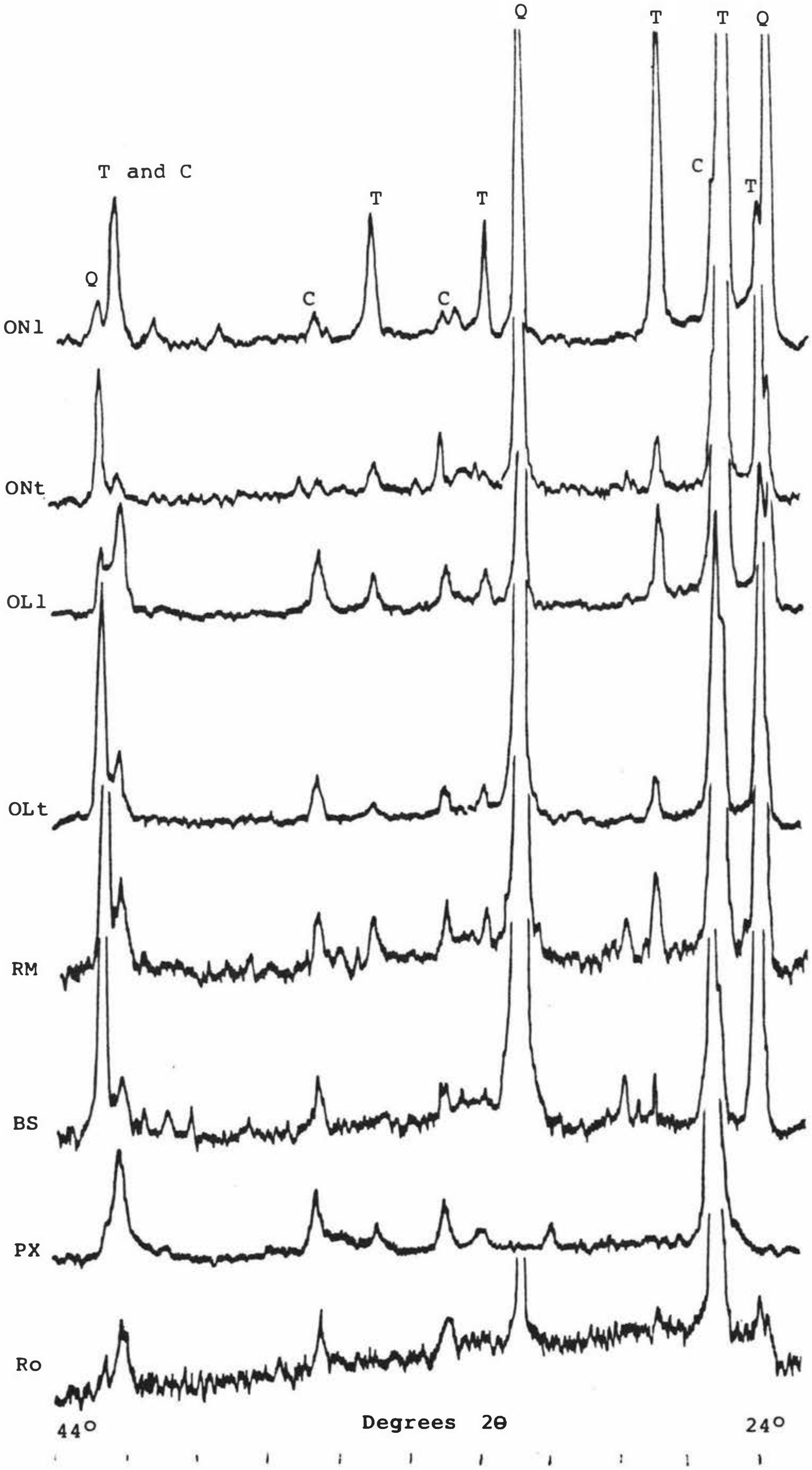

Figure 3.26: XRD spectra of cristobalite (C) and tridymite (T) in some eruptives associated with the Okataina Volcanic Centre. The Okareka Ash (O) from two sites (L - Loop Road; N - Ngongataha; Benny 1982), both with the tephra (t) and overlying tephric loess (l), are shown. Cristobalite and tridymite bearing eruptives associated with the 1886 Tarawera eruption are also shown: (1) Rotomahana Mud (RM), (2) Base surge deposits associated with the mud (BS), and (3) pumiceous xenoliths (PX) within Tarawera Basalt. Trace Ro is from the Rotoma Ash.

(63-20 µm versus <20 µm respectively) so the different sizes of the reflections could be due to this effect, but if the trends of the Hamilton basin soil samples apply, then tridymite would be concentrated in the 63-20 µm fraction. The use of the 63-20 µm fraction from the ash should therefore favour higher abundances of tridymite. The relative concentration of cristobalite and tridymite in the loess may be related to the grain size, density, and morphology of these phases, all of which combine to permit the grains to be winnowed preferentially from the ash. Benny (1982) suggested that some of the loess may have been derived from the Mamaku Ignimbrite and this is another possible source of cristobalite and tridymite.

Of the other volcanogenic materials examined from this centre:

- the Rotomahana Mud contains both opal-C and tridymite-M (Fig. 3.26),
- the base surge deposits associated with the Rotomahana Mud contain opal-C with variable amounts of tridymite (Fig. 3.26),
- the Rotoma Ash contains opal-C (Fig. 3.26),
- the Rotoehu Ash has a very weak cristobalite spectrum, and
- the phases produced by thermal metamorphism and devitrification of pumice xenoliths in the Tarawera Basalt contain opal-C. A weak tridymite spectrum contains the 3.0 and 3.25 but not the 3.85Å reflections.

OTHER COMPONENTS IN THE SOILS

While processing the samples to investigate the cristobalite and tridymite distribution, the mineral compositions of some of the "by-product" fractions were noted. Some of these data are only qualitative but they supply information relevant to interpreting the genesis of cristobalite and tridymite.

(a) Quartz: The quartz content of the three soils from the Hamilton basin was determined along with the cristobalite and tridymite. In the Hamilton soil (Fig. 3.27) quartz in the silts increases in a zone at 40-60 cm deep from low values in deeper horizons to c. 5%, 9% and 1.5% in the coarse, medium and fine silts respectively. In the <2 µm fraction the quartz content is relatively uniform (1.3%) but there is a zone of reduced values at 70-90 cm.

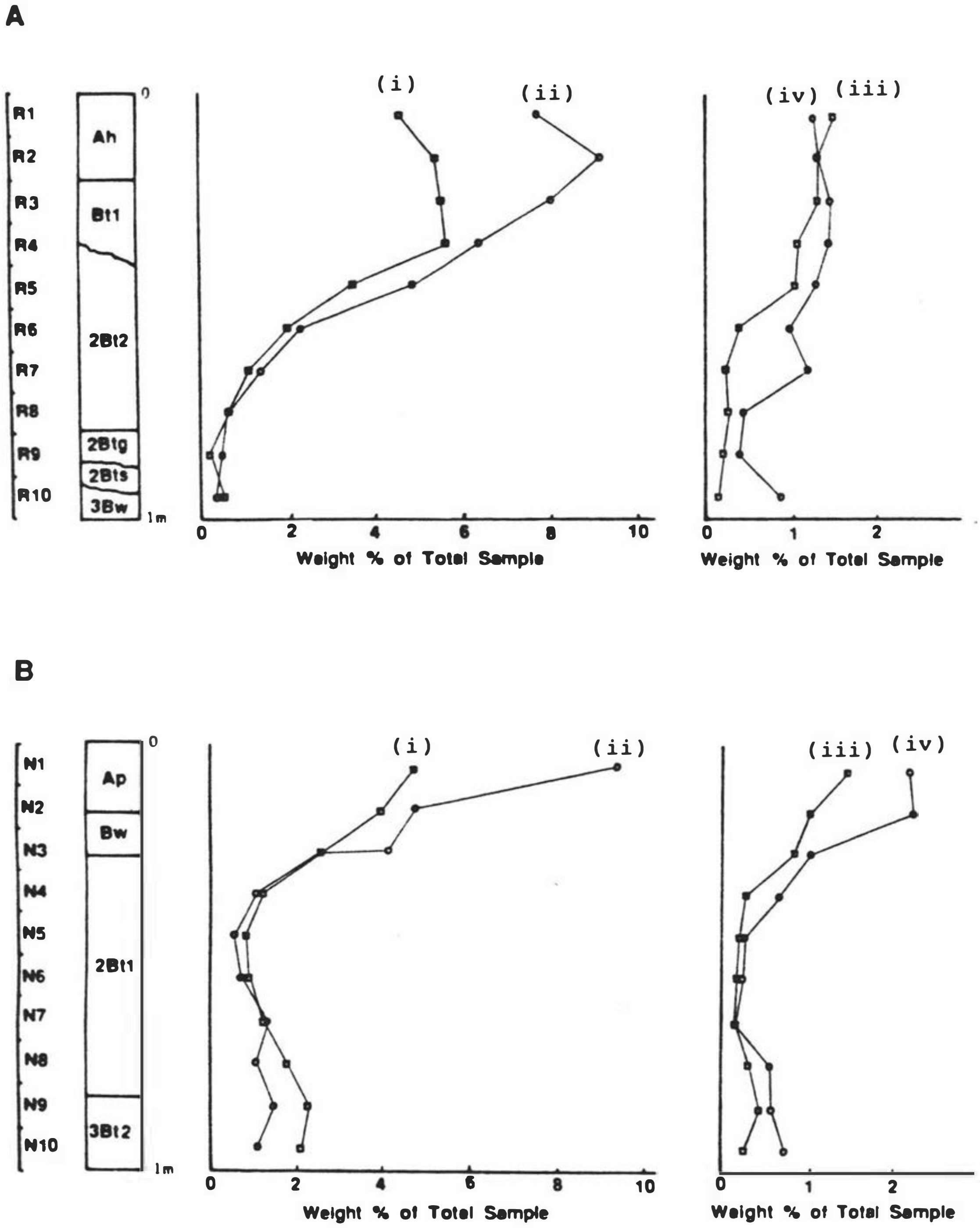

Figure 3.27: Quartz distribution in the silt and clay fractions of the Hamilton (A) and Naike (B) soils. Symbols (i) coarse silt, (ii) medium silt, (iii) fine silt, (iv) clay.

In the silts and clays from the Naike soil there is a dramatic increase in the quartz content in the A and Bw horizons (Fig. 3.27). Much of the 2Bt1 horizon has lower quartz content than the Ap and Bw horizons but there is an increase in the 3Bt2 horizon at the base of the profile.

In the Te Kowhai soil the quartz content of the upper horizons is much lower than for similar horizons in the Hamilton and Naike soils (Fig. 3.28). There is more quartz in the top 30 cm of the medium and fine silts compared with deeper levels and there appears to be a pulse of increased quartz content at sample TK8 in the coarse and medium silts.

(b) Ferromagnesian Mineralogy: During the preliminary treatment of the fine and very fine sands bromoform (S.G. 2.87 Mg m^{-3}) was used to remove the ferromagnesian silicates and the iron oxides. The distributions of this heavy fraction as a proportion of (1) the specific size fraction, and (2) the total sample are illustrated in figures 3.29 to 3.31. In these figures the general trends for the Te Kowhai soil are similar using both approaches (1) and (2). Although the stratification of the Hamilton soil and Naike soil profiles is preserved using methods (1) and (2) the relative concentrations of the heavy fraction is reversed. This occurs because there are significant variations in the sand content down the profiles and demonstrates that relative trends within fractions which are themselves only minor components (e.g. the sands in the lower horizons of the Hamilton soil and Naike soil) should be interpreted with caution.

In the Hamilton soil there is a marked change in the heavy component of the total sample at 50 cm (Fig. 3.29b). This change is less obvious in figure 3.29a but is thought to be significant as it corresponds with a change in the mineralogy of the heavy fraction. The mineralogy of the heavy fraction above 50 cm is dominated by ferromagnesian silicates whereas these are rare or absent at deeper levels where the heavy fraction is composed entirely of iron oxides, together with zircons. There is a significant increase in the heavy fraction in sample R10 and although this is not accompanied by a dramatic change in mineralogy this sample contains orange-brown highly corroded and porous grains which are interpreted as the remnants of pyroxenes or amphiboles.

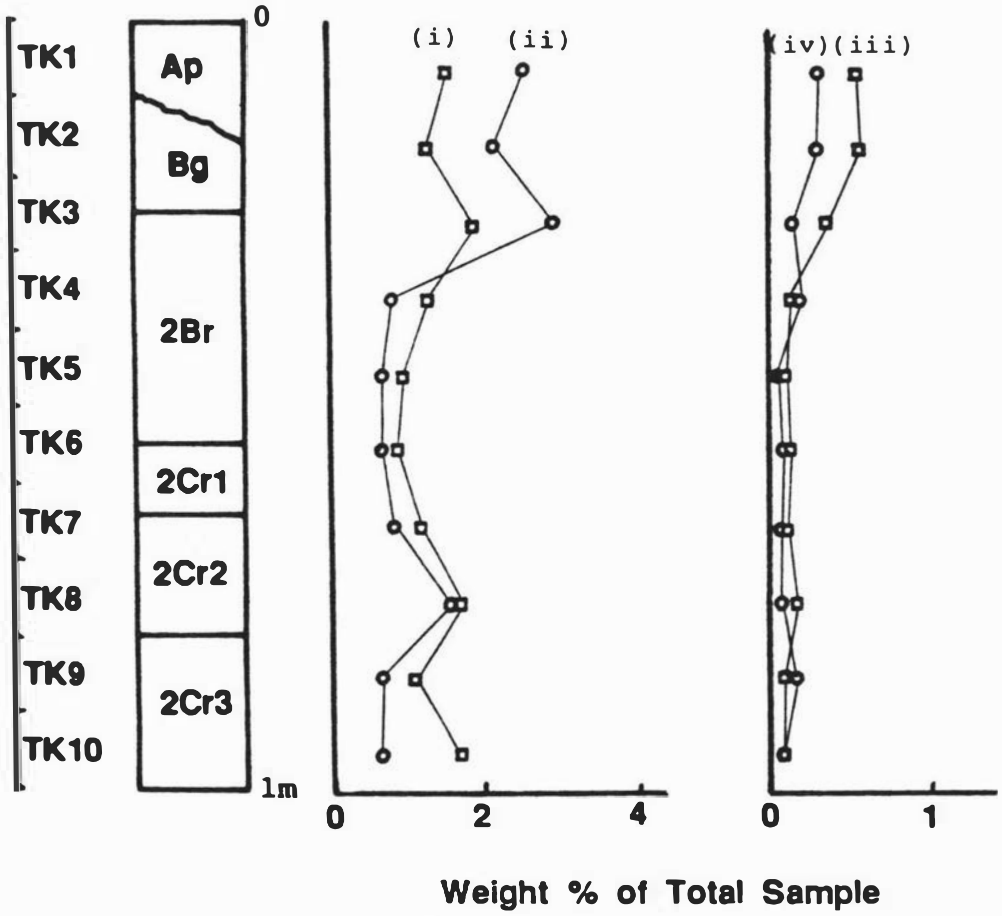

Figure 3.28: Quartz distribution in the silt and clay fractions of the Te Kowhai soil. Symbols (i) coarse silt, (ii) medium silt, (iii) fine silt, (iv) clay.

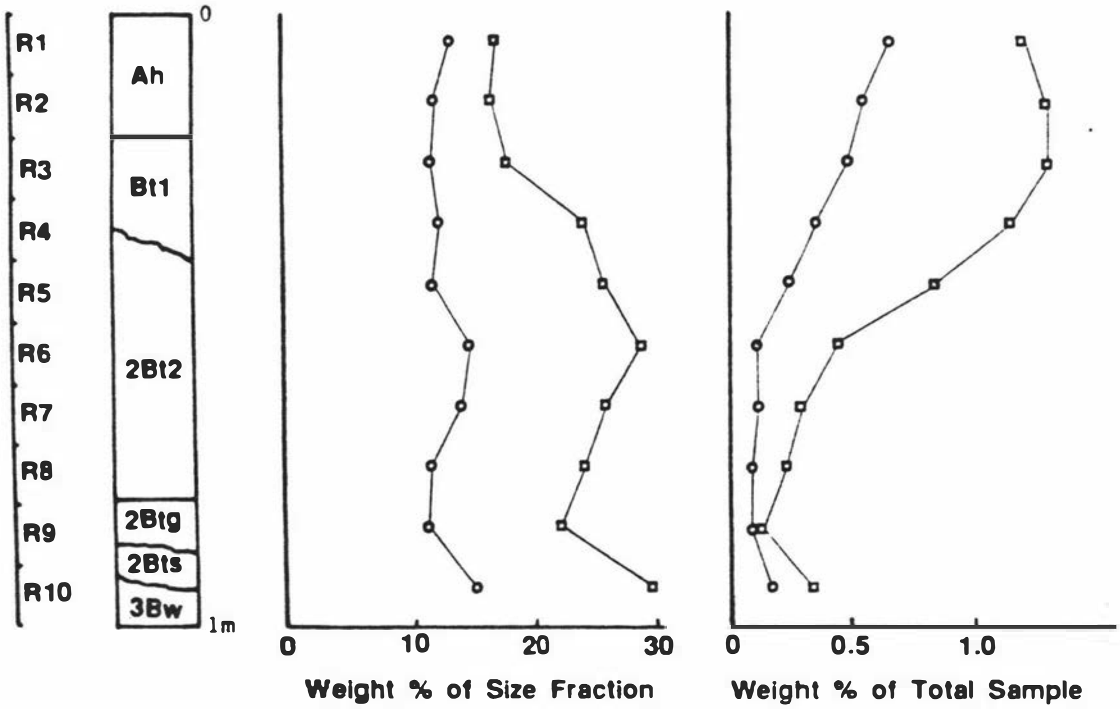

Figure 3.29: Distribution of the heavy fraction in the fine (o) and very fine sand (□) fractions of the Hamilton soil. Data are expressed as both a proportion of the size fraction and the total sample.

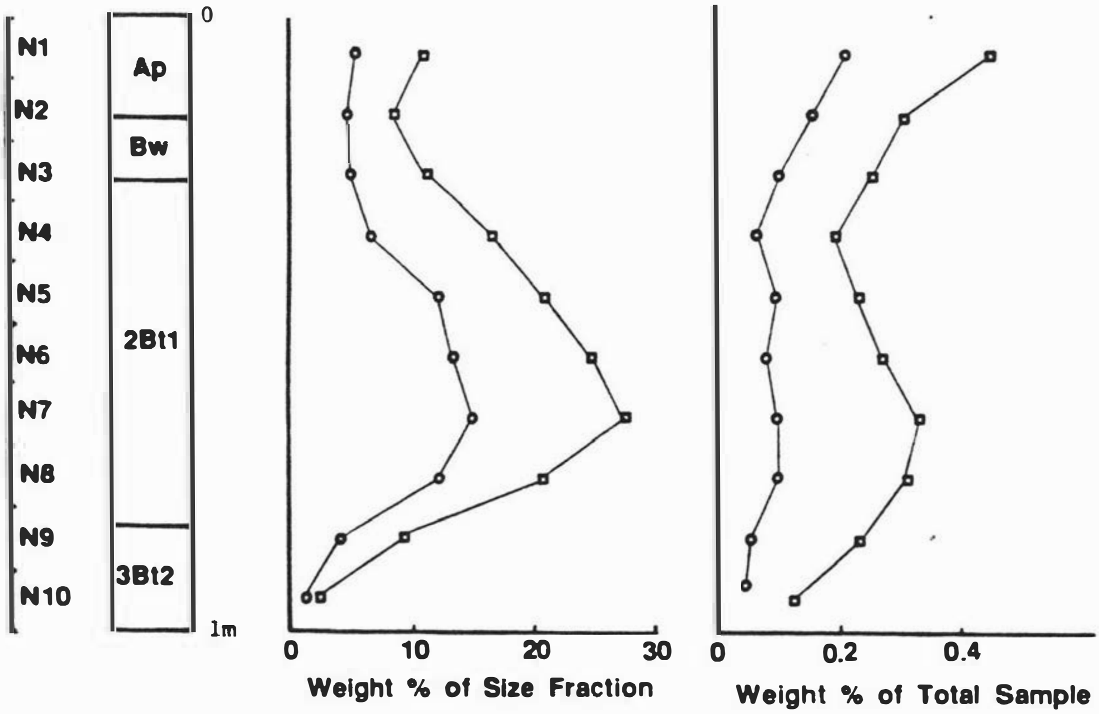

Figure 3.30: Distribution of the heavy fraction in the fine (o) and very fine sand (□) fractions of the Naike soil. Data are expressed as both a proportion of the size fraction and the total sample.

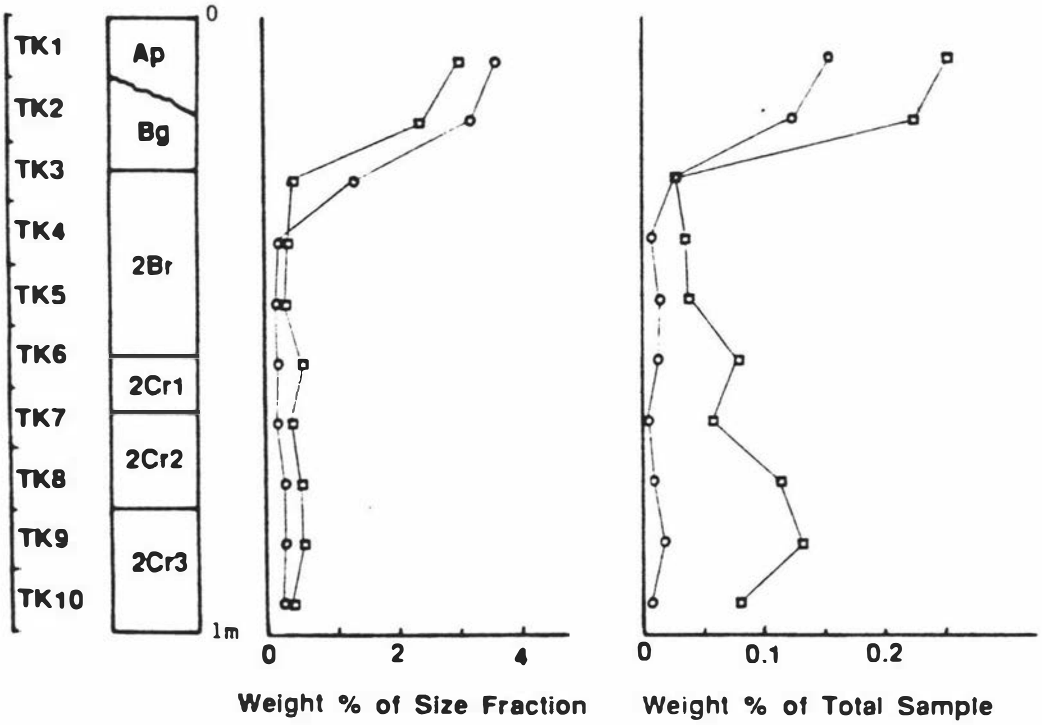

Figure 3.31: Distribution of the heavy fraction in the fine (o) and very fine sand (□) fractions of the Te Kowhai soil. Data are expressed as both a proportion of the size fraction and the total sample.

In the Naike soil there is an increase in the heavy component of the total soil in the top 20-30 cm and in a zone between 60 and 80 cm particularly in the very fine sand (Fig. 3.30). In the top 20-30 cm the heavy fraction is composed of ferromagnesian silicates and iron oxides in approximately equal proportions but between 40 and 90 cm the silicates are almost totally absent and this fraction is dominated by iron oxides. The mineralogy between 30-40 cm is transitional between these two zones. At the base of the profile, N10 and to a less extent N9 are still dominated by iron oxides but zircon and biotite (both euhedral) are much more evident. The biotite flakes are often partly or fully expanded to vermiculite. Many of the expanded grains are totally bleached and appear very similar to halloysite grains.

The distribution of the heavy component in the fine and very fine sands of the Te Kowhai soil (Fig. 3.31) illustrates that the top 20 cm are of significantly different provenance to deeper horizons. This is reinforced by the mineralogy of the heavy fraction which changes markedly from biotite domination below 30 cm to pyroxene+amphibole domination in the top 20 cm. There is a transition zone between 20-30 cm.

(c) Other trends which have been observed in the three Hamilton profiles but for which there is only qualitative data include:

(i) Hamilton soil

- in the coarse and medium silt fractions plant phytoliths are only common in the top 30 cm,
- in the coarse silt cristobalite concentrates, glass shards are common in the top 30 cm, are rare between 30 and 60 cm and absent below 60 cm,
- in the medium silt cristobalite concentrates, zircon grains are suddenly evident in the two bottom samples (R9 and R10).

(ii) Naike soil

- In the coarse silt fraction mafic minerals and phytoliths are only common in the top thirty cm,
- glass shards are significant in the top thirty cm, are minor between 30 and 50 cm and become absent below 50 cm.

- large halloysite nodules (up to 2 cm diameter) are common in N10 (90-100 cm). They occur in a pinkish white to pale yellowish brown horizon that contrasts with the overlying reddish brown horizons.

(iii) Te Kowhai soil

- in the coarse silt, phytoliths are common in the top 30 cm but rare below this level,
- in the medium silts, diatom tests are common below 30 cm.

DISCUSSION

TRIDYMITE IN NEW ZEALAND SOILS

Cristobalite has frequently been reported from New Zealand soils but this study is the first to report significant amounts of tridymite. This is perhaps because most researchers studying the mineralogy of New Zealand soils use the JCPDS (1974) data set for reference spectra (see also Brown 1980) and this set has few tridymite examples. These reference spectra show I_{100} to I_{90} reflections at c. 4.33Å and c. 4.11Å and only a limited number of other peaks with relative intensities greater than I_{10} (i.e. at 3.85Å, 2.99Å and 2.52Å). Quartz, which is a major component in soils where tridymite commonly occurs, has major reflections at 4.26Å and 2.46Å which are very close to those of tridymite. Furthermore the relative intensity of tridymite reflections can be quite variable (Hill and Roy 1958b; Sato 1963a, 1963b; Tada and Iijima 1983), e.g. the 4.33Å reflection is commonly an I_{20} peak rather than I_{90}. These factors, coupled with the absence of tridymite in the clay fractions, are suggested as the causes of this oversight. In the present project it was only when samples were analysed with newly acquired x-ray diffraction equipment that two separate peaks were resolved in the 4.1Å region. Tridymite had, nevertheless, been identified on the basis of the 3.85Å reflection.

SOIL STRATIGRAPHY AND PARENT MATERIALS

(1) Hamilton Soil

Previous detailed investigations of the Hamilton soil (Lowe 1981; Joe 1986) have documented dramatic changes at the boundary between the upper zone (post-Hamilton Ash Group) and the lower zone (weathered Hamilton Ash Group). The data from the Hamilton soil presented here, supports this division (see Fig. 3.32). Changes in (1) the grain size distribution, (2) the size and mineralogy of the heavy mineral fraction, and (3) opal-C and tridymite-M in the silt fractions indicate that there is a dramatic change at 50 cm depth, between R5 and R6.

(i) Upper Zone: Within the upper zone the common occurrence of volcanic glass, euhedral opaques and ferromagnesian silicates supports the conclusion of Lowe (1981) that this is a zone of tephra accumulation. Lowe identified minerals indicative of several specific tephras in this zone and determined that the Rotoehu Ash (c. 50 ka) and Kawakawa Tephra (a correlative of the c. 20 ka Aokautere Ash) occurred at 45-50 cm and at c. 35 cm depth respectively. The opal-C and tridymite-M distribution is quite variable in the upper zone but there is a consistent maximum of tridymite-M in the silts at R4 (30-40 cm). This sample corresponds to the region from which Lowe (1981) describes the Kawakawa Tephra. In the current studies it has been shown that the Aokautere Ash contains tridymite and cristobalite so the increased tridymite-M in R4 may reflect the influence of this tephra. The Okareka Ash is another tephra shown to be dominated by tridymite in some fractions, and because it was erupted soon after the Aokautere Ash it may also contribute to R4 and cannot be excluded as a possible tridymite source. The Okareka Ash is known to have been deposited throughout the Waikato region (Pullar and Birrell 1973a).

As well as the minerals with demonstrable tephric origins there is considerable quartz in the upper zone. This quartz may be tephric, but Stewart (1982) has demonstrated that tephric quartz most commonly

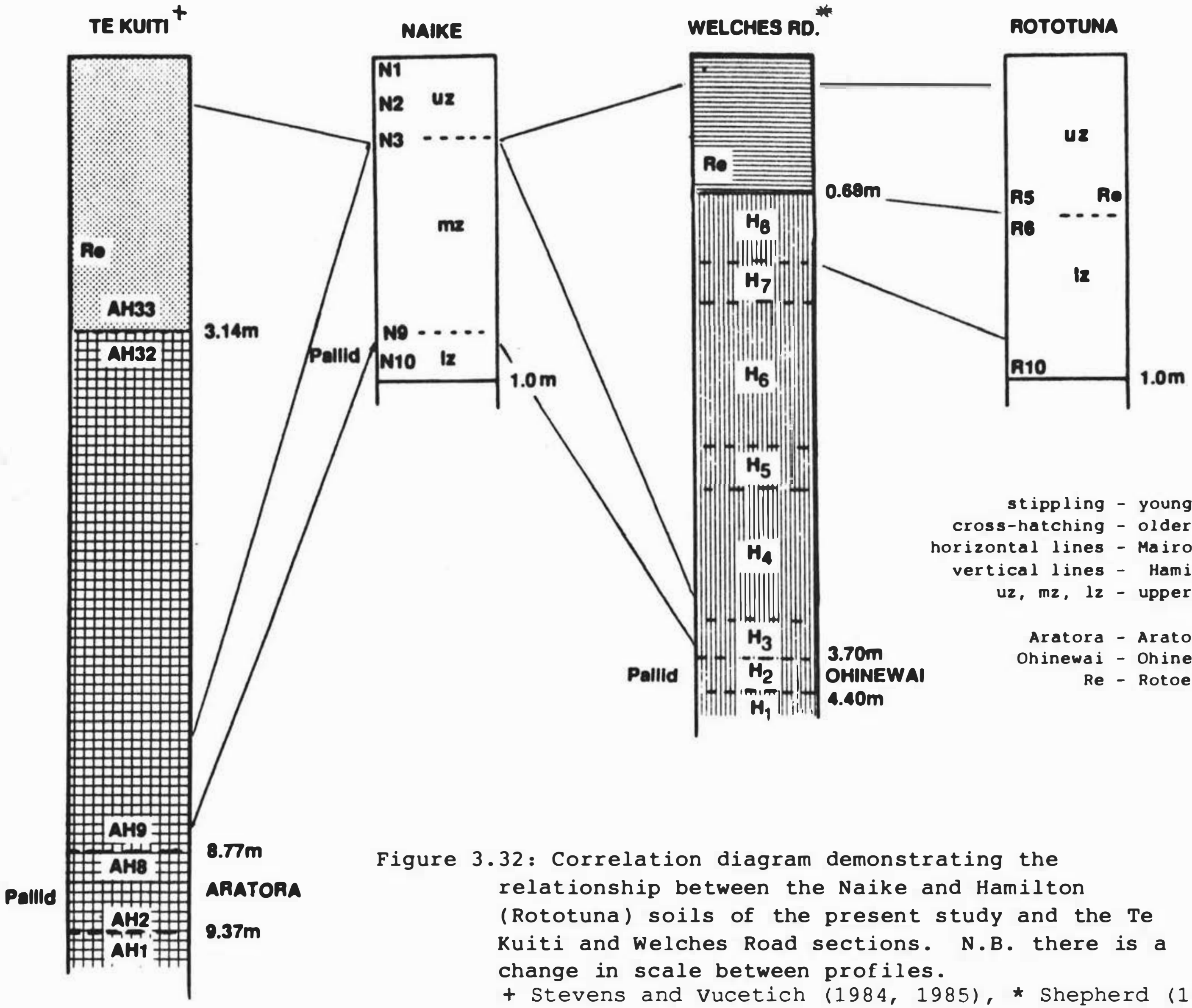

stippling - younger beds
cross-hatching - older beds
horizontal lines - Mairoa Ash
vertical lines - Hamilton Ash Group
uz, mz, lz - upper, middle and lower zones

Aratora - Aratora Tephra
Ohinewai - Ohinewai Tephra Formation
Re - Rotoehu Ash

Figure 3.32: Correlation diagram demonstrating the relationship between the Naike and Hamilton (Rototuna) soils of the present study and the Te Kuiti and Welches Road sections. N.B. there is a change in scale between profiles.
+ Stevens and Vucetich (1984, 1985), * Shepherd (1984).

occurs in grain sizes coarser than 63 µm. As a percentage of total sample however, quartz is most common in the silt sizes in the upper zone. Here it is interpreted that this quartz was loessial in origin, derived from local Tertiary sediments during stadial periods of the late Quaternary.

The aggregate thickness of tephras that have been preserved in favourable sites in the Waikato suggests that approximately 1.5 m of tephra has been deposited in the region of the Rototuna site in the last 50 ka. This is considerably more than the thickness of the upper zone. The common occurrence of weatherable minerals (plagioclase, ferromagnesian silicates and glass) indicates that the removal of material by strong weathering and leaching cannot be considered a significant factor in the thinning of the upper zone. A period of erosion is therefore inferred.

(ii) Lower Zone: Lowe (1981) identified a mixed transition zone (50-70 cm) in the top of the lower zone. The gradual change of some properties demonstrated in the present study (e.g. trends in opal-C, tridymite-M and quartz in the clays and medium and coarse silts), as shown in samples R6-R7, may support this conclusion. In this transition zone however, the clay content is very high and the sand content low, being similar to the basal lower zone, and there may be an alternative explanation. Shepherd (1984) reports significant quartz and cristobalite in some members of the Hamilton Ash Group and demonstrates that the distribution of these phases throughout the Ash is quite variable. It may be that the gradual changes in R6-R7 represent the "normal" level of these components in specific members of the Hamilton Ash Group.

Lowe (1981) shows the upper zone lying disconformably on members H_5 and H_6 of the Hamilton Ash Group in the road cutting adjacent to the Hamilton soil site. These two members cannot be those in the lower zone from the site under investigation however, because the data from R6-R10 are incompatible with those for H_5 or H_6 (Shepherd 1984). Shepherd (1984) shows that H_5 and H_6 have increased cristobalite and quartz abundances in their silt fractions, and an increased heavy fraction in the sands compared with adjacent beds. When compared with the Hamilton Ash Group members below H_5, R6-R10 in general have (1) less opal-C and tridymite-M in the silts, (2) lower quartz content in the silts and to a lesser extent the clays, and (3) very low levels of opaque minerals (exemplified by the heavy fraction as a percent of the total soil). These data are more compatible with the uppermost Hamilton Ash Group member, H_8. The increased zircon content in R9-R10 is in accord with the slightly increasing zircon content of the heavy sand fraction in H_7 (Shepherd 1984). Also, the increasing values of total quartz (in the coarse silt and clay size fraction) and total heavies (in the sands) in R10 are consistent with it being correlated with H_7.

It is here concluded that the lower zone at the sample site in this study is a sequence of beds similar to the upper Hamilton Ash Group beds (H_7 and H_8) at Welches Road. The upper zone is composed of tephra and loess deposits deposited since about 50 ka B.P.

(2) Naike Soil

Most of the data from the Naike soil are consistent with a division of this profile into three units, an upper zone (Ap-Bw, N1-N3), a middle zone (2Bt1, N4-N8) and a lower zone (3Bt2, N9-N10), see figure 3.32.

(i) Upper Zone. Mineralogically the upper zone is markedly different to the middle zone because it has distinctly more glass and ferromagnesian silicates (i.e. weatherable minerals). The change in abundance of weatherable minerals at the upper zone/middle zone boundary could arise as a result of differential weathering of a uniform parent material and indeed the middle zone is obviously highly weathered, but this interpretation is inconsistent with the reduction in quartz in the middle zone. Quartz is relatively resistant to weathering and so would increase in a zone of maximum weathering. There is such a marked contrast between the degree of weathering in the upper and middle zones that they cannot have both developed during the same weathering cycle from a common parent material, and it is concluded that there is a significant disconformity between the upper and middle zones.

The upper zone represents organic and mineral accretions which are much younger than the middle zone. It is not possible to specifically identify the source of the upper zone material. The increased quartz content of the silt and clay fractions suggests that some at least is derived from the Tertiary sediments adjacent to the site. This quartz is unlikely to have a dominantly tephric origin as Stewart (1982) has suggested that quartz from tephric sources is dominantly coarser than 63 µm. In the Naike soil there is more quartz in the silt fractions than in the sand fraction, particularly in the medium silt. The opaques, pyroxenes and amphiboles which are prevalent in the sand fraction of the upper zone are euhedral and occasionally have glass selvedges. This, together with the common occurrence of volcanic glass, indicates that they are derived from volcanic sources (both rhyolitic and andesitic). Based on a study of tephras in lake sediments in the Waikato (Lowe 1987), and extrapolating data from Pullar (1967) it is estimated that since *c.* 15 ka B.P. approximately 20-25 cm of distal tephras could have accumulated at the Naike site and it is suggested that the upper zone represents the bulk of this material. There was expansion of the forest in the Hamilton Basin after 15 ka B.P. (Harris 1963; M^{c}Glone *et al.* 1978; Green and Lowe 1985; Lowe 1987) and the increase in phytoliths in the soil at *c.* 30 cm is thought to represent this expansion. If the upper zone does represent material accumulated during the post-glacial then not only has the upper Hamilton Ash Group (H_4-H_8) been eroded from this site but so too has material chronostratigraphically equivalent to the lower parts of the Mairoa Ash and the upper zone at Rototuna.

(ii) Middle and Lower Zones. The material below the upper zone is part of the Hamilton Ash Group and using morphological, mineralogical and chemical criteria it is possible to relate the middle and lower zones to the tephra sequences described by Shepherd (1984) and Stevens and Vucetich (1984; 1985). It is demonstrated that N10 is a possible correlative of the upper levels of the Ohinewai Tephra Formation (Vucetich *et al.* 1978), see figure 3.32.

At a site near Te Kuiti, Stevens and Vucetich (1984; 1985) described 42 tephric and loessial beds. These can be broadly subdivided into (1) relatively clay-rich beds below 3.15 m (here referred to as the "older beds") and (2) shallower beds with markedly less clay (the "younger beds"). The Rotoehu Ash occurs towards the base of the "younger beds" so these beds are considered possible chronostratigraphic equivalents of the upper zone at Rototuna, and of the Mairoa Ash at Welches Road. Shepherd (1984) concluded that the Rotoehu Ash occurred in the lower Mairoa Ash at Welches Road. Towards the base of the Te Kuiti section (samples AH2-8) is the Aratora Tephra (Vucetich *et al.* 1981) which has been correlated with the c. 250 ka B.P. Mount Curl Tephra (Vucetich *et al.* 1981; Froggatt 1983).

In a detailed study of the Hamilton Ash Group at Welches Road, Shepherd (1984) described a "platy mineral" (here interpreted as partially altered biotite) from two levels within the Group, (1) In H_7 and H_8 at the top of the Group, and (2) towards the base of the Group in a pallid zone associated with the H_2 beds (Ohinewai Tephra Formation). At the Te Kuiti site the K_2O distribution has two significant maxima, at AH25-30 and AH4-10 (which incorporates the Aratora Tephra), i.e. towards the top and the base of the "older beds" respectively. These maxima have a very similar relative stratigraphic position to the biotite-bearing H_7-H_8 and H_2 beds of the Hamilton Ash Group. It is here suggested that the zones of higher potassium are correlatives of the zones of increased biotite content. The Te Kuiti section is highly weathered and Stevens and Vucetich (1984) show that most elements (K_2O included) have been significantly leached so that the soil chemistry might be expected to be a poor pointer to parent material mineralogy. If the profile is strongly leached, however, any increases in a leached element must reflect either the presence of a resistant phase containing that element or a fortuitous accumulation zone. Biotite and vermiculitised biotite remain in the highly weathered Hamilton Ash Group at Welches Road, in the weathered lower zone at the Naike site, and in other highly weathered tephras e.g. at Omahina Road, Waverley, so the zones of increased potassium in the "older beds" at Te Kuiti are here considered to reflect the presence of biotite. In support of this supposition, Vucetich *et al.* (1981) report a "strongly discoloured mica - presumed ..... to be altered biotite" from the Aratora Tephra i.e. within the lower potassic zone.

The "platy mineral" of Shepherd (1984) and "strongly discoloured mica" of Vucetich *et al.* (1981) are very similar to the mica from the lower zone of the Naike soil. Total element data for the Naike soil (Anon. 1981) show that compared with overlying horizons there are increased values for potassium in a halloysite nodule-bearing horizon at the level of the lower zone. At Te Kuiti the Aratora Tephra immediately underlies a halloysite-rich pallid zone. Based on (1) the presence of biotite and (2) relatively increased potassium values, the lower zone of the Naike soil is correlated with either (a) the Ohinewai Tephra Formation and the Aratora Tephra, or (b) the H_7-H_8 and AH25-AH30 beds. These correlations assume that there has not been significant erosion between these beds at the Welches Road or Te Kuiti sites. It is improbable that the lower zone of the Naike soil is correlated with the H_7-H_8 or AH25-AH30 beds because it is overlain by a far greater thickness of Hamilton Ash Group than any of the other sections, which are all closer to volcanic sources. A pallid zone and halloysite concretions thought to be similar to those in the lower zone at Naike are associated with the Ohinewai Tephra Formation throughout the Waikato and Bay of Plenty regions (Vucetich *et al.* 1978; 1981). Based on the coincidence of mica, halloysite concretions and pallid zones it is suggested that the lower zone at Naike is a correlative of the Ohinewai Tephra Formation and the Aratora Tephra. Vucetich *et al.* (1981) and Froggatt (1983) correlated the Aratora Tephra with the Mount Curl Tephra, so the lower zone at Naike is a possible correlative of the Mount Curl Tephra. Milne (1973) documented 2% quartz and 0.5% biotite in the Mount Curl Tephra at its type section and a preliminary investigation by the present author shows that the biotite is more abundant in the upper layers of the Tephra compared with lower layers. This biotite forms hexagonal euhedral to subhedral plates that are often a very pale straw brown colour due to their ultra-thin nature. The pale brown mica in the lower zone at Naike, and in the Aratora Tephra at Te Kuiti, plus the "platy mineral" described by Shepherd (1984) in the Ohinewai Tephra Formation are here interpreted as representing weathered equivalents of this biotite.

Other mineralogical data from the present study support the correlations between sites documented above. For example residual minerals may be of considerable use in correlation. Shepherd (1984) separated the heavy components from the sand fraction of the beds within the Hamilton Ash Group at Welches Road. His data show that between H_2 and H_3 the heavy component in the sands increases from 2% to 32% while between H_7/H_8 and the Mairoa Ash this component decreases from 27% to 2%. The silt magnetic fractions show similar trends with high values directly above H_2 and low values above H_8. In the sands of the Naike soil the lower zone has 2-5% heavy fraction, rising to 25% in the middle zone i.e. compatible with the H_2/H_3 relationship. This mineralogical trend is also reflected in the chemical data. The Naike soil has increasing TiO_2 and Fe_2O_3 levels in the middle zone compared with the lower zone (Anon. 1981), indicating an increasingly andesitic provenance. In the Te Kuiti section there are pulses of increased TiO_2 content, concomitant with higher Fe_2O_3 values, above the Aratora Tephra. At the Welches Road section the TiO_2 and Fe_2O_3 contents increase above the Ohinewai Tephra Formation, mirroring the mineralogical data.

In the Naike soil profile description, (Anon. 1981) "prominent clean quartz grains" are described from a zone directly below the lowermost horizon sampled in the present investigation. Similar clear euhedral quartz crystals are common in the base of the Ohinewai Tephra Formation (Vucetich *et al.* 1981) and Stevens and Vucetich (1984) report coarse, faceted quartz crystals from the base of the Aratora Tephra. Quartz distribution in the silt fraction of the Hamilton Ash Group allows discrimination between the H_2/H_3 coupling compared with the H_7-H_8/Mairoa Ash coupling. Quartz in H_2 is greater than in H_3 whereas quartz in H_7-H_8 is generally low and equal to that in the Mairoa Ash. In the silts of the Naike soil the quartz in the lower zone is greater than in the middle zone, i.e. in agreement with the $H_2:H_3$ relationship. At Te Kuiti an increase in SiO_2 content in AH4-10 compared with the overlying beds is in accord with increasing levels of SiO_2 in the lower zone at Naike (Anon. 1981). This is consistent with increasing quartz content in the silts and clays towards the base of the Naike soil.

Assuming that there are no significant members missing at the Welches Road or Te Kuiti sites, this evidence indicates that the pallid lower zone of the Naike soil may be correlated with the pallid zone associated with Ohinewai Tephra Formation and Aratora Tephra. An increased heavy mineral fraction in the middle zone of the Naike soil is correlated with H_3 in the Hamilton Ash Group and the andesitic tephras that overlie the Aratora Tephra at Te Kuiti. The correlatives of the H_4-H_8 beds and the lower part of the Mairoa Ash are missing at the Naike soil site. This is probably restricted to this site because at other sites variable amounts of material may have been removed.

Interpretation of the mineralogical variations within the Naike soil demonstrate a complex history. After deposition of mixed rhyolitic and andesitic tephras and loess beginning *c.* 250 ka B.P. there were periods of intense weathering and major erosion. The last of these occurred prior to *c.* 15 ka B.P. During the Holocene there have been additions to the profile from both tephric and quartzo-feldspathic sedimentary sources.

(3) Te Kowhai Soil

Although the grain size distribution down this profile is highly variable this is consistent with an alluvial parent material. There is significant mineralogical data to show, however, that the top 20-30 cm has a different parent material from that at deeper levels. Not only does the heavy fraction increase in the Ap and Bg horizons compared with the C horizons (similar to Joe, 1986) but there is also a significant change in mineralogy. Biotite dominates the heavy fraction below 30 cm and pyroxenes + amphiboles dominant above 20 cm. In addition to these variations, the quartz content of the silts increases in the top 30 cm. Quartz content also increases in the coarse and medium silts of sample TK8 (70-80 cm deep) which is in accordance with a significant increase in the coarse silt fraction of the soil. Compared with the changes in the other minerals there is less contrasting stratification of opal-C and tridymite-M in the Te Kowhai soil. In general the top 30 cm contain higher concentrations of these minerals, except in the coarse silt. In this fraction opal-C is significantly lower in the top 20 cm. The stratification is also reflected in some of the data from other sources. The feldspar data of M^{C}Queen (1975) shows that in the sands there is more plagioclase in the top 20 cm while the total element chemistry of Joe (1986) documents increasing MnO, TiO_2, CaO, MgO, Cr, V, Ni, Nb, and Ga and decreasing Ba and Rb in the top 22 cm.

The Te Kowhai soil is the poorly drained member of the Horotiu-Te Kowhai complex so this stratigraphy might be interpreted as a weathering phenomenon, with the absence of pyroxenes and amphiboles below 30 cm being interpreted as reflecting reducing conditions below this level. This is not, however, consistent with the reduction in quartz and, in general, opal-C and tridymite-M with depth. It is here suggested that the zone below c. 30 cm represents alluvium of the Hinuera Formation while the top 30 cm is formed from material subsequently added to the profile. Comminuted diatoms are common below 30 cm. Similar diatoms are found in lakes in the central North Island. In the Te Kowhai soil they probably represent material transported along with the alluvium. The biotite common below 30 cm in the heavy fraction is similarly thought to be from an alluvial source.

The top 30 cm represents a zone of accumulated tephra dustings. Evidence for this includes (1) the finer grain size of this zone, (2) the manner in which the amount of heavy fraction reduces towards the finer grain sizes (similar to the tephric data of M^{C}Queen (1975), and the tephric component in the Tokomaru soil, chapter 4), and (3) the euhedral nature of acicular pyroxenes and amphiboles. Recent studies of distal tephras in lake sediments and peats (Lowe 1987), and known tephra distribution in the Waikato (Pullar 1967) demonstrate that since *c.* 15 ka B.P. approximately 30 cm of rhyolitic and andesitic tephras have been deposited in the proximity of the Te Kowhai site. As the final phase of the Hinuera Formation aggradation ceased at 15 ka B.P. (Green and Lowe 1985; Lowe 1987) these tephras might be expected to be preserved in the Te Kowhai soil. In the Waikato region after 15 ka B.P. there was significant climatic amelioration and expansion of the forest (Harris 1963; McGlone *et al.* 1978; Green and Lowe 1985).

The sudden upsurge in phytolith content of the soil at 30 cm is interpreted to represent the cessation of alluvial accumulation at this site and the development of a post-glacial vegetation cover.

In the Te Kowhai soil the stratification of the primary minerals is here interpreted as reflecting two parent materials, (1) a lower alluvial deposit derived from predominantly pumiceous materials from the Taupo Volcanic Zone, and (2) an overlying tephric cover of rhyolitic and andesitic dustings which have accumulated since about 15 ka B.P.

THE ORIGIN OF CRISTOBALITE AND TRIDYMITE IN SOILS

During weathering silica is released to the soil solution. It may be removed from solution either by combining with other elements to produce secondary minerals (e.g. precipitation with Al to form allophane) or by plants (phytoliths) and the soil fauna (see Jones and Hay 1975). Studies of soil leachates, however, show that much silica remains in solution and is lost entirely from the soil (see Mitchell 1975; Wilding *et al*. 1977). Although there is dispute over the forms of silica in natural waters (see discussion in Mitchell 1975) it is thought to occur mainly as silicic acids. Ginzburg and Kabanova (1960) recognised five forms of silica in natural waters, (1) ionic and molecular, (2) colloidal, (3) absorbed to oxides of Mg, Ca, Fe and Al, (4) organic silica (humites), and (5) in skeletal material but White *et al*. (1956) and Krauskopf (1976) concluded that silica in natural waters was mainly in the form of monomeric silicic acid.

The polymeric nature of silica in solution allows it to readily form "weak" or "thin" colloids or gels. Polymerisation of the monomeric silicic acid, which is enhanced by decreasing pH, increasing temperature and increasing degree of silica supersaturation, produces silica hydrosols. These may change progressively to hydrogels and eventually to relatively brittle amorphous silica during dehydration. It is known from studies of amorphous silica (opal-A) in geological environments that given time and slightly raised temperatures opal-A is transformed to opal-CT (cristobalite) and it has been suggested that cristobalite observed in soils may also be derived from amorphous silica (see Mitchell 1975; Lowe 1986). Lowe has suggested that under conditions of poor drainage, relatively high concentrations of silica in the soil solution might result, leading to hydrogel formation. He suggests that dehydration of these hydrogels would lead to cristobalite forming.

(i) Drainage: The upper horizons in the Hamilton, Naike and Te Kowhai soils all have their highest concentrations of opal-C and tridymite-M in zones relatively close to the surface where alternating wet and dry conditions and desiccation are maximised, the most favourable environment for the mechanism proposed by Lowe (1986). It may be particularly applicable to the Hamilton soil as this soil has relatively poor drainage, resulting from its location on a flat terrace underlain by the more compact and impermeable Hamilton Ash Group. It is less likely to apply to the Naike soil, as this site occurs on a low spur where natural run-off lessens the possibility of water perching on the Hamilton Ash Group and the consequent build up of silica in solution. The Te Kowhai soil occurs in low lying swales where there is often a shallow water table, also favouring the suggested mechanism. The Te Kowhai silt loam, however, forms a complex with the Horotiu silt loam, a well drained soil (M^{c}Queen 1975; Jessen 1977; Joe 1986) which is reported to contain common amounts of cristobalite (M^{c}Queen 1975; Jessen 1977; Joe 1986). Comparative data for these two soils (Joe 1986) shows that the Te Kowhai soil does have slightly more cristobalite than the Horotiu soil, suggesting that their differing drainage status may be significant if cristobalite forms in the soil, but it cannot be the dominant factor.

As more mineralogical data becomes available in New Zealand cristobalite is being described from many more soils, e.g. Mamaku sandy loam, Patumahoe silt loam (Anon. 1981); Otorohanga silt loam, Rukuhia peat, Netherton clay loam (Joe 1986); Hamilton Ash Group (Shepherd 1984). Many of these are well drained soils. Furthermore many soils from Japan which contain cristobalite are commonly well drained (Mizota and Aomine 1975; Mizota *et al.* 1987).

An increase in the concentration of silica in the soil solution can also be induced by vegetation (Mitchell 1975; Lowe 1986) and soil desiccation so these processes may therefore promote the formation of cristobalite. In the Horotiu-Te Kowhai complex, however, the soils form such a complicated inter-relationship that the observed variability of cristobalite in the soil cannot be reasonably explained by these mechanisms.

(ii) Crystallinity: During the diagenesis of deep sea siliceous deposits there is a gradual increase in the structural order from opal-A to opal-CT, and eventually to quartz, and a similar range of structural order might be expected during the maturation of gels in soils. Such a range is not apparent in the soils investigated during the present study. The cristobalite in the soils is all opal-C except for rare samples (e.g. R9), but even in these samples it can be demonstrated that the weak development of the peaks is due to reduced absolute abundance of opal-C rather than reduced crystallinity. Tada and Iijima (1983) have demonstrated that in poorly crystalline opal-CT, not only are the reflections at 2.85Å and 3.14Å absent but also there is marked peak broadening of the c. 4.1Å peak. Comparison of the peakedness of the opal-C and quartz in figure 3.17 indicates that they both have similar peak shape. Any slight broadening of the 4.1Å opal-C peak can be attributed to associated tridymite which can readily be identified in the XRD spectra. These results are similar to the limited data from Lowe (1981) which depicts an XRD spectrum in which cristobalite has similar peakedness to quartz in a silt sample from approximately the level of the Aokautere Ash at the Rototuna site.

The relative homogeneity of the opal-C crystallinity data indicate that all the opal-C originates from similar sources, and the multiple reflections of the spectra indicates that the opal-C originates from environments where highly ordered structures can develop.

(iii) Oxygen Isotopes: The oxygen isotope values for opal-C and tridymite-M range from 7.22 to 8.74 $^{o}/_{oo}$ and although they are limited in number, they demonstrate that these minerals are of a high temperature origin, e.g. they are similar to values of c. 8.4 $^{o}/_{oo}$ for Taupo Volcanic Zone quartz (Stewart 1982; P. Blattner *pers. comm.*). The data are similar to those of Henderson *et al.* (1972) who determined $\delta^{18}O$ values of 8.3 to 9.1 $^{o}/_{oo}$ for three cristobalite concentrates from a podzol in north Auckland. Four values for cristobalite and "tridymite" in ando soils and a podzolic soil in Japan (Mizota *et al.* 1987) range from 5.3 to 8.4 $^{o}/_{oo}$ with one markedly higher value of 11.0 $^{o}/_{oo}$. It is noticeable that the yield for this sample is much lower (88%) than for their others and it is suggested that the higher value is due to contamination. During the present study $\delta^{18}O$ values from the clay size fraction of sample TK1 were high (17.5 $^{o}/_{oo}$ and 21.7 $^{o}/_{oo}$), but the yields were low (72% and 80% respectively) and subsequent detailed examination determined that the samples were contaminated.

The $\delta^{18}O$ fractionation for the samples from the Hamilton basin appears to be independent of density and grain size. Although the opal-C:tridymite-M ratio changes markedly with grain size and density the $\delta^{18}O$ values do not (variations in samples R1, R4 and R9 are within the limits of the experimental error). This indicates that both tridymite and cristobalite have similar oxygen isotope fractionation equilibria.

Notwithstanding that the samples analysed during the present investigation are from soils and may therefore be composites from various sources, the oxygen isotope abundance from the silt fractions have a restricted range and there is a grouping between 7.22 and 7.76 $^{o}/_{oo}$. The fractionation of O^{18} and O^{16} between a crystal and water is temperature dependent and, other things being equal, a lower $\delta^{18}O$ value indicates a higher equilibrium temperature. Therefore if the partitioning of O^{18} and O^{16} between cristobalite and "tridymite" and water is similar to that of quartz and water then this data (7.22-7.76 $^{o}/_{oo}$) indicates that cristobalite and "tridymite" either formed at a higher temperature, or were in equilibrium with water of different oxygen isotope chemistry to that of the quartz (8.4$^{o}/_{oo}$, Stewart 1982; P. Blattner *pers. comm.*). They may therefore record a magmatic event different to that recorded by the quartz.

Four data, 8.02, 8.18, 8.40 and 8.74 $^{o}/_{oo}$ are significantly different to the group noted above. Excepting TK5 (8.40 $^{o}/_{oo}$) these data are from deeper levels in the profiles. It has been argued above that these deeper horizons are in general much older than those containing the 7.22-7.76$^{o}/_{oo}$ grouping. Thus it could be argued that the higher $\delta^{18}O$ values are the result of post-depositional exchange with ambient water over a longer period of time, particularly considering that the highest $\delta^{18}O$ data, (N4), is from the oldest sample. Samples R9 and R10 are adjacent samples in the Hamilton soil yet they have contrasting $\delta^{18}O$ values. Shepherd (1984) documents a palaeosol between H_8 and H_7 (correlatives of R9 and R10 respectively) so sample R10 may have had a longer period in contact with ambient water, but this does not satisfactorily explain the difference between the two samples. It is suggested that the difference therefore reflects the temperature of formation of the cristobalite and "tridymite" and may indicate a change in magmatic processes or source at this time.

Sample TK5 is chronostratigraphically within the age range of the 7.22-7.76 $^{o}/_{oo}$ group so either it represents cristobalite from a slightly cooler environment or this sample is contaminated. Sample TK5 is from a poorly drained soil profile where the parent material is dominated by glass and as a consequence it was not possible to obtain a pure mineral concentrate. Although it has been argued that the glass should not influence the $\delta^{18}O$ significantly it is suggested that hydration of the glass may have occurred (Hodder 1978; Lowe *et al.* 1984) and the $\delta^{18}O$ value may be higher as a consequence.

Although the oxygen isotopes from the soils may represent an "average" value of cristobalite and "tridymite", potentially derived from many sources, the distribution of the data indicates that there may have been a significant change in the nature of the source with time. It is suggested that variations in $\delta^{18}O$ values of cristobalite and tridymite may be useful in investigation of magmatic processes, particularly as they may reflect processes occurring at, or immediately prior to eruption.

(iv) Sources: The distributions of opal-C and tridymite-M in the Hamilton, Naike and Te Kowhai soils are highly stratified with, in general, higher abundances in the upper horizons. The stratification is also reflected in the distribution of other components e.g. glass, ferromagnesian silicates and opaques. These other components represent a change in parent material in the top of the profiles and it is concluded that the changes in the distribution of opal-C and tridymite-M are related to changes in parent material. The concomitant increase in opal-C and tridymite-M and relatively unweathered materials of demonstrable volcanogenic origin suggest that the opal-C and tridymite-M are derived from volcanic sources. α-cristobalite and α-tridymite are closely associated with volcanicity and the oxygen isotope and crystallinity data of the opal-C and tridymite-M are consistent with this origin. The morphology of the crystals (euhedral to subhedral) is in general compatible with this interpretation. The variability in form, however, even within the same soil sample, suggests that the opal-C and tridymite-M in some samples are from multiple sources. A limited investigation has identified opal-C and tridymite-M from several diverse and contrasting volcanic environments, e.g. andesitic lavas, rhyolitic tephras and hydrothermally altered material. This variability probably accounts for the variety in crystal shape.

(v) Distribution: If the cristobalite in the soils is derived from an igneous source and transported to a site in association with tephric materials then cristobalite should be a common mineral in tephric soils. In the Waikato, Lowe (1981, 1986) has concluded that this does not appear to be the case and that while cristobalite is common near Hamilton, e.g. Rototuna, it "was rarely detected in any samples from the other three sites" (i.e. the Tapapa, Taotaoroa and Kakepuku sites). M^{c}Queen (1975), Anon. (1981) and Joe (1986) also show cristobalite distribution to be variable. This variability could be due to difficulty in identifying cristobalite where it occurs with plagioclase and quartz because of peak overlap, or it could be due to winnowing effects during transport. Opal-C and tridymite-M occur in the finer grain sizes and selective deposition may effect distribution. Cristobalite can form via pneumatolytic processes (Bernard and Guern 1986; Hampton and Bailey 1985; Sarna-Wojcicki *et al.* 1981) so crystals can grow very quickly. Many of the plinian rhyolites from the central North Island have multiple phases of eruption, each of which may have a different distribution pattern. It is possible that conditions suitable for cristobalite formation may occur prior to, or during, a specific phase of eruption. Cristobalite will consequently only occur in this phase of eruption, and because in distal deposits separate phases are seldom able to be differentiated the cristobalite distribution will appear variable. Notwithstanding these possibilities the main factor controlling the distribution of opal-C and tridymite-M in soils is the variability in distribution between tephras. It has been shown that opal-C and tridymite-M are common in some fractions of the Okareka, Aokautere and Rotoma ashes but rare or absent in other tephras (Rotoehu, Taupo, Waimihia). This data is supported by Lowe (1981). At the Tapapa site cristobalite is reported as common in the silts and sands of the tephra, loess and palaeosols associated with the Okareka, Aokautere and Tahuna ashes but absent or in only trace amounts at the level of the Rotoehu Ash, and at other levels where no specific tephras are identified. The variable distribution of cristobalite can be explained by the distribution and proportion of cristobalite-bearing and non-cristobalite-bearing ashes in each soil.

CRISTOBALITE AS A TRACER FOR TEPHRAS

If it can be shown, as the preliminary work presented here suggests, that cristobalite is associated with particular eruptions then there exists the possibility of using cristobalite for correlation of ashes. Cristobalite not only has the advantage of being resistant to weathering (it is still common in the H_1 bed of the Hamilton Ash Group, and in the underlying Kauroa Ash Formation (Davoren 1976)) but it occurs in a relatively narrow range of grain sizes. It is also readily detected by XRD, and beneficiation with fluorosilicic acid (Henderson et *al*. 1972) removes feldspar, the major phase that interferes with the cristobalite spectrum. The cristobalite identified in the Aokautere Ash from the West Coast confirms that cristobalite has travelled significant distances. By using the most advantageous grain size and treating a sample with fluorosilicic acid it may be possible to quantify what are only trace amounts of cristobalite in a sample.

In an investigation of a marine core east of the North Island, Stewart and Neall (1984) determined the biogenic opal content by converting it to cristobalite and quantifying the cristobalite by XRD. They also determined the distribution of tephric components in the core. The trends of the biogenic silica distribution from their analysis are quite variable but there are markedly increased values for biogenic silica at 3.8 and 5.5 m sub-bottom depth. These depths correspond to the levels of the Aokautere and Okareka ashes respectively and it is here suggested that these increases in biogenic silica are related to relatively high initial cristobalite levels (i.e. volcanogenic cristobalite) in these samples. A detailed inspection of other data (in Stewart 1982) from this core indicates that synchronised increases in volcanic glass and biogenic silica content occur:

(1) Immediately below the Aokautere Ash at the level correlated with the Poihipi Tephra (Stewart 1982).

(2) Below the Okareka Ash, at the level of Tephra 5 of Stewart (1982).

(3) At the levels of the Waiohau, Rotoma and Whakatane Tephras where there are small but potentially significant increases in biogenic silica.

The distribution of cristobalite may thus be a useful parameter to use to identify small tephric additions to sedimentary sequences.

AMORPHOUS SILICA IN HAMILTON BASIN SOILS

Although there is no evidence from the present investigation for the involvement of cristobalite with the precipitation of silica from the soil solution, some of the opal-A may have formed by this pathway. The morphologies of the opal-A grains in (1) the A and upper Bt1 horizons of the Hamilton soil, (2) the A and Bw horizons of the Naike soil, and (3) the Te Kowhai soil, are of phytoliths and microfossils, consistent with a biogenic origin. The dusty and concentric opal-A have morphologies consistent with inorganic origins and they are here thought to have formed in the soil. IR spectra for the dusty and concentric opal-A (Fig. 3.13) are both similar to those from opal (Yoshida *et al.* 1959; Kamatani 1971) except for a pronounced inflection at approximately wave number 960 cm^{-1} probably related to a Si-OH bond.

Knauth and Epstein (1982) have shown that oxygen isotope analysis of opal-A is difficult because of the differential release of adsorbed, occluded and structural water (see also Jones and Segnit 1969; Bartoli 1985). This may be further complicated by (1) the evaporation effect, where O^{16} is preferentially lost during evaporation (Stewart and Taylor 1981) so $\delta^{18}O$ increases in the remaining water, (2) the temperature effect, $\delta^{18}O$ decreases with increasing temperature, and (3) post-depositional exchange with younger ambient water. These problems, together with the possibility that oxygen isotope equilibrium may deviate from linearity at low temperatures (Kawabe 1978) suggest that only broad generalities arising from differences in $\delta^{18}O$ should be made, particularly considering the size of the data set.

Comparison of the $\delta^{18}O$ values of the four samples of opal-A analysed indicates that there is a significantly wide range of values. Equilibrium temperatures calculated using different calibrations (Clayton *et al.* 1972; Knauth and Epstein 1975; Kita *et al.* 1985) range from 9°C to 37°C with estimated temperatures from the same sample being highly variable, depending on the particular calibration used. This range is too broad to warrant detailed interpretation but in general the calibrations predict that the soil phytoliths formed in an environment approximately 10°C cooler than the concentric and dusty opal-A (assuming that all formed in equilibrium with waters that had similar isotope chemistry).

The factors which are thought to lead to the formation of hydrogels and opal-A include high temperature, low pH, and silica supersaturation. As the dusty and concentric opal-A content appears to be stratified in the soil, changes in the controlling factor(s) should occur at the boundaries of the opal-A-bearing zone. There are no significant contrasts of pH in the profiles. pH values in the soils range from 5.6 in topsoil to 5.3 at one metre depth in the Naike soil (Anon. 1981) and from 5.7 in topsoil to 5.2 at one metre depth in the

Hamilton soil (Joe 1986). At depths greater than 50 cm the temperature differential and variability of the two soils would be minimal, so current pH and temperature are not considered critical factors in the occurrence of inorganic opal-A in the soil. Silica supersaturation of the soil solution is probably most readily induced where water table fluctuations and desiccation are most marked i.e. in the topsoil, but the distribution of acid oxalate-soluble silica indicates that there is no marked change in silica distribution down the profile (Anon. 1981; Joe 1986). These factors, taken together with the contrasting morphologies of the opal-A in two soils which have similar physical and chemical environments, suggests that opal-A is either an artifact of, or at least initially developed during, an earlier weathering cycle.

If the correlation of the stratigraphy of the Hamilton and Naike soils to the Hamilton Ash Group is correct then the concentric and dusty opal-A-bearing zones occur in parent materials that are of considerably different ages. The beds in which the *dusty* opal-A is found have been correlated with the upper Ohinewai Tephra Formation + H_3 beds and with the 250 ka Mount Curl Tephra. Shepherd (1984) describes a palaeosol developed in the H_3 bed and Ohinewai Tephra Formation, so it is concluded that the middle and lower zones of the Naike soil (i.e. those zones containing the *dusty* opal-A) were initially weathered during this period.

The *concentric* opal-A occurs in horizons which are overlain by the Rotoehu Ash so they are at least 50 ka old. If the correlation between the Hamilton soil site, the Welches Road section and the Te Kuiti section is tenable then the Hamilton soil lower zone (i.e. the zone containing the *concentric* opal-A) is tentatively correlated with the upper horizons of the "older beds" at Te Kuiti. Stevens and Vucetich (1984), assuming a uniform accumulation rate, inferred these horizons to have been deposited c. 80-110 ka BP. If it can be assumed that opal-A formed (or began to form) during weathering soon after deposition of the associated parent materials (Ward 1967; Stevens and Vucetich 1984) then the dusty opal-A is considered older than the concentric opal-A.

Although the dusty and concentric opal-A have significant morphological differences and have been interpreted to be of markedly different ages, the $\delta^{18}O$ and IR data suggests that they comprise similar materials and that they formed at low temperatures. An ordered internal structure was not observed in the dusty opal-A but the concentric opal-A comprises particles that are c. 1600Å in diameter and which appear to be very similar to the microspheres identified in precious opals (Jones *et al*. 1964, 1966; Darragh *et al*. 1966; Sanders 1968). These are thought to form by the aggregation of flocs in thin hydrogels with subsequent desiccation "setting" the structure (Darragh *et al*. 1966). The same process probably produced the dusty and concentric opal-A. The marked contrast in refractive index between zones probably reflects a significant change in either the size of the individual flocs or in the water content. Darragh *et al*. (1966) considered that the presence of open cavities was a significant prerequisite for the formation of opal and the form of inorganic opal-A identified here is consistent with this. Although the dusty opal-A has fine inclusions throughout the grains they are not in sufficiently high concentrations to demonstrate that the opal-A had enclosed a soil aggregate. It is concluded that these grains developed in pores within the soil.

The concentric structure of the opal-A suggests a rhythmic deposition sequence. Of the three main factors identified with the formation of opal-A it is improbable that pH by itself would be cyclic so the main factors involved with the deposition of opal-A are probably related to temperature and silica saturation. If they are related to temperature these cycles could be climatic, on a scale of a decade, a millennium or perhaps of stadial proportions. It is improbable that they could be annual cycles unless the growth period of the grains was very short, as the grains have only five zones at most. Aridity was considered a major factor in the formation of opal in Australia (Darragh *et al*. 1966) and it may be that a similar factor, either as droughts or stadials produced the desiccation required to form the opal-A. Judging by the variations in the numbers of zones not all grains have undergone the same number of cycles.

Variable silica supply is another factor which could be cyclical. Studies of recently erupted ashes showed that there may be large increases in the silica leached from an ash soon after eruption (White and Claasen 1980). It is possible therefore that immediately after an eruption a sudden increase of silica in solution produces silica supersaturation and given the appropriate desiccating environment this may produce opal-A.

While this project has demonstrated that the cristobalite identified in the soils studied is derived from igneous sources it has also identified a low temperature form of inorganic opal-A in the soil. It is thought that weathering of andesitic and rhyolitic tephras provided a relatively continuous source of silica in solution which with polymerisation produced hydrogels. These accumulated at specific sites in the soil and subsequent dehydration produced opal-A. Repetition of this process produced the concentric zoning.

CHAPTER FOUR

SAND AND SILT MINERALOGY AND GEOCHEMISTRY OF THE TOKOMARU SILT LOAM

INTRODUCTION

PREVIOUS WORK

The Tokomaru silt loam is a soil developed on the high terrace of the east bank of the Manawatu River (Fig. 4.1) near Palmerston North. It has formed in the youngest of a sequence of silty units which overlie interdigitating gravels and sands that were deposited on a marine bench (Te Punga, 1962). This is the Tokomaru marine bench (Hesp and Shepherd 1978) which was cut during a period of higher sea level.

One of the earliest geological descriptions of the area (Crawford 1886) noted that "the drift gravels form terraces" and suggested that the gravels were raised beaches. Park (1887) included the surficial deposits in a "Drift Formation". In 1910 he included the surficial deposits in the "Rangitikei fan" (still part of the Drift Formation), a "maritime" fan built from material transported down the larger rivers between the Manawatu and "Wangaehu" (*sic*) Rivers. Marshall and Murdock (1920) noted that there were large muscovite flakes (unknown in the local North Island basement rocks) in the Plio-Pleistocene "papa" underlying the Drift Formation and described extra-regional pebbles with granitic and schistose affinities in the raised beach deposits. They suggested that these extra-regional pebbles were evidence for a late Pleistocene land bridge with northwest Nelson and that a climatic cooling had occurred at that time.

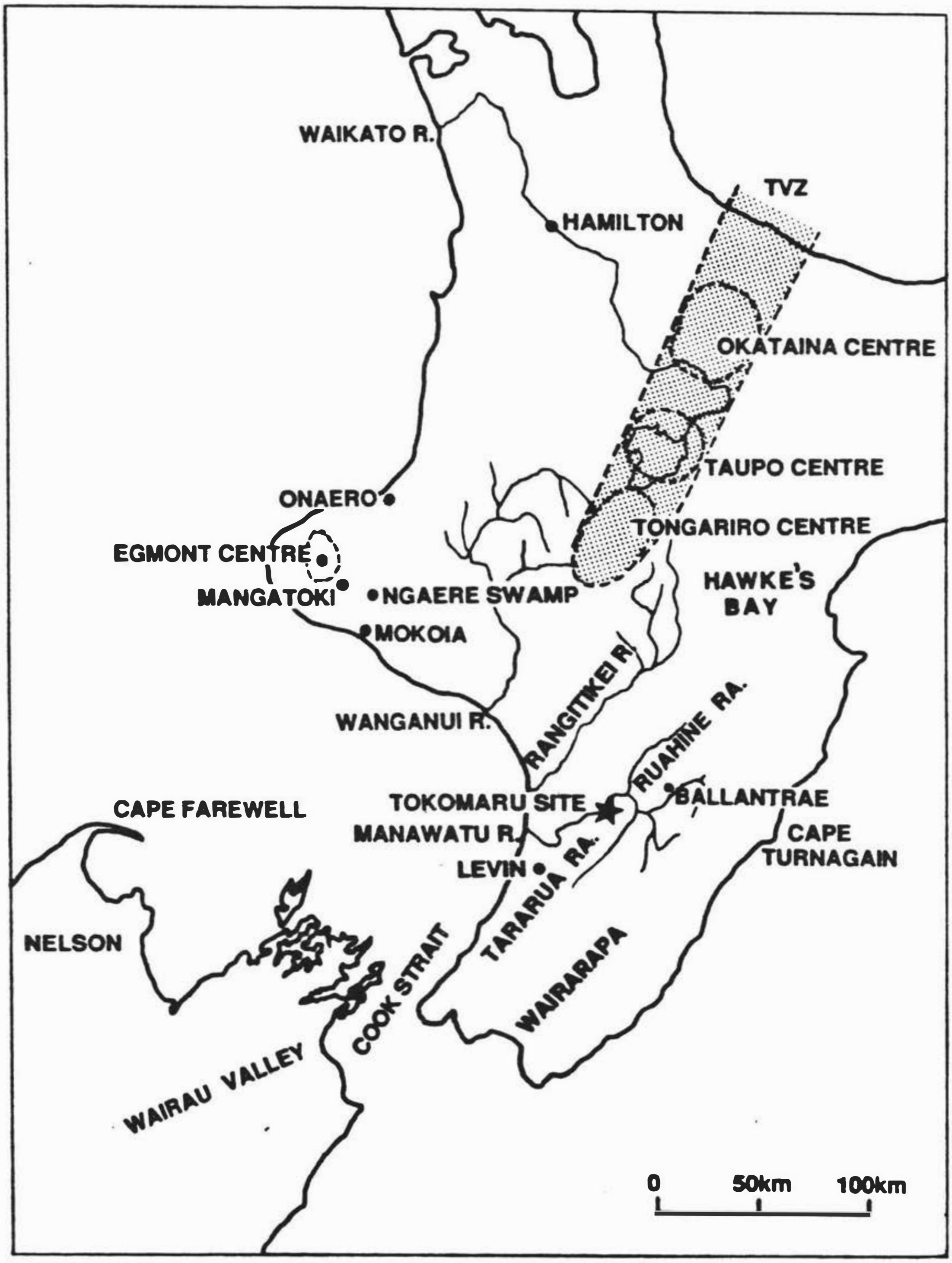

Figure 4.1: Location map of part of central New Zealand showing the location of the Tokomaru site. TVZ refers to Taupo Volcanic Zone.

Hudson and Fife (1940) were the first to report on the soils of the terraces. This work (on mole drainage) was in response to a major limitation of the soil for agricultural purposes. It has a perched water table which results in poor drainage in winter. They documented the grain size distribution down the profile and showed that the soil was dominated by their fine sand (0.2 - 0.002 mm) fraction. They also noted the "clay bulge" between 44 and 60 cm depth and described iron concretions (see also Te Punga 1954) which commonly occur in a zone above the "clay bulge". Hudson and Fife were also the first to note "the presence of a narrow sandy layer an inch or two in thickness", (the Aokautere Ash of Cowie 1964) at approximately 2.2 m depth. They regarded the origin of the silt as "marine sediments now forming an elevated coastal plain". Fife (1945) in studying a "yellow-grey loam" (*sic*) (Grange 1945; Pohlen *et al.* 1947) in the Manawatu (the Tokomaru silt loam) provided the first data on the chemistry of the soil. Using pH and base exchange chemistry he showed a marked change in the chemical properties within the B horizon and between the B and C horizons. His data came from an untopdressed profile among forest remnants and although the exact site is unknown, (it is believed to be in the vicinity of grid reference T24/306879, J.A. Pollok *pers. comm.* 1986), it probably represents the best chemical data for a virgin forest soil of this terrace.

Taylor (1948) grouped the yellow-grey loams of the North Island (Grange 1945) with the South Island Lowland Tussock Soils (Grange 1946) and changed the name to yellow-grey earths to emphasis the zonal nature of the group. It was not until the 1:253440 North Island soil map (Soil Survey Staff 1954) was published however that the group was formally described and the Tokomaru silt loam identified as belonging to the group. The group is characterised by "greyish topsoils, yellowish subsoils with a hard, massive pan" below the subsoil. Greyish bands of gleyed soil immediately above the pan pass down into vertical cracks in the pan. Although they describe the parent material for the Tokomaru silt loam as alluvium, the parent material for the yellow-grey earth group is given as, amongst others "drift deposits including fine volcanic ash and other loess like beds". They also state " examination of the minerals of the sand fraction has shown

......the parent material of the soil is stratified and that there has been some accumulation of airborne material during soil formation" (Soil Survey Staff 1954). A comprehensive summary of the physical and chemical properties of the yellow-grey earths was given in a symposium on this soil group in 1958 (New Zealand Soil News 6:206-230).

In a detailed study of the sediments on the marine bench south of Palmerston North, Oliver (1948) described a sandstone (Otaki Sandstone) equivalent at least in part to the Drift Formation of Park (1910). He included the overlying silts in the Otaki Formation. According to Oliver most of the Otaki Formation was deposited in a shallow marine to beach environment with much of the sand being derived from reworked Tertiary sediments to the north. Te Punga (1953) in a study of the Rangitikei Valley correlated the alluvium (greywacke derived conglomerates plus sands) overlying the Castlecliffian sediments (i.e. the Drift formation) with the Hawera Series of Thomson (1916).

Rich (1959) in a study of the Cenozoic geology of the lower Manawatu Valley included the gravels and overlying silts in the Tiritea Formation. He described approximately 40 metres of rarely fossiliferous interlaminated gravels, sands and silts, which often have ripple marks, capped by 6 metres of yellow-grey silt. He suggested that this capping of "thin, yellow, and in places sandy, silt layers may represent alluvial or aeolian deposition. A sheet of yellow-gray silt forms the top member of the Tiritea Formation in most places. ...... a distinct vertical parting invites comparison with loess. An aeolian origin is suggested by a lack of stratification and by a persistent 3 to 6" band of gray-white pumice ash 3 to 5 feet below the top .... Thickness decreases away from Anzac Park but the silt with the ash band persists southwards to the vicinity of Linton." In the north he traced the ash to an area northeast of Colyton and suggested that the "pumice material was probably air-borne to site of deposition" and "pumiceous material came originally from the Taupo volcanic zone". On the greywacke along the inner (east) edge of the Tiritea Formation, Rich also describes outcrops of sands with "steeper cross bedding, 17-30° ...... suggesting some of the sand is wind blown". He finally concludes that "The widespread silt forming the topmost member of the formation suggests that the final phase of the Tiritea deposition may have been the aeolian distribution of loess-like silt". Earlier, Birrell (1956) had also referred to the youngest unit on the Tokomaru marine bench as "loess-like silts".

Cowie (1963,1964a) realised that the thin sand of Hudson and Fife (1940) and the ash of Rich (1959) were parts of a much more extensive unit that formed a thin veneer mantling the landscape. He named it the Aokautere Ash. At its type section (1.5 km east of the Tokomaru silt loam site of this study) the ash consists of 1.5 cm of fine pinkish pumiceous silt overlain (with a sharp boundary) by 11 cm of a normally graded coarse pumiceous sand which grades into the overlying silt. The base of the lower pumiceous silt is sharp and undulating. The ash is relatively continuous in the road cutting at its type section but elsewhere in the Manawatu is discontinuous. Isopachs show that the Aokautere Ash increases in thickness towards the central North Island. Vucetich and Howarth (1976) have proposed that the Aokautere Ash, Scinde Island Ash and Oruanui Breccia are members of the Kawakawa Formation, a c. 20,000 year old rhyolitic eruptive from Lake Taupo. Recent work (Self 1983; Self and Healy 1987) would group the above members with the Wairakei Breccia (Grindley 1965) and proposed the name Wairakei Formation. The problem of correlation and nomenclature has not been satisfactorily resolved so for the purposes of this work the term Aokautere Ash *sensu stricto* (Cowie 1964a) is used.

Cowie (1964b) demonstrated that the Aokautere Ash and therefore the enclosing silts must have been deposited subaerially so that the silts were of a loessial origin. He showed that the loess was thin or absent on the Ohakean Terrace (Te Punga 1953b) and that the post-Aokautere Ash loess thinned and became finer towards the southeast away from each major river, so drawing the conclusion that the loess was derived from material blown off the terraces built during the Ohakean aggradation. This terrace formed during the aggradation phase of the last stadial (Milne 1973a, 1973b). It is now recognised that in the southwestern North Island the silty material overlying the terrace gravels (all part of the drift regime of earlier workers) is composed of multiple loess units each separated by a palaeosol (Cowie and Milne

1973; Leamy *et al.* 1973; Milne 1973a, 1973b) . During colder stadial periods aggradation occurs in the river valleys as a consequence of devegetation and accelerated erosion (Vella 1963; Leamy *et al.* 1973) and with the relatively colder, windier and drier conditions silt size material can be removed from the aggradation surfaces and deposited as loess on older and higher terraces. During interglacials or interstadials soils develop as the climatic conditions improve, only to be buried by loess deposited during a subsequent cooling. On the Tokomaru marine bench between two and four periods of loess accumulation are preserved (Cowie 1973; McIntyre 1975; Milne and Smalley 1979; Anthony 1984) with the Tokomaru silt loam developed in the youngest of these.

Since Cowie (1964b) there has been a series of detailed studies undertaken on various aspects of the pedological properties of the Tokomaru silt loam. The distribution of Fe, Mn, V, Ni, Cr, Co and Ti between the concretions and soil (Brooks 1965) showed that there was a marked concentration of all these elements except Ti in the concretions. Comparison between the parent soil and the gleyed cracks showed a loss of all these elements (Co was beyond detection limit) in the gleyed material. Symes and Wells (1973) in an X-ray study of the topsoil mineralogy from Mount Egmont to Palmerston North reported only trace amounts of ash in the Tokomaru silt loam. Their method however was unsuitable for identifying minor amounts of volcanic components but they did show a systematic increase in quartz content away from Mount Egmont. Kirkman (1973a, 1973b) showed that the occurrence of amorphous Si, Al and Fe reached a maximum in the B horizon.

Soil water and related soil physical parameters in the Tokomaru silt loam were investigated by Gradwell (1974) and Scotter *et al.* (1979). Their work confirmed inferences from the morphological description of the Tokomaru silt loam in that quantitative measurements were obtained to show the gradual change in bulk density and water properties down to the pan which is relatively dense and impervious. Below the pan the data indicate little further change until the zone of influence of the Aokautere Ash.

In 1975 Pollok published the first results of an ongoing investigation of the pedology of the Tokomaru silt loam. He (see Pollok, 1984) designated a pseudogley horizon in the B horizon and the dense pan a fragipan in the C horizon. Using extractable chemistry, clay mineralogy and micromorphology he demonstrated (like Fife 1945) that there was a marked difference between the B and C horizons. The Tokomaru silt loam has a measure of variable charge and Pollok (1984) suggested that this was due to ferrolysis. Pollok concluded that the soil is the product of polygenesis with the early formation of the fragipan in the loess followed by subsequent pseudogleying which is the prominent current process.

During a survey of Kairanga County, Cowie (1978) studied a site adjacent to the one presently being investigated and presented data similar to that of Fife (1945) and Pollok (1975). In studying the relationship between the yellow-grey earths and adjacent yellow-brown earth/yellow-brown loam intergrades he concluded that the difference between the groups was not due to different parent materials. Rather they were the result of variations in climatic factors, with seasonal wetting and drying producing the compact fragipan of the yellow-grey earth. Initial results of this investigation (Wallace and Neall 1982, 1984) presented the sand mineralogy of the Tokomaru silt loam and identified significant rhyolitic and andesitic tephra components (other than the Aokautere Ash). These results showed a marked stratigraphic break at approximately 0.5 m which is thought to be related to an hiatus in loess accumulation marking the end of the Otiran Glacial stage. A threefold division for the post-Aokautere Ash loess was proposed: (1) an upper mixed tephra/loess unit, (2) a middle quartzofeldspathic loess, (3) a lower tephric loess down to the ash. In a study of the relationship between the yellow-grey earths and the yellow-brown earth/yellow-brown loam intergrades Parfitt *et al.* (1984) presented limited mineralogical data on the Tokomaru silt loam. Like Cowie (1978) they suggested that the differences between the yellow-grey earths and intergrades were due to climatic factors. High summer water deficits in the yellow-grey earths exert hydraulic suction that produces the increase in bulk density. This impedes drainage leading to separate weathering paths and different soils.

The Tokomaru silt loam, an Aeric Fragiaqualf in U.S. Soil Taxonomy, is a member of the central zone of yellow-grey earth soils (see Bruce 1984; Cowie 1984). It has developed in last stadial Ohakean loess which probably started accumulating approximately 23,000 years ago (at least prior to the 20,000 year old Aokautere Ash) and may have continued until approximately 9760 years B.P. (based on a radiocarbon date in the Rangitikei River, Milne and Smalley 1979).

THE PRESENT STUDY

The purpose of the current investigation was to study the accumulation of aeolian materials from various sources (including loessic, aerosolic and tephric) in the development of the Tokomaru silt loam. The sample site (informally known as Pollok's Pit) is located on one of the Massey University farms adjacent to Clifton Terrace at T24/329881. Clearance of the original broadleaf/podocarp forest began in the 1880s and after the initial grass was sown "the area where the profile pit is located was kept as a museum piece" (Pollok 1975). It has not been actively topdressed or cultivated and a well-defined charcoal layer at approximately 5 cm (the burnt remains of the original bush clearing phase), the preservation of granules in planes parallel to the surface, and mineralogically discrete layers indicate that the soil has only been minimally disturbed.

Samples were fractionated into grain sizes and whereas the sands and coarse silt were subjected to detailed optical investigations, dissolution techniques were employed to determine mineralogical trends in the finer fractions. The first stage of the dissolution which involved repeated heating in HCl removed micas and mafic minerals (Brindley 1957; Henderson *et al.* 1972). After this the samples were treated repeatedly with H_2SiF_6 so removing the feldspar (Chapman *et al.* 1969) and leaving a residue of quartz (plus minor cristobalite in some cases).

Optical investigation showed that there were numerous tephra additions to the soil and that these were concentrated in the sand fraction. This fraction was therefore analysed for major and trace elements in an attempt to support the mineralogical evidence of volcanic additions to the loess. Chemical analyses were also carried out on the whole soil in an attempt to locate chemical translocations due to pedogenic processes.

Phosphorus is relatively immobile in the soil, it being readily fixed by amorphous Al-Fe compounds. As it is a major plant nutrient phosphorus is removed from the subsoil during plant growth and accumulates in the A horizon, therefore if a surface is stable there is a gradual accumulation of P. This P is normally retained if the soil is buried (e.g. by tephra, loess, colluvium etc.) and the subsequent palaeosol may have a relatively high P content. This property has been used (Walker 1965; Leamy and Burke 1973; Tonkin *et al.* 1974; Runge *et al.* 1974; M^{c}Intyre 1975) to identify palaeosols. Phosphorus distribution was therefore determined in a search for palaeosols in the upper zones of the soil.

Trace element chemistry of minerals in tephras has been used (Rankin 1973; Kohn 1970; Kohn and Neall 1973) to characterise individual tephras. Apart from the Aokautere Ash, the tephric materials in the Tokomaru silt loam occur as dustings diluted by loess, so that bulk sampling methods are inappropriate. An alternative is to analyse individual minerals on an electron microprobe (Westgate *et al.* 1970; Westgate and Gorton 1981; Froggatt 1983). Such an investigation of the volcanogenic components in the Tokomaru silt loam was undertaken for correlation with potential sources.

Although pollens are not preserved in the loess due to the oxidising environment, the occurrence of different forms of phytoliths (plant opal) hinted at a potential for discerning the vegetative history. Phytoliths are composed of biogenic silica that forms replicas of plant cells or crystals within plant cells. These are released when the cell decays. It is unclear whether silica is an essential element for plant growth or even advantageous to the plant but Japanese workers believe that silica deposited within rice plant cells makes the plant more resistant to fungal and insect attack (Yoshida *et al.* 1962a, 1962b). Phytoliths are formed when silica in solution moves through the plant system until water loss due to transpiration allows the silica to precipitate, most commonly in the leaves. Struve (1835) was one of the earliest workers to investigate silica in plants and Ehrenberg (1847) used the term phytolitharia for some dust constituents he described. It was Ruprecht (1866) who first used the term phytolith for "minute stoney parts of plants". Subsequent work (e.g. Jones and Handreck 1967; Twiss *et al.* 1969) has shown that phytolith shape may be identified with particular plants and that they are commonly preserved in soils (Baker 1958; Beavers and Stephen 1958; Wilding and Drees 1971; Bartoli and Guillet 1977). Ecological reconstructions based on phytoliths have also been attempted (Baker 1959; Rovner 1971). In New Zealand Raeside (1964a) described plant opal (phytoliths) from loesses and later attempted to relate these to those he extracted from various tussocks and sedges (Raeside 1970). Potentially, phytoliths may be used like pollens and as the loess parent material to the Tokomaru silt loam accumulated on a grass/shrub dominated surface compared with the pre-European bush cover, phytoliths were extracted from samples T17 to T24 seeking this change in vegetation. In an attempt to identify the soil phytoliths, wood and leaves from elements of the present bush on the Tokomaru terrace, kahikatea (*Podocarpus dacrydioides*), rimu (*Dacrydium cupressinum*), totara (*Podocarpus totara*), black beech (*Nothofagus solandri*) and tawa (*Beilschmiedia tawa*) were processed. Two peats representative of forest communities were also studied. Pollen data indicated one peat (from Maruia, South Island) to be beech dominated while the other (from Mt. Egmont) is from a mixed podocarp association (C.M. Lees *pers. comm.* 1986).

RESULTS

GRAIN SIZE DATA

The relative proportions of the various size fractions are presented in Appendix 4. The textures of all samples are silt loams except for T1 and T17 which are silts and T20 which is a silty clay loam. Even the Aokautere Ash is of silt loam texture. This is due to significant amounts of non-volcanic material in the silt size fractions in the ash. The grain size data are very similar to those of Hudson and Fife (1940) and Pollok (1975). Like Hudson and Fife continuous sampling was used (in contrast to the horizon sampling of Pollok), which gives much improved definition to the patterns of changes down the profile.

(i) CLAYS: The main feature of the clay distribution down the profile is the "clay bulge" described by Hudson and Fife (1940) and Pollok (1975). It is here reflected in the high clay content of sample T20 (Fig. 4.2) which is located towards the top of the Bgt2 horizon. Above this there is a variable clay content with a minor increase just below the surface. In the Cxg horizon the clay content is relatively constant and it should be noted that this uniformity continues above the cap of the fragipan into the middle of the Btg2 horizon. Below the Cxg horizon there is a rise in clay content at sample T8 followed by a general fall in clay content to the Aokautere Ash. This trend

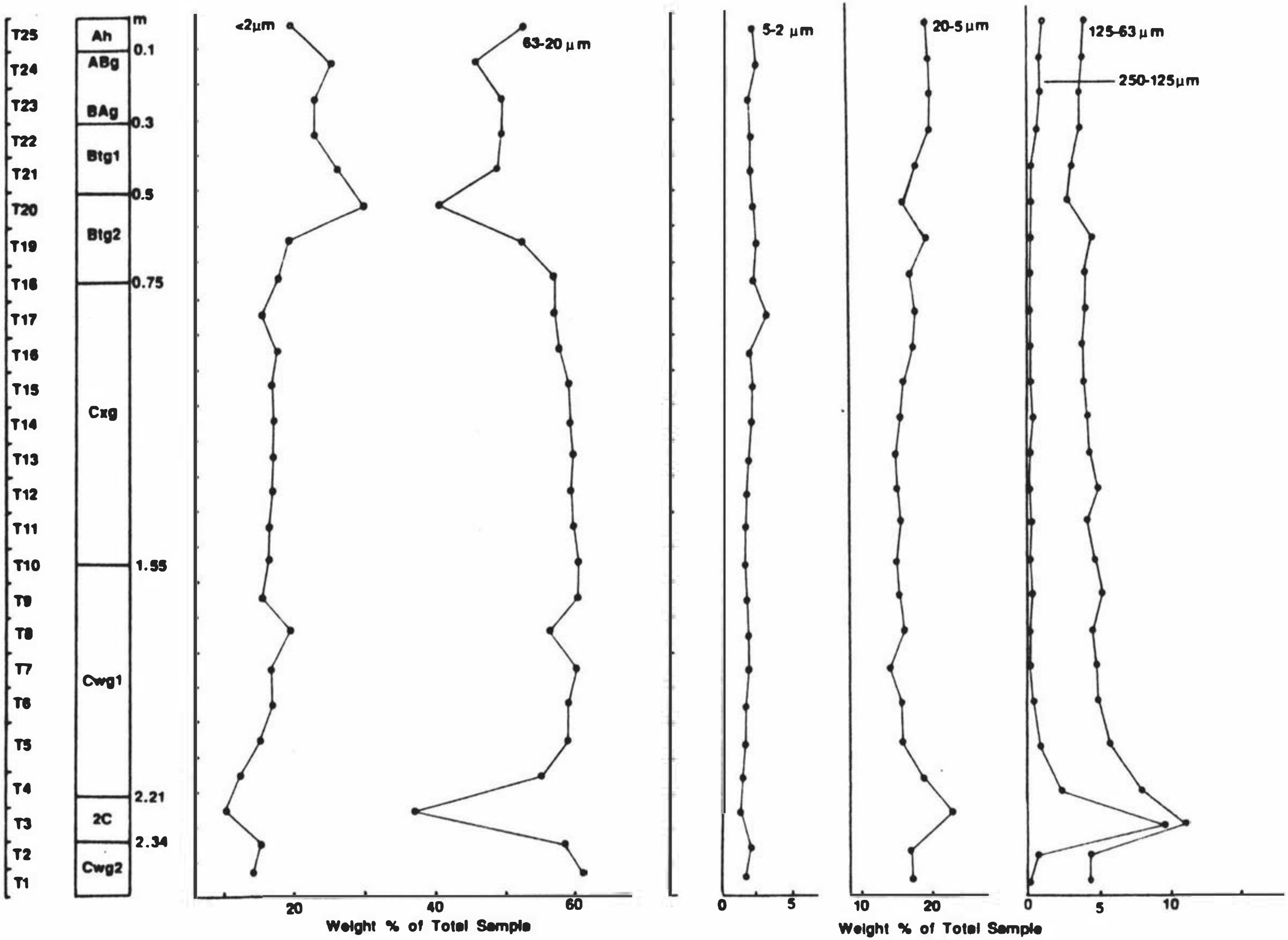

Figure 4.2: Variation in grain size distribution for the Tokomaru silt loam.

parallels the rising glass content in this region of the profile (see mineralogy section). Below the ash the clay content rises to levels similar to those of the Cxg horizon.

(ii) SILTS: Silt distribution is broadly antipathetic to the clay distribution (Fig. 4.2). The **5-2** μm fraction, taken to represent global aerosolic dust (Mokma *et al*. 1972), has a relatively uniform distribution throughout although there are perturbations at the Aokautere Ash. In the **20-5** μm fraction there is a marked decrease between samples T19 and T20, a slight increase from samples T15 to T19 and higher values in the Aokautere Ash. The Aokautere Ash has a bimodal grain size distribution (modes at 250 μm and 20-5 μm) so that the increase in the 20-5 μm fraction for the Ash, compared with the loess is attributed to increased medium silt sized glass shards. The higher H_2SiF_6 soluble material in this fraction of the ash (compared with adjacent samples) supports this conclusion. The mode of the loess is in the **63-20** μm fraction. At the level of the Aokautere Ash in this fraction there is a lower coarse silt content compared with the adjacent Cwg horizons. The top seven samples, particularly the ABg (T24) and top of the Btg2 (T20), have a lower coarse silt content than in the C horizon. Samples T16-T18 (the cap of the fragipan) have coarse silt levels slightly below those of the underlying C horizons.

(iii) SANDS: The sand fraction forms up to 6% of the loess (excluding the influence of the Aokautere Ash) and although samples T9 and T12-T13 appear to be above background the only significant shift in trend is between samples 19 and 20 where there is a general lowering of the total sand content (Fig. 4.2). Individually the various divisions of the sands present quite different trends. In the very fine sands (125-63 μm) there is a maximum at the Aokautere Ash. The top six samples (T20-T25) trend at slightly lower levels compared with the Cxg-Cwg horizons. The trends for the fine sand (250-125 μm) show a maximum at the level of the Ash and the top four samples (T22-T25) have fine sand contents above those of the Cxg-1Cwg1 horizons. There are also slight increases at the levels of samples T9 and T13. The medium sand (500-250 μm) content is at a maximum at the Ash and there is an increase in this fraction above sample T21. Although the coarser sand fractions are only a minor component they are considered significant because they reflect important trends in the mineralogy. Further, Hudson and Fife (1940) also demonstrated a change in the coarse sand fraction at approximately 45 cm depth.

OPTICAL MINERALOGY

The mafic content of the samples is low, so to improve the quality of the data the various sand fractions were split into magnetic and non-magnetic fractions. The mineral proportions were determined on both grain mounts and thin sections prepared from these fractions, but grain mounts of only whole samples were studied for the coarse silt (63 - 20 µm). The mineral proportions are recorded in appendix 5. Minerals or mineral groupings showing repeatable and/or systematic trends are plotted against depth (sample number). Although variations in trends within a particular fraction seem significant they can be biased by variations in the proportions of that fraction in the total sample (e.g. hornblende dominating a magnetic fraction is insignificant, where the magnetic fraction is a very minor amount of the whole sample). To obviate this, data are usually presented as proportions of the total sample but some data are presented as a proportion of the particular fraction. When plotted as a percentage of the total sample variations may seem small, but they are highly significant because they are based on a much wider data base than is apparent. Absolute proportions (percent of total sample) of minerals or mineral associations of demonstrably volcanic origin are used to identify possible tephric additions to the loess, while variations in the loess are investigated using the relative proportions (percent of fraction) of non-volcanogenic minerals. Although the sand content of the samples is low it is important as much of the volcanic material is in this fraction.

FINE SAND FRACTION

Non-Magnetic Fraction: In this fraction the volcanic plagioclase is above background levels in samples T9-T10 and T13 while there are significant peaks at samples T5 and T22-T25 (Fig. 4.3). Volcanic lithics (monomineralic aggregates of plagioclase) increase at the level of the Aokautere Ash (sample T3) and again in samples T10, T13 and in the top 50 cm with maxima at samples T22 and T25 (Fig. 4.3). The glassy material has been subdivided into shards and pumice in figure 4.3. The Aokautere Ash (with approximately 9% of the whole sample being glass in this fraction) dominates and the influence of the ash continues for at least 40 cm (up to sample T8) and perhaps 90 cm (up to sample T12) above the visible top of the ash. The sample immediately underlying the ash (sample T2) is also influenced. Above the Aokautere Ash there are significant increases in total glass content at sample 14 and in the top 50 cm, particularly samples T22 and T25. There is also a marked change in the morphology of the glasses at 50 cm. Below this level shards dominate, although in the Aokautere Ash shards and pumice are approximately equal, while in the top of the profile pumice dominates.

Excluding the influence of the Aokautere Ash, minerals of a sedimentary origin range from 75% in the Cxg to 55% in the top 50 cm. There is a significant and systematic increase in the proportion of sedimentary lithics (quartz-feldspar greywacke and illite greywacke) with depth (Fig. 4.4). Also, although there is a problem with obtaining representative data for the micas, the data in appendix 5 indicate a reduction in mica content in the top 40-50 cm.

Magnetic Fraction: The magnetic fraction of the fine sand varies between 4% and 39% (Fig. 4.6). Generally a high magnetic content reflects a higher proportion of grains from volcanic sources. The pyroxene and hornblende content increase at the Aokautere Ash and at

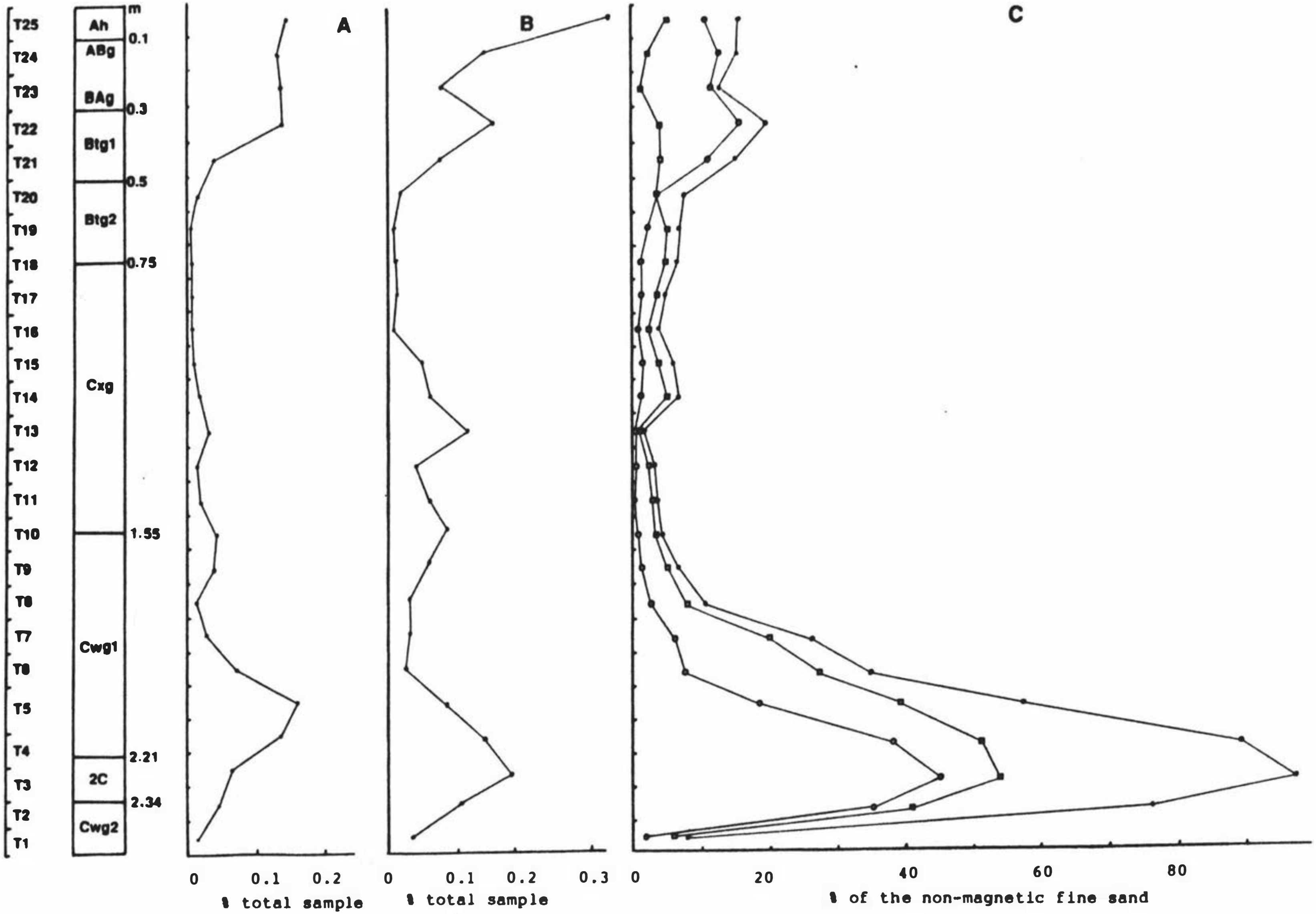

Figure 4.3: Tokomaru soil - Abundance of volcanic plagioclase (A), plagioclase volcanic lithic (B), and glass (C) in the non-magnetic fraction of the fine sands. In C the total glass (•) has been subdivided into pumiceous (o) and non-pumiceous (□) fractions.

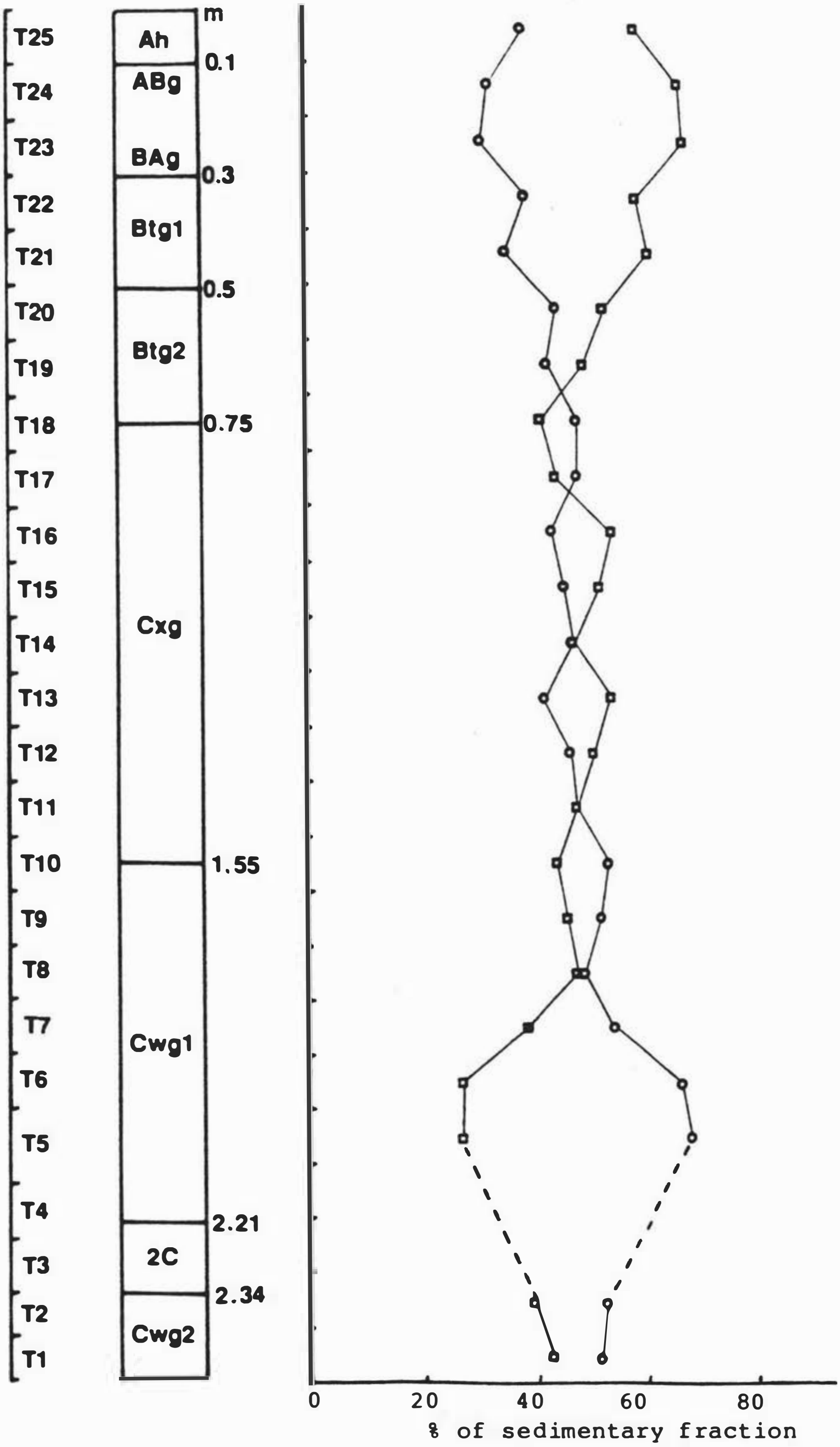

Figure 4.4: Distribution of the illite greywacke lithic (o) and quartz + sedimentary plagioclase (□) as a proportion of the sedimentary fraction in the non-magnetic fraction of the fine sand in the Tokomaru soil.

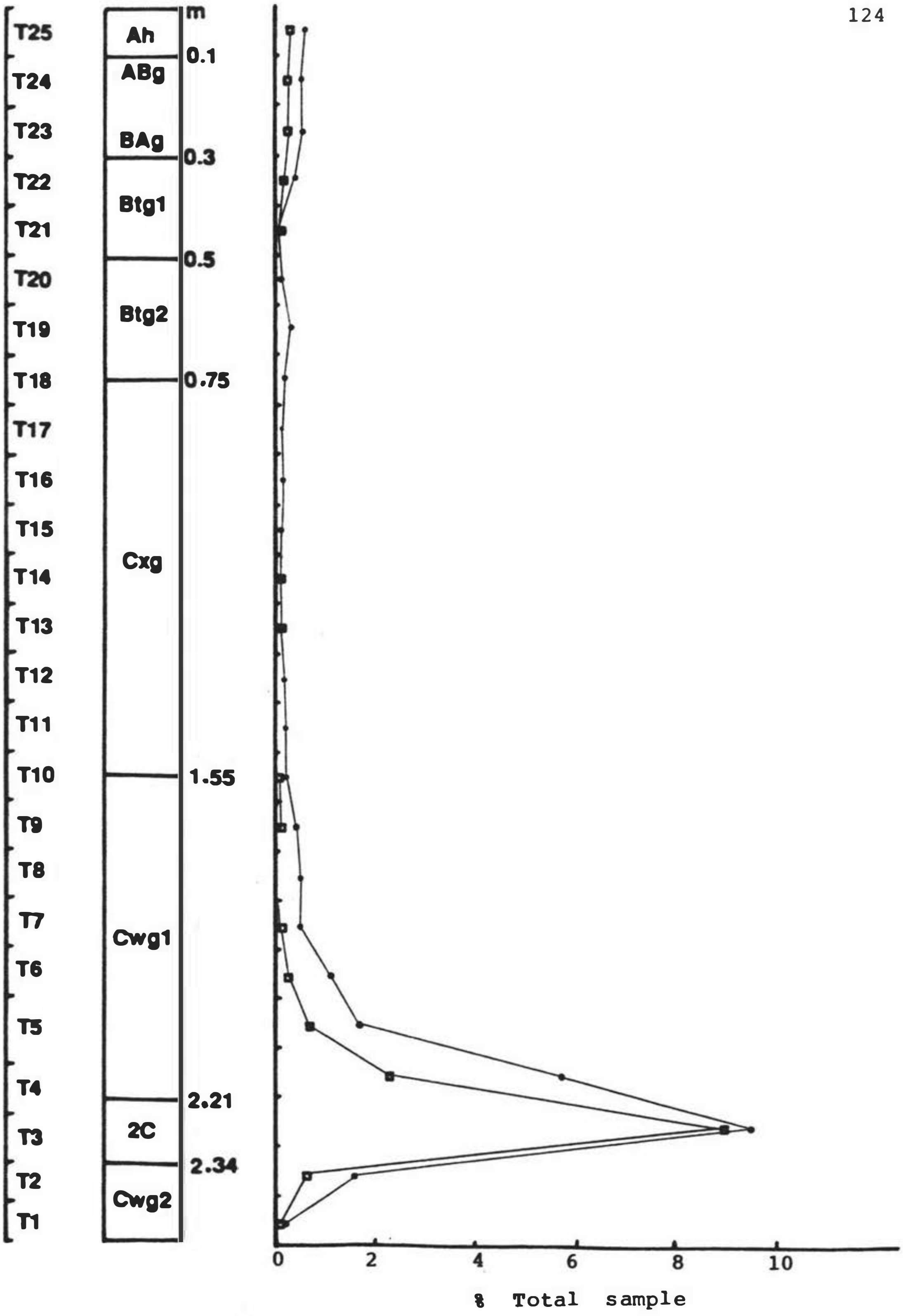

Figure 4.5: Variation in the total volcanic component of the non-magnetic very fine sand (•) and fine sand (□) fractions of the Tokomaru soil.

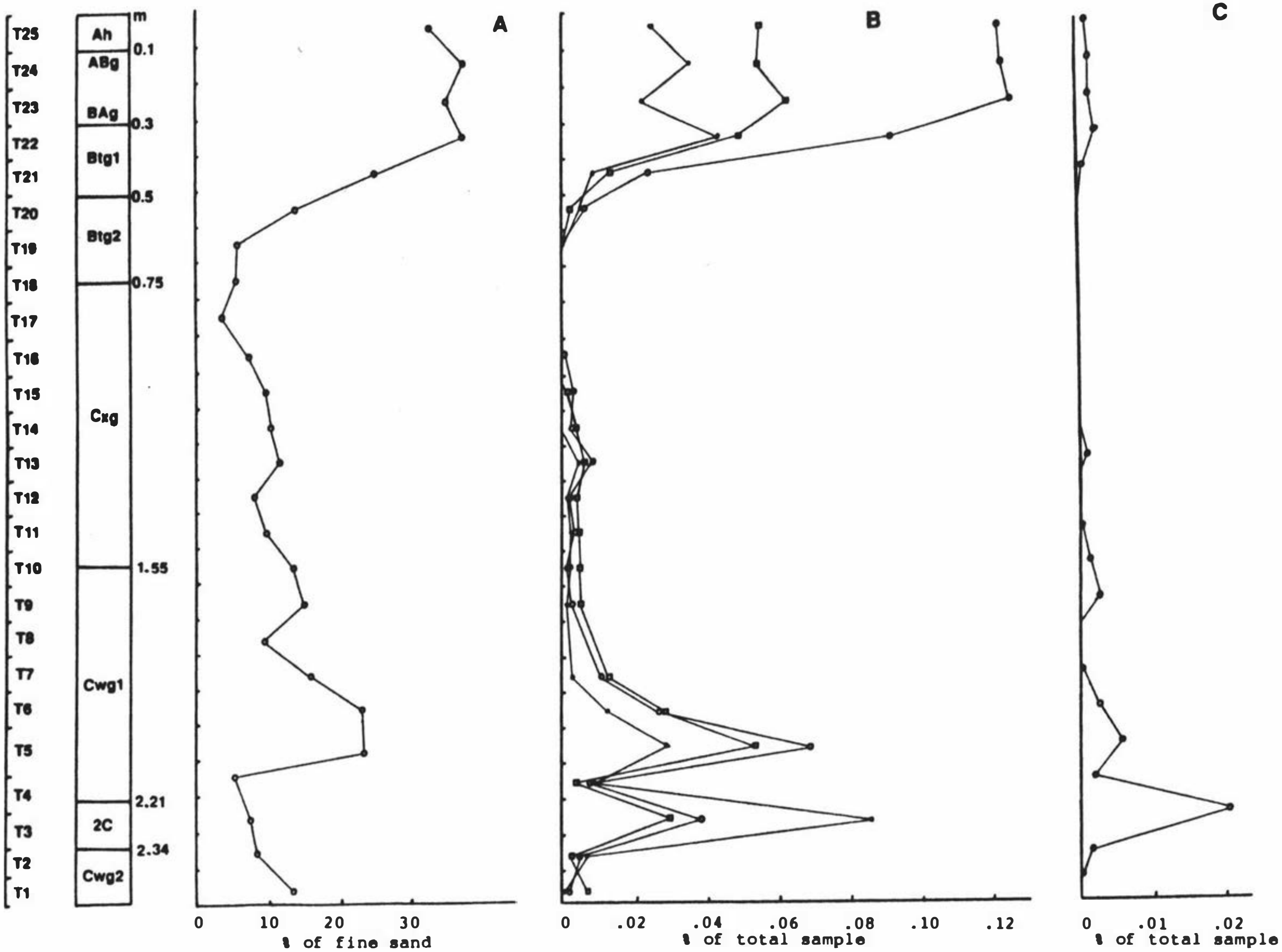

Figure 4.6: Distribution of mineral phases in the magnetic fraction of the fine sand of the Tokomaru soil. A - magnetic fraction ; B - hornblende (□), orthopyroxene (·), clinopyroxene (o), and C - volcanic plagioclase.

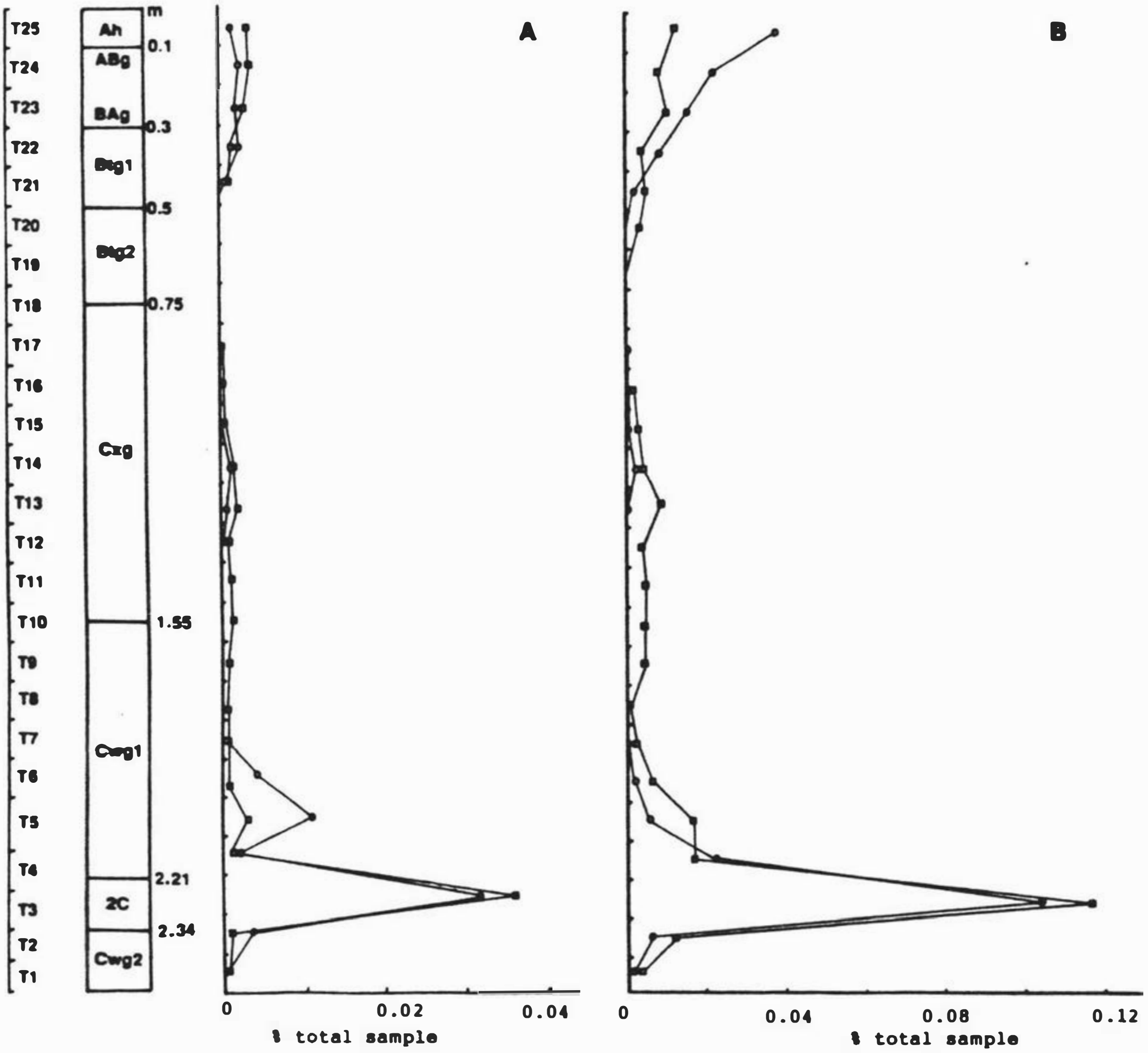

Figure 4.7: Tokomaru soil - Further abundance of volcanic components in the magnetic fraction of the fine sand. A - opaques (o), plagioclase volcanic lithic (□); B - obsidian (o) and plagioclase-opaque volcanic lithic (□).

samples T5, T13-T14 and T21-T25 (Fig. 4.6). The relative proportions of the minerals also changes. At the Aokautere Ash orthopyroxene dominates with less clinopyroxene and hornblende lowest. In contrast clinopyroxene dominates samples T5 and T21-T25 and orthopyroxene is lowest. At sample T13 the clinopyroxene dominates but at sample T14 both hornblende and clinopyroxene diminish while orthopyroxene increases slightly. The distribution of opaques (mainly titanomagnetite and ilmenite) is highly variable with peaks at samples T3 and T5, a high opaque content in T22-T25 and a broad zone of higher opaque content for samples T12 to T14. Volcanic plagioclase (drawn into the magnetic fraction because of magnetic inclusions) shows a marked increase at the top of the profile and at samples T3, T5 and T9 and a slight increase at sample T13. The distribution of obsidian (Fig. 4.7) increases at samples T3, T14 and T21-T25 (particularly T25). Data for two varieties of volcanic lithic fragments (monomineralic plagioclase and plagioclase + opaque varieties) are documented in figure 4.7. The plagioclase volcanic lithics contribute to samples T3 and T5 and there are minor additions to broad zones encompassing samples T10-T14 and T20-T25. The plagioclase + opaque volcanic lithic is highlighted in samples T3-T5, T13 and T23-T25. Figure 4.8 indicates that other than the Aokautere Ash the magnetic fine sand fraction contributes approximately 0.25% volcanic material to a total sample.

Trends within the sedimentary fraction are difficult to identify because at the level of the Aokautere Ash and in the top 50 cm the sedimentary data set is too small. There is a general trend of decreasing micas, epidote greywacke lithics and chlorite greywacke lithics towards the top of the profile (see appendix 5).

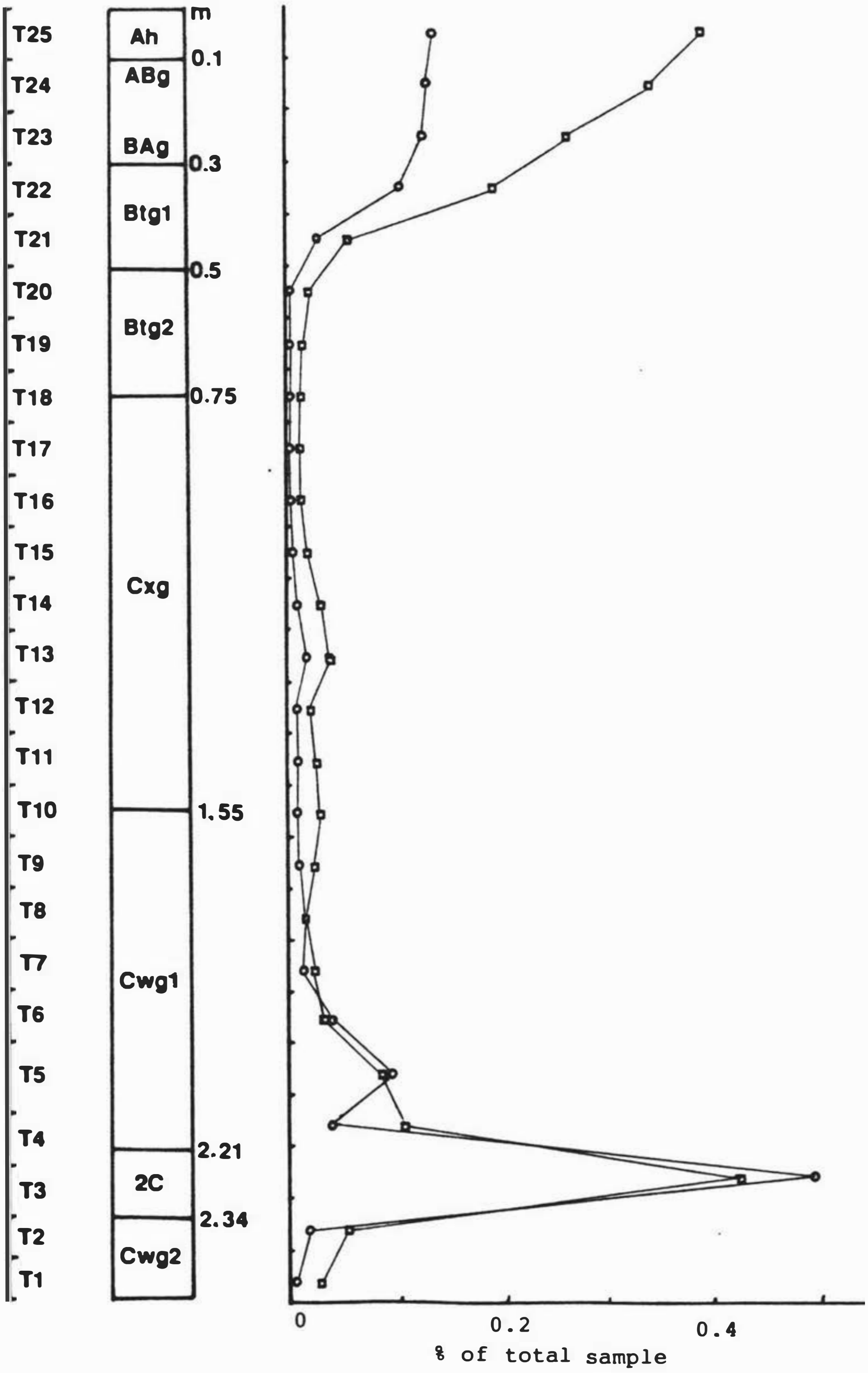

Figure 4.8: Abundances of the total volcanogenic component in the magnetic fractions of the fine (o) and very fine (□) sands in the Tokomaru soil.

VERY FINE SAND FRACTION

Both grain mounts of the whole fraction and thin sections of the magnetic and non-magnetic fractions were used to investigate trends in the very fine sands.

Non-magnetic fraction: Except for the influence of the Aokautere Ash, minerals with a volcanic association are minor (*c*. 5% of the fraction rising to *c*. 18% in the top 40 cm) and consist of glass and volcanic plagioclase. At the level of the Aokautere Ash glass dominates this fraction and constitutes 9% of the total sample (Fig. 4.9) but for the remainder of the profile glass represents *c*. 0.4% of the total sample and the sum of the volcanogenic material is *c*. 0.5% of the sample. The volcanic plagioclase, although only a trace constituent, indicates volcanic additions to samples T3, T5 and T22-T25 (Fig. 4.9).

In the materials of a sedimentary origin there is a gradual increase in the proportion of illite greywacke lithics and a decline in the proportion of quartz with depth (Fig. 4.9).

Magnetic Fraction: Unlike the fine sand the magnetic fraction of the very fine sand is a relatively constant component at approximately 3%, rising to 10% for samples T21 to T25. The distributions of the pyroxenes and hornblende (Fig. 4.10) are similar to those in the fine sand with significant increases in samples T3, T5, and T21 to T25. A change at samples T13-T14 is also evident but additionally there is a significant increase in hornblende content in samples T9 and T10. Orthopyroxene dominates the Aokautere Ash but its contribution to the very fine sand has been halved compared with the fine sand and while hornblende contributes similar amounts to both size fractions the clinopyroxene content of the very fine sand is greatly reduced. At sample T5 hornblende now dominates (although reduced) and the

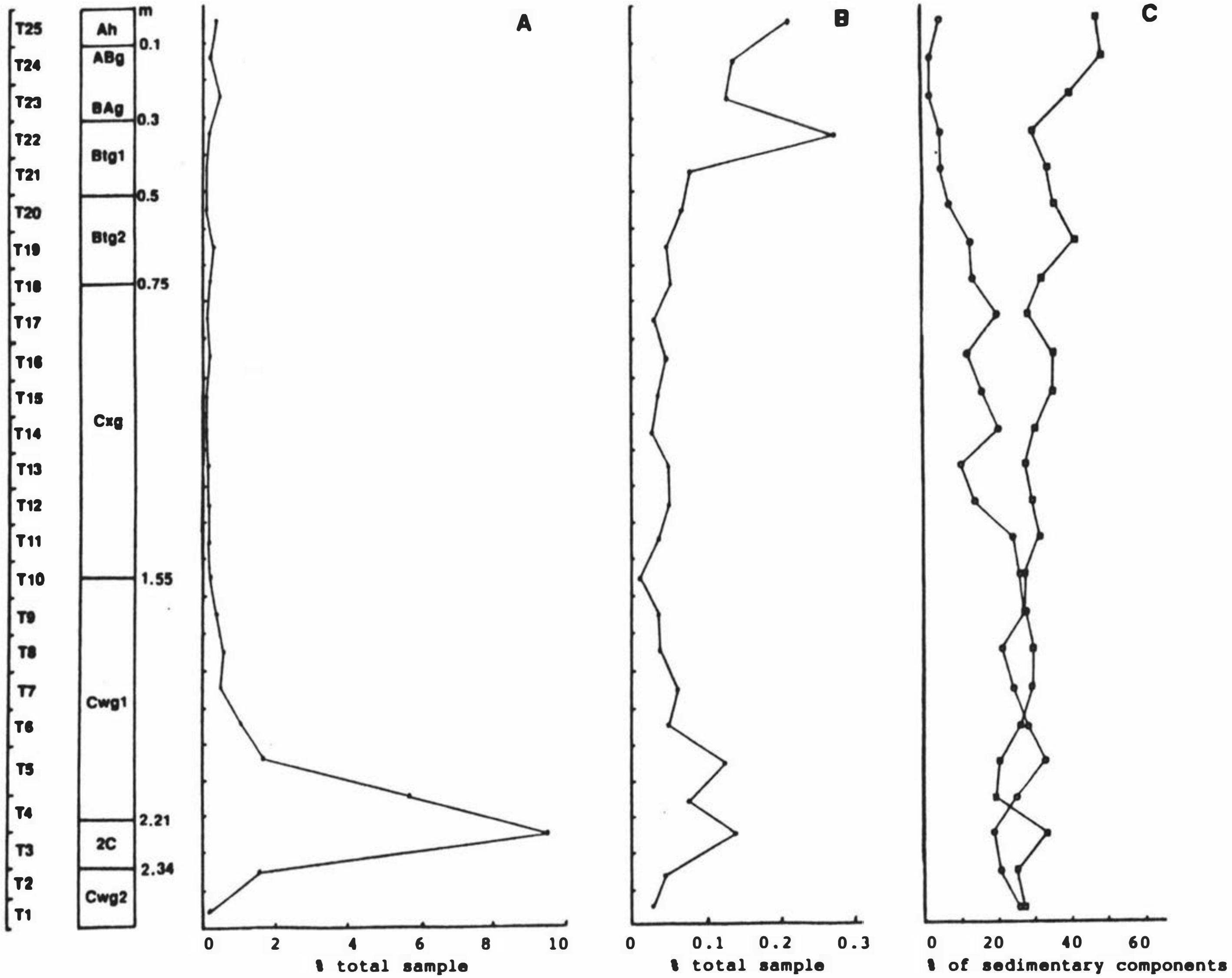

Figure 4.9: Tokomaru soil - Mineral distribution in the non-magnetic fraction of the very fine sand. A - glass; B - volcanic plagioclase; C - proportion of illite-greywacke lithic (o) and quartz + sedimentary plagioclase (▫) in the sedimentary component.

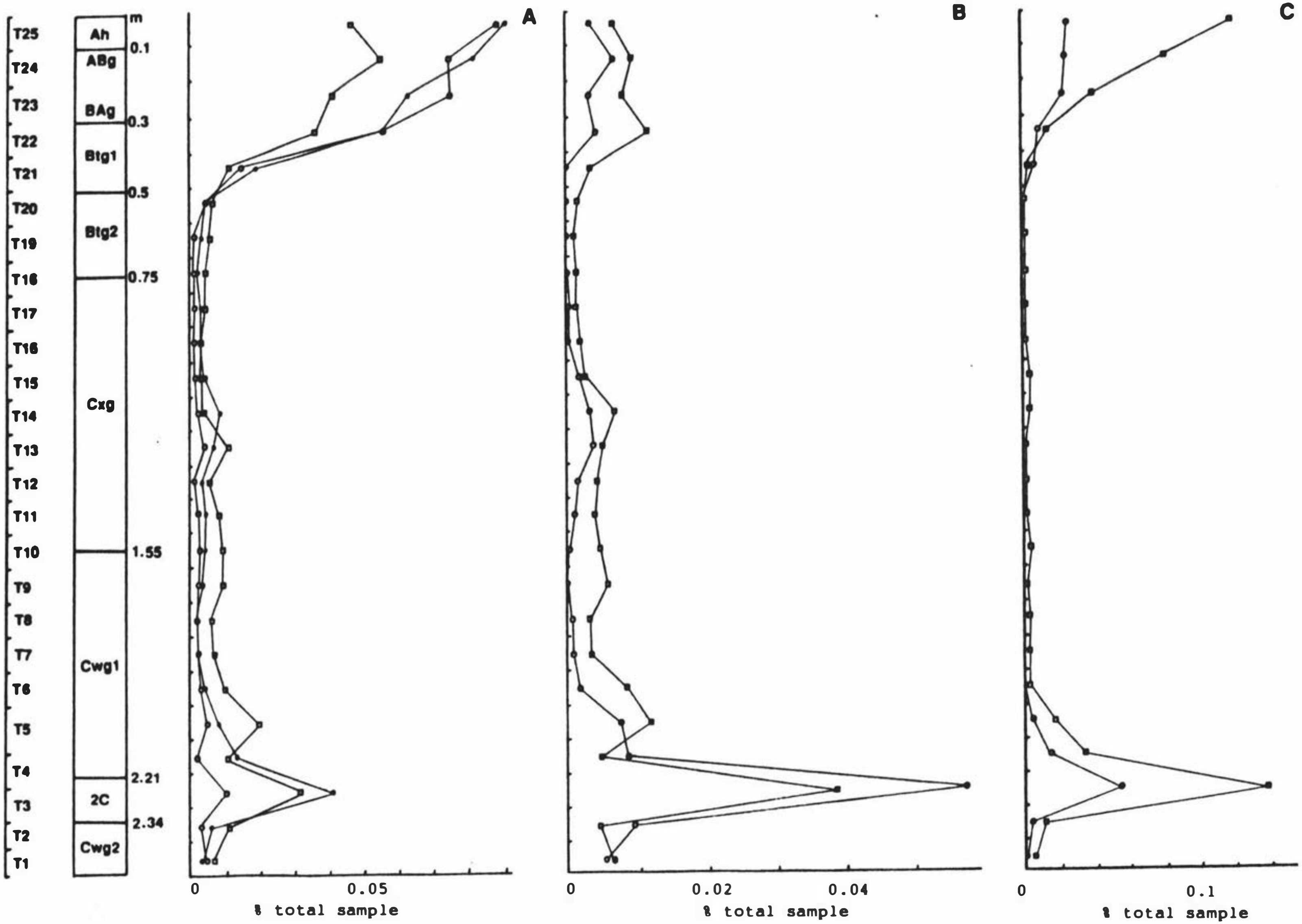

Figure 4.10: Abundances of minerals in the magnetic fraction of the very fine sand in the Tokomaru silt loam. A - hornblende (□), orthopyroxene (·), clinopyroxene (o); B - plagioclase-opaque volcanic lithic (o), opaques (□); C - glass (o), obsidian (□).

pyroxenes are greatly reduced. Hornblende dominates sample T13 but, as in the fine sand, orthopyroxene dominates sample T14. In the top 50 cm the amount of orthopyroxene has increased and the clinopyroxene decreased compared with the fine sand and they are co-dominant in the very fine sand. The hornblende content of both fractions is similar. The opaques trend (Fig. 4.10) indicates increases at samples T3, T5, T9, T14 and T22-T25 which excepting for T9 is similar to the fine sand. The glass and obsidian contents (both are microlitic varieties) have increased values for samples T3 and T22-T25 (Fig. 4.10). The major volcanic lithic present is a plagioclase + opaque variety and although it shows a similar distribution to that in the fine sand, with peaks at T3, T5 (a shoulder on T3), T13 and T22-T25 (Fig. 4.10) it contributes only half that of the fine sand. The total volcanic component (Fig. 4.5) for the magnetic fraction of both the fine sand and very fine sand fractions are similar.

The distribution of the sedimentary components is complex. One striking feature is a drop in the biotite+chlorite, and chlorite greywacke lithic content in the top four samples (T22-T25), see appendix 5.

Very Fine Sand Grain Mounts: The glass content of this fraction reaches *c*. 9% of the whole sample at the Aokautere Ash and then declines gradually reaching an average value of 0.1 - 0.2% for most of the profile (Fig. 4.11). There is significant glass mixed with loess for at least 40 cm (to sample T8) and perhaps 90 cm (sample T12) above the visible top of the ash, if the broad rise in glass content at samples T9-T10 is related to the Aokautere Ash. As in the fine sand fraction there is a consistent pattern in the morphology of the glass with shards being greater than, or co-dominant with pumice at the base of the section while pumice dominates in the top 40 cm (Appendix 5).

The amounts of other volcanic minerals are too low to warrant individual plotting, however it is noticeable (see appendix 5) that the sum of hornblende + pyroxenes and the volcanic plagioclase are both higher in the top 50 cm of the profile.

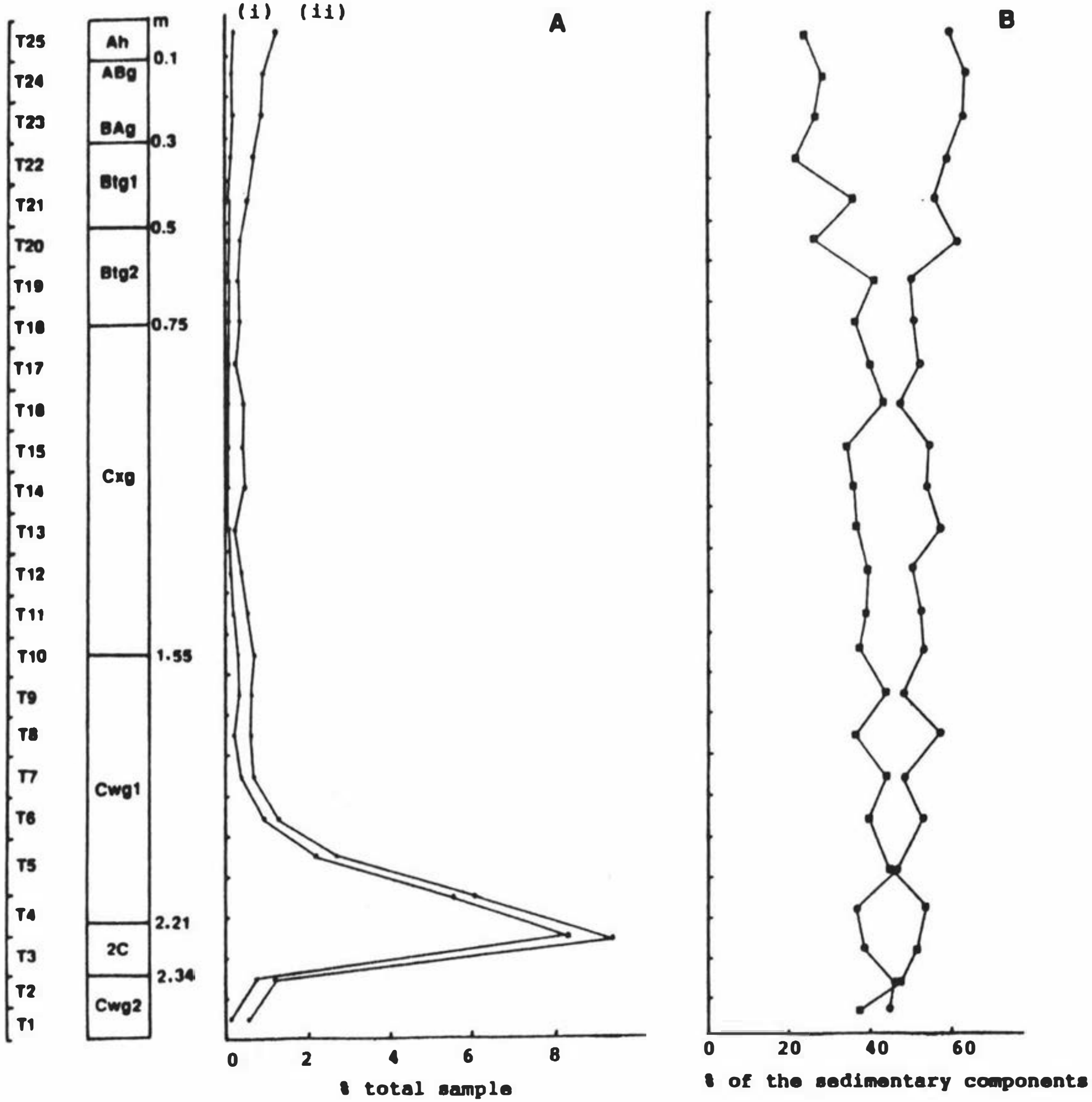

Figure 4.11: Tokomaru soil - Mineralogical variations within the very fine sand as determined on grain counts. A - (i) glass, (ii) sum of the volcanic components; B - greywacke (□), quartz + feldspar (o).

Figure 4.11 charts the variation of the sum of the volcanic components and demonstrates that this fraction normally contributes between 0.5 and 1% to the total sample. At the level of the Aokautere Ash this contribution reaches over 9%.

Grains with a demonstrably sedimentary origin form between 70 and 90% of this fraction (reducing to 15% at the Aokautere Ash) and there are systematic trends within this sedimentary grouping. The proportion of epidote greywacke and mica greywacke lithics (plotted as greywacke lithics), increase with depth and there is a corresponding decrease in the proportion of quartz + sedimentary feldspar (Fig. 4.11). Also, muscovite and biotite/chlorite are reduced in the top 40 cm.

COARSE SILT

The coarse silt is the modal interval for the Tokomaru silt loam so mineral trends in this fraction have significant influence. Figure 4.12 plots the proportion of minerals which are from volcanic and sedimentary provenances together with various plagioclase types whose sources are equivocal. The fraction is dominated by sedimentary material and even at the Aokautere Ash c. 45% of the coarse silts (c. 15% of the total sample) are from a sedimentary source. Such material must have been translocated since the ash was deposited. The glassy material of the Aokautere Ash provides *c.* 18% of the total sample (Fig. 4.12) and glass content gradually decreases to sample T8. The glass content is constant between samples T10 and T21 with slightly higher values (up to 1.4% of whole sample) between samples T22 - T25. The total volcanic component (glasses + hornblende + pyroxenes + volcanic plagioclase + high R.I. plagioclase + opaques + obsidians + volcanic lithics) shown in the same diagram increases gradually from approximately sample T16 and contributes 7 - 10% towards the top of the profile. Although the amounts of individual components are low there is: (1) a slight increase in hornblende + pyroxenes in the top

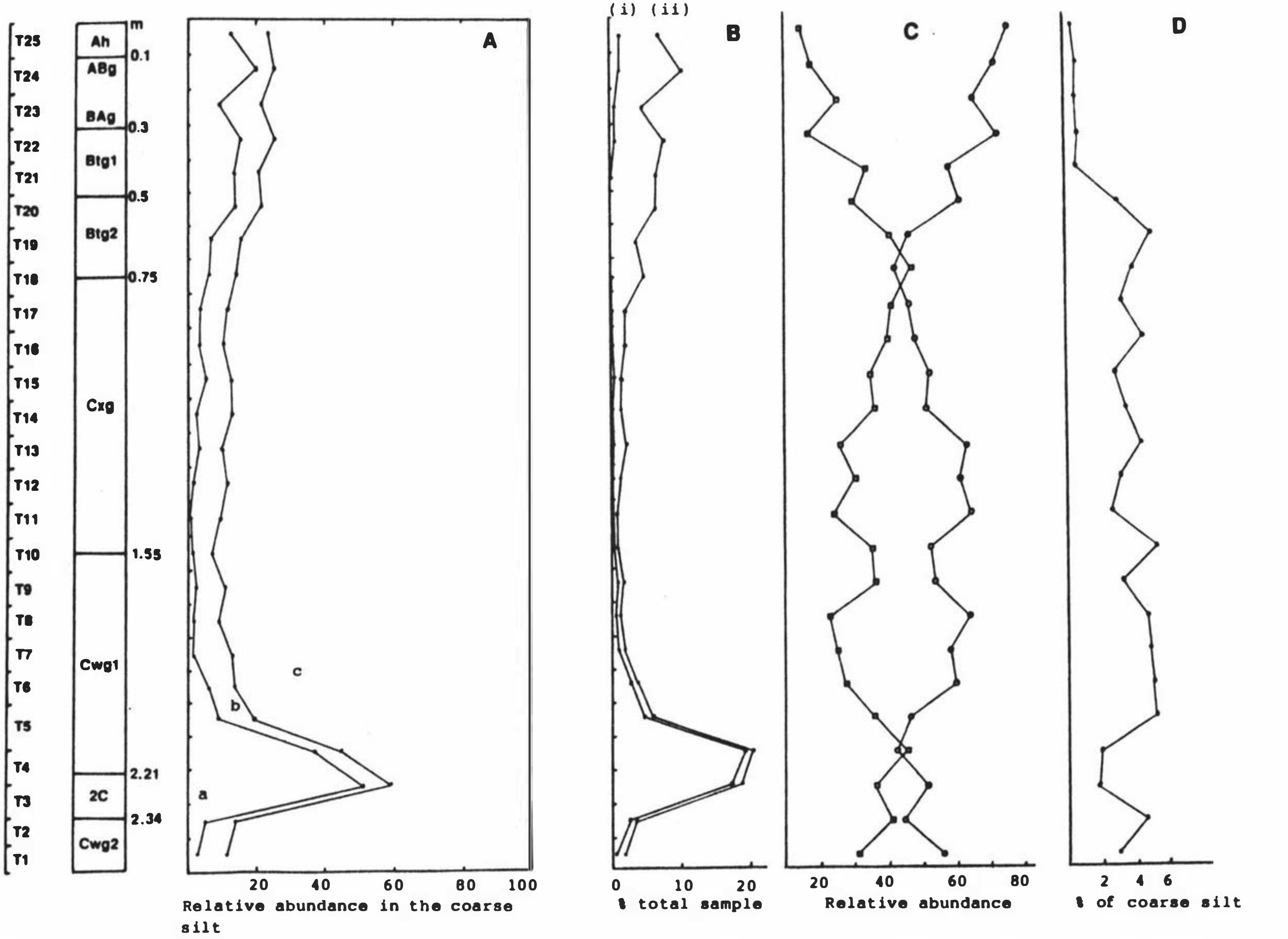

Figure 4.12: Variation in the mineralogy of the coarse silt of the Tokomaru soil. A - Relative amounts of glass (area a), sum of volcanogenic component (area b) and sum of the sedimentary components (area c); B - Absolute abundance of glass (i) and total volcanic component (ii); C - Relative abundance of lithics (□) and quartz + plagioclase (o) in the sedimentary component; D - Distribution of micas within the coarse silt.

50 cm, (2) an increase in the volcanic plagioclase at samples T5-T6 and T19-T25, and (3) an increase in the high R.I. plagioclase in the top half of the profile (appendix 5).

Trends in the sedimentary components are similar to those identified in the coarser fractions. There is a reduction in the sedimentary lithic component and increase in the quartz + sedimentary plagioclase towards the top (Fig. 4.12). The mineral data in indicate a significant reduction in mica in the top 50 cm.

MINERAL CHEMISTRY

During the optical investigation in the present study several mineralogical components were identified that were consistent with derivation from a volcanogenic source (such as glass selvedges and inclusions, euhedral crystal outlines). If the source of this material can be identified then time planes are provided which enable the dating of soil parent materials and calculation of soil accumulation rates. The potential sources for these volcanic components are eruptions from Mt. Egmont volcano or from the Taupo Volcanic Zone. In the latter source this would include rhyolitic tephras from the Taupo and Okataina centres and andesitic tephras from the Tongariro centre (Fig. 4.1). Although these centres have different mineralogies (Table 4.1) it is not possible to identify unequivocally these different sources on mineralogy alone. The chemistries of the sources vary from basalt to rhyolite and they are situated in different tectonic environments so the mineral chemistry from each centre might be expected to be different.

Mineral chemistries have been used by, among others, Howarth and Rankin (1975), Westgate and Fulton (1975), Kohn (1970) and Froggatt (1983) to identify igneous sources. Initial techniques e.g. Kohn and Neall (1973) involved the concentration of a phase from bulk samples

Table 4.1: Summary of the mineralogy of tephra from some North Island volcanic centres.

TAUPO CENTRE --- Clear glass + sodic plagioclase + orthopyroxene + opaques(m*) + clinopyroxene(m)

OKATAINA CENTRE --- Clear glass + sodic plagioclase + orthopyroxene + hornblende ± cummingtonite ± biotite + clinopyroxene(m) + opaques(m)

TONGARIRO CENTRE --- Orthopyroxene + clinopyroxene + calcic plagioclase + opaques ± olivine ± hornblende(tr*)

EGMONT CENTRE --- Clinopyroxene + hornblende + calcic plagioclase + opaques ± orthopyroxene(m) ± biotite

* m = Minor; tr = Trace

for which both major and trace elements were analysed. Where there is possible contamination e.g. dilution of tephras in soils, mixing of tephras from various sources, or phases intimately intergrown or exsolved, then the concentration process is critical and bulk sampling techniques are unsuitable. The use of the electron microprobe obviates this problem because individual phases can be analysed. This is an advance in that small quantities of sample will suffice. However, complicating factors include: (1) only major elements can practicably be analysed and (2) variations due to chemical zoning in individual grains can be determined, so enlarging the compositional range to which any unknown is referred.

In the present study chemistries of phases from various sources were determined by electron microprobe in order to identify chemical discriminating factors (Appendix 7). Aokautere Ash (*c.* 20 ka B.P.), which is a readily identifiable marker horizon throughout the North Island occurs in the C horizon within the Tokomaru silt loam at 2.2 m depth, so potential reference tephras above the ash were sampled. Minerals were separated from pumice and lithic fragments because this reduced the potential for contamination and also because these fragments could readily be unambiguously correlated with known tephras. The chemistries of the pyroxenes, amphiboles, plagioclases, titanomagnetites and glasses were then determined with the electron microprobe and plots of element pairs (one element plotted against another) were constructed.

In a study of Eltham County, Franks (1984) showed that the post-Aokautere Ash sequence of tephras from Mt. Egmont was thickest to the southeast (i.e. towards Palmerston North). Minerals from twelve of the larger eruptions in this sector were thus sampled to attempt correlation with the tephric components in the Tokomaru silt loam. This data set was extended by the whole rock data of Neall *et al.* (1986). Reference electron microprobe mineral data from the Taupo Volcanic Zone was obtained from Howorth (1976) and Froggatt (1982) and augmented with whole rock data for basaltic to dacitic compositions from Cole (1979), Reid and Cole (1983) and Froude and Cole (1985). In an attempt to exclude possible differences in operator techniques with the microprobe analyses, minerals from the Waimihia Lapilli (Taupo centre) and Rotoma and Whakatane eruptives (Okataina centre) were analysed as reference material to best represent these centres. Major element mineral chemistry of tephras from the Tongariro centre is not available so the chemistries of the lava minerals (Hackett 1985) are used.

When it had been established that it was possible to discriminate between potential sources using mineral chemistry, minerals from the soil were analysed for comparison with these sources. The minerals and glasses in the fine sand fraction from samples that have a demonstrable volcanogenic component (samples T1, T3, T5, T6, T9, T10, T13-T16 and T21-T25) were investigated with the electron microprobe (Appendix 12).

PLAGIOCLASE: Plagioclase chemistry is usually sensitive to the composition of the magma from which it crystallises, (calcic plagioclases form in more basic magma types and sodic plagioclases form in more acidic magmas) so plagioclase composition should help differentiate sources. However it is of limited use in the present study because chemical zoning produces a very wide range in composition (An_{31} to An_{90} with typical ranges of 25% anorthite within a grain). Further, zones of corrosion parallel to crystal outlines occur within plagioclases in the soil environments as the more calcic zones are preferentially removed.

Notwithstanding these problems plagioclases associated with samples T1 and T3 (average plagioclase composition An_{44} and An_{40} respectively) have lower anorthite content than shallower samples. Average composition for sample T6 is An_{55}, sample T13 is An_{55}, sample T24 is An_{49} and sample T25 is An_{52}.

AMPHIBOLES: The amphiboles are pargasite to pargasitic hornblende in Mt. Egmont tephras and magnesio-hornblende, edenitic hornblende or edenite in the rhyolitic tephras from the central North Island. Amphiboles are absent or very rare in material from the Tongariro centre. Most major elements in the amphiboles produce a good discrimination between magma types. Potassium in particular, together with silicon, iron and titanium produce a distinction between andesites and rhyolites so Egmont sourced material can be readily identified (Figs. 4.13). It is not possible to differentiate between the Okataina and Taupo centres.

When the amphiboles from the soils are compared with the reference material (Fig. 4.13) the dominant source of amphiboles in samples above the Aokautere Ash is shown to be Mt. Egmont. There is however a significant proportion of the amphiboles in the top of the profile (e.g. T21 and T25) that have a Taupo Volcanic Zone signature. As expected the chemistry of the amphiboles in the Aokautere Ash is consistent with a Taupo Volcanic Zone source.

ORTHOPYROXENE: In eruptives from Mt. Egmont orthopyroxenes are relatively rare (Tonkin 1970; Kohn and Neall 1973; Franks 1984; Neall *et al*. 1986; Lowe 1987) and only 12 orthopyroxenes were identified in the *c*. 1000 pyroxenes investigated within the fine sand fraction of the Egmont reference data in this study. If the references cited above and the data presented here are representative of the mineralogy of the Egmont volcano then orthopyroxene is only a trace constituent in tephras from this source. It is therefore probably very rare in distal tephras. In contrast to the Egmont source orthopyroxenes are the dominant mafic mineral in rhyolites and are common in andesites from the Taupo Volcanic Zone. A detailed comparison of the orthopyroxene chemical data from the Taupo Volcanic Zone and Egmont centre (Froggatt 1982; Hackett 1985; Lowe 1987; this study) indicates that there is a limited discrimination between these two source areas. This comparison has however identified significant trends with respect to the relationship between MnO, FeO and MgO within the eruptives from the Taupo and Tongariro centres.

Most orthopyroxenes from the Taupo centre have MnO contents that trend from c. 1.9% to 1.3% as MgO increases (Fig. 4.14). This group is here referred to as high Mn orthopyroxenes. In figure 4.14 there is however another trend parallel to the high Mn orthopyroxene trend, with MnO between 0.4% and 1.3%. These are here referred to as the low Mn orthopyroxenes. The high Mn orthopyroxenes also have relatively higher FeO (En_{40}-En_{55}) and lower CaO, Al_2O_3, MgO and TiO_2

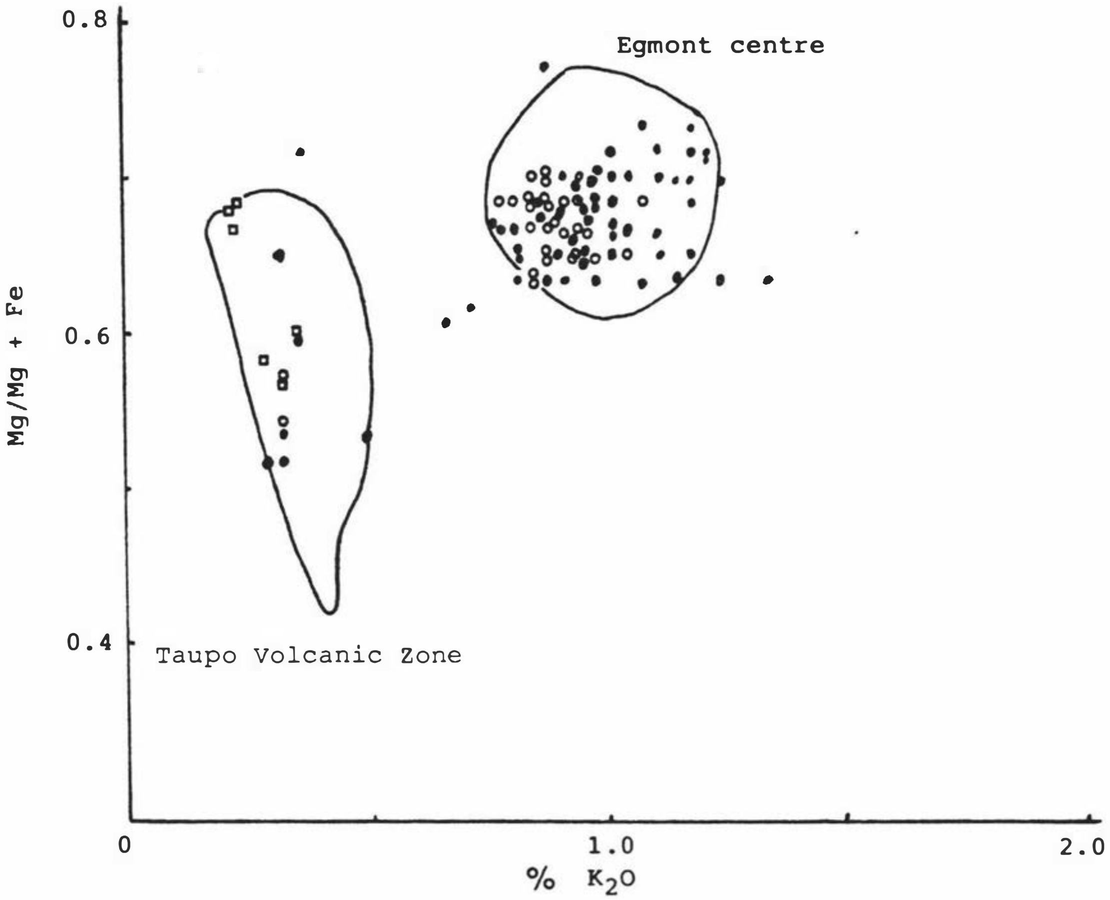

Figure 4.13: Comparison of the chemistries of the amphiboles from the Tokomaru soil with those from possible volcanic sources. Symbols - sample T3 (□); samples T1, T5, T6, T9, T13, T14 (○), and T21-T25 (·).

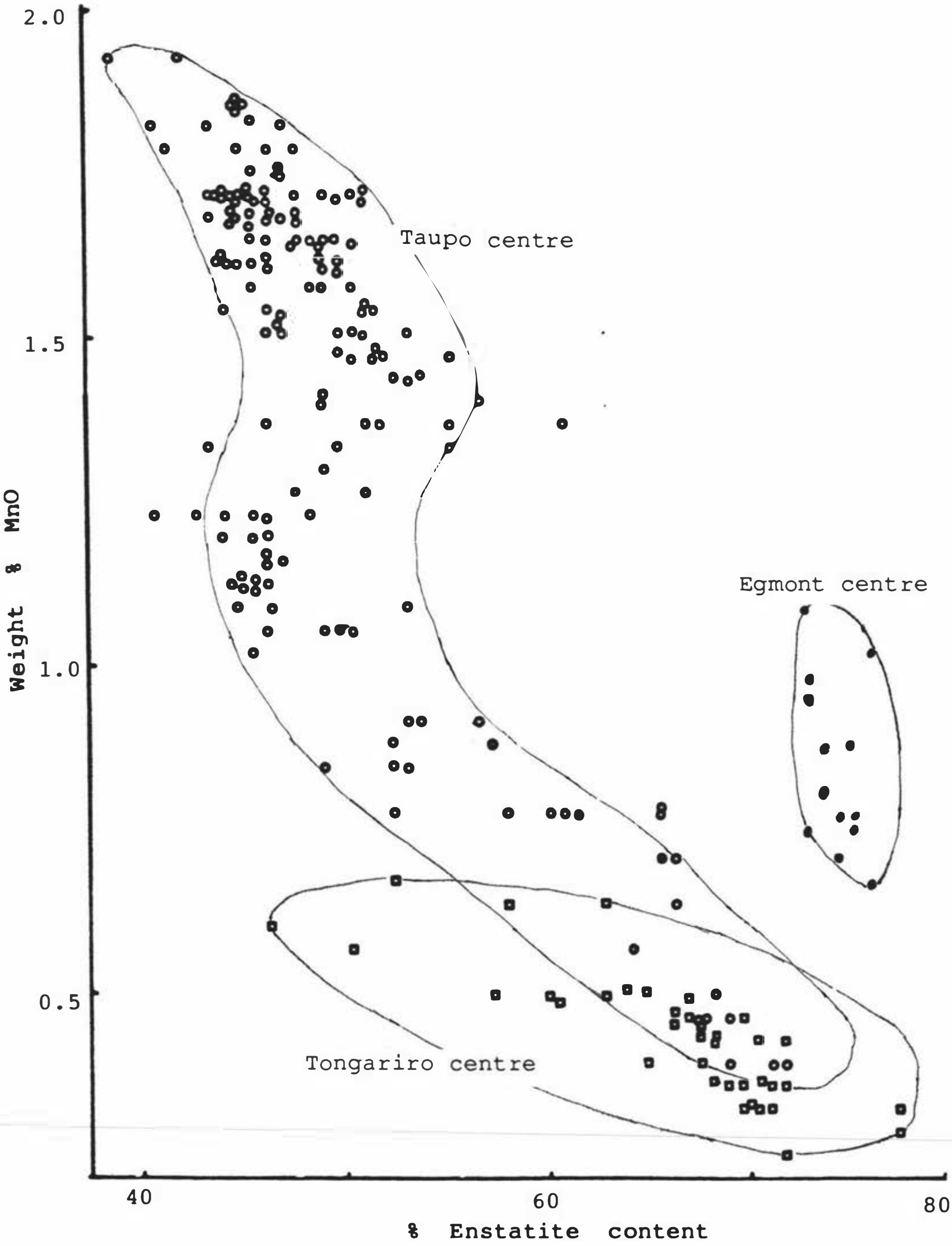

Figure 4.14: Bi-variant plot of MnO and enstatite content for orthopyroxenes from the Taupo centre (o), Tongariro centre (□) and Egmont centre (•).

compared with the low Mn orthopyroxenes. This dichotomy of MnO data is also reflected in data from the Aokautere Ash and its correlative, the Kawakawa Tephra Formation of Howorth (1976).

Froggatt and Solloway (1986) attributed the bimodal nature of the chemistry of the orthopyroxenes in some Taupo centre eruptives to andesitic contamination but the orthopyroxenes in the reference material from the present study were separated from rhyolitic pumiceous lapilli that were collected from the middle of multiple shower units. These factors combined with an association with glasses more acidic than those known from Tongariro centre andesites (Appendix 7) preclude an andesitic origin.

The orthopyroxenes with low MnO have relatively high enstatite content (En_{50}-En_{75}) and in those that have glass inclusions the glasses are commonly dacitic (Appendix 7). This chemical data suggests that the low Mn orthopyroxenes formed in equilibrium with a magma of more basic composition than that with which they were erupted. The low Mn orthopyroxenes are presently known to occur in deposits from four formations (Taupo, Hinemaiaia, and Waimihia tephra formations and the Aokautere Ash; Froggatt 1982; this study). Of the eleven major rhyolitic eruptions from the Taupo centre in the last 20 ka these four are the largest (Latter 1985; Lowe 1986). It is here suggested that whereas the smaller eruptions tap only the more evolved upper area of the magma chamber, the larger eruptions (i.e. those with the more enstatitic orthopyroxenes) are derived from deeper levels in the system. The chemistry of the orthopyroxenes and their associated glasses suggests that the magma chambers associated with the rhyolitic eruptions from the Taupo centre may be zoned.

The orthopyroxene data from the soils indicates that within the framework of the potential sources considered here the orthopyroxenes originate mainly from either the Taupo or Tongariro centres. The absence of evidence for orthopyroxenes from the Okataina centre supports results obtained from the glass chemistry which showed that glasses from Okataina are rare. The rarity of orthopyroxenes with chemical characteristics similar to those of Mt. Egmont may be a reflection of the grain size used in this investigation (fine sand) as

Kohn and Neall (1973) record orthopyroxene from Mt. Egmont smaller than this. However Tonkin (1970), Kohn and Neall (1973), Franks (1974) and Neall *et al.* (1986) support the findings of this study, i.e. pyroxenes from Egmont are dominated by augite. Most of the orthopyroxenes from the soil plot within the fields of the high Mn and low Mn orthopyroxene identified in figure 4.15. The soil orthopyroxenes which correspond to the high Mn orthopyroxenes probably originated from the Taupo centre, but the low Mn orthopyroxene field overlaps with that of the Tongariro field so in these cases it is not possible to differentiate between the two sources. In the reference data from the Taupo centre the low Mn orthopyroxene group forms a relatively small proportion of the total orthopyroxenes, whereas in the soil this group is a much greater proportion of the orthopyroxene population analysed. It is here suggested that this enrichment is due to the addition of orthopyroxenes from the Tongariro centre andesites.

CLINOPYROXENE: Clinopyroxenes are common in Egmont eruptives. Within the Taupo Volcanic Zone they are rare in the rhyolites and common in the andesites. As in Lowe (1987) it is only possible to confidently discriminate between Egmont and Tongariro centre sourced material using CaO. Minor amounts of Cr are however common in Taupo Volcanic Zone clinopyroxenes and rare in those from Egmont so Cr in clinopyroxenes probably indicates a Taupo Volcanic Zone source. Lowe (1987) showed that Tongariro sourced clinopyroxenes averaged Wo_{42} while Egmont sourced material had Wo_{45}.

In samples T1,T5, T24 and T25 the chemistry indicates that the clinopyroxenes are derived from both Mt. Egmont and Taupo Volcanic Zone (Fig. 4.16). It is not possible to distinguish between the Tongariro and Taupo centres using clinopyroxene chemistry, however clinopyroxenes are rare in rhyolitic tephras and there are too many with Taupo Volcanic Zone signatures in samples T24 and T25 for them all to be derived from the Taupo centre. It is therefore likely that some must be from Tongariro centre, possible derived from the Ngauruhoe volcano which began its present cone building phase c. 2.5 ka B.P. (Latter 1985).

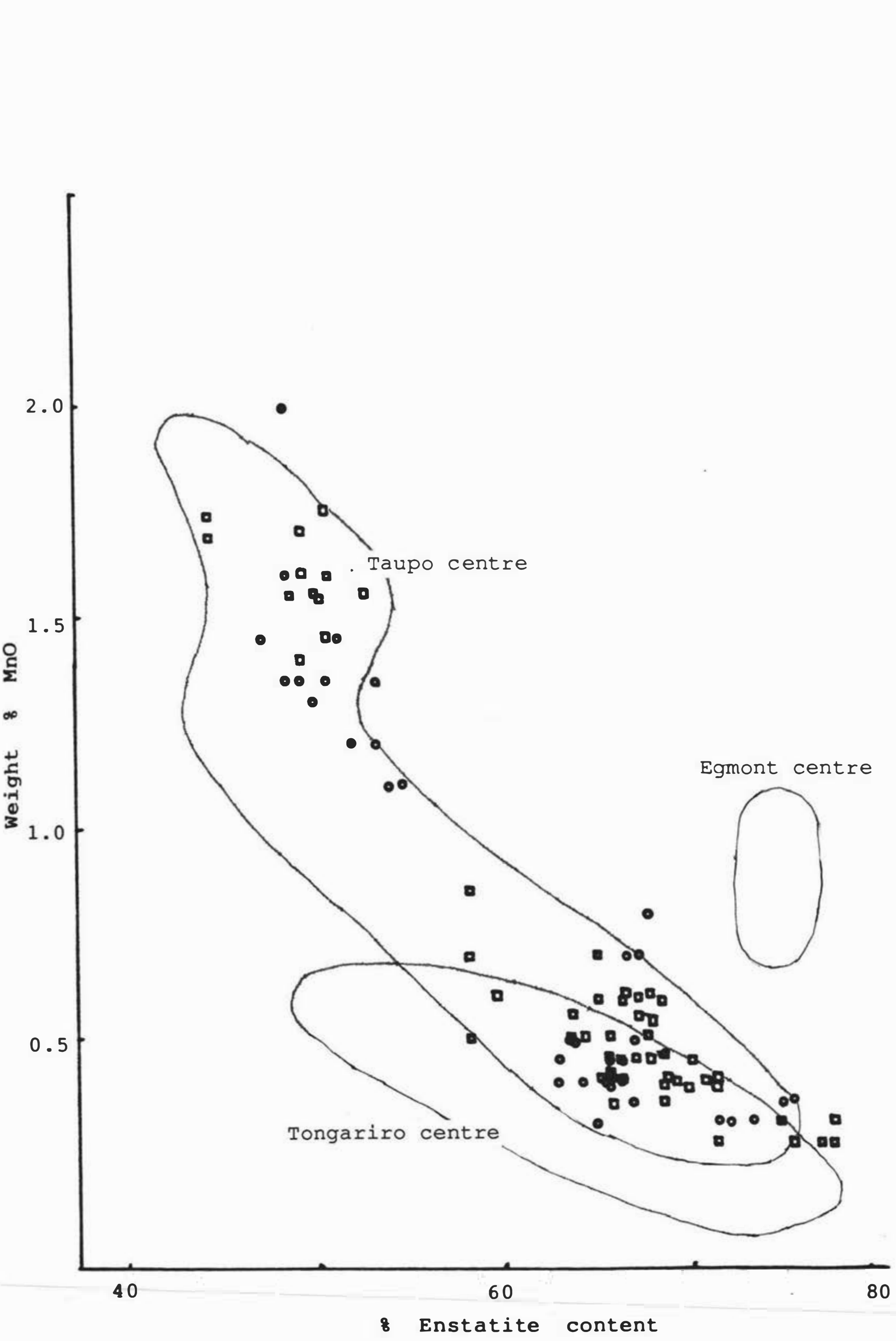

Figure 4.15: Distribution of orthopyroxene from the Tokomaru soil on an MnO - enstatite plot. Symbols T21-T25 (◘), and T1, T3, T5 (o).

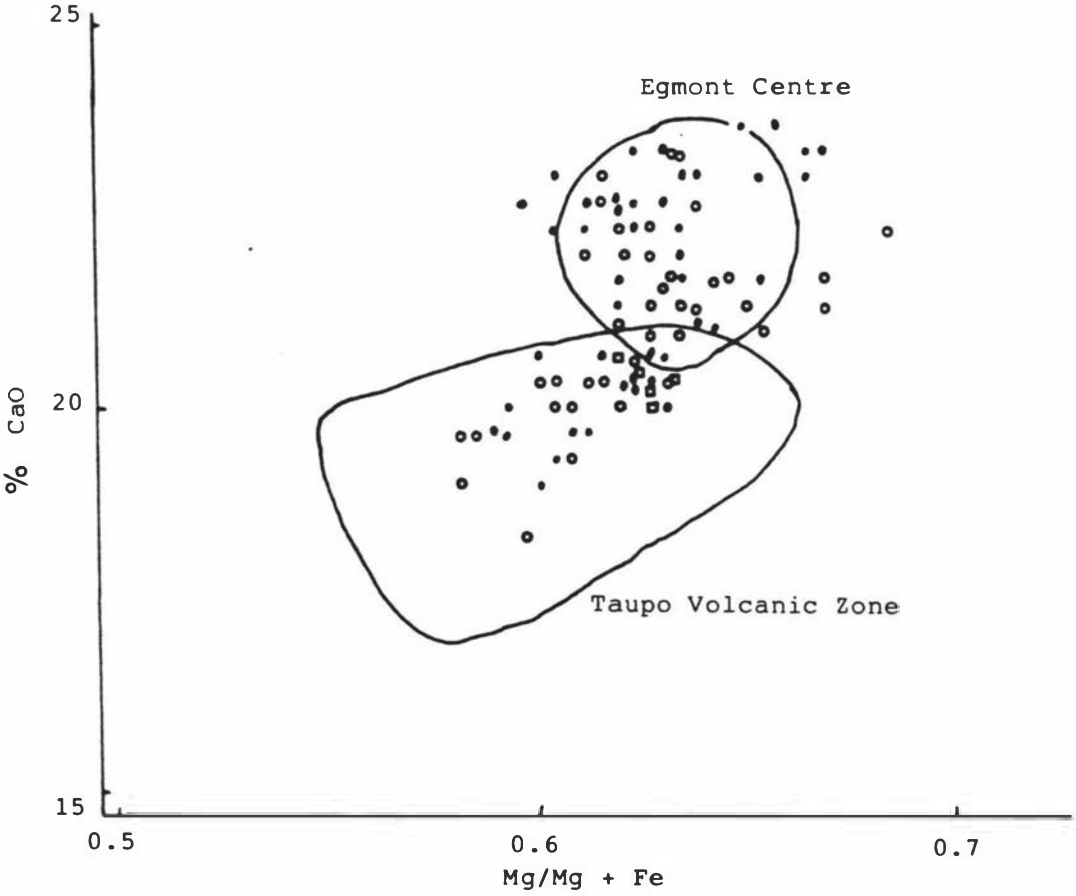

Figure 4.16: Comparison between the chemistry of the clinopyroxenes from the soil and those from possible source regions. Symbols - sample T3 (□); samples T1, T5, T6, T9, T13, T14 (o), and T21-T25 (•).

GLASSES: The Mt. Egmont volcano and the members of the Taupo Volcanic Zone occur in two different tectonic settings (Cole 1986) and have evolved along separate chemical lineages (Neall *et al*. 1986; Cole 1979; Reid and Cole 1983; Froude and Cole 1985). While XRF analyses can characterise the chemistry of whole rock samples these represent only the less to moderately evolved members of a series as the most evolved members are represented by interstitial glasses. These glasses require the microprobe for analysis. Microprobe analyses of glasses in rocks are consistent with the XRF data of whole samples from the same suite and clearly extend the trends to more highly evolved end points (Fig. 4.17). Utilising chemical data from the two environments, it can be shown that while the Taupo Volcanic Zone eruptives follow the basalt-andesite-dacite-rhyolite lineage, those from Mt. Egmont are higher in alkalis and follow a basalt-trachyandesite-trachyte-rhyolite trend (Wallace *et al*. 1986). The two trends plot in distinct fields (Fig. 4.17) so microprobe analyses of glasses should distinguish between these two sources. Recent data on the chemistry of glasses from tephras in lake sediments in Waikato (Lowe 1987) are consistent with these distinct fields. Within the Taupo Volcanic Zone there are several eruptive centres and Froggatt (1983) has demonstrated that among the rhyolites, pumiceous glasses erupted from the Okataina centre are chemically distinct from those erupted from the Taupo centre (see also Lowe 1987). Additionally, while the <10 ka eruptives from Taupo (the Holocene Taupo eruptives) are indistinguishable from each other they are chemically different to glasses of the Kawakawa Formation (i.e. Aokautere Ash) (P.W. Froggatt *pers. comm*. 1984). Within the given time frame (<20 ka) it is possible to use the chemical variations in FeO, CaO and K_2O to distinguish between rhyolitic glasses from the Okataina centre, the Holocene tephras from the Taupo centre, and the Aokautere Ash (Fig. 4.18).

The clear glass fragments in the soil have chemistries consistent with a Taupo Volcanic Zone source. In the lower third of the profile the glass composition is consistent with that of the Aokautere Ash and there is a significant Aokautere Ash component up to

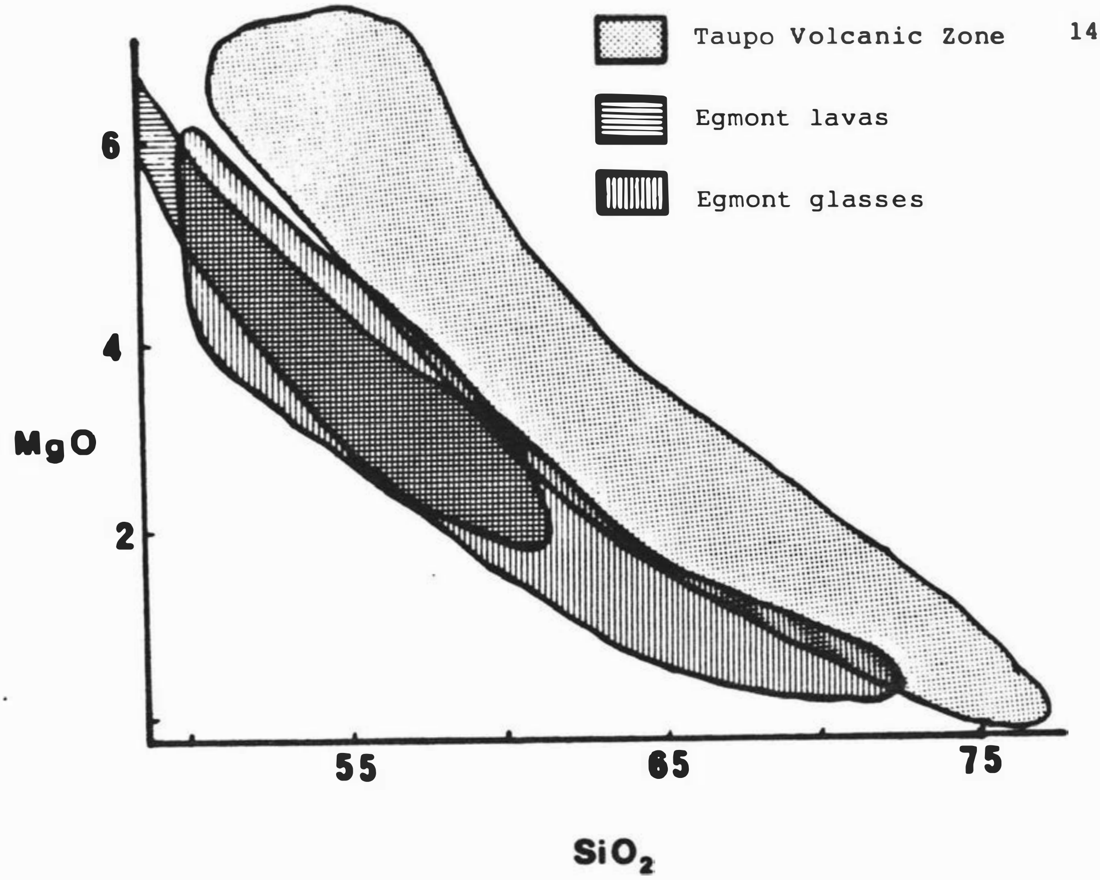

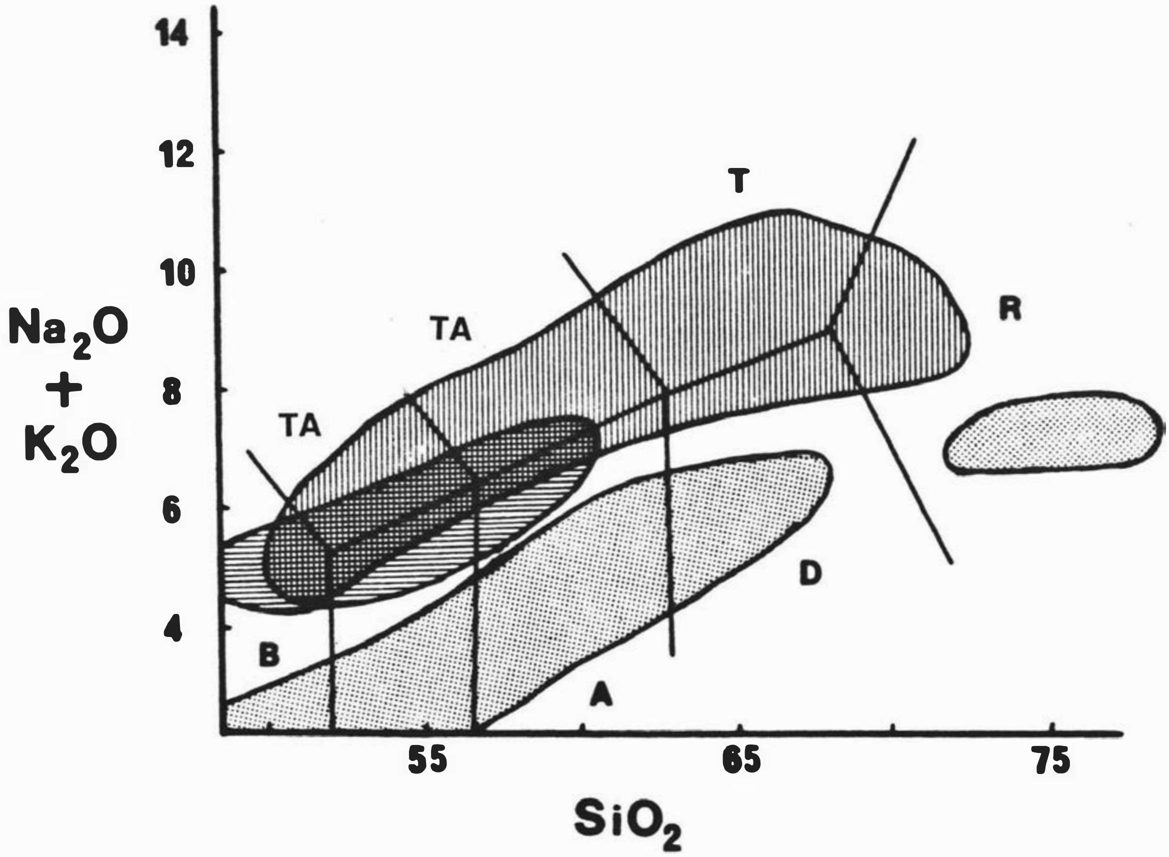

Figure 4.17: Harker diagrams demonstrating the discrete nature of the chemical trends between Egmont centre and the Taupo Volcanic Zone. B - basalt, TA - trachyandesite, T - trachyte, R - rhyolite, D - dacite, A - andesite.

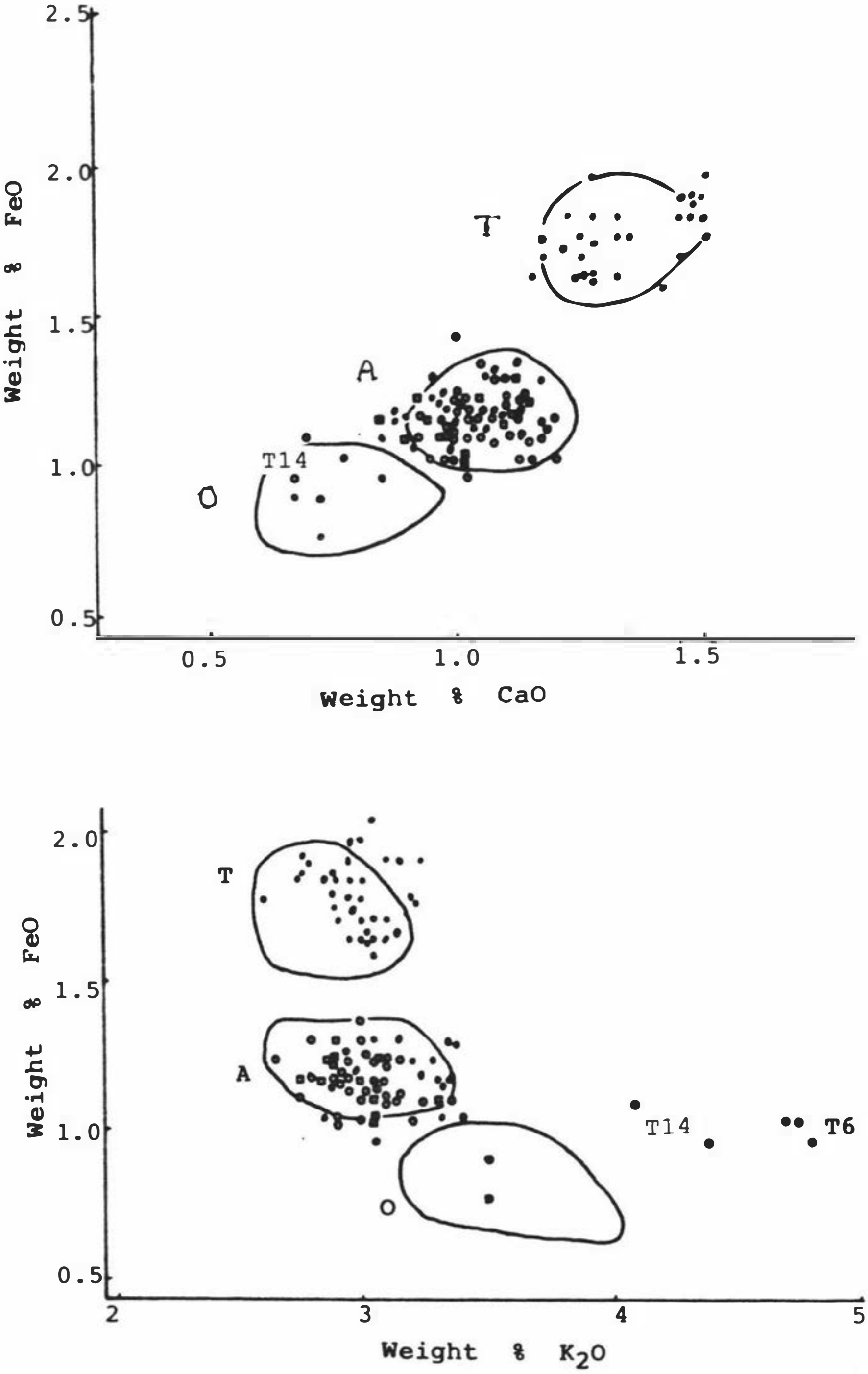

Figure 4.18: Chemical variation diagrams demonstrating the similarity between the compositions of glasses in the Tokomaru soil and possible sources. Symbols - sample T3 (□); samples T1, T5, T6, T9, T13, T14 (o), and T21-T25 (•). O = field of glasses from the Okataina centre; T = field of glasses for Holocene ashes from the Taupo centre; A - pre-Holocene ashes from Taupo centre. N.B. - Other mineralogic evidence indicates that T6 has had a dusting from an andesitic source.

sample T10. Three data points from T6 are consistent with an Egmont source. A general increase in glass content towards the top of the profile begins at sample T21. The glass in sample T21 has a Holocene Taupo eruptive signature and although the data set is small there is no indication of glass from the Okataina centre. Above sample T21 the glasses have multiple sources with chemical signatures consistent with derivation from Holocene Taupo eruptives, the Aokautere Ash and perhaps the Okataina centre (sample T25). The amount of glass above sample T21 with Aokautere Ash chemistry is significant and may represent the reactivation of Aokautere Ash glass by erosion in the landscape.

DISSOLUTION TECHNIQUES

Optical methods are not appropriate to investigate mineralogical trends in the finer fractions and although the mineralogy of the HCl and H_2SiF_6 soluble fractions cannot be precisely identified, variations in amounts of this fraction are informative. The pretreatment of the samples removes most amorphous materials so the HCl soluble portion is thought to be dominated by micas + mafic minerals with the H_2SiF_6 soluble fraction dominated by feldspars + glass. The unreactive residue is quartz except for four samples in the 5-2 µm fraction where cristobalite occurs (sample 3 has 4% and samples T24 and T25 have approximately 1% cristobalite).

Coarse Silt: The HCl soluble fraction (Fig. 4.19) decreases at samples T3 and T8 and in the top 70 cm (but particularly the top 50 cm). There may also be a tendency to decrease slightly up the profile. The H_2SiF_6 soluble fraction decreases slightly in T3 and T8 and excepting sample T25 there is a reduction towards the top of the profile. Quartz distribution emphasises the Aokautere Ash and tends to be reduced in the top 90 cm.

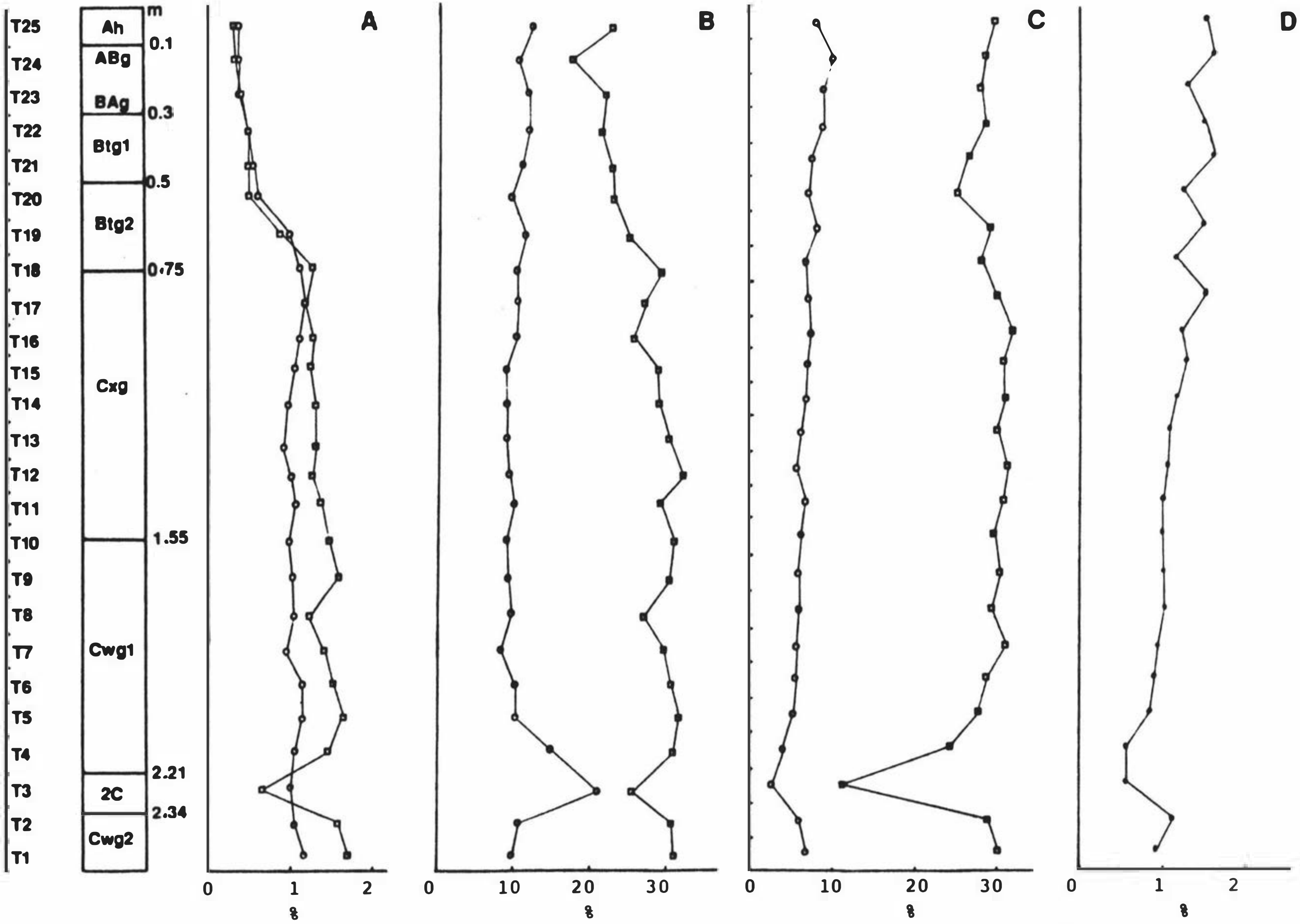

Figure 4.19: Proportion of the Tokomaru soil removed during the acid dissolution sequence. A - HCl soluble; B - H_2SiF_6 soluble; C and D remainder (quartz). Symbols - coarse silt (□); medium silt (o); fine silt (·).

Medium Silt: In the medium silt (Fig. 4.19) the HCl soluble fraction drops significantly in the top 60 cm. The trends of the H_2SiF_6 soluble material and quartz both highlight the Aokautere Ash and are relatively uniform or increase slightly up the profile.

Fine Silt: Only the quartz content was determined in this fraction and it is reduced at the level of the Aokautere Ash and increases up the profile becoming irregular in the top third (Fig. 4.19).

MAJOR AND TRACE ELEMENT CHEMISTRY OF THE SOIL

The sand fraction and whole soil were analysed (Appendix 6) with the objective of determining chemical variations in soil parent materials in order to provide some evidence of translocations due to pedogenic processes. The carbon, and to a significant degree, water contents, are later additions to the primary parent material and as these are incorporated in the loss on ignition (LOI) in the major element analyses the plotting of the data is on a LOI free basis with the data normalised to 100%. Adjusting the analyses in this manner ignores some primary water bound in micas, amphiboles and glasses but this is a relatively minor component. No such adjustments were made for the trace elements.

MAJOR ELEMENTS

SiO_2: The SiO_2 content of the whole soil is relatively constant (Fig. 4.20) except for a slight reduction at samples T5 and T6 and the rise in the top 40 cm. SiO_2 in the sand fraction is more variable with low values for the Aokautere Ash and a rise to sample T8. The decrease at T9-T10 is small but is significant as it mimics changes in the rest of the major elements. There is also an increase in SiO_2 at T20-T22.

Al_2O_3: The soil Al_2O_3 content (Fig. 4.20) increases at the Aokautere Ash (T3-T7) and the "clay bulge" (T20-T21). There are trends of increasing aluminium up to T20-T21 and reducing aluminium above this level. The aluminium content of the sands has a maximum at the Aokautere Ash, gradually reducing to sample T8, a slight increase at T10 and a dramatic reduction in the top 60 cm.

TiO_2: In the top of the soil profile TiO_2 (Fig. 4.20) has a distribution similar to Al_2O_3, rising with depth to a maximum at sample T20. At the level of the Aokautere Ash however TiO_2 is at a minimum. The TiO_2 distribution in the sand fractions indicates increased values at samples T5-T6 and T9-T10 but reduced values at T19-T21.

Total Iron: This element is expressed by calculating total iron as Fe_2O_3. As a consequence of the variable distribution of iron concretions in the soil, iron is highly variable (Fig. 4.20). Soil iron increases from the surface reaching a maximum at the base of the Btg1 (sample T21) and is higher than background at the base of the Btg2 (T18-T19) and into the fragipan (T16-T17), even perhaps down to sample T13. The iron content of the Aokautere Ash is low but there is a slight increase at sample T5. The iron content in the sand fraction is also variable with small peaks at T3, T5, and perhaps T10 and trough at T20-T21. There are relatively higher iron values in samples T23-T25.

MgO: The soil MgO content (Fig. 4.20) shows a dramatic drop at the Aokautere Ash and also between 40 and 70 cm depth. It is uniform above 40 cm. In the sand fraction there is an increase in samples T5 and T9-T10, a decrease in sample T20 followed by increasing values to a high plateau in the topsoil.

CaO: The soil CaO values diminish from the basal samples to sample T20, with slight increases at T3, T5 and T10. There is a general increase in calcium in the soil from sample T20 to the surface. This increasing calcium content in the surface sample could be due to the addition of lime or superphosphate, however the sand also shows a high CaO content (pre-treatment of sand samples involved an acid wash) and the mineralogical evidence indicates increasing calcic minerals in the top of the profile. Fertiliser and lime influence on CaO levels (and P_2O_5 levels) is therefore discounted. The sand fraction CaO levels parallel the soil CaO in the central portion of the loess but towards the base samples T3 and T5 have increased calcium and the top samples (T22-T25) have high CaO contents.

Na_2O: The Na_2O values are similar for both the sand fraction and total soil except for (a) the influence of the Aokautere Ash, which has higher values in the sand fraction and (b) the top 5 samples where the sand fraction is lower (Fig. 4.20).

K_2O: Except for at the level of the Aokautere Ash where the K_2O level in the sand fraction and the total soil are the same, the trend of the sands parallels that of the soil (Fig. 4.20). The trends are relatively uniform but for a slight increase in samples T9-T10 and a generally lower K_2O content above sample T18, particularly evident above samples T20-T21.

Loss on Ignition (LOI): The LOI for the sand fraction reflects water bound in hydrous minerals and is relatively low and uniform except at the Aokautere Ash level where the water in the glass reached 3.9% (Fig. 4.20). The top samples, T21-T25, have significantly lower

LOI (water?) levels. The LOI component in the total soil samples is dominated by the carbon supplied by the organic matter in the top soil and water associated with clay minerals in samples T20-T21.

P_2O_5: Phosphorus forms only a minor component of the sand fraction and in the total soil samples has a distribution profile typical of the yellow-grey earths with high phosphorus in the topsoil but much lower values in the Btg horizons (Fig. 4.20). The P_2O_5 content then increases to a relatively uniform level in the C horizon. The Aokautere Ash is notably lower in phosphorus.

Total Soil Phosphorus: The distribution of total soil phosphorus (Walker and Adams 1958) at 5 cm intervals in the top of the profile is similar to the trend in soil P_2O_5 (see Appendix 10).

TRACE ELEMENTS

Vanadium: In the sand fraction the V values are relatively constant with decreases at samples T3-T4 and T20-T21 (Fig. 4.21). In the soil the V content is low in the Aokautere ash but above the ash there is a gradual build up in V to sample T21 then a continuous reduction to the surface.

Barium: The Ba distribution for the sands and soil are generally similar although the soil has slightly higher values for most of the C horizon (Fig. 4.21). The Ba increases at the Aokautere Ash and there is a systematic reduction in Ba levels above sample T17. The Ba content of the sand fraction in T17 increase dramatically. The Ba content of the sand also increases in T9.

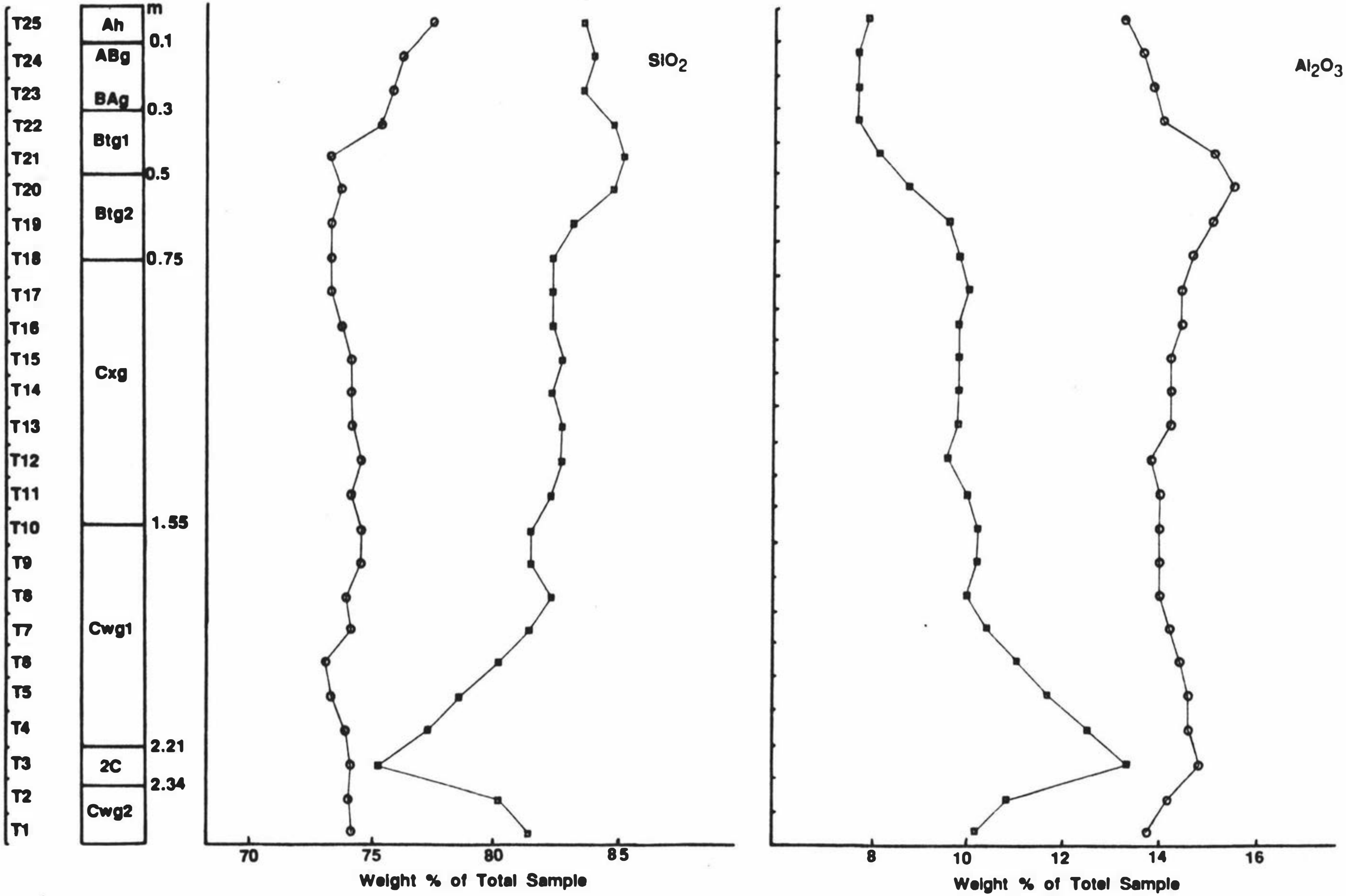

Figure 4.20: Distribution of the major elements in the sand fraction (□) and total soil (o) of the Tokomaru silt loam.

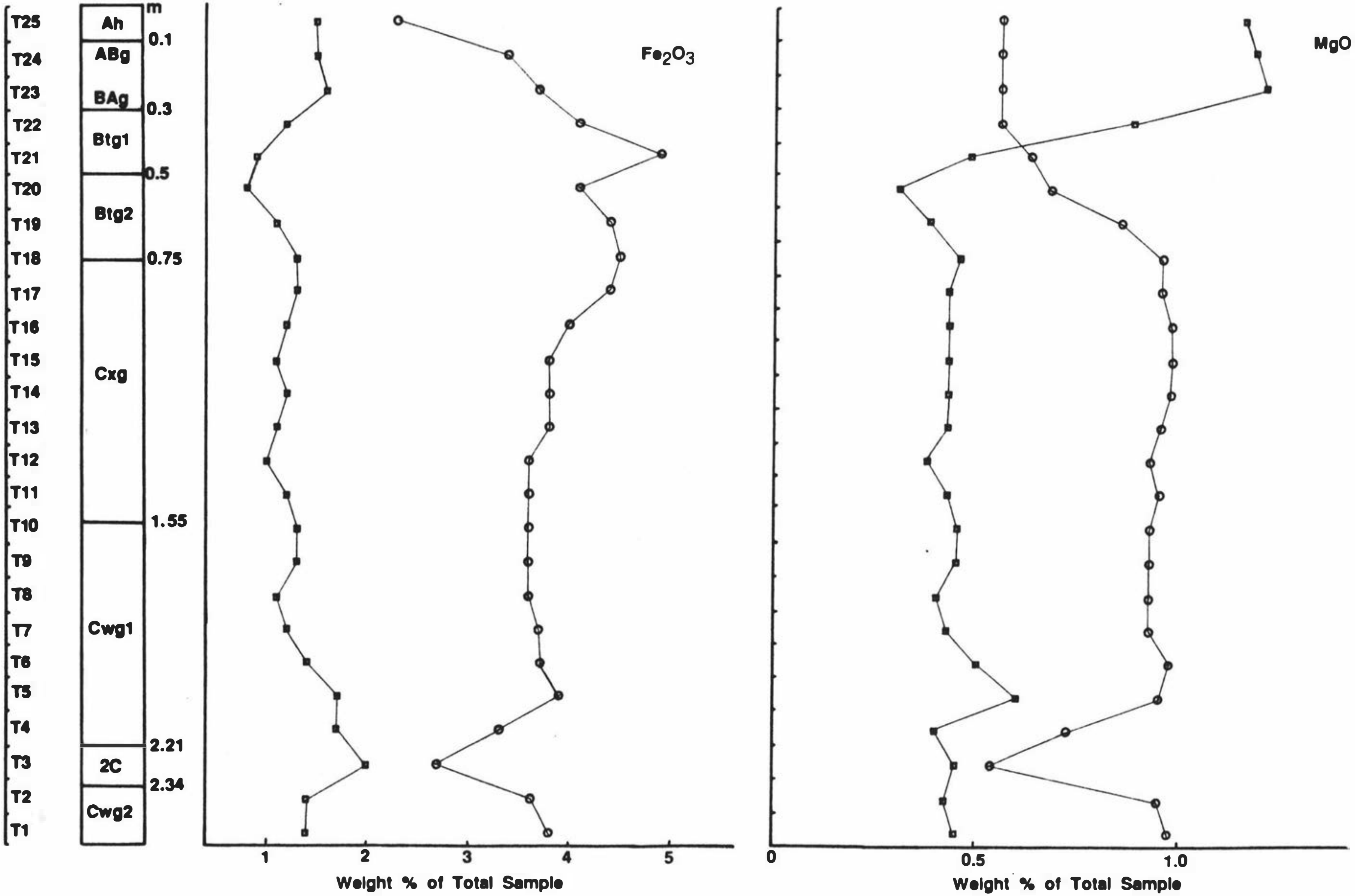

Figure 4:20 continued

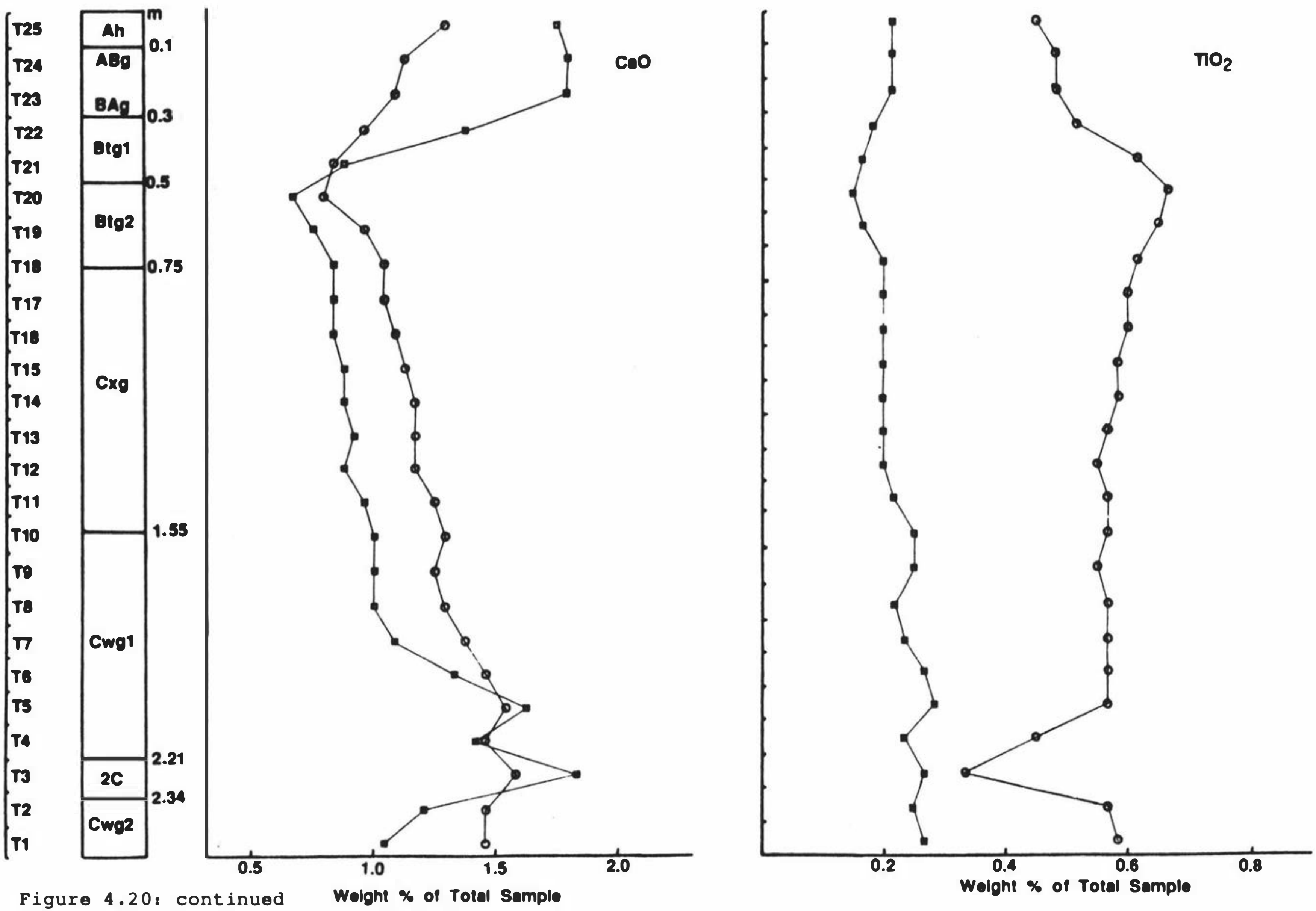

Figure 4.20: continued

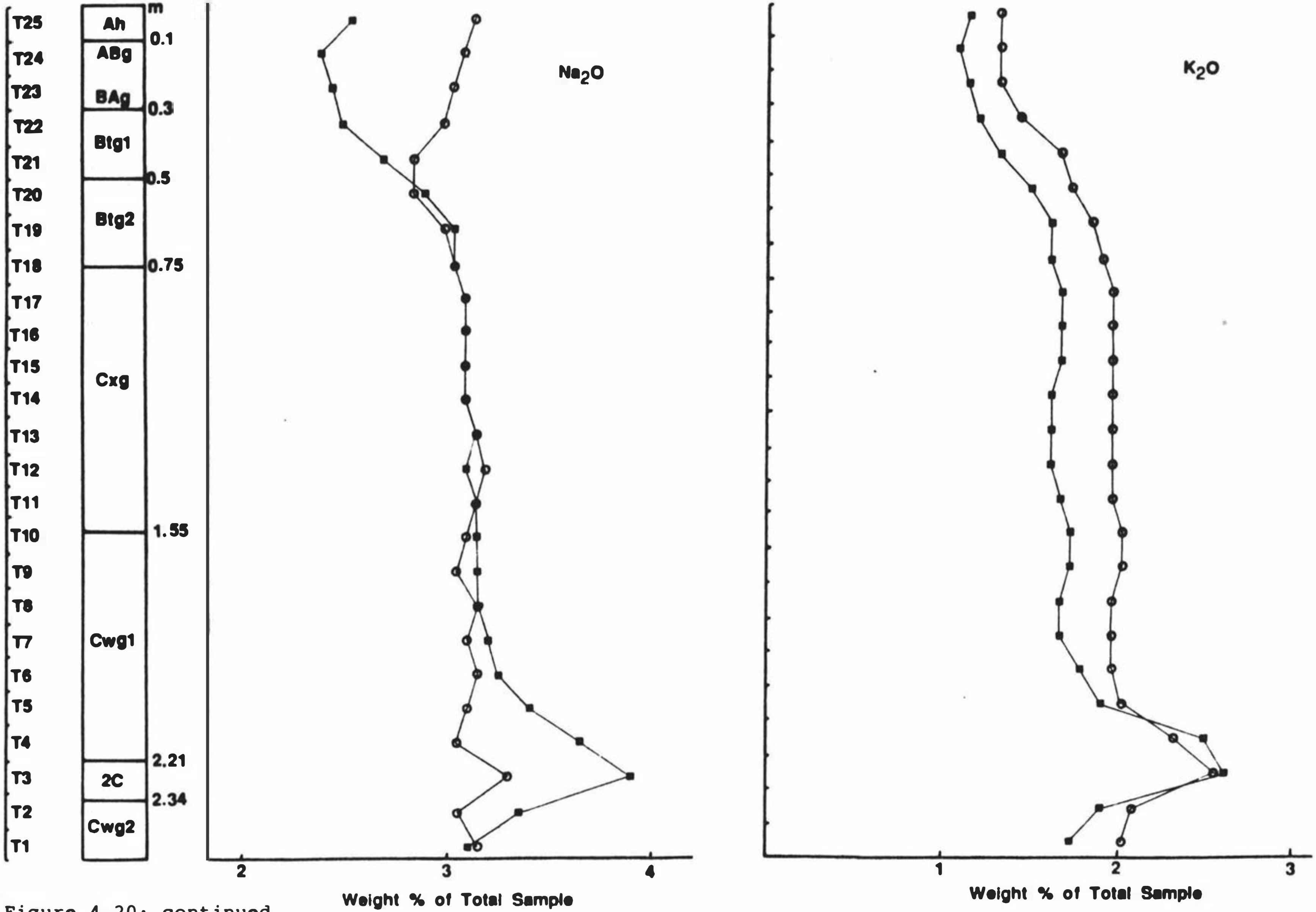

Figure 4.20: continued

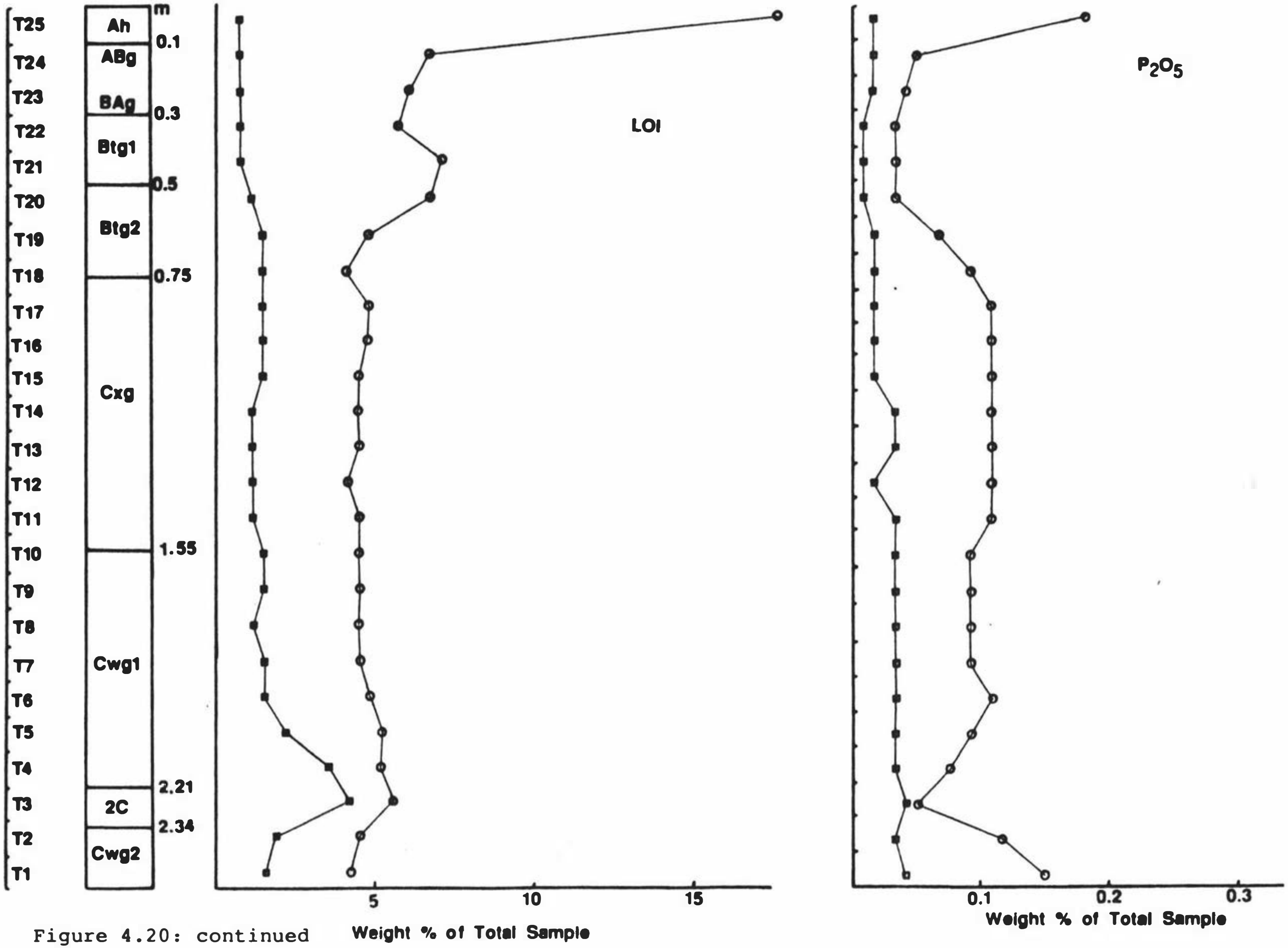

Figure 4.20: continued

Manganese: In the sands the Mn is relatively uniform except for increased values at the Aokautere Ash and in the top four samples (Fig. 4.21). Values in the soil are more variable with significant increases in Mn content at samples T2, T10 and in the top three samples.

Zirconium: Zirconium is an important trace element and as it is mainly concentrated in the highly stable phase zircon, Zr is often used as an index of weathering assuming that the parent materials were originally uniform in Zr content. The Zr contents of the sands are very uniform except for increased values at the Aokautere Ash and in the top of the profile. In the soil, Zr is uniform for most of the fragipan, excepting the low values at the Aokautere Ash, but there is a decrease in the very top of the fragipan and Btg2 and an increase in samples T22-T24 (Fig. 4.21).

Yttrium: Yttrium distribution in the sand fraction is uniform except for the increase in the Aokautere Ash (Fig. 4.21). The distribution in the soil however shows no relationship to soil boundaries and increases gradually to a maximum in sample T15 then diminishes to a relatively low value below sample T11.

PHYTOLITHS

The yield of phytoliths from the soil is low (*c.* 0.5%) with slightly higher yields in the upper samples (T22-T24). The phytoliths have low refractive indices (approximately 1.45) and although most are clear and transluscent there are pale brown varieties and occasionally fragments with a pale green or pink iridescence similar to that of precious opal.

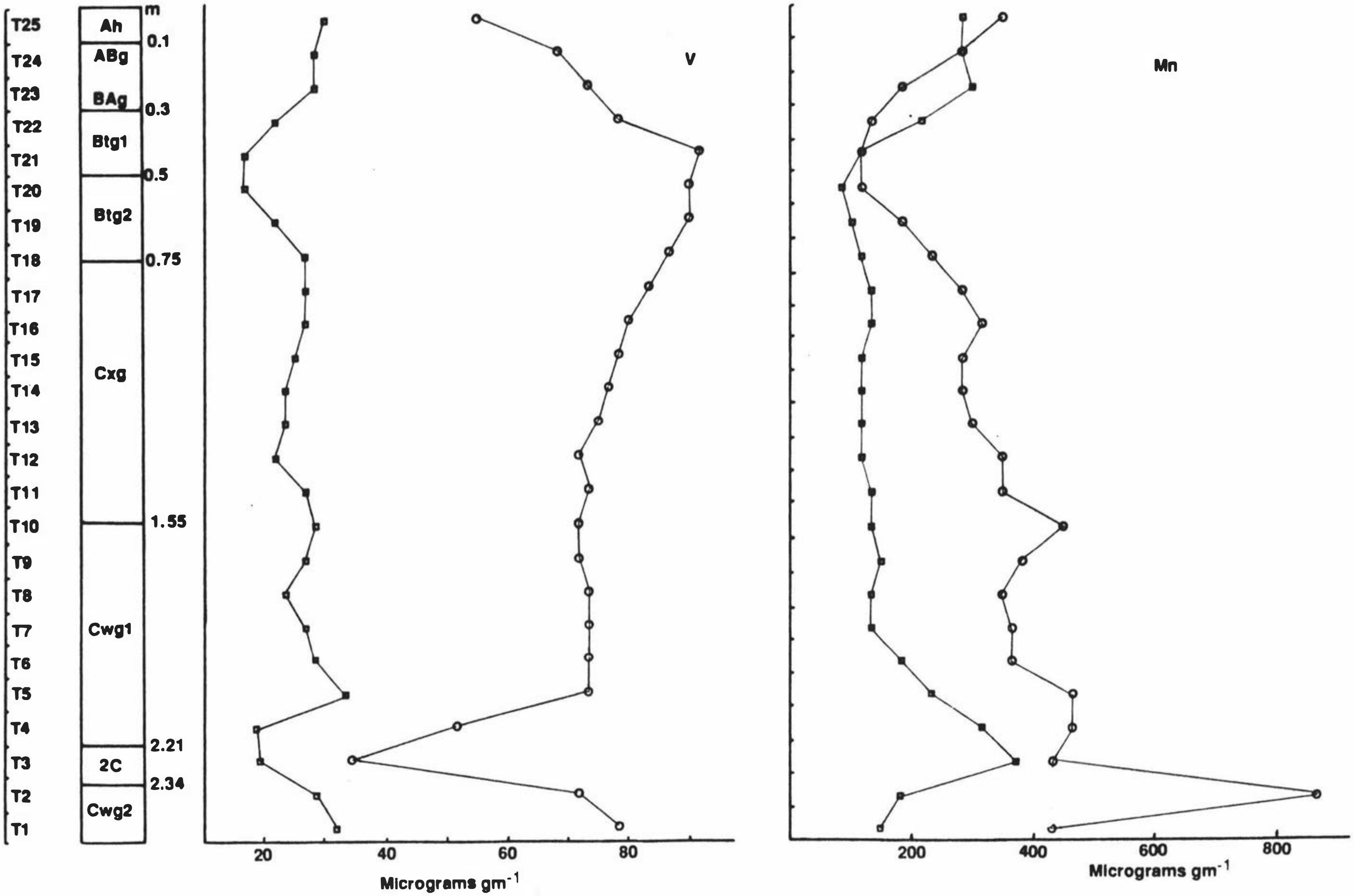

Figure 4.21: Distribution of V, Mn, Ba, Y, and Zr in the sand fraction (□) and total soil (o) of the Tokomaru silt loam. See the text for an explanation of areas "a" and "b" in the Y distribution.

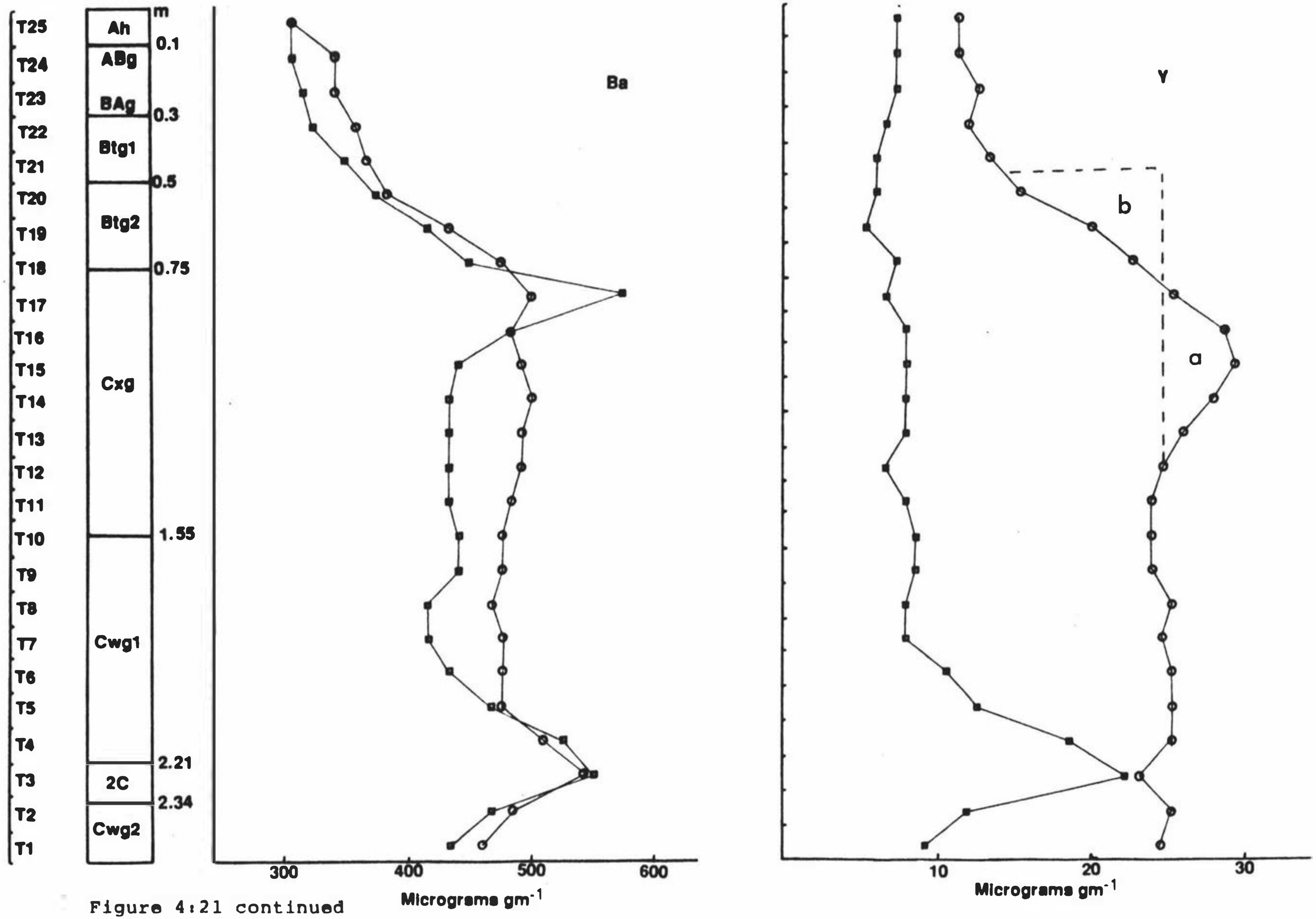

Figure 4:21 continued

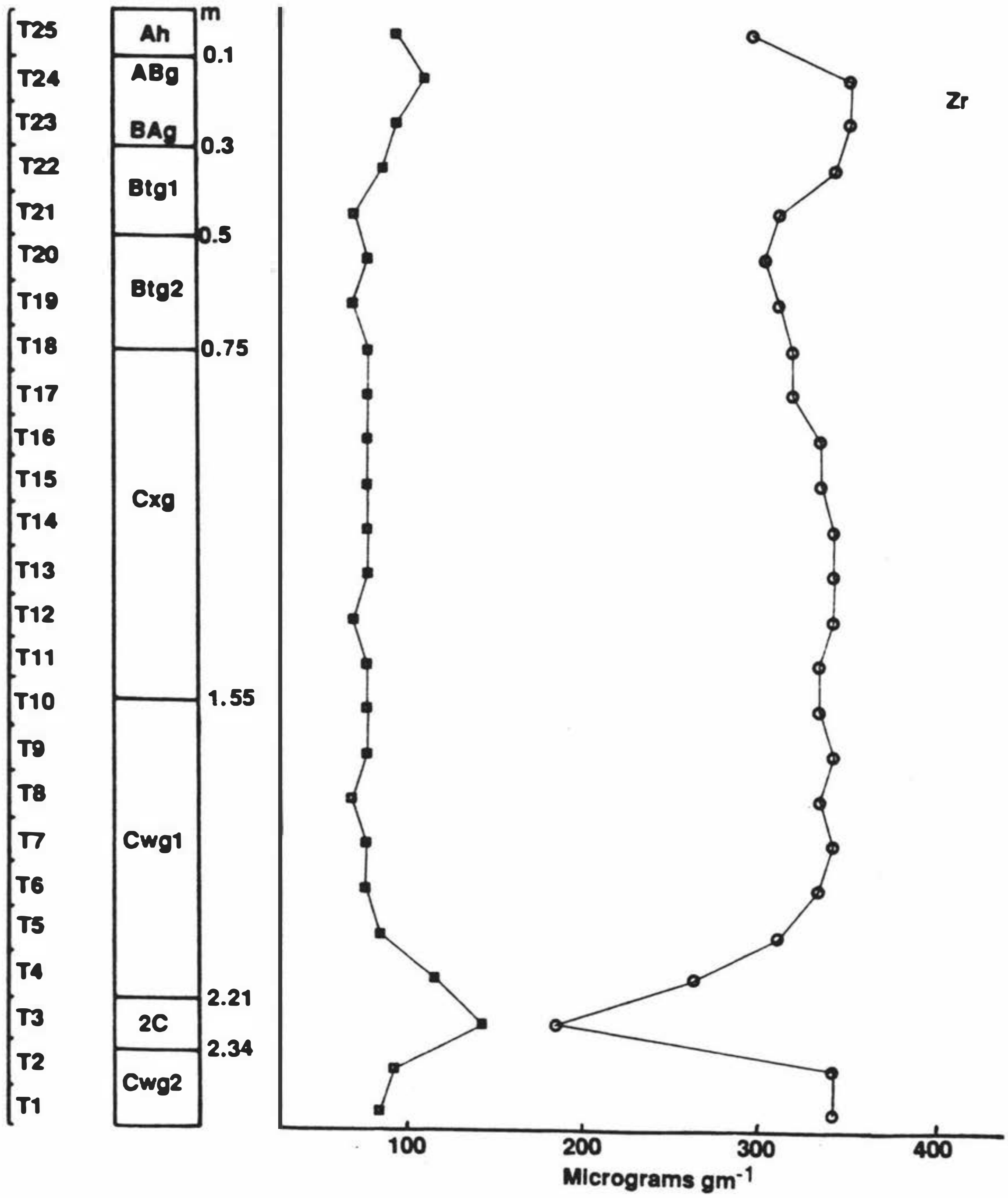

Figure 4:21 continued

There is a wide variety of material concentrated in the low density fraction but only the biogenic opal is reported here. Microfossils are common and sponge spicules dominate some samples. There is no established nomenclature to cover the considerable range in phytolith shapes so purely descriptive terms have been used. Prismatic and tabular forms (Fig. 4.22) are common, frequently serrated (with pointed or rounded serrations), or are ribbed, or have rows of turrets. Microspheres are common (Fig. 4.22) and are composed of spheres approximately 10 µm in diameter that appear to be concentrically zoned in transmitted light. Also common is a flower-shaped variety (Fig. 4.22) which has a rough lobate outline (Fig. 4.22). Rarer shapes include those like bicycle seats (Fig. 4.22), smooth rounded forms (Fig. 4.22), jigsaw puzzle pieces, hour glass, discs, and kidney or sausage forms (depending on the length/width ratio).

A comparison of the phytolith assemblages in the top and base of the profile (Fig. 4.23) indicated that there were large differences, so the relative proportions of the various shapes were quantified (Table 4.2) and the distribution plotted (Fig. 4.24). This shows that above sample T19 there is a significant reduction in the microfossils and spicules and concomitant increase in the flower and microspherical shapes. The tabular and prismatic shapes show little change in the same interval. Further, it was apparent during optical scanning of the samples that samples T19 and T20 had much more fine grained, irregular, nondescript debris compared with the rest.

The beech and tawa vegetation and the two peats all gave good phytolith yields. The beech phytoliths are relatively uniform being composed of 10 µm diameter microspheres which the electron microscope shows to be semi-spherical bodies composed of even smaller spheres (approximately 3000 Å in diameter, Fig. 2.25). Tawa vegetation has a range of phytolith shapes. Some have multi-ribbed shapes but the most common shape is a smooth rounded "eye" with or without an outer shell (Fig. 4.25). In transmitted light some of these "eyes" are concentrically zoned and have apparently formed by the growth of additional shells. The other vegetation species (kahikatea, rimu, and

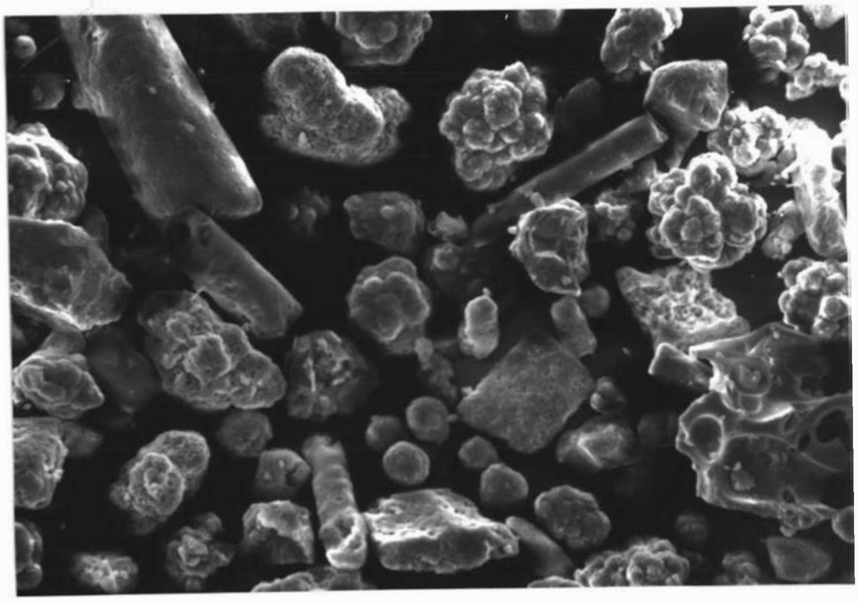

a

50 microns

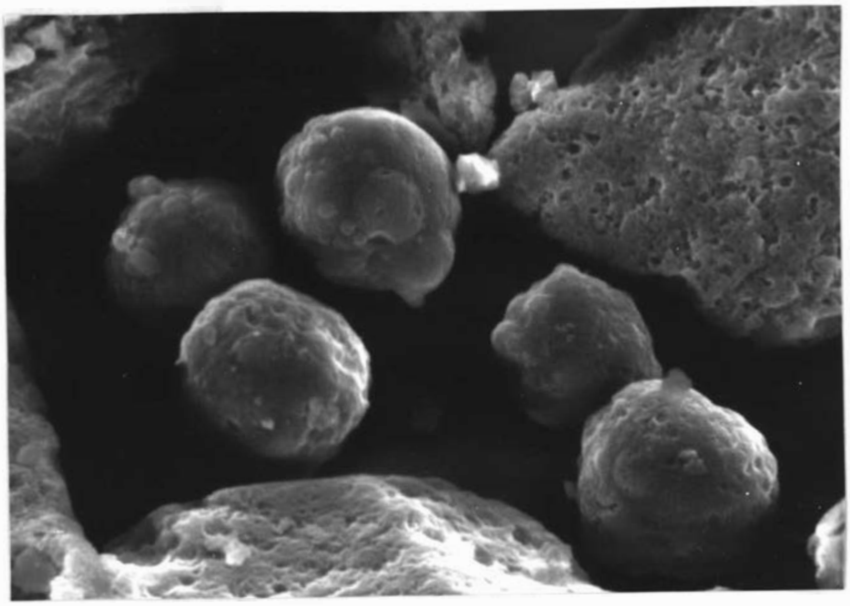

b

20 microns

Figure 4.22: Typical phytoliths extracted from the Tokomaru soil. (a) prismatic, tabular, microspheres; (b) microspheres, (c) flower shape (in transmitted light); (d) external morphology of the flower shape showing the rough lobate outline; (e) smooth surfaced form; (f) bicycle seat form.

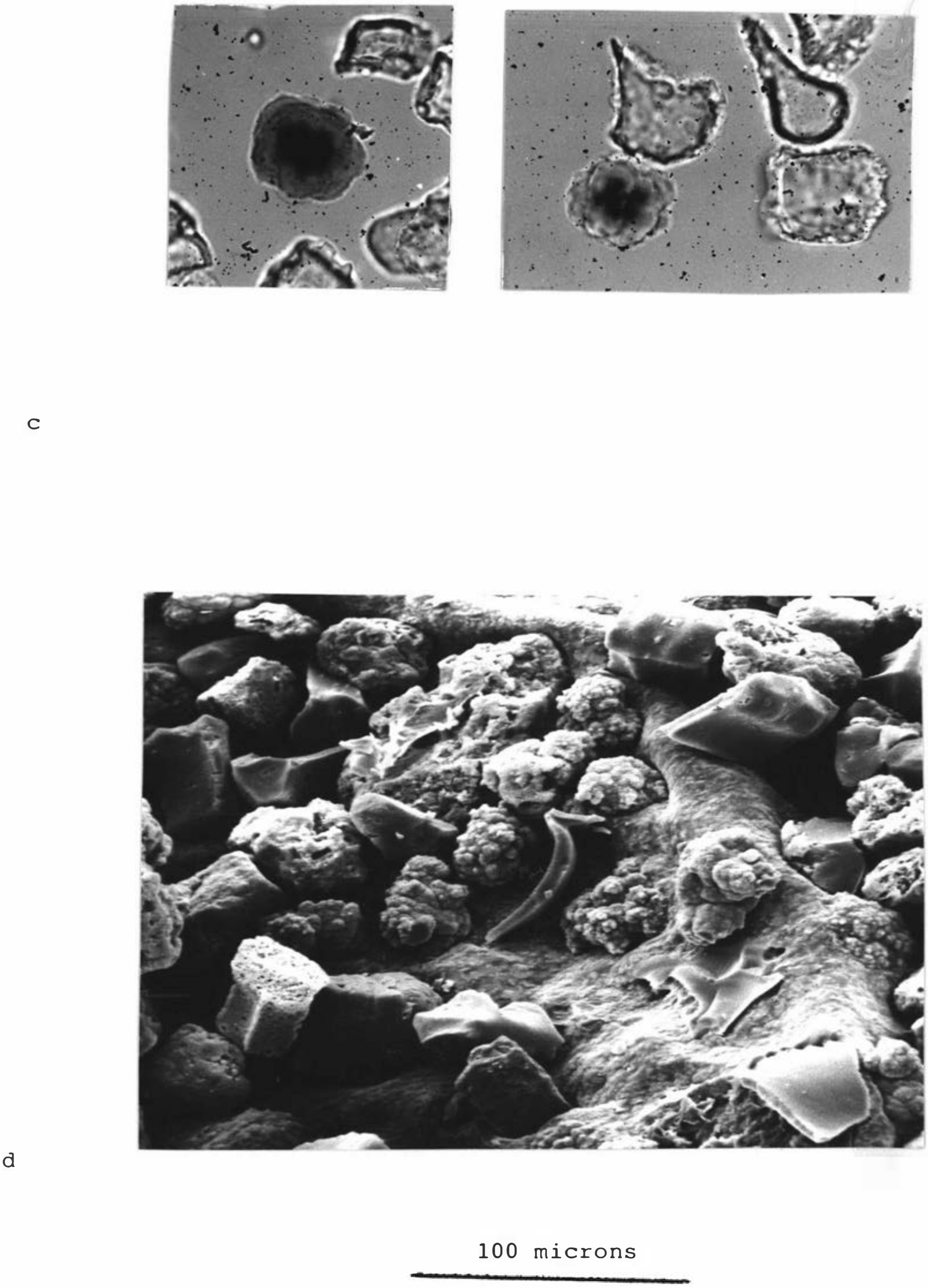

Figure 4.22: continued

(c) flower shape (in transmitted light); (d) external morphology of the flower shape showing the rough lobate outline.

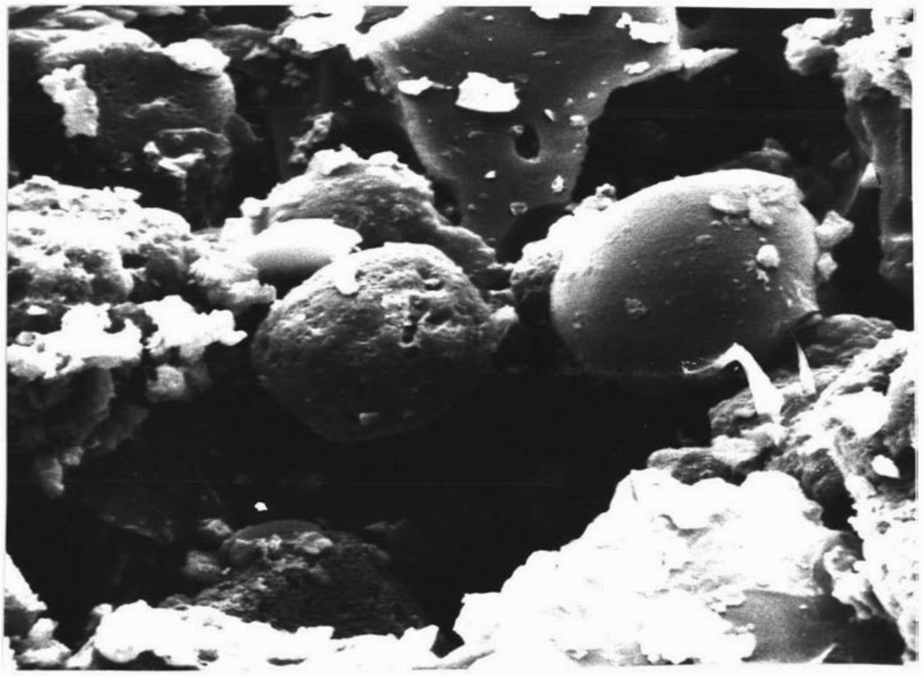

e

20 microns

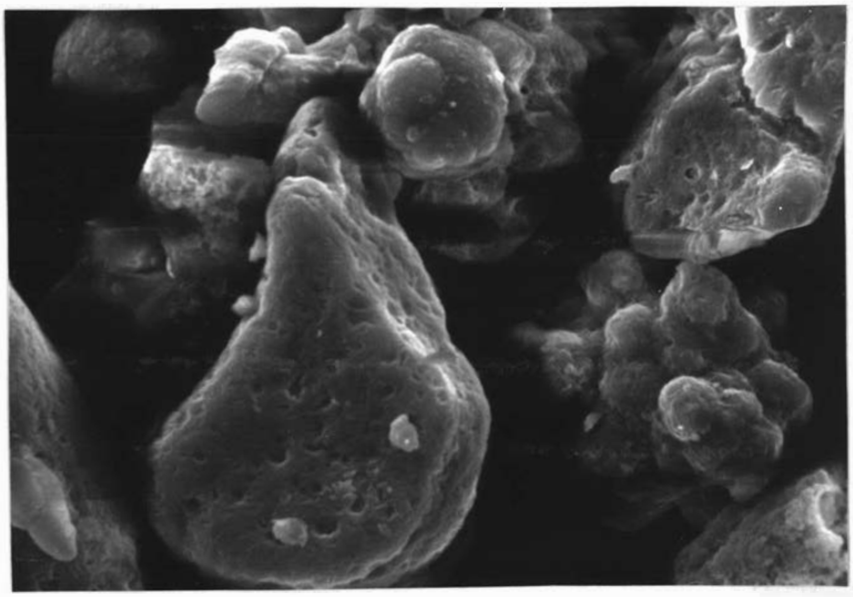

f

30 microns

Figure 4.22: continued

(e) smooth surfaced form; (f) bicycle seat form.

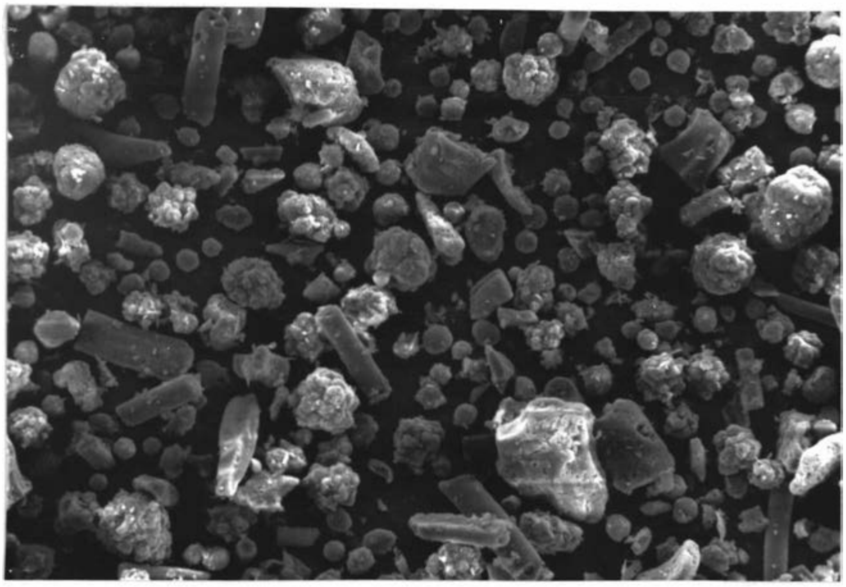

a

b

Figure 4.23: General view of the low density fraction from T23(a) and T18(b). This fraction of T23 is dominated by phytoliths in contrast with T18 which is dominated by sponge spicules and mica flakes.

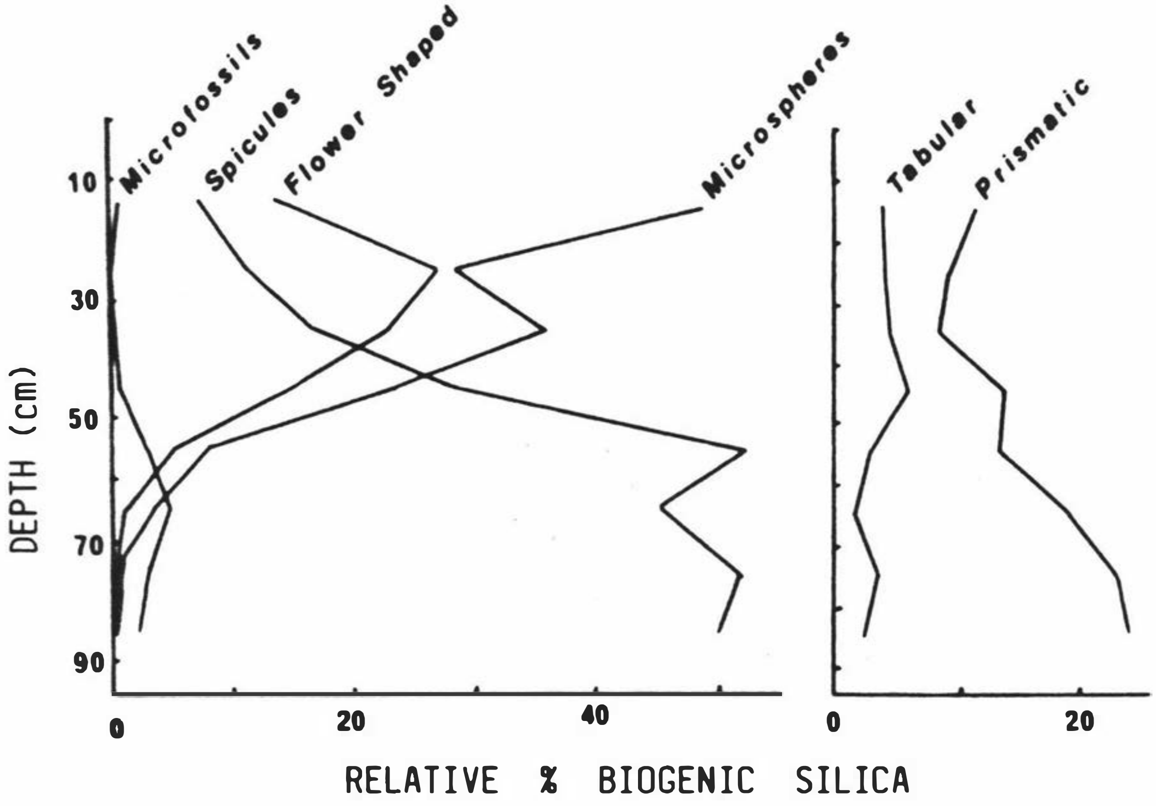

Figure 4.24: Relative distribution of the more common forms of biogenic silica between 10 and 90 cm depth in the Tokomaru silt loam.

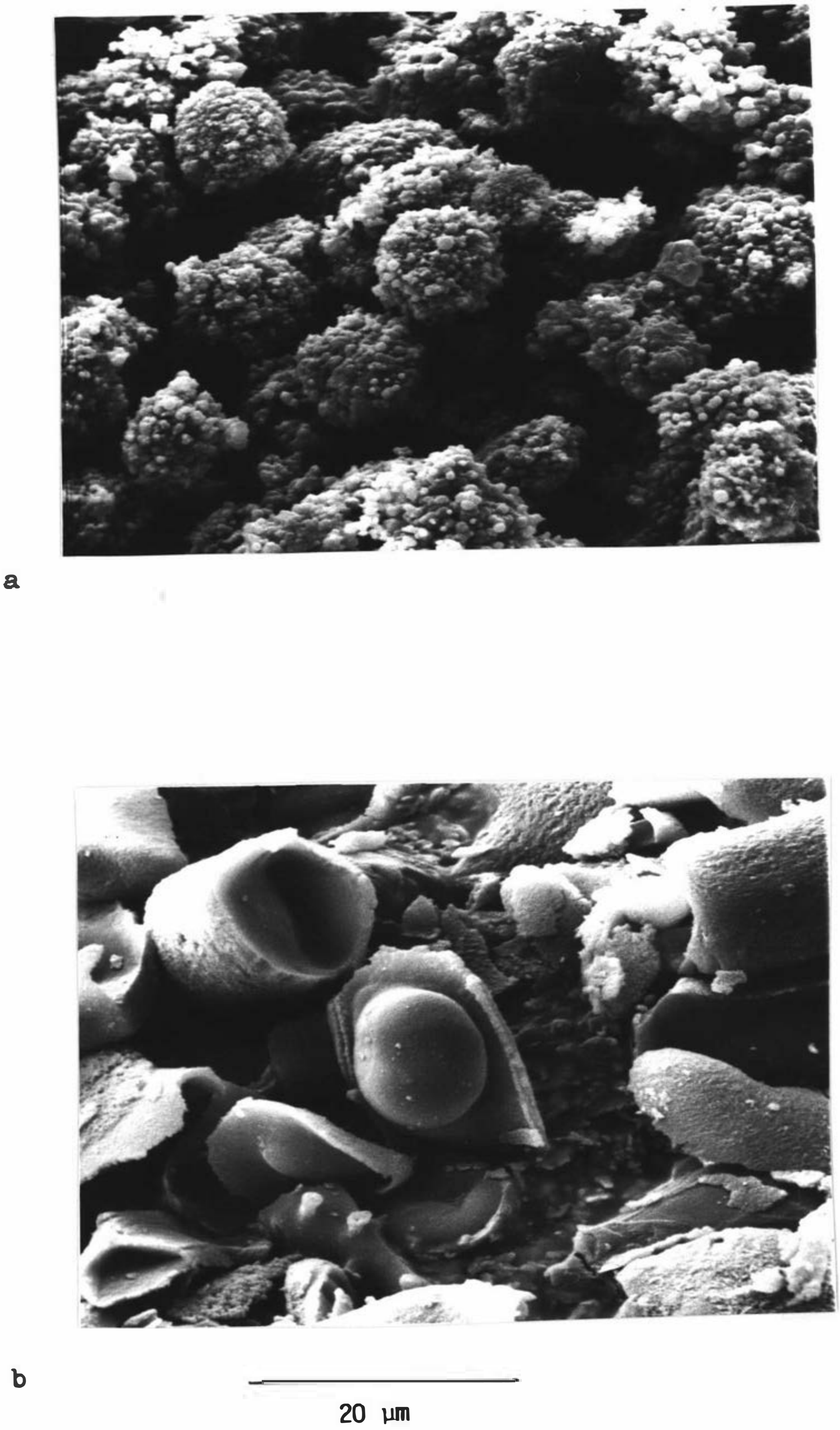

Figure 4.25: Phytoliths extracted from vegetation. (a) Round phytoliths from beech vegetation. These are composed of small spherical bodies which are less than one micron in diameter; (b) tawa phytoliths with an outer shell and a central bulge.

Table 4.2: Relative proportions of the various shapes identified in the low density fraction from the Tokomaru soil.

Sample	T17	T18	T19	T20	T21	T22	T23	T24
Microspheres	0.51	0.49	3.72	8.22	23.70	35.82	25.70	49.04
Tabular	2.05	3.25	1.12	3.18	5.96	4.15	3.75	3.65
Prismatic	24.17	22.89	18.96	13.27	12.97	8.13	9.38	11.30
Seat	0.77	0.65	1.86	0.56	1.04	1.00	1.13	1.04
Flower	0.64	-	1.49	5.61	14.90	22.39	27.20	12.87
Kidney	-	0.65	-	0.19	0.30	-	-	0.17
Others+	9.85	6.33	5.58	9.91	9.39	8.62	19.89	11.30
Microfossil	2.05	2.92	4.83	2.99	0.60	0.83	-	1.57
Spicules	50.26	52.76	44.98	53.08	28.32	16.58	11.26	7.30
Others*	7.92	10.39	17.11	2.99	2.83	2.49	1.69	1.91

+ Other forms of phytoliths.
* Other minerals identified (e.g. micas, glass).

totara) did not yield phytoliths but did yield significant mineral matter (mainly quartz and feldspars) and diatoms when the foliage was washed.

The beech peat contained a phytolith population that was dominated by microspheres (Fig. 4.26) whereas the podocarp peat has tabular and prismatic forms together with many forms very similar to the flower shapes in the soil (Fig. 4.26).

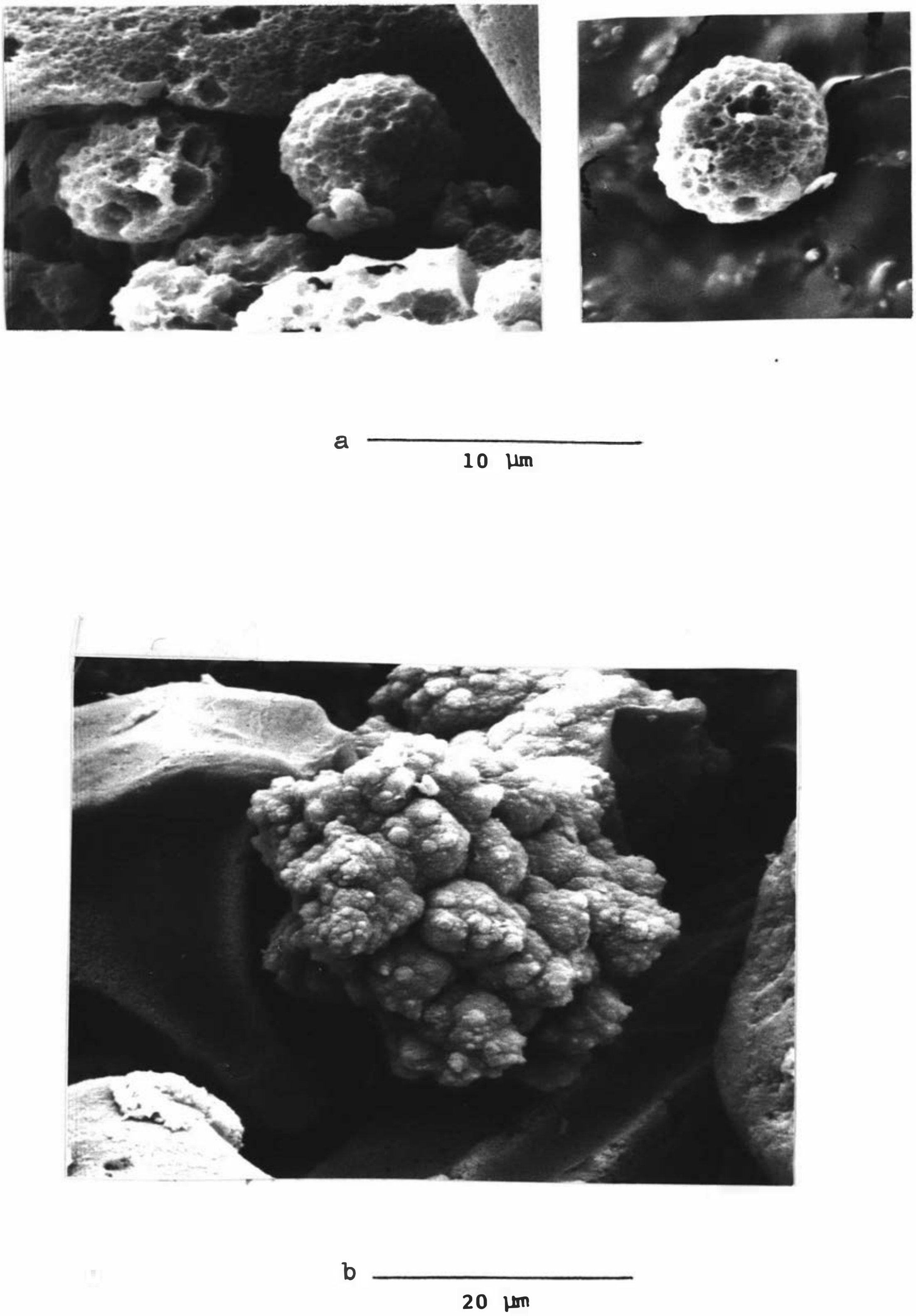

Figure 4.26: Typical phytoliths extracted from peats. (a) Corroded microspheres from a peat dominated by beech pollen. (b) A knobbly form extracted from a peat dominated by mixed podocarp pollen.

DISCUSSION

TEPHRA IN THE OHAKEAN LOESS IN THE MANAWATU

Although the Ohakean loess in the Manawatu is dominated by quartz and feldspar, there are stratigraphic levels at which there are increased amounts of minerals that clearly derive from volcanogenic sources. Cowie (1964) demonstrated that the loess in the Manawatu was formed from silts blown off the major river aggradational surfaces, so any volcanogenic material in the Tokomaru soil could feasibly be blown in as loess. The sources of the sediments on these aggradation surfaces include (1) greywackes from the Tararua and Ruahine ranges, and (2) the Plio-Pleistocene sediments, (plus older terrace coverbeds) from the Dannevirke-Pahiatua and Manawatu regions. All of these contain volcanogenic materials (Te Punga 1953; Kingma 1962, 1967; Milne 1973; Suggate et *al.* 1978; Roser 1983; Marden 1984). The volcanogenic material in the greywackes however is usually at least slightly weathered (Roser 1983; Marden 1984) and the ashes in the Plio-Pleistocene sediments and older terrace cover beds are frequently pumiceous. Thus these types of volcanogenic materials are probably not sufficiently robust to withstand major river transportation and abrasion. Furthermore, Lithgow (1986) did not report glass in the present Manawatu River sediments. The volcanogenic grains identified in the soil are inconsistent with transport that would produce significant abrasion because they frequently have glass selvedges and euhedral outlines. Thus the pulses of volcanogenic material described in the soil are interpreted as being derived from late Quaternary North Island tephras.

Tephras are a common feature of the coverbed stratigraphy of the North Island, producing excellent chronostratigraphic units that provide reliable markers for correlation between regions (e.g.

Aokautere Ash in loesses of the Rangitikei, Manawatu, Wairarapa and Wairau valleys and Westland). The eruption that produced the Aokautere Ash was particularly large and the ash is usually well preserved so there is little doubt about its identification (Cowie 1964; Mew *et al.* 1986), but it can also appear as grains dispersed in loess (Neall *et al.* 1983). Smaller tephras fall as light dustings in distal regions and will be mixed to a greater or lesser extent with the material at the surface on which they fall. To utilise the chronostratigraphic potential of these dustings it is important to establish if this mixing is significant.

Tephra Preservation: The C horizons of the Tokomaru soil accumulated during the last stadial, when the environmental conditions of the last Glacial were most severe (CLIMAP 1976; Thompson 1981; Pedersen 1983; Stewart and Neall 1984; McGlone 1985). Climatic conditions throughout this period were probably much drier, windier and colder than at present (Fleming 1970; McGlone *et al.* 1978; McGlone 1980, 1985; Salinger *et al.* 1985; Soons 1976). This is supported by the palynological evidence which indicates that the flora was dominated by grasses with rare *Nothofagus* and shrubs (McIntyre 1970; McGlone and Topping 1983; Lewis *et al.* 1985), particularly in exposed locations. Under these conditions the range of soil biota may have significantly contracted (Lee 1959; Ross 1984) and activity suppressed (Lee 1968; Sparling *et al.* 1986). It is suggested that there would have been very little biological activity in the surface layers that were accumulating at this time. This is consistent with the lack of bioturbation of the Aokautere Ash, particularly the very fine base, at its type section. An environment of a rather restricted flora and minimal fauna is in accord with the findings of Birrell and Pullar (1973), who demonstrated that palaeosols which developed in the central North Island at this time were only slightly weathered. Further, M^{c}Intyre (1975) and Blakemore (1984) demonstrated that phosphorus in the C horizons of the Tokomaru soil is dominated by inorganic P also indicating weak weathering. In addition, the clay mineralogy, especially the absence of interstratified clays in the Cxg and Cwg horizons (Pollok 1975), can be interpreted to indicate minimal weathering. It is therefore concluded that during the last stadial there was very little pedological activity at the surface on which any ash fell and that below *c.* 60-70 cm there was minimal post-depositional redistribution of ash in the loess.

In the top of the profile there are indications of more pronounced biological activity and thus a greater potential for mixing. In the top *c.* 50 cm the volcanogenic component is high and relatively uniformly distributed rather than in pulses. This uniformity could (1) reflect homogenisation by pedological processes (2) indicate an increased rate of tephric addition and/or (3) reflect a reduction in the loess accumulation rate. The preservation of quartz granules in planes parallel to the soil surface and the irregular variations in depth of changes in mineralogical and chemical trends indicate that the Ah to Btg1 horizons have not been significantly homogenised and that some of the original stratigraphy may be preserved, as shown for example by variations in XRF analyses (Figs. 4.20, 4.21), HCl soluble fractions (Fig. 4.19), grain size (Fig. 4.2) and mineralogy (Figs. 4.4 - 4.12). The change at 50 cm is sudden rather than gradual. Many parameters indicate that there is little mixing across this boundary, yet there is no impediment to root penetration at this level e.g. grain size distribution (Fig. 4.2) and bulk density values (Scotter *et al.* 1979) are similar across this zone.

It is concluded that there has been little translocation or mixing of volcanogenic materials, particularly below 50 cm. The levels of the samples with a higher volcanogenic component are taken as the level at which individual tephras were deposited. Using this criterion the mineralogical data identify tephric additions to the loess at the level of samples T5, T9-T10, T13, T14, and T21 to T25 (mainly T22 to T25) as well as sample T3 (the Aokautere Ash). The mineralogy is also reflected in the sand chemistry with higher than background levels of TiO_2, reflecting increased hornblende, clinopyroxene, and titanomagnetite content; higher MgO and FeO reflecting increased pyroxenes and hornblende content; higher CaO reflecting increased plagioclase and clinopyroxene content; decreasing SiO_2 and increasing Al_2O_3 and alkalis reflecting the presence of rhyolitic glass, and higher K_2O reflecting increased hornblende and glass content (see Fig. 4.20).

IDENTIFICATION OF TEPHRA SOURCES

The sources for these tephric additions are the andesitic centres of Egmont and Tongariro and the rhyolitic Okataina and Taupo centres, but unless one of the more unusual minerals from any of these sources is identified in the soil (e.g. abundant cummingtonite indicating a source in the Okataina Volcanic Centre), mineralogy alone cannot uniquely identify a source (Table 4.1). The relative proportions of minerals can nevertheless give an indication of source. For example significant hornblende reflects an Egmont centre source; significant orthopyroxene indicates a Taupo Volcanic Zone source; significant clinopyroxene or opaques indicate an andesitic source and increased transluscent glass content reflects a rhyolitic source. The tephra additions to the soil have been initially classified as to source on this basis; T5, T9, T13 and T21-T25 have andesitic additions while T3, T14 and T21-T25 contain rhyolitic ashes.

When mineralogy is used in conjunction with mineral chemistry however, it is possible to uniquely identify sources. Utilising the chemistry of the amphiboles it is possible to discriminate between Egmont and Taupo centres, and where amphiboles form a significant component of the profile (T5, T6, T9, T10, T13, T21-T25) they are usually from the Egmont centre (Fig. 4.13). The exception is sample T3 which has a Taupo centre source. There are also rare amphiboles in samples T21 and T25 which have demonstrable Taupo centre chemistry.

The chemistry of clinopyroxenes from selected samples in which they are more common (e.g. T3, T5, T24, T25) indicate that they originate from both the Taupo Volcanic Zone and Mt. Egmont (Fig. 4.16). The clinopyroxenes in sample T3 are consistent with those from the Aokautere Ash but the clinopyroxenes in the remaining samples predominantly originate from Mt. Egmont. It is not possible to identify a specific centre from within the Taupo Volcanic Zone using the chemistry of the clinopyroxenes, however clinopyroxenes are rare in rhyolites so soil samples with a high proportion of clinopyroxenes are unlikely to be derived from rhyolitic eruptions. In the topsoil, clinopyroxenes with Taupo Volcanic Zone chemistry are relatively common, so some are most likely derived from andesitic sources, probably the Tongariro centre. This would be consistent with reports of ashes from Mount Ruapehu (Tongariro centre) reaching Wellington in historic times (Latter *et al.* 1981). The data on clinopyroxenes from T9, T10, T13, T14 and T21-T23 indicate that these are divided between an Egmont and Taupo Volcanic Zone sources.

Orthopyroxenes are rare in the sand grain size in tephras from Mt. Egmont and examples with Egmont chemistry are rare in the Tokomaru samples (3 orthopyroxenes in samples T22 and T25 have an Egmont chemistry). Further, orthopyroxenes with an Okataina centre chemistry are absent, which is to be expected as glass grains with an Okataina signature are rare. Most of the orthopyroxenes analysed plot on trends consistent with either a Taupo or Tongariro centre source and preserve the separation into low Mn and high Mn varieties identified in the section on results (Fig. 4.14). The high Mn orthopyroxenes are derived from the Taupo centre but there is overlap between the Taupo centre low Mn orthopyroxenes, and Tongariro orthopyroxenes. In the reference tephras from the Taupo centre there was a greater proportion of high Mn orthopyroxenes compared with the low Mn orthopyroxenes but in the Tokomaru samples these groups are approximately equally represented. If the analysed grains from the soil are a reasonable representation of the total soil population then there is an excess of low Mn orthopyroxenes and some are derived from Tongariro.

The analyses of the glasses in the soil indicate that but for rare exceptions (in T6, T24 and T25) they are rhyolitic and therefore from the Taupo or Okataina centres. The mineralogy demonstrated that rhyolitic glass is a significant component of the loess for up to 40 cm (sample T8) above the Aokautere Ash and this is supported by the reduced SiO_2 and increased Al_2O_3 in the sand fraction above the Ash. Microprobe analyses of the glass grains demonstrate that the glass up to T8 and even trace amounts of glass up to T13 has a chemical signature identical to that of the Ash. It is known that the compositions of the glasses in the rhyolitic eruptives from the central North Island are cyclical (P.C. Froggatt *pers. comm.*; B.J. Pillans *pers. comm.*) and that it is possible to have glasses with chemistries equivalent to the Aokautere Ash in older rhyolitic tephras. The simplest explanation is however, that this glass represents grains of Aokautere Ash blown in as loess.

Based on the presence of glass, obsidian, orthopyroxenes, opaques and iron content of the sand fraction, sample T14 was identified as containing rhyolitic tephra material. Only three grains of glass were analysed from T14 so the data set is unacceptably small but the glass composition is similar to that erupted from the Okataina centre.

The chemistries of the glasses in samples T21 to T25 are highly variable with (Fig. 4.18):

(1) the Holocene Taupo centre signature common in all samples,
(2) sample T21 and perhaps T25 have glass chemistry consistent with the Okataina centre although the data set is small,
(3) samples T22 to T25 contain a significant amount of glass with an Aokautere Ash signature.

There are no known eruptions since the Aokautere Ash with a similar chemistry, (Latter 1985; Froggatt and Solloway 1986), so the recurrence of glass with this chemistry probably reflects the reactivation of the Aokautere Ash glass in the landscape due to erosion, although reactivation of older tephras with similar chemistry cannot be precluded.

Using the above chemical parameters (together with mineralogy) it is possible to identify the sources of the tephra additions to the loess. T3 is Taupo centre; T5, T9 and T13 are from the Egmont centre; T14 is from the Okataina centre and T21-T25 are mixed Tongariro, Taupo and Egmont centres.

TEPHRA CORRELATION

(i) Andesitic: Potentially the andesitic additions from Mt. Egmont can be correlated with specific eruptions. Post-Aokautere Ash isopachs of Mt. Egmont tephras indicate that there is a lobed distribution to the southeast (Franks 1984). In the Manawatu and Taranaki regions the wind is from the north to west quadrant for *c.* 55% of the time at a height corresponding to the summit of Mt. Egmont and increases to *c.* 75% of the time at 16 km height (Reid and Penny 1982). Larger eruptions from Mt. Egmont might therefore be expected to be carried to the Palmerston North region. Modern evidence for long carry distances of ashes is provided by the 1980 eruption sequence of

Mt. St. Helens. The ash clouds from these eruptions contained glasses of comparable composition to those of Mt. Egmont and reached heights of 25 km and travelled 1200 km, depositing more than 5 mm of ash up to 600 km from source (Harris *et al.* 1981; Sarna-Wojcicki *et al.* 1981).

In southeastern Taranaki the post-Aokautere Ash coverbeds may be subdivided into a lower tephric loess unit and an upper tephric unit (see Stewart *et al.* 1977 and Franks 1984). In regions close to Mt. Egmont these two units are separated by a marked disconformity (Franks 1984; B.V. Alloway *pers. comm.*) which formed approximately 11-12 ka B.P., and at which time there was significant erosion. There is also evidence that a rudimentary soil developed on the tephric loess at this time (Franks 1984). Further from Mt. Egmont the disconformity is less obvious but is readily identified on mineralogical grounds (Stewart *et al.* 1977). Within the loessial unit there are numerous tephras and southeast of Mt. Egmont at the Mangatoki Stream section (Fig. 4.1) of Franks (1984), there are three prominent tephras in the lower part of the unit, above the Aokautere Ash (Table 4.3). These tephras are here referred to informally from oldest to youngest as ME1, ME2 and ME3. ME1 is dark brown and dominated by lithic lapilli while ME2 and ME3 are yellowish brown and composed of coarse pumiceous lapilli (Franks 1984). ME2 and ME3 are thought to be members of the Carrington Tephras (Neall 1972). The tephras (ME1, ME2, ME3) are here correlated with the three lower andesitic layers identified in the Tokomaru soil (i.e. T5, T9 and T13 respectively). This correlation cannot be substantiated on mineralogical grounds as the tephras have similar mineralogies but the sand chemistry indicates that T5 has higher levels of MgO, total Fe and TiO_2 than T9 or T13. While this could be related to the relative amount of material reaching the Tokomaru site, it could also be because these elements are concentrated in the ferromagnesian mineral fraction and so are higher in lithic fragments than in pumice. Furthermore the ratios of the distances between the Aokautere Ash and T5, T9 and T13 are similar to those between the Ash and ME1, ME2 and ME3 and all three tephras occur in the lower portions of a last stadial loess unit. In a detailed mineralogical study of a section at Mokoia (Fig. 4.1), Stewart *et al.* (1977) demonstrated that within the last stadial loess unit there are

Table 4.3: Chronology of the larger post-20 ka eruptions from four volcanic centres in the North Island.

	TAUPO CENTRE	OKATAINA CENTRE	TONGARIRO CENTRE	EGMONT CENTRE
0*				
		Kaharoa Ash (c. 0.85 ka)	Ngauruhoe Tephra (0-1.8ka)	Kaupokanui tephra (1.2 ka)
	Taupo Pumice (1.8 ka)		Mangatawai Tephra (1.8-2.5 ka)	
	Mapara Tephra (2.2 ka)			
	Whakaipo Tephra (2.8 ka)			Maketawa tephra (3.1 ka)
	Waimihia Lapilli (3.4 ka			Manganui tephra (3.5 ka)
				Inglewood tephra (4.0 ka)
	Hinemaiaia Ash (4.5 ka)	Whakatane Ash (4.8 ka))		Korito tephra (4.5 ka)
5*				
	Motutere Tephra (5.4 ka)			Mangatoki tephra (5.5 ka)
				Tariki tephra
			Papakai Tephra	
		Mamaku Ash (7.0 ka)		Waipuku tephra
		Rotoma Ash (8.5 ka)		
	Opepe Tephra (8.9 ka)			Kaponga tephra
	Poronui Tephra (9.2 ka)			
			Mangamate Tephra (9.6-9.9 ka)	Konini tephra
10*	Karapiti Lapilli (9.8 ka)			
				Mahoe tephra (10.5-11 ka)
			Okupata Tephra (c. 11 ka)	
		Waiohau Ash (12.4 ka)		
		Rotorua Ash (13.5 ka)	Rotoaira Lapilli (13.8 ka)	Unnamed ash (c. 13.3 ka)
15*		Rerewhakaaitu Ash (14.7 ka)		
				Unnamed ash (pumiceous)
		Okareka Ash (c. 17 ka)		Unnamed ash (pumiceous)
		Te Rere Ash (c. 19 ka)		Unnamed ash (lithic)
20*	Aokautere Ash (c. 20 ka)			

* ka B.P.

Compiled from data in Topping and Kohn (1973), Stewart (1982), Franks (1984), Latter (1985), Froggatt and Solloway (1986), Lowe (1987), Alloway (*pers. comm.*) and Neall (*pers. comm.*).

small tephra pulses together with one macroscopic "marker lapilli" horizon composed of "andesite pebbles". The lapilli occurs at a level in the loessial unit which is *c.* 85% of the distance between a paraconformity and the Aokautere Ash. This proportion is similar for that of ME1 and T5 in their respective profiles, so this lapilli is correlated with the tephra in T5 identified in the present study.

The upper tephric unit in Taranaki represents a period of much more active volcanism (Stewart *et al.* 1977; Franks 1984) and Stewart *et al.* (1977) have correlated pulses in andesitic glasses and plagioclase at Mokoia with a sequence of 7 major tephras preserved in the Ngaere Swamp (Fig. 4.1), southeast of Mt. Egmont. The peat at the level of a concentration of these tephras towards the base of a core obtained from the swamp has been radiocarbon dated at 10450 ± 100 yr B.P. (Stewart *et al.* 1977). This upper tephric unit is correlated with the increase in andesitic additions to the top of the Tokomaru soil on the basis of (1) the lower tephras in the Ngaere Swamp core are amongst the thickest and coarsest (and therefore perhaps largest) post-13,000 yr B.P. ashes and (2) Stewart *et al.* (1977) document a marked change in the detrital components in the soil at the base of the tephric unit (quartz, micas, epidote and microcline content decrease dramatically). A similar change in the proportion of the detrital components occurs at c. 50 cm in the Tokomaru soil.

The three andesite tephras in T5, T9 and T13 are estimated to have been erupted approximately 19, 17 and 15.2 ka B.P., assuming uniform sedimentation rates during this period. The andesitic material in the top 50 cm represents tephra dustings that have accumulated during the last 10.5 ka.

(ii) Rhyolitic eruptions are much more explosive than those associated with andesites (see Self 1983; Wilson 1985; Wilson and Walker 1985; Self and Healy 1987) with much greater quantities of ash convected to greater altitudes and dispersed over a wider area. In addition to the Aokautere Ash some of the post 20 ka B.P. rhyolitic tephras reached the Manawatu and Elder (1965) described up to 7 tephras from peats in the northern Ruahine Range (Fig. 4.1). The Taupo and Waimihia tephras have been described from peats in the Ruahine

Range (Elder 1965; Hubbard and Neall 1980; Lees 1986) and recently a rhyolitic tephra radiocarbon dated at *c.* 5900 years B.P. (D.J. Lowe *pers. comm.*) has been described in lake sediments near Levin (M.S. McGlone *pers. comm.*).

The Aokautere Ash at 2.21-2.34 m depth in the Tokomaru profile is a major rhyolitic tephra addition to the loess in the Manawatu but there is evidence of other small dustings of rhyolitic material. Sample T14 has a mineral signature compatible with a rhyolitic origin and the glass chemistry is consistent with an origin from the Okataina centre. Given its position in the centre of a last stadial loess there are four possible correlatives, the Okareka, Waiohau, Rotoma and Rerewhakaaitu ashes (Table 4.3). The Okareka Ash at *c.* 17 ka (Pullar 1980; Stewart and Neall 1984) would be expected to occur at levels closer to the Aokautere Ash than T14 (assuming relatively constant accumulation rates). Furthermore cristobalite, which is common in the Okareka Ash, (see chapter 3) was not identified in T14. Waiohau and Rotoma ashes have dispersal patterns inconsistent with transport to the south and Froggatt and Solloway (1986) failed to find the Waiohau Ash southeast of Lake Taupo. Sample T14 is therefore tentatively correlated with the Rerewhakaaitu Ash because in the central North Island this ash is associated with the last phase of loess accumulation (McGlone *et al.* 1984; Froggatt and Solloway 1986). The Rerewhakaaitu Ash has been dated at 14.7 ka B.P. (Pullar *et al.* 1973; Green and Lowe 1985) therefore, if the correlation to T14 is correct, there is evidence in the Tokomaru soil for considerable loess accumulation after *c.* 14.7 ka, which is in contrast to the central North Island (Kennedy 1980). Data in Stewart (1982) showed that the proportion of quartz in a marine core continued at higher than Holocene levels for c. 2 ka after the Rerewhakaaitu Ash was erupted before declining to levels typical of the Holocene. This is consistent with the data from the Tokomaru soil.

In the top 40-50 cm there is a large increase in rhyolitic components. The glasses in these samples indicate that the source of this volcanic material is the Taupo centre but it is not possible to identify individual tephras. After 10 ka B.P. there was a resurgence in activity at the Taupo centre (Table 4.3) and two of the largest eruptions during this period, the Taupo and Waimihia tephra formations, have been identified in peats of the southern Ruahine Range (Hubbard and Neall 1980; Lees 1986) and might well have reached Palmerston North. Glass from the c. 5.9 ka rhyolitic tephra near Levin would also probably have been deposited throughout the Manawatu. Recent work has shown that the Hinemaiaia Tephra was also a very large eruption and has been correlated with an ash in southern Hawke's Bay (Lowe 1986). Froggatt and Solloway (1986) have recently redefined the Karapiti Tephra to incorporate the previous distribution of the Papanetu Tephra, thus enlarging the size of this eruption. They describe an upper fine ash unit of the Karapiti Tephra that has a distribution pattern directed to the south.

Amongst the ashes from the Taupo centre it is possible that any or all of these five tephra could have contributed to the soil of the present study. The increase in the rhyolitic components in the topsoil is therefore attributed to the resurgence of activity from the Taupo centre *c.* 10 ka ago.

One sample (T21) of this upper unit has a glass chemistry consistent with an Okataina centre source. It is not possible to positively identify the source tephra, but its position towards the base of a zone of increased tephric additions is consistent with the identification of the Rotoma Ash towards the base of the upper tephric unit at Mokoia (Stewart *et al.* 1977).

The distribution of volcanogenic minerals in the Tokomaru soil allows the profile to be subdivided into three units (1) an upper unit of mixed rhyolitic and andesitic ashes younger than *c.* 10.5 ka, (2) a middle unit with minor inputs from volcanic sources and (3) a lower unit of tephras and tephric loess dominated by the Aokautere Ash. The Aokautere Ash and sample T14 allow time planes at *c.* 20 ka and *c.* 14.7 ka to be established.

THE SIGNIFICANCE OF BIOGENIC SILICA IN THE TOKOMARU SOIL

In the present study the various forms of biogenic silica have been divided into two broad groups (1) animal tests and (2) plant phytoliths.

The animal test group is composed of diatoms and radiolaria (or parts thereof), fragments of sponge spicules and sponge sterrasters. Most of the grains have suffered abrasion and are thought to have been transported to the site as loess. At the time the animal tests were deposited there was a land bridge between the North and South Islands (Lewis and Eade 1974) with the exposed continental shelf traversed by the Manawatu, Rangitikei and Wanganui rivers which flowed out through Cook Strait (Lewis 1979). The spicules and microfossils probably originated from material deposited on the shelf. The sudden reduction in the proportion of spicules (and to a lesser extent microfossils) at 50 cm depth in the Tokomaru soil (Fig. 4.24) may represent the cessation of supply from this source area which occurred when the rising sea level covered the continental shelf during the post-glacial transgression. Given the very low angle of slope on the continental shelf (van der Linden 1969; Norris 1972; Lewis and Eade 1974; Lewis 1979), possible downwarping of the south Wanganui Basin (Milne 1976; Anderton 1981) and the possibility of sea level still stands before the land bridge was breached (Andrews 1973) the final stages of this transgression may have been relatively fast resulting in a sharp cutoff of the source area. The rapid rise in sea level has been estimated to have occurred 11-12 ka B.P. (Cullen 1967; Norris 1972; Lewis and Eade 1974). Norris (1972) also reported some elements of a cold water fauna dated at 10.6 ka B.P. from the South Taranaki Bight. The presence of this fauna may reflect a short cold episode and sea level still stand during the climatic amelioration, also recently documented in pollen stratigraphy from Tierra del Fuego (Heusser and Rabassa 1987).

Phytoliths have been identified in palaeosols (Beavers and Stephens 1958), in loess (Baker 1959), deep sea cores (Kolbe 1957) and in atmospheric dust (Baker 1959). They are relatively common in soils (Baker 1959; Jones and Beavers 1964; Wilding and Drees 1971), and have been used in palaeoecological reconstructions (Rovner 1971; Wilding and Drees 1971; Bartoli and Guillet 1977). Historically pollens have been used in this role and although phytoliths are not as uniquely specific as pollens (Rovner 1971; Bartoli and Guillet 1977) there is good differentiation of phytoliths between major plant groups and they are probably less mobile (at least in a forest situation) and more stable in an oxidising environment, common in soils.

In New Zealand Raeside (1964) identified phytoliths in loess from the South Island and separated phytoliths from some tussock and sedge species (Raeside 1970). These phytolith forms allowed identification of sedge species but could only identify tussock at the family level. "Silica grains" (i.e. phytoliths) have also been identified in *Nothofagus* (Patel 1986) and other New Zealand woods (B.G. Butterfield *pers. comm.*).

Of the phytoliths identified in the present study some of the serrated prismatic forms are similar to those described by Raeside (1970) and in general the prismatic forms are similar to those described from grasslands (Jones et *al.* 1963; Twiss *et al.* 1969; Rovner 1971). The microspheres are similar to phytoliths from the North American *Fagus* group (Wilding et *al.* 1977), are very similar to those from the beech peat and could readily be slightly corroded relics of the beech vegetation. Among the New Zealand *Nothofagus* species silica grains only occur in *Nothofagus truncata, Nothofagus solandri* and *Nothofagus solandri* var. *cliffordioides* (Patel 1986). The flower shape phytolith is similar to some phytoliths of unknown origin in Australia (Baker 1959) and is very similar to those from the mixed podocarp association investigated in the present study. The smooth-surfaced form in sample T24 is thought to be equivalent to the central "eye" type from tawa vegetation. Although the distribution of phytoliths in different parts of the plant has not been investigated in the present study Lanering et *al.* (1958) and Baker (1959) report that silica is not usually deposited in underground parts of plants, so the phytoliths in the soil are interpreted as the residue left after decomposition of vegetable matter on the soil surface. In the soil profile of the present study there is a significant change in the phytolith population down the profile (e.g. compare Figures 4.23 and

4.24). The population dominated by microspheres, the flower shape and the smooth-surfaced form are interpreted to represent forest species or a forest association. Thus the change in phytolith population at *c.* 50 cm depth reflects a significant change in the flora and is associated with the Aranuian afforestation. There is no palynological data for this time period in the Manawatu west of the main axial ranges but in the central North Island the afforestation began *c.* 14.5 ka ago (McGlone and Topping 1977; McGlone 1980), in Taranaki it occurred at approximately 12-13 ka B.P. (McGlone 1980; McGlone and Neall *pers. comm.*) and in the Wellington region *c.* 10 ka B.P. (Mildenhall and Moore 1983; Lewis *et al.* 1985). This decreasing age of forest expansion with increasing latitude in the south of the North Island follows the general trend for New Zealand (McGlone 1980), and an age for the afforestation in the Manawatu is thus inferred to be 11-12 ka B.P.

Palynological data (Lees 1986) showed that there was an assemblage dominated by *Leptospermum* and *Cyathea* with minor *Podocarpus spicata* (matai) on a 13 ka B.P. terrace related to Ohakean aggradation (Marden *et al.* 1986) at Ballantrae (Fig. 4.1). This is apparently inconsistent with the grass-scrub assemblage inferred for Palmerston North at this time. The type of flora in a region may, however, be very dependant on site, particularly in relation to aspect, (McGlone and Neall *pers. comm.*) and it is suggested that forest conditions developed earlier at Ballantrae because of the sheltering effects of the Ruahine Range.

The change in the phytolith population at 50 cm depth in the Tokomaru soil, interpreted to have occurred 11-12 ka B.P., is consistent with an 11-12 ka age for the rise in sea level that resulted in the diminution in supply of sponge spicules, suggesting that the two events were strongly climatically interrelated.

LOESS PROVENANCE

The Tokomaru soil is located in a region surrounded by indurated Mesozoic sediments of the Torlesse terrain (Suggate *et al.* 1978) and poorly consolidated Tertiary sediments of the South Wanganui Basin (Te

Punga 1953; Kingma 1962, 1967). Minerals from both these domains are therefore potential source materials for loess. A third potential source area is atmospheric dust from Australia. The distribution of quartz, kaolin and illite in the Tasman Sea and western Pacific Ocean sediments (Windom 1975; Thiede 1979) and the historic falls of Australian dust in New Zealand (Marshall and Kidson 1928) demonstrate that Australian-derived aeolian material can reach New Zealand under favourable circumstances (see also Gagosian *et al.* 1987). Cowie (1964b) however, has shown that the loess in the Manawatu thins dramatically on the eastern banks of the major rivers, clearly demonstrating that most of the aeolian materials are locally derived. The lithologies of the Torlesse terrain range from greywackes (feldsarenites and litharenites) to argillites. Mineralogically the coarser lithologies are composed of plagioclase (albite), quartz, lithic fragments and alkali feldspar (in decreasing order of abundance) in a fine-grained matrix (<15 µm) which is often recrystallised to sericite or chlorite (Reed 1957; Rowe 1980; Roser 1983; Graham 1985). Coarse mica grains are rare (Reed 1957; Rowe 1980; Graham 1985; Marden 1984). The Tertiary sediments include mudstones, siltstones and sandstones (all of which are micaceous) and rare greywacke conglomerates (Fleming 1953; Te Punga 1953; Graham 1985). Mineralogically the coarser members of this set comprise quartz and muscovite in a muddy matrix; feldspar and lithic fragments are less common (Graham 1985; Lithgow 1986). The Tertiary sediments are thought to be derived from the local greywackes (supplying quartz, feldspar and lithic fragments) with quartz, feldspars and mica supplied by the basement rocks of the northwest Nelson area (Te Punga 1953; Anderton 1981; Graham 1985). A distinction between the Tertiary and Mesozoic sediment provenances is therefore difficult. They do have minor differences in mineralogy and whereas the Tertiary sediments have a high proportion of coarse muscovite and fewer lithic fragments, the reverse is true in the greywackes.

The mineralogy of the detrital fraction of the loess is dominated by quartz, feldspar and greywacke lithics, reflecting the two major sources highlighted above. In the coarser fractions quartz dominates over feldspar while in the finer fractions feldspar dominates. The lithic fragments are a significant component at 25% to 40% of the sand and coarse silt fractions. These values are not dissimilar to the sum of "lithic" plus "sericite" determined by Palmer (1982) in loess in the Wairarapa.

Quartz distribution in the silts and very fine sands down the profile demonstrates that there are greater abundances of quartz in the top 50 cm (particularly the fine silt) compared with the underlying loess. The SiO_2 content of the soil supports this conclusion. The quartz content of the coarse silt as determined by the point count method is low (Appendix 5) and apparently at variance with that determined by the dissolution techniques (Appendix 8). Lithics are often dominated by quartz and when the matrix of the lithics is dissolved out this quartz contributes to the total quartz.

Lithic fragments decrease as a concomitant increase in quartz+feldspars occurs towards the top of the profile, particularly above 50 cm depth (Figs. 4.4, 4.9, 4.11, 4.12). It might be argued that the reduction in lithics is related to weathering, specifically the matrix of the lithics. This, however, appears not to be the case because such weathering would release the fine and medium silt-sized grains from the lithics and there are no increases in the 5-2 µm or 20-5 µm fractions, concomitant with the reduction in lithic content. There is an increase in the quartz content of the 5-2 µm fraction but this occurs in samples above 50 cms whereas the maximum weathering is between 51 and 64 cm (Pollok 1975). The present data is not able to demonstrate a cause of reduction in the lithic component towards the top of the profile.

Micas are minor phases among the detrital components, and although it is acknowledged that it is difficult to obtain representative data on micas because of their platy nature, there is a reduction in the mica content of the coarse fractions above 50 cm. This trend is supported by the chemical analyses which show a decrease in K_2O and Al_2O_3 content above 50 cms. LOI in the sands also decreases above 50 cms. The potassic phases that contribute to the K_2O in the sands are potassium feldspar, hornblende, micas and glass. The sand mineralogy demonstrated that hornblende and glass increase above 50 cms and there is no change in potassium feldspar content at 50 cm so the reduction in K_2O content must be due to a reduced mica content. The LOI component in the sands is probably due to structural water in the hydrous phases (micas, hornblende and glasses) so a reduced LOI content also reflects a reduction in the mica content. Furthermore, if the HCl-soluble component of the medium and coarse silts is mainly mica (optical data indicate that amphiboles, pyroxenes and opaques are rare in the coarse silt fraction), then the results of the HCl dissolution supports the conclusion that there is a lowered mica content above 50 cms. The data demonstrates that this occurs for the full range of grain sizes >5 μm. The lowering of the mica content may be due to weathering but several factors are inconsistent with this:

(1) The top 50 cm is a zone richer in relatively weatherable pyroxenes which are comparatively unetched and euhedral compared with the highly etched pyroxenes in the Cxg and Cwg horizons where micas are common. It is difficult to envisage a situation where, given similar parent materials and pHs (4.9 - 5.3 in the topsoils, compared with 5.0 - 5.2 in the Cxg; Pollok 1975) micas would be weathered in preference to the readily weathered pyroxenes at one level and not at another.

(2) Micas are still identifiable in the highly weathered tephras in the Hamilton basin (chapter 3) whereas the pyroxenes and glass are almost completely weathered.

(3) Compared with levels below 50 cm, mica content in the top 50 cm is lowered almost uniformly across the range of grain sizes >5 μm.

(4) The level of maximum weathering (Pollok 1984) and hence the zone of maximum degradation of minerals is between 51 - 64 cm depth *i.e.* below the zone of lowered mica content.

It is therefore thought that the change in mica content does not reflect pedogenic processes but rather a change in parent material. Parfitt *et al.* (1984) document a reduction in epidote and chlorite in the top of the Tokomaru soil. There is also a reduction in mica and epidote content at the boundary between tephric loess (with micas) and an overlying tephric unit in yellow-brown loams from south Taranaki (Stewart 1982). The greywackes and the Plio-Pleistocene sediments are the two possible major sources for the micas in the loess, although Australia cannot be totally excluded as Marshall and Kidson (1928) describes "flakey" *sic* minerals (probably micas) in historic dust-storm debris. In the greywackes, however, the micas are either fine-grained (< c. 20 µm) or, when coarser, are deformed and relatively rare, while in the Plio-Pleistocene sediments micas are more common and coarser (up to sand-sized grains). This is good evidence for the micas to have been eroded from the Plio-Pleistocene sediments and deposited on the Ohakean aggradation surfaces, from where they were removed by aeolian processes. The sudden reduction in mica content of the loess may be due to the loess source being inundated by the sea and/or expansion of the forest at the end of the stadial. At the end of the last stadial De Angelis *et al.* (1987) document a similar decrease in aluminosilicates (mainly illite; Windom 1975) in aerosols trapped in an Antarctic ice core.

The reduced mica content may also be reflected in the chemical data of Childs and Searle (1975). They show a pattern of reduced K_2O content in A and B horizons compared with C horizons in yellow-grey earths and yellow-brown loams and attribute the lowered K_2O levels to loss of potassium during weathering. An alternative explanation to weathering is that it represents a different parent material. Under acid conditions in soils chlorite is more readily weathered than micas yet it is still present in significant quantities in yellow-brown loam/yellow-brown earth intergrades (e.g. Parfitt *et al.* 1984) so the potassium decrease which also occurs in the upper horizons of these soils (unpublished data, C.W. Childs *pers. comm.*) may not be due to mica weathering. Even where mica degradation does occur the potassium fixing properties of the clays will tend to minimise K leaching. In the Table Flat silt loam the K_2O content is very low towards the base where the parent material is demonstrably different, *i.e.* the "Tongariro" tephra (Leamy *et al.* 1973; Childs and Searle 1975) mixed with loess. It is suggested that the decrease in potassium reflects a reduction in potassium-bearing minerals (micas). In some of the Holocene portions of deep-sea sediments and ice cores (De Angelis *et al.* 1986; Griggs *et al.* 1983; Nelson *et al.* 1985) there is a decrease in the mica content which is inferred to reflect a decreased aeolian content in the atmosphere as a consequence of climatic amelioration. The cyclical reduction in potassium in loessial sequences (e.g. Childs and Searle 1975) may be a reflection of the provenance of loessial materials that accumulated between stadial periods.

<u>Chemical trends</u> which are due to tephra in the loess have been discussed above but some trends evident may not be related to tephra additions but rather to variations in the detrital mineralogy.

Zircon is a particularly stable mineral and has commonly been used as an index of relative change in provenance and pedological studies (Khangarat *et al.* 1971; Rutledge *et al.* 1975). Changes in Zr content in a sedimentary sequence may be taken as reflecting changes due to either weathering or changes in parent materials. In the Tokomaru soil the Zr content of the Ohakean loess is relatively uniform, except in the Aokautere Ash, but there is a marked increase for samples T22-T24. This increase could be due to either an additional parent material or the removal of a fraction that does not include zircon (i.e. weathering). The fresh but weatherable minerals in T22-T24 suggest that minimal material has been translocated so the increase in Zr in these samples is thought to be due to a change in parent material. The increase in Zr cannot be due to the more volcanic nature of the top 50 cm, for although the sands which are dominated by volcanics do have an increased Zr content in the top 50 cm the increase is insufficient to account for the increased levels in the soil. It is concluded that the increased Zr content of T22-T24 is therefore a reflection of increased zircon content of the loess at this level.

Based on the significantly different quartz, lithics, mica and Zr content in the top of the profile it is here suggested that the top 50 cm represent loess with a different provenance to that below 50 cm. It has been argued above that the top unit accumulated during the last 10-11 ka so it is here referred to as post-glacial loess.

POST-GLACIAL LOESS SOURCE

In the South Island post-glacial loess is relatively common east of the main divide, but of local extent, (Bruce *et al.* 1973) and at the present time storms frequently blow dust (loess) from braided river systems onto adjacent terraces (Cox *et al.* 1973; Ives and Stevenson 1973). In the North Island post-glacial loess is less extensive (Cowie and Milne 1973; M^{c}Craw 1975) although in the central North Island this apparent absence may be an identification problem due to the difficulty of differentiating thin, shower bedded tephras from tephric loess (Pullar and Pollok 1973; Lowe 1980). Holocene loess has been reported at Lake Ferry in the Wairarapa (Palmer 1982) and Pullar (1980) described tephric loess derived from pumice of the Taupo Tephra Formation in the Rangitaiki River valley.

In the Manawatu dust can be observed blowing from the Manawatu River flood plain during storms. The sand mineralogy of the present day Manawatu River sediments has a quartz:feldspar:lithics ratio similar to the post-glacial loess so the flood plain is a possible loess source. Micas are common in the present overbank deposits from the river however, and river sediment clays are currently dominated by micas (J.G. Churchman *pers. comm.*). A source with a relatively high mica content would be expected to produce loess with a high mica content, particularly if one considers the ease with which a platy mineral like mica can be lifted (Souster *et al.* 1985) and the forest present at this time would have provided an excellent loess trap. The scarcity of micas in the post-glacial loess at the Tokomaru site may be due to either:

(1) Weathering - micas may have been removed by weathering. It has been argued above however, that this is not the cause of the dearth of micas in the Ah to Btg1 horizons and data of Parfitt *et al.* (1984) indicate that micas are even absent in the Ap horizon.

(2) Non-deposition - Souster *et al.* (1985) show that for grain sizes >20 µm the relative proportion of micas in loess increases with distance from source because micas tend to

be transported further than other mineral grains. Notwithstanding the trapping ability of the forest, micas may have blown beyond the "Pollok's Pit" site which is quite close to source.

(3) Proximity of any accumulation site down wind from extensive, sparsely vegetated flood plain areas.

(4) Scarcity of micas in the loess source.

Rhyolitic glass with chemistry similar to that of the Aokautere Ash reappears in the post-glacial loess. There are no known tephras with similar chemistry to the Aokautere Ash after 20 ka. B.P. so this glass must represent recycled material. Glass is fragile and would not survive abrasion in the river and Lithgow (1986) did not record glass in the sand fraction of the Manawatu River sediments. The source of the glass in the post-glacial loess must therefore have been relatively localised.

Based on these factors it is suggested that the major sources of the post-glacial loess are (1) the thinly vegetated cliffs that were exposed in the valley as the river was downcutting, and (2) the river flood plain. Such cliffs are common in the Manawatu River valley and its tributaries (e.g. the Tiritea valley) today. In the Rangitikei River valley Milne (1973) also considered the exposed valley sides might be local sources for loess. The slightly coarser nature of the post-glacial loess, even with reduced wind intensities can be reconciled if the following points are considered:

(1) much of the energy used in transporting dust is expended in lifting grains from a surface (Bagnold 1973; Thorson and Bender 1985) so where this energy is not required e.g. when grains fall naturally from a cliff, weaker winds may transport larger grains;

(2) the orographic effects of the cliffs might increase wind speeds locally. A.S. Palmer (*pers. comm.*) reports observing quartz granules being blown from cliffs onto terraces in the southern Wairarapa.

If valley-side cliffs are considered the dominant source of the post-glacial loess in the Manawatu then the loess should be slightly more mature than the Ohakean loess. Increases in quartz content are thought to reflect increasing maturity in sediments (Folk 1974) so the slight increase in quartz content and decrease in lithic content in the post-glacial loess are compatible with increasing maturity. Similarly the slight increase in the Zr content in the post-glacial loess could be interpreted as representing a more mature parent material for this unit.

THE PALAEOSOL IN THE OHAKEA LOESS

The Tokomaru marine bench and coverbeds form an extensive terrace out of which numerous valleys and gullies have been eroded (Hesp and Shepherd 1978). Towards the head of one of these gullies (GR T24/344886) there is a disconformable relationship between the upper *c.* 60 cm and the underlying loesses which contain the Aokautere Ash (Fig. 4.27). This upper unit is inclined at a shallow angle on the gully side and shows an apparent constancy and continuity of pedological horizons from the terrace tread into the gully. Charcoal is restricted to the top 10 cm of the upper unit, and this, together with an absence of organic debris throughout the top 60 cm in the gully, indicates that the mass movement events described in the area by Jane (1980) probably have not affected this profile. This unit was not emplaced by mass wasting processes but rather is a unit mantling the contours of the landscape. It is thought to be of aeolian origin and is correlated with the post-glacial loess identified in the present study. If this correlation is correct then there was a significant hiatus between the Ohakean and post-glacial loesses during which time there was erosion of the Ohakean and older loesses.

In the previous sections it has been demonstrated that the loess sequence being studied consists of a post-glacial loess overlying Ohakean loess in a disconformable relationship. In the Tokomaru soil at Pollok's Pit there is a transition zone between *c.* 50 cm depth and the cap of the fragipan at *c.* 80 cm (the Btg2 horizon) where the mineralogical and chemical trends change from those of the Cxg and Cwg horizons, which have reasonably constant properties, to those typical of the post-glacial loess. The samples immediately below the post-

Figure 4.27: A thin layer of post-glacial loess (above arrow heads) unconformably overlying older loess units. The Aokautere Ash is visible at the level of the horizontal line to the left.

glacial loess have the highest clay content of the soil (note also the increased aluminium, titanium and vanadium levels which are related to the clays). They happen to correspond to the two samples in the sequence prepared for the phytolith studies where there were significant nondescript fragments of biogenic material. These fragments may represent highly corroded biogenic silica.

In other areas of New Zealand a disconformity is commonly preserved in deposits that were laid down during the transition from stadial to post-glacial conditions. In the vicinity of Mt. Egmont a soil is developed below a disconformity of similar age to that described above (Franks 1984). In Canterbury at Barrhill, Ives (1973) described a post-glacial loess (probably a correlative of that described here) that overlies an indistinct palaeosol developed in a deflated late Pleistocene loess. In wetter areas of Southland, Bruce (1973) recognised a poorly defined palaeosol below the modern soil and he reports that in drier areas this palaeosol is represented by a textural change. In central North Island there is evidence for a period of erosion and soil development at the end of the last stadial. There is therefore evidence from other areas of New Zealand for a period of soil development towards the close of the last stadial and it is here suggested that the zone of increased clay content below the post-glacial loess (i.e. the Btg2 horizon) is a relic of a soil that formed in the Manawatu at this time. This conclusion is supported by the clay mineralogy of Pollok (1974) which shows a marked increase in interstratified clays and heat collapsible 14 Å clays at 51 - 64 cm depth.

The tephric nature of the post-glacial loess and proximity of the buried soil to the present topsoil masks many of the chemical properties that have traditionally been used to identify buried soils (Runge *et al.* 1973; Tonkin *et al.* 1974; Childs and Searle 1975) but the trends of Fe, Ba and Y are informative. Down the profile the iron content of the soil increases towards the base of the post-glacial loess but decreases at sample T20 (top of Btg2) before increasing towards the base of the Btg2 horizon. These two iron maxima are interpreted as being related to two periods of iron mobility and precipitation. Childs and Searle (1975) demonstrated that there was an increase in the Ba content in the B horizons of palaeosols due to the presence of barite. The higher Ba content of the sands in sample T17 may be related to this phenomenon. Y levels are low in the A and B horizons and rise to a maximum in the Cxg (data from A.S. Palmer, *pers. comm.*, in the Wairarapa commonly show higher Y values in the top of C horizons). The increase in Y might reflect a relatively Y-rich parent material but the uniformity of soil Zr and sand Y distributions at this level tends to counter this possibility and there are no mineralogical or chemical trends similar to that of Y. Most commonly Y substitutes for Ca in phosphates (Taylor 1969; Lambert and Holland 1974) so the low Y values in the A and B horizons may be due to weathering of apatite and the leaching of Y. The high Y levels in the Cxg may represent Y released from the upper horizons during weathering. If the levels of Y in samples T5-T11 reflect the levels in unweathered loess, and the Y distribution was approximately uniform prior to weathering as indicated by the distribution of Y in the sands above the Aokautere Ash, then the amount of Y added to samples T13-T17 (area A in Fig. 4.21) approximately equals that removed from samples T18-T20 (area B in Fig. 4.21). It is proposed that Y added to samples T13-T17 represents Y released by weathering of phosphates in the very top of the Ohakean loess.

FRAGIPAN GENESIS

DEFINING PROPERTIES OF FRAGIPANS: Fragipans are sufficiently important soil features that they are used for classification in the US Soil Taxonomy at the great group level in Alfisols, Inceptisols, Spodosols and Ultisols yet there is still debate about what criteria should be used to define a fragipan (Grossman and Carlisle 1969; Smalley and Davin 1982; Veneman and Lidbo 1986). This problem has led to a diverse range of suggested mechanisms for fragipan formation (*e.g.* see Smalley and Davin 1982).

In pedology the concept of a pan involves an horizon that restricts root penetration. The term "fragipan" was introduced by G.D. Smith (Grossman and Carlisle 1969) to distinguish uncemented compact loam to silt loam soilpans from hardpans (cemented), clay pans (clay dominated) and duripans (silica cemented). Later Smith *et al.* (1975) introduced the term "densipan" to describe a dense albic horizon. The important factor differentiating a fragipan from the other soil hardpans is that it is hard but uncemented *i.e.* the apparent induration disappears on wetting as the material slakes or disperses. The range of properties of fragipans was extended to encompass indurated "drift" deposits by Fitzpatrick (1956, see also Fitzpatrick 1976 and De Kimp 1970, 1976) but more recently Mathews (1976), Romans (1976) and Avery (1980) concluded that at least some of the "fragipans" of Fitzpatrick (1956) failed to slake and were mainly cemented. Fitzpatrick (1976) acknowledged that "there are probably at least two different horizons that have been called fragipans hence the lack of agreement and confusion that exists". Recently Veneman and Lidbo (1986) stated that "there exists a clear need to better define the term fragipan".

Soil Survey Staff (1975) describe fragipans as compact loamy subsurface horizons of high bulk density which are hard to extremely hard when dry, and firm to very firm when wet. They are brittle when dry or wet. This definition is used here. In New Zealand fragipans or related massive horizons are integral parts of the yellow-grey earth soil group (Cowie 1984). Their physical properties are typified by:

(1) a low porosity (Scotter *et al.* 1979),
(2) a high bulk density, between 1.5 and 1.8 Mg/m^3 (Gradwell 1974; Scotter *et al.* 1979,
(3) a relatively well-sorted particle size distribution with a silt mode,
(4) columns that are polygonal in cross-section with grey veins (gammations) between the columns (Bruce 1972), and
(5) skeletal grains which are closely packed.

MECHANISMS OF FRAGIPAN FORMATION: The primary characteristics of fragipans are (1) high bulk densities, and (2) low porosities, both of which influence the drainage properties of any overlying horizons. The most plausible theories on fragipan formation involve either chemical pathways or soil desiccation processes to produce a high bulk density (see Grossman and Carlisle 1969; and Smalley and Davin 1982 for a detailed discussion of these theories).

Nikiforoff (1955) and Fitzpatrick (1956) invoked desiccation and freeze-thaw processes respectively to explain the increase in density. More recently Fitzpatrick (1976) and Langohr (1987) have developed the freeze-thaw principle further and suggest that in a permafrost environment, near-surface frozen ground draws water from deeper levels so compressing the layers at those levels and producing a high bulk density. Parfitt and Milne (1984) and Parfitt *et al.* (1984) working in New Zealand suggested that under a high soil-water deficit, plant root suction would desiccate the subsoil placing it under high compressive stresses and so produce compaction.

Investigators using dissolution techniques to study possible chemical pathways for reducing porosity in fragipans concluded that there were bridges of Si, Al and Fe between skeletal grains (Harlan *et al.* 1977; Hallmark and Smeck 1979; Veneman and Lidbo 1986; Bull and Bridges 1978). They also noted that there was a reduction in the number of voids in a fragipan compared with the underlying loess. Using the scanning electron microscope Norton *et al.* (1983) identified thin Si, Al and Fe coatings that they thought were probably acting as cementing agents although they acknowledged that clays had been rearranged and could be the binding agent. Grossman and Carlisle (1969) also favoured clays as the bonding agents but they did not exclude thin chemical films as possible bonding agents.

FRAGIPANS IN NEW ZEALAND: Fragipans in New Zealand have not been studied in sufficient detail to be able to determine if amorphous coatings are common but data of Kirkman (1973) and Parfitt *et al.* (1984) show that if amorphous Si, Al and Fe are present they are only minor. Barratt (1981) describes ultra thin pale coatings that "could act as cement" and the iron distribution (plus Ba and Y) in the Tokomaru soil indicates that there are increased levels of these elements in the top of the fragipan compared with lower horizons. The ease with which the fragipan slakes however indicates that the strength of any chemical coatings is easily overcome, so it seems improbable that they are major factors in fragipan strength. Any chemical coatings almost certainly post-date fragipan formation because where they have been identified they form thin coatings that cover grains that are already in a very dense configuration and so do not cause the densification. Barratt (1984) after studying the micromorphology of some New Zealand fragipans concluded that they resulted mainly from physical processes and it is here concluded that fragipans in New Zealand formed by some form of densification due to desiccation.

Although a systematic study of fragipans has not been undertaken in the present investigation, properties observed in the Tokomaru soil that may be pertinent to the origin of the fragipan include:

(1) A grain size distribution dominated by silts (mean grain size of 14 µm for the whole sample or 28 µm on a clay-free basis) but with significant clay content (15 - 17%).

(2) Joints divide the loess into polygonal columns and commonly extend for the full thickness of the Ohakean loess *i.e.* they are continuous from the cap of the fragipan through the Cwg1, Aokautere Ash and Cwg2 (Fig. 4.28).

(3) The top of individual columns (*i.e.* the top of the fragipan) often have a rounded cap (c. 10 cm thick) which is noticeably stronger than lower portions of the column. During the present study the initial disaggregation of samples taken from loess columns involved crushing with a hydraulic press, and although only qualitative it was noted that the sample from the cap of the fragipan withstood significantly higher pressures before yielding.

(4) Remnants of the fragipan are discernible in the overlying Btg2 horizon.

(5) Loess from the fragipan slakes readily in water. This happens when small exfoliation bursts occur from ped surfaces. There is often no accompanying release of gas.

(6) Chemically the fragipan is relatively homogenous for the major elements except for an increase in Fe in the cap of the pan. There is more variation in the trace elements

Figure 4.28: Well developed columnar structure formed in loess near the Tokomaru site. The Aokautere Ash is at the level of the arrowheads.

with V increasing towards the cap while there are higher values for Y in the centre of the fragipan. The sand fraction Ba content increases in the cap.

To establish how the fragipan forms it is important to establish a time frame within which the process occurred. The Tokomaru soil profile is capped by a post-glacial loess which is underlain by a Btg2 horizon, here interpreted as a buried soil that formed *c.* 12 ka B.P. The Btg2 incorporates fragments of the fragipan and is continuous with gammations that fill joints in the fragipan, so the major features of the fragipan were probably established by this time, (although it is acknowledged that expansion and contraction within the gammations continues today). Raeside (1956, 1964a, 1964c) and others (see Bruce 1984) also inferred that the fragipan was an inherited feature.

The opening of joints that are polygonal in plan section is a common natural phenomenon in geological materials, e.*g*. mudcracks (Dunbar and Rodgers 1958), sandstones (Splettstoesser and Jirsa 1985; Kocurek and Hunter 1986), surface sediments of arid regions (Hunt *et al*. 1966; Neal *et al*. 1979; Alaily 1986), columnar jointing in igneous rocks (Press and Siever 1974; Healy 1982; Tarbuck and Lutgens 1984) and fragipans. In igneous rocks these joints are thought to be the result of shrinkage due to cooling and where they occur in sediments they are interpreted as the result of shrinkage and densification due to desiccation. Langohr (1987) has argued that the joints in fragipans are the result of permafrost and ice wedges. In New Zealand, however, this is an unlikely pathway because it is improbable that there was permafrost at this altitude in New Zealand during the Ohakean. M^{c}Glone (1985) and Soons (1976) have estimated that there was a temperature depression of between 6^{o}C and 4^{o}C during the last stadial. Furthermore, joints and gammations in New Zealand loesses are never as wide as similar types of features formed from ice wedges. Fitzpatrick (1976) agreed that New Zealand fragipans lack some of the ancillary features associated with permafrost and concluded that the polygons in many European pseudogleys and New Zealand yellow-grey earths were the result of shrinkage.

It is improbable that plants caused desiccation and development of the fragipan as the loess accumulated, (Parfitt and Milne 1984; Parfitt *et al.* 1984) because:

(1) The contraction joints are continuous across the Aokautere Ash so the Ohakean loess has probably acted as a whole unit during the desiccation and compaction process and the deeper levels would be beyond the reach of the plant roots.

(2) The Aokautere Ash does not appear to have fallen down the joints as might be expected if the fragipan formed when the ash was only thinly covered by loess.

(3) A report by M^{C}Intyre (1975) on the P distribution in a yellow-grey earth 15 km south of "Pollok's Pit" showed a similar P distribution to that in figure 4.20. The P in the stadial loess had not been translocated by vegetation as has happened in the Btg horizons and the P in the C horizons is dominated by inorganic P i.e. it is relatively unweathered. The unweathered nature of the phosphorus at this level is also demonstrated by Blakemore (1984) and suggests that there had been minimal weathering during loess accumulation. It has been argued above that there was probably minimal biological activity while the loess accumulated. Micromorphological data of Barratt (1981, 1984) also indicate that the fragipan formed when weathering and biological activity were at a minimum, so the vegetation was probably sparse.

(4) If this desiccation theory applied today to loess deposits, a fragipan should perhaps be developing under the Barrhill fine sandy loam. This does not appear to be occurring.

A MODEL FOR FRAGIPAN FORMATION: The desiccation and densification exemplified by mudcracks is here used as a model for fragipan formation. The model invokes natural drying to impose the stress that results in densification.

In well-sorted material like loess, densification and low porosity cannot occur unless there is finer grained material or some form of chemical "cement" to seal off the pores. The grain size distribution in the Tokomaru fragipan is dominated by silts but there is significant clay content. Many investigations (e.*g*. Syers *et al*. 1969; Smith *et al*. 1970; Windom 1975; Duce *et al*. 1980; De Angelis *et al*. 1987) have shown that aerosolic dust contains clays, and the upper horizons of the presently accumulating Barrhill fine sandy loam contain *c*. 13% clay. Whalley (1979) and Derbyshire (1983) have identified silt-sized aggregates of clay-sized minerals in loess and the 15-17% clay in the fragipan of the Tokomaru soil is thus interpreted as being aeolian in origin. The fragipan parent materials were thought to comprise silt-sized mineral grains (with or without clay coatings) and silt-sized clay aggregates. This material accumulated under relatively dry conditions with very low biological activity, but the actual nature of the environment is little understood. It is difficult to envisage how loess or ash is stabilised in the landscape during windy conditions and with limited vegetation. It may be that the limited vegetation was of a form that produced a canopy that provided shelter from the wind but without significant surface activity.

At some stage the loess becomes wetted. This may have been a repeated process during accumulation and therefore explains why the loess was trapped. There could not have been many cycles of significant wetting then drying however, as this would probably have produced repeated dispersion cycles and under such conditions the voids in the Aokautere Ash might be expected to fill with translocated clays and silts when the ash was thinly covered with loess. For example, at the present time tile drains in the Btg horizon may fill with silt and clay. The pumice lapilli in the Aokautere Ash only contain minor illuviated clays and silts. During the wetting the silt-sized clay aggregates collapse and are redistributed as clay coatings or bridges between the coarser grains. Dispersion may have been assisted by the presence of cyclic salts which were more common constituents of aerosols during stadial periods than during the Holocene (De Angelis *et al*. 1987) and would have been deposited with the loess. Consequently the density is increased and in the process many of the airways are blocked to produce closed voids. This gives a wet homogenous unit and natural drying results in a columnar polygonal shrinkage pattern and increased density similar to those formed by mudcracks (see Fig. 2 in Bishop *et al.* 1984). As a consequence of the lack of bioturbation because of the low biological activity, high densities may be maintained at comparatively shallow depths. The drying phase further increases the density due to the forces induced by the low matric potential (Croney and Coleman 1953; Croney and Jacobs 1967). This process may also pressurise the closed voids and explain the bursts which release material from the loess surface on rewetting.

It is difficult to determine the conditions and time required for fragipan formation. Columnar structures have been recorded such as figure 4.29 developing under present climatic conditions in a matter of months rather than years (J.A. Pollok *pers. comm.*) and in a similar time frame polygonal structures are produced from the dewatering of loess slurries from German coal mines (J.A. Pollok *pers. comm.*).

It has been shown above that there was a period of erosion and pedogenesis when the climate improved at the end of the deposition of last stadial loess. This probably happened before colonisation by the forest. It is here suggested that it was during this time that the final properties of the fragipan developed due to natural drying. The fragipan is now being destroyed during the current phase of pedogenesis.

YELLOW-GREY EARTH AND YELLOW-BROWN EARTH/YELLOW-BROWN LOAM INTERGRADE RELATIONSHIPS

In New Zealand, soils derived from loess embrace a wide range of morphological, physical and chemical characteristics ranging from brown-grey earths (more arid environments) through yellow-grey earths to yellow-brown earths (more humid environments). In the Manawatu

Figure 4.29: These columnar structures developed in a few months in a spoil heap left after building foundations were excavated. Photographer Dr. J.A. Pollok.

district a transition occurs between the yellow-grey earths and intergrades between yellow-brown earths and yellow-brown loams (soils formed mainly from volcanic ash parent materials). The two soil groupings can be found on the same terrace, have similar textures (dominated by silt), similar age and apparently formed from similar parent materials, yet have dramatically contrasting properties (see Neall 1982, and Bruce 1984).

The yellow-grey earths of the Manawatu typically have a fragipan with high dry bulk densities (1.5 - 1.85 Mg/m^3) and very low permeability (Gradwell 1974, 1978; Scotter *et al.* 1979). Thus they become waterlogged in winter to produce reduced, pale, grey B horizons (often with large iron concretions). They have "yellow" C horizons with orange mottles. The soils that are classified as being intergrades between yellow-brown earths and yellow-brown loams (hereafter referred to as YBE-YBL) have moderate dry bulk densities (1.2 - 1.5 Mg/m^3), are permeable, do not have a fragipan and have brown B and C horizons, i.e. have a more uniform profile form. YBE-YBL are free draining with significantly more ferrihydrite and allophane distributed uniformly throughout the profile, creating greater macroporosity which maintains free drainage. Further, they are commonly found in areas with slightly more rainfall and at slightly higher elevations than the yellow-grey earths. The fundamental difference between the yellow-grey earths and the YBE-YBL is the impeded drainage of the former caused by a comparatively impermeable fragipan.

PAST EXPLANATIONS: Milne (1973) suggested that the difference between the two soil groupings was caused by summer drying which produced a dense subsoil in yellow-grey earths. Later he completed a detailed map of the transition between yellow-grey earths and YBE-YBL (Milne 1981) and showed that the soils were juxtaposed in an irregular, interdigitating pattern. He proposed that local site factors had an influence in developing this pattern and that these factors acted early in pedogenesis to force the system along either a YBE-YBL or yellow-grey earth weathering path. Vegetation was a possible factor and Milne (1981) suggested that the area which is at an elevation of *c.* 200 m straddled the Pleistocene tree line and that the yellow-grey earths developed under shrubs and trees and the YBE-YBL under tussock. Vegetation may have been a factor but, judging from the palynological evidence in Taranaki and south of Levin, the last stadial vegetation on the low terraces in the region was probably dominated by grasses with minor scrub (e.g. *Dacrydium bidwillii*, *Dracophyllum*, *Leptospermum* and *Hebe*) and rare forest trees (*Nothofagus menziesii*) (M^c^Glone and Neall *pers. comm.*; M^c^Intyre 1970). According to Fleming (1979) the Manawatu was beyond the forest vegetation zone during the last stadial. The uniform and relatively low phosphorus content of the YBE-YBL subsoils yet high proportion of organic P (Anon. 1981), the more disrupted nature of the Aokautere Ash, and the less contrasting nature of YBE-YBL soil horizons in successive loessial units indicate a significant degree of mixing or biological activity during accumulation. Such mixing is more compatible with a scrub or bush environment. At least one member of the soil fauna, worms, are more numerous under forest vegetation and almost absent in dry tussock vegetation, especially during stadial conditions (Lee 1959). If the presence or absence of forest was a determining factor then it is more probable that the YBE-YBL formed under bush.

Parfitt and Milne (1984) and Parfitt *et al.* (1984) attributed the differences between the soils to increasing impermeability towards the yellow-grey earth end member. They proposed that desiccation and densification was induced by hydraulic suction from plant roots during periods of high soil-water deficit. As discussed above, this particular mechanism does not adequately explain some features of fragipan formation and it cannot easily account for the complexity of the boundary relationship to the YBE-YBL soils. The theory also requires that the subtle variations in soil-water deficit observed at the present time operated during the last stadial. This is unlikely given the different wind regime probably operating during that period and the changed environmental conditions consequent upon a lowered sea level.

A MODEL TO EXPLAIN THE YELLOW-GREY EARTH, YELLOW-BROWN EARTH/YELLOW-BROWN LOAM INTERGRADE RELATIONSHIP: Where a terrace is covered by multiple loess units the repetitive occurrence of either yellow-grey earth or YBE-YBL soil profiles suggests that once a particular soil formation pathway is established it is maintained. Only one exception has been observed; 4 km south of Massey University a yellow-grey earth profile has developed after a possible YBE-YBL profile precursor.

Many parameters (e.g. morphology, chemistry, mineralogy and physical properties) indicate that yellow-grey earth formation results in an efficient differentiation into horizons and that this pattern is repeated for each new cycle (e.g. Dashing Rocks, Timaru), whereas in the YBE-YBL there is much less differentiation into horizons within loess cycles and even between cycles. The distribution of phosphorus in YBE-YBL profiles emphasises this. In the Dannevirke and Kiwitea silt loams (Anon. 1981) and Shannon silt loam (M^{c}Intyre 1975) much of the phosphorus in the profile is in the upper horizons with subsoils and palaeosols having low and uniform phosphorus levels. This is in contrast with the yellow-grey earths where phosphorus distribution is more variable. Here P is relatively high in topsoils and palaeosols, decreases markedly in B horizons, but increases to a constant level in C horizons (Fig. 4.20; see also Childs and Searle, 1975; M^{c}Intyre 1975). If the soils originally had similar levels of phosphorus, and phosphorus in topsoils represents P translocated to the surface by biological activity while the loess was accumulating, then YBE-YBL have probably undergone more active pedogenesis throughout all stages of accumulation than yellow-grey earths. This conclusion is supported by the form of the phosphorus because in the C horizons of the yellow-grey earths the P is dominantly inorganic P while at deeper levels in the YBE-YBL organic P is a higher proportion of total P.

This continual pedogenesis may also explain why the Aokautere Ash tends to be more diffuse in YBE-YBL profiles compared with in the yellow-grey earths. In contrast the yellow-grey earths have experienced more stop-start cyclical pedogenesis. Therefore although the conditions that produced the yellow-grey earths (fragipan formation) are repeated at the end of each stadial, the factors that lead to the YBE-YBL path were established at the first appearance of YBE-YBL in a sequence of loesses and were maintained to the present.

To investigate the factors that lead to the formation of the YBE-YBL it is necessary to search for the first level where similar aged loesses develop along YBE-YBL or yellow-grey earth weathering paths.

In the Manawatu the cycle of YBE-YBL soil formation begins with a tephric palaeosol on comparatively well-drained sands or gravelly alluvium and the allophane and ferrihydrite present produced a free-draining soil. The volcanic centres of Egmont, Tongariro and Taupo have erupted intermittently at least since the Tokomaru marine bench was cut (Latter 1985) so have probably regularly supplied tephra dustings to the region. It is proposed that there was slightly increased weathering and biological activity in the YBE-YBL, even during stadial periods so even though the accumulating loess was probably mainly quartzofeldspathic the weathering of the occasional tephra provided sufficient allophane and ferrihydrite to maintain good drainage. Both allophane and ferrihydrite are highly reactive and have large surface areas so small amounts have a disproportionate effect on the soil. Parfitt *et al.* (1984) report 1-5% allophane in YBE-YBL in the Manawatu (excluding the influence of the Aokautere Ash) and based on Fe_{ox} it has been estimated that there is 1-3 % ferrihydrite (C.W. Childs *pers. comm.*)

In contrast the formations underlying the basal yellow-grey earth in a sequence of yellow-grey earths is often relatively impermeable or poorly drained. In the Rangitikei River valley the yellow-grey earth sequences are frequently underlain by thin layers of aggradational gravels that rest on impervious mudstones. Judging by the seepage from along the contact between these gravels and the mudstones, the gravels have a shallow water table and are poorly drained. Although many yellow-grey earth sequences are underlain by the highly permeable Otaki Sandstone in the Manawatu, the loesses are often separated from the sandstone by silts or are underlain by silty alluvium so that they are initially poorly drained. Once a yellow-grey earth weathering path has developed, tephras falling on this surface during an interstadial will be subjected to redox reactions. Iron is translocated to form concretions while the aluminium and silicon form halloysite (Milne 1981; Parfitt *et al.* 1984). Allophane is absent from the Tokomaru soil (except in the Aokautere Ash) and there is less than

0.5% ferrihydrite in the B and C horizons. During stadial periods the tephras are "sealed" in the loess at the position where they fall and there is little weathering or translocation.

At the site where there is a switch in the sequence of soil formation the change is from a YBE-YBL type to a yellow-grey earth. Although this section has not been studied in detail the change occurs at a level where there is a particularly reduced and clay-rich layer. This may have reduced the drainage and initiated a yellow-grey earth sequence.

The theory suggested here to explain the origins of the differing weathering paths maintains that the YBE-YBL path has been followed at least since soon after the Tokomaru bench was cut, whereas the yellow-grey earth path has been re-established at the end of each stadial cycle. Like Milne (1973) it is suggested that flora may have influenced the soil patterns. It is proposed that the YBE-YBL parent materials which were darker (warmer), freer draining (promoting longer growing cycles) and with higher phosphorus were more favourable for some specific flora-fauna association compared with yellow-grey earths. These slight site advantages would be maximised during the stadial periods. It is not possible to ascertain if the interdigitating relationship of the soils in the boundary area is solely a function of the present pedogenesis or a relic feature, but under the scenario developed above it is proposed that the complexity of the boundary relationship is an inter-relationship between the flora-fauna association and drainage.

SEDIMENTATION HISTORY OF THE TOKOMARU SOIL

The history of sedimentation revealed in a deep sea core from 120 km east of Cape Turnagain (Stewart 1982) may be relevant to the history of the Tokomaru soil. Close examination of the mineralogical components at the level of the stadial/Holocene transition in this core shows that there were two stages in the change at the boundary. Initially there was a marked reduction in accumulation rate at *c.* 14.2 ka (after the Rerewhakaaitu Ash). A decrease in quartz content in the coarse and fine silts at *c.* 12 ka. (after the Waiohau Ash) is here interpreted as reflecting a reduction in the aerosolic component of the sediments. After *c.* 12 ka the sedimentation rates were relatively low and uniform. These data indicate that changes in environmentally sensitive factors may not have been synchronised. Absence of synchronisation of changes in sediments at the stadial/post-glacial transition is substantiated by recent data from separate marine cores east of the North Island (R.B. Stewart *pers. comm.*) which show a change in *Globigerina bulloides* and *Neogloboquadrina pachyderma* c. 40 cm above the major colour change in these cores. Furthermore, data from Antarctic ice cores (Petit *et al.* 1987; Raisbeck *et al.* 1987), Tierra del Fuego (Heusser and Rabassa 1987) and the North Atlantic (Ruddiman and M^{c}Intyre 1981) indicate that there was an inflection in the general trend of climatic amelioration at the end of the last stadial. The marked change in sedimentation rates at 14.2 ka has been interpreted as reflecting the southward migration of the westerly wind system (Stewart and Neall 1984) marking the beginning of a climatic amelioration while the change at *c.* 12 ka is here interpreted as reflecting the termination of the loess source due to the rising sea level or spreading forest. In the Tokomaru soil there is a reduction in microfossils and sponge spicules and increase in forest phytoliths at 50 cm and this has been interpreted as reflecting a change in sea level and/or afforestation. Furthermore, as well as the change in biogenic silica at 50 cm depth there is a reduction in mica content and slight increase in sand content. Griggs *et al.* (1983) record a similar reduction in micas and increase in sands in the Holocene sections of marine cores east of the South Island. The age of the level where this change occurs is c. 12 ka, after adjusting for the effects of sediment bioturbation (Stewart 1982).

In the Manawatu a combination of ameliorating climate and a reduced accumulation rate led to the development of a soil at the close of the Ohakean sub stage. If the correlation between the loess and cores is sound then loess was still accumulating at this latitude at *c.* 12 ka. This is inconsistent with an absence of loess above the Rotoaira Lapilli (13.8 ka B.P.) from an area southeast of Lake Taupo (Topping 1973; Froggatt and Solloway 1986) or above the Rerewhakaaitu Ash (14.7 ka B.P.) north of Taupo (Kennedy 1982). Thus loess ceased accumulating in the central North Island earlier than in the southern North Island.

ACCUMULATION AND SEDIMENTATION RATES

As a result of the Deep Sea Drilling Projects there have been numerous investigations studying the palaeontology and sedimentology of marine cores to identify trends in palaeoceanography and palaeoclimatology (Burn *et al.* 1973; Kennett *et al.* 1975, 1985; Stewart and Neall 1984; Nelson *et al.* 1985). Variations in the biogenic components of marine sediments (silica and carbonate content) are interpreted in terms of changes in productivity due to variations in the nutrient status of water masses, while variations in the aerosolic dust accumulation and sedimentation rates have been interpreted either in terms of changes in source areas (marine transgressions inundating or afforestation stablising source areas) or changes in transport mechanisms (shifts in wind patterns).

After correlating features in the Tokomaru soil profile with events for which there is temporal control it is possible to determine sedimentation rates (thickness of sediment/time, cm/ka.) and accumulation rates (weight of mineral flux, $gm/cm^2/ka.$) for the loess parent materials. The temporal controls used include:

(1) the Aokautere Ash (20 ka at 2.21 m depth),
(2) the changes in mineralogy (micas), grain size (sands), and inversion of the dominance of marine microfossils over phytoliths (12 ka at 50 cm depth),
(3) the tentative correlation of the tephra dusting at 1.15 m with the Rerewhakaaitu Ash (14.7 ka), and

(4) the increase in volcanogenic materials toward the top of the profile (10.5 ka at 40-50 cm depth).

It is unrealistic to expect changes in sedimentation rates (and resultant accumulation rates) to be isochronous with tephras, and the major changes at tephras may be relics of these temporal controls, so the distribution pattern should be smoothed across these zones. Changes that occur across boundaries that have environmental significance (e.g. changes in biogenic component, changes in the distribution of the detrital components), or general trends within a zone of uniform sedimentation rate are more representative of real changes or trends in accumulation rates.

The sedimentation rates for the Tokomaru soil range from 4.55 cm ka $^{-1}$ for the post-glacial loess to 50 cm ka $^{-1}$ for Ohakean loess. Sedimentation rates in loess are very dependent on proximity to source, so rates from different areas are not directly comparable, but the ranges of rates from the Tokomaru soil are similar to those from other areas of New Zealand (calculated from Bruce 1973; Kennedy 1982), United States (Ruhe *et al.* 1971; Kleiss 1973), and marine cores east of New Zealand (Stewart 1982; Griggs *et al.* 1983; Nelson *et al.* 1985). Historic sedimentation rates on the Canterbury Plains (Cox *et al.* 1973; Ives and Stevenson 1973) are 2-7 cm ka^{-1}.

Quartz accumulation rates in the Tokomaru soil (Fig. 4.30) are higher than those from a marine core east of Cape Turnagain (Stewart and Neall 1984). The much higher rates for the Tokomaru soil 63-20 µm fraction which represents the loessial component of aeolian materials (Bagnold 1941; Ruhe 1969; Jackson *et al.* 1971) are a reflection of proximity to source. This conclusion is supported by the grain size data which shows that the modal interval for the soil profile is 28 µm while that of the core is finer (*c.* 8 µm). The rates for the 5-2 µm fraction from both sources are similar, reflecting the more global nature of this aerosolic component (Rex and Goldberg 1962; Walker and Costin 1970; Jackson *et al.* 1971, 1973).

The distributions of quartz in the 63-20 µm and 5-2 µm fractions are taken to represent the loessial and aerosolic dust components respectively. These demonstrate that there is an increasing

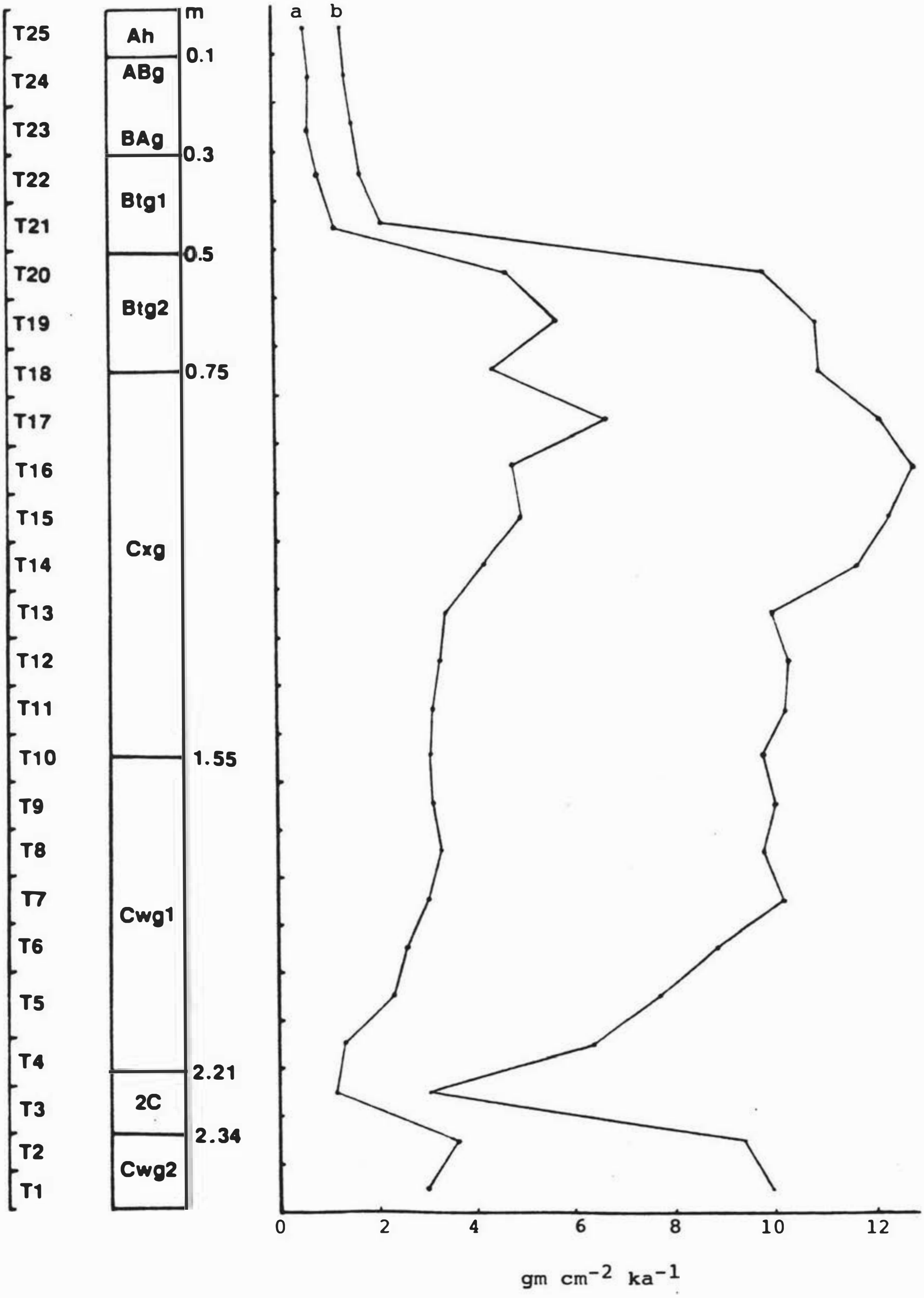

Figure 4.30: Quartz accumulation rates in the fine silt (a) and coarse silt (b) in the Tokomaru soil.

accumulation rate towards the end of the Ohakean stadial before a dramatic drop to Holocene accumulation rates (Fig. 4.30). These results are consistent with the documented increasing rates of aeolian sedimentation towards the end of the last stadial in North America (Ruhe *et al.* 1971; Kleiss 1973), in tephric loess in Taranaki (B.V. Alloway *pers. comm.*) and in marine sediments to the east of the North Island (Stewart and Neall 1984). In the Tokomaru soil the highest rates occur between 14.2 ka and *c.* 12 ka. Data in Stewart (1982) also show that sedimentation of the terrestrial components in a marine core east of Cape Turnagain continued at a relatively high rate until approximately 12 ka when a Holocene rate began. Major factors that may contribute to the increases towards the end of the stadial include: (1) increased source area, (2) increased severity of the transport mechanism, and (3) increased sediment supply. In the South Island the glacial maximum occurred at *c.* 18 ka. (Suggate and Moar 1970; M^{c}Glone 1985) and sea level began to rise after this time so an increased source area is improbable. Stewart and Neall (1984) have suggested a contraction in the circum-polar wind system as part of the amelioration at approximately this time, so an increasingly severe wind system is a doubtful cause of the continuing high accumulation rate. It is concluded that the increasing rates reflect increasing sediment supply. East of the Ruahine Range Hubbard and Neall (1980) and Marden *et al.* (1986a, 1986b) concluded that large volumes of gravels were moved during a period towards the culmination of the Ohakean. Richmond (1962), Wellman (1972), Ives (1973) and Tonkin *et al.* (1974) theorised that the maximum loess accumulation should be associated with the recessional stage of a glacier and the data presented here supports this thesis.

During the last stadial, mass movement and solifluction processes were common in the southern North Island and valleys probably infilled with debris because of a declining load:discharge ratio of the rivers brought about by the lowered rainfall. The climatic amelioration increased rainfall before the expanding forest stabilised the land surface and the debris was flushed down the valleys to form broad unstable aggradation surfaces which were the source of the loess. Eventually a rising sea level, expanding bush cover and a diminution of source material curtailed the high loess accumulation rate at c. 12 ka B.P.

CHAPTER FIVE

SUMMARY AND CONCLUSIONS

CRISTOBALITE GENESIS

1. **Cristobalite origin**: This study has shown by means of oxygen isotope analysis, degree of mineral crystallinity, and grain morphology that cristobalite has not formed *in situ* in the soils investigated here. These data indicate that the cristobalite crystallised at a relatively high temperature, consistent with magmatic origins.

2. **Tridymite**: XRD spectra from silt fractions of the soils indicate that cristobalite is usually accompanied by tridymite. Although some of the tridymite may occur as a discrete phase, SEM studies suggest that it more often occurs intimately intergrown with cristobalite.

3. **Cristobalite sources**: Investigation of selected possible high temperature sources (tephras from the Taupo Volcanic Zone, lavas from the Egmont Volcanic Centre and hydrothermal deposits) indicate that cristobalite and or tridymite is common in hydrothermal deposits but only in <u>some</u> tephras and <u>some</u> lavas. Cristobalite and tridymite in the soils of the Hamilton basin are derived from the Taupo Volcanic Zone and have been transported to the region by aerial tephra deposition.

4. **Cristobalite distribution**: The variable distribution of cristobalite in topsoils is related to the dispersal pattern and depth of burial of cristobalite-bearing tephras.

5. **Cristobalite as a tephra tracer**: Cristobalite is deduced to be a stable phase in the pedosphere and this, together with the narrow grain size limits within which it occurs and the ease of beneficiation indicates that it may have a use as a tracer for tephras.

6. **Inorganic opal-A**: Inorganic opal-A (amorphous silica) has been identified from the Hamilton Ash Group zone of the Hamilton and Naike soils. Grain morphology indicates that this was formed in the soil and oxygen isotope data are consistent with this interpretation. Silica released during weathering of tephras develops into silica gels and desiccation of these gels produces opal-A.

TOKOMARU SOIL

1. **Tephric additions**: Based on chemistry, mineral proportions and mineral chemistry of the sand fraction in the Tokomaru soil, it is possible to identify pulses of tephric additions to the loess, and to identify their sources:

0-50 cm	0-11 ka	Mixed rhyolitic and andesitic tephras from the Egmont Volcanic Centre and the Taupo Volcanic Zone.
1.1-1.2 m	14.7 ka	Rhyolitic ash, possibly the Rerewhakaaitu Ash from the Okataina Volcanic Centre.
1.2-1.3 m	e[*] 15.2 ka	Andesitic tephra from the Egmont Volcanic Centre.
c. 1.6 m	e[*] 17 ka	Andesitic tephra from the Egmont Volcanic Centre.
c. 2.0 m	e[*] 19 ka	Andesitic tephra from the Egmont Volcanic Centre.
2.21-2.34 m	20 ka	Aokautere Ash, a major eruption from the Taupo Volcanic Centre.

[*] estimated age assuming a constant accumulation rate between the Aokautere and Rerewhakaaitu ashes.

2. **Biogenic silica**: In the Tokomaru soil there is a dramatic change in the form of biogenic silica down the profile with sponge spicules and microfossils prevalent below 50 cm and phytoliths dominant above this level. The change is interpreted to represent post-glacial afforestation and is inferred to have occurred at 11-12 ka. B.P. The dramatic change in biogenic silica morphology with depth suggests a potential use of phytoliths to investigate both spatial and temporal variations in vegetation in "normal" parent materials.

3. **Soil Stratigraphy**: Three stratigraphic units are recognised above the Aokautere Ash in the Tokomaru soil:

   (I) Post-glacial Loess - The upper 0.5 m, while still dominantly quartzofeldspathic, is characterised by increased rhyolitic glass, obsidian, volcanic lithics, volcanic minerals (which are mainly unetched), SiO_2, CaO, Zr, and decreased micas, greywacke lithics, TiO_2, Al_2O_3 , K_2O, Cr, V and Y compared with the underlying loess. The post-glacial loess has accumulated during the past c. 11-12 ka.

   (II) Quartzofeldspathic loess: Between 0.5 and 1.7 m there is more mica in the silt and sand fractions compared with the post-glacial loess and much less volcanogenic material compared with the adjacent units. Notwithstanding the general low volcanogenic contributions to this unit there are two distinct pulses of Egmont-derived tephra and a dusting of rhyolitic material with Okataina Volcanic Centre affinities.

   (III) Tephric loess: The zone between 1.7 m and 2.21 m (i.e. immediately overlying the Aokautere Ash) is one wherein there is a transition in mineralogical and chemical properties from those of the Aokautere Ash to those of the quartzofeldspathic loess, particularly in the coarser grain sizes. There is a pulse of Egmont-derived tephra at 2.0-2.1 m.

4. **Initial soil development**: While it is acknowledged that the Btg2 horizon is within the region where weathering is currently occurring, this horizon is interpreted as resulting from weathering that initially developed in the quartzofeldspathic loess at c. 12 ka B.P. It represents the soil that began to develop after the dramatic reduction in accumulation rates at about that time. There is also evidence for localised gullying in the quartzofeldspathic loess at that time.

5. **Fragipan formation**: It is inferred that the fragipan formed by a process that initially involved the wetting of material composed of well sorted silt-sized quartz, feldspars and clay aggregates, and the collapse of the clay aggregates to produce a close packed homogenous silt. Subsequent desiccation resulted in shrinkage cracks and columnar structures. The fragipan is inferred to have formed towards the end of the last stadial.

6. **Yellow-grey earth to Yellow-brown loam/Yellow-brown earth intergrade relationships**: It is concluded that the complexity of the yellow-grey earth to yellow-brown loam/yellow-brown earth relationship is a function of drainage and a soil flora+fauna association. These two soils have developed along fundamentally different weathering paths:
   (I) Yellow-brown loam/yellow-brown earth intergrades are well drained low bulk density soils, where the formation of allophane and ferrihydrite has occurred essentially *in situ* as primary minerals weather so that they are evenly distributed throughout the profile.
   (II) Yellow-grey earths are poorly drained and waterlogging is common so as the ferromagnesian minerals weather, Fe is translocated and precipitated at specific sites as mottles and/or concretions.

   Once these two soil patterns are established they tend to be maintained through different climatic cycles. To understand the paramount factors that govern which weathering path will dominate it is necessary to investigate the cover beds where the two paths were established, i.e. in most cases in the Manawatu, the Tokomaru marine bench. It is concluded that the initial drainage status is important in determining the weathering path and that once established a combination of drainage and a specific flora+fauna association maintains the separate paths. The complexity of the present boundary perhaps reflects competition between the two mechanisms.

7. **Variations in accumulation rates**: The quartz accumulation rates in the silt fractions demonstrate that there are increasing rates from the level of the Aokautere Ash up to the top of the quartzofeldspathic loess, with markedly higher rates between 14.7 ka and 12 ka. At the base of the post-glacial loess there is a dramatic reduction in accumulation rates. The loess that accumulated between 14.7 ka and 12 ka may not be related to cold climate conditions but rather to the increased supply of suitable source material.

8. **Chronology**: The following chronology is therefore suggested for the Tokomaru soil:

20-14.7 ka	Continued accumulation of loess from a quartzofeldspathic source with diminishing input from Aokautere Ash-derived glass and occasional dustings from eruptions at Egmont Volcanic Centre and the Okataina Volcanic Centre. All these aeolian materials fell on a surface where there was comparatively little biological activity. Towards the end of this period there was slow climatic amelioration.
14.7-12 ka	Increased climatic amelioration although the vegetation is still dominated by grass and scrub. There is large scale aggradation, possibly towards the end of this period. Within this zone there is an increase in quartz accumulation rates, either for the full period or towards the top of the zone.
12-11 ka	Dramatic reduction in quartz accumulation rates due to a reduction in source area. Erosion occurs near the edge of the Tokomaru terrace and there is increased biological activity and increased weathering. Forest expands over the area.
11 - 0 ka	Post-glacial loess accumulated from more restricted and localised sources. There are significant dustings from both the Egmont Volcanic Centre and Taupo Volcanic Zone.

Appendix 1: Grain size data for the Waiareka, Hamilton, Naike and Te Kowhai soils (gm).

Waiareka clay

Sample	W1	W2	W3	W4	W5	W6	W7
Initial*	139.00	109.80	126.10	95.10	114.20	86.10	145.70
+1 mm	-	-	-	6.4	-	28.25	42.63
1000-500 µm	1.27	2.05	4.00	4.43	17.62	6.73	31.42
500-250 µm	0.55	0.91	2.25	5.66	11.78	4.59	27.40
250-125 µm	1.65	1.68	2.95	4.90	8.75	4.75	16.64
125-63 µm	2.56	2.96	3.47	2.95	4.14	3.76	9.12
63-20 µm	9.54	9.83	7.16	5.90	6.96	3.62	2.91
20-5 µm	14.06	11.52	10.60	5.80	4.94	2.87	2.42
5-2 µm	3.06	2.69	2.33	1.06	0.68	0.54	0.43
< 2 µm	44.70	36.20	42.60	22.20	18.70	4.30	2.20
Sum	77.39	67.84	75.36	59.30	73.57	59.41	135.17

Te Kowhai silt loam

Sample	TK1	TK2	TK3	TK4	TK5	TK6	TK7	TK8	TK9	TK10
Initial*	71.00	72.40	79.70	68.60	69.80	85.80	76.20	71.50	96.00	105.80
+1 mm	0.11	0.08	-	tr	tr	0.41	0.05	tr	0.04	-
1000-500µ m	0.30	0.26	0.04	0.01	0.10	0.16	0.01	0.03	0.05	tr
500-250 µm	0.58	0.58	0.17	0.20	1.26	1.86	0.20	0.21	0.51	0.10
250-125 µm	2.05	1.98	1.19	2.15	7.50	6.82	2.07	2.65	6.31	3.64
125-63 µm	4.02	4.79	4.23	6.57	9.75	9.89	9.98	11.10	17.02	20.03
63-20 µm	8.50	8.30	13.50	10.60	11.90	12.26	14.70	16.43	17.20	24.30
20-5 µm	16.60	18.00	21.50	17.30	10.34	16.20	13.90	13.00	14.70	14.00
5-2 µm	3.70	5.60	4.90	2.60	1.66	2.30	1.70	1.60	2.00	1.70
<2 µm	13.70	14.30	15.20	12.60	9.60	11.90	9.50	4.50	7.40	10.80
Sum	49.56	53.89	60.73	52.03	52.11	61.80	52.11	49.52	65.23	74.57

Hamilton clay loam

Sample	R1	R2	R3	R4	R5	R6	R7	R8	R9	R10
Initial*	91.38	89.36	91.92	71.87	74.20	72.84	73.70	81.20	83.40	71.50
1000-500µ m	1.25	0.35	0.23	0.25	0.10	0.07	0.04	0.05	0.08	0.11
500-250 µm	1.30	1.27	1.18	0.50	0.51	0.20	0.20	0.20	0.26	0.42
250-125 µm	2.87	2.98	2.69	1.30	0.91	0.38	0.31	0.30	0.31	0.55
125-63 µm	4.18	5.08	4.60	2.17	1.44	0.64	0.44	0.38	0.26	0.58
63-20 µm	9.57	9.63	8.59	5.10	3.67	2.00	1.40	1.10	0.23	0.93
20-5 µm	15.94	17.55	15.39	9.50	7.28	3.80	2.59	2.00	1.76	2.24
5-2 µm	3.59	3.39	3.63	2.90	2.10	1.10	0.93	0.80	0.80	1.18
<2 µm	18.93	22.56	25.87	24.90	29.45	34.10	32.83	37.50	42.17	47.86
Sum	57.63	62.81	62.18	46.62	45.46	42.29	38.74	42.33	45.87	53.87

Naike clay

Sample	N1	N2	N3	N4	N5	N6	N7	N8	N9	N10
Initial*	110.00	94.20	86.40	70.90	70.60	80.10	91.60	78.90	83.20	73.90
+ 1mm	0.18	0.08	tr	tr	tr	tr	tr	tr	0.07	0.28
1000-500µ m	0.22	0.22	0.05	0.02	0.02	0.01	0.02	0.07	0.24	0.62
500-250 µm	0.57	0.52	0.21	0.09	0.05	0.09	0.08	0.14	0.44	1.10
250-125µ m	2.83	2.20	1.26	0.41	0.34	0.30	0.30	0.37	0.77	1.77
125-63 µm	3.03	2.31	1.33	0.51	0.48	0.56	0.65	0.67	1.22	2.09
63-20 µm	7.46	6.02	3.42	1.42	1.33	1.52	1.95	1.97	2.73	2.92
20-5 µm	16.06	12.85	7.48	3.99	3.71	4.58	5.12	4.80	5.39	6.58
5-2 µm	3.29	2.18	2.59	1.72	2.16	2.13	2.01	2.47	2.54	2.52
<2 µm	38.80	35.80	42.60	36.10	36.80	41.30	44.20	35.60	36.00	27.80
Sum	72.44	62.18	58.94	44.26	44.89	50.49	54.33	46.09	49.40	45.68

* Initial weight. tr - trace.

Appendix 2: Weight percent(cristobalite + tridymite) and quartz in the Hamilton, Naike and Te Kowhai silt and clay fractions.

	--- 63-20 µm ----			---- 20-5 µm -----			---- 5-2 µm ----			-- < 2 µm -	
	C+T	R	Q	C+T	R	Q	C+T	R	Q	C	Q
R1	18	14	28	25.0	73	34.6	27.1	64	24	8.8	3.9
R2	16	26	35	29.5	71	33.3	21.0	71	24	8.9	3.6
R3	11	26	40	30.2	79	32.7	25.0	76	23	9.1	3.5
R4	22	19	42	35.6	63	31.6	29.0	58	26	6.9	2.7
R5	20	38	43	37.9	70	31.0	16.1	65	22	5.7	2.0
R6	22	43	41	34.3	62	25.8	7.6	58	15	3.9	1.2
R7	26	52	30	31.0	71	19.8	16.0	66	11	3.0	1.4
R8	18	42	24	28.8	77	13.6	3.3	69	12	2.7	0.5
R9	14	54	22	20.3	35	12.5	7.0	48	10	1.7	0.4
R10	12	55	25	4.3	28	8.4	4.0	64	5	1.3	1.0
N1	10	24	46	26.0	72	42.5	15.4	83	33	5.9	4.1
N2	13	19	41	34.8	68	23.2	18.5	75	28	5.9	3.9
N3	11	42	45	23.8	67	32.9	16.6	72	18	2.7	1.4
N4	13	22	38	17.3	35	11.5	5.9	52	5.9	1.8	0.8
N5	10	33	27	10.7	38	6.3	4.5	58	3.1	1.2	0.3
N6	6	37	30	10.8	63	7.8	3.7	58	3.0	1.3	0.3
N7	6	38	34	9.4	63	13.0	2.3	56	3.4	1.8	0.2
N8	7	33	41	11.7	10	9.7	1.8	57	5.2	1.5	0.7
N9	6	33	40	12.1	50	13.2	4.4	60	7.8	1.6	0.8
N10	4	30	32	6.9	20	7.4	1.9	64	3.8	1.8	1.2
TK1	18	26	10	19.5	67	7.6	25.4	71	7.2	7.9	1.1
TK2	19	20	8	24.6	71	6.5	13.9	63	5.4	7.6	1.1
TK3	23	36	8	21.5	76	8.4	17.0	79	4.3	4.4	0.5
TK4	25	44	6	11.0	70	2.4	9.4	65	2.8	3.0	0.7
TK5	20	45	4	9.5	74	3.0	1.1	47	2.3	2.7	0.2
TK6	20	50	4	9.0	76	2.7	7.5	72	3.5	2.2	0.4
TK7	22	36	4	12.0	70	3	7.5	53	2.5	2.1	0.3
TK8	21	53	5	13.7	76	5.9	15.4	66	4.9	3.7	0.6
TK9	18	47	4	14.4	75	2.9	8.4	58	2.6	2.9	1.5
TK10	15	42	5	10.4	71	3.3	5.7	55	2.7	2.8	0.6

Q = Quartz; C = Cristobalite; C+T = Cristobalite plus Tridymite; R = C/(C+T) ratio.

APPENDIX 3: Description of the minerals identified in the Tokomaru silt loam.

(1) QUARTZ: Quartz occurs as discrete grains broadly in two forms: (1) rounded frosted grains (occasionally with dusty inclusions) that can be up to 3 mm in diameter. This form is of a sedimentary origin; (2) conchoidally fractured euhedral fragments or bipyramidal crystals, both of which often have glass selvedges and/or inclusions. This form is of volcanic origin. Quartz is also common in lithic fragments (see below).

(2) PLAGIOCLASE: Grains of plagioclase are divided into two broad categories:

(1) Slightly rounded, usually untwinned grains that have a relatively low refractive index (<1.54) and are commonly cloudy or dusty due to very fine-grained alteration products. This type has been albitised and is referred to as a sedimentary plagioclase;

(2) Clear, high relief, highly angular fragments or euhedral tabular crystals of a complexly zoned (normal, reverse and oscillatory zoning) plagioclase that varies in composition up to An_{80} (labradorite). They commonly have anomalous brownish interference colours, glassy re-entrants and selvedges of glass or volcanic lithic material. They frequently contain pyroxene, opaque and/or glassy (both clear or brown glass) inclusions. Occasionally the cores, which are usually more calcic, have preferentially weathered out in zones parallel to the optical zoning or grain outline. Within the silt-size fractions where fragments are usually not sufficiently large to be able to recognise zoning or inclusions two additional forms of plagioclase have been recognised. One is referred to as "low R.I. plagioclase", being composed of clear, low refractive index (approximately equal to that of the mounting medium) grains which often have grey

interference colours. These grains often have glass selvedges. The second form, referred to as "high R.I. plagioclase" is clear and has a relatively high refractive index compared with Canada balsam but without anomalous interference colours. This group also often has glass selvedges. Because of their obvious volcanic origin all of these forms of plagioclase are referred to as volcanic plagioclase.

Plagioclase is also common in lithic fragments (see below).

(3) MICROCLINE: Microcline occurs as clear to slightly dusty, rounded to subrounded (often approximately square in outline) single grains or as the coarser grains in a silty matrix of a greywacke lithic. No other potassium feldspar was identified on a routine basis.

(4) LITHIC FRAGMENTS: Lithic fragments of various types are common in the loess. Previous investigations of the sand and silt mineralogy of soils have employed grain mounts to determine the mineral content and so have not been able to unambiguously identify the various rock types. In this study thin sections were used enabling this difficulty to be overcome.

Grains that have been described as lithic fragments have been divided into three groups.

(1) The first group comprises sub-rounded silt to fine sand size quartz, quartz + feldspar or epidote in a clay to fine silt matrix. This matrix is composed of either colourless micas (sericite or illite) which are aligned and often draped over the coarser grains, or is an orange-yellow material (chlorite or vermiculite and iron oxide coatings). Occasionally the matrix is absent and the fragments are composed of interlocking quartz and/or feldspar and/or epidote grains. There are also rare chert and argillite fragments. This group is consistent with derivation from greywacke.

(2) The second form of lithic fragment is rare, occurring only in the top 10 cms of the profile. It is commonly oblate, up to 5 x 3 mm in size and grey under natural light. In

thin section it is seen to comprise mainly quartz and feldspar in a clayey matrix, cemented by an iron oxide in a very open spongey texture. It is different from concretions in the Btg horizons and is resistant to repeated deferration. But for the iron oxide cement the texture is very similar to that in the natural topsoil. Because of this factor and the association of this form of lithic with charcoal remaining from the original forest burning it is suggested that this form has resulted from soil fusion during this burning.

(3) The third form of lithic fragment comprises euhedral to subhedral silt sized plagioclase with or without opaque grains. Occasionally pyroxene or amphibole grains are present. Usually these minerals form a holocrystalline interlocking mosaic but a thin zone of glass may be present between grains. The mineralogy is consistent with derivation from a volcanic source and these grains are therefore referred to as "volcanic lithics".

(5) MICAS: Muscovite, biotite and chlorite form rounded slightly deformed flakes which, because they have strong electrostatic forces, are difficult to sample representatively. This problem is compounded as the pre-treatment given the samples may exploit any weathering-induced weakness in the micas and split thick flakes into thinner sheets.

Muscovite appears to be the most stable mica and forms clear buckled flakes which are almost isotropic but with a birefringent rim due to deformation and expansion at the edge of the flake. Biotite comprises pleochroic brown and green varieties which are often altered to chlorite. Like muscovite, biotites have deformed rims. Occasionally biotite is euhedral, undeformed and with a hexagonal outline. As well as occurring closely associated with biotite, a green variety of chlorite also occurs as distinct monocrystalline grains.

(6) EPIDOTE GROUP: For the purpose of the mineralogical analysis individual epidote group minerals were not differentiated from each other. "Epidote" occurs as rounded equidimensional colourless to pale lemon grains of high relief. "Epidote" as individual grains is relatively rare in the coarser grain sizes; it is more common in the silts. It is common, however, as the larger grains in greywacke lithics in the coarser fractions.

(7) CLINOPYROXENE: Clinopyroxenes form colourless to pale green grains that are often chemically and optically concentrically zoned and twinned. Grains often contain apatite, glass and opaque inclusions, and sometimes are partially enclosed by selvedges of glass or volcanic lithic material. In the upper portions of the profile (above c. 50 cm) clinopyroxenes form euhedral stubby crystals whereas at deeper levels they have very irregular outlines due to weathering and show coxcomb terminations and etched prism faces.

(8) ORTHOPYROXENE: Orthopyroxene is represented by pleochroic green to pink hypersthene that occasionally has dark brown oxidised ("burned") rims. Grains can contain glass and/or opaque inclusions and frequently have glassy selvedges. Like the clinopyroxenes the orthopyroxenes are euhedral in the upper portions of the profile (although more prismatic in form than the clinopyroxenes) and at depth are etched with coxcomb terminations.

(9) AMPHIBOLES: Although they are only a relatively minor component of the soil there is a wide variety of amphibole types. Pleochroic green-brown and green hornblendes are the common forms but there are minor red-brown oxy-hornblendes and rare blue-green varieties. Grains are occasionally twinned and are more commonly euhedral and less altered compared with the pyroxenes. They may contain glass and opaque inclusions and sometimes have glassy selvedges.

Rarely the amphibole is a twinned, non-pleochroic pale brown variety that has very thin (micron thick) transverse exsolution lamellae and a relatively low extinction angle. This amphibole may be cummingtonite, but none with a suitable orientation for positive optical identification was found.

(10) OPAQUES: The opaque minerals are magnetite, ilmenite and titanomagnetite or their oxidised equivalents. They are usually black but there are grains with thin orange oxidised rims. Their morphology can vary from rounded frosted grains through to perfect euhedral octahedra (titanomagnetite) or hexagonal plates (ilmenite). The euhedral varieties may contain glass inclusions or selvedges and, rarely, volcanic lithic selvedges. Some opaques are exsolved.

(11) VOLCANIC GLASSES: The term glass has been used for irregular, colourless, isotropic material that has a low refractive index. Where this material has a brown colour it is referred to as obsidian (glass and obsidian from the same sample are usually chemically equivalent). Grains form (a) keel or slightly curved platelette shapes derived from the breakup of glass bubbles, (b) irregular solid glass (or obsidian) forms with conchoidally fractured surfaces and (c) rounded pumice fragments where the vesicles are preserved. Where there is a high density of vesicles or the vesicles form long tubes the pumice grains have a translucent "white" colour. The coarser pumice fragments commonly have layers of clays deposited in the vesicles or silt grains trapped at constrictions in elongate vesicles. At the level of the Aokautere Ash and in the uppermost 50 cm of the profile the pumice fragments are up to 5 mm in diameter.

Where there are crystallites present in the glasses the adjective microlitic is used. These crystals are very fine prismatic grains of pyroxenes and amphiboles or more equant plagioclase and opaques. As the crystal content increases the microlitic glasses grade towards the volcanic lithic group.

(12) TRACE CONSTITUENTS: Minerals that have been identified in trace amounts include titanite, garnets (some with spiral trails of inclusions), zircons, tourmaline, allanite and (?)perovskite. Also cristobalite forms fine needles in close association with fibrous feldspar in pale brown grains with a fibro-radiating spherulitic texture similar to those in devitrified ignimbrites and rhyolites.

Rarely fossils (biogenic opal) were noted. These include spherical, cylindrical and disc-like radiolaria, sponge sterrasters and spicules, diatoms and plant phytoliths. A more detailed description of the phytoliths is given in chapter 4.

Appendix 4: Tokomaru silt loam grain size distribution (gm).

Sample	T1	T2	T3	T4	T5	T6	T7	T8	T9
Initial*	52.32	63.60	114.40	64.30	61.40	59.00	63.00	62.50	62.73
>500µm	0.01	0.02	1.50	0.04	-	0.01	0.01	-	-
500-250µm	0.01	0.13	5.90	0.29	0.11	0.04	0.01	0.01	0.01
250-125µm	0.08	0.34	10.76	1.37	0.49	0.20	0.12	0.07	0.15
125-63µm	2.21	2.31	12.29	4.61	3.05	2.59	2.74	2.72	2.99
63-20µm	30.70	31.20	40.40	31.80	31.30	31.30	34.10	33.00	34.70
20-5µm	8.70	9.00	25.30	10.90	8.40	8.50	8.30	9.50	9.00
5-2µm	1.70	1.80	2.90	1.70	1.70	1.70	2.00	2.10	1.80
<2µm	7.10	8.20	11.40	7.10	8.00	9.00	9.50	11.50	8.90
Sum	50.49	53.00	110.45	57.81	53.05	53.33	56.77	58.90	57.54

Sample	T10	T11	T12	T13	T14	T15	T16	T17
Initial*	67.70	66.00	56.00	59.10	115.30	62.70	67.30	62.10
>500µm	0.01	-	-	-	-	-	-	0.01
500-250µm	0.01	0.01	0.01	0.01	0.01	0.01	0.01	0.01
250-125µm	0.14	0.14	0.11	0.17	0.27	0.10	0.07	0.07
125-63µm	2.83	2.45	2.57	2.31	4.46	2.23	2.32	2.23
63-20µm	36.20	35.10	30.60	32.20	62.40	33.90	34.90	31.90
20-5µm	9.40	10.00	8.00	8.40	17.10	9.40	11.00	10.30
5-2µm	1.80	1.90	1.70	1.90	3.90	2.34	2.20	3.30
<2µm	9.80	9.60	8.70	9.10	17.40	9.60	10.70	8.60
Sum	60.17	59.19	51.68	54.08	105.53	57.58	61.19	56.41

Sample	T18	T19	T20	T21	T22	T23	T24	T25
Initial*	65.10	108.20	64.40	63.90	62.12	61.30	64.20	56.90
>500µm	-	-	-	0.04	0.01	0.01	0.01	0.02
500-250µm	0.01	0.01	0.02	0.01	0.04	0.06	0.05	0.06
250-125µm	0.07	0.09	0.09	0.13	0.34	0.41	0.41	0.44
125-63µm	2.18	4.52	1.54	1.63	1.87	1.90	2.16	1.78
63-20µm	31.00	50.50	26.30	25.40	28.00	26.20	25.70	23.60
20-5µm	9.70	19.20	9.20	9.60	11.70	10.90	11.50	9.00
5-2µm	2.20	4.40	2.10	1.90	2.00	1.70	2.50	1.70
<2µm	9.60	18.40	16.60	13.60	12.90	12.20	14.20	8.60
Sum	54.75	97.11	55.85	52.31	56.85	53.37	56.52	45.20

* Initial weight

Appendix 5: Modal data from the sand and coarse silt fractions of the Tokomaru silt loam. Data are based on 700 counts unless otherwise specified and are expressed in the tables as frequency percent.

Abbreviations of the mineral categories identified:

Cpx	Clinopyroxene
Opx	Orthopyroxene
Hblde	Hornblende
V lithic	Volcanic lithic
PO lithic	Plagioclase-opaque volcanic lithic
P lithic	Plagioclase volcanic lithic
O volc	Other volcanic types
S plag	Sedimentary plagioclase
V plag	Volcanic plagioclase
HRI plag	High refractive index plagioclase
LRI plag	Low refractive index plagioclase
C gwke	Chlorite greywacke lithic
E gwke	Epidote greywacke lithic
I gwke	Illite greywacke lithic
M gwke	Mica greywacke lithic
QF gwke	Quartzofeldspathic greywacke lithic
O sed	Other grains of sedimentary origin
tr	Trace amounts

O sed includes titanite, garnet, zircon, tourmaline, allanite, fossils and phytoliths.

Appendix 5.1 - Magnetic fraction of the fine sand.

Sample	T1	T2	T3	T4	T5	T6	T7	T8*	T9
Hblde	3.1	5.0	4.0	3.0	25.5	32.3	36.7	23.8	14.3
Cpx	5.6	8.4	5.1	6.4	32.3	30.0	29.8	17.1	5.0
Opx	5.9	12.8	11.2	7.0	13.7	14.2	8.7	18.6	2.8
V plag	2.7	2.4	2.7	1.4	2.6	2.6	1.4	-	6.0
P lithic	5.0	1.6	4.8	1.7	1.4	0.6	1.1	1.3	1.9
PO lithic	13.6	20.5	15.3	14.2	7.5	6.3	5.8	26.0	9.1
Opaque	0.3	4.9	4.4	1.5	5.1	4.3	2.0	2.2	0.5
Pumice	0.1	1.2	3.6	9.3	-	-	-	-	1.5
Glass	1.4	2.0	6.9	6.7	1.4	0.2	0.2	0.4	8.0
Obsidian	3.0	8.6	13.7	18.4	1.9	1.5	0.9	6.1	0.7
O volc	2.2	13.5	10.8	7.9	3.1	0.7	2.0	1.9	1.9
C gwke	46.8	12.3	14.4	17.8	3.7	6.0	6.2	-	38.4
E gwke	9.3	4.3	1.8	1.7	1.2	0.8	4.7	-	8.0
Epidote	-	-	0.1	-	-	-	0.2	0.4	-
Micas	0.7	0.8	0.3	2.6	0.4	0.5	0.5	1.9	2.2
O sed	-	1.2	0.8	0.2	-	-	0.2	0.2	-
Counts								270	
% magnetic	14	8	8	5	24	24	16	9	15

Sample	T10	T11	T12	T13	T14	T15	T16	T17	T18
Hblde	15.8	17.4	18.8	18.0	13.0	7.9	8.5	2.2	5.4
Cpx	4.9	10.5	9.2	18.9	11.1	14.2	5.8	3.4	3.2
Opx	6.0	9.3	7.8	11.9	15.5	10.4	13.0	3.4	4.3
V plag	4.1	1.5	2.2	2.2	1.1	0.7	-	1.4	0.5
P lithic	4.3	4.7	6.6	3.8	3.2	1.8	2.4	0.8	1.6
PO lithic	11.1	16.8	20.3	20.6	14.5	14.4	18.4	5.0	9.2
Opaque	0.4	1.0	2.7	1.3	2.4	1.3	1.4	0.2	-
Pumice	1.0	0.3	0.4	-	0.2	0.2	-	-	1.6
Glass	2.5	1.9	2.6	0.6	3.5	1.5	2.3	2.2	2.1
Obsidian	1.8	1.7	2.8	0.7	5.2	2.5	5.8	1.0	2.7
O volc	2.0	1.4	1.5	4.3	3.0	6.8	6.1	6.0	9.7
C gwke	37.7	23.7	16.1	8.6	18.4	25.5	23.2	64.3	53.0
E gwke	7.1	8.2	8.1	7.6	3.5	9.1	12.6	6.0	6.5
Epidote	-	-	-	0.1	-	0.3	-	-	-
Micas	1.1	1.3	0.9	1.3	5.4	3.5	1.0	4.0	0.5
O sed	0.1	-	-	-	-	-	0.3	-	0.5
Counts							285	289	499
% magnetic	14	10	8	14	13	11	7	4	6

Sample	T19	T20*	T21	T22	T23	T24	T25
Hblde	7.0	12.3	22.1	22.0	23.2	20.4	17.2
Cpx	12.8	25.7	38.4	41.1	46.5	45.3	37.9
Opx	6.2	25.7	13.9	19.5	8.1	13.2	7.6
V plag	0.8	-	1.2	1.0	0.7	0.7	0.4
P lithic	2.3	4.1	1.7	0.7	0.9	1.1	0.9
PO lithic	7.5	13.7	5.5	1.3	3.6	2.7	3.6
Opaque	0.6	1.4	0.4	0.9	0.6	0.8	0.4
Pumice	0.6	-	3.2	2.2	1.7	0.4	0.7
Glass	3.5	1.4	3.3	3.0	4.8	5.6	6.4
Obsidian	6.6	3.0	2.2	3.1	5.4	7.9	11.5
O volc	4.0	6.8	2.5	1.5	3.1	1.3	5.7
C gwke	36.2	-	4.3	2.2	0.6	0.4	6.6
E gwke	6.4	-	0.4	1.7	0.1	0.1	0.5
Epidote	0.9	-	0.1	-	0.4	-	0.2
Micas	4.6	-	0.7	0.1	0.1	-	0.2
O sed	-	6.0	-	-	0.2	-	-
Counts	530	273	690	1005	803	740	916
% magnetic	6	14	25	39	35	38	33

* Determined on the total fine sand fraction.

Appendix 5.2 - Non-magnetic fraction of the fine sand.

Sample	T1	T2	T3	T4	T5	T6	T7	T8*	T9
E gwke	1.6	-	-	tr	0.3	0.5	0.6	1.2	0.7
I gwke	22.4	2.1	0.2	tr	5.7	16.9	15.2	18.7	18.0
QF gwke	20.0	5.7	0.3	1.7	7.2	10.4	13.3	17.6	20.7
V plag	8.2	7.3	0.7	6.0	22.7	23.9	18.9	14.1	16.1
S plag	4.3	0.6	-	-	1.1	1.1	2.9	7.3	4.2
Quartz	30.9	5.0	0.2	2.6	3.8	9.9	17.6	28.5	29.6
P lithic	2.5	1.8	0.2	0.6	1.2	0.9	1.8	0.3	2.7
Pumice	1.6	35.0	44.8	38.0	18.2	7.4	6.1	2.5	1.2
Glass	5.6	40.7	53.8	50.9	38.8	27.2	20.1	7.9	5.1
Micas	2.2	tr	-	tr	0.9	1.4	2.0	1.2	0.7
Microcline	0.5	0.4	-	-	tr	0.3	0.7	0.8	0.9
O sed	-	-	-	-	tr	0.2	0.5	-	0.1
O volc	-	1.1	-	-	1.0	-	-	-	-

Sample	T10	T11	T12	T13	T14	T15	T16	T17	T18
E gwke	0.9	1.5	1.3	1.9	1.1	1.5	1.1	1.6	0.4
I gwke	24.3	21.7	18.1	15.8	19.5	19.0	23.9	25.5	22.2
QF gwke	13.9	19.4	22.5	19.6	17.3	20.5	15.6	16.4	19.4
V plag	19.4	9.1	6.9	9.5	8.3	4.2	3.7	4.6	4.5
S plag	3.3	5.9	6.6	6.4	7.4	7.3	7.4	7.7	5.7
Quartz	28.2	34.6	38.1	39.4	30.8	37.5	41.9	30.5	30.6
P lithic	4.2	2.8	2.1	4.5	2.6	3.1	0.8	1.1	0.9
Pumice	0.6	-	0.6	0.1	1.1	1.4	0.8	1.5	1.0
Glass	3.6	3.0	2.5	0.8	5.0	4.0	2.8	5.1	6.9
Micas	1.2	1.3	0.4	1.1	6.1	1.2	1.3	5.6	7.9
Microcline	0.2	0.7	0.9	0.7	0.8	0.1	0.6	0.3	0.3
O sed	0.2	-	-	0.1	-	0.1	-	0.1	0.4

Sample	T18	T19	T20*	T21	T22	T23	T24	T25
E gwke	1.0	0.7	1.7	0.1	0.1	0.6	0.1	1.2
I gwke	24.3	20.4	18.6	9.1	5.7	8.0	7.8	11.2
QF gwke	18.9	16.4	17.2	12.8	10.1	10.4	9.4	10.8
V plag	5.0	4.2	9.5	19.5	35.5	26.5	28.3	21.7
S plag	5.8	5.3	7.8	7.2	3.8	5.1	3.0	2.8
Quartz	30.1	36.6	34.9	30.4	20.2	34.9	32.5	30.5
P lithic	0.4	1.0	1.4	4.0	4.1	1.5	3.1	5.2
Pumice	0.9	1.9	3.7	10.9	15.8	11.4	12.9	10.7
Glass	6.7	7.0	3.6	4.1	3.8	1.2	2.2	5.0
Micas	6.2	5.9	1.1	1.3	0.5	-	0.2	0.3
Microcline	0.6	0.3	0.3	0.4	0.3	0.3	0.5	0.6
O sed	0.2	0.3	-	0.1	0.2	-	-	0.1

* Determined on the total sample.
Number of grains counted; T8 = 310; T20 = 360.

Appendix 5.3 - Magnetic fraction of the very fine sand.

Sample	T1	T2	T3	T4	T5	T6	T7	T8	T9
Hblde	4.9	9.0	5.7	4.9	10.0	8.3	7.7	6.6	6.4
Cpx	1.8	2.2	1.8	0.8	2.2	2.3	2.2	1.6	1.3
Opx	1.1	4.4	7.4	5.8	3.9	2.6	2.0	1.2	2.0
Glass	0.8	2.4	9.8	6.6	2.1	1.7	0.8	1.0	0.4
Obsidian	3.4	9.3	25.1	15.9	9.1	2.7	3.1	1.9	1.0
Opaque	2.5	3.6	7.0	2.1	6.1	7.4	3.8	3.6	4.1
V plag	1.6	1.6	1.4	1.3	2.2	1.5	0.5	1.0	0.6
PO lithic	4.0	7.8	10.6	3.9	3.7	1.4	1.1	1.5	0.4
P lithic	0.4	1.2	0.4	0.3	0.2	0.6	0.6	0.3	0.1
V lithic	1.5	2.2	3.2	1.4	0.6	0.3	0.3	0.2	0.1
O volc	0.5	0.8	4.9	7.8	4.4	2.4	3.4	3.1	1.8
C gwke	33.0	17.9	11.2	21.8	22.6	29.1	27.2	33.1	33.6
E gwke	16.5	14.2	2.5	10.6	12.1	15.9	17.4	16.6	15.9
Epidote	9.0	5.4	0.8	2.3	4.1	8.7	10.5	10.7	7.6
Micas	16.5	16.2	5.7	13.5	16.6	12.7	16.6	14.8	20.3
O sed	2.6	1.5	0.2	0.7	0.4	2.4	2.6	2.8	3.7
% magnetic	2.9	2.8	5.0	2.7	3.4	2.3	1.8	1.9	2.5

Sample	T10	T11	T12	T13	T14	T15	T16	T17
Hblde	9.1	5.6	4.0	7.9	2.4	3.6	3.5	4.9
Cpx	2.2	1.4	0.6	2.9	1.4	1.3	0.5	0.8
Opx	3.2	2.6	2.3	4.8	5.2	4.1	3.5	3.1
Glass	0.9	0.4	-	1.4	0.3	0.7	0.8	0.9
Obsidian	2.7	1.0	1.0	1.4	1.5	2.8	2.0	1.1
Opaque	4.5	2.9	3.1	3.8	4.7	2.9	2.6	1.6
V plag	0.3	0.6	0.6	1.2	0.6	0.3	0.5	0.3
PO lithic	0.5	1.0	0.9	2.9	1.5	2.4	1.1	0.8
P lithic	-	0.3	0.5	0.8	0.5	-	0.3	-
V lithic	0.2	0.3	0.8	0.5	0.8	0.3	-	0.4
O volc	3.7	3.5	2.2	3.0	3.8	3.2	2.8	1.8
C gwke	26.0	41.2	43.2	35.2	40.5	33.0	32.0	39.1
E gwke	14.0	17.4	15.7	15.0	13.2	10.2	13.6	13.1
Epidote	5.6	5.5	6.0	5.7	5.6	5.7	8.7	8.8
Micas	24.0	12.5	16.3	12.1	15.4	27.4	24.2	19.9
O sed	2.9	3.9	2.6	1.7	2.6	2.1	3.0	2.2
% magnetic	2.2	3.5	2.8	3.1	3.5	2.2	2.0	2.0

Sample	T18	T19	T20	T21	T22	T23	T24	T25
Hblde	5.1	7.8	12.9	13.0	16.6	14.7	15.2	11.2
Cpx	1.2	0.8	8.5	15.3	25.2	26.4	20.1	21.3
Opx	1.8	3.3	8.5	19.6	25.2	22.2	22.0	21.7
Glass	1.4	1.1	3.1	6.4	4.0	7.8	6.4	6.2
Obsidian	1.3	2.3	2.3	3.2	6.6	14.3	22.3	28.8
Opaque	1.9	1.4	3.5	4.0	5.4	2.9	2.6	1.6
V plag	0.1	0.1	1.5	0.8	0.5	0.9	0.6	0.5
PO lithic	0.9	0.4	0.6	1.0	2.0	1.2	1.9	0.9
P lithic	-	0.1	-	-	-	-	-	0.2
V lithic	-	0.3	-	-	0.8	1.2	0.7	1.2
O volc	1.7	2.4	3.6	1.8	2.0	1.7	2.1	1.8
C gwke	36.1	26.0	14.7	7.6	2.2	0.9	0.5	2.3
E gwke	10.5	14.2	8.5	5.1	1.5	1.4	1.4	0.7
Epidote	7.3	11.0	11.3	8.1	4.1	2.1	2.4	0.9
Micas	28.7	25.1	17.3	10.3	1.4	0.5	0.2	0.2
O sed	2.1	3.6	2.9	2.6	1.3	1.4	1.3	0.6
% magnetic	2.0	1.6	1.7	3.0	6.7	8.0	9.7	10.6

Appendix 5.4 - Non-magnetic fraction of the very fine sand.

Sample	T1	T2	T3	T4	T5	T6	T7	T8	T9
Glass	5.0	37.3	89.7	73.1	32.2	22.7	10.5	12.9	7.2
Obsidian	-	-	-	-	0.1	-	-	-	-
V plag	0.6	1.0	1.3	1.0	2.2	1.0	1.2	0.8	0.7
LRI plag	0.3	-	2.0	1.5	0.7	0.7	1.0	1.0	0.5
V lithic	0.3	0.1	-	-	0.1	0.1	-	-	-
I gwke	24.1	12.4	1.3	5.9	21.6	21.0	20.9	17.5	25.0
QF gwke	23.7	17.6	2.4	9.0	17.7	17.0	17.4	17.8	20.2
Quartz	26.0	15.6	2.4	4.8	13.9	20.1	25.5	25.4	25.4
S plag	18.4	15.6	0.9	4.4	12.8	15.7	22.3	23.7	19.7
Microcline	0.4	0.1	0.2	-	-	-	0.2	-	-
Micas	1.3	0.3	-	0.1	0.6	1.1	0.8	0.6	1.0
O sed	0.1	-	-	0.1	0.1	0.4	0.3	0.3	0.2

Sample	T10	T11	T12	T13	T14	T15	T16	T17
Glass	4.5	4.4	3.1	3.5	2.2	2.9	5.2	3.0
Obsidian	-	-	-	-	-	-	-	-
V plag	0.2	0.9	1.0	1.2	0.6	2.2	1.6	0.7
LRI plag	0.2	0.9	0.6	0.5	0.6	0.9	0.8	-
V lithic	0.2	-	-	0.3	0.2	0.4	0.2	-
I gwke	24.1	21.8	13.0	9.4	19.3	14.6	11.8	19.3
QF gwke	25.4	21.6	33.3	21.6	18.7	15.3	27.4	21.3
Quartz	26.4	29.3	28.3	25.6	29.1	32.9	32.6	27.3
S plag	18.1	17.0	17.4	32.5	24.0	26.0	16.5	23.7
Microcline	0.2	-	-	0.5	0.4	-	0.6	0.2
Micas	0.4	0.4	0.4	0.7	-	0.5	1.0	0.7
O sed	0.4	3.7	2.9	4.2	4.7	4.2	2.3	3.7

Sample	T18	T19	T20	T21	T22	T23	T24	T25
Glass	5.6	8.3	3.4	3.0	5.8	12.6	6.8	10.3
Obsidian	-	-	-	-	-	-	-	0.2
V plag	1.3	1.0	2.5	2.6	8.9	3.9	4.0	6.0
LRI plag	-	0.4	0.2	0.2	-	1.1	0.7	0.2
V lithic	-	-	0.2	-	-	-	-	-
I gwke	12.1	11.3	6.4	4.2	3.7	1.5	1.3	3.6
QF gwke	28.9	13.9	25.6	23.1	22.0	12.8	14.2	24.4
Quartz	29.5	37.0	33.2	31.4	25.5	32.8	43.4	31.3
S plag	21.1	25.7	25.6	29.6	25.9	29.6	25.0	20.6
Microcline	-	-	0.7	0.7	0.2	0.2	0.4	-
Micas	0.6	1.4	0.2	0.7	-	0.2	-	0.2
O sed	0.8	1.0	1.9	4.4	8.0	5.2	4.2	3.0

Appendix 5.5 - Grain mounts of the very fine sand.

Sample	T1	T2	T3	T4	T5	T6	T7	T8	T9
Quartz	31.3	23.5	2.9	4.6	13.3	24.3	19.8	24.8	22.5
M gwke	34.4	33.8	7.0	12.7	16.2	25.5	26.1	25.7	25.7
E gwke	8.2	1.7	1.0	0.6	7.9	4.2	11.9	6.3	13.1
S plag	9.0	12.0	3.2	4.5	13.0	17.3	22.6	26.3	21.8
Micas	3.6	2.5	1.1	1.4	2.4	3.0	5.3	3.2	3.9
Microcline	0.9	0.4	0.3	-	0.2	0.4	0.7	0.4	0.1
Epidote	0.8	0.3	-	0.1	0.1	0.1	0.3	0.4	0.4
O sed	0.3	0.8	0.1	0.6	0.6	-	0.1	0.3	0.1
LRI plag	2.2	2.6	4.2	2.7	3.7	2.9	3.5	4.9	4.5
HRI plag	4.1	2.0	0.8	1.2	1.1	0.3	0.9	0.1	1.0
V plag	1.8	2.0	1.7	0.6	1.1	2.7	0.9	1.3	0.3
Hblde	0.5	-	0.2	0.1	0.1	0.2	0.3	0.6	0.1
Cpx	-	0.1	0.1	-	0.1	0.1	-	-	-
Opx	-	0.1	0.2	-	-	0.3	-	-	-
Opaque	-	0.2	0.3	0.1	0.1	-	0.3	0.2	0.5
Pumice	1.0	10.8	33.8	39.6	19.4	6.9	3.1	1.3	2.3
Glass	1.4	5.2	40.8	31.1	18.1	11.2	3.7	3.9	2.5
Obsidian	-	0.1	0.6	0.4	0.6	0.4	-	0.2	0.1
PO lithic	0.1	0.2	0.2	-	0.2	-	-	0.1	-
V lithic	-	1.3	1.3	0.5	1.0	0.2	0.3	0.1	0.8
P lithic	0.1	0.1	0.1	-	0.1	-	0.1	-	-

Sample	T10	T11	T12	T13	T14	T15	T16	T17	T18
Quartz	23.5	20.7	25.1	28.2	26.8	20.1	17.2	23.4	20.0
M gwke	24.2	28.1	24.7	28.7	24.0	27.1	37.1	29.9	30.3
E gwke	7.6	6.7	11.8	5.7	9.4	4.2	2.6	8.0	2.7
S plag	23.9	28.0	23.9	28.0	25.9	34.0	28.3	27.9	27.5
Micas	4.9	1.8	3.5	1.4	1.5	3.0	4.6	3.5	6.4
Microcline	0.7	1.3	2.1	0.5	2.4	0.7	0.5	0.2	3.3
Epidote	0.5	0.2	0.1	0.2	0.1	0.6	0.2	-	0.4
O sed	-	0.4	0.1	0.7	0.4	0.2	0.2	0.3	0.2
LRI plag	4.9	4.3	5.2	3.2	6.3	6.0	6.3	4.1	4.4
HRI plag	0.5	1.3	-	-	0.4	0.9	0.2	0.5	1.0
V plag	1.4	2.0	0.4	2.0	0.5	0.5	0.2	0.7	0.4
Hblde	0.1	-	0.2	-	0.2	0.1	-	-	0.2
Cpx	0.1	-	-	-	-	-	0.1	-	0.2
Opx	0.1	-	-	-	0.1	0.1	0.1	-	-
Opaque	0.2	0.4	0.5	-	0.4	0.2	0.4	0.2	0.4
Pumice	1.9	1.1	0.2	0.7	0.5	1.0	0.2	0.8	0.3
Glass	4.2	3.1	1.7	0.5	0.7	0.6	1.4	0.7	1.9
Obsidian	0.4	-	-	-	-	-	0.1	-	-
PO lithic	0.1	-	-	0.2	0.1	0.1	-	-	-
V lithic	0.6	0.2	0.3	0.2	0.4	0.5	0.2	-	0.4
P lithic	-	-	-	-	-	-	-	-	-

Sample	T19	T20	T21	T22	T23	T24	T25
Quartz	17.6	21.3	29.8	23.1	22.3	37.0	15.8
M gwke	34.4	20.4	26.8	17.2	21.5	21.0	16.9
E gwke	2.6	3.3	4.2	1.3	-	1.7	0.6
S plag	30.7	36.2	19.6	29.5	31.1	14.8	33.6
Micas	2.5	2.5	1.5	0.4	0.6	0.2	0.4
Microcline	0.2	4.7	2.1	9.1	1.0	1.4	2.1
Epidote	0.1	0.6	0.3	0.4	0.4	0.5	0.2
O sed	0.2	0.4	0.1	-	0.6	-	1.5
LRI plag	7.5	3.9	8.3	5.9	5.3	6.6	10.9
HRI plag	0.4	1.1	0.1	4.0	1.4	0.7	0.6
V plag	-	0.6	2.1	2.3	4.0	4.7	3.4
Hblde	0.2	0.6	0.4	0.6	0.2	1.1	0.9
Cpx	0.2	0.2	0.3	-	1.2	1.8	0.9
Opx	0.4	0.1	0.3	1.3	2.6	1.8	1.1
Opaque	0.2	-	0.1	0.4	0.4	0.1	0.4
Pumice	0.4	0.9	1.5	3.6	4.2	2.0	3.6
Glass	1.1	2.6	1.9	0.2	2.0	2.1	2.6
Obsidian	-	0.1	-	0.4	0.8	1.2	3.6
PO lithic	-	-	-	-	-	-	-
V lithic	0.1	0.5	0.4	-	0.6	1.1	0.4
P lithic	-	-	-	-	-	-	-

Appendix 5.6 - Grain mounts of the coarse silt fraction.

Sample	T1	T2	T3	T4	T5	T6	T7	T8	T9
Quartz	6.8	8.2	3.9	6.0	7.9	9.3	6.4	9.5	5.1
M gwke	26.8	34.5	13.6	23.6	25.7	21.1	20.2	19.8	31.5
E gwke	1.6	1.9	1.6	2.2	3.4	2.9	2.0	1.2	1.6
S plag	36.4	28.1	16.4	17.3	28.0	41.6	43.1	46.8	41.8
Epidote	6.3	6.9	2.9	4.2	7.2	5.7	8.0	6.7	4.3
Micas	2.4	4.4	1.7	1.8	5.1	4.9	4.7	4.6	3.1
Microcline	6.8	2.6	1.2	0.7	1.9	1.3	2.1	2.5	1.4
O sed	1.9	0.3	2.4	0.4	1.5	0.5	1.4	1.1	0.9
Hblde	0.4	0.4	0.2	0.1	-	0.2	0.1	0.3	0.4
Cpx	0.1	-	0.1	-	0.2	0.2	-	0.3	-
Opx	0.1	-	0.2	0.1	-	-	-	-	-
Opaque	0.1	0.3	0.3	0.1	-	0.2	0.3	0.3	0.4
Glass	0.5	4.0	47.4	35.0	7.4	4.2	1.3	0.8	1.3
V plag	0.9	0.6	0.5	0.2	1.3	1.0	0.5	0.3	0.3
HRI plag	0.4	-	0.9	1.1	0.5	0.2	0.4	0.3	0.1
LRI plag	8.1	7.3	4.4	6.3	9.8	6.1	9.5	5.1	7.2
O volc	0.3	0.4	1.9	0.5	0.2	0.9	0.1	-	0.1
Counts	790	680	800	814	623	590	750	640	830

Sample	T10	T11	T12	T13	T14	T15	T16	T17
Quartz	7.6	5.1	6.9	9.6	7.1	20.6	9.5	14.4
M gwke	31.1	21.9	24.2	21.8	31.4	29.2	34.6	34.4
E gwke	1.6	1.7	3.2	2.0	0.8	2.0	1.9	2.4
S plag	39.3	50.2	43.7	46.5	34.2	24.5	28.9	24.0
Epidote	4.9	4.8	3.0	4.3	5.2	5.7	4.6	6.1
Micas	5.1	2.5	3.0	4.2	3.4	2.8	4.4	3.2
Microcline	2.5	3.7	3.8	1.1	4.0	1.0	5.2	2.9
O sed	1.0	1.4	1.7	0.9	1.5	1.4	0.7	1.3
Hblde	0.2	0.3	0.3	0.4	-	-	0.2	0.5
Cpx	0.2	-	-	-	-	0.1	-	0.1
Opx	0.2	-	-	-	-	0.1	-	-
Opaque	-	0.4	0.3	0.5	0.3	0.9	0.3	0.3
Glass	0.2	0.1	0.3	0.6	0.5	0.7	0.2	0.5
V plag	-	-	0.3	0.4	0.6	0.1	0.7	0.4
HRI plag	0.4	-	0.8	1.6	1.1	6.0	2.2	2.0
LRI plag	5.3	7.7	8.4	5.8	9.7	4.2	6.6	6.7
O volc	0.6	0.1	-	0.1	-	0.1	-	0.3
Counts	514	700	600	800	618	680	590	735

Sample	T18	T19	T20	T21	T22	T23	T24	T25
Quartz	11.6	14.1	14.1	24.8	9.3	9.3	10.0	8.0
M gwke	38.1	33.6	21.5	26.3	12.0	20.3	12.9	10.6
E gwke	2.9	1.3	2.5	1.3	1.0	0.4	0.5	0.7
S plag	23.4	23.4	33.0	20.2	43.6	38.8	41.5	48.1
Epidote	3.9	4.9	3.6	4.2	5.8	4.9	5.6	6.4
Micas	3.8	4.9	3.0	0.7	0.7	0.6	0.7	0.4
Microcline	1.3	1.8	1.1	1.0	1.6	2.9	1.9	1.8
O sed	1.6	0.9	0.3	0.5	0.9	1.4	1.2	1.0
Hblde	0.3	0.3	0.3	0.6	0.9	0.8	0.7	0.5
Cpx	0.5	0.2	-	0.7	0.4	1.2	0.5	0.9
Opx	-	0.2	-	0.1	0.2	-	-	-
Opaque	0.5	0.2	0.2	0.1	0.4	0.5	0.4	0.1
Glass	0.5	0.6	0.5	0.6	1.3	0.9	1.3	1.1
V plag	1.0	1.8	1.3	2.4	1.7	1.3	2.5	1.7
HRI plag	5.6	3.7	11.6	8.8	10.6	5.2	14.3	7.0
LRI plag	5.2	8.1	7.0	6.9	9.2	11.2	5.1	10.3
O volc	-	0.2	-	0.2	0.3	0.1	0.7	0.8
Counts	612	616	610	570	770	750	824	823

Appendix 6: GEOCHEMICAL DATA FROM THE TOKOMARU SILT LOAM.

6.1: Major element analyses of the whole soil.

Sample	T1	T2	T3	T4	T5	T6	T7	T8	T9	T10	T11	T12	T13
SiO_2	70.28	70.38	69.66	70.14	69.70	70.21	70.12	70.74	71.15	70.89	70.71	71.20	70.61
Al_2O_3	13.11	13.37	13.85	13.72	13.89	13.80	13.46	13.38	13.34	13.21	13.35	13.15	13.38
TiO_2	0.55	0.54	0.33	0.42	0.54	0.55	0.54	0.54	0.53	0.54	0.54	0.53	0.54
Fe_2O_3	3.65	3.38	2.61	3.10	3.73	3.53	3.51	3.44	3.47	3.38	3.41	3.45	3.57
MnO	0.05	0.10	0.05	0.06	0.05	0.05	0.04	0.04	0.05	0.05	0.04	0.04	0.03
MgO	0.92	0.90	0.52	0.69	0.90	0.93	0.88	0.88	0.88	0.89	0.91	0.89	0.90
CaO	1.38	1.38	1.49	1.38	1.46	1.38	1.29	1.22	1.20	1.21	1.18	1.13	1.11
Na_2O	2.99	2.92	3.03	2.91	2.96	3.09	2.96	2.98	2.93	2.97	2.98	3.04	3.00
K_2O	1.94	1.97	2.39	2.19	1.93	1.88	1.88	1.90	1.93	1.93	1.91	1.91	1.89
P_2O_5	0.14	0.11	0.05	0.07	0.09	0.11	0.09	0.09	0.09	0.09	0.10	0.10	0.10
LOI	4.04	4.31	5.28	5.09	4.93	4.65	4.43	4.27	4.18	4.26	4.25	4.16	4.33
Total	99.05	99.36	99.26	99.77	100.18	100.18	99.20	99.48	99.75	99.42	99.38	99.60	99.46

Sample	T14	T15	T16	T17	T18	T19	T20	T21	T22	T23	T24	T25
SiO_2	70.86	70.43	69.89	69.56	69.37	68.97	68.78	68.59	71.08	71.31	71.79	63.89
Al_2O_3	13.57	13.49	13.63	13.73	13.80	14.10	14.41	14.09	13.13	12.92	12.71	10.86
TiO_2	0.55	0.56	0.57	0.57	0.58	0.61	0.62	0.58	0.49	0.46	0.45	0.37
Fe_2O_3	3.59	3.59	3.84	4.14	4.28	4.14	3.86	4.57	3.86	3.47	3.15	1.93
MnO	0.04	0.04	0.04	0.03	0.03	0.02	0.01	0.02	0.02	0.02	0.03	0.04
MgO	0.93	0.92	0.92	0.91	0.89	0.79	0.64	0.59	0.52	0.51	0.51	0.46
CaO	1.10	1.06	1.03	0.99	0.97	0.89	0.75	0.76	0.92	1.00	1.07	1.05
Na_2O	2.97	2.93	2.92	2.95	2.87	2.84	2.67	2.66	2.84	2.87	2.91	2.58
K_2O	1.88	1.89	1.90	1.86	1.83	1.77	1.66	1.56	1.37	1.28	1.25	1.13
P_2O_5	0.10	0.10	0.10	0.10	0.09	0.06	0.03	0.03	0.03	0.04	0.05	0.15
LOI	4.35	4.44	4.56	4.83	4.05	4.60	6.66	6.84	5.70	6.02	6.51	17.81
Total	99.94	99.45	99.40	99.67	98.76	98.79	100.09	100.29	99.96	99.90	100.43	100.27

Appendix 6.2: Major element analyses of the sand fraction (weight precent).

Sample	T1	T2	T3	T4	T5	T6	T7	T8	T9	T10	T11	T12	T13
SiO_2	80.33	78.92	72.28	75.03	77.03	79.43	80.62	81.64	81.04	80.91	81.66	82.56	82.06
Al_2O_3	10.04	10.63	12.87	12.05	11.51	10.80	10.17	9.87	10.16	10.16	9.80	9.55	9.66
TiO_2	0.26	0.25	0.25	0.23	0.27	0.26	0.23	0.21	0.25	0.25	0.22	0.20	0.20
Fe_2O_3	1.37	1.34	1.92	1.61	1.65	1.37	1.19	1.07	1.33	1.27	1.17	1.04	1.12
MnO	0.02	0.02	0.05	0.04	0.03	0.02	0.02	0.02	0.02	0.02	0.02	0.02	0.02
MgO	0.45	0.41	0.44	0.39	0.58	0.50	0.41	0.40	0.44	0.44	0.41	0.37	0.43
CaO	1.04	1.20	1.74	1.35	1.61	1.31	1.07	0.98	0.99	0.99	0.93	0.86	0.92
Na_2O	3.07	3.27	3.72	3.52	3.31	3.22	3.17	3.12	3.14	3.14	3.11	3.09	3.12
K_2O	1.72	1.87	2.53	2.40	1.89	1.76	1.66	1.66	1.72	1.71	1.65	1.63	1.63
P_2O_5	0.04	0.03	0.04	0.03	0.03	0.03	0.03	0.03	0.03	0.03	0.03	0.02	0.03
LOI	1.18	1.67	3.90	3.25	1.93	1.47	1.21	1.11	1.21	1.19	1.07	1.01	1.01
Total	99.52	99.61	99.74	99.90	99.84	100.17	99.78	100.11	100.33	100.11	100.07	100.35	100.20

Sample	T14	T15	T16	T17	T18	T19	T20	T21	T22	T23	T24	T25
SiO_2	81.75	81.99	81.55	81.38	81.70	81.72	83.65	84.77	84.37	83.22	83.39	82.92
Al_2O_3	9.71	9.70	9.77	9.87	9.76	9.38	8.70	8.17	7.72	7.73	7.64	7.94
TiO_2	0.20	0.19	0.20	0.19	0.19	0.16	0.15	0.16	0.18	0.21	0.21	0.22
Fe_2O_3	1.15	1.12	1.20	1.26	1.29	1.06	0.78	0.88	1.21	1.58	1.51	1.52
MnO	0.02	0.02	0.02	0.01	0.01	0.01	0.01	0.02	0.03	0.04	0.04	0.04
MgO	0.43	0.43	0.43	0.43	0.44	0.36	0.29	0.46	0.87	1.20	1.17	1.13
CaO	0.88	0.85	0.84	0.83	0.81	0.73	0.64	0.85	1.36	1.79	1.76	1.72
Na_2O	3.09	3.08	3.04	3.06	3.00	2.99	2.87	2.70	2.51	2.45	2.36	2.51
K_2O	1.64	1.67	1.68	1.67	1.64	1.59	1.48	1.36	1.19	1.14	1.11	1.18
P_2O_5	0.03	0.02	0.02	0.02	0.02	0.02	0.01	0.01	0.01	0.02	0.02	0.02
LOI	1.11	1.18	1.30	1.36	1.37	1.19	0.92	0.77	0.57	0.58	0.65	0.76
Total	100.01	100.25	100.05	100.08	100.23	99.21	99.50	100.15	100.02	99.96	99.86	99.96

Appendix 6.3: Trace element data for the total soil (µg/g).

Sample	T1	T2	T3	T4	T5	T6	T7	T8	T9	T10	T11	T12	T13
Cr	58.0	51.0	27.0	33.0	55.0	55.0	55.0	53.0	56.0	53.0	56.0	51.0	54.0
V	78.0	71.0	36.0	52.0	74.0	73.0	74.0	74.0	72.0	72.0	74.0	72.0	75.0
Ba	458.0	482.0	547.0	509.0	479.0	472.0	472.0	470.0	471.0	478.0	482.0	489.0	495.0
Sc	9.0	9.0	8.0	6.0	10.0	9.0	9.0	9.0	8.0	7.0	8.0	9.0	9.0
Mn	433.0	860.0	410.0	470.0	460.0	373.0	367.0	352.0	385.0	456.0	352.0	355.0	295.0
Ti	3261.0	3171.0	1863.0	2395.0	3098.0	3235.0	3275.0	3243.0	3277.0	3215.0	3244.0	3229.0	3264.0
Zn	51.4	53.6	47.8	50.7	54.3	52.2	53.3	52.5	52.7	52.3	54.6	54.0	55.3
Cu	6.9	6.3	6.2	6.7	6.9	5.9	6.0	5.3	6.1	6.1	6.8	7.3	6.5
Ni	16.0	14.6	11.9	14.5	18.4	17.7	15.4	13.5	17.8	15.5	15.4	16.3	13.5
Nb	7.1	7.0	5.9	6.7	6.2	7.0	6.6	5.8	7.1	6.0	6.5	6.5	6.3
Zr	347.0	340.0	197.0	265.0	311.0	333.0	340.0	336.0	340.0	336.0	334.0	341.0	345.0
Y	24.8	25.2	24.1	25.2	25.2	25.3	24.8	25.0	23.8	24.0	23.9	24.4	25.9
Sr	274.0	264.0	162.0	208.2	257.0	266.0	267.0	267.0	266.0	264.0	265.0	263.0	263.0
Rb	83.5	83.6	92.4	91.6	84.7	82.1	81.0	81.6	82.2	82.8	82.0	79.7	77.7
Pb	11.8	12.2	14.7	14.0	13.5	13.7	13.0	12.7	13.2	13.7	13.3	13.0	12.7
Ga	12.5	15.1	14.8	14.3	15.2	14.0	13.9	15.0	14.9	13.9	14.6	14.5	14.0

Sample	T14	T15	T16	T17	T18	T19	T20	T21	T22	T23	T24	T25
Cr	54.0	57.0	57.0	57.0	59.0	56.0	56.0	52.0	47.0	45.0	44.0	38.0
V	77.0	78.0	80.0	83.0	86.0	90.0	90.0	92.0	78.0	73.0	69.0	55.0
8a	496.0	490.0	484.0	496.0	476.0	432.0	385.0	369.0	359.0	343.0	338.0	305.0
Sc	9.0	9.0	9.0	10.0	9.0	10.0	8.0	8.0	6.0	6.0	6.0	5.0
Mn	288.0	280.0	316.0	284.0	238.0	191.0	124.0	115.0	140.0	180.0	276.0	348.0
Ti	3305.0	3332.0	3420.0	3515.0	3544.0	3778.0	3906.0	3728.0	2968.0	2842.0	2696.0	2228.0
Zn	53.2	53.4	53.8	54.2	49.0	44.1	36.8	34.4	33.6	35.3	36.1	73.3
Cu	7.0	7.7	7.8	6.6	5.1	6.6	5.3	4.6	4.1	2.3	3.2	6.5
Ni	13.7	13.7	13.0	13.4	12.6	12.8	9.8	8.4	7.4	6.7	6.0	6.2
Nb	6.2	6.7	6.9	8.1	7.7	7.8	8.5	7.2	7.0	5.9	5.9	4.7
Zr	345.0	338.0	334.0	320.0	322.0	314.0	306.0	314.0	342.0	353.0	349.0	300.0
Y	27.9	29.1	28.7	25.4	22.6	20.0	15.2	13.0	12.2	12.5	11.4	11.0
Sr	263.0	259.0	257.0	254.0	251.0	240.0	218.0	214.0	231.0	236.0	236.0	217.0
Rb	78.1	78.7	79.0	77.4	75.4	73.5	72.3	73.1	69.7	69.0	70.6	55.5
Pb	13.1	13.1	13.8	13.2	14.0	13.3	13.2	12.6	12.0	11.1	11.6	15.5
Ga	14.2	14.3	17.0	15.0	17.0	17.4	17.2	16.3	13.0	13.6	13.0	11.0

Appendix 6.4: Trace element data of the sand fraction (μg/g).

Sample	T1	T2	T3	T4	T5	T6	T7	T8	T9	T10	T11	T12	T13
Cr	24.0	23.0	14.0	16.0	24.0	22.0	21.0	23.0	23.0	25.0	23.0	20.0	22.0
V	32.0	28.0	18.0	19.0	33.0	29.0	26.0	24.0	27.0	28.0	26.0	22.0	24.0
Ba	437.0	463.0	543.0	524.0	465.0	437.0	418.0	419.0	441.0	438.0	435.0	437.0	433.0
Sc	5.0	4.0	6.0	5.0	5.0	4.0	3.0	4.0	5.0	4.0	3.0	4.0	4.0
Mn	143.0	178.0	370.0	315.0	230.0	178.0	137.0	133.0	142.0	141.0	128.0	116.0	120.0
Ti	1455.0	1381.0	1313.0	1262.0	1536.0	1414.0	1230.0	1169.0	1319.0	1342.0	1220.0	1046.0	1105.0
Zn	29.0	26.7	44.7	37.2	28.4	23.3	21.6	20.9	21.6	22.2	20.8	18.6	20.5
Cu	14.8	7.3	15.6	8.2	5.7	6.1	4.6	7.5	8.6	4.7	6.1	5.9	5.2
Ni	4.5	5.2	3.7	2.5	6.2	6.0	3.2	3.3	5.9	5.5	4.5	5.0	4.0
Nb	3.4	3.7	6.3	4.5	4.0	4.0	3.7	2.2	2.7	1.8	2.0	1.8	2.9
Zr	81.0	91.3	141.0	117.2	86.7	80.3	74.2	72.8	75.5	78.7	73.9	71.8	75.6
Y	9.3	11.7	22.2	18.5	12.8	10.7	8.2	8.2	8.4	8.8	8.3	6.9	7.8
Sr	248.2	231.3	147.1	170.4	246.2	250.9	235.0	241.7	228.6	244.2	241.4	241.6	248.6
Rb	57.8	65.1	95.0	91.1	68.0	60.4	53.3	52.5	52.9	55.8	51.7	49.3	50.6
Pb	8.0	9.4	14.5	11.9	8.4	8.1	7.8	7.5	7.6	8.4	7.6	6.8	8.5
Ga	9.7	10.0	13.7	12.8	11.8	10.0	9.6	8.8	8.4	8.9	8.7	7.9	7.6

Sample	T14	T15	T16	T17	T18	T19	T20	T21	T22	T23	T24	T25
Cr	22.0	23.0	24.0	26.0	25.0	20.0	19.0	19.0	24.0	26.0	25.0	26.0
V	23.0	25.0	26.0	27.0	26.0	22.0	17.0	17.0	22.0	29.0	28.0	30.0
Ba	435.0	443.0	486.0	576.0	450.0	419.0	372.0	346.0	322.0	314.0	305.0	312.0
Sc	3.0	2.0	2.0	2.0	2.0	2.0	2.0	2.0	4.0	5.0	6.0	4.0
Mn	117.0	115.0	126.0	126.0	121.0	98.0	86.0	122.0	211.0	303.0	290.0	285.0
Ti	1086.0	1043.0	1084.0	1085.0	1052.0	911.0	773.0	894.0	963.0	1129.0	1126.0	1180.0
Zn	20.3	20.9	23.3	23.4	23.8	17.8	11.5	12.4	11.5	17.7	17.2	50.7
Cu	5.0	5.5	5.0	5.4	6.9	5.3	8.3	5.5	7.8	7.0	8.4	8.9
Ni	3.0	4.2	3.1	5.0	2.6	1.7	0.3	2.5	2.7	5.5	4.3	2.3
Nb	2.3	2.0	2.1	2.6	2.4	4.1	1.7	1.4	1.6	2.1	1.5	1.9
Zr	78.6	78.0	79.9	77.9	74.7	71.4	75.7	72.2	82.9	92.2	107.3	94.2
Y	7.7	7.7	8.2	6.6	7.5	5.3	5.7	5.8	6.4	7.1	7.3	7.4
Sr	240.6	239.3	239.3	240.8	234.5	223.4	209.9	203.6	207.8	217.1	213.8	213.0
Rb	50.4	52.2	53.0	54.2	52.9	48.8	43.6	39.2	33.8	32.7	31.8	34.9
Pb	6.9	6.7	7.0	8.9	8.3	7.1	6.2	5.5	7.3	6.4	6.1	16.6
Ga	8.1	7.6	8.6	8.5	8.4	8.5	7.0	5.8	6.4	5.5	7.0	5.8

Appendix 7: Electron microprobe data of tephra minerals

Sample localities.

(1) Aokautere Ash, from the type section.
89 very fine ash base.
90 coarse base of the graded unit.
91 fine ash overlying the graded unit.
92 upper part of the graded unit (between samples 90 and 91).

(2) Waimihia Tephra Formation, De Bretts section.
sample numbers 10 and 19.

(3) Egmont tephras from Mangatoki Strean section (Franks 1984).
In stratigraphic order:
MnP Pumiceous block from the Manganui tephra.
MnL Lithic crystals from the Manganui tephra.
Il Inglewood tephra.
222 (E5, Franks 1984)
228u (E4, Franks 1984)
228m
228l
235 (E3, Franks 1984)
243 (E2, Franks 1984)
246 (E1, Franks 1984)
251 Mahoe tephra.
256 Unamed lithic tephra directly above Aokautere Ash.

(4) Okataina Volcanic Centre tephras.
84 Rotoma Ash, Kawerau (I.Nairn *pers. comm.*).
87 Whakatane Ash, Kawerau (I.Nairn *pers. comm.*).

Abbreviations:
a - associated with b - brown c - clinopyroxene
d - corona around f - olivine g - glass
h - hornblende i - inclusion k - core
o - orthopyroxene p - plagioclase q - quartz
r - rim s - selvedge t - titanomagnetite
z - zone n.d. not determined
v - vesicular

APPENDIX 7.1: GLASS

Sample	MnP	MnP	MnP	MnP	MnP	MnP	MnP	MnP	MnP	MnP	MnP	MnP	MnP
Code	ih2	it3	v	st5	it7	it8	sc10	sc11	sh13	sh14	ic15	ic16	v
SiO_2	63.24	56.43	61.22	61.04	64.13	60.35	64.60	61.00	62.99	61.81	61.57	66.77	61.06
Al_2O_3	16.91	16.35	16.82	17.25	16.35	16.40	16.42	21.22	16.72	17.91	16.64	13.49	16.52
TiO_2	0.61	0.92	0.59	0.46	0.58	0.73	0.49	0.42	0.51	0.72	0.54	0.64	0.58
FeO^*	3.56	5.82	3.66	4.39	3.73	5.25	2.90	2.22	3.47	4.31	3.06	2.87	4.15
MnO	0.00	0.21	0.16	0.23	0.10	0.14	0.17	0.00	0.17	0.00	0.14	0.00	0.16
MgO	1.11	1.92	1.52	1.30	1.08	1.70	0.95	0.72	1.15	1.44	0.91	0.56	1.47
CaO	2.71	7.58	3.29	3.07	2.62	5.96	2.50	5.99	2.26	3.26	1.92	1.67	3.37
Na_2O	5.13	4.41	5.22	5.35	5.14	4.52	4.73	5.87	5.00	5.18	4.81	4.01	5.52
K_2O	4.09	2.38	4.08	4.08	3.50	2.54	4.40	2.23	5.13	3.90	4.02	4.43	3.60
Cl	0.35	0.13	0.16	0.26	0.15	0.10	0.11	0.10	0.19	0.18	0.19	0.09	0.13
Total	97.71	96.15	96.72	97.43	97.38	97.69	97.27	99.77	97.59	98.71	93.80	94.53	96.56

Sample	MnP	MnL	MnL	MnL	MnL	MnL	MnL	MnL	MnL	MnL	MnL	MnL	MnL
Code	v	ic1	sc1	it2	it3	it3	it4	it5	it6	it6	ih9	ic11	sc12
SiO_2	61.91	54.16	53.59	49.36	54.30	53.23	53.91	53.26	53.21	48.17	48.64	52.49	61.15
Al_2O_3	16.60	19.18	19.11	18.15	15.65	18.48	18.48	18.10	18.18	17.65	16.44	18.99	18.53
TiO_2	0.65	0.89	0.99	1.03	1.17	0.97	0.87	0.85	0.99	1.10	1.33	0.89	0.56
FeO^*	4.01	7.78	8.12	7.68	9.50	8.46	8.15	8.68	8.26	9.37	9.55	6.70	3.18
MnO	0.00	0.16	0.13	0.00	0.24	0.00	0.00	0.23	0.13	0.24	0.00	0.22	0.00
MgO	1.47	3.33	3.48	3.60	4.92	3.69	3.46	3.29	3.23	3.85	5.80	2.97	0.99
CaO	2.67	7.83	7.73	11.02	7.81	8.59	7.91	7.54	7.92	10.62	9.04	7.36	4.74
Na_2O	5.37	3.65	3.89	2.71	3.91	4.47	4.65	4.72	4.03	2.83	3.37	4.35	5.52
K_2O	4.26	2.08	1.96	1.33	2.38	2.45	3.07	2.86	2.69	1.71	1.93	2.28	2.99
Cl	0.10	0.00	0.14	0.13	0.15	0.13	0.17	0.17	0.13	0.11	0.10	0.13	0.17
Total	97.04	99.06	99.14	95.01	100.03	100.47	100.67	99.70	98.77	95.65	96.20	96.38	97.83

Sample	MnL	MnL	MnL	MnL	Ing	Ing	Ing	Ing	Ing	Ing	Ing	Ing	Ing
Code	ic1	it2	ic27	ic29	sh15	ih16	sh17	ih18	ih20	sh21	sc5	sc23	ic23
SiO_2	53.23	47.99	52.87	53.27	69.70	67.02	66.91	68.43	70.88	70.46	71.31	69.88	67.73
Al_2O_3	19.19	17.57	16.59	19.07	15.10	15.82	16.61	14.79	15.55	15.28	15.52	15.25	14.45
TiO_2	0.87	1.06	0.88	0.64	0.28	0.29	0.34	0.36	0.41	0.44	0.42	0.37	0.42
FeO^*	7.43	7.51	6.85	7.89	1.96	2.30	1.99	1.85	1.94	2.14	1.86	2.00	1.81
MnO	0.12	0.15	0.15	0.12	0.00	0.15	0.12	0.16	0.19	0.17	0.14	0.22	0.00
MgO	3.30	3.60	3.40	2.94	0.34	0.49	0.47	0.43	0.35	0.42	0.46	0.31	0.30
CaO	7.87	10.84	6.32	7.81	1.85	2.51	3.04	1.57	1.84	1.91	1.76	1.97	1.66
Na_2O	4.26	3.14	4.24	4.14	4.66	4.56	4.93	4.18	4.74	4.59	4.91	4.69	4.17
K_2O	2.02	1.53	2.70	2.16	4.47	4.05	3.75	4.49	4.39	4.47	4.40	4.28	4.32
Cl	0.12	0.12	0.20	0.16	0.21	0.16	0.20	0.15	0.16	0.23	0.21	0.23	0.21
Total	98.41	93.51	94.20	98.20	98.57	97.35	98.36	96.41	100.45	100.11	100.99	99.20	95.07

APPENDIX 7.1: Continued.

Sample Code	Ing Sc24	Ing v	Ing b2	Ing b2	Ing sp6	Ing sh	Ing st8	222 bic15	222 bic15	222 bic16	222 bic16	222 bic17	222 lc17
SiO_2	70.54	68.95	71.19	69.93	70.46	70.43	70.10	67.10	65.04	67.10	65.72	66.82	68.68
Al_2O_3	15.25	14.58	15.28	15.09	15.05	15.34	15.22	14.39	18.12	14.57	14.62	13.95	13.81
TiO_2	0.44	0.33	0.46	0.46	0.39	0.46	0.48	0.48	0.29	0.39	0.45	0.48	0.40
FeO^*	1.95	1.76	1.70	1.73	2.14	1.83	1.92	1.88	1.52	2.19	2.26	2.04	2.16
MnO	0.16	0.14	0.22	0.00	0.00	0.00	0.14	0.16	0.11	0.13	0.15	0.00	0.00
MgO	0.37	0.42	0.35	0.39	0.41	0.42	0.40	0.33	0.22	0.38	0.42	0.44	0.30
CaO	1.92	1.64	1.77	1.76	1.99	1.77	1.80	1.26	3.54	1.59	1.61	1.45	1.17
Na_2O	4.56	4.49	4.77	4.31	4.94	4.82	4.72	3.97	4.41	4.04	4.04	3.70	3.87
K_2O	4.60	4.45	4.44	4.54	4.39	4.40	4.30	4.37	3.36	4.52	4.47	4.48	4.45
Cl	0.24	0.19	0.19	0.19	0.14	0.18	0.22	0.17	0.14	0.18	0.18	0.16	0.17
Total	100.03	96.95	100.37	98.40	99.91	99.65	99.30	94.11	96.75	95.09	93.84	93.52	95.01

Sample Code	222 sh18	222 sh19	222 sh20	222 ic21	222 sc21	222 st23	222 s	222 ih25	222 ic26	222 ic26	222 ic27	222 st28	222 sh9
SiO_2	70.42	70.78	68.97	64.62	69.94	71.35	69.30	67.49	67.85	67.14	68.75	69.30	70.54
Al_2O_3	14.13	15.35	16.08	12.80	15.05	14.88	15.05	14.73	14.81	14.88	14.49	15.22	15.30
TiO_2	0.44	0.57	0.41	0.42	0.47	0.45	0.41	0.36	0.41	0.40	0.36	0.42	0.43
FeO^*	1.68	1.94	2.09	2.54	2.15	2.02	2.18	2.11	1.76	2.10	2.04	2.48	1.90
MnO	0.11	0.11	0.11	0.17	0.15	0.14	0.13	0.12	0.00	0.14	0.17	0.19	0.12
MgO	0.31	0.50	0.44	2.12	0.51	0.42	0.47	0.34	0.47	0.49	0.31	0.49	0.55
CaO	1.21	1.63	2.54	5.10	1.74	1.32	1.79	1.47	1.53	1.66	1.19	1.58	1.60
Na_2O	4.01	4.65	4.64	3.76	4.60	4.79	4.77	4.22	4.13	4.03	4.07	4.97	4.85
K_2O	4.95	5.01	4.37	4.04	4.94	4.85	4.65	4.60	4.62	4.56	4.61	4.84	4.86
Cl	0.11	0.14	0.16	0.18	0.21	0.15	0.19	0.18	0.06	0.23	0.20	0.20	0.17
Total	97.37	100.68	99.81	95.75	99.76	100.37	98.94	95.62	95.64	95.63	96.19	99.69	100.32

Sample Code	222 sp11	222 v	228u st13	228u st13	228u it25	228u st25	228u ic26	228u ic27	228u ic27	228u sc27	228u sc29	228u ic29	228u ic30
SiO_2	71.57	67.93	68.59	69.09	66.78	68.64	66.76	67.24	66.96	68.53	67.82	65.55	68.11
Al_2O_3	15.19	14.18	15.60	15.73	15.56	15.89	14.73	13.94	14.62	15.12	15.45	15.08	15.67
TiO_2	0.36	0.30	0.59	0.41	0.57	0.53	0.40	0.33	0.52	0.63	0.67	0.62	0.63
FeO^*	1.74	1.33	2.97	2.81	3.27	2.68	2.39	2.16	2.42	2.30	2.12	2.22	2.24
MnO	0.10	0.12	0.00	0.00	0.16	0.00	0.16	0.00	0.15	0.14	0.00	0.17	0.13
MgO	0.47	0.27	0.62	0.60	0.65	0.62	0.55	0.44	0.56	0.55	0.59	0.64	0.69
CaO	1.40	1.28	1.80	1.75	2.08	1.84	2.12	1.75	1.93	1.61	1.75	1.71	1.78
Na_2O	4.39	4.42	4.77	4.81	4.53	5.02	3.78	3.42	3.98	4.41	5.03	4.10	4.90
K_2O	4.83	4.77	5.01	4.74	4.00	4.83	4.56	4.25	4.35	5.19	4.88	4.59	4.81
Cl	0.20	0.14	0.15	0.16	0.18	0.20	0.24	0.24	0.30	0.24	0.14	0.07	0.06
Total	100.25	94.74	100.10	100.10	97.78	100.25	95.69	93.77	95.79	98.72	98.45	94.75	99.02

APPENDIX 7.1: Continued.

Sample Code	228u ic30	228u ic32	228u ih33	228u sc34	228u s	228m ic1	228m sc5	228m sf4	228m ic6	228m sc6	228m bic7	228m it9	228m it9
SiO_2	66.90	66.51	64.77	67.99	67.59	66.95	64.91	64.80	68.31	66.27	65.19	66.26	64.27
Al_2O_3	15.44	15.20	15.29	15.71	15.87	14.28	16.55	16.10	14.01	15.50	14.73	15.61	16.10
TiO_2	0.57	0.66	0.49	0.71	0.70	0.29	0.39	0.58	0.33	0.48	0.40	0.68	0.50
FeO^*	2.28	2.59	3.07	2.48	2.65	2.98	1.89	3.52	2.13	2.54	3.11	3.75	3.78
MnO	0.00	0.00	0.00	0.15	0.00	0.25	0.19	0.13	0.00	0.00	0.17	0.00	0.11
MgO	0.50	0.86	0.87	0.58	0.72	0.67	0.43	1.03	0.53	0.69	0.90	0.68	0.80
CaO	1.57	2.06	2.53	1.83	2.31	2.08	2.63	2.65	1.69	2.05	2.42	2.38	2.70
Na_2O	4.78	4.49	4.21	4.92	4.91	3.97	4.78	4.84	3.96	4.53	4.38	4.66	4.46
K_2O	4.68	4.43	4.23	4.87	4.58	4.28	4.08	4.39	4.27	4.29	3.66	4.13	4.05
Cl	0.28	0.17	0.24	0.20	0.19	0.16	0.11	0.22	0.17	0.19	0.14	0.17	0.22
Total	97.00	96.97	95.70	99.44	99.52	95.91	95.96	98.26	95.40	96.54	95.10	98.32	96.99

Sample Code	228m ic11	228m sc11	228m sh12	228m ih13	228L ih1	228L ih2	228L ic3	228L ic4	228L ic4	228L ic18	228L ic30	228L st10	228L sc
SiO_2	67.40	65.46	66.29	67.19	65.80	63.52	64.16	66.25	66.03	64.16	66.24	68.25	68.09
Al_2O_3	14.74	15.92	16.54	15.25	15.59	16.87	15.72	15.69	16.23	15.79	15.10	15.92	16.12
TiO_2	0.52	0.50	0.48	0.66	0.49	0.36	0.49	0.47	0.51	0.52	0.55	0.51	0.52
FeO^*	2.51	2.75	2.88	2.60	2.37	2.69	2.30	2.28	2.39	2.67	2.35	3.09	2.21
MnO	0.00	0.15	0.23	0.00	0.00	0.16	0.00	0.17	0.00	0.00	0.11	0.00	0.12
MgO	0.71	0.74	0.74	0.56	0.42	0.46	0.71	0.57	0.65	0.87	0.56	0.57	0.58
CaO	1.87	2.04	2.45	1.90	1.94	2.34	2.14	1.79	2.02	2.56	1.81	1.82	1.78
Na_2O	4.30	4.55	2.89	4.84	5.04	4.11	4.12	4.12	5.03	4.20	4.00	4.86	5.06
K_2O	4.32	4.44	3.80	4.77	4.42	4.06	4.15	4.32	4.63	4.23	4.63	4.70	4.90
Cl	0.00	0.16	0.19	0.20	0.26	0.31	0.14	0.23	0.21	0.13	0.21	0.17	0.27
Total	96.37	96.71	96.49	97.97	96.33	94.88	93.93	95.89	97.70	95.13	95.56	99.89	99.65

Sample Code	228L ic31	228L ip32	235 sh3	235 ic24	235 sh4	235 ih6	235 sh6	235 1c25	235 so8	235 sc27	235 1c28	235 sh9	235 so11
SiO_2	65.43	67.62	69.16	65.97	68.37	65.42	64.52	67.37	67.58	68.42	66.87	67.92	68.87
Al_2O_3	15.70	15.98	16.00	15.27	15.88	15.23	17.94	15.45	15.98	16.16	15.57	15.98	16.15
TiO_2	0.55	0.42	0.47	0.39	0.42	0.48	0.36	0.47	0.48	0.44	0.49	0.46	0.44
FeO^*	2.30	2.09	2.43	2.47	2.68	2.24	1.92	2.85	2.70	2.51	2.39	2.80	2.70
MnO	0.14	0.00	0.00	0.00	0.14	0.12	0.00	0.00	0.16	0.12	0.16	0.12	0.13
MgO	0.53	0.60	0.58	0.56	0.69	0.73	0.48	0.61	0.65	0.71	0.57	0.72	0.61
CaO	1.81	1.79	1.90	1.93	2.43	1.93	3.48	2.16	2.16	2.10	1.83	2.18	1.97
Na_2O	4.75	4.62	4.79	4.38	4.54	3.75	4.71	4.37	4.89	4.77	4.63	4.71	4.93
K_2O	4.42	4.75	4.52	4.33	4.14	4.15	3.46	4.40	4.16	4.39	4.36	4.44	4.69
Cl	0.20	0.17	0.20	0.21	0.24	0.18	0.11	0.21	0.16	0.19	0.15	0.20	0.22
Total	95.83	98.04	100.05	95.51	99.53	94.23	96.98	97.89	98.92	99.81	97.02	99.53	100.71

APPENDIX 7.1: Continued.

Sample Code	235 st20	235 st22	235 sp29	235 sp32	235 ip32	243 sc1	243 ic2	243 ic3	243 sc4	243 ic6	243 sc7	243 v	243 ic8
SiO_2	67.75	67.42	69.40	69.40	65.98	65.51	63.40	63.56	63.58	66.43	65.68	63.50	63.73
Al_2O_3	16.24	15.96	15.85	15.93	14.74	16.63	16.28	16.26	16.72	14.94	16.36	19.33	15.90
TiO_2	0.44	0.54	0.42	0.44	0.38	0.67	0.61	0.54	0.64	0.41	0.59	0.43	0.60
FeO*	3.06	3.19	2.29	2.55	2.74	3.28	3.21	3.07	3.26	2.27	3.37	2.24	3.16
MnO	0.12	0.12	0.13	0.00	0.00	0.18	0.20	0.14	0.18	0.13	0.21	0.17	0.00
MgO	0.61	0.60	0.65	0.82	0.72	1.14	1.00	0.72	1.09	0.56	0.88	0.65	0.96
CaO	2.21	2.14	1.96	1.87	1.89	2.75	2.60	1.90	2.88	1.89	2.39	4.62	2.81
Na_2O	4.82	4.26	4.74	4.69	4.15	4.96	4.18	5.58	5.20	3.71	4.94	5.48	4.30
K_2O	4.33	4.10	4.46	4.28	4.66	4.27	4.20	4.26	4.23	4.80	4.69	3.54	4.44
Cl	0.23	0.21	0.19	0.20	0.23	0.23	0.20	0.24	0.21	0.26	0.25	0.14	0.24
Total	99.81	98.54	100.09	100.18	95.49	99.62	95.88	96.27	97.99	95.40	99.36	100.10	96.14

Sample Code	243 sh9	243 ic11	243 ic12	243 ih13	246 ip12	246 s	246 s	246 st1	246 ih15	246 ih16	246 bic17	246 sh17	246 bic18
SiO_2	64.68	64.12	63.65	63.36	64.03	65.78	65.27	64.60	64.68	63.49	64.53	63.57	62.12
Al_2O_3	16.37	16.50	16.44	16.52	16.67	16.76	17.08	16.67	17.02	16.32	15.82	16.80	15.95
TiO_2	0.70	0.58	0.49	0.66	0.59	0.50	0.69	0.68	0.66	0.65	0.63	0.71	0.63
FeO*	3.40	3.39	2.91	3.02	3.18	3.31	3.35	3.70	3.30	3.07	3.11	3.68	3.12
MnO	0.00	0.17	0.22	0.13	0.17	0.14	0.17	0.00	0.20	0.12	0.00	0.12	0.00
MgO	1.09	1.11	0.90	0.91	1.10	1.20	1.21	1.06	0.82	0.88	0.71	1.08	1.03
CaO	2.67	2.42	2.50	2.30	2.96	2.64	2.55	2.56	2.53	2.20	2.99	2.63	2.34
Na_2O	5.18	5.61	4.76	4.76	4.96	5.14	5.12	5.41	5.82	5.86	4.07	5.77	5.08
K_2O	4.55	4.53	4.59	4.49	4.11	4.14	4.46	4.65	4.72	4.25	4.52	4.31	4.33
Cl	0.25	0.27	0.25	0.25	0.21	0.17	0.22	0.25	0.26	0.24	0.17	0.21	0.21
Total	98.89	98.70	96.71	96.40	97.98	99.78	100.12	99.58	100.01	97.08	96.55	98.88	94.81

Sample Code	246 bic18	246 bic19	246 sc20	246 ic20	246 io21	251 ic2	251 ic2	251 sc3	251 sc5	251 ic6	251 s	251 sc9	251 ic9
SiO_2	62.78	63.17	66.46	64.52	65.02	61.68	61.59	62.43	63.75	61.12	62.86	63.05	60.14
Al_2O_3	16.02	16.53	15.77	16.57	15.92	15.96	15.87	16.41	16.66	16.23	16.40	16.78	16.49
TiO_2	0.56	0.51	0.63	0.63	0.53	0.72	0.65	0.77	0.74	0.72	0.72	0.71	0.66
FeO*	3.22	3.30	3.42	3.07	3.08	3.93	4.14	4.00	3.82	3.86	3.75	3.85	3.96
MnO	0.12	0.00	0.12	0.00	0.12	0.20	0.15	0.16	0.16	0.13	0.00	0.00	0.17
MgO	0.96	1.04	1.51	1.11	0.82	1.27	1.22	1.42	1.17	1.23	1.17	1.25	1.46
CaO	2.44	2.56	2.11	2.96	2.44	2.85	2.75	3.12	2.76	2.87	2.82	2.87	3.36
Na_2O	4.45	4.87	4.83	5.26	4.69	4.68	4.84	5.25	4.90	4.75	4.96	5.45	4.40
K_2O	4.07	4.14	4.93	4.71	4.25	4.06	4.04	4.44	4.99	4.40	4.50	4.70	4.02
Cl	0.29	0.20	0.24	0.23	0.22	0.15	0.17	0.19	0.12	0.13	0.13	0.15	0.16
Total	94.91	96.32	100.02	99.06	97.09	95.50	95.42	98.19	99.07	95.44	97.31	98.81	94.82

APPENDIX 7.1: Continued.

Sample Code	251 io10	251 sc11	251 it22	251 it20	251 st14	251 sp23	251 v	251 v	251 ip27	251 s	256 if1	256 ic39
SiO_2	61.55	64.32	62.24	62.03	61.26	62.99	60.62	63.87	59.67	63.46	53.06	59.11
Al_2O_3	16.59	16.77	16.77	16.67	16.12	16.69	20.46	16.93	17.65	16.57	18.94	16.87
TiO_2	0.68	0.74	0.78	0.79	0.99	0.66	0.53	0.74	0.72	0.79	0.80	0.80
FeO*	3.47	3.85	4.26	5.06	5.25	3.71	2.87	3.54	3.36	3.59	5.38	4.47
MnO	0.09	0.18	0.16	0.17	0.15	0.17	0.14	0.00	0.00	0.00	0.21	0.13
MgO	1.36	1.16	1.21	1.34	1.20	1.26	1.15	1.08	1.04	1.20	2.07	1.44
CaO	2.65	2.70	2.95	3.37	2.64	2.86	5.93	2.73	3.63	2.83	7.77	3.78
Na_2O	4.71	4.93	4.96	5.02	4.98	5.23	5.35	4.99	4.79	4.99	4.41	4.50
K_2O	4.14	4.82	4.29	4.63	4.56	4.76	3.04	4.29	3.99	4.68	2.52	3.69
Cl	0.16	0.14	0.18	0.20	0.19	0.16	0.08	0.14	0.18	0.13	0.15	0.17
Total	95.40	99.61	97.80	99.28	97.34	98.49	100.17	98.31	95.03	98.24	95.31	94.96

Sample Code	256 s	256 sc14	256 sc44	256 ic45	256 ic46	256 sc46	256 ic47	256 ic48	256 ic49	256 ip7	256 v
SiO_2	61.83	62.14	60.95	61.67	65.84	60.78	59.60	60.15	63.40	60.20	64.71
Al_2O_3	17.57	17.15	17.20	16.99	13.95	17.28	16.76	16.76	16.12	16.80	14.52
TiO_2	0.68	0.76	0.75	0.61	0.35	0.63	0.65	0.64	0.49	0.66	0.65
FeO*	4.85	4.55	5.47	3.42	4.77	4.87	4.29	4.44	4.09	4.73	4.11
MnO	0.19	0.17	0.17	0.18	0.18	0.15	0.17	0.13	0.11	0.11	0.16
MgO	1.69	1.30	1.48	0.86	0.93	1.48	1.78	1.23	0.68	1.76	0.83
CaO	4.49	3.38	3.72	3.12	3.33	3.81	4.55	2.96	2.24	3.45	1.15
Na_2O	5.54	5.21	5.03	4.67	3.32	5.13	4.72	4.84	4.93	4.12	4.92
K_2O	3.15	4.32	4.10	3.58	3.26	3.75	3.38	3.68	3.89	3.65	5.58
Cl	0.17	0.19	0.18	0.21	0.16	0.22	0.17	0.20	0.15	0.17	0.14
Total	100.16	99.17	99.05	95.31	96.09	98.10	96.07	95.03	96.10	95.65	96.77

APPENDIX 7.1: Continued.

Sample Code	19 io1	19 io2	19 so2	19 io3	19 io3	19 so3	19 io4	19 bio5	19 bio6	19 io7	19 bio8
SiO_2	76.27	72.96	76.81	72.77	74.41	74.06	74.49	69.68	73.00	74.77	73.28
Al_2O_3	12.79	12.24	12.80	12.35	12.44	12.24	12.45	13.33	12.13	12.49	12.02
TiO_2	0.17	0.43	0.28	0.13	0.14	0.00	0.21	0.40	0.13	0.28	0.15
FeO^*	2.28	2.52	1.83	2.39	2.14	1.80	2.02	3.48	2.45	2.35	1.86
MnO	0.17	0.18	0.00	0.15	0.00	0.00	0.00	0.00	0.10	0.00	0.16
MgO	0.14	0.19	0.15	0.16	0.13	0.17	0.10	0.49	0.23	0.13	0.15
CaO	1.25	1.29	1.29	1.26	1.24	1.29	1.26	2.34	1.26	1.23	1.24
Na_2O	4.04	3.18	4.29	2.44	3.88	3.40	4.02	3.81	3.55	4.08	3.15
K_2O	2.96	2.80	2.87	2.82	2.89	2.85	2.85	2.45	2.85	2.77	2.91
Cl	0.12	0.13	0.11	0.00	0.12	0.11	0.00	0.14	0.12	0.13	0.10
Total	100.19	95.92	100.43	94.47	97.39	95.92	97.40	96.12	95.82	98.23	95.02

Sample Code	19 bio9	19 so9	19 io11	19 so11	19 io12	19 so12	19 sp25	19 g27	19 g28	10 bio41	10 bst42
SiO_2	74.06	75.44	73.44	76.21	75.23	76.19	75.62	76.16	75.36	73.90	76.97
Al_2O_3	12.19	12.36	12.04	12.54	12.53	12.61	12.20	12.49	12.45	12.35	12.89
TiO_2	0.19	0.15	0.09	0.14	0.17	0.11	0.21	0.20	0.15	0.23	0.16
FeO^*	1.90	1.87	2.33	1.91	1.87	1.86	1.73	1.73	1.79	1.82	1.88
MnO	0.12	0.00	0.13	0.00	0.00	0.00	0.00	0.00	0.00	0.00	0.00
MgO	0.14	0.13	0.17	0.18	0.14	0.14	0.16	0.17	0.19	0.16	0.13
CaO	1.17	1.26	1.25	1.36	1.34	1.31	1.20	1.24	1.34	1.17	1.29
Na_2O	3.92	4.26	3.42	4.03	4.06	3.99	3.72	3.90	3.79	3.91	4.27
K_2O	2.80	2.73	2.59	2.85	2.88	2.85	2.80	2.80	2.86	2.85	2.75
Cl	0.08	0.13	0.11	0.12	0.12	0.12	0.11	0.12	0.16	0.13	0.10
Total	96.57	98.33	95.77	99.34	98.34	99.18	97.75	98.81	98.09	96.52	100.44

APPENDIX 7.1: Continued.

Sample Code	10 bst43	10 st43	10 st44	10 bio45	10 so45	10 bio46	10 bio80	10 so80	10 bit48	10 st48	10 s81	10 i82
SiO_2	76.29	76.92	76.46	74.47	76.52	73.09	76.57	76.86	76.05	75.96	76.21	73.42
Al_2O	12.62	12.78	12.86	12.45	12.59	12.32	12.69	12.83	12.75	12.61	12.78	12.05
TiO_2	0.24	0.21	0.22	0.15	0.16	0.10	0.12	0.17	0.36	0.18	0.30	0.25
FeO^*	2.12	1.76	2.00	2.20	1.78	2.62	1.89	1.93	1.92	1.78	1.59	2.00
MnO	0.00	0.00	0.00	0.00	0.00	0.00	0.00	0.00	0.14	0.00	0.00	0.00
MgO	0.16	0.17	0.17	0.14	0.18	0.14	0.14	0.13	0.17	0.18	0.20	0.15
CaO	1.21	1.23	1.29	1.20	1.30	1.19	1.22	1.24	1.24	1.34	1.27	1.17
Na_2O	4.22	4.50	4.36	4.29	4.36	4.08	4.20	4.25	4.49	4.28	4.04	3.83
K_2O	2.80	2.92	2.91	2.79	2.88	2.82	2.94	2.94	2.70	3.03	3.21	2.78
Cl	0.13	0.16	0.17	0.16	0.15	0.13	0.15	0.14	0.16	0.12	0.12	0.12
Total	99.79	100.65	100.44	97.85	99.92	96.49	99.92	100.49	99.98	99.48	99.72	95.77

Sample Code	10 io83	10 so83	10 io49	10 so84	10 g50	10 bk50	10 g51	10 g52	10 b53	10 v54	10 v56
SiO_2	75.59	77.58	74.89	76.82	77.52	76.87	77.25	76.63	75.95	76.73	76.64
Al_2O	12.64	12.63	12.28	12.78	12.71	12.67	12.86	12.33	12.69	12.67	12.97
TiO_2	0.11	0.18	0.24	0.21	0.22	0.25	0.12	0.23	0.19	0.22	0.23
FeO^*	2.20	1.91	2.13	1.76	1.70	1.83	1.76	1.81	1.72	1.79	1.77
MnO	0.00	0.00	0.11	0.00	0.00	0.12	0.00	0.00	0.00	0.11	0.00
MgO	0.14	0.15	0.11	0.17	0.13	0.18	0.17	0.16	0.19	0.19	0.18
CaO	1.28	1.32	1.15	1.21	1.46	1.30	1.28	1.32	1.28	1.32	1.38
Na_2O	4.27	4.22	3.71	4.15	3.73	4.48	4.28	4.26	4.32	4.39	4.38
K_2O	2.64	2.78	3.30	3.02	3.03	2.77	2.89	3.07	2.78	2.97	3.06
Cl	0.15	0.17	0.17	0.13	0.00	0.07	0.11	0.13	0.11	0.11	0.08
Total	99.02	100.94	97.09	100.25	100.50	99.54	100.72	99.94	99.23	100.50	100.69

APPENDIX 7.1: Continued.

Sample Code	87 io14	87 g33	87 bgk34	87 bgk34	87 bgR34	87 bg35	87 v36	87 bv37	87 g38	87 sp39	87 sq40	87 su41	87 iu41
SiO_2	74.78	78.58	77.49	76.94	77.03	78.70	78.29	78.88	79.08	78.42	79.37	79.01	74.92
Al_2O_3	11.71	12.03	11.81	11.80	11.72	11.85	11.92	12.41	11.94	12.00	12.12	12.02	11.35
TiO_2	0.14	0.12	0.08	0.12	0.00	0.12	0.00	0.16	0.14	0.08	0.00	0.09	0.00
FeO^*	1.31	0.85	1.13	0.84	0.93	0.78	0.77	0.90	0.92	0.80	0.98	1.04	1.59
MnO	0.04	0.00	0.00	0.00	0.00	0.00	0.00	0.13	0.00	0.12	0.00	0.00	0.13
MgO	0.10	0.10	0.21	0.05	0.20	0.16	0.09	0.10	0.09	0.14	0.10	0.07	0.13
CaO	0.95	0.70	0.70	0.74	0.77	0.90	0.64	0.96	0.59	0.61	0.70	0.65	0.92
Na_2O	2.34	3.59	3.30	3.73	3.36	5.55	3.62	4.26	3.85	3.84	3.75	3.58	2.97
K_2O	3.02	3.58	3.97	3.85	4.03	1.09	3.70	3.18	3.67	3.74	3.53	3.67	2.97
Cl	0.13	0.08	0.12	0.13	0.06	0.07	0.05	0.00	0.00	0.10	0.10	0.10	0.08
Total	94.52	99.63	98.81	98.15	98.10	99.22	99.08	100.98	100.28	99.85	100.65	100.23	95.06

Sample Code	84 ip30	84 bg36	84 bsp37	84 gk39	84 gk39	84 gR39	84 g	84 gk40	84 gR40	84 v	84 su42	84 v
SiO_2	78.64	79.21	64.65	78.37	77.10	76.94	78.21	78.10	78.15	77.67	77.57	76.46
Al_2O_3	11.94	12.16	21.03	12.12	11.86	11.97	12.02	11.95	11.83	12.00	11.93	11.63
TiO_2	0.11	0.00	0.22	0.16	0.13	0.13	0.12	0.00	0.07	0.12	0.15	0.00
FeO^*	0.89	0.35	0.87	0.97	0.93	0.84	0.86	0.91	0.84	0.86	1.05	0.91
MnO	0.00	0.00	0.00	0.00	0.14	0.00	0.00	0.00	0.00	0.09	0.00	0.00
MgO	0.13	0.08	0.13	0.10	0.11	0.13	0.14	0.08	0.13	0.13	0.11	0.14
CaO	0.79	0.90	5.76	0.87	0.76	0.77	0.80	0.75	0.81	0.78	0.79	0.82
Na_2O	3.71	4.99	5.97	3.81	3.91	3.99	3.66	3.69	3.78	3.82	3.78	3.57
K_2O	3.39	0.69	1.30	3.26	3.40	3.38	3.40	3.38	3.45	3.40	3.41	3.33
Cl	0.12	0.00	0.00	0.00	0.08	0.06	0.00	0.10	0.10	0.06	0.14	0.13
Total	99.72	98.38	99.93	99.66	98.28	98.21	99.21	98.96	99.16	98.93	98.93	96.99

APPENDIX 7.1: Continued.

Sample Code	92 g20	92 g1	92 g2	92 g3	92 g4	92 g5	92 g7	92 g8	92 g9	92 g10	92 g11	92 g12	92 g13
SiO_2	75.24	75.64	75.66	75.78	76.40	75.78	74.30	75.33	75.47	74.22	75.98	75.17	75.47
Al_2O_3	11.43	11.78	11.38	11.87	11.53	11.37	11.50	11.26	11.44	11.36	11.33	11.11	11.46
TiO_2	0.11	0.11	0.12	0.17	0.17	0.14	0.10	0.15	0.09	0.11	0.11	0.16	0.10
FeO^*	1.14	1.18	1.05	1.11	1.02	1.20	1.03	1.07	1.05	1.06	1.09	1.13	1.26
MnO	0.00	0.00	0.00	0.00	0.00	0.11	0.09	0.00	0.00	0.00	0.00	0.00	0.13
MgO	0.12	0.09	0.13	0.14	0.10	0.11	0.13	0.10	0.12	0.11	0.07	0.12	0.11
CaO	1.02	1.03	0.96	1.01	0.92	0.97	0.94	0.92	0.88	1.01	1.01	1.01	0.93
Na_2O	3.11	3.34	3.43	3.57	3.71	3.01	3.44	3.38	3.47	3.39	3.12	3.20	3.30
K_2O	3.02	3.11	2.90	2.89	2.90	3.10	2.78	2.62	3.08	2.67	2.57	3.02	2.93
Cl	0.15	0.11	0.14	0.13	0.13	0.20	0.15	0.12	0.16	0.14	0.13	0.16	0.12
Total	95.34	96.39	95.77	96.67	96.88	95.99	94.46	94.95	95.76	94.07	95.41	95.08	95.81

Sample Code	92 g14	92 g15	92 g16	92 g17	92 g18	92 g19	89 sh4	89 sh8	89 it11	89 st14	89 sh24	89 ih29	89 bio32
SiO_2	75.78	76.01	75.65	75.59	75.08	75.99	75.59	75.16	74.02	73.97	75.59	73.33	65.26
Al_2O_3	11.31	11.37	11.40	11.47	11.38	11.38	12.13	11.70	11.39	11.42	12.11	12.75	15.61
TiO_2	0.00	0.11	0.10	0.10	0.11	0.17	0.14	0.00	0.49	0.12	0.10	0.13	0.97
FeO^*	1.33	1.04	1.07	1.26	1.04	0.85	1.22	1.23	1.76	1.17	1.21	1.16	3.39
MnO	0.00	0.00	0.00	0.00	0.00	0.00	0.00	0.00	0.00	0.00	0.00	0.11	0.00
MgO	0.14	0.11	0.12	0.11	0.08	0.15	0.10	0.12	0.12	0.11	0.12	0.17	1.14
CaO	1.00	1.08	1.07	0.98	0.97	0.92	1.11	1.18	0.96	1.06	1.02	1.10	3.39
Na_2O	3.41	3.19	3.61	3.41	3.35	3.36	3.19	3.40	2.97	2.53	3.37	3.21	5.16
K_2O	3.08	2.74	2.90	2.72	3.17	3.60	2.75	2.98	2.82	2.95	2.83	2.79	1.88
Cl	0.16	0.16	0.12	0.16	0.14	0.13	0.09	0.00	0.08	0.00	0.09	0.10	0.08
Total	96.21	95.81	96.04	95.80	95.32	96.55	96.32	95.77	94.61	93.33	96.44	94.85	96.88

Sample Code	89 bio39	89 bio39	89 so40	89 9	89 9	89 9	89 9	89 9	89 9	89 9	89 9	89 9	89 9
SiO_2	58.67	58.85	73.34	73.75	73.73	73.62	74.82	74.43	74.59	73.88	73.82	73.89	74.41
Al_2O_3	15.82	15.38	11.52	11.54	11.85	11.66	11.66	11.84	11.38	11.58	11.37	11.54	12.04
TiO_2	0.98	1.00	0.13	0.07	0.13	0.16	0.00	0.20	0.13	0.15	0.11	0.00	0.13
FeO^*	6.12	5.79	1.49	1.14	1.18	1.14	1.19	1.24	1.14	1.25	1.05	1.18	1.15
MnO	0.00	0.00	0.09	0.09	0.00	0.00	0.00	0.00	0.00	0.00	0.00	0.00	0.00
MgO	2.02	2.19	0.11	0.11	0.09	0.17	0.13	0.13	0.13	0.13	0.09	0.14	0.13
CaO	5.05	5.23	0.99	0.98	1.05	1.13	1.18	1.20	1.00	1.01	0.88	1.09	1.08
Na_2O	3.56	3.67	3.05	2.56	3.01	3.39	3.41	3.46	3.19	3.35	2.94	3.00	3.40
K_2O	1.98	1.81	2.87	2.76	2.57	2.66	2.93	2.69	2.83	2.71	2.89	2.78	2.72
Cl	0.13	0.08	0.11	0.11	0.07	0.17	0.13	0.08	0.09	0.12	0.07	0.12	0.11
Total	94.33	94.00	93.70	93.11	93.68	94.10	95.45	95.27	94.48	94.18	93.22	93.74	95.17

APPENDIX 7.1: Continued.

Sample	89	89	89	89	89	89	90	90	90	90	90
Code	9	9	9	9	9	9	ih1	sh7	sh10	g	g
SiO_2	74.52	73.62	74.28	75.16	73.83	74.00	71.14	72.81	73.43	73.49	73.14
Al_2O_3	11.44	11.48	11.71	11.50	11.50	11.55	11.45	11.61	11.66	11.49	11.38
TiO_2	0.00	0.11	0.08	0.12	0.14	0.11	0.24	0.13	0.21	0.15	0.10
FeO^*	0.95	1.26	1.20	1.03	1.03	1.11	2.19	1.04	1.26	1.09	1.09
MnO	0.12	0.00	0.00	0.00	0.00	0.00	0.10	0.00	0.00	0.00	0.00
MgO	0.11	0.13	0.13	0.13	0.10	0.11	0.58	0.09	0.09	0.09	0.15
CaO	0.95	1.11	1.05	0.99	1.07	0.98	1.49	0.95	0.94	1.02	1.03
Na_2O	3.14	3.06	3.22	3.39	2.92	3.27	3.21	3.52	3.42	2.94	3.33
K_2O	2.80	2.46	2.62	2.95	2.73	2.93	3.18	2.72	2.83	2.93	2.87
Cl	0.10	0.12	0.15	0.12	0.12	0.10	0.11	0.15	0.07	0.08	0.11
Total	94.13	93.35	94.44	95.39	93.44	94.16	93.69	93.02	93.91	93.29	93.20

Sample	90	90	90	90	90	90	90	90	90	90	90
Code	g	g	g	g	g	g	g	g	g	g	so11
SiO_2	74.46	73.39	74.61	74.91	72.86	74.26	73.16	73.70	73.25	72.84	74.40
Al_2O_3	11.64	11.62	11.49	11.37	11.74	11.51	11.57	11.64	11.63	11.85	11.55
TiO_2	0.11	0.12	0.13	0.11	0.17	0.09	0.12	0.15	0.10	0.10	0.15
FeO^*	1.05	1.07	1.08	1.17	1.19	1.12	1.12	1.06	1.09	1.07	1.27
MnO	0.00	0.00	0.09	0.00	0.00	0.00	0.00	0.00	0.00	0.00	0.00
MgO	0.10	0.14	0.13	0.09	0.14	0.11	0.11	0.12	0.12	0.10	0.14
CaO	0.98	0.90	1.06	1.00	1.01	0.94	1.02	0.95	1.10	1.05	1.02
Na_2O	3.30	3.46	3.25	2.93	3.41	3.39	3.34	3.47	2.93	3.34	3.38
K_2O	2.81	3.01	2.73	2.96	2.79	3.07	2.63	2.97	2.88	2.66	2.43
Cl	0.00	0.11	0.00	0.09	0.08	0.09	0.00	0.10	0.09	0.09	0.09
Total	94.45	93.82	94.57	94.63	93.39	94.58	93.07	94.16	93.19	93.10	94.43

Sample	90	90	90	90	90	90	90	90	90	90
Code	io12	st15	sh19	io20	io21	io22	io23	io23	sh27	ih
SiO_2	73.24	74.23	73.64	71.22	72.72	72.40	72.30	72.33	73.61	71.23
Al_2O_3	11.66	11.56	11.57	12.88	11.75	11.71	11.70	11.40	11.39	12.84
TiO_2	0.16	0.16	0.10	0.17	0.15	0.20	0.17	0.15	0.10	0.08
FeO^*	1.69	1.24	1.22	1.92	1.27	1.66	1.56	1.47	1.19	1.28
MnO	0.00	0.00	0.00	0.10	0.00	0.00	0.00	0.00	0.00	0.00
MgO	0.13	0.11	0.13	0.15	0.15	0.12	0.14	0.13	0.13	0.19
CaO	0.99	0.99	1.03	1.36	1.17	1.05	0.95	0.89	1.04	0.90
Na_2O	3.39	3.35	3.12	3.03	2.96	2.87	2.92	2.91	2.99	3.49
K_2O	2.79	2.97	2.98	2.70	2.82	2.99	3.65	3.78	2.69	3.60
Cl	0.11	0.12	0.23	0.00	0.12	0.00	0.00	0.09	0.08	0.09
Total	94.16	94.73	94.02	93.53	93.11	93.00	93.39	93.15	93.22	93.70

APPENDIX 7.2: AMPHIBOLES

Sample Code	MnP ifl	MnP 26	MnP 27	MnP 2	MnP -	MnP 13	MnP 14	MnP 31	MnP a28	MnP a29	MnP a30	MnL 7	MnL 10	MnL 9	IL 1	IL 2	IL 10	IL 11	IL 12	IL 13
SiO_2	40.51	38.86	39.08	40.14	39.45	40.27	39.85	40.04	40.30	39.99	39.77	40.88	39.93	39.90	42.90	43.39	42.38	43.15	43.10	44.46
Al_2O_3	13.62	14.06	14.63	13.37	14.74	13.14	14.59	13.81	13.65	14.19	14.25	14.02	14.14	14.68	10.67	10.00	11.41	10.75	10.88	9.83
TiO_2	1.57	2.66	2.41	2.69	2.30	2.70	2.33	2.10	2.55	2.10	2.35	2.79	2.82	2.30	3.11	2.91	2.79	3.40	2.97	2.85
FeO^*	9.20	12.58	11.53	11.83	11.03	12.05	11.17	9.75	11.42	10.08	11.10	10.48	10.56	10.82	12.93	12.64	13.70	10.93	12.55	11.69
MnO	0.10	0.22	0.12	0.21	0.14	0.20	0.00	0.00	0.17	0.00	0.00	0.00	0.00	0.00	0.47	0.50	0.45	0.29	0.39	0.41
MgO	16.31	12.84	13.97	13.62	13.95	13.78	13.82	15.11	13.60	14.43	13.59	14.38	14.37	13.77	13.04	13.65	12.67	14.41	13.48	14.20
CaO	11.45	12.21	12.42	12.19	12.49	12.13	12.31	12.35	12.06	12.27	12.22	12.06	11.89	12.31	11.52	11.54	11.49	11.54	11.93	11.80
Na_2O	2.58	2.49	2.30	2.49	2.38	2.48	2.34	2.18	2.42	2.16	2.24	2.53	2.46	2.39	2.39	2.38	2.51	2.56	2.38	2.28
K_2O	0.92	0.93	1.00	0.94	0.88	0.94	0.93	1.19	0.90	1.12	0.94	0.93	0.89	1.00	1.17	0.87	1.07	0.83	1.00	0.93
Total	96.26	96.85	97.46	97.48	97.36	97.69	97.34	96.53	97.07	96.34	96.46	98.07	97.06	97.17	98.20	97.88	98.47	97.86	98.68	98.45
Cations on the basis of 23 oxygens																				
Si	6.040	5.860	5.822	5.979	5.861	5.990	5.914	5.963	6.004	5.968	5.952	5.992	5.923	5.923	6.350	6.422	6.277	6.335	6.332	6.500
Al	2.370	2.499	2.569	2.347	2.581	2.304	2.552	2.424	2.397	2.496	2.514	2.422	2.472	2.568	1.861	1.744	1.992	1.860	1.884	1.694
Ti	0.177	0.302	0.270	0.301	0.257	0.302	0.260	0.235	0.286	0.236	0.265	0.308	0.315	0.257	0.346	0.324	0.311	0.375	0.328	0.313
Fe	1.128	1.587	1.437	1.474	1.371	1.499	1.386	1.214	1.423	1.258	1.389	1.285	1.310	1.343	1.601	1.565	1.697	1.342	1.542	1.429
Mn	0.012	0.028	0.015	0.026	0.018	0.025	0.000	0.000	0.021	0.000	0.000	0.000	0.000	0.000	0.059	0.063	0.056	0.036	0.049	0.051
Mg	3.598	2.886	3.102	3.024	3.089	3.055	3.056	3.354	3.020	3.209	3.031	3.141	3.177	3.047	2.876	3.011	2.797	3.153	2.952	3.094
Ca	1.822	1.973	1.983	1.946	1.988	1.933	1.957	1.971	1.925	1.962	1.960	1.894	1.890	1.958	1.827	1.830	1.824	1.815	1.878	1.848
Na	0.750	0.728	0.664	0.719	0.686	0.715	0.673	0.630	0.699	0.625	0.650	0.719	0.708	0.688	0.686	0.683	0.721	0.729	0.678	0.646
K	0.176	0.179	0.190	0.179	0.167	0.178	0.176	0.226	0.171	0.213	0.179	0.174	0.168	0.189	0.221	0.164	0.202	0.155	0.187	0.173
Mg No.	0.761	0.641	0.681	0.668	0.690	0.667	0.688	0.734	0.676	0.718	0.686	0.710	0.708	0.694	0.634	0.649	0.615	0.696	0.650	0.676

APPENDIX 7.2: Continued.

Sample Code	IL 15	IL 16	IL 17	IL 18	222 K6	222 Z6	222 Z6	222 Z6	222 Z6	222 R6	222 7	222 8	222 9	222 K10	222 Z10	222 Z10	222 R10	222 11	222 25
SiO_2	43.78	42.68	41.42	44.27	43.76	41.84	43.30	42.29	46.06	43.40	40.79	43.30	43.13	43.39	42.67	43.57	43.55	41.38	41.40
Al_2O_3	10.21	11.48	12.77	9.43	9.87	11.10	9.71	10.86	8.50	10.11	12.36	10.35	10.36	10.33	10.97	10.28	9.88	13.14	11.78
TiO_2	3.17	2.96	2.53	3.20	2.88	3.32	2.93	3.16	2.15	3.36	3.05	3.37	3.50	2.93	3.47	3.32	3.34	2.08	3.59
FeO^*	12.09	13.02	13.16	11.61	11.38	12.55	11.66	12.21	10.96	11.71	11.95	11.58	11.52	11.55	11.48	11.16	11.41	9.88	11.75
MnO	0.41	0.33	0.32	0.00	0.44	0.45	0.34	0.55	0.36	0.48	0.36	0.29	0.29	0.27	0.39	0.31	0.38	0.00	0.31
MgO	14.14	13.56	12.45	14.42	14.66	13.38	14.32	13.30	15.57	14.12	13.37	14.42	14.08	14.62	14.13	14.59	14.35	15.20	13.73
CaO	11.59	11.42	11.82	11.08	11.52	11.57	11.42	11.60	11.50	11.42	11.90	11.51	11.25	11.58	11.61	11.59	11.40	12.18	11.64
Na_2O	2.42	2.37	2.57	2.41	2.39	2.49	2.40	2.41	2.10	2.41	2.40	2.45	2.40	2.40	2.52	2.54	2.50	2.47	2.54
K_2O	0.93	1.01	0.93	0.19	0.86	0.95	0.85	0.93	0.76	0.90	0.83	0.93	0.91	0.85	0.91	0.90	0.88	1.11	0.94
Total	98.74	98.83	97.97	96.61	97.76	97.65	96.93	97.31	97.96	97.91	97.01	98.20	97.44	97.92	98.15	98.26	97.69	97.44	97.68
Cations on the basis of 23 oxygens																			
Si	6.403	6.266	6.154	6.546	6.441	6.227	6.439	6.300	6.709	6.394	6.098	6.356	6.373	6.381	6.275	6.379	6.419	6.093	6.139
Al	1.760	1.986	2.236	1.643	1.712	1.947	1.702	1.907	1.459	1.755	2.178	1.791	1.804	1.790	1.901	1.774	1.716	2.280	2.059
Ti	0.349	0.327	0.283	0.356	0.319	0.372	0.328	0.354	0.236	0.372	0.343	0.372	0.389	0.324	0.384	0.366	0.370	0.230	0.400
Fe	1.479	1.599	1.635	1.436	1.401	1.562	1.450	1.521	1.335	1.443	1.494	1.422	1.424	1.420	1.412	1.366	1.407	1.217	1.457
Mn	0.051	0.041	0.040	0.000	0.055	0.057	0.043	0.069	0.044	0.060	0.046	0.036	0.036	0.034	0.049	0.038	0.047	0.000	0.039
Mg	3.082	2.967	2.757	3.178	3.216	2.968	3.174	2.953	3.380	3.100	2.979	3.155	3.100	3.204	3.097	3.183	3.152	3.336	3.034
Ca	1.816	1.796	1.882	1.755	1.817	1.845	1.820	1.852	1.795	1.803	1.906	1.810	1.781	1.825	1.829	1.818	1.800	1.922	1.849
Na	0.686	0.675	0.740	0.691	0.682	0.719	0.692	0.696	0.593	0.688	0.696	0.697	0.688	0.684	0.719	0.721	0.715	0.705	0.730
K	0.174	0.189	0.176	0.036	0.162	0.180	0.161	0.177	0.141	0.169	0.158	0.174	0.172	0.159	0.171	0.168	0.165	0.209	0.178
Mg No.	0.668	0.644	0.622	0.689	0.688	0.647	0.680	0.650	0.710	0.674	0.659	0.684	0.680	0.688	0.680	0.694	0.684	0.733	0.670

APPENDIX 7.2: Continued.

Sample Code	228u 33	228u 37	228u 31	228u 38	228u 39	228m 2	228m 12	228m 13	228m 14	228m 15	228m 21	228L 22	228L ic4	228L 24	228L 25	228L 26	228L 27	228L 28	228L K29
SiO_2	41.79	43.69	42.99	40.90	42.19	40.02	42.42	42.09	39.33	43.51	40.11	43.83	40.60	44.13	40.44	42.63	41.75	41.70	41.26
Al_2O_3	11.72	9.72	10.50	12.87	11.52	14.14	10.61	10.47	13.62	10.24	13.42	9.71	12.03	9.09	13.23	10.65	11.44	11.00	11.82
TiO_2	3.04	3.10	3.79	2.98	2.09	2.42	3.47	2.51	2.78	2.89	2.55	2.35	3.17	2.83	2.73	3.38	2.93	3.42	2.95
FeO^*	12.62	11.66	10.94	11.55	9.85	13.03	12.12	13.44	12.74	11.14	12.28	12.57	11.84	11.25	11.76	11.48	11.79	11.05	12.22
MnO	0.28	0.37	0.33	0.21	0.13	0.15	0.39	0.34	0.26	0.34	0.18	0.42	0.43	0.50	0.21	0.28	0.36	0.37	0.36
MgO	13.59	14.46	14.60	13.28	15.35	12.91	13.91	12.08	12.43	14.74	13.20	13.23	13.65	15.03	13.45	14.48	14.16	14.70	14.06
CaO	11.75	11.44	11.60	11.97	12.08	12.01	11.08	11.45	12.21	11.39	11.76	11.47	11.75	11.47	11.78	11.59	11.75	11.38	11.78
Na_2O	2.62	2.31	2.67	2.50	2.51	2.34	2.43	2.04	2.37	2.39	2.40	2.14	2.58	2.29	2.52	2.55	2.49	2.43	2.46
K_2O	0.85	0.93	0.95	0.97	1.09	0.91	0.96	1.05	1.01	0.89	0.89	0.94	1.01	0.83	0.90	0.96	0.92	0.98	0.94
Total	98.26	97.78	98.37	97.23	96.81	97.93	97.39	95.47	96.75	97.53	96.79	96.66	97.06	97.42	97.02	98.00	97.59	97.03	97.85
Cations on the basis of 23 oxygens																			
Si	6.178	6.444	6.296	6.087	6.253	5.951	6.300	6.415	5.938	6.409	6.015	6.550	6.080	6.512	6.037	6.281	6.195	6.203	6.125
Al	2.042	1.690	1.812	2.258	2.012	2.478	1.857	1.881	2.423	1.778	2.372	1.710	2.123	1.581	2.328	1.849	2.001	1.928	2.068
Ti	0.338	0.344	0.417	0.334	0.233	0.271	0.388	0.288	0.316	0.320	0.288	0.264	0.357	0.314	0.306	0.375	0.327	0.383	0.329
Fe	1.560	1.438	1.340	1.438	1.221	1.621	1.505	1.713	1.609	1.372	1.540	1.571	1.483	1.388	1.468	1.415	1.463	1.375	1.517
Mn	0.035	0.046	0.041	0.026	0.016	0.019	0.049	0.044	0.033	0.042	0.023	0.053	0.055	0.062	0.027	0.035	0.045	0.047	0.045
Mg	2.994	3.179	3.186	2.946	3.390	2.861	3.079	2.744	2.797	3.236	2.950	2.946	3.046	3.305	2.992	3.180	3.132	3.259	3.110
Ca	1.861	1.808	1.820	1.909	1.918	1.914	1.763	1.870	1.975	1.798	1.890	1.837	1.885	1.814	1.884	1.830	1.868	1.814	1.874
Na	0.751	0.661	0.758	0.721	0.721	0.675	0.700	0.603	0.694	0.683	0.698	0.620	0.749	0.655	0.729	0.729	0.716	0.701	0.708
K	0.160	0.175	0.177	0.184	0.206	0.173	0.182	0.204	0.195	0.167	0.170	0.179	0.193	0.156	0.171	0.180	0.174	0.186	0.178
Mg No.	0.652	0.682	0.698	0.668	0.733	0.636	0.665	0.610	0.630	0.696	0.654	0.645	0.665	0.695	0.667	0.687	0.675	0.696	0.666

APPENDIX 7.2: Continued.

Sample Code	228L Z29	228L Z29	228L Z29	228L 1	228L 2	235 1	235 2	235 3	235 4	235 5	235 6	235 9	235 10	243 14	243 15	243 16	243 13
SiO_2	41.56	41.93	41.91	39.71	39.89	43.24	42.79	40.16	41.70	42.79	42.87	42.18	42.68	43.01	42.16	42.73	43.10
Al_2O_3	11.75	10.95	10.97	13.70	13.70	10.24	10.73	13.29	11.38	11.14	10.42	10.92	10.45	10.54	11.11	11.31	11.08
TiO_2	2.97	3.22	3.30	2.85	2.61	3.35	3.16	2.38	2.79	3.02	3.05	2.88	3.44	3.07	3.82	3.45	3.82
FeO^*	11.52	10.90	11.91	12.05	11.92	10.98	11.95	12.06	12.03	11.58	10.82	11.43	11.10	12.37	10.91	11.04	10.52
MnO	0.35	0.24	0.40	0.19	0.00	0.38	0.38	0.17	0.24	0.39	0.29	0.31	0.34	0.34	0.28	0.24	0.32
MgO	13.87	14.58	13.72	13.42	13.54	15.07	14.33	13.32	13.95	14.32	14.29	14.36	14.76	13.62	14.13	14.54	14.87
CaO	11.75	11.84	11.56	11.93	12.23	11.44	11.44	11.99	11.83	11.53	11.30	11.77	11.51	11.46	11.36	11.58	11.46
Na_2O	2.47	2.48	2.48	2.57	2.57	2.48	2.39	2.33	2.39	2.41	2.30	2.47	2.38	2.36	2.57	2.47	2.57
K_2O	0.98	0.91	0.96	0.94	0.94	0.91	0.86	0.89	0.82	0.84	0.82	0.77	0.83	1.19	1.01	0.94	0.96
Total	97.22	97.05	97.21	97.36	97.40	98.09	98.03	96.59	97.13	98.02	96.16	97.09	97.49	97.96	97.35	98.30	98.70

Cations on the basis of 23 oxygens

Si	6.184	6.231	6.246	5.929	5.947	6.341	6.305	6.031	6.216	6.293	6.394	6.270	6.303	6.360	6.238	6.254	6.268
Al	2.061	1.918	1.927	2.411	2.407	1.770	1.863	2.352	1.999	1.931	1.832	1.913	1.819	1.837	1.938	1.951	1.899
Ti	0.332	0.360	0.370	0.320	0.293	0.369	0.350	0.269	0.313	0.334	0.342	0.322	0.382	0.341	0.425	0.380	0.418
Fe	1.434	1.355	1.484	1.505	1.486	1.347	1.473	1.515	1.500	1.424	1.350	1.421	1.371	1.530	1.350	1.351	1.280
Mn	0.044	0.030	0.050	0.024	0.000	0.047	0.047	0.022	0.030	0.049	0.037	0.039	0.043	0.043	0.035	0.030	0.039
Mg	3.076	3.229	3.047	2.986	3.008	3.294	3.147	2.981	3.099	3.138	3.176	3.181	3.248	3.002	3.116	3.171	3.223
Ca	1.873	1.885	1.846	1.909	1.954	1.798	1.806	1.929	1.890	1.817	1.806	1.875	1.821	1.816	1.801	1.816	1.786
Na	0.713	0.715	0.717	0.744	0.743	0.705	0.683	0.678	0.691	0.687	0.665	0.712	0.681	0.677	0.737	0.701	0.725
K	0.186	0.173	0.183	0.179	0.179	0.170	0.162	0.171	0.156	0.158	0.156	0.146	0.156	0.225	0.191	0.176	0.178
Mg No.	0.675	0.700	0.665	0.661	0.669	0.703	0.674	0.660	0.669	0.681	0.696	0.685	0.697	0.656	0.692	0.697	0.710

APPENDIX 7.2: Continued.

Sample Code	246 23	246 15	246 16	246 17	246 df27	246 df27	251 33	251 34	251 35	251 36	251 37	256 18	256 19	256 20	256 21	256 23	256 25	256 25	256 df31	256 e32
SiO_2	42.75	42.33	42.49	42.64	40.84	40.23	40.37	42.45	39.98	40.70	40.72	41.27	42.11	40.44	41.28	42.02	41.24	41.50	41.55	42.26
Al_2O_3	11.08	12.20	11.31	10.92	13.71	13.95	14.13	11.14	13.54	13.72	12.91	11.49	11.82	14.50	13.26	11.59	12.96	12.66	13.35	11.38
TiO_2	3.70	2.56	3.74	3.83	2.50	2.16	2.75	3.66	2.66	2.75	2.83	3.76	3.87	2.16	2.45	3.90	2.71	2.59	2.34	3.57
FeO^*	11.83	11.46	11.33	11.22	10.44	10.41	11.63	11.01	11.27	11.58	11.38	12.07	11.44	10.51	12.85	11.79	12.76	12.29	9.66	11.16
MnO	0.29	0.16	0.22	0.28	0.14	0.14	0.13	0.27	0.00	0.00	0.18	0.20	0.17	0.20	0.18	0.34	0.25	0.27	0.00	0.26
MgO	14.31	14.51	14.91	14.74	14.27	14.57	14.01	14.81	13.83	13.66	13.79	13.87	14.33	13.63	13.68	13.87	13.00	13.52	15.23	14.15
CaO	11.36	11.76	11.19	11.31	11.76	12.22	12.26	11.62	12.20	12.13	12.07	11.36	11.41	11.83	12.34	11.37	12.10	11.72	11.40	11.36
Na_2O	2.56	2.57	2.61	2.59	2.50	2.43	2.52	2.57	2.27	2.43	2.41	2.62	2.71	2.36	2.38	2.75	2.55	2.59	2.61	2.66
K_2O	1.00	0.94	1.03	0.99	0.98	0.97	0.83	0.88	0.86	0.98	0.88	1.06	0.93	0.92	0.90	0.90	0.91	0.76	0.92	0.95
Total	98.88	98.49	98.83	98.52	97.14	97.08	98.63	98.41	96.61	97.95	97.17	97.70	98.79	96.55	99.32	98.53	98.48	97.90	97.06	97.75

Cations on the basis of 23 oxygens

Si	6.246	6.197	6.199	6.239	6.043	5.970	5.926	6.214	5.980	6.008	6.059	6.131	6.151	6.017	6.044	6.170	6.090	6.139	6.113	6.230
Al	1.908	2.105	1.945	1.883	2.391	2.440	2.445	1.922	2.387	2.387	2.264	2.012	2.035	2.543	2.288	2.006	2.256	2.207	2.315	1.977
Ti	0.407	0.282	0.410	0.421	0.278	0.241	0.304	0.403	0.299	0.305	0.317	0.420	0.425	0.242	0.270	0.431	0.301	0.288	0.259	0.396
Fe	1.446	1.403	1.382	1.373	1.292	1.292	1.428	1.348	1.410	1.430	1.416	1.499	1.398	1.308	1.574	1.448	1.576	1.520	1.189	1.376
Mn	0.036	0.020	0.027	0.035	0.018	0.018	0.016	0.033	0.000	0.000	0.023	0.025	0.021	0.025	0.022	0.042	0.031	0.034	0.000	0.032
Mg	3.116	3.166	3.242	3.214	3.147	3.222	3.065	3.231	3.083	3.005	3.058	3.071	3.120	3.022	2.985	3.035	2.861	2.980	3.339	3.109
Ca	1.779	1.845	1.749	1.773	1.864	1.943	1.928	1.823	1.955	1.919	1.924	1.808	1.786	1.886	1.936	1.789	1.915	1.858	1.797	1.795
Na	0.725	0.729	0.738	0.735	0.717	0.699	0.717	0.730	0.658	0.696	0.695	0.755	0.768	0.681	0.676	0.783	0.730	0.743	0.745	0.760
K	0.186	0.176	0.192	0.185	0.185	0.184	0.155	0.164	0.164	0.185	0.167	0.201	0.173	0.175	0.168	0.169	0.171	0.143	0.173	0.179
Mg No.	0.678	0.690	0.697	0.695	0.706	0.711	0.680	0.701	0.686	0.678	0.680	0.668	0.687	0.694	0.652	0.671	0.640	0.657	0.737	0.688

APPENDIX 7.2: Continued.

Sample Code	89 1	89 2	89 3	89 4	89 8	89 9	89 10	89 18	89 19	89 20	89 21	89 22	89 23	89 24	89 28	89 30	89 Ro35
SiO_2	46.10	44.00	47.58	47.36	45.86	47.61	43.86	43.95	42.90	46.61	45.82	46.43	43.90	44.85	44.12	44.04	45.71
Al_2O_3	7.03	8.98	5.92	6.23	7.46	6.60	8.78	9.31	9.96	6.62	7.40	6.80	8.58	8.09	8.74	8.70	8.05
TiO_2	1.41	2.31	1.18	1.28	1.67	1.44	2.10	2.54	2.72	1.34	1.76	1.55	2.27	1.72	2.08	2.35	1.77
FeO^*	18.62	15.09	15.00	17.44	18.52	15.77	16.89	14.32	14.39	16.34	16.50	15.98	16.70	18.09	17.45	15.14	11.92
MnO	0.43	0.43	0.38	0.45	0.55	0.49	0.51	0.47	0.53	0.43	0.47	0.38	0.49	0.43	0.59	0.38	0.24
MgO	11.63	12.60	14.04	12.38	11.41	13.00	11.43	13.17	13.09	13.02	12.52	12.98	12.00	11.03	11.44	12.86	14.96
CaO	10.38	10.73	10.64	10.41	10.31	10.67	10.80	10.79	11.11	10.55	10.70	10.86	10.23	10.48	10.37	10.82	11.29
Na_2O	1.51	2.14	1.34	1.51	1.79	1.45	2.02	2.21	2.49	1.51	1.69	1.53	2.00	1.76	1.96	2.10	3.48
K_2O	0.37	0.31	0.40	0.25	0.25	0.33	0.34	0.27	0.26	0.33	0.32	0.32	0.31	0.32	0.28	0.31	0.31
Total	97.48	96.69	96.48	97.31	97.82	97.36	96.73	97.03	97.45	96.75	97.19	96.83	96.48	96.77	97.03	96.70	97.73

Cations on the basis of 23 oxygens

Si	6.937	6.619	7.099	7.080	6.879	7.061	6.648	6.561	6.408	6.991	6.864	6.954	6.654	6.802	6.669	6.622	6.720
Al	1.247	1.592	1.041	1.098	1.319	1.154	1.568	1.638	1.753	1.170	1.307	1.200	1.533	1.446	1.557	1.542	1.395
Ti	0.160	0.261	0.132	0.144	0.188	0.161	0.239	0.285	0.306	0.151	0.198	0.175	0.259	0.196	0.236	0.266	0.196
Fe	2.343	1.899	1.872	2.180	2.323	1.956	2.141	1.788	1.798	2.050	2.067	2.002	2.117	2.294	2.206	1.904	1.466
Mn	0.055	0.055	0.048	0.057	0.070	0.062	0.065	0.059	0.067	0.055	0.060	0.048	0.063	0.055	0.076	0.048	0.030
Mg	2.608	2.825	3.122	2.758	2.551	2.873	2.582	2.930	2.914	2.910	2.795	2.897	2.711	2.493	2.577	2.882	3.278
Ca	1.674	1.730	1.701	1.667	1.657	1.696	1.754	1.726	1.778	1.695	1.718	1.743	1.661	1.703	1.680	1.743	1.778
Na	0.441	0.624	0.388	0.438	0.521	0.417	0.594	0.640	0.721	0.439	0.491	0.444	0.588	0.518	0.574	0.612	0.992
K	0.071	0.059	0.076	0.048	0.048	0.062	0.066	0.051	0.050	0.063	0.061	0.061	0.060	0.062	0.054	0.059	0.058
Mg No.	0.521	0.591	0.619	0.552	0.516	0.587	0.539	0.613	0.610	0.580	0.568	0.586	0.554	0.515	0.530	0.596	0.687

APPENDIX 7.2: Continued.

Sample	89	90	90	90	90	90	90	90	90	90	90	90	90	90	90	90	90
Code	a38	1	1	2	4	5	7	8	9	10	18	19	24	18	27	29	32
SiO_2	45.99	43.98	45.48	44.72	43.46	43.88	42.66	46.12	46.64	45.16	45.68	46.84	46.79	45.55	46.55	42.65	47.54
Al_2O_3	8.56	9.38	7.42	8.46	9.05	9.91	10.87	7.24	6.64	7.72	7.15	6.44	6.87	7.38	6.54	10.60	6.29
TiO_2	1.76	2.19	1.78	2.15	2.34	2.47	2.69	1.62	1.55	1.81	1.59	1.32	1.60	1.76	1.54	2.88	1.17
FeO^*	13.82	15.70	16.26	15.16	15.85	13.81	12.70	17.23	15.36	17.47	16.84	15.17	15.73	16.74	15.40	12.38	16.28
MnO	0.30	0.36	0.48	0.48	0.41	0.36	0.36	0.58	0.33	0.42	0.51	0.32	0.43	0.41	0.30	0.25	0.38
MgO	14.26	12.19	12.58	12.79	12.27	13.38	13.87	11.76	13.79	12.31	12.09	13.12	12.81	12.42	12.84	13.95	13.41
CaO	10.97	10.79	10.58	10.76	10.48	11.00	11.07	10.64	11.04	10.85	10.57	10.98	10.81	10.48	10.88	11.19	10.23
Na_2O	1.62	2.21	1.68	1.92	2.10	2.29	2.46	1.63	1.46	1.77	1.67	1.44	1.63	1.63	1.54	2.32	1.25
K_2O	0.43	0.34	0.24	0.27	0.28	0.31	0.24	0.35	0.32	0.37	0.38	0.35	0.32	0.30	0.36	0.23	0.31
Total	97.71	97.14	96.50	96.71	96.24	97.41	96.92	97.17	97.13	97.88	96.48	95.98	96.99	96.67	95.95	96.45	96.86
Cations on the basis of 23 oxygens																	
Si	6.762	6.596	6.854	6.708	6.586	6.511	6.347	6.928	6.944	6.763	6.907	7.044	6.983	6.863	7.015	6.365	7.088
Al	1.483	1.658	1.318	1.496	1.616	1.733	1.906	1.282	1.165	1.363	1.274	1.141	1.208	1.310	1.162	1.864	1.105
Ti	0.195	0.247	0.202	0.243	0.267	0.276	0.301	0.183	0.174	0.204	0.181	0.149	0.180	0.199	0.175	0.323	0.131
Fe	1.699	1.969	2.049	1.902	2.009	1.714	1.580	2.165	1.913	2.188	2.129	1.908	1.963	2.109	1.941	1.545	2.030
Mn	0.037	0.046	0.061	0.061	0.053	0.045	0.045	0.074	0.042	0.053	0.065	0.041	0.054	0.052	0.038	0.032	0.048
Mg	3.125	2.725	2.825	2.859	2.771	2.959	3.076	2.633	3.060	2.747	2.724	2.940	2.849	2.789	2.884	3.103	2.980
Ca	1.728	1.734	1.708	1.729	1.702	1.749	1.765	1.713	1.761	1.741	1.712	1.769	1.729	1.692	1.757	1.789	1.634
Na	0.462	0.643	0.491	0.558	0.617	0.659	0.710	0.475	0.421	0.514	0.490	0.420	0.472	0.476	0.450	0.671	0.361
K	0.081	0.065	0.046	0.052	0.054	0.059	0.046	0.067	0.061	0.071	0.073	0.067	0.061	0.058	0.069	0.044	0.059
Mg No.	0.643	0.575	0.572	0.593	0.573	0.627	0.654	0.540	0.610	0.551	0.554	0.601	0.585	0.563	0.593	0.663	0.589

APPENDIX 7.2: Continued.

Sample	84	84	84	84	84	84	84	84	87	87	87	87	87
Code	11	K12	R12	K12	R12	15	18	19	17	K18	R18	19	21
SiO_2	49.17	46.10	48.41	47.87	48.23	48.69	44.25	45.09	48.40	48.36	44.98	48.70	48.07
Al_2O_3	5.21	7.35	5.73	6.37	5.84	5.76	7.91	7.81	6.47	6.25	9.20	6.04	6.64
TiO_2	0.94	1.67	1.16	1.23	1.14	1.09	2.00	1.64	1.46	1.43	2.09	1.37	1.47
FeO^*	14.45	15.06	14.96	14.57	15.05	13.86	18.44	17.38	14.41	15.00	16.09	14.32	14.18
MnO	0.87	0.67	0.67	0.53	0.61	0.79	0.83	0.44	0.64	0.45	0.49	0.67	0.57
MgO	14.84	12.77	13.72	13.97	13.73	14.68	10.95	11.31	13.97	13.72	11.91	14.04	14.10
CaO	9.70	10.38	10.18	10.45	10.53	10.38	10.17	10.55	10.52	10.57	10.73	10.39	10.60
Na_2O	1.31	1.66	1.37	1.46	1.37	1.34	1.72	1.62	1.04	1.05	1.27	1.13	1.46
K_2O	0.17	0.29	0.19	0.20	0.27	0.18	0.43	0.55	0.27	0.31	0.49	0.25	0.31
Total	96.48	95.69	96.39	96.65	96.77	96.77	96.70	96.39	97.18	97.14	97.25	96.91	97.40

Cations on the basis of 23 oxygens

Si	7.265	6.938	7.203	7.101	7.164	7.184	6.750	6.848	7.122	7.138	6.716	7.180	7.068
Al	0.907	1.304	1.005	1.114	1.022	1.002	1.422	1.398	1.122	1.087	1.619	1.050	1.151
Ti	0.104	0.189	0.130	0.137	0.127	0.121	0.229	0.187	0.162	0.159	0.235	0.152	0.163
Fe	1.785	1.896	1.862	1.808	1.870	1.710	2.353	2.207	1.773	1.852	2.009	1.766	1.744
Mn	0.109	0.085	0.084	0.067	0.077	0.099	0.107	0.057	0.080	0.056	0.062	0.084	0.071
Mg	3.268	2.864	3.042	3.088	3.039	3.228	2.489	2.560	3.064	3.018	2.650	3.085	3.090
Ca	1.536	1.674	1.623	1.661	1.676	1.641	1.662	1.717	1.659	1.672	1.717	1.641	1.670
Na	0.375	0.484	0.395	0.420	0.395	0.383	0.509	0.477	0.297	0.300	0.368	0.323	0.416
K	0.032	0.056	0.036	0.038	0.051	0.034	0.084	0.107	0.051	0.058	0.093	0.047	0.058
Mg No.	0.633	0.591	0.610	0.622	0.610	0.641	0.503	0.531	0.623	0.613	0.561	0.625	0.630

APPENDIX 7.3: CLINOPYROXENE

Sample Code	MnP 25	MnP 10	MnP 11	MnP 11	MnP 15	MnP 16	MnP 16	MnP K32	MnP R32	MnP 33	MnP 34	MnP -	MnP -	MnP -	MnP 24	MnL ih10	MnL K13	MnL Z13	MnL Z13
SiO_2	49.02	50.57	48.90	49.75	51.06	n.d.	51.33	51.47	50.39	50.10	48.38	48.57	52.19	50.10	47.45	n.d.	51.02	49.55	50.19
Al_2O_3	4.55	2.68	4.32	3.59	2.33	1.00	1.35	2.21	3.45	3.36	5.58	5.08	1.90	3.44	6.31	4.62	3.76	5.21	4.32
TiO_2	0.60	0.40	0.57	0.47	0.54	n.d.	0.19	0.47	0.56	0.53	0.93	0.63	0.40	0.68	0.98	0.70	0.79	0.96	0.74
FeO^*	6.29	7.58	7.04	7.14	7.42	13.76	11.58	7.24	7.87	8.21	8.07	7.41	7.56	6.77	7.85	6.90	7.77	7.05	8.21
MnO	0.00	0.42	0.18	0.13	0.33	0.33	0.47	0.48	0.29	0.46	0.17	0.15	0.41	0.26	0.00	0.25	0.24	0.00	0.27
MgO	14.56	15.46	13.47	14.41	15.47	11.27	12.66	14.78	13.81	13.99	12.90	14.16	16.15	14.34	13.66	14.51	14.57	14.15	13.89
CaO	23.42	21.80	23.30	23.27	21.86	20.58	20.99	22.52	22.69	21.03	22.79	23.33	20.59	22.41	23.31	23.07	21.77	23.26	22.23
Na_2O	0.29	0.45	0.28	0.27	0.30	n.d.	0.31	0.35	0.43	0.34	0.30	0.26	0.30	0.32	0.30	n.d.	0.43	0.26	0.36
Total	98.73	99.36	98.06	99.03	99.31	-	98.88	99.52	99.49	98.02	99.10	99.59	99.50	98.32	99.86	-	100.35	100.44	100.21
Cations on the basis of 6 oxygens																			
Si	1.846	1.896	1.861	1.874	1.911	-	1.961	1.924	1.891	1.904	1.827	1.824	1.940	1.892	1.782	-	1.889	1.836	1.869
Al	0.202	0.118	0.194	0.159	0.103	-	0.061	0.097	0.153	0.150	0.248	0.225	0.083	0.153	0.279	-	0.164	0.228	0.190
Ti	0.017	0.011	0.016	0.013	0.015	-	0.005	0.013	0.016	0.015	0.026	0.018	0.011	0.019	0.028	-	0.022	0.027	0.021
Fe	0.198	0.238	0.224	0.225	0.232	-	0.370	0.226	0.247	0.261	0.255	0.233	0.235	0.214	0.247	-	0.241	0.218	0.256
Mn	0.000	0.013	0.006	0.004	0.010	-	0.015	0.015	0.009	0.015	0.005	0.005	0.013	0.008	0.000	-	0.008	0.000	0.009
Mg	0.817	0.864	0.764	0.809	0.863	-	0.721	0.823	0.772	0.792	0.726	0.793	0.895	0.807	0.765	-	0.804	0.781	0.771
Ca	0.945	0.876	0.950	0.939	0.877	-	0.859	0.902	0.913	0.856	0.922	0.939	0.820	0.907	0.938	-	0.864	0.924	0.887
Na	0.021	0.033	0.021	0.020	0.022	-	0.023	0.025	0.031	0.025	0.022	0.019	0.022	0.023	0.022	-	0.031	0.019	0.026
Sum	4.047	4.050	4.036	4.043	4.033	-	4.015	4.027	4.032	4.018	4.033	4.055	4.018	4.024	4.061	-	4.022	4.033	4.028
Wo	48.2	44.3	49.0	47.6	44.5	43.8	44.1	46.2	47.2	44.8	48.5	47.8	42.1	47.0	48.1	47.4	45.3	48.0	46.4
En	41.7	43.7	39.4	41.0	43.8	33.4	37.0	42.2	40.0	41.5	38.1	40.4	45.9	41.9	39.2	41.5	42.1	40.6	40.3
Fs	10.1	12.0	11.6	11.4	11.8	22.9	19.0	11.6	12.8	13.7	13.4	11.8	12.1	11.1	12.6	11.1	12.6	11.4	13.4

APPENDIX 7.3: Continued.

Sample Code	MnL Z13	MnL Z13	MnL Z13	MnL R13	MnL 14	MnL 18	MnL 20	MnL 25	MnL 25	MnL 26	MnL R1	MnL 12	MnL 11	MnL 8	MnL 27	MnL 28	MnL 29	IL 14	IL K26
SiO_2	51.54	48.99	n.d.	50.88	49.11	48.30	50.19	48.16	49.56	49.63	48.58	51.73	48.98	48.79	49.53	46.94	50.69	53.78	n.d.
Al_2O_3	3.29	5.55	3.81	4.48	5.56	6.42	4.66	4.54	5.09	4.95	5.58	2.14	5.10	5.59	4.78	6.94	3.94	0.71	1.41
TiO_2	0.57	1.18	0.58	0.66	0.85	0.86	0.85	1.20	0.73	0.75	0.81	0.49	0.84	1.26	0.82	1.17	0.44	0.18	0.26
FeO^*	5.90	7.86	6.46	6.93	8.32	8.32	6.71	7.83	7.50	7.04	8.02	7.59	8.16	8.01	7.13	8.39	6.52	7.03	7.86
MnO	0.12	0.17	0.13	0.16	0.21	0.24	0.00	0.25	0.00	0.17	0.17	0.41	0.18	0.16	0.00	0.00	0.17	0.90	0.72
MgO	15.14	13.80	15.47	14.71	13.09	13.19	14.36	13.33	14.33	14.38	13.51	15.09	13.40	13.59	14.49	12.64	14.73	15.12	14.77
CaO	23.12	22.54	22.96	22.80	23.10	22.63	23.44	21.04	22.11	22.45	23.02	22.26	22.37	22.20	22.34	22.12	22.59	22.84	22.40
Na_2O	0.20	0.39	n.d.	0.32	0.34	0.38	0.31	0.42	0.33	0.33	0.40	0.34	0.45	0.40	0.30	0.33	0.32	0.33	0.44
Total	99.88	100.48	-	100.94	100.58	100.34	100.52	96.77	99.65	99.70	100.09	100.05	99.48	100.00	99.39	98.53	99.40	100.89	-
Cations on the basis of 6 oxygens																			
Si	1.905	1.821	-	1.870	1.830	1.804	1.855	1.856	1.849	1.850	1.819	1.924	1.841	1.823	1.851	1.785	1.888	1.979	-
Al	0.143	0.243	-	0.194	0.244	0.283	0.203	0.206	0.224	0.217	0.246	0.094	0.226	0.246	0.211	0.311	0.173	0.031	-
Ti	0.016	0.033	-	0.018	0.024	0.024	0.024	0.035	0.020	0.021	0.023	0.014	0.024	0.035	0.023	0.033	0.012	0.005	-
Fe	0.182	0.244	-	0.213	0.259	0.260	0.207	0.252	0.234	0.219	0.251	0.236	0.257	0.250	0.223	0.267	0.203	0.216	-
Mn	0.004	0.005	-	0.005	0.007	0.008	0.000	0.008	0.000	0.005	0.005	0.013	0.006	0.005	0.000	0.000	0.005	0.028	-
Mg	0.834	0.765	-	0.806	0.727	0.734	0.791	0.765	0.797	0.799	0.754	0.836	0.751	0.757	0.807	0.716	0.818	0.829	-
Ca	0.916	0.898	-	0.898	0.922	0.905	0.928	0.869	0.884	0.897	0.923	0.887	0.901	0.889	0.895	0.901	0.902	0.901	-
Na	0.014	0.028	-	0.023	0.025	0.028	0.022	0.031	0.024	0.024	0.029	0.025	0.033	0.029	0.022	0.024	0.023	0.024	-
Sum	4.015	4.038	-	4.026	4.037	4.045	4.031	4.022	4.031	4.032	4.050	4.028	4.038	4.033	4.031	4.038	4.025	4.012	-
Wo	47.4	47.1	46.4	46.8	48.3	47.7	48.2	46.0	46.2	46.8	47.9	45.3	47.2	46.9	46.5	47.8	46.9	46.3	45.6
En	43.2	40.1	43.5	42.0	38.1	38.6	41.1	40.6	41.6	41.7	39.1	42.7	39.3	39.9	41.9	38.0	42.5	42.6	41.9
Fs	9.4	12.8	10.2	11.1	13.6	13.7	10.8	13.4	12.2	11.5	13.0	12.0	13.4	13.2	11.6	14.2	10.6	11.1	12.5

APPENDIX 7.3: Continued.

Sample Code	IL Z26	IL Z26	IL Z26	IL Z26	IL R26	IL K14	IL S14	IL Z14	IL Z14	IL Z14	IL R14	IL 22	IL 22	IL 23	IL 24	IL 25	222 df1	222 2	222 K3
SiO_2	n.d.	n.d.	51.83	n.d.	53.20	52.26	53.34	52.80	n.d.	n.d.	53.26	51.87	53.37	n.d.	53.02	52.68	52.81	52.13	52.27
Al_2O_3	2.83	2.03	2.70	1.45	1.25	2.23	1.21	1.62	0.89	1.15	1.13	2.30	1.17	1.62	1.39	1.72	1.54	2.27	1.62
TiO_2	0.54	0.44	0.50	0.37	0.28	0.50	0.33	0.37	0.30	0.27	0.30	0.49	0.19	0.32	0.30	0.38	0.40	0.57	0.45
FeO^*	7.94	8.32	8.63	7.66	6.95	7.90	7.23	7.67	7.38	7.17	7.04	7.63	8.13	8.44	7.50	7.52	7.41	7.78	7.39
MnO	0.33	0.57	0.48	0.67	0.67	0.68	0.85	0.71	0.67	0.75	0.68	0.59	0.70	0.72	0.66	0.68	0.72	0.46	0.79
MgO	14.23	13.96	13.42	14.69	15.20	14.33	15.27	14.52	15.72	15.24	14.96	14.59	14.62	14.27	14.77	14.25	15.55	14.74	15.57
CaO	23.16	22.77	22.87	22.56	22.90	22.46	22.31	22.58	22.22	22.61	22.83	22.49	22.16	22.33	22.19	22.07	21.91	22.50	21.47
Na_2O	0.31	0.46	0.39	0.40	0.39	0.44	0.38	0.42	0.37	0.36	0.35	0.47	0.54	0.53	0.42	0.51	0.39	0.36	0.39
Total	-	-	100.82	-	100.84	100.80	100.92	100.69	-	-	100.55	100.43	100.88	-	100.25	99.81	100.73	100.81	99.50
Cations on the basis of 6 oxygens																			
Si	-	-	1.923	-	1.959	1.933	1.962	1.952	-	-	1.966	1.924	1.970	-	1.964	1.961	1.947	1.925	1.942
Al	-	-	0.118	-	0.054	0.097	0.052	0.071	-	-	0.049	0.101	0.051	-	0.061	0.075	0.067	0.099	0.071
Ti	-	-	0.014	-	0.008	0.014	0.009	0.010	-	-	0.008	0.014	0.005	-	0.008	0.011	0.011	0.016	0.013
Fe	-	-	0.268	-	0.214	0.244	0.222	0.237	-	-	0.217	0.237	0.251	-	0.232	0.234	0.228	0.240	0.230
Mn	-	-	0.015	-	0.021	0.021	0.026	0.022	-	-	0.021	0.019	0.022	-	0.021	0.021	0.022	0.014	0.025
Mg	-	-	0.742	-	0.834	0.790	0.837	0.800	-	-	0.823	0.807	0.804	-	0.815	0.79	0.854	0.811	0.862
Ca	-	-	0.909	-	0.903	0.890	0.879	0.895	-	-	0.903	0.894	0.876	-	0.881	0.880	0.865	0.890	0.855
Na	-	-	0.028	-	0.028	0.032	0.027	0.030	-	-	0.025	0.034	0.039	-	0.030	0.037	0.028	0.026	0.028
Sum	-	-	4.018	-	4.021	4.021	4.016	4.017	-	-	4.013	4.029	4.019	-	4.012	4.009	4.023	4.022	4.024
Wo	47.1	46.8	47.4	46.1	46.3	46.3	45.4	46.3	44.6	45.8	46.5	46.1	45.4	45.8	45.7	46.2	44.4	45.8	43.9
En	40.3	39.9	38.7	41.7	42.7	41.0	43.2	41.4	43.9	42.9	42.3	41.6	41.6	40.7	42.3	41.5	43.9	41.8	44.3
Fs	12.6	13.3	14.0	12.2	11.0	12.7	11.5	12.3	11.6	11.3	11.2	12.2	13.0	13.5	12.0	12.3	11.7	12.4	11.8

APPENDIX 7.3: Continued.

Sample Code	222 K4	222 K5	222 Z5	222 Z5	222 Z5	222 Z5	222 R5	222 12	222 13	222 16	222 K21	222 27	228u K16	228u Z16	228u Z16	228u Z16	228u R16	228u 34	228u 32
SiO_2	53.05	52.43	50.31	52.28	50.51	50.42	53.02	52.19	52.49	52.57	51.24	53.01	n.d.	n.d.	53.45	n.d.	n.d.	52.20	51.91
Al_2O_3	1.40	1.54	3.40	1.79	2.51	3.01	1.35	1.81	1.05	1.86	2.77	1.62	2.18	1.23	1.38	1.31	1.51	1.87	1.77
TiO_2	0.47	0.50	0.75	0.41	0.52	0.55	0.33	0.31	0.36	0.46	0.60	0.41	0.29	0.38	0.31	0.34	0.34	0.57	0.50
FeO^*	7.67	7.51	8.46	7.83	8.10	7.85	7.28	8.62	7.20	7.62	7.62	7.10	8.80	6.95	7.30	7.12	7.15	7.22	7.09
MnO	0.60	0.51	0.33	0.51	0.17	0.31	0.61	0.75	0.77	0.66	0.28	0.60	0.78	0.51	0.47	0.72	0.51	0.65	0.60
MgO	15.66	16.08	13.59	14.89	14.36	14.33	15.43	14.62	15.41	15.18	14.21	15.51	14.61	15.55	15.92	16.03	16.00	15.50	15.41
CaO	21.42	21.38	22.56	21.97	22.47	22.68	21.57	20.44	21.70	21.53	23.15	21.60	21.35	21.75	21.62	21.42	21.74	21.49	21.79
Na_2O	0.35	0.38	0.28	0.29	0.31	0.27	0.43	0.57	0.32	0.44	0.32	0.41	0.51	0.31	0.43	0.33	0.35	0.38	0.42
Total	100.62	100.33	99.68	99.97	98.95	99.42	100.02	99.31	99.30	100.32	100.19	100.26	-	-	100.88	-	-	99.88	99.49
Cations on the basis of 6 oxygens																			
Si	1.955	1.938	1.889	1.944	1.907	1.894	1.963	1.955	1.961	1.945	1.907	1.956	-	-	1.960	-	-	1.938	1.936
Al	0.061	0.067	0.150	0.078	0.112	0.133	0.059	0.080	0.046	0.081	0.122	0.070	-	-	0.060	-	-	0.082	0.078
Ti	0.013	0.014	0.021	0.011	0.015	0.016	0.009	0.009	0.010	0.013	0.017	0.011	-	-	0.009	-	-	0.016	0.014
Fe	0.236	0.232	0.266	0.244	0.256	0.247	0.225	0.270	0.225	0.236	0.237	0.219	-	-	0.224	-	-	0.224	0.221
Mn	0.019	0.016	0.010	0.016	0.005	0.010	0.019	0.024	0.024	0.021	0.009	0.019	-	-	0.015	-	-	0.020	0.019
Mg	0.860	0.886	0.760	0.825	0.808	0.802	0.851	0.816	0.858	0.837	0.788	0.853	-	-	0.870	-	-	0.857	0.857
Ca	0.846	0.847	0.908	0.875	0.909	0.913	0.856	0.821	0.869	0.854	0.923	0.854	-	-	0.850	-	-	0.855	0.871
Na	0.025	0.027	0.020	0.021	0.023	0.020	0.031	0.041	0.023	0.032	0.023	0.029	-	-	0.031	-	-	0.027	0.030
Sum	4.014	4.028	4.025	4.015	4.034	4.034	4.014	4.017	4.017	4.017	4.027	4.012	-	-	4.017	-	-	4.019	4.026
Wo	43.5	43.1	46.9	45.0	46.1	46.5	44.3	43.0	44.5	44.3	47.4	44.3	44.0	44.6	43.7	43.5	43.9	44.1	44.7
En	44.3	45.1	39.3	42.4	41.0	40.9	44.1	42.8	44.0	43.5	40.4	44.3	41.9	44.3	44.8	45.2	44.9	44.3	44.0
Fs	12.2	11.8	13.7	12.5	13.0	12.6	11.7	14.2	11.5	12.2	12.2	11.4	14.2	11.1	11.5	11.3	11.3	11.6	11.3

APPENDIX 7.3: Continued.

Sample Code	228u 29	228u 30	228m 16	228m 18	228m 1	228m 3	228m 5	228m 6	228m 7	228m 8	228m 11	228m 24	228m 25	228m K31	228m Z31	228m Z31	228m R31	228L 18	228L 19
SiO_2	49.74	52.66	52.54	51.36	52.26	51.99	50.23	52.74	51.21	50.81	52.01	51.54	51.09	51.89	49.00	50.92	51.27	51.94	52.41
Al_2O_3	4.42	2.04	1.47	2.16	1.05	1.58	3.28	1.28	2.87	2.97	1.14	2.26	2.39	1.30	4.11	3.04	2.59	1.90	1.77
TiO_2	0.83	0.55	0.29	0.49	0.24	0.40	0.64	0.33	0.64	0.60	0.24	0.70	0.56	0.25	0.70	0.54	0.42	0.50	0.41
FeO^*	8.29	7.38	7.51	7.02	8.07	7.53	7.80	7.79	7.41	7.16	7.36	6.57	7.62	7.60	9.03	7.72	7.70	7.17	7.34
MnO	0.29	0.53	0.74	0.44	0.69	0.48	0.17	0.74	0.45	0.35	0.64	0.34	0.31	0.76	0.44	0.28	0.31	0.43	0.51
MgO	13.52	15.12	15.32	15.08	15.30	15.63	15.36	15.93	14.42	14.56	15.35	15.50	15.03	15.05	13.35	14.23	14.58	15.49	15.83
CaO	23.17	21.85	21.32	21.64	21.68	21.26	22.03	21.15	21.57	22.34	21.67	22.19	22.85	21.75	22.24	22.37	22.78	22.78	22.18
Na_2O	0.37	0.41	0.40	0.32	0.39	0.40	0.17	0.34	0.38	0.28	0.36	0.37	0.26	0.51	0.33	0.30	0.31	0.36	0.42
Total	100.63	100.54	99.59	98.51	99.68	99.27	99.68	100.30	98.95	99.07	98.77	99.47	100.11	99.11	99.20	99.40	99.96	100.57	100.87

Cations on the basis of 6 oxygens

Si	1.853	1.942	1.957	1.932	1.954	1.943	1.877	1.952	1.920	1.906	1.956	1.919	1.904	1.950	1.857	1.907	1.912	1.921	1.930
Al	0.194	0.089	0.065	0.096	0.046	0.070	0.144	0.056	0.127	0.131	0.051	0.099	0.105	0.058	0.184	0.134	0.114	0.083	0.077
Ti	0.023	0.015	0.008	0.014	0.007	0.011	0.018	0.009	0.018	0.017	0.007	0.020	0.016	0.007	0.020	0.015	0.012	0.014	0.011
Fe	0.258	0.228	0.234	0.221	0.252	0.235	0.244	0.241	0.232	0.225	0.231	0.205	0.237	0.239	0.286	0.242	0.240	0.222	0.226
Mn	0.009	0.017	0.023	0.014	0.022	0.015	0.005	0.023	0.014	0.011	0.020	0.011	0.010	0.024	0.014	0.009	0.010	0.013	0.016
Mg	0.751	0.831	0.850	0.845	0.853	0.871	0.855	0.879	0.806	0.814	0.860	0.860	0.835	0.843	0.754	0.794	0.810	0.854	0.869
Ca	0.925	0.863	0.851	0.872	0.869	0.851	0.882	0.839	0.867	0.898	0.873	0.885	0.912	0.876	0.903	0.898	0.910	0.903	0.875
Na	0.027	0.029	0.029	0.023	0.028	0.029	0.012	0.024	0.028	0.020	0.026	0.027	0.019	0.037	0.024	0.022	0.022	0.026	0.030
Sum	4.040	4.013	4.017	4.018	4.030	4.025	4.039	4.023	4.012	4.022	4.025	4.025	4.037	4.033	4.043	4.021	4.031	4.036	4.035
Wo	47.8	44.9	44.0	45.0	44.0	43.5	44.5	42.8	45.5	46.4	44.4	45.4	46.0	44.7	46.5	46.4	46.4	45.6	44.4
En	38.8	43.2	43.9	43.6	43.2	44.5	43.2	44.9	42.3	42.0	43.8	44.1	42.1	43.1	38.8	41.1	41.3	43.2	44.1
Fs	13.4	11.8	12.1	11.4	12.8	12.0	12.3	12.3	12.2	11.6	11.8	10.5	12.0	12.2	14.7	12.5	12.2	11.2	11.5

APPENDIX 7.3: Continued.

Sample Code	228L 20	228L 21	228L 22	228L 23	228L K30	228L Z30	228L Z30	228L Z30	228L R30	228L 3	228L 4	228L 30	235 7	235 e22	235 16	235 24	235 25	235 26	235 R27	235 28
SiO_2	51.61	52.10	51.92	50.44	52.33	51.97	50.25	51.64	51.97	51.14	52.11	52.06	52.13	52.13	51.83	52.09	50.78	51.97	52.08	51.61
Al_2O_3	1.87	1.99	1.40	3.26	0.78	1.75	3.28	1.78	1.46	2.42	1.40	1.30	1.86	1.62	1.83	1.51	3.15	1.79	1.95	1.71
TiO_2	0.49	0.42	0.32	0.58	0.22	0.39	0.54	0.42	0.43	0.54	0.34	0.33	0.48	0.36	0.49	0.40	0.49	0.43	0.52	0.44
FeO^*	7.15	7.52	7.93	7.84	8.19	6.82	7.76	7.08	6.78	7.80	7.64	6.86	7.99	7.63	8.02	7.77	7.90	8.13	8.03	7.73
MnO	0.61	0.46	0.81	0.22	0.80	0.51	0.18	0.44	0.53	0.34	0.67	0.64	0.44	0.45	0.53	0.62	0.33	0.49	0.76	0.56
MgO	15.75	14.65	14.77	14.00	14.94	15.75	14.26	15.49	15.67	15.69	15.58	15.91	15.22	15.52	15.20	15.43	14.19	15.04	15.82	15.68
CaO	21.47	23.04	22.40	23.10	21.99	22.06	22.97	22.13	22.23	21.95	21.72	22.04	21.54	21.04	20.96	21.17	22.97	21.42	20.24	20.93
Na_2O	0.39	0.35	0.41	0.32	0.34	0.43	0.25	0.33	0.34	0.28	0.47	0.31	0.40	0.35	0.37	0.37	0.25	0.42	0.36	0.33
Total	99.34	100.53	99.96	99.76	99.59	99.67	99.49	99.31	99.41	100.16	99.93	99.45	100.06	99.10	99.23	99.36	100.06	99.69	99.76	98.99
Cations on the basis of 6 oxygens																				
Si	1.928	1.931	1.941	1.889	1.962	1.933	1.886	1.931	1.939	1.902	1.941	1.942	1.937	1.949	1.940	1.947	1.895	1.940	1.937	1.936
Al	0.082	0.087	0.062	0.144	0.034	0.077	0.145	0.078	0.064	0.106	0.061	0.057	0.081	0.071	0.081	0.067	0.139	0.079	0.085	0.076
Ti	0.014	0.012	0.009	0.016	0.006	0.011	0.015	0.012	0.012	0.015	0.010	0.009	0.013	0.010	0.014	0.011	0.014	0.012	0.015	0.012
Fe	0.223	0.233	0.248	0.246	0.257	0.212	0.244	0.221	0.212	0.243	0.238	0.214	0.248	0.239	0.251	0.243	0.247	0.254	0.250	0.242
Mn	0.019	0.014	0.026	0.007	0.025	0.016	0.006	0.014	0.017	0.011	0.021	0.020	0.014	0.014	0.017	0.020	0.010	0.015	0.024	0.018
Mg	0.877	0.809	0.823	0.782	0.835	0.873	0.798	0.863	0.871	0.869	0.865	0.885	0.843	0.865	0.848	0.860	0.789	0.837	0.877	0.877
Ca	0.859	0.915	0.897	0.927	0.883	0.879	0.924	0.887	0.889	0.875	0.867	0.881	0.858	0.843	0.841	0.848	0.919	0.857	0.806	0.841
Na	0.028	0.025	0.030	0.023	0.025	0.031	0.018	0.024	0.025	0.020	0.034	0.022	0.029	0.025	0.027	0.027	0.018	0.030	0.026	0.024
Sum	4.031	4.026	4.034	4.034	4.027	4.033	4.035	4.030	4.029	4.040	4.036	4.031	4.023	4.017	4.019	4.022	4.031	4.024	4.019	4.026
Wo	43.9	46.7	45.6	47.4	44.7	44.8	47.0	45.0	45.1	44.0	44.0	44.5	44.0	43.3	43.3	43.5	47.0	44.0	41.7	42.9
En	44.7	41.3	41.8	40.0	42.3	44.4	40.6	43.8	44.2	43.8	43.9	44.7	43.3	44.4	43.7	44.1	40.4	43.0	45.4	44.7
Fs	11.4	11.9	12.6	12.6	13.0	10.8	12.4	11.2	10.7	12.2	12.1	10.8	12.7	12.3	12.9	12.5	12.6	13.0	12.9	12.4

APPENDIX 7.3: Continued.

Sample Code	243 i	243 ih9	243 12	243 17	243 18	243 19	243 2	243 4	243 11	243 24	246 K22	246 Z22	246 Z22	246 Z22	246 R22	246 24	246 21	246 K25
SiO_2	51.94	51.74	52.13	53.07	51.99	52.07	52.48	52.11	52.33	52.32	n.d.	52.25	n.d.	51.53	n.d.	53.35	52.30	51.96
Al_2O_3	2.36	1.68	1.85	1.44	1.94	1.98	1.93	3.05	2.11	2.15	2.72	2.70	1.79	3.42	2.41	1.48	1.79	2.39
TiO_2	0.50	0.44	0.33	0.38	0.51	0.47	0.39	0.68	0.47	0.69	0.66	0.55	0.46	0.61	0.51	0.37	0.39	0.40
FeO^*	7.51	7.89	8.03	7.63	7.83	8.01	7.11	7.79	7.38	8.60	7.86	7.54	7.69	7.84	7.69	6.96	7.71	7.56
MnO	0.39	0.57	0.59	0.68	0.53	0.52	0.35	0.45	0.48	0.41	0.50	0.35	0.52	0.28	0.42	0.59	0.51	0.35
MgO	15.62	15.01	14.75	15.89	15.42	15.11	15.67	14.90	15.34	15.67	15.62	14.69	15.83	14.48	15.64	15.03	15.17	14.92
CaO	21.35	20.79	21.43	21.36	20.91	21.46	22.20	21.31	21.48	20.76	21.60	22.10	21.82	22.42	22.17	22.58	22.21	22.86
Na_2O	0.40	0.43	0.48	0.34	0.37	0.30	0.38	0.40	0.45	0.38	0.47	0.35	0.36	0.30	0.43	0.40	0.44	0.41
Total	100.07	98.55	99.59	100.79	99.50	99.92	100.51	100.69	100.04	100.98	-	100.35	-	100.88	-	100.76	100.52	100.85
Cations on the basis of 6 oxygens																		
Si	1.924	1.949	1.947	1.952	1.938	1.937	1.935	1.919	1.938	1.926	-	1.928	-	1.900	-	1.962	1.936	1.919
Al	0.103	0.075	0.081	0.062	0.085	0.087	0.084	0.132	0.092	0.093	-	0.117	-	0.149	-	0.064	0.078	0.104
Ti	0.014	0.012	0.009	0.011	0.014	0.013	0.011	0.019	0.013	0.019	-	0.015	-	0.017	-	0.010	0.011	0.011
Fe	0.233	0.249	0.251	0.235	0.244	0.249	0.219	0.240	0.229	0.265	-	0.233	-	0.242	-	0.214	0.239	0.233
Mn	0.012	0.018	0.019	0.021	0.017	0.016	0.011	0.014	0.015	0.013	-	0.011	-	0.009	-	0.018	0.016	0.011
Mg	0.862	0.843	0.821	0.871	0.857	0.838	0.861	0.818	0.847	0.860	-	0.808	-	0.796	-	0.824	0.837	0.821
Ca	0.847	0.839	0.858	0.842	0.835	0.855	0.877	0.841	0.852	0.819	-	0.874	-	0.886	-	0.890	0.881	0.904
Na	0.029	0.031	0.035	0.024	0.027	0.022	0.027	0.029	0.032	0.027	-	0.025	-	0.021	-	0.029	0.032	0.029
Sum	4.025	4.017	4.020	4.018	4.018	4.017	4.026	4.011	4.019	4.022	-	4.011	-	4.019	-	4.010	4.030	4.033
Wo	43.6	43.5	44.4	43.2	43.1	44.0	44.8	44.3	44.2	42.1	43.7	45.6	43.8	46.1	44.4	46.2	45.0	46.2
En	44.4	43.7	42.6	44.7	44.2	43.1	44.0	43.1	43.9	44.2	43.9	42.2	44.2	41.4	43.6	42.7	42.8	41.9
Fs	12.0	12.9	13.0	12.1	12.6	12.8	11.2	12.6	11.9	13.6	12.4	12.2	12.0	12.6	12.0	11.1	12.2	11.9

APPENDIX 7.3: Continued.

Sample	246	246	246	246	246	246	246	251	251	251	251	251	251	251	251	251	251	251
Code	Z25	Z25	R25	20	19	K18	178	ip27	38	Z	K41	Z41	Z41	Z41	R41	11	9	6
SiO_2	50.79	51.94	51.64	52.42	52.44	52.49	51.45	50.22	52.09	52.36	51.48	51.50	52.15	51.80	52.68	51.72	51.34	51.71
Al_2O_3	3.07	2.42	2.18	1.81	1.62	1.85	2.98	2.63	1.79	2.12	3.18	2.68	2.45	2.19	1.76	2.05	2.61	2.11
TiO_2	0.69	0.60	0.59	0.42	0.44	0.53	0.48	0.77	0.48	0.55	0.68	0.59	0.45	0.53	0.52	0.53	0.58	0.60
FeO^*	8.08	7.74	7.56	7.57	7.66	7.12	8.73	7.78	7.75	7.85	7.70	7.57	7.39	7.13	7.64	7.53	7.40	7.45
MnO	0.37	0.42	0.25	0.58	0.54	0.40	0.51	0.37	0.47	0.49	0.34	0.36	0.36	0.44	0.50	0.43	0.26	0.31
MgO	14.72	15.13	15.73	15.61	15.50	16.17	13.67	15.23	15.82	15.40	14.94	15.44	15.52	15.51	15.89	15.97	15.49	15.71
CaO	22.07	21.93	21.52	21.42	21.72	21.55	22.26	21.32	20.65	21.39	22.02	21.78	22.18	21.10	20.70	20.84	22.37	21.67
Na_2O	0.41	0.41	0.40	0.33	0.38	0.34	0.58	0.48	0.36	0.41	0.35	0.35	0.32	0.38	0.37	0.40	0.31	0.39
Total	100.20	100.59	99.87	100.16	100.30	100.45	100.66	98.80	99.41	100.57	100.69	100.27	100.82	99.08	100.06	99.47	100.36	99.95
Cations on the basis of 6 oxygens																		
Si	1.892	1.920	1.919	1.941	1.942	1.934	1.913	1.894	1.941	1.933	1.900	1.908	1.920	1.934	1.948	1.927	1.902	1.920
Al	0.135	0.105	0.095	0.079	0.071	0.080	0.131	0.117	0.079	0.092	0.138	0.117	0.106	0.096	0.077	0.090	0.114	0.092
Ti	0.019	0.017	0.016	0.012	0.012	0.015	0.013	0.022	0.013	0.015	0.019	0.016	0.012	0.015	0.014	0.015	0.016	0.017
Fe	0.252	0.239	0.235	0.234	0.237	0.219	0.271	0.245	0.242	0.242	0.238	0.235	0.228	0.223	0.236	0.235	0.229	0.231
Mn	0.012	0.013	0.008	0.018	0.017	0.012	0.016	0.012	0.015	0.015	0.011	0.011	0.011	0.014	0.016	0.014	0.008	0.010
Mg	0.817	0.833	0.871	0.861	0.855	0.888	0.757	0.856	0.879	0.847	0.822	0.853	0.851	0.863	0.876	0.887	0.855	0.870
Ca	0.881	0.869	0.857	0.850	0.862	0.851	0.887	0.862	0.825	0.846	0.871	0.865	0.875	0.844	0.820	0.832	0.888	0.862
Na	0.030	0.029	0.029	0.024	0.027	0.024	0.042	0.035	0.026	0.029	0.025	0.025	0.023	0.028	0.027	0.029	0.022	0.028
Sum	4.036	4.026	4.031	4.020	4.024	4.023	4.030	4.043	4.019	4.021	4.024	4.030	4.026	4.017	4.013	4.028	4.036	4.031
Wo	45.2	44.7	43.7	43.7	44.1	43.4	46.3	43.9	42.4	43.7	45.1	44.3	44.8	43.7	42.4	42.6	45.0	43.9
En	41.9	42.9	44.4	44.3	43.8	45.3	39.5	43.6	45.2	43.8	42.6	43.7	43.6	44.7	45.3	45.4	43.4	44.3
Fs	12.9	12.3	12.0	12.0	12.1	11.2	14.2	12.5	12.4	12.5	12.3	12.0	11.6	11.5	12.2	12.0	11.6	11.8

APPENDIX 7.3: Continued.

Sample Code	256 11	256 7	256 K12	256 R12	256 13	256 15	256 16	256 17	256 26	256 28	256 K29	256 Z29	256 Z29	256 Z29	256 Z29	256 Z29	256 Z29	256 R29
SiO_2	48.31	52.23	n.d.	51.13	51.72	51.93	52.07	49.88	52.12	51.27	50.21	48.76	51.09	51.75	50.36	50.89	51.20	51.87
Al_2O_3	5.86	2.53	2.52	2.92	2.90	2.54	2.71	4.55	1.87	2.73	4.73	5.34	2.92	3.00	3.73	3.09	3.32	2.93
TiO_2	0.82	0.62	0.67	0.67	0.69	0.55	0.62	0.66	0.50	0.57	0.61	0.81	0.56	0.50	0.68	0.61	0.59	0.57
FeO^*	8.00	7.72	8.17	8.38	8.05	7.71	7.86	7.68	7.38	7.87	6.99	8.10	7.53	7.75	7.97	7.78	8.03	7.44
MnO	0.21	0.36	0.35	0.35	0.38	0.29	0.35	0.30	0.41	0.41	0.00	0.24	0.33	0.29	0.28	0.31	0.32	0.47
MgO	12.96	15.46	15.40	15.05	14.86	15.19	14.92	13.42	15.89	15.25	14.25	13.43	14.99	14.91	14.64	14.79	14.59	15.08
CaO	22.62	21.14	21.55	21.31	21.35	21.64	20.84	22.59	21.23	21.39	23.64	22.44	21.95	21.72	21.59	21.69	21.34	21.52
Na_2O	0.27	0.38	0.53	0.48	0.40	0.39	0.43	0.38	0.36	0.42	0.27	0.37	0.37	0.41	0.41	0.42	0.47	0.36
Total	99.05	100.44	-	100.29	100.35	100.24	99.80	99.46	99.76	99.91	100.70	99.49	99.74	100.33	99.66	99.58	99.86	100.24

Cations on the basis of 6 oxygens

Si	1.824	1.926	-	1.900	1.915	1.922	1.932	1.870	1.935	1.908	1.855	1.833	1.904	1.915	1.882	1.901	1.906	1.918
Al	0.261	0.110	-	0.128	0.127	0.111	0.119	0.201	0.082	0.120	0.206	0.237	0.128	0.131	0.164	0.136	0.146	0.128
Ti	0.023	0.017	-	0.019	0.019	0.015	0.017	0.019	0.014	0.016	0.017	0.023	0.016	0.014	0.019	0.017	0.017	0.016
Fe	0.253	0.238	-	0.260	0.249	0.239	0.244	0.241	0.229	0.245	0.216	0.255	0.235	0.240	0.249	0.243	0.250	0.230
Mn	0.007	0.011	-	0.011	0.012	0.009	0.011	0.010	0.013	0.013	0.000	0.008	0.010	0.009	0.009	0.010	0.010	0.015
Mg	0.729	0.850	-	0.833	0.820	0.838	0.825	0.750	0.879	0.846	0.785	0.753	0.833	0.822	0.815	0.823	0.809	0.831
Ca	0.915	0.835	-	0.849	0.847	0.858	0.828	0.907	0.845	0.853	0.936	0.904	0.877	0.861	0.864	0.868	0.851	0.853
Na	0.020	0.027	-	0.035	0.029	0.028	0.031	0.028	0.026	0.030	0.019	0.027	0.027	0.029	0.030	0.030	0.034	0.026
Sum	4.032	4.015	-	4.035	4.017	4.021	4.007	4.025	4.023	4.031	4.034	4.039	4.029	4.021	4.032	4.029	4.022	4.015
Wo	48.2	43.4	43.7	43.7	44.2	44.4	43.7	47.8	43.2	43.9	48.3	47.3	45.1	44.8	44.8	44.9	44.6	44.6
En	38.4	44.2	43.4	42.9	42.8	43.3	43.5	39.5	45.0	43.5	40.5	39.4	42.8	42.8	42.3	42.6	42.4	43.4
Fs	13.3	12.4	12.9	13.4	13.0	12.3	12.9	12.7	11.7	12.6	11.2	13.3	12.1	12.5	12.9	12.6	13.1	12.0

APPENDIX 7.3: Continued.

Sample Code	256 K30	256 Z30	256 Z30	256 Z30	256 Z30	256 Z30	256 Z30	256 R30	256 eh32	256 et42	256 K49	256 48	256 47	256 46	256 44	256 41	256 -
SiO_2	52.12	50.95	50.13	51.36	50.47	51.21	51.47	51.43	51.32	n.d.	53.15	51.85	51.11	51.69	51.71	51.52	50.57
Al_2O_3	1.95	2.84	3.89	2.70	3.56	3.00	2.89	2.72	2.54	2.08	1.40	2.22	3.27	2.54	2.83	2.99	3.94
TiO_2	0.45	0.54	0.59	0.53	0.70	0.60	0.61	0.53	0.69	0.50	0.20	0.52	0.72	0.50	0.59	0.57	0.56
FeO^*	7.69	8.61	8.37	7.81	7.99	7.76	7.97	7.47	8.00	8.47	7.81	7.50	8.23	8.26	7.92	7.58	6.42
MnO	0.34	0.29	0.29	0.30	0.26	0.41	0.39	0.30	0.42	0.38	0.62	0.33	0.37	0.38	0.39	0.35	0.00
MgO	15.56	14.87	14.16	15.22	14.52	15.15	15.05	14.92	15.18	15.61	14.29	15.39	14.91	14.88	15.01	15.08	14.53
CaO	21.49	21.33	21.45	21.70	21.67	21.83	21.43	22.04	21.53	21.05	23.01	21.54	21.49	21.61	21.39	21.66	23.48
Na_2O	0.39	0.39	0.39	0.41	0.44	0.39	0.38	0.38	0.39	0.42	0.44	0.38	0.43	0.36	0.42	0.40	0.26
Total	99.99	99.82	99.27	100.03	99.61	100.35	100.19	99.79	100.07	-	100.92	99.73	100.53	100.22	100.26	100.15	99.76

Cations on the basis of 6 oxygens

Sample Code	256 K30	256 Z30	256 Z30	256 Z30	256 Z30	256 Z30	256 Z30	256 R30	256 eh32	256 et42	256 K49	256 48	256 47	256 46	256 44	256 41	256 -
Si	1.934	1.904	1.883	1.909	1.887	1.899	1.910	1.914	1.909	-	1.962	1.928	1.894	1.920	1.916	1.909	1.880
Al	0.085	0.125	0.172	0.118	0.157	0.131	0.126	0.119	0.111	-	0.061	0.097	0.143	0.111	0.124	0.131	0.173
Ti	0.013	0.015	0.017	0.015	0.020	0.017	0.017	0.015	0.019	-	0.006	0.015	0.020	0.014	0.016	0.016	0.016
Fe	0.239	0.269	0.263	0.243	0.250	0.241	0.247	0.233	0.249	-	0.241	0.233	0.255	0.257	0.245	0.235	0.200
Mn	0.011	0.009	0.009	0.009	0.008	0.013	0.012	0.009	0.013	-	0.019	0.010	0.012	0.012	0.012	0.011	0.000
Mg	0.861	0.828	0.793	0.843	0.809	0.837	0.832	0.828	0.842	-	0.786	0.853	0.823	0.824	0.829	0.833	0.805
Ca	0.855	0.854	0.863	0.864	0.868	0.867	0.852	0.879	0.858	-	0.910	0.858	0.853	0.860	0.849	0.860	0.935
Na	0.028	0.028	0.028	0.030	0.032	0.028	0.027	0.027	0.028	-	0.031	0.027	0.031	0.026	0.030	0.029	0.019
Sum	4.025	4.033	4.028	4.032	4.031	4.033	4.024	4.025	4.030	-	4.017	4.022	4.030	4.023	4.021	4.024	4.027
Wo	43.7	43.8	45.0	44.3	45.1	44.6	44.1	45.3	44.0	42.6	47.0	44.1	44.2	44.3	44.1	44.6	48.2
En	44.0	42.4	41.3	43.2	42.0	43.0	43.1	42.7	43.2	44.0	40.6	43.9	42.6	42.5	43.1	43.2	41.5
Fs	12.2	13.8	13.7	12.4	13.0	12.4	12.8	12.0	12.8	13.4	12.4	12.0	13.2	13.2	12.8	12.2	10.3

APPENDIX 7.3: Continued.

Sample	89	90	90	90	84	84	84	84
Code	36	25	13	6	10	11	K12	R12
SiO_2	49.70	50.61	52.27	53.24	51.97	52.17	52.63	51.69
Al_2O_3	2.95	2.68	2.48	2.55	1.52	1.51	1.32	2.06
TiO_2	0.38	0.79	0.21	0.24	0.43	0.35	0.34	0.50
FeO^*	7.49	12.05	4.81	5.47	10.37	9.50	9.32	9.06
MnO	0.16	0.26	0.18	0.00	0.63	0.61	0.59	0.45
MgO	16.04	14.53	17.08	17.68	14.02	13.94	15.25	14.71
CaO	20.18	18.63	21.91	20.61	20.30	21.01	19.52	19.85
Na_2O	0.38	0.43	0.24	0.30	0.31	0.34	0.23	0.28
Cr_2O_3	0.28	0.18	0.25	0.17	0.00	0.00	0.00	0.00
Total	97.56	99.56	99.43	100.26	99.55	99.43	99.20	98.70

Cations on the basis of 6 oxygens

Sample	89	90	90	90	84	84	84	84
Code	36	25	13	6	10	11	K12	R12
Si	1.890	1.902	1.926	1.938	1.956	1.961	1.970	1.948
Al	0.132	0.119	0.108	0.109	0.067	0.067	0.058	0.092
Ti	0.011	0.022	0.006	0.007	0.012	0.010	0.010	0.014
Fe	0.238	0.379	0.148	0.167	0.326	0.299	0.292	0.286
Mn	0.005	0.008	0.006	0.000	0.020	0.019	0.019	0.014
Mg	0.909	0.814	0.938	0.959	0.786	0.781	0.851	0.826
Ca	0.822	0.750	0.865	0.804	0.819	0.846	0.783	0.802
Na	0.028	0.031	0.017	0.021	0.023	0.025	0.017	0.020
Cr	0.008	0.005	0.007	0.005	0.000	0.000	0.000	0.000
Sum	4.043	4.030	4.020	4.009	4.010	4.008	3.999	4.002
Wo	41.7	38.6	44.3	41.7	42.4	43.9	40.7	41.9
En	46.2	41.9	48.1	49.7	40.7	40.6	44.2	43.2
Fs	12.1	19.5	7.6	8.6	16.9	15.5	15.2	14.9

APPENDIX 7.4: ORTHOPYROXENE

Sample	256	251	251	251	246	243	235	235	235	228m	228u	228u	222
SiO_2	52.91	54.18	53.77	54.14	54.60	53.78	53.34	53.08	53.42	54.38	-	-	54.16
Al_2O_3	1.82	1.02	1.22	0.89	0.86	1.40	0.72	1.29	0.74	0.55	0.84	0.99	1.10
TiO_2	0.28	0.31	0.29	0.17	0.20	0.28	0.24	0.21	0.20	0.11	0.15	0.00	0.20
FeO^*	16.27	15.04	15.57	14.97	16.08	14.65	16.38	16.04	16.42	16.35	15.90	15.06	13.95
MnO	0.83	0.83	0.73	0.77	0.87	0.80	0.98	0.94	1.04	1.27	0.92	0.69	1.20
MgO	26.01	27.14	26.69	27.12	26.99	26.71	25.75	26.35	25.79	26.68	27.45	28.88	28.07
CaO	1.38	1.39	1.43	1.26	1.17	1.35	1.35	1.24	1.28	1.08	1.06	0.82	0.92
Total	99.50	99.91	99.70	99.32	100.77	98.97	98.76	99.15	98.98	100.42	-	-	99.60
Cations on the basis of 6 oxygens													
Si	1.936	1.960	1.954	1.968	1.965	1.960	1.967	1.947	1.968	1.971	-	-	1.956
Al	0.078	0.043	0.052	0.038	0.036	0.060	0.031	0.056	0.032	0.023	-	-	0.047
Ti	0.008	0.008	0.008	0.005	0.005	0.008	0.007	0.006	0.006	0.003	-	-	0.006
Fe	0.498	0.455	0.473	0.455	0.484	0.447	0.505	0.492	0.506	0.496	-	-	0.421
Mn	0.026	0.025	0.022	0.024	0.027	0.025	0.031	0.029	0.032	0.039	-	-	0.037
Mg	1.418	1.463	1.446	1.469	1.448	1.451	1.416	1.441	1.416	1.441	-	-	1.511
Ca	0.054	0.054	0.056	0.049	0.045	0.053	0.053	0.049	0.051	0.042	-	-	0.036
Sum	4.017	4.010	4.012	4.008	4.011	4.002	4.010	4.019	4.010	4.015	-	-	4.014
En	74.0	76.3	75.3	76.3	74.9	76.5	73.7	74.5	73.7	74.4	75.5	77.4	78.2

APPENDIX 7.4: Continued.

Sample	90	90	90	90	90	90	90	90	90	90	90	89	89	89	89	89	89	89	89	89
SiO_2	50.81	50.97	50.28	51.25	50.88	52.25	50.13	50.89	50.99	51.21	52.47	51.58	51.79	52.50	50.81	53.13	50.98	52.38	51.85	51.05
Al_2O_3	0.32	0.44	0.41	0.47	0.31	0.19	0.39	0.39	0.42	0.27	1.16	0.88	1.85	1.44	0.95	0.90	0.45	2.77	0.33	0.42
TiO_2	0.10	0.15	0.12	0.11	0.00	0.00	0.10	0.00	0.00	0.00	0.29	0.12	0.41	0.34	0.24	0.11	0.13	0.20	0.00	0.00
FeO	27.59	27.18	28.62	28.38	27.97	26.37	28.14	27.68	27.37	26.07	22.23	25.49	20.45	16.33	25.21	17.20	26.00	16.57	27.30	26.40
MnO	1.33	1.37	1.44	1.52	1.37	1.40	1.60	1.37	0.99	1.33	0.98	1.34	0.43	0.42	1.15	0.79	1.33	0.31	1.45	1.19
MgO	17.84	17.69	16.93	16.81	17.08	18.09	17.19	17.64	18.72	18.75	21.78	19.06	22.72	25.52	18.30	23.88	18.89	25.64	18.27	18.73
CaO	0.78	1.14	0.95	1.05	1.13	0.74	0.81	1.00	1.16	0.75	1.30	1.00	1.77	2.15	1.11	0.97	0.93	1.31	0.73	0.82
Total	98.77	98.94	98.75	99.59	98.74	99.04	98.36	98.97	99.65	98.38	100.21	99.47	99.42	98.70	97.77	97.10	98.71	99.18	99.93	98.61

Cations on the basis of 6 oxygens

Si	1.980	1.980	1.973	1.988	1.988	2.012	1.973	1.981	1.966	1.988	1.959	1.973	1.934	1.940	1.977	1.995	1.974	1.920	1.990	1.980
Al	0.015	0.020	0.019	0.021	0.014	0.009	0.018	0.018	0.019	0.012	0.051	0.040	0.081	0.063	0.044	0.040	0.021	0.120	0.015	0.019
Ti	0.003	0.004	0.004	0.003	0.000	0.000	0.003	0.000	0.000	0.000	0.008	0.003	0.012	0.009	0.007	0.003	0.004	0.006	0.000	0.000
Fe	0.899	0.883	0.939	0.921	0.914	0.849	0.926	0.901	0.883	0.846	0.694	0.816	0.639	0.505	0.820	0.540	0.842	0.508	0.876	0.856
Mn	0.044	0.045	0.048	0.050	0.045	0.046	0.053	0.045	0.032	0.044	0.031	0.043	0.014	0.013	0.038	0.025	0.044	0.010	0.047	0.039
Mg	1.036	1.024	0.990	0.972	0.995	1.038	1.008	1.023	1.076	1.085	1.212	1.087	1.264	1.405	1.061	1.336	1.090	1.401	1.045	1.082
Ca	0.033	0.047	0.040	0.044	0.047	0.031	0.034	0.042	0.048	0.031	0.052	0.041	0.071	0.085	0.046	0.039	0.039	0.051	0.030	0.034
Sum	4.010	4.005	4.014	3.998	4.004	3.984	4.015	4.010	4.024	4.006	4.007	4.003	4.014	4.020	3.994	3.987	4.012	4.015	4.003	4.011
En	53.5	53.7	51.3	51.4	52.1	55.0	52.1	53.2	54.9	56.2	63.6	57.1	66.4	73.6	56.4	71.2	56.4	73.4	54.4	55.8

APPENDIX 7.4: Continued.

Sample	89	89	89	89	89	89	89	10	10	10	10	10	10	10	10	10	10	10	10	10
SiO_2	51.50	50.68	51.16	51.94	49.45	51.44	50.07	50.43	50.29	52.73	50.45	50.33	53.63	50.59	50.83	50.45	50.70	50.54	50.35	50.95
Al_2O_3	1.01	1.07	0.41	0.54	0.34	0.35	1.03	0.39	0.42	1.19	0.36	0.65	1.34	0.42	0.47	0.45	0.32	0.73	0.51	0.42
TiO_2	0.24	0.20	0.00	0.00	0.00	0.00	0.32	0.15	0.18	0.24	0.10	0.21	0.21	0.12	0.14	0.16	0.16	0.22	0.00	0.19
FeO	19.63	24.94	27.57	27.03	30.32	27.16	31.04	30.15	31.05	17.42	30.45	30.02	18.25	30.02	29.59	30.10	30.06	29.41	29.86	30.51
MnO	0.55	1.15	1.24	1.14	1.63	1.23	0.85	1.67	1.87	0.43	1.82	1.72	0.52	1.68	1.65	1.80	1.66	1.62	1.73	1.67
MgO	23.78	19.27	18.33	18.23	15.37	18.43	14.34	15.07	14.36	24.98	14.95	15.02	24.91	14.92	15.54	14.86	14.87	15.58	14.93	14.71
CaO	1.42	1.16	0.70	0.98	0.84	0.75	2.00	1.24	1.35	1.46	1.24	1.42	1.55	1.25	1.24	1.25	1.21	1.35	1.31	1.29
Total	98.13	98.47	99.41	99.86	97.95	99.36	99.65	99.10	99.52	98.45	99.37	99.37	100.41	99.00	99.46	99.07	98.98	99.45	98.69	99.74

Cations on the basis of 6 oxygens

Si	1.944	1.957	1.978	1.990	1.977	1.984	1.968	1.988	1.985	1.957	1.987	1.979	1.957	1.994	1.989	1.990	1.999	1.978	1.992	1.996
Al	0.045	0.049	0.019	0.024	0.016	0.016	0.048	0.018	0.020	0.052	0.017	0.030	0.058	0.020	0.022	0.021	0.015	0.034	0.024	0.019
Ti	0.007	0.006	0.000	0.000	0.000	0.000	0.009	0.004	0.005	0.007	0.003	0.006	0.006	0.004	0.004	0.005	0.005	0.006	0.000	0.006
Fe	0.620	0.806	0.891	0.866	1.014	0.876	1.020	0.994	1.025	0.541	1.003	0.987	0.557	0.990	0.968	0.993	0.991	0.962	0.988	1.000
Mn	0.018	0.038	0.041	0.037	0.055	0.040	0.028	0.056	0.063	0.014	0.061	0.057	0.016	0.056	0.055	0.060	0.055	0.054	0.058	0.055
Mg	1.337	1.109	1.056	1.041	0.916	1.060	0.840	0.885	0.845	1.382	0.878	0.880	1.355	0.877	0.906	0.874	0.874	0.909	0.880	0.859
Ca	0.057	0.048	0.029	0.040	0.036	0.031	0.084	0.052	0.057	0.058	0.052	0.060	0.061	0.053	0.052	0.053	0.051	0.057	0.056	0.054
Sum	4.027	4.012	4.013	3.998	4.015	4.008	3.998	3.998	4.000	4.010	4.001	4.000	4.009	3.992	3.996	3.995	3.989	3.999	3.997	3.989
En	68.3	57.9	54.2	54.6	47.5	54.7	45.2	47.1	45.2	71.9	46.7	47.1	70.9	47.0	48.3	46.8	46.9	48.6	47.1	46.2

Appendix 8: Proportion of the silt fraction removed from the Tokomaru silt loam during the acid dissolution treatments.

	5-2μm	------ 20-5μm -------			------ 63-20μm ------		
No.	Residue	HCl	H_2SiF_6	Residue	HCl	H_2SiF_6	Residue
T1	27.2	7.1	53.7	39.2	2.8	47.5	50.0
T2	32.3	6.5	58.5	35.0	2.7	48.2	49.0
T3	21.3	4.5	85.3	10.2	1.8	66.7	31.5
T4	18.8	5.7	73.3	21.1	2.7	52.5	44.8
T5	26.2	7.3	60.1	32.6	2.8	50.1	47.1
T6	27.0	7.0	57.6	35.4	2.6	48.5	49.0
T7	26.5	6.8	53.6	39.6	2.4	46.0	51.6
T8	28.5	6.6	55.9	37.6	2.2	45.0	52.8
T9	30.7	6.7	55.4	38.0	2.6	46.8	50.6
T10	31.9	6.5	54.3	39.3	2.5	47.7	49.7
T11	30.0	6.5	54.5	38.9	2.3	45.6	52.2
T12	31.2	6.4	55.9	37.7	2.2	49.3	52.5
T13	30.3	6.0	53.1	40.9	2.3	46.9	50.8
T14	31.0	6.0	51.3	42.8	2.3	45.1	52.6
T15	30.8	6.5	50.8	42.7	2.1	45.3	52.5
T16	33.4	6.2	52.4	41.4	2.3	41.5	56.3
T17	28.6	6.6	53.4	40.5	2.2	44.3	53.4
T18	28.4	6.4	53.8	39.8	2.3	47.8	49.9
T19	32.5	5.0	53.0	42.1	1.7	44.6	53.8
T20	32.2	3.8	53.0	43.2	1.1	44.9	54.0
T21	43.6	2.9	54.6	42.5	1.0	43.2	55.8
T22	41.9	2.3	53.7	44.0	1.0	40.1	58.9
T23	40.1	1.8	52.4	45.8	0.8	41.4	57.8
T24	36.4	1.9	47.8	50.3	0.7	35.5	63.9
T25	40.0	2.0	56.3	41.8	0.6	42.0	57.4

Appendix 9: Key to sample depths (m).

Tokomaru silt loam	
T1	2.42-2.50
T2	2.34-2.42
T3	2.24-2.34
T4	2.14-2.24
T5	2.00-2.14
T6	1.90-2.00
T7	1.80-1.90
T8	1.70-1.80
T9	1.60-1.70
T10	1.50-1.60
T11	1.40-1.50
T12	1.30-1.40
T13	1.20-1.30
T14	1.10-1.20
T15	1.00-1.10
T16	0.90-1.00
T17	0.80-0.90
T18	0.70-0.80
T19	0.60-0.70
T20	0.50-0.60
T21	0.40-0.50
T22	0.30-0.40
T23	0.20-0.30
T24	0.10-0.20
T25	0.00-0.10

Hamilton clay loam	
R1	0.0-0.1
R2	0.1-0.2
R3	0.2-0.3
R4	0.3-0.4
R5	0.4-0.5
R6	0.5-0.6
R7	0.6-0.7
R8	0.7-0.8
R9	0.8-0.9
R10	0.9-1.0

Naike clay	
N1	0.0-0.1
N2	0.1-0.2
N3	0.2-0.3
N4	0.3-0.4
N5	0.4-0.5
N6	0.5-0.6
N7	0.6-0.7
N8	0.7-0.8
N9	0.8-0.9
N10	0.9-1.0

Te Kowhai silt loam	
TK1	0.0-0.1
TK2	0.1-0.2
TK3	0.2-0.3
TK4	0.3-0.4
TK5	0.4-0.5
TK6	0.5-0.6
TK7	0.6-0.7
TK8	0.7-0.8
TK9	0.8-0.9
TK10	0.9-1.0

Waiareka clay	
W1	0.0-0.1
W2	0.1-0.2
W3	0.2-0.3
W4	0.3-0.4
W5	0.4-0.5
W6	0.5-.55

Appendix 10: Analyses of phosphorus and carbon from selected depths and samples in the Tokomaru silt loam.

Depth(cm)	μg/g P+	Sample	%C*
0-5	562	T25	7.70
5-10	446	T24	1.45
10-15	390	T23	1.02
15-20	306	T22	0.63
20-25	243	T21	0.51
25-30	196	T20	0.48
30-35	150	T19	0.30
35-40	108	T18	0.15
40-45	60	T17	0.12
45-50	40	T16	0.1
50-55	33	T15	0.1
55-60	34	T13	0.1
60-65	31	T11	0.1
65-70	55	T9	0.1
70-75	124	T8	0.1
75-80	313	T7	0.1
80-90	341	T5	0.1
90-100	351	T3	0.1
100-110	340	T1	0.1

\+ Walker and Adams (1958)   * A. West analyst

Appendix 11: The percent heavy minerals in the fine and very fine sand fractions from the Hamilton, Naike and Te Kowhai soils.

Sample	250-125 μm	125-63 μm
R1	13.0	16.4
R1	11.5	16.1
R3	11.2	17.5
R4	12.0	24.2
R5	11.3	25.8
R6	14.4	28.7
R7	13.8	25.9
R8	11.5	24.3
R9	11.1	22.2
R10	15.1	29.6

Sample	250-125 μm	125-63 μm
N1	5.2	10.6
N2	4.4	8.4
N3	4.8	11.1
N4	6.6	16.6
N5	12.1	21.0
N6	13.3	24.8
N7	14.9	27.7
N8	12.2	21.0
N9	4.0	9.3
N10	1.3	2.7

Sample	250-125 μm	125-63 μm
TK1	3.7	3.1
TK2	3.3	2.5
TK3	1.4	0.4
TK4	0.1	0.3
TK5	0.1	0.2
TK6	0.1	0.5
TK7	0.1	0.3
TK8	0.2	0.5
TK9	0.2	0.5
TK10	0.2	0.3

Appendix 12: Electron microprobe analyses of soil minerals.

12.1: Glasses.

Sample	T1	T1	T1	T1	T1	T1	T1	T1
SiO_2	74.34	73.80	73.15	74.71	74.07	73.97	76.00	73.13
Al_2O_3	11.27	11.19	11.11	11.35	11.10	11.28	11.59	12.09
TiO_2	0.16	0.09	0.00	0.17	0.10	0.12	0.15	0.17
FeO	1.02	1.14	1.28	1.10	1.12	1.04	1.13	1.95
MnO	0.14	0.00	0.00	0.00	0.12	0.00	0.00	0.00
MgO	0.11	0.10	0.13	0.11	0.09	0.10	0.09	0.10
CaO	0.87	0.95	1.03	1.02	0.98	0.95	0.94	1.07
Na_2O	3.21	3.46	2.96	3.27	2.98	2.97	3.60	4.15
K_2O	3.64	2.88	2.79	2.90	2.90	3.05	3.74	3.33
Cl	0.00	0.08	0.09	0.09	0.10	0.06	0.11	0.10
Total	94.76	93.69	92.54	94.72	93.56	93.54	97.35	96.09

Sample	T3	T3	T3	T3	T3	T3	T3	T3
SiO_2	66.80	64.28	62.00	74.80	73.12	74.50	75.19	73.77
Al_2O_3	13.77	15.37	14.38	11.18	11.27	11.32	11.44	11.15
TiO_2	1.18	1.17	0.96	0.00	0.13	0.12	0.11	0.13
FeO	5.05	5.35	5.54	1.07	1.18	1.00	1.21	1.07
MnO	0.04	0.00	0.11	0.00	0.00	0.00	0.00	0.00
MgO	1.14	1.26	2.00	0.10	0.11	0.13	0.12	0.10
CaO	3.43	5.38	5.04	0.92	1.07	0.97	1.07	0.83
Na_2O	3.75	3.96	3.25	3.50	3.55	3.54	3.43	3.53
K_2O	3.33	2.29	2.56	2.87	2.71	3.14	2.76	2.86
Cl	0.00	0.07	0.10	0.07	0.07	0.10	0.09	0.10
Total	98.49	99.13	95.94	94.51	93.21	94.82	95.42	93.54

Sample	T5	T5	T5	T5	T5	T5	T5	T5
SiO_2	74.63	75.02	73.75	67.97	68.52	68.34	75.54	74.15
Al_2O_3	11.34	11.41	11.29	13.04	13.14	14.57	11.34	11.26
TiO_2	0.10	0.00	0.14	0.80	0.77	1.04	0.13	0.00
FeO	1.15	1.08	0.94	3.18	3.87	3.63	0.98	1.01
MnO	0.00	0.00	0.00	0.13	0.15	0.00	0.00	0.14
MgO	0.15	0.14	0.09	0.87	0.83	1.31	0.09	0.13
CaO	1.04	1.06	0.68	3.50	2.90	2.77	0.74	0.93
Na_2O	3.20	3.17	2.49	3.53	3.27	5.55	2.76	2.83
K_2O	2.69	2.77	4.51	3.33	3.39	1.49	4.55	2.95
Cl	0.15	0.17	0.18	0.12	0.00	0.00	0.20	0.00
Total	94.45	94.82	94.07	96.47	96.84	98.70	96.33	93.40

Appendix 12.1: continued.

Sample	T6	T6	T6	T6	T6	T6	T6
SiO_2	75.11	62.44	74.56	74.83	74.14	74.72	74.37
Al_2O_3	11.38	15.87	11.40	11.28	11.30	11.32	11.33
TiO_2	0.08	0.56	0.13	0.11	0.15	0.11	0.00
FeO	1.03	3.12	1.07	1.09	0.97	1.01	1.15
MnO	0.00	0.16	0.00	0.00	0.00	0.00	0.00
MgO	0.11	1.23	0.12	0.11	0.08	0.10	0.13
CaO	1.10	2.76	1.04	1.04	0.88	0.93	1.09
Na_2O	2.96	4.10	2.90	2.84	2.59	2.90	2.82
K_2O	2.62	4.14	2.92	2.91	2.81	3.13	2.84
Cl	0.08	0.11	0.00	0.10	0.10	0.11	0.08
Total	94.47	94.49	94.14	94.31	93.02	94.33	93.81

Sample	T6	T6	T6	T6	T13	T13	T14
SiO_2	74.91	75.17	75.07	74.42	73.02	72.98	73.56
Al_2O_3	11.29	11.47	11.24	11.22	11.50	11.63	11.71
TiO_2	0.09	0.14	0.13	0.12	0.08	0.14	0.09
FeO	1.15	1.08	1.18	1.13	1.11	1.02	0.94
MnO	0.00	0.00	0.00	0.00	0.00	0.00	0.00
MgO	0.12	0.12	0.10	0.11	0.11	0.12	0.08
CaO	0.95	0.99	0.97	1.05	1.12	1.07	0.63
Na_2O	2.93	3.19	2.79	2.52	3.16	2.61	3.41
K_2O	2.50	2.68	2.69	2.93	2.83	2.82	4.25
Cl	0.09	0.10	0.09	0.07	0.11	0.08	0.13
Total	94.09	94.94	94.44	93.57	93.04	92.47	94.80

Sample	T14	T14	T16	T16	T16	T16
SiO_2	74.09	74.63	73.18	73.44	74.26	71.67
Al_2O_3	11.75	11.71	11.74	11.68	12.08	12.67
TiO_2	0.11	0.11	0.09	0.00	0.14	0.26
FeO	1.05	1.35	1.15	1.08	1.04	1.76
MnO	0.00	0.00	0.00	0.00	0.00	0.00
MgO	0.07	0.04	0.13	0.16	0.08	0.23
CaO	0.67	0.59	1.04	1.05	0.98	1.40
Na_2O	3.53	3.92	3.26	3.41	3.32	3.71
K_2O	4.03	3.76	2.85	2.76	3.82	2.64
Cl	0.14	0.09	0.13	0.12	0.19	0.00
Total	95.44	96.20	93.57	93.70	95.91	94.34

Appendix 12.1: Continued.

Sample	T24	T24	T24	T24	T24	T24	T24	T24
SiO_2	75.18	75.45	72.01	75.27	73.13	73.43	74.52	75.04
Al_2O_3	12.62	11.69	12.37	12.65	12.57	11.23	11.50	12.38
TiO_2	0.18	0.11	0.27	0.20	0.26	0.13	0.16	0.22
FeO	1.57	1.23	1.78	1.86	1.82	1.06	1.21	1.68
MnO	0.00	0.00	0.00	0.00	0.11	0.00	0.00	0.00
MgO	0.18	0.13	0.24	0.18	0.23	0.12	0.13	0.17
CaO	1.39	1.03	1.42	1.47	1.43	0.94	1.02	1.60
Na_2O	3.96	3.71	3.80	4.05	3.99	3.01	3.72	3.96
K_2O	2.98	3.02	2.58	2.93	2.69	3.23	2.93	2.95
Cl	0.12	0.08	0.10	0.07	0.09	0.11	0.10	0.08
Total	98.18	96.45	94.57	98.68	96.32	93.26	95.29	98.08

Sample	T24	T24	T24	T24	T24	T24	T24	T24
SiO_2	74.82	72.69	76.36	76.40	76.84	77.23	73.01	74.16
Al_2O_3	11.51	12.31	11.92	11.73	11.78	11.78	13.28	13.35
TiO_2	0.00	0.24	0.16	0.11	0.10	0.12	0.52	0.40
FeO	1.06	1.77	1.27	1.25	1.17	1.05	2.65	2.39
MnO	0.00	0.00	0.00	0.00	0.00	0.00	0.00	0.00
MgO	0.11	0.25	0.14	0.12	0.10	0.14	0.39	0.35
CaO	1.08	1.42	1.15	0.93	1.08	0.98	2.19	2.10
Na_2O	3.55	4.32	3.64	3.80	3.69	3.96	4.15	3.64
K_2O	3.41	2.65	3.34	3.29	3.25	3.35	2.81	2.79
Cl	0.09	0.09	0.11	0.10	0.05	0.10	0.07	0.05
Total	95.63	95.74	98.09	97.73	98.06	98.71	99.07	99.23

Sample	T24	T24	T24	T24	T24	T24	T24	T24
SiO_2	75.31	68.32	62.22	74.56	70.26	66.61	62.50	74.32
Al_2O_3	12.55	14.45	15.79	12.30	12.28	15.18	14.97	11.41
TiO_2	0.19	0.39	1.05	0.14	0.24	0.42	1.02	0.00
FeO	1.59	1.79	6.11	1.47	3.00	2.19	5.89	1.07
MnO	0.00	0.24	0.00	0.00	0.15	0.12	0.00	0.00
MgO	0.14	0.40	2.05	0.10	0.38	0.51	2.15	0.10
CaO	1.25	1.58	5.57	1.15	1.73	2.01	5.17	1.02
Na_2O	5.51	4.40	3.98	3.84	3.17	4.20	3.96	2.98
K_2O	1.57	4.88	2.28	3.89	2.33	4.48	2.43	2.76
Cl	0.06	0.10	0.04	0.08	0.11	0.18	0.06	0.09
Total	98.17	96.55	99.09	97.53	93.65	95.90	98.15	93.75

Appendix 12.1: Continued.

Sample	T25	T25	T25	T25	T25	T25	T25	T25
SiO_2	67.64	67.36	63.67	77.52	74.63	75.06	75.20	75.99
Al_2O_3	11.25	14.69	15.86	12.08	11.73	11.37	11.18	12.83
TiO_2	0.65	0.31	0.61	0.09	0.00	0.16	0.10	0.15
FeO	5.85	1.91	3.10	1.24	0.94	1.00	0.96	1.63
MnO	0.13	0.00	0.00	0.10	0.00	0.00	0.00	0.00
MgO	3.96	0.33	0.93	0.15	0.12	0.11	0.08	0.18
CaO	2.27	1.72	2.65	0.94	0.81	0.92	0.74	1.24
Na_2O	2.34	3.39	4.45	3.80	2.97	2.87	2.88	3.68
K_2O	3.09	4.27	4.19	3.12	2.88	2.69	2.88	2.98
Cl	0.11	0.14	0.15	0.10	0.10	0.09	0.09	0.11
Total	97.29	94.12	95.61	98.14	94.18	94.27	94.11	98.79

Sample	T25	T25	T25	T25	T25	T25	T25	T25
SiO_2	75.33	77.67	76.21	75.14	60.65	65.44	64.72	64.23
Al_2O_3	11.36	11.85	12.43	12.70	18.37	14.06	14.19	13.91
TiO_2	0.10	0.00	0.20	0.19	0.63	0.63	0.63	0.54
FeO	1.13	1.12	1.73	1.96	4.65	5.63	6.53	6.15
MnO	0.00	0.00	0.11	0.00	0.15	0.19	0.17	0.00
MgO	0.10	0.14	0.18	0.28	1.61	1.37	1.41	1.49
CaO	0.84	0.86	1.17	1.26	7.14	3.83	3.91	4.17
Na_2O	3.16	3.41	3.65	3.73	3.91	3.63	3.64	3.57
K_2O	2.81	3.32	2.90	2.89	1.72	1.99	1.83	1.92
Cl	0.10	0.14	0.07	0.06	0.06	0.08	0.07	0.00
Total	94.93	98.51	98.65	98.21	98.89	96.85	97.10	95.98

Sample	T25	T25	T25	T25	T25	T25	T25	T25	T25
SiO_2	59.85	62.26	70.97	64.37	56.40	75.70	70.21	64.22	67.78
Al_2O_3	19.50	16.31	14.80	14.76	23.85	13.68	13.85	13.72	17.53
TiO_2	0.53	0.76	0.34	0.78	0.28	0.23	0.88	0.53	0.57
FeO	4.28	5.93	1.70	6.58	2.54	0.44	1.41	5.33	1.83
MnO	0.00	0.16	0.15	0.00	0.00	0.00	0.00	0.17	0.00
MgO	1.73	2.27	0.29	1.32	0.64	0.00	0.11	3.11	0.11
CaO	7.95	6.22	1.51	4.72	10.01	2.27	1.39	4.50	5.49
Na_2O	3.86	3.87	5.15	4.64	4.15	4.52	3.22	3.99	5.09
K_2O	1.41	1.93	4.17	1.93	0.97	1.87	5.96	1.02	0.41
Cl	0.00	0.00	0.18	0.09	0.00	0.00	0.00	0.08	0.00
Total	99.11	99.71	99.26	99.19	98.84	98.71	97.03	96.67	98.81

Appendix 12.2: Amphiboles.

Sample	T3	T3	T3	T3	T3	T3	T5	T5
SiO_2	47.32	47.58	47.17	47.24	47.64	48.27	39.38	41.90
Al_2O_3	6.33	6.20	6.37	7.30	7.46	6.90	13.37	11.84
TiO_2	1.30	1.30	1.53	1.57	1.49	1.42	2.45	3.11
FeO	16.39	15.91	15.32	12.75	11.94	12.60	11.42	12.53
MnO	0.37	0.44	0.36	0.26	0.18	0.23	0.20	0.29
MgO	12.72	12.83	13.29	14.48	14.87	15.09	13.22	12.92
CaO	10.48	10.49	10.75	11.10	11.20	11.03	12.08	11.60
Na_2O	1.51	1.40	1.55	1.13	1.21	1.16	2.52	2.56
K_2O	0.31	0.27	0.32	0.20	0.21	0.20	0.82	0.92
Total	96.73	96.42	96.66	98.13	96.20	96.90	95.46	97.67

Sample	T5	T5	T5	T5	T5	T5	T5	T5
SiO_2	42.89	40.74	41.58	42.37	42.36	41.24	38.89	42.74
Al_2O_3	11.03	12.57	11.90	10.96	11.02	12.85	13.55	11.16
TiO_2	3.83	2.76	2.59	3.59	3.60	2.77	2.73	3.63
FeO	10.90	12.09	11.21	11.17	10.92	11.88	11.70	11.26
MnO	0.32	0.26	0.40	0.34	0.32	0.18	0.14	0.32
MgO	14.25	13.08	14.37	14.36	14.18	13.98	13.08	14.05
CaO	11.46	11.90	11.38	11.39	11.06	12.09	12.02	11.51
Na_2O	2.64	2.35	2.60	2.54	2.62	2.47	2.43	2.47
K_2O	0.94	0.85	0.87	0.83	0.85	0.85	0.82	0.86
Total	98.26	96.60	96.90	97.55	96.93	98.31	95.36	98.00

Sample	T5	T5	T5	T5	T5	T5	T5	T5
SiO_2	40.06	42.94	39.78	39.94	39.99	41.94	42.13	39.82
Al_2O_3	10.83	11.42	14.49	13.42	13.60	11.66	10.96	13.80
TiO_2	3.57	3.31	2.42	2.46	2.68	3.54	3.45	2.36
FeO	11.81	11.13	11.28	11.46	11.77	12.43	11.55	11.34
MnO	0.36	0.28	0.00	0.14	0.17	0.34	0.30	0.18
MgO	13.61	14.45	13.62	13.44	13.46	13.06	14.12	13.63
CaO	11.19	11.54	12.26	12.30	12.06	11.36	11.32	12.25
Na_2O	2.48	2.53	2.32	2.39	2.45	2.47	2.46	2.48
K_2O	0.89	0.82	1.06	0.90	0.95	0.92	0.82	0.92
Total	94.80	98.42	97.23	96.45	97.13	97.72	97.11	96.78

Appendix 12.2: Continued.

Sample	T6	T6	T6	T6	T6	T6	T6	T6
SiO_2	41.83	41.30	40.72	42.96	40.74	42.21	42.08	42.35
Al_2O_3	11.60	13.07	13.46	11.05	13.10	11.06	12.07	10.86
TiO_2	3.07	2.37	2.02	3.34	2.43	3.62	3.09	3.48
FeO	11.92	11.57	11.87	11.89	11.65	10.88	11.71	11.28
MnO	0.23	0.15	0.00	0.32	0.17	0.26	0.21	0.27
MgO	13.67	13.68	13.24	13.93	13.44	14.14	13.30	14.27
CaO	11.70	12.02	11.96	11.36	12.04	11.42	11.82	11.45
Na_2O	2.50	2.33	2.48	2.66	2.39	2.47	2.50	2.42
K_2O	0.86	0.80	0.84	0.93	0.84	0.95	0.82	0.80
Total	96.93	97.29	96.59	98.44	96.80	97.01	97.60	97.18

Sample	T6	T6	T6	T6	T6	T6	T6	T6
SiO_2	42.54	42.96	42.44	42.41	42.41	42.49	42.37	41.47
Al_2O_3	10.80	10.93	10.97	10.80	10.80	10.89	10.48	11.50
TiO_2	3.39	3.51	3.69	3.15	3.15	3.51	3.49	3.26
FeO	11.60	11.18	11.84	12.27	12.27	11.13	12.07	12.08
MnO	0.33	0.26	0.31	0.28	0.28	0.26	0.29	0.28
MgO	13.95	14.07	13.85	13.73	13.73	14.08	13.68	13.21
CaO	11.31	11.46	11.42	11.20	11.20	11.32	11.12	11.39
Na_2O	2.51	2.61	2.56	2.38	2.38	2.55	2.63	2.48
K_2O	0.85	0.81	0.88	0.87	0.87	0.89	0.96	0.98
Total	97.28	97.79	97.96	97.09	97.09	97.12	97.09	96.65

Sample	T6	T6	T6	T6	T6	T6	T6
SiO_2	40.40	40.77	42.16	42.53	41.69	42.77	42.53
Al_2O_3	12.10	12.08	10.92	11.07	11.75	10.92	11.14
TiO_2	2.92	2.83	3.54	3.62	3.51	3.48	3.41
FeO	12.57	12.45	10.87	11.02	11.62	11.30	11.55
MnO	0.25	0.31	0.21	0.32	0.28	0.30	0.32
MgO	12.69	12.58	13.90	14.35	13.53	14.29	13.79
CaO	11.73	11.77	11.40	11.52	11.54	11.32	11.22
Na_2O	2.47	2.35	2.61	2.52	2.57	2.63	2.54
K_2O	0.84	0.82	0.79	0.82	0.94	0.76	0.85
Total	95.97	95.96	96.40	97.77	97.43	97.77	97.35

Appendix 12.2: Continued.

Sample	T24	T24	T24	T24	T24	T24	T24	T24
SiO_2	42.25	43.28	41.31	43.08	42.56	40.64	40.46	41.46
Al_2O_3	12.17	10.14	13.00	10.30	11.00	12.48	13.59	13.08
TiO_2	2.78	3.31	2.11	3.17	3.16	2.80	2.34	2.91
FeO	13.61	11.43	9.60	12.23	11.84	12.79	11.58	12.24
MnO	0.30	0.42	0.00	0.36	0.29	0.30	0.18	0.00
MgO	11.91	13.77	14.92	13.47	13.55	12.50	13.55	13.68
CaO	11.79	11.44	12.27	11.42	11.63	11.77	12.40	12.16
Na_2O	2.29	2.33	2.37	2.35	2.50	2.54	2.29	2.53
K_2O	0.87	0.83	1.01	0.85	0.87	0.71	0.92	0.85
Total	97.97	96.95	96.59	97.23	97.40	96.53	97.31	98.91

Sample	T24	T24	T24	T24	T24	T24	T24	T24
SiO_2	40.31	40.44	42.21	43.06	42.08	43.77	39.99	39.58
Al_2O_3	13.80	13.81	11.42	10.55	11.00	10.28	14.06	14.27
TiO_2	2.30	2.36	2.89	3.30	3.64	2.68	1.44	2.49
FeO	11.16	11.21	14.19	12.34	11.17	12.47	12.14	12.07
MnO	0.00	0.00	0.44	0.33	0.33	0.47	0.16	0.00
MgO	13.60	13.64	11.87	13.58	14.19	13.24	12.86	12.90
CaO	12.21	12.26	11.58	11.27	11.36	11.56	12.11	12.01
Na_2O	2.37	2.43	2.38	2.45	2.53	2.32	2.37	2.42
K_2O	0.95	1.00	0.90	0.87	0.89	0.92	0.97	0.93
Total	96.70	97.15	97.88	97.75	97.19	97.71	96.10	96.67

Sample	T24	T24	T24	T24	T24	T24	T24	T24
SiO_2	41.50	39.78	40.23	42.68	40.11	43.07	43.72	43.76
Al_2O_3	13.56	14.47	13.91	10.89	15.90	10.09	9.91	10.16
TiO_2	2.86	2.32	2.87	2.78	2.11	3.19	3.05	3.00
FeO	11.18	11.73	11.05	12.33	10.71	11.51	12.33	11.43
MnO	0.00	0.13	0.00	0.35	0.00	0.45	0.43	0.37
MgO	14.30	13.18	13.86	13.31	13.63	13.76	14.02	13.72
CaO	11.80	12.12	12.05	11.75	12.83	11.50	11.50	11.59
Na_2O	2.51	2.43	2.43	2.44	2.37	2.31	2.45	2.41
K_2O	0.87	0.92	0.86	0.83	0.64	0.82	0.87	0.83
Total	98.64	97.08	97.26	97.36	98.30	96.70	98.28	97.27

Appendix 12.2: Continued.

Sample	T25	T25	T25	T25	T25	T25	T25	T25	T25
SiO_2	45.20	45.80	40.95	41.81	41.76	42.39	40.49	41.07	41.09
Al_2O_3	7.70	6.84	11.98	13.53	10.95	11.02	13.44	13.62	13.54
TiO_2	1.97	1.54	2.88	1.68	3.50	3.72	2.60	2.45	2.05
FeO	17.06	18.33	12.48	10.24	12.87	12.76	10.69	10.89	10.09
MnO	0.48	0.38	0.24	0.13	0.30	0.28	0.00	0.00	0.00
MgO	11.49	11.46	13.01	14.53	13.03	12.96	14.16	14.20	14.74
CaO	10.63	10.34	11.83	12.16	10.79	11.02	12.01	12.18	12.21
Na_2O	1.86	1.49	2.45	2.40	2.38	2.30	2.51	2.48	2.39
K_2O	0.29	0.31	0.87	0.33	1.14	1.34	0.91	0.97	1.11
Total	96.68	96.49	96.69	96.81	96.72	97.79	96.81	97.86	97.22

Sample	T25	T25	T25	T25	T25	T25	T25	T25	T25
SiO_2	42.82	43.60	43.45	41.55	41.82	42.62	42.11	42.86	40.90
Al_2O_3	10.17	9.72	10.10	11.48	11.54	10.41	11.12	10.34	13.56
TiO_2	3.07	3.05	3.01	2.68	2.55	3.34	2.77	3.25	2.49
FeO	12.19	12.40	12.22	12.92	12.47	11.64	13.33	11.39	10.87
MnO	0.41	0.45	0.42	0.30	0.29	0.31	0.33	0.29	0.00
MgO	13.72	13.68	13.66	12.59	13.06	14.00	12.83	13.77	13.76
CaO	11.66	11.69	11.63	11.80	11.89	11.32	11.88	11.49	12.18
Na_2O	2.36	2.32	2.38	2.41	2.38	2.40	2.30	2.47	2.26
K_2O	0.92	0.89	0.88	0.80	0.81	1.00	0.89	0.91	1.04
Total	97.32	97.80	97.75	96.53	96.81	97.04	97.56	96.77	97.06

Sample	T25	T25	T25	T25	T25	T25	T25	T25	T25
SiO_2	42.38	42.47	42.73	43.03	42.62	40.99	42.56	42.15	42.32
Al_2O_3	10.46	10.20	10.12	10.26	10.45	12.97	10.43	10.96	12.70
TiO_2	3.40	3.29	3.16	3.16	3.31	1.80	3.38	3.66	1.98
FeO	12.04	12.11	12.11	11.96	11.88	9.67	11.47	11.20	8.77
MnO	0.37	0.31	0.38	0.40	0.32	0.00	0.35	0.27	0.00
MgO	13.51	13.62	13.76	13.81	13.73	15.03	13.72	14.26	15.53
CaO	11.90	11.54	11.56	11.38	11.35	12.36	11.56	11.30	12.32
Na_2O	2.35	2.38	2.39	2.48	2.58	2.12	2.45	2.53	2.39
K_2O	0.92	0.95	0.91	0.79	0.81	1.06	0.80	0.78	0.86
Total	97.33	96.87	97.12	97.27	97.05	96.00	96.73	97.11	96.87

Appendix 12.3: Clinopyroxene.

Sample	T5	T5	T5	T5	T5	T5	T5	T5
SiO_2	51.90	47.57	52.52	52.04	49.51	51.17	52.20	51.46
Al_2O_3	2.29	6.78	2.80	1.80	5.23	2.11	2.07	2.45
TiO_2	0.80	1.06	0.34	0.52	0.80	0.64	0.45	0.64
FeO	11.43	7.72	6.70	9.80	7.20	11.92	7.85	7.91
MnO	0.29	0.15	0.19	0.16	0.14	0.37	0.45	0.40
MgO	14.79	12.74	16.37	14.68	13.19	13.77	15.83	15.08
CaO	18.37	22.25	21.08	20.34	23.41	19.10	20.85	20.29
Na_2O	0.44	0.28	0.29	0.30	0.26	0.35	0.32	0.39
Cr_2O_3	0.39	0.00	0.00	0.00	0.00	0.00	0.00	0.00
Total	100.70	98.55	100.29	99.64	99.74	99.43	100.02	98.62

Sample	T5	T5	T5	T5	T5	T5	T5	T5
SiO_2	51.13	50.75	50.10	50.33	49.74	51.83	51.29	49.92
Al_2O_3	2.58	3.48	4.38	3.49	2.43	2.40	2.81	4.11
TiO_2	0.64	0.82	0.85	0.73	0.61	0.50	0.65	0.90
FeO	9.25	7.96	8.78	8.11	7.71	6.17	7.59	8.30
MnO	0.16	0.40	0.44	0.30	0.28	0.46	0.28	0.28
MgO	14.32	14.57	13.49	14.43	15.18	15.16	14.74	13.75
CaO	20.21	21.31	21.93	20.87	21.24	21.46	21.81	21.98
Na_2O	0.36	0.33	0.40	0.36	0.40	0.38	0.39	0.32
Cr_2O_3	0.00	0.00	0.00	0.00	0.00	0.00	0.00	0.00
Total	98.65	99.62	100.37	98.62	97.59	98.36	99.56	99.56

Appendix 12. 3 Continued.

Sample	T24	T24	T24	T24	T24	T24	T24	T24
SiO_2	52.56	50.28	52.43	49.79	52.12	49.74	50.60	52.35
Al_2O_3	1.58	3.91	1.63	3.72	3.03	4.54	2.80	1.40
TiO_2	0.43	0.83	0.41	0.81	0.45	0.84	0.67	0.39
FeO	11.02	8.52	8.17	8.49	5.73	6.42	9.93	10.78
MnO	0.25	0.29	0.62	0.54	0.00	0.00	0.27	0.26
MgO	15.00	14.28	15.58	13.29	15.42	14.16	13.68	14.91
CaO	18.96	21.23	20.82	22.19	23.04	23.67	20.51	19.39
Na_2O	0.29	0.38	0.46	0.42	0.26	0.25	0.40	0.29
Total	100.09	99.72	100.12	99.25	100.05	99.62	98.86	99.77

Sample	T24	T24	T24	T24	T24	T24	T24	T24
SiO_2	51.29	51.84	48.03	51.23	51.00	51.87	53.60	52.10
Al_2O_3	3.07	2.27	6.04	2.67	2.37	2.40	1.20	1.54
TiO_2	0.59	0.57	0.93	0.56	0.59	0.45	0.28	0.43
FeO	8.02	11.16	9.02	8.94	11.03	5.67	7.40	9.93
MnO	0.17	0.26	0.30	0.41	0.23	0.00	0.61	0.25
MgO	13.66	14.09	12.01	13.01	14.15	15.72	15.02	15.04
CaO	22.76	19.84	22.73	22.43	19.64	23.44	22.28	19.59
Na_2O	0.25	0.29	0.47	0.33	0.31	0.23	0.39	0.28
Total	99.81	100.32	99.53	99.58	99.32	99.78	100.78	99.15

Appendix 12.3: Continued.

Sample	T25	T25	T25	T25	T25	T25	T25	T25
SiO_2	51.67	50.85	51.63	50.25	50.30	48.86	51.42	52.09
Al_2O_3	2.60	3.10	2.54	3.66	3.62	5.13	2.14	3.66
TiO_2	0.43	0.51	0.46	0.63	0.55	0.74	0.32	0.30
FeO	8.43	7.41	7.62	8.48	8.68	7.02	9.06	6.48
MNO	0.39	0.29	0.51	0.35	0.35	0.07	0.24	0.16
MgO	14.35	14.14	14.97	13.03	13.34	13.82	14.35	15.31
CaO	21.54	22.70	21.60	22.26	22.28	23.03	20.67	21.64
Na_2O	0.33	0.30	0.39	0.52	0.49	0.31	0.33	0.37
Total	99.74	99.36	99.72	99.18	99.61	98.98	98.53	100.01

Sample	T25	T25	T25	T25	T25	T25	T25	T25
SiO_2	53.26	52.14	51.12	52.80	51.25	50.87	51.17	51.11
Al_2O_3	1.72	3.29	2.58	1.06	2.48	2.67	2.81	2.52
TiO_2	0.19	0.42	0.35	0.22	0.43	0.46	0.47	0.40
FeO	4.49	5.11	8.31	7.26	8.05	11.22	9.03	8.91
MNO	0.13	0.14	0.28	0.65	0.40	0.31	0.22	0.15
MgO	16.44	15.31	13.52	14.83	13.65	13.83	14.46	14.78
CaO	22.50	23.43	22.80	22.04	22.68	19.69	20.74	20.35
Na_2O	0.24	0.33	0.36	0.36	0.35	0.35	0.16	0.38
Total	98.97	100.17	99.32	99.22	99.29	99.40	99.06	98.60

Sample	T25	T25	T25	T25	T25	T25	T25	T25
SiO_2	52.26	52.25	50.37	50.47	48.31	48.31	51.99	51.62
Al_2O_3	2.02	2.62	4.02	3.54	5.82	5.65	2.44	3.26
TiO_2	0.44	0.39	0.42	0.40	0.69	0.70	0.44	0.39
FeO	8.38	8.52	7.27	7.17	8.87	8.30	9.95	6.06
MNO	0.20	0.17	0.22	0.21	0.13	0.15	0.25	0.00
MgO	15.51	15.09	13.42	13.84	12.35	12.32	14.68	14.83
CaO	20.03	20.61	23.28	23.05	22.89	22.80	19.72	23.65
Na_2O	0.35	0.33	0.31	0.31	0.36	0.42	0.45	0.25
Total	99.19	99.98	99.31	98.99	99.42	98.65	99.92	100.06

Appendix 12.4: Orthopyroxenes.

Sample	T3	T3	T3	T3	T3	T3	T3	T3
SiO_2	51.46	51.34	54.22	53.53	51.14	54.25	53.75	53.55
Al_2O_3	0.35	0.38	1.41	1.49	0.28	2.48	1.66	2.54
TiO_2	0.10	0.12	0.14	0.14	0.00	0.10	0.16	0.12
FeO	28.60	29.41	16.23	15.34	29.70	11.72	14.96	11.86
MnO	1.33	1.59	0.29	0.33	1.44	0.21	0.33	0.22
MgO	16.99	16.18	25.79	26.08	15.60	29.45	27.12	28.74
CaO	0.80	0.89	1.45	1.19	0.83	1.42	1.54	1.47
Total	99.63	99.91	99.53	98.10	98.99	99.79	99.52	98.50

Sample	T3	T3	T3	T3	T3	T3	T3	T3
SiO_2	54.13	51.63	51.86	50.87	51.45	51.31	51.59	53.47
Al_2O_3	2.48	0.34	0.30	0.35	0.42	0.33	0.42	0.79
TiO_2	0.12	0.05	0.09	0.06	0.12	0.08	0.00	0.11
FeO	11.67	28.15	26.68	28.35	26.70	28.56	27.35	20.42
MnO	0.22	1.44	1.35	1.32	1.19	1.34	1.18	0.70
MgO	28.96	17.39	18.20	16.73	17.95	16.37	17.52	23.45
CaO	1.47	0.83	0.79	0.83	1.27	0.86	1.30	0.79
Total	99.05	99.83	99.27	98.51	99.10	98.85	99.36	99.73

Sample	T3	T3	T3
SiO_2	53.46	52.98	53.54
Al_2O_3	0.68	1.82	1.43
TiO_2	0.00	0.13	0.25
FeO	19.89	17.51	16.98
MnO	0.72	0.28	0.32
MgO	23.57	24.92	24.95
CaO	0.89	1.51	1.95
Total	99.21	99.15	99.42

Appendix 12.4: Continued.

Sample	T24	T24	T24	T24	T24	T24	T24	T24
SiO_2	50.68	52.38	53.39	51.12	51.26	52.51	52.85	52.92
Al_2O_3	1.16	1.52	1.36	0.37	0.40	1.79	1.07	3.64
TiO_2	0.23	0.31	0.27	0.13	0.19	0.20	0.25	0.00
FeO	28.20	19.70	18.02	30.62	30.73	19.27	20.12	14.09
MnO	1.39	0.47	0.46	1.71	1.77	0.46	0.37	0.26
MgO	16.27	22.98	24.16	14.45	14.41	23.50	22.47	27.04
CaO	1.91	1.28	1.32	1.18	1.25	1.33	1.77	1.35
Total	99.84	98.64	98.98	99.58	100.01	99.06	98.90	99.30

Sample	T24	T24	T24	T24	T24	T24	T24	T24
SiO_2	54.40	52.38	52.82	51.56	50.63	52.14	52.06	54.15
Al_2O_3	2.26	1.20	0.74	0.68	0.44	0.69	0.82	0.88
TiO_2	0.17	0.31	0.21	0.18	0.13	0.23	0.26	0.20
FeO	13.78	20.96	18.84	24.27	28.42	24.41	24.15	18.55
MnO	0.26	0.52	0.58	0.84	1.57	0.50	0.72	0.39
MgO	27.52	21.73	24.05	19.79	15.78	19.33	19.40	23.85
CaO	1.13	1.53	1.58	1.33	1.29	1.32	1.61	1.85
Total	99.52	98.63	98.82	98.65	98.26	98.62	99.02	99.87

Sample	T24	T24	T24	T24	T24	T24	T24	T24
SiO_2	51.01	51.78	53.45	51.62	52.24	52.53	53.61	53.39
Al_2O_3	0.52	0.43	0.88	0.51	3.46	1.25	1.99	1.23
TiO_2	0.17	0.19	0.22	0.18	0.22	0.00	0.23	0.35
FeO	28.05	26.74	20.59	27.98	18.73	21.57	17.40	19.54
MnO	1.54	1.57	0.59	1.54	0.37	0.52	0.25	0.36
MgO	16.50	17.61	22.71	16.74	23.64	21.75	24.98	22.83
CaO	1.32	1.26	1.67	1.20	1.21	1.56	1.43	2.14
Total	99.11	99.58	100.11	99.77	99.87	99.18	99.89	99.84

Appendix 12.4: Continued.

Sample	T25	T25	T25	T25	T25	T25	T25	T25
SiO_2	51.48	51.06	52.78	53.09	53.95	52.83	52.94	53.79
Al_2O_3	0.43	0.42	1.35	1.06	1.06	1.49	1.23	1.31
TiO_2	0.13	0.11	0.29	0.31	0.20	0.24	0.23	0.00
FeO	28.64	28.58	20.43	20.97	18.99	19.59	20.40	17.36
MnO	1.58	1.69	0.50	0.40	0.39	0.62	0.47	0.39
MgO	16.29	16.42	22.57	22.35	23.96	23.02	22.97	24.92
CaO	1.21	1.24	1.44	1.55	1.34	1.51	1.56	1.48
Total	99.76	99.52	99.36	99.73	99.89	99.30	99.80	99.25

Sample	T25	T25	T25	T25	T25	T25	T25	T25
SiO_2	53.39	52.56	52.44	52.76	53.20	52.95	52.56	52.48
Al_2O_3	1.03	3.97	4.07	1.43	3.15	1.12	1.21	1.00
TiO_2	0.21	0.14	0.17	0.22	0.17	0.19	0.26	0.26
FeO	20.01	14.70	15.14	19.75	13.50	19.55	18.77	20.34
MnO	0.46	0.25	0.31	0.60	0.31	0.61	0.41	0.47
MgO	23.54	25.93	26.02	23.05	27.28	22.87	23.55	22.69
CaO	1.67	1.09	1.10	1.55	1.33	1.52	1.66	1.71
Total	100.31	98.64	99.25	99.36	98.94	98.81	98.42	98.95

Sample	T25	T25	T25	T25	T25	T25	T25	T25
SiO_2	52.69	52.58	53.11	52.96	53.79	52.97	53.62	51.89
Al_2O_3	0.99	1.35	1.19	0.79	0.96	1.00	1.30	0.42
TiO_2	0.21	0.24	0.25	0.16	0.17	0.23	0.12	0.00
FeO	19.75	20.28	19.23	23.36	18.67	17.69	18.14	27.95
MnO	0.41	0.42	0.52	0.62	0.46	0.42	0.45	1.75
MgO	22.91	22.70	23.52	19.95	23.56	24.36	24.35	16.95
CaO	1.70	1.70	1.64	2.01	1.82	2.12	1.52	1.12
Total	98.66	99.27	99.46	99.85	99.43	98.79	99.50	100.08

Ager, T.A. 1983: Glacial and floral changes in southern Argentina since 14000 years ago. *National geographic research report 15*:457-479.

Alaily, F. 1986: Cracks in sandy soils of the extreme arid part of the Sahara. *Abstracts of the 13th Congress of the International Society of Soil Science, 1986, Hamburg III*:1023-1024.

Anderson, R.B.; Hallet, B. 1986: Sediment transport by wind: towards a general model. *Geological society of America bulletin 97*:523-535.

Anderton, P.W. 1981: Structure and evolution of the south Wanganui Basin. *New Zealand journal of geology and geophysics 24*:39-63.

Andrews, J.T. 1982: On the reconstruction of the Pleistocene ice sheets: a review. *Quaternary sciences review 1*:1-31.

Anonymous 1981: Post-conference tour, North Island. *in* Pollok, J.A.; Parfitt, R.L.; Furket, R.J. *eds*. Guide book 4. *Soils with Variable Charge Conference, 1981, Palmerston North*.

Anthony, J.C. 1984: The stratigraphy and mineralogy of a Late Pleistocene loess sequence in southern Manawatu. Unpublished B.Sc. (Hons.) dissertation held in the Department of Soil Science, Massey University.

Aoyagi, K.; Kazama, T. 1980: Transformational changes of clay minerals, zeolites and silica minerals during diagenesis. *Sedimentology 27*:178-188.

Appleman, D.E.; Nissen, H.U.; Stewart, D.B.; Clark, J.R.; Dowty, E.; Huebner, J.S. 1971: Studies of Lunar plagioclases, tridymite and cristobalite. *Proceedings of the Second Lunar Conference 1*:11-133.

Arrhenius, G.O. 1952: Sediment cores from the east Pacific. Chapter 5. *In* Pettersson, H. *ed*. Reports of the Swedish Deep-sea Expedition. 227pp.

Backett, W. 1985: Geology and petrology of Ruapehu Volcano and related vents. Unpublished Ph.D. thesis held in the Library, Victoria University of Wellington.

Bagnold, R.A. 1973: The physics of blown sand and desert dunes. New York, Methuen. 265p.

Bailey, J.M. 1971: Extraction and radiocarbon dating of dispersed organic material from loess in the South Island of New Zealand. *New Zealand journal of science 14:*490-503.

Baker, G. 1959: Opal phytoliths in some Victorian soils and "Red Rain" residues. *Australian journal of botany* 7:64-87.

Baker, G. 1960: Hook-shaped opal phytoliths in the epidermal cells of oats. *Australian journal of botany 8*:69-74.

Balsam, W. 1981: Late Quaternary sedimentation in the western north Atlantic: stratigraphy and palaeoecology. *Palaeogeography, palaeoclimatology, palaeoecology 35*:215-240.

Barnett, R. 1984: Upper Quaternary stratigraphy in the Otaki district. Unpublished B:Sc.(Hons) thesis, held in the Library, Victoria University of Wellington.

Barratt, B.C. 1981: Micromorphology of a yellow-grey earth to yellow-brown earth soil sequence on loess in Canterbury, Otago and Southland, New Zealand. *New Zealand Soil Bureau scientific report 45*.

Barratt, B.C. 1984: Micromorphology of yellow-grey earths. Pp 59-64. *In* Bruce, J.G. *(ed.)*. *Soil Groups of New Zealand. Part 7. Yellow-grey earths.* Lower Hutt, New Zealand Society of Soil Science.

Barron, E.J.; Washington, W.M. 1982: Atmospheric circulation during warm geologic periods: Is the equator-to-pole surface-temperature gradient the controlling factor. *Geology 10*:633-636.

Bartoli, F. 1985: Crystallochemistry and surface properties of biogenic opal. *Journal of soil science 36*:335-350.

Bartoli, F.; Guillet, B. 1977: Etude compareie des phytilithiques et polliniques d'un podzol des vosges Greseuses. *Acadimie des Science Comptes Rendus 284D*:353-356.

Bartoli, F.; Wilding, L.P. 1980: Dissolution of biogenic opal as a function of its physical and chemical properties. *Journal of the Soil Science Society of America 44*:873-878.

Beavers, A.H.; Stephen, I. 1958: Some features of the distribution of plant-opal in Illinois soils. *Soil science 86*:1-5.

Beget, J.E. 1983: Radiocarbon-dated evidence of world wide early Holocene climatic change. *Geology 11*:389-393.

Benny, L.A. 1982: A mineralogical and textural study of the central North Island tephra, Okareka Ash and its overlying tephric loess deposit. Unpublished M.Sc. thesis, held in the Library, Massey University.

Bernard, A.; Guern, F. 1986: Condensation of volatile elements in high temperature gases of Mount St. Helens. *Journal of volcanology and geothermal research 28*:91-105.

Birrell, K.S. 1956: Soil conditions in relation to engineering in New Zealand. *Proceedings of the 2nd Australia-New Zealand Conference on Soil Mechanics and Foundation Engineering, 1956, Christchurch*. Pp 17-19.

Birrell, K.S. 1972: The physical properties of loess soils and the influence of cultivation. *In* Watt, J.P.C. *ed*. Loess Soils and Land use on the Downlands of the South Island of New Zealand, with particular reference to the North Otago area. *Otago Catchment Board Publication 4*:29-44.

Birrell, K.S.; Packard, R.Q. 1953: Some Physical properties of New Zealand "loess". *New Zealand journal of science and technology B35*:30-35.

Birrell, K.S.; Pullar, W.A. 1973: Weathering of paleosols in Holocene and Late Pleistocene tephras in central North Island, New Zealand. *New Zealand journal of geology and geophysics 16*:687-702.

Bishop, D.G.; Lindqvist, J.K.; Ritchie, D.D.; Turnbull, I.M. 1984: Modern sedimentation at Falls Dam, upper Manuherikia River, Central Otago, New Zealand. *New Zealand journal of geology and geophysics 27*:305-312.

Blakemore, L.C. 1958: Chemistry of the yellow-grey earths in the North Island, New Zealand. *New Zealand soil news 6*:218-225.

Blakemore, L.C. 1984: Survey chemistry of yellow-grey earths. Pp. 66-70. *In* Bruce, J.G. *ed*. Soil Groups of New Zealand. Part 7, Yellow-grey earths. New Zealand Society of Soil Science, Lower Hutt, New Zealand.

Blattner, P.; Bird, G.W. 1974: Oxygen isotope fractionation between quartz and K-feldspar at 600°C. *Earth and planetary science letters 23*:21-27.

Bleeker, P.; Parfitt, R.L. 1974: Volcanic ash and its clay mineralogy at Cape Hoskins, New Brittain, Papua New Guinea. *Geoderma 11*:123-135.

Bloom, A.L. 1971: Glacial eustatic and isostatic controls of sea level since the last glaciation. Pp 355-379. *In* Turekian, K.K. *ed*. Late Cenozoic glacial ages. New Haven,Yale University Press.

Bloom, A.L. 1983: Sea level movements during the last interglacial hemicycle. *International geological correlation program report No. 11*.

Bloom, A.L.; Broecker, W.S.; Chappel, J.M.A.; Mathews, R.K.; Mesolella, K.J. 1974: Quaternary sea level fluctuations on a tectonic coast: New $^{230}Th/^{234}U$ dates from Huon Peninsula, New Guinea. *Quaternary research 4*:185-205.

Bottinga, Y.; Javoy, M. 1973: Comments on oxygen isotope geothermometry. *Earth and planetary science letters 20*:250-265.

Brazier, J.D.; Franklin, G.L. 1961: Identification of hardwoods; a microscopic key. *Forest Products research bulletin 46*.

Brindley, G.W. 1957: Fullers earth from near Dry Branch, Georgia - a montmorillonite-cristobalite clay. *Clay mineralogy bulletin 3*:167-169.

Bronger, A. 1986: Argillic horizons in modern loess soils in an ustic soil moisture regime in the temperate climatic zone. *Abstracts of the 13th International Soil Science Society Congress, 1986, Hamburg III*:1068-1069.

Brooks, R.R. 1965: The distribution of elements in gleyed and concretionary material in a New Zealand yellow-grey earth. *New Zealand journal of science 8*:88-92.

Brown, G. 1980: Associated Minerals. Pp 361-411. *In* Brindley, G.W.; Brown, G. *eds*. Crystal structures of clay minerals and their X-ray identification. London, Mineralogical Society.

Bruce, J.G. 1972: Loess soils in the South Island. *In* Watt, J.P.C. *ed*. Loess Soils and Land use on the Downlands of the South Island of New Zealand, with particular reference to the North Otago area. *Otago Catchment Board Publication 4*:1-28.

Bruce, J.G. 1973a: A time-stratigraphic sequence of loess deposits on near coastal surfaces in the Balclutha district. *New Zealand journal of geology and geophysics 16*:549-556.

Bruce, J.G. 1973b: Loessial deposits in southern South Island, with a definition of Stewarts Claim Formation. *New Zealand journal of geology and geophysics 16*:533-548.

Bruce, J.G. 1978a: Loess content of soils in South Island, New Zealand; scale 1:1,000,000. Map to accompany Watt, J.P.C. *ed.* Loess Soils and Land use on the Downlands of the South Island of New Zealand, with particular reference to the North Otago area. *Otago Catchment Board Publication 4*.

Bruce, J.G. 1978b: Soils of part of Raglan county, South Auckland, New Zealand. *New Zealand Soil Bureau bulletin 41*.

Bruce, J.G. 1983: Effect of climate on morphological features of soils from loess in the southern part of South Island, New Zealand. *Australian journal of soil science 21*:359-371.

Bruce, J.G. 1984a: Yellow-grey earths of Southland and West Otago. Pp 46-51. *In* Bruce, J.G. *ed.* Soil Groups of New Zealand Part 7. Yellow-grey earths. Lower Hutt, New Zealand Society of Soil Science.

Bruce, J.G. *ed.* 1984b: Soil Groups of New Zealand. Part 7. Yellow-grey earths. Lower Hutt, New Zealand Society of Soil Science.

Bruce, J.G.; Ives, P.W.; Leamy, M.L. 1973: Maps and sections showing the distribution and stratigraphy of South Island loess deposits, New Zealand 1:1,000,000. *New Zealand soil survey report 7*.

Buerger, M.J. 1954: The stuffed derivatives of the silica structure. *American mineralogist 39*:600-614.

Bull, P.A.; Bridges, E.M. 1978: Micromorphological and genetic properties of a gleyic brown podzolic soil from South Wales, United Kingdom. *Abstracts of the 11th International Society of Soil Science Congress, 1978, Edmonton*. P 34.

Burns, R.E.; Andrews, J.E, *et al* 1973: Initial report of the deep sea drilling project, 21. Washington, United States Government Printing Office.

Butzer, K.W. 1983: Global sea level stratigraphy. *Quaternary science review 2*:1-17.

Buurman, P. 1972: Mineralisation of fossil wood. *Scripta geologica 12*:1-43.

Calvert, S.E. 1971a: Composition and origin of North Atlantic deep sea cherts. *Contributions to mineralogy and petrology 33*:273-288.

Calvert, S.E. 1971b: Nature of silica phases in deep sea cherts of the North Atlantic. *Nature, physical sciences 234*:33-34.

Campbell, I.B. 1979: Occurrence of Kawakawa Tephra near Nelson - Note. *New Zealand journal of science 22*:133-136.

Carpenter, M.A.; Wennemer, M. 1985: Characterisation of synthetic tridymite by transmission electron microscopy. *American mineralogist 70*:517-528.

Carter, L. 1980: Ironsands in continental shelf sediments off western New Zealand - a synopsis. *New Zealand journal of geology and geophysics 23*:455-468.

Champness, P.E.; Durham, A.C.; Gibb, F.G.F.; Giles, H.N.; M^{ac}Kenzie, W.S.; Stumpfl, E.F.; Zussman, J. 1971: Mineralogy and petrology of some Apollo 12 Lunar samples. *Proceedings of the Second Lunar Conference 1*:359-376.

Chapman, S.L.; Syers, J.K.; Jackson, M.L. 1969: Quantitative determination of quartz in soils, sediments and rocks by pyrosulfate fusion and hydrofluorosilicic acid treatment. *Soil science 107*:348-355.

Childs, C.W. 1973: Patterns of total element concentration in Quaternary loess columns. *Abstracts of the 9th INQUA Conference 1973, Christchurch*. P 61.

Childs, C.W.; Leslie, D.M. 1977: Interelement relationships in Fe-Mn concretions from a catenary of yellow-grey earth soils in loess. *Soil science 123*:369-376.

Childs, C.W.; Searle, P.L. 1975: Element distributions in loess columns at Claremont, Table Flat, and Stewarts Claim, New Zealand. *New Zealand Soil Bureau Scientific Report 20*.

Christie, J.M.; Lally, J.S.; Heuer, A.H.; Fisher, R.M.; Griggs, D.T.; Radcliffe, S.V. 1971: Comparative electron petrography of Apollo 11, Apollo 12 and terrestrial rocks. *Proceedings of the Second Lunar Science Conference 1*:69-89.

Claridge, G.G.C.; Weatherhead, A.V. 1978: Mineralogy of the silt fraction of New Zealand soils. *New Zealand journal of science 21*:413-423.

Clayton, L.; Moran, S.R. 1982: Chronology of Late Wisconsin glaciation in middle North America. *Quaternary science review 1*:55-82.

Clayton, R.N.; Epstein, S. 1958: The relationship between $O^{18}:O^{16}$ ratios in coexistng quartz, carbonate, and iron oxides from various geological deposits. *Journal of geology 66*: 352-373.

Clayton, R.N.; Mayeda, T. 1963: The use of bromine pentafluoride in the extraction of oxygen from oxides and silicate minerals for isotopic analysis. *Geochimica et cosmochimica acta 27*:43-52.

Clayton, R.N.; O'Neil, J.R.; Mayeda, T.K. 1972: Oxygen isotope exchange between quartz and water. *Journal of geophysical research* 77: 3057-3063.

CLIMAP Project Members, 1976: The surface of the ice-age Earth. *Science 191*:1131-1137.

Cole, J.W. 1970: Description and correlation of Holocene volcanic formations in the Tarawera-Rerewhakaaitu region. *Transactions of the Royal Society of New Zealand, earth science 8*:93-107.

Cole, J.W. 1979: Structure, petrology and genesis of Cenozoic volcanism, Taupo Volcanic Zone, New Zealand - a review. *New Zealand journal of geology and geophysics 22*:631-657.

Cophen, T.B.; Kendall, C.; Hopple, J. 1983: Comparison of stable isotope reference samples. *Nature 302*:235-238.

Cornish, R. 1983: Glacial erosion in an ice divide zone. *Nature 301*:413-415.

Cortez, A.; Franzmeier, D.P. 1972: Weathering of primary minerals in volcanic ash-derived soils of the central cordillera of Columbia. *Geoderma 9*:165-176.

Cotton, C.A. 1917: The geomorphology of the coastal district of south western Wellington. *Transactions and proceedings of the New Zealand Institute 50*:212-222.

Cowie, J.D. 1963: Dune-building phases in the Manawatu District, New Zealand. *New Zealand journal of geology and geophysics 6*:268-280.

Cowie, J.D. 1964a: Aokautere Ash in the Manawatu district. *New Zealand journal of geology and geophysics* 7:67-77.

Cowie, J.D. 1964b: Loess in the Manawatu district, New Zealand. *New Zealand journal of geology and geophysics* 7:389-396.

Cowie, J.D. 1973: Pretoria Road Site section (p 83) *In* IX INQUA Congress Guidebook for Excursion A2, Central North Island, New Zealand.

Cowie, J.D. 1978: Soils and agriculture of Kairanga County. *New Zealand Soil Bureau bulletin 33.*

Cowie, J.D. 1984: Yellow-grey earths - definition and classification. Pp.7-10. *In* Bruce, J.G. *ed.* Soil Groups of New Zealand. Part 7, Yellow-grey earths. New Zealand Society of Soil Science, Lower Hutt, New Zealand.

Cowie, J.D.; Milne, J.D.G. 1973: Maps and sections showing the distribution and stratigraphy of North Island loess and associated deposits, New Zealand. 1:1,000,000. *New Zealand soil survey report 6.*

Cowie, J.D.; Wellman, H.W. 1962: Age of Ohakean Terrace, Rangitikei River. *New Zealand journal of geology and geophysics 5*:617-619.

Cox, J.E.; Vucetich, C.G.; Mead, C.B., Owers, W.R.; Daly, B. 1973: Loess fallout measurements near Barrhill, Canterbury, New Zealand 1959-64. *Abstracts of the 9th INQUA Conference 1973, Christchurch.* Pp 70-71.

Craig, H. 1961: Standard for reporting concentrations of deuterium and oxygen-18 in natural waters. *Science 133*:1833.

Crawford, J.C. 1869: On the geology of the province of Wellington. *Transactions of the New Zealand Institute 2*:343-360.

Crawford, J.C. 1886: Geology of the North Island, New Zealand. *Transactions of the New Zealand Institute 1*:305-328.

Croney, D.; Coleman, J.D. 1953: Soil moisture suction properties and their bearing on the moisture distribution in soils. *Proceedings of the 3rd International Conference on Soil Mechanics and Foundation Engineering 1*: 13-18.

Croney, D.; Jacobs, J.C. 1967: The frost susceptibility of soils and road materials. *Road Research Laboratory, Report LR 90.* 68 p.

Cronin, T.M. 1982: Rapid sea level and climatic changes: evidence from continental and island margins. *Quaternary science review 1*:177-215.

Cui, B.; Kromar, P.D.; Baba, J. 1983: Settling velocities of natural sand grains in air. *Journal of sedimentary petrology 53*:1205-1211.

Cullen, D.J. 1967: Submarine evidence from New Zealand of a rapid rise in sea level at 11,000 years B.P. *Palaeogeography, palaeoclimatology and palaeoecology 3*:289-298.

Darragh, P.T.; Gaskin, A.J.; Terrell, B.C,; Sanders, J.V. 1966: Origin of precious opal. *Nature 209*:13-16.

Davis, J.C. 1970: Petrology of Cretaceous Mowry Shale of Wyoming. *American association of petroleum geologists 54*:487-502.

Davoren, A. 1976: A pedological study of the Kauroa Ash Formation. Unpublished M.Sc. thesis, held in the Library, University of Waikato.

De Angelis, M.; Barkov, N.I.; Petrov, V.N. 1986: Aerosol concentrations over the last climate cycle (160 kyr) from an Antarctic ice core. *Nature 325*:318-321.

Deer, W.A.; Howie, R.A.; Zussman, J. 1967: Rock-forming minerals, V.4 Framework silicates. London, Longmans.

De Kimp, C. 1970: Chemical, physical and mineralogical properties of a podzol soil with fragipan derived from glacial till in the province of Quebec. *Canadian journal of soil science 50*:317-330.

De Kimp, C.R. 1976: Influence of parent material and moisture regime on soils genesis in the Appalachian Highlands, Quebec. *Canadian journal of soil science 56*:271-283.

Denton, G.H.; Prentice, M.L.; Kellogg, D.E.; Kellogg, T.B. 1984: Late Tertiary history of the Atlantic ice sheet: evidence from the Dry Valleys. *Geology 12*:263-267.

Derbyshire, E. 1983: The loess at Jiuzhoutai, Lanzhour, People's Republic of China. *Loess Letter 9*:10-13.

Dethier, D.P.; Pevear, D.R.; Frank, D. 1981: The 1980 eruptions of Mount St Helens Washington: Alteration of new volcanic deposits. *United States Geological Survey professional paper 1250:*649-665.

Duce, R.A.; Unui, C.K.; Ray, B.J.; Prospero, J.M.; Merrill, J.T. 1980: Long range atmospheric transport of soil dust from Asia to tropical North Pacific: temporal variability. *Science 209*:1522-1524.

Dunbar, C.O.; Rodgers, J. 1958: Principles of Stratigraphy. John Wiley and Sons, London.

Duplessey, J.C.; Arnold, M.; Maurice, P.; Bord, E.; Duprat, J.; Moyes, J. 1986: Direct dating of the oxygen isotope record of the last glaciation by ^{14}C accelerator mass spectrometry. *Nature 320*:350-352.

Dutch, M.E.; Miller, R.B. 1965: Rate of breakdown of Beech litter. *New Zealand soil news 13*:130-131.

Egunjobi, J.K. 1969: Primary productivity and nutrient cycling in terrestrial ecosystems. *Tuatara 17*:49-67.

Ehrenberg, C.G. 1847: Passatstaub und Blutregen. Deutsche Academie Wissenschafte, Berlin Abhandlungen:269-460.

Eitel, W. 1954: The physical chemistry of the silicates. Chicago, University of Chicago Press.

Elder, N.L. 1965: Vegetation of the Ruahine Range: An introduction. *Transactions of the Royal Society of New Zealand, botany 3*:13-66.

Emery, K.O. 1969: The continental shelves. *Scientific american 221*:106-128.

Emery, K.O.; Kuhn, G.G. 1982: Sea cliffs: Their processes, profiles and classification. *Geological Society of America bulletin 93*:644-654.

Emiliani, C. 1966: Paleotemperature analysis of Caribbean cores P6304-8 and P6304-9 and a generalised temperature curve for the past 425,000 years. *Journal of geology 75*:109-126.

Engel, A.E.J.; Clayton, R.N.; Epstein, S. 1958: Variations in isotopic composition of oxygen and carbon in Leadville limestone (Mississippian, Colorado) and its hyrothermal and metamorphic phases. *Journal of geology, 66*:374-393.

Epstein, S.; Buchsbaum, R.; Lowenstam, H.A.; Urey, H.C. 1953: Revised carbonate-water isotopic temperature scale. *Geological society of America bulletin 64*:1315-1326.

Epstein, S.; Taylor, H.P.(Jr.) 1967: Variation of $^{18}O:^{16}O$ in minerals and rocks. Pp 29-62. *In* Abelson, P.H. *ed.* Researches in geochemistry II. New York.

Ernst, W.G.; Calvert, S.E. 1969: An experimental study of the recrystallisation of porcelanite and its bearing on the origin of some cherts. *American journal of science 267A*:114-133.

Ewart, A. 1965: Mineralogy and petrogenesis of the Whakamaru ignimbrite in the Maraeti area of the Taupo Volcanic Zone, New Zealand. *New Zealand journal of geology and geophysics 8*:611-677.

Ewart, A. 1971: Chemical changes accompanying spherulitic crystallisation in rhyolitic lava, central volcanic region, New Zealand. *Mineralogical magazine 38*:424-434.

*

Ewart, A. 1968: The petrography of the central North Island lavas. Part 2. Regional petrography including notes on associated ash-flow pumice deposits. *New Zealand journal of geology and geophysics 11:478-545.*

Fairbridge, R.W. 1982: The Pleistocene-Holocene boundary. *Quaternary science review 1*:215-244.

Fenner, C.N. 1913: Stability relations of the silica minerals. *American journal of science 36*:331-384.

Fieldes, M. 1952: Abnormal behaviour of alpha-quartz from some New Zealand soils. *Nature 170*:366-367.

Fieldes, M. 1958: Clay mineralogy of yellow-grey earths. *New Zealand soil news 6*:225-227.

Fieldes, M. 1966: The nature of allophane in soils. Part 1: Significance of structural randomness in pedogenesis. *New Zealand journal of science 9*:599-607.

Fieldes, M.; Furkert, R.J. 1966: The nature of allophane in soils, Part 2. Differences in composition. *New Zealand journal of science 9*:608-622.

Fieldes, M.; Swindale, L.D. 1954: Chemical weathering of silicates in soil formation. *New Zealand journal of science and technology B36*:140-154.

Fieldes, M.; Walker, I.K.; Williams, P.P. 1956: Clay mineralogy of New Zealand soils: Part 3- Infrared absorption spectra of soil clays. *New Zealand journal of science and technology B38*:31-43.

Fieldes, M.; Weatherhead, A.V. 1966: Mineralogy of sand fractions of New Zealand Soils. *New Zealand journal of science 9*:1006-1021.

Fieldes, M.; Weatherhead, A.V. 1968: Mineralogy of the sand fraction. Pp 8-21. *In* New Zealand Soil Bureau. 1968: Soils of New Zealand. *New Zealand Soil Bureau bulletin* 26(2).

Fieldes, M.; Williamson, K.I. 1955: Clay mineralogy of New Zealand soils: Part 1 - Electron microscopy. *New Zealand journal of science and technology B37*:314-335.

Fife, C.V. 1945: Study of a yellow-grey loam in the Manawatu. *New Zealand journal of science and technology A26*:281-293.

Fitzpatrick, E.A. 1956: An indurated soil horizon formed by permafrost. *Journal of soil science* 7:248-254.

Fitzpatrick, E.A. 1976: Cryons and isons. *Proceedings of the North England soils discussion group (1974) 11*:31-43.

Fleming, C.A. 1970: Radiocarbon dating and pollen analyses from Otiran periglacial fans in western Wellington. *Transactions of the Royal Society of New Zealand, earth science* 7:197-208.

Fleming, C.A. 1979: The geological history of New Zealand. Auckland University Press. 141p.

Florke, O.W. 1955: Zur frage des "hoch"-cristobalite in opalel, bentoniten und glasern. *Neues Jahrbuch fur Mineralogie 1955*:217-223.

Florke, O.W.; Hollmann, R.; von Rad, U.; Rosch, H. 1976: Intergrowth and twinning in opal-CT lepispheres. *Contributions to mineralogy and petrology 58*:235-242.

Florke, O.W.; Jones, J.B.; Segnit, E.R. 1975: Opal-CT crystals. *Neues Jahrbuch fur Mineralogie Mn. H8*:369-377.

Folk, R.L. 1974: Petrology of Sedimentary Rocks. Hemphill, Austin, Texas. 182p.

Franks, A.M. 1984: Soils of Eltham County and the tephrachronology of Central Taranaki. Unpublished Ph.D. thesis held in the Library, Massey University.

Froggatt, P.C. 1982: A study of some aspects of the volcanic history of the Lake Taupo Area, North Island, New Zealand. Unpublished Ph.D.thesis held at the Library, Victoria University of Wellington.

Froggatt, P.C. 1983: Towards a comprehensive Upper Quaternary tephra and ignimbrite stratigraphy in New Zealand using electron microprobe analysis of glass shards. *Quaternary Research 19*:188-200.

Froggatt, P.C.; Solloway, G.J. 1986: Correlation of Papanetu Tephra to Karapiti Tephra, central North Island, New Zealand. *New Zealand journal of geology and geophysics 29*:303-313.

Frondel, C. 1962: Dana's system of mineralogy. Volume III. Silica minerals. John Wiley and Sons, New York.

Froude, D.O. 1985: Petrography, mineralogy and chemistry of Titiraupenga Volcano, North Island, New Zealand. *New Zealand journal of geology 28*: 487-496.

Fruchter, J.S.; Robertson, D.E.; Evans, J.C. *et al*. 1980: Mount St. Helens ash from the 18 May 1980 eruption - chemical, physical, mineralogical and biological properties. *Science 209*:1116-1125.

Gage, D.R.; Jernegan, M.F.; Farwell, S.O. 1981: Characteristics and quantification of inhalable particulate volcanic ash from Mt St Helens. *Mt St Helens: One Year Later Conference, Washington, May 1981*.

Gage, M. 1957: The geology of Waitaki Division. *New Zealand Geological Survey bulletin 55*.

Gagosian, R.B.; Peltzer, E.T.; Merril, J.T. 1987: Long-range transport of terrestrially derived lipids in aerosols from the South Pacific. *Nature 325*:800-803.

Galehouse, J.S. 1969: Counting grain mounts:number percentages versus number frequency. *Sedimentary petrology 39*:812-815.

Garlick, G.D.; Epstein, S. 1967: Oxygen isotope ratios in coexistng minerals of regionally metamorphosed rocks. *Geochimica et cosmochimica acta 31*: 181-214.

Gibb, J.G. 1979: Late Quaternary shoreline movements in New Zealand. Unpublished Ph.D. thesis, held in the Library, Victoria University of Wellington.

Gibb, J.G. 1983: Sea levels during the past 10,000 years B.P. from the New Zealand region - South Pacific Ocean. Pp 28-31. *Abstracts of the International Symposium of Coastal Evolution in the Holocene, Tokyo*. Japanese Society for the Promotion of Science.

Gibb, J.G. 1986: A New Zealand regional Holocene eustatic sea level curve and its application to determination of vertical tectonic movements. *Royal Society of New Zealand bulletin 24*:377-397.

Gibbs, H.S. 1964: Some reflections on soil formation and loess. *New Zealand soil news 12*:222-225.

Gibbs, H.S. 1980: New Zealand soils. Wellington, Oxford University Press.

Ginzburg, I.I.; Kabanova, E.S. 1960: Silica content and its form in natural waters. Kora Vyvetrivaniya, Akad. Nauk SSSR, Inst. Geol. Gudnykh Mestorozhden., Petrog., *Mineral. i Geokhim. 3*:313.

Goh, K.M.; Tonkin, P.J.; Rafter, T.A. 1978: Implications of improved radiocarbon dates of Timaru peats on Quaternary loess stratigraphy. *New Zealand journal of geology and geophysics 21*:463-466.

Gradwell M.W. 1974: The available-water capacities of some southern and central zonal soils of New Zealand. *New Zealand journal of agricultural research 17*:465-478.

Gradwell, M.W. 1978a: Pore size distributions of some New Zealand soil groups. *New Zealand journal of agricultural research 21*:603-614.

Gradwell, M.W. 1978b: Subsoil hydraulic conductivities of major New Zealand soil groups at water content near field capacity. *New Zealand journal of agricultural research 22*:603-614.

Graham, I.V. 1985: Petrochemical and Sr isotopic studies of lavas and xenoliths from Tongariro Volcanic Centre - Implications for crustal contamination of calc-alkaline magmas. Unpublished Ph.D. thesis held in the Library, Victoria University, Wellington.

Grange, L.I. 1945: Farming in New Zealand. North Island Soils. *New Zealand journal of agriculture 70*:387-397.

Grange, L.I. 1946: Farming in New Zealand. South Island soils. *New Zealand journal of agriculture 72*:583-591.

Green, J.D.; Lowe, D.J. 1985: Stratigraphy and development of *c*.17,000 year old Lake Maratoto, North Island, New Zealand, with some inferences about postglacial climatic change. *New Zealand journal of geology and geophysics 28*:675-701.

Greenwood, R. 1973: Cristobalite: its relationship to chert formation in selected samples from the deep sea drilling project. *Journal of sedimentary petrology 43*:700-808.

Greig, J.W. 1932: The existence of the high-temperature form of cristobalite at room temperature and the crystallinity of opal. *Journal of the American chemical society 54*:2846-2849.

Griggs, G.B.; Carter, L.; Kennett, J.P.; Carter, R.V. 1983: Late Quaternary marine stratigraphy southeast of New Zealand. *Geological Society of America bulletin 94*:791-797.

Grossman, R.B.; Carlisle, F.J. 1969: Fragipan soils of the eastern United States. *Advances in agronomy 21*:237-276.

Guven, N.; Grim, R.E. 1972: X-ray diffraction and electron optical studies on smectite and alpha-cristobalite associations. *Clays and clay minerals 20*:89-92.

*
Hall, R.D.; Canepa, A.P.; Ruhe, R.V. 1973: Paleosols of southwestern Indiana. *Abstracts of the 9th INQUA Congress, 1973, Christchurch*. Pp 133-134.

Hallmark, C.T.; Smeck, N.E. 1979: The effect of extractable aluminium, iron and silicon on strength and bonding of fragipans of northeastern Ohio. *Journal of the Soil Science Society of America 43*:145-150.

* Hackett, W. 1985: Geology and petrology of Ruapehu volcano and related vents. Unpublished Ph.D. thesis held in the Library, Victoria University.

Hampton, C.M.; Bailey, D.K. 1985: Sublimates obtained during fusion of volcanic glass. *Journal of volcanology and geothermal research 25*:145-155.

Hardjosoesastro, R.R. 1956: Preliminary note on cristobalite in clay fractions of volcanic glass. *Journal of soil science* 7:185-188.

Harlan, P.W.; Franzmeier, D.P.; Roth, C.B. 1977: Soil formation on loess in southwestern Indiana. I. Loess stratigraphy and soil morphology. *Journal of the Soil Science Society of America 41*:93-98.

Harland, W.B. 1981: Chronology of Earths glacial and tectonic record. *Journal of the geological society of London 138*:197-203.

Harris, D.M.; Rose, W.I.; Roe, R.; Thompson, M.R. 1981: The 1980 eruptions of Mt. St. Helens, Washington: radar observations of ash eruptions. *United States Geological Survey professional paper 1250*:323-333.

Harris, W.F. 1963: Paleoecological evidence from pollens and spores. *New Zealand Ecological Society proceedings 10*:38-55.

Harvey, C.C. 1980: A study of the alteration products of acid volcanic rocks from Northland, New Zealand. Unpublished Ph.D. thesis. Indiana University.

Healy, J. 1982: Central Volcanic Region. *In* Soons, J.M.; Sleby, M.J. *eds*. Landforms of New Zealand. Longman-Paul, Auckland.

Heath, G.R.; Moberly, R. 1971: Cherts from the western Pacific, Leg 7, deep sea drilling project. Pp 991-1007. *In* Winterer *et al*. (*eds*.) Initial reports of the deep sea drilling project VII. Washington, United States Government Printing Office.

Hein, J.R. 1981: Siliceous deposits of the Pacific region. *International geological correlation program report 10*:38-39.

Hein, J.R.; Scholl, D.W.; Baron, J.A.; Jones, M.G.; Miller, J. 1978: Diagenesis of late Cenozoic diatomaceous deposits and formation of the bottom simulating reflector in the southern Bering Sea. *Sedimentology 25*:155-181.

Hein, J.R.; Yeh, H. 1981: Oxygen isotope composition of chert from the mid Pacific Mountains and Hesse Rise, Deep Sea Drilling Project, Leg 62. Initial reports of the deep sea drilling project, Leg 62. Washington D.C., United States Government Printing Office.

Hemley, J.J.; Meyer, C.; Richter, D.H. 1961: Some alteration reactions in the system Na_2O-Al_2O_3-SiO_2-H_2O. *United States Geological Survey professional paper 424D*:388-340.

Henderson, J.H.; Clayton, R.N.; Jackson, M.L.; Syers, J.K.; Rex, R.W.; Brown, J.L.; Sachs, I.B. 1972: Cristobalite and quartz isolation from soils and sediments by hydrofluorosilicic acid treatment and heavy liquid separation. *Soil Science Society of America proceedings 36*:830-835.

Henderson, J.H.; Jackson, M.L.; Syers, J.K.; Clayton, R.N.; Rex, R.W, 1971: Cristobalite authigenic origin in relation to montmorillonite and quartz origin in bentonites. *Clays and clay minerals 19*:229-238.

Henmi, T.; Parfitt, R.L. 1980: Laminar opaline silica from volcanic ash soils in New Zealand. *Clays and clay minerals 28*:57-60.

Hesp, P.A.; Shepherd, M.J. 1978: Some aspects of the late Quaternary geomorphology of the lower Manawatu valley, New Zealand. *New Zealand journal of geology and geophyics 21*:403-412.

Heusser, C.J.; Rabassa, J. 1987: Cold climate episode of younger Dryas age in Tierra del Fuego. *Nature 328*:609-611.

Heydemann, A. 1964: Untersuchunge uber die bildungsbedingungen van quartz im temperaturbereich zwaschen 100°C und 250°C. *Beitrage vur mineralogie und petrographie 10*:242-259.

Hill, V.G.; Roy, R. 1958a: Silica structure studies: V. the variable inversion of cristobalite. *Journal of the American ceramic society 41*:532-537.

Hill, V.G.; Roy, R. 1958b: Silica structure studies. VI on tridymite. *Transactions of the British ceramic society* 57:496-510.

Hodder, A.P.W. 1978: Refractive index and hydration of rhyolitic glass from Holocene tephras, North Island, New Zealand. *New Zealand journal of geology and geophysics 21*:155-166.

Hogg, A.G. 1979: Identification and correlation of thinly bedded Late Quaternary tephras of the Coromandel Peninsula, New Zealand. Unpublished D. Phil. thesis, held in the Library, University of Waikato.

Hogg, A.G.; McCraw, J.D. 1983: Late Quaternary tephras of Coromandel Peninsular, New Zealand: a mixed peralkaline and calcalkaline tephra sequence. *New Zealand journal of geology and geophysics 26*:163-187.

Holmquist, S.B. 1961: Conversion of quartz to tridymite. *Journal of the American Ceramic Society 44*:82-86.

Howorth, R. 1976: Late Pleistocene tephras of the Taupo and Bay of Plenty regions. Unpublished Ph.D. thesis held at the Library, Victoria University of Wellington.

Hubbard, C.B.; Neall, V.E. 1980: A reconstruction of Late Quaternary erosional events in the West Tamiki River catchment, Southern Ruahine Range, North Island, New Zealand. *New Zealand journal of geology and geophysics 23*: 587-593.

Hudson, A.W.; Fife, C.V. 1940: Mole drainage investigations in New Zealand. *New Zealand journal of science and technology A22*:197-208.

Hume, T.M.; Nelson C.S. 1986: Distribution and origin of clay minerals in surficial shelf sediments, western North Island, New Zealand. *Marine geology 69*:289-308.

Hume, T.M.; Sherwood, A.M.; Nelson, C.S. 1975: Alluvial sedimentology of the Upper Pleistocene Hinuera Formation, Hamilton basin, New Zealand. *Journal of the Royal Society of New Zealand 5*:421-462.

Huut C.B.; Robinson T.W.; Bowles W.A.; Washburn A.L. 1966: Hydrolic Basin Death Valley California. *United States geological survey professional paper* 494-B.

Iijima, A.; Matsumoto, R.; Tada, R. 1980a: Zeolite and silica diagenesis and sandstone petrography at sites 438 and 439 off Sanriku, northwest Pacific. Pp 1143-1158. *In* Lee, M.; Stout, L.N. *ed*. Initial reports of the deep sea drilling project, leg 57. Washington, United States Government Printing Office.

Iijima, A.; Matsumoto, R.; Tada, R. 1980b: Zeolite and silica diagenesis and sandstone petrography at sites 438 and 439 off Sanriku, northwest Pacific. Pp 56-57. *In* Lee, M.; Stout, L.N. *ed*. Initial reports of the deep sea drilling project, leg 57. Washington, United States Government Printing Office.

Iijima, A.; Tada, R. 1981: Silica diagenesis of neogene diatomaceous and volcaniclastic sediment in northern Japan. *Sedimentology 28*:185-200.

Isaacs, C.M. 1982: Influence of rock composition on kinetics of silica phase changes in the Monterey Formation, Santa Barbara area, California. *Geology 10*:304-308.

Ives, D. 1973: Nature and distribution of loess in Canterbury, New Zealand. *New Zealand journal of geology and geophysics 16*:587-610.

Ives, D.; Stevenson, E. 1973: Recent loess sedimentation on the Canterbury Plains and its implications in terms of Late Quaternary loess deposits. *Abstracts of the 9th INQUA Congress, 1973, Christchurch*. Pp 186-189.

Jackson, M.L. 1956: Soil chemical analysis - advanced course. Department of Soil Science, University of Wisconsin, Madison, Wisconsin.

Jackson, M.L.; Clayton, R.N.; Fujii, N.; Henderson, J.H. 1977: Cristobalite morphology and oxygen isotope composition variation under hydrothermal alteration. *Clays and clay minerals 25*:31-38.

Jackson, M.L.; Gillette, D.A.; Danielson, E.F.; Blifford, I.H.; Byron, R.A.; Syers, J.K. 1973: Global dust fall during the Quaternary as related to environments. *Soil science 116*:135-145.

Jackson, M.L.; Levett, W.M.; Syers, J.K.; Rex, R.W.; Clayton, R.N.; Sherman, G.D.; Uehara, G. 1971: Geomorphological relationships of tropospherically derived quartz in the soils of the Hawaiian Islands. *Soil Science Society of America Proceedings 35*:515-525.

Jane, D.S. 1980: Slope morphology, soils and erosion of a terrace scarp at the Fitzherbert site, Palmerston North. Dip.Ag.Sc. dissertation held in the Department of Soil Science, Massey University.

JCPDS. 1974: Selected powder diffraction data for minerals. Joint Committee on Powder Diffraction Standards. Pennsylvania.

Jeans, C.V. 1978: Silicifications and associated clay assemblages in the Cretaceous marine sediments of southern England. *Clay mineralogy 13*:101-125.

Jessen, M.R. 1977: Horotiu and Waihou silt loams, a comparative study. Unpublished M.Sc. thesis, held in the Library, University of Waikato.

Joe, E.N. (Compiler) 1986: Soil water characterisation studies of 6 soils in the Waikato district New Zealand. *New Zealand Soil Bureau SWAMP data sheets 1984*:1-6.

JOIDES 1967: *American association of petroleum geologists bulletin 51*.

Jones, J.B.; Biddle, J.; Segnit, E.R. 1966: Opal genesis. *Nature 210*:1353-1354.

Jones, J.B.; Sanders, J.V.; Segnit, E.R. 1964: Structure of opal. *Nature 204*:990-991.

Jones, J.B.; Segnit, E.R. 1969: Water in sphere-type opal. *Mineralogical magazine 37*:357-361.

Jones, J.B.; Segnit, E.R. 1971: The nature of opal: I. Nomenclature and constituent phases. *Journal of the geological society of Australia 18*:57-68.

Jones, J.B.; Segnit, E.R. 1975: Nomenclature and the structure of natural disordered (opaline) silica. *Contributions to mineralogy and petrology 51*:231-234.

Jones, J.B.; Segnit, E.R.; Nickson, N.M. 1963: Differential thermal and X-ray analysis of opal. *Nature 198*:1191.

Jones, L.H.P.; Handreck, K.A. 1967: Silica in soils, plants and animals. *Advances in Agronomy 19*:107-149.

Jones, L.H.P.; Milne, A.A.; Wadham, S.M. 1963: Studies of silica in the oat plant. II. Distribution of silica in the plant. *Plant and soil 18*:358-371.

Jones, R.C.; Uehara, G. 1973: Amorphous coatings on mineral surfaces. *Soil Science Society of America proceedings 37*:792-798.

Jones, R.L.; Beavers, A.H. 1963: Some mineralogical and chemical properties of plant opal. *Soil science 96*:375-79.

Jones, R.L.; Beavers, A.H. 1964: Aspects of catenary and depth distribution of opal phytoliths in Illinois soils. *Soil Science Society of American proceedings 28*:413-416.

Jones, R.L.; Hay, W.W. 1975: Bioliths. Pp. 481-496. *In* Gieseking, J.E. *ed*. Soil Components: Volume 2, Inorganic Components. New York, Springer-Verlag.

Kadko, D.; Blueford, J.R.; Burckle, L.H.; Barron, J. 1983: Selective dissolution of siliceous microfossils observed in a box core from the north east equatorial Pacific. *Nature 302*:139-141.

Kamatani, A. 1971: Physical and chemical characteristics of biogenous silica. *Marine biology 8*:89-95.

Kastner, M.; Keene, J.B.; Gieskes, J.M. 1977: Diagenesis of siliceous oozes - 1. Chemical control on the rate of opal-A to opal-CT transition - an experimental study. *Geochimica et cosmochimica acta 41*:1041-1059.

Kawabe I. 1978: Calculation of oxygen isotope fractionation in quartz-water system with special reference to the low temperature fractionation. *Geochimica et cosmochimica acta 42*:613-621.

Keil, K.; Prinz, M. 1971: Mineralogy, petrology and chemistry of some Apollo 12 samples. *Proceedings of the Second Lunar Conference 1*:319-341.

Keller, M.A.; Isaacs, C.M. 1985: An evaluation of temperature scales for silica diagenesis in diatomaceous sequences in the Miocene Monterey Formation, California. *Geo-marine letters* 5:31-35.

Kennedy, N.M. 1980: Field recognition of tephric loess (c.42,000 - c.15,000 years B.P.) in central North Island. *New Zealand soil news 28*:55-58.

Kennedy, N.M. 1982: Tephric loess in the Rotorua-Bay of Plenty region, North Island, New Zealand. Pp 119-122. *In* Wasson, R.J. *ed.* Quaternary dust mantles of China, New Zealand and Australia. Canberra, Australia National University.

Kennedy, N.M.; Pullar, W.A. 1977: Loess on the Mamaku Plateau. *New Zealand soil news 25*:91.

Kennett, J.P.; Houtz, R.E. *et al* 1975: Initial reports of the deep sea drilling program 29. Washington, United States Government Printing Office.

Kennett, J.P.; van der Borch, C.C. *et al* 1985: Initial reports of the deep sea drilling program 90. Washington, U.S. Government Printing Office.

Khangarat, A.S.; Wilding, L.P.; Hall, G.F. 1971: Composition and weathering of loess mantled Wisconsin and Illinoian-age terraces in central Ohio. *Soil Science Society of America proceedings 35*:621-626.

Kihara, K. 1978: Thermal change in unit-cell dimensions, and a hexagonal structure of tridymite. *Zeitschrift fur kristallographie 148*:237-253.

Kihara, K. 1980: On the split-atom model for hexagonal tridymite. *Zeitschrift fur kristallographie 152*:95-101.

Kingma, J.T. 1962: Geological map of New Zealand. 1:250,000 Sheet 11-Dannevirke. Department of Scientific and Industrial Research, Wellington.

Kingma, J.T. 1967: Geological map of New Zealand. 1:250,000. Sheet 12-Wellington. Department of Scientific and Industrial Research, Wellington.

Kirkman, J.H. 1971a: Amorphous inorganic materials in three soils formed from loess. 1. Application of selective dissolution techniques. *New Zealand journal of science 16*:79-93.

Kirkman, J.H. 1971b: Amorphous inorganic materials in three soils formed from loess. 2. Amounts and distribution. *New Zealand journal of science 16*: 95-100.

Kirkman, J.H. 1973: Amorphous inorganic materials in the soils formed from loess. 2.Amounts and distribution. *New Zealand journal of science 16*:95-100.

Kita I.; Taguchi S.; Matsubaga O. 1985: Oxygen isotope fractionation between amorphous silica and water at 34-93°C. *Nature 314:*83-84.

Klein, C,; Drake, J.C.; Frondel, C. 1971: Mineralogical, petrological and chemical features of four Apollo 12 Lunar microgabbros. *Proceedings of the second Lunar conference 1*:265-284.

Klein, C.; Hurlbut, C.S. 1985: Manual of mineralogy. New York, John Wiley & Sons.

Kleiss, H.J. 1973: Loess distribution along the Illinois soil-development sequence. *Soil science 115*:194-198.

Knauth, L.P.; Epstein, S. 1975: Hyrogen and oxygen isotope ratios in silica from the JOIDES deep sea drilling project. *Earth and planetary science letters 25*:1-10.

Knauth, L.P.; Epstein, S. 1976: Hydrogen and oxygen isotope ratios in nodular and bedded cherts. *Geochimica et cosmochimica acta 40*:1095-1108.

Knauth, L.P.; Epstein, S. 1982: The nature of water in hydrous silica. *American mineralogist 67*:510-520.

Kocurek, G.; Hunter, R.E. 1986: Origin of polygonal fractures in sand, uppermost Navajo and Page sandstones, Page, Arizona. *Journal of sedimentary petrology 56*:895-904.

Kohn, B.P. 1970: Identification of New Zealand tephras by emmission spectrograph analysis of their titanomagnetites. *Lithos 3*:361-368.

Kohn, B.P.; Neall, V.E. 1973: Identification of Late Quaternary tephras for dating Taranaki lahar deposits. *New Zealand journal of geology and geophysics 16 (3)*:781-792.

Kolbe, R.W. 1957: Fresh water diatoms from Atlantic deep-sea sediments. *Science 126*:1053-1056.

Krauskopf, K.B. 1967: Introduction to geochemistry. McGraw-Hill Book Co., New York.

Kuno, H. 1933: On silica minerals occurring in the groundmass of common Japanese volcanic rocks. *Earthquake Research Institute bulletin 11*:382-390.

Kuntz, M.A.; Rowley, P.D., M^{ac}Leod, N.S.; Reynolds, R.L.; M^{c}Broome, L.A.; Kaplan, A.M.; Lidke, D.J. 1981: The 1980 eruptions of Mount St Helens, Washington: Petrography and particle-size distribution of pyroclastic-flow, ash-cloud, and surge deposits. *United States Geological Survey professional paper 1250*:525-639.

Labeyie, L.D.; Pichon, J.J.; Labracherie, M.; Ippolito, P.; Duprat, J.; Duplessey, J. 1986: Melting history of Antarctica during the past 60,000 years. *Nature 322*:701-706.

Laffan, M.D. 1979: Slope stability in the Charleston-Punakaiki region, South Island, New Zealand. 2. Soil disturbance by windthrow and podocarp logging on steepland soils formed from micaceous silty sandstone. *New Zealand journal of science 22*:193-201.

Lanering, F.C.; Pannaiya, B.W.N.; Crumption, C.F. 1958: The chemical nature of silica in plants. *Plant physiology 33*:339-343.

Langer, K.; Florke, O.W. 1974: Near infrared adsorption spectra (4000-9000cm-^{1}) of opals and the role of "water" in these $SiO_2.nH_2O$ minerals. *Fortschritte der mineralogie 52*:17-51.

Langohr, R. 1987: Consolidated horizons (fragipans?) in loess soils of western Europe: their characteristics, impact on root penetration and water percolation and their use as paleoenvironmental markers. *Abstracts for International Symposium on Loess, 1987, New Zealand*. p15.

Latter, J.H. 1985: Frequency of eruptions at New Zealand volcanoes. *Bulletin of the New Zealand national society for earthquake engineering 18*:55-110.

Latter, J.H.; Houghton, B.F.; Hackett, W.R. 1981: Volcanic risk assessment at Ruapehu volcano. Chapter 4. *in* Houghton, B.F.; Smith, I.E.M. *ed.* Volcanologic Workshop, 1981. *Proceedings of the New Zealand volcanologic workshop, 1981, Turangi.*

Leamy, M.L. 1973: Paleosol identification and soil stratigraphy in South Island, New Zealand. *Abstracts of the 9th INQUA Congress, 1973, Christchurch.* Pp 204-205.

Leamy, M.L.; Burke, A.S. 1973: Identification and significance of paleosols in cover deposits in Central Otago. *New Zealand journal of geology and geophysics 16 (3)*:623-635.

Leamy, M.L.; Clayden, B.; Hewitt, A.E. 1983: Soil classification in the New Zealand Soil Bureau. *New Zealand soil news 31*:183-185.

Leamy, M.L.; Milne, J.D.G.; Pullar, W.A.; Bruce, J.G. 1973: Paleopedology and soil sratigraphy in the New Zealand Quaternary succession. *New Zealand journal of geology and geophysics 16*:723-744.

Lee, K.E. 1959: The earthworm fauna of New Zealand. *New Zealand Department of Scientific and Industrial Research bulletin 130.*

Lee, K.E. 1968: A preliminary study of soil animals and their relationship to some New Zealand soils. *New Zealand Soil Bureau bulletin 26*:168-183.

Lee, R.; Bailey, J.M.; Northey, R.D.; Blake, P.R.;Gibson, E.J. 1975: Variations in some chemical and physical properties of three related soil types: Dannevirke silt loam, Kiwitea silt loam and Marton silt loam. *New Zealand journal of agricultural research 18*:29-36.

Lees, C.M. 1981: Some Aranuian (Postglacial) organic deposits in the south eastern Ruahine Range, North Island, New Zealand, investigated by palynological methods. Unpublished M.Sc. thesis, held in the Library, Massey University.

Lees, C.M. 1986: Late Quaternary palynology of the southern Ruahine Range, North Island, New Zealand. *New Zealand journal of botany 24*:315-329.

Lewis, K.B. 1979: A storm-dominated inner shelf, western Cook Strait, New Zealand. *Marine geology 31*:31-43.

Lewis, K.B.; Eade, J.V. 1974: Sedimentation in the vicinity of the Maui gas field. *New Zealand Oceanographic Institute oceanography summary 6.*

Lewis, K.B.; Mildenhall, D.C.; Clowes, C.D. 1985: The Late Quaternary seismic, sedimentary and palynological stratigraphy beneath Evans Bay, Wellington Harbour. *New Zealand journal of geology and geophysics 28*:129-152.

Lipman, P.W.; Norton, D.R.; Taggart, J.E.; Brandt, E.L.; Engleman, E.E. 1981: The 1980 eruption of Mount St. Helens, Washington: Compositional variations in 1980 magmatic deposits. *United States Geological Survey professional paper 1250*:631-640.

Lithgow, N.A. 1986: A textural and mineralogical study of the beach sands along the southwest coast of the North Island. Unpublished M.Sc. thesis, held in the Library, Massey University.

Lofgrens, J. 1981: Analysis of volcanic ash from Mt. St. Helens by X-ray diffraction. *Mt St Helens:One Year Later Conference, Washington,May 1981.*

Lorius, C.; Merlivat, L.; Jouzel, J.; Pourchet, M. 1979: A 30,000 year isotope climatic record from Antarctic ice. *Nature 280*:644-648.

Lovering, T.S. 1959: Significance of accumulator plants in rock weathering. *Geological Society of America bulletin 70*:781-800.

Lowe, D.J. 1980: Tephric Loess. *New Zealand soil news 28*:217-220.

Lowe, D.J. 1981: Origin and composite nature of Late Quaternary airfall deposits, Hamilton Basin. Unpublished M.Sc. thesis, held in the Library, University of Waikato.

Lowe, D.J. 1986: Controls on the rates of weathering and clay mineral genesis in airfall tephras: a review and New Zealand case study. Pp 265-330. *In* Coleman, S.; Dethier, D. *ed.* Rates of chemical weathering of rocks and minerals. New York, Academic Press.

Lowe, D.J. 1987: Studies on Late Quaternary tephras in the Waikato and other regions in the northern North Island, New Zealand. Based on distal deposits in lake sediments and peats. Unpulished Ph.D. thesis, held in the Library, Waikato University.

Lowe, J.P.; Lowe, D.J.; Hodder, A.P.W.; Wilson, A.T. 1984: A tritium-exchange method for obsidian hydration shell measurements. *Isotope geoscience 2*: 351-363.

M^{C}Craw, J.D. 1967: The surface features and soil pattern of the Hamilton Basin. *Earth science journal 1*:59-74.

M^{C}Craw, J.D. 1975: Quaternary airfall deposits of New Zealand. Pp. 35-44. *In* Suggate, R.P.; Cresswell, M.M. *eds*. Quaternary Studies. The Royal Society of New Zealand, Wellington.

M^{C}Glone, M.S. 1980: The history of New Zealand Lowland forest since the glaciation. *Proceedings of the Symposium on Lowland Forest in New Zealand, 1980, Hamilton*. Pp 1-18.

M^{C}Glone, M.S. 1985: Biostratigraphy of the last interglacial-glacial cycle, southern North Island, New Zealand. *Proceedings of the 2nd CLIMANZ conference, 1985, Harihari, New Zealand*. Pp 17-32.

M^{C}Glone, M.S.; Howarth, R.; Pullar, W.A. 1984: Late Pleistocene stratigraphy, vegetation and climate of Bay of Plenty and Gisborne regions, New Zealand. *New Zealand journal of geology and geophysics 27*:327-350.

M^{C}Glone, M.S.; Nelson, C.S.; Hume, T.M. 1978: Palynology, age and environmental significance of some peat beds in Upper Pleistocene Hinuera Formation, south Auckland, New Zealand. *Journal of the Royal Society of New Zealand 8*:385-393.

M^{C}Glone, M.S.; Topping, W.W. 1973: Late Otiran/early Aranuian vegetation in the Tongariro area, central North Island, New Zealand. *New Zealand journal of botany 11*:283-290.

M^{C}Glone, M.S.; Topping, W.W. 1977: Aranuian (Postglacial) pollen diagrams from the Tongariro region, North Island, New Zealand. *New Zealand journal of botany 15*:749-760

M^{C}Glone, M.S.; Topping, W.W. 1983: Late Quaternary vegetation, Tongariro region, central North Island, New Zealand. *New Zealand journal of botany 21*:53-76.

M^{C}Intyre, B.M. 1975: Upper Quaternary loess stratigraphy at two exposures in southern Manawatu. Unpublished B.Sc. (Hons.) dissertation held in the Geography Department, Massey University.

M^{C}Intyre, D.J. 1963: Pollen analyses of a peat in Koputaroa dune sands. *New Zealand journal of geology and geophysics 6*:278-280.

M^{C}Intyre, D.J. 1970: Pollen analyses from the Lindale section, Paraparaumu. *Transactions of the Royal Society of New Zealand, earth science* 7:203-206.

M^{C}Keague, J.A. and Cline, M.G. 1963: Silica in soils. *Advances in Agronomy 15*: 339-396.

M^{C}Kee, E.D. 1983: Eolian sand bodies of the world. Pp. 1-25. *In* Brookfield, M.E. *et al. eds*. Eolian Sediments and Processes. Elsevier, Amsterdam.

M^{C}Millan, P.F.; Remmele, R.L. 1986: Hydroxyl sites in SiO$_2$ glass: a note on infrared and raman spectra. *American mineralogist 71*:772-778.

M^{C}Queen, D.J. 1975: A study of the Horotiu - Te Kowhai soil complex. Unpublished M.Sc. thesis, held in the Library, University of Waikato.

Mahood, G.A.; Gilbert, C.M.; Carmichael, I.S.E. 1985: Peralkaline and metaluminous mixed liquid ignimbrites of the Guadalajara Region, Mexico. *Journal of volcanology and geothermal research 25*:259-271.

Marden, M. 1984: Geology and its relationship to erosion in the southern Ruahine Range, North Island, New Zealand. Unpublished Ph.D. thesis, held in the Library, Massey University.

Marden, M.; Paintin, I.K.; Lees, C.M.; Neall, V.E. 1986: Woodville neotectonics and Quaternary stratigraphy fieldtrip. *Geological Society of New Zealand miscellaneous publication 35B*:B3.1-B3.20.

Marshall, P.; Kidson, E. 1928: The duststorm of October, 1928. *New Zealand journal of science and technology 10*:291-299.

Marshall, P.; Murdoch, R. 1920: Tertiary rocks near Wanganui. *Transactions of the New Zealand Institute 52*:115-128.

Mason, B. 1955: Notes on some New Zealand minerals. *New Zealand journal of science and technology B36*:557.

Mason, B. 1966: Principles of geochemistry. New York. John Wiley & Sons.

Mathews, B. 1976: Soils with discontinuous induration in the Penrith area of Cumbria. *Proceedings of the North of England Soils Discussion Group (1974) 11*:11-19.

Mew, G.; Hunt, J.L.; Froggatt, P.C.; Eden, D.N.; Jackson, R.J. 1986: An occurrence of Kawakawa tephra from the Grey River valley, South Island, New Zealand. *New Zealand journal of geology and geophysics 28*:315-323.

Mildenhall, D.C. 1979: Holocene pollen diagrams from Pauatahanui Inlet, Porirua, New Zealand. *New Zealand journal of geology and geophysics 22*:585-591.

Mildenhall, D.C.; Moore, P.R. 1983: A late Holocene pollen sequence at Turakirae Head, and climatic and vegetational changes in the Wellington area in the last 10,000 years. *New Zealand journal of science 26*:447-459.

Miller, R.B. 1961: The chemical composition of rainwater at Taita, New Zealand, 1956-58. *New Zealand journal of science 4*:844-853.

Miller, R.B. 1963a: Plant nutrients in hard beech. I. The immobilisation of nutrients. *New Zealand journal of science 6*:365-377.

Miller, R.B. 1963b: Plant nutrients in hard beech. II. Seasonal variation in leaf composition. *New Zealand journal of science 6*:378-387.

Miller, R.B. 1963c: Plant nutrients in hard beech. III. The cycle of nutrients. *New Zealand journal of science 6*:388-413.

Miller, R.B. 1965: Cycles of energy, minerals, water and organic matter in an ecosystem with hard beech. *New Zealand soil news 13*:113-119.

Miller, R.B. 1978: Soil Taxonomy. *New Zealand soil news 26*:176-79.

Milne, J.D.G. 1973a: Maps and sections of river terraces in the Rangitikei basin, North Island, New Zealand. *New Zealand soil survey report 4*.

Milne, J.D.G. 1973b: Upper Quaternary geology of the Rangitikei drainage basin, North Island, New Zealand. Unpublished Ph.D. thesis, held in the Library, Victoria University of Wellington.

Milne, J.D.G. 1973c: Mount Curl Tephra, A 230,000-year-old marker bed in New Zealand, and its implication for Quaternary chronology. *New Zealand journal of geology and geophysics 16*:519-532.

Milne, J.D.G. 1976: Upper Quaternary geology of the Rangitikei valley. Pp 60-62. *Excursion guide no. 55A and 56C. 25th International Geological Congress, 1976, Sydney*. Christchurch, Progress Press.

Milne, J.D.G. 1981: Yellow-grey earths and yellow-brown earths formed from loess with tephra additions. Pp. 14-18. *In* Soils with Variable Charge Conference Guidebook for Tour 4. Government Printer, Wellington.

Milne, J.D.G.; Smalley, I.J. 1979: Loess deposits in the southern part of the North Island of New Zealand. An outline stratigraphy. *Acta Geological Academiae Scientiarum Hungaricae, Tomus 22 (1-4)*:197-204.

Mitchell, B.D. 1975: Oxides and hydrous oxides of silicon. Pp 395-432. *In* Gieseking, J.E. *ed*. Soil components, Volume 2.Inorganic components. New York, Springer-Verlag.

Mitchell, R.S. 1967: Tridymite pseudomorphs after wood in Virginian Lower Cretaceous sediments. *Science 158*:9095-9106.

Mitchell, R.S.; Tuft, S. 1973: Wood opal - A tridymite-like mineral. *American mineralogist 58*:717-720.

Miyauchi, N.; Aomine, S. 1964: Does "allophane B" exist in Japanese soils? *Soil Science and plant nutrients 10*:199-203.

Mizota, C. 1976: Relationship between the primary mineral and the clay mineral compositions of some recent andosols. *Soil science and plant nutrients 22*:257-268.

Mizota, C.; Aomine, S. 1975: Clay mineralogy of some volcanic ash soils in which cristobalite predominates. *Soil science and plant nutrition 21*:327-335.

Mizota, C.; Toh, N.; Matsuhia, Y. 1987: Origin of cristobalite in soils derived from volcanic ash in temperate and tropical regions. *Geoderma 39*:323-330.

Mizutani, S. 1977: Progressive ordering of cristobalitic silica in the early stages of diagenesis. *Contributions to mineralogy and petrology 61*:129-140.

Moar, N.T. 1961: Contributions to the Quaternary history of the New Zealand flora. 4:Pollen diagrams from the western Ruahine Range. *New Zealand journal of science 4*:350-359.

Moar, N.T. 1967: Contributions to the Quaternary history of the New Zealand flora. 5:Pollen diagrams from No Man's Land bog, northern Ruahine Range. *New Zealand journal of botany* 5:394-399.

Moar, N.T. 1973: A pollen diagram from a buried peat in loess at Timaru, South Island, New Zealand. *Abstracts of the 9th INQUA Congress, 1973, Christchurch*. Pp 245-246.

Moar, N.T. 1980: Late Otiran and early Aranuian grassland in central South Island. *New Zealand journal of ecology 3*:4-12.

Mokma, D.L.; Syers, J.K.; Jackson, M.L.; Clayton, R.N.; Rex, R.W. 1972: Eolian additions to soils and sediments in the South Pacifica area. *Journal of soil science, 23:*147-162.

Molina-Cruz, A. 1977: The relation of the southern trade wind to the upwelling processes during the last 75,000 years. *Quaternary research 8*:324-338.

Molloy, B.P.J.; Cox, J.E. 1965: The role of Beech forest in the development of the yellow-brown earth to podzol sequence of eastern South Island. *New Zealand soil news 13:*95-103.

Molloy, L.F.; Speir, T.W. 1977: Studies on the climosequence of soils in tussock grassland. 12.Constituents of the soil light fraction. *New Zealand journal of science 20*:167-177.

Moncure, G.K.; Surdam, R.C.; M^{c}Kaque, H.L. 1981: Zeolite diagenesis below Pahute Mesa, Nevada test site. *Clays and clay minerals 29*:385-396.

Moore, T.C.; Hatson, W.H.; Kipp, N.; Hays, J.D.; Prell, W.; Thompson,; Boden, G. 1981: The biological record of the ice age ocean. *Palaeogeography, palaeoclimatology, palaeoecology 35*:357-370.

Mullineaux, D.R.; Crandell, D.R. 1962: Recent lahars from Mount St. Helens, Washington. *Geological Society of America bulletin 73*:855-870.

Mullins, C.E.; Panayiotopoulas, K. 1980: Why are compact horizons unusual. *North of England soils discussion group (1979) proceedings 16*:127-130.

Murata, K.J.; Friedman, I.; Gleason, J.D. 1977: Oxygen isotope relations between diagenetic silica minerals in Monterey shale, Temblar Range, California. *American journal of science 277*:259-272.

Murata, K.J.; Larson, R.R. 1975: Diagenesis of Miocene siliceous shales, Temblar Range, California. *Journal of research of the United States Geological Survey 3*:553-566.

Murata, K.J.; Nakata, J.K. 1974: Cristobalitic stage in the diagenesis of diatomaceous shale. *Science 184*:567-568.

Murray, H.H.; Harvey, C.; Smith, J.M. 1977: Mineralogy and geology of the Maungaporerua halloysite deposit in New Zealand. *Clays and clay minerals 25*:1-5.

Neal J.T.; Langer A.M.; Kerr P.F. 1979: Giant desiccation polygons of Great Basin Playas. *Geological society of America bulletin 79*:69-90..

Neall, V.E. 1972: Tephrachronology and tephrastratigraphy of western Taranaki. *New Zealand Journal of Geology and Geophysics 15 (4)*:507-557.

Neall, V.E. 1982: Yellow-brown loams of Taranaki. Pp. 34-36. *In* Neall, V.E. *ed.* Soil Groups of New Zealand. Part 6, Yellow-brown loams. New Zealand Society of Soil Science, Wellington, New Zealand.

Neall, V.E.; Stewart, R.B.; Smith, I.E.M. 1986: History and petrology of the Taranaki volcanoes. Pp 251-263. *In* Smith, I.E.M. *ed.* Late Cenozoic Volcanism in New Zealand. *Royal Society of New Zealand bulletin 23.*

Neall, V.E.; Stewart, R.B.; Wallace, R.C.; Mew, G. 1983: The origin of quartz and associated soil mineralogy in relation to terrace ages at Kumara, Westland, New Zealand. *Abstracts, Pacific Science Association 15th Congress, Dunedin, New Zealand. Volume 1*:174.

Nelson, C.S. 1985: Lithostratigraphy of DSDP leg 90 drill sites in the southwest Pacific: An overview. Pp. 1471-1491. *In* Kennett, J.P.; van der Borch, C.C. *et al. ed.* Initial Reports of the DSDP, vol. XC. Washington, United States Government Printing Office.

Nelson, C.S.; Froggatt, P.C.; Gosson, G.J. 1985: Nature, chemistry, and origin of Late Cenozoic megascopic tephras in leg 90 cores from the southwest Pacific. Pp. 1161-1173. *In* Kennett, J.P.; van der Borch, C.C. *et al. eds.* Initial Reports of the DSDP, vol. XC. Washington, United States Government Printing Office.

Nelson, C.S.; Hendy, C.H.; Cuthbertson, A.M.; Jarrett, G.R. 1985: Late Quaternary carbonate and isotope stratigraphy, subantarctic site 594, southwest Pacific. Pp. 1425-1435. *In* Kennett, J.P.; van der Borch, C.C. *et al. ed.* Initial Reports of the DSDP, vol. XC. Washington, United States Government Printing Office.

Nelson, C.S.; Hendy, C.H.; Jarrett, G.R.; Cuthbertson, A.M. 1985: Near-synchroneity of New Zealand alpine glaciation and northern hemisphere continental glaciations during the past 750 kyr. *Nature 318*:361-363.

Netolitsky, F. 1929: Die Kieselkorpen. *Linsbauers Handb. der Pflanzenanatomie Berlin.* 3/1a:1-80.

New Zealand Soil Bureau, 1954: General survey of the soils of North Island, New Zealand. *New Zealand Soil Bureau bulletin 5.*

New Zealand Soil Bureau, 1968: Soils of New Zealand. *New Zealand Soil Bureau bulletin 26*: 3 volumes.

Nikiforoff, C.C. 1955: Hardpan soils of the coastal plain of southern Maryland. *United States Geological Survey Professional Paper 267B.*

Norris, R.M. 1972: Shell and gravel layers, western continental shelf, New Zealand. *New Zealand journal of geology and geophysics 15*:572-589.

Norton, L.D.; Bigham, J.M.; Hall, G.F.; Smeck, N.E. 1983: Etched thin sections for coupled optical and electron microscopy and microanalysis. *Geoderma 30*:55-64.

Oehler, J.H. 1973: Tridymite like crystals in cristobalite "chert". *Nature, physical sciences 241*:64-65.

Oliver, R.L. 1948: The Otaki sandstone and its geological history. *Department of Scientific and Industrial Research geological memoir* 7.

O'Neil, J.R.; Epstein, S. 1966: Oxygen isotope fractionation in the system dolomite-calcite-carbon dioxide. *Science 152*:198-200.

O'Neil, J.R.; Taylor, H.P. 1967: The oxygen isotope and cation exchange chemistry of feldspars. *American mineralogist 52*:1414-1437.

Packard, R. 1958: Physical properties of the yellow-grey earths. *New Zealand soil news 6*:227-230.

Pain, C.F. 1975: Some tephra deposits in the south-west Waikato area, North Island, New Zealand. *New Zealand journal of geology and geophysics 18*:541-550.

Palmer, A.S.: The stratigraphy and selected properties of loess in Wairarapa, New Zealand. Unpublished Ph.D. thesis held in the Library, Victoria University of Wellington.

Papike, J.J.; Hodges, F.N.; Bence, A.E.; Cameron, M.; Rhodes, J.M. 1976: Mare basalts: crystal chemistry, mineralogy and petrology. *Reviews of geophysics and space physics 14*:475-540.

Parfitt, R.L. 1975: Clay minerals in recent volcanic soils from Papua New Guinea. Pp 241-245. *In* Suggate, R.P.; Cresswell, M.M. *eds.* Quaternary studies. Wellington, Royal Society of New Zealand.

Parfitt, R.L.; Milne, J.D.G. 1984: An hypothesis on the formation of yellow-grey earths. p. 65. *In* Bruce, J.G. *ed.* Soil Groups of New Zealand. Part 7, Yellow-grey earths. New Zealand Soceity of Soil Science, Lower Hutt, New Zealand.

Parfitt, R.L.; Russell, M.; Orbell, G.E. 1983: Weathering sequences of soils from volcanic ash involving allophane and halloysite, New Zealand. *Geoderma 29*:41-57.

Parfitt, R.L.; Saigusa, M.; Eden D.N. 1984: Soil development processes in an aqualf-ochrept sequence from loess with admixtures of tephra, New Zealand. *Journal of soil science 35*:625-640.

Park, J. 1910: The geology of New Zealand. Whitcombe & Tombs Ltd. Dunedin.

Patel, R.N. 1986: Wood anatomy of the dicotyledons indigenous to New Zealand. 15. Fagaceae. *New Zealand journal of botany 24*:189-203.

Paul, M.A. 1980: The compaction of soil: a geological and geotechnical analysis. *Proceedings of the North of England soils discussion group 16*: 63-82.

Pedersen, T.F. 1983: Increased productivity in the eastern equatorial Pacific during the last glacial maximum (19,000 to 14,000 years B.P.). *Geology 11*:16-19.

Peterson, M.N.A.; von der Borch, C.C. 1965: Chert: modern inorganic deposition in a carbonate precipitating locality. *Science 149*:1501-1503.

Petit, J.R.; Duval, P.; Lorius, C. 1987: Long-term climatic changes indicated by crystal growth in polar ice. *Nature 325*:62-64.

Pettijohn, F.J.; Potter, P.E.; Siever, R. 1972: Sands and sandstones. New York, Spring-Verlag. 618 p.

Pewe, T.L. 1981: Desert dust: origin, characteristics and effects on Man. *Geological Society of America special paper* 186.

Pillans, B.J. 1985: Southwest North Island paleoenvironments 150,000 years B.P. to present. Pp 37-43. *In* Pillans, B.J. *ed.* The second symposium of results and discussions concerned with Late Quaternary climatic history of Australia New Zealand and surrounding seas. Geology Department, Victoria Univerity of Wellington Publication 31.

Pillans, B.J. 1986: A Late Quaternary uplift map for North Island, New Zealand. *Royal Society of New Zealand bulletin 24*:409-417.

Pisciotto, K.A. 1978: Basinal sedimentary facies and diagenic aspects of the Monterey Shale, California. Unpublished Ph.D. thesis, held at the University of California, Santa Cruz. 450 p.

Pisciotto, K.A. 1981: Diagenetic trends in the siliceous facies of the Monterey Shale in the Santa Maria region, California. *Sedimentology 28*:547-571.

Pohlen, I.J.; Harris, C.S.; Gibbs, H.S.; Raeside, J.D. 1947: Soils and some related agricultural aspects of mid Hawke's Bay. *New Zealand Department of Scientific and Industrial Research Bulletin 94*. 176 p.

Pollok, J.A. 1975: A comparative study of certain New Zealand and German soils formed from loess. Published Ph.D. thesis, Institue fur Badenkunde, Rheinischen Friedrich-Wilhelms-Univeritat, Bonn.

Pollok, J.A. 1981: Changes in pedogenic processes and soil properties of the junction between the fragipan and horizons above in a sequence of four New Zealand yellow-grey earths (fragiochrepts to fragiaqualfs). *Abstracts of the Soils With Variable Charge Conference, 1981, Palmerston North*. p 190.

Pollok, J.A. 1984: Development of variable charge properties in Tokomaru silt loam. Pp 76-79. *In* Bruce, J.G. *ed*. Soil groups of New Zealand. Part 7 yellow-grey earths. Lower Hutt, New Zealand Society of Soil Science.

Pollok, J.P. 1976: Towards a definitive account of the Tokomaru silt loam, (Summary). *New Zealand soil news 24*:135-136.

Press, F.; Siever, R. 1974: Earth. W.H. Freeman and Co. San Francisco.

Pullar, W.A. 1967: Volcanic ash beds in the Waikato district. *Earth science journal 1*:17-30.

Pullar, W.A. 1980: Tephra and loess cover deposits of Kaiangaroa Plateau including detailed lithology of upper Taupo Pumice. *New Zealand Soil Bureau scientific report 44*.

Pullar, W.A.; Birrell, K.S. 1973a: Age and distribution of late Quaternary pyroclastic and associated cover deposits of the Rotorua and Taupo area, North Island, New Zealand. *New Zealand soil survey reports 1*.

Pullar, W.A.; Birrell, K.S. 1973b: Age and distribution of late Quaternary pyroclastic and associated cover deposits of the Rotorua and Taupo area, North Island, New Zealand. *New Zealand soil survey reports 2*.

Pullar, W.A.; Birrell, K.S.; Heine, J.C. 1973: Named tephras and tephra formations occurring in the central North Island, with notes on derived soils and buried paleosols. *New Zealand journal of geology and geophysics 16*:497-518.

Pullar, W.A.; Pollok, J.A. 1973: Palaeosols and tephric loess associated with the Okareka and Te Rere Tephra formations. *New Zealand soil news 21*:186-188.

Pye, K. 1984: Some perspectives on loess accumulation. *Loess letter 11*:5-10.

Pye, K.; Sperling, C.H.B. 1983: Experimental investigation of silt formation by static breakage processes: the effect of temperature, moisture and salt on quartz dune sand and granite regoliths. *Sedimentology 30*:49-63.

Raeside, J.D. 1956: Yellow-grey earths of South Island, New Zealand an example of polygenesis in soil development. *Rapports 6e Congress International de la Science du Sol, 1965, Paris.* Pp 665-672.

Raeside, J.D. 1958: The yellow-grey earths of the South Island. *New Zealand soil news 6*:206-208.

Raeside, J.D. 1964a: Loess deposits of the South Island, New Zealand, and soils formed on them. *New Zealand journal of geology and geophysics* 7:811-838.

Raeside, J.D. 1964b: Loess and soil formation. *New Zealand soil news 12*:99-102.

Raeside, J.D. 1964c: Further comment on loess and yellow-grey earths. *New Zealand soil news 12*:226-228.

Raeside, J.D. 1970: Some New Zealand plant opal. *New Zealand journal of science 13*:122-132.

Raisbeck, G.M.; Yiou F.; Bourles, D. *et al*. 1987: Evidence for two intervals of enhanced ^{10}Be deposition in Antarctic ice during the last glacial period. *Nature 326*:273-277.

Rankin, P.C. 1973: Correlation of volcanic glasses in tephras and soils using micro-element compositions. *New Zealand journal of geology and geophysics 16 (3)*:637-641.

Reed, J.J. 1957: Petrology of the lower Mesozoic rocks of the Wellington district. *New Zealand geological survey bulletin 57*. 60 p.

Reid, J.S. 1947: Silica in Beech timbers. *New Zealand journal of forestry 4*:330-331.

Reid, J.S. 1955: Beech timbers. *New Zealand Forest Service information series 17*.

Reid, S.J. 1982: Surface wind frequencies in the southwest Pacific estimated from radar-wind data. *New Zealand journal of science 25*:303-311.

Reid, S.J.; Penny, A.C. 1982: Upper-level wind frequencies and mean speeds for New Zealand and Pacific island station. *New Zealand meteorological service miscellaneous publication 174*.

Rex, R.W. 1969: X-ray mineralogical studies. pp 354-368. *In* Ewing *et. al*. 1969: Initial reports of the deep sea drilling project leg 1, 672pp.

Rex, R.W.; Goldberg, E.D. 1962: Insolubles. *In* Hill, M.N. *ed*. The Sea. Interscience, London 1:295-304.

Reynolds, W.R. 1970: Mineralogy and stratigraphy of Lower Tertiary clays and claystones of Alabama. *Journal of sedimentary petrology 40*:829-840.

Rich, C.C. 1958: Occurrence of sterrasters of the Geodiidae (Demospongea, Choristida) in late Cenozoic strata of western Wellington province, New Zealand. *New Zealand journal of geology and geophysics 1*:641-646.

Rich, C.C. 1959: Late Cenozoic geology of the lower Manawatu valley, New Zealand. Unpublished Ph.D. thesis, Harvard University.

Richmond, G.M. 1962: Quaternary stratigraphy of the La Sal Mountains, Utah. *United States Geological Survey professional paper 32*: 135 p.

Riezebos, P.A.; Lustenhouwer, W.J. 1983: Characteristics and significance of composite particles derived from a Columbian andosol profile. *Geoderma 30*:195-217.

Rockett, T.J.; Foster, W.R. 1967: The thermal stability of purified tridymite. *American mineralogist 52*:1233-1240.

Rogers, A.F. 1928. Natural history of the silica minerals. *American mineralogist 13*:73-90.

Romans, J.C.C. 1976: Indurated layers. *Proceedings of the North of England soils discussion group (1974) 11*:20-30.

Roser, B.P. 1983: Comparative studies of copper and manganese mineralisation in Torlesse, Waipapa and Haast Schist terrains, New Zealand. Unpublished Ph.D. thesis, held in the Library, Victoria University of Wellington.

Ross, D.J. 1984: Some biochemical properties of two southern yellow-grey earths under tussock grassland. Pp 104-107. *In* Bruce, J.G. *ed.* Soil Groups of New Zealand Part 7 Yellow-grey earths. Lower Hutt, New Zealand Soil Science Society.

Rovner, I. 1971: Potential of opal phytoliths for use in paleoecological reconstructions. *Quaternary research 1*:343-359.

Rowe, G.H. 1980: Applied geology of Wellington rocks for aggregates and concrete. Unpublished Ph.D. thesis held at the Library, Victoria University of Wellington.

Roy, D.M.; Roy, R. 1964: Tridymite-cristobalite relations and stable solid solution. *American mineralogist 49*:953-962.

Ruddiman, W.F.; Duplessey, J.C. 1985: Conference on the last deglaciation: timing and mechanism. *Quaternary research 23*:1-17.

Ruddiman, W.F.; M^{C}Intyre, A. 1981: The North Atlantic Ocean during the last glaciation. *Palaeogeography, palaeoclimatology, palaeoecology 35*:145-214.

Ruddiman, W.F.; M^{C}Intyre, A. 1982: Severity and speed of Northern Hemisphere glaciation pulses: the limiting case. *Geological Society of America bulletin 93*:1273-1279.

Ruhe, R.V. 1969: Application of pedology to Quaternary research pp 1-23. *In* Pawluk, S. *ed.* Pedology and Quaternary Research. National Research Council of Canada and University of Alberta.

Ruhe, R.V.; Miller, G.A.; Vreeken, W.J. 1971: Paleosols, loess sedimentation and soil stratigraphy. Pp 41-60. *In* Yaalon, D.H. *ed.* Paleopedology - Origin, natue and dating of paleosols. Jerusalem, International Society of Soil Science and Israel University Press.

Runge, E.C.A.; Goh, K.M.; Rafter 1973: ^{14}C chronology and problems in their interpretation for Quaternary loess deposits - Timaru, New Zealand. *Soil Science Society of America proceedings 37*:742-646.

Runge, E.C.A.; Walker, T.W.; Howorth, D.T. 1974: A study of the Late Pleistocene loess deposits, South Canterbury, New Zealand. Part 1:Forms and amounts of phosphorus compared with other techniques for identifying paleosols. *Quaternary research 4*:76-84.

Ruprecht, I. 1866: Geobotanical investigations on Chernozem. St. Petersburg Imperiale Academie des Sciences.

Rutledge, E.M.; Wilding, L.P.; Hall, G.F.; Holowaychuk, N. 1975: Loess in Ohio in relation to several possible source areas: II element and mineralogical compositions. *Soil Science Society of America proceedings 39*:1133-1139.

Salinger, M.J. *et al.* 1985: Modelling the Last Glacial/Interglacial transition: Implications for New Zealand climate (note). Proceedings of the Second CLIMANZ Conference, 1985, Westland, New Zealand. *Geology Department, Victoria Univeristy of Wellington publication 31*.

Sanders, J:V. 1968: Diffraction of light by opals. *Acta cyrstallographic A24*:427-434.

Sarna-Wojcicki, A.M.; Shipley, S.; Waitt, R.B.; Dzurisin, D.; Word, S.H. 1981: The 1980 eruptions of Mount St. Helens, Washington: area distribution, thickness, mass, volume and grain size of airfall ash from the six major eruption of 1980. *United States Geological Survey professional paper 1250*:577-600.

Sato, M. 1963a: X-ray studies of tridymite (1) on tridymite-M and tridymite-S. *Mineralogical journal 4*:115-130

Sato, M. 1963b: X-ray studies of tridymite (2) structure of low tridymite, type M. *Mineralogical journal 4*:131-146.

Sato, M. 1963c: X-ray studies of tridymite (3) unit cell dimensions and phase transitions of tridymite, type S. *Mineralogical journal 4*:215-225.

Savin, S.M.; Epstein, S. 1970: The oxygen isotopic compositions of coarse grained sedimentary rocks and minerals. *Geochimica et cosmochimica acta 34*: 323-329.

Schofield, J.C. 1965: The Hinuera Formation and associated Quaternary events. *New Zealand journal of geology and geophysics 8*:772-791.

Scotter, D.R.; Clothier, B.E.; Corker, R.B. 1979: Soil water in a fragiaqualf. *Australian journal of soil research 17*:443-453.

Scurfield, G.; Segnit, E.R. 1984. Petrification of wood by silica minerals. *Sedimentary geology 39*:149-167.

Segnit, E.R.; Anderson, C.A. Jones, J.B 1970: A scanning electron microscope study of the morphology of opal. *Search 1*:349-351.

Selby, M.J. 1976: Loess. *New Zealand journal of geography 61*:1-18.

Self, S. 1983: Large-scale phreatomagmatic silicic volcanism: a case study from New Zealand. *Journal of volcanology and geothermal research 17*:433-469.

Self, S. Healy, J. 1987: Wairakei Formation, New Zealand: Stratigraphy and correlation. *New Zealand journal of geology and geophysics 30*:73-86.

Senkayi, A.L.; Dixon, J.B.; Hossner, L.R.; Yerima, B.P.K.; Wilding, L.P. 1985: Replacement of quartz by opaline silica during weathering of petrified wood. *Clays and clay minerals 33*:525-531.

Shackleton, N.J.; Opdyke, N.D. 1973: Oxygen isotope and paleomagnetic stratigraphy of equatorial Pacific core V28-238: oxygen isotope temperatures and ice volumes on a 10^4 year scale. *Quaternary research 3*: 39-55.

Shepherd, G.T. 1984: A pedological study of the Hamilton Ash Group at Welches Road, Mangawara, north Waikato. Unpublished M.Sc. thesis, held in the Library, Waikato University.

Shoji, S.; Saigusa, M. 1978: Occurrence of laminar opaline silica in some Oregon andosols. *Soil science and plant nutrition 24*:157-160.

Shoji, S.; Takahashi, T.; Saigusa, M.; Yamada, I.; Ugolini, F.C. 1986: Climo- and biosequences of tephra derived soils in Towada District, Northeastern Japan - chemical and mineralogical properties. *Abstracts of the 13th International Soil Science Society Congress, 1986, Hamburg III*:1274-1275.

Siever, H.C.; Stein, C.L. 1976: Models for the transformation of biogenic silica to chert. *Transactions of the America Geophysical Union, EOS* 57:256.

Sippel, R.F. 1971: Luminescence petrography of the Apollo 12 rocks and comparitive features of terrestrial rocks and meteorites. *Proceedings of the second lunar conference 1*:247-263.

Sjarif, S.; Gilkes, R.J. 1986: Some properties of Indonesian andosols and their sorption of phosphorus. *New Zealand soil news 34*:180.

Skinner, H.C. 1963: Precipitation of calcium dolomite and magnesium calcite in the southeast of South Australia. *American journal of science 261*:449-472.

Smalley, I.J. 1978: The New Zealand loess and the major categories of loess classification. *Search 9*:281-282.

Smalley, I.J. 1981a: Formation of a fragipan in a loess soil: An assumption, a speculation and a simple mathematical model (Pt 1). *New Zealand soil news 29*:167-169.

Smalley, I.J. 1981b: Formation of a fragipan in a loess soil: An assumption, a speculation and a simple mathematical model (Pt 2). *New Zealand soil news 29*:192-195.

Smalley, I.J. 1982a: Formation of a fragipan in a loess soil: An assumption, a speculation and a simple mathematical model (Pt 3). *New Zealand soil news 30*:27-29.

Smalley, I.J. 1982b: The New Zealand loess in a world setting. Pp 99-109. *In* Wasson, R.J. *ed.* Quaternary dust mantles of China, New Zealand and Australia. Canberra, Australia National University.

Smalley, I.J.; Davin, J.E. 1982: Fragipan horizons in soils: a bibliographic study and review of some of the hard layers in loess and other materials. *New Zealand Soil Bureau Bibliographic Report 30*. 122p.

Smalley, I.J.; Krinsley, D.H. 1981: The Urloss concept, and changing ideas on loess formation. *New Zealand soil news 29*:57-59.

Smith, G.D.; Ayra, L.M.; Stark, J. 1975: The densipan, a diagnostic horizon of Densiaqualfs for Soil Taxonomy. *Soil Science Society of America Proceedings 39*:369-370.

Smith, R.M.; Twiss, P.C.; Kraus, R.K.; Brown, M.J. 1970: Dust deposition in relation to site, season and climatic variations. *Soil Science Society of America proceedings 34*:112-117.

Soil Survey Staff, 1954: General survey of the soils of the North Island, New Zealand. *New Zealand Soil Bureau bulletin 5*.

Soil Survey Staff, 1975: Soil Taxonomy; A basic system of soil classification for making and interpreting soil surveys. *United States Department of Agriculture, Soil Conservation Service, Agriculture Handbook 436*. 754p.

Soons, J.M. 1976: Late Quaternary environments in the South Island of New Zealand. *Abstract of the 25th International Geological Congress 2*:511.

Sosman, R.B. 1932: The inversion of cristobalite. *Journal of the American chemical society 54*:3015-3016.

Souster, W.E.; Arnaud, R.J.St.; Huang, P.M. 1985: Mineral sorting through aeolian processes. *Loess letter 13*:5-10.

Sparling G.P.; Milne J.D.G.; Vincent, K.W. 1986: Effect of soil moisture regime on the microbial contribution to Olsen P values. *In* Abstracts, New Zealand Society of Soil Science Conference. *New Zealand soil news 34*:180.

Splettstoesser J.F.; Jirsa M.A. 1985: Columnar jointed sandstone in Beacon supergroup, Britannia Range, Antarctica. *New Zealand journal of geology and geophysics 28*:761-764.

Sridhar, K.; Jackson, M.L.; Clayton, R.N. 1975: Quartz oxygen isotope stability in relation to isolation from sediments and diversity of source. *Soil Science Society of America proceedings 39*:1209-1213.

Stein, C.L. 1982: Silica recrystallisation in petrified wood. *Journal of sedimentary petrology 52*:1277-1282.

Stein, C.L.; Kirkpatrick, R.J. 1976: Experimental porcelanite recrystallisation kinetics: A nucleation and growth model. *Journal of sedimentary petrology 46*:430-435.

Steinhaedt, G.C.; Fransmeier 1979: Chemical and mineralogical properties of the fragipan of the Cincinnati catena. *Journal of the Soil Science Society of America 43*:1008-1013.

Stevens, K.F.; Vucetich, C.G. 1984: Pedogenic weathering of Upper Quaternary tephras in New Zealand 1. Isovolumetric geochemical evidence of cation movement. *Chemical geology 47*:285-302.

Stevens, K.F.; Vucetich, C.G. 1985: Weathering of Upper Quaternary tephras in New Zealand. Clay minerals and their climatic interpretation. *Chemical geology 53*:237-247.

Stewart M.K.; Taylor C.B. 1981: Environmental isotopes in New Zealand hydrology. I. Introduction: The role of oxygen-18, deuterium, and tritium in hydrology. *New Zealand journal of sedimentology 24*:295-311.

Stewart, R.B. 1982: Origin of selected soil parent materials and sediments in North Island, New Zealand. Unpublished Ph.D. thesis, held in the Library, Massey University.

Stewart, R.B.; Neall, V.E. 1984: Chronology of palaeoclimatic changes at the end of the last glaciation. *Nature 311*:47-48.

Stewart, R.B.; Neall, V.E.; Pollok, J.A.; Syers, J.K. 1977: Parent material stratigraphy of an Egmont loam profile, Taranaki, New Zealand. *Australian journal of soil research 15*:177-190.

Stewart, R.B.; Neall, V.E.; Syers, J.K. 1986a: Accumulation of aerosolic quartz in an andept chronosequence, North Island, New Zealand. *Geoderma 37*:331-340.

Stewart, R.B.; Neall, V.E.; Syers, J.K. 1986b: Origin of quartz in selected soils and sediments, North Island, New Zealand. *New Zealand journal of geology and geophysics 29*:147-152.

Struve, G.A. 1835: De silica in plantis nounullis. Diss Berlin.

Suggate, R.P. 1985: The glacial/interglacial sequence of north Westland, New Zealand. *New Zealand Geological Survey record* 7.

Suggate, R.P.; Moar, N.T. 1970: Revision of the chronology of the late Otira Glacial. *New Zealand journal of geology and geophysics 13*: 742-746.

Suggate, R.P.; Stevens, G.R.; Te Punga, M.T. *ed.* 1978: Geology of New Zealand. Wellington, Government Printer.

Swindale, L.D.; Jackson, M.L. 1960: A mineralogical study of soil formation in four rhyolitic derived soils from New Zealand. *New Zealand journal of geology and geophysics 3*:141-183.

Syers, J.K.; Jackson, M.L.; Berkheiser, V.E.; Clayton, R.N.; Rex, R.W. 1969: Eolian sediment influence on pedogenesis during the Quaternary. *Soil science* 1-7:421-427.

Symes, R.E.; Wells, N. 1973: Mineral content of topsoils on coastal terraces from Mount Egmont to Palmerston North, New Zealand. *New Zealand journal of geology and geophysics 16*:651-656.

Tada, R.; Iijima, A. 1983: Identification of mixtures of opaline silica phases and its implication for silica diagenesis. Pp 229-244. *In* Iijima, A.; Hein,J.R.; Siever, H.C. *ed.* Siliceous deposits in the Pacific region. Amsterdam, Elsevier.

Tarbuck, E.J.; Lutgens, F.K. 1984: The Earth, an introduction to physical geology. Charles E. Merrill, Columbus, Ohio.

Taylor, B.E.; Dunbar, N.; Kyle, P.R. 1986: Stable isotope studies of the volatile history and degassing of rhyolitic magmas in the Taupo Volcanic Zone, New Zealand. *Abstracts of the International Volcanologic Congress, 1986, Auckland.* P 217.

Taylor, H.P.; Epstein, S. 1962: Relationship between $O^{18}:O^{16}$ ratios in coexisting minerals of igneous and metamorphic rocks. Part 2. Application to petrological problems. *Bulletin of the geological society of America 73*:675-694.

Taylor, H.P.; Epstein, S. 1970: Stable isotope geochemistry of lunar samples. *Geological Society of America Abstracts. In* Henderson et al. (1972) *Soil Science Society American proceedings 36*:830-835.

Taylor, N.H. 1948: Soil map of New Zealand. *New Zealand Soil Bureau map No. S.B. 280.*

Taylor, N.H. 1953: The ecological significance of the central North Island ash showers - the soil pattern. *New Zealand ecological society proceedings 1*:11-12.

Te Punga, M.T. 1953a: A late Pleistocene land bridge across Cook Strait, New Zealand. *New Zealand journal of science and technology 35B*:161-192.

Te Punga, M.T. 1953b: Radiocarbon dating of a Rangitikei River terrace. *New Zealand journal of science and technology B35*:45-48.

Te Punga, M.T. 1953c: The geology of Rangitikei valley. *New Zealand Geological Survey memoir 8.*

Te Punga, M.T. 1954: Late Pleistocene Buckshot Gravels from western Wellington, New Zealand. *New Zealand journal of science and technology B36*:1-13.

Te Punga, M.T. 1957: Live anticlines in Western Wellington. *New Zealand journal of science and technology B38*:433-446.

Te Punga, M.T. 1958: Evidence for a low sea level 9900 years ago. *New Zealand journal of geology and geophysics 1*:92-94.

Te Punga, M.T. 1962: Some geological features of the Otaki-Waikanae district. *New Zealand journal of geology and geophysics 5 (4)*:517-530.

Thiede, J. 1979: Wind regimes over the late Quaternary southwest Pacific Ocean. *Geology* 7:259-262.

Thompson, C.S. 1981: The climate and weather of the Taranaki region. *New Zealand meteorological service miscellaneous publication 115.*

Thompson, L.G.; Mosley-Thompson, E. 1981: Temporal variablity of microparticle properties in polar ice sheets. *Journal of volcanology and geothermal research 11*:11-27.

Thomson, J.A. 1916: The Hawera Series or the so-called "Drift Formation" of Hawera. *Transactions of the New Zealand Institute 49*:414-417.

Thorson, R.M.; Bender, G. 1985: Eolian deflation by ancient katabatic winds: A Late Quaternary example from the North Alaska Range. *Geological Society of America 96*:702-709.

Tokashiki, T; Wada, K. 1975: Weathering implications of the mineralogy of clay fractions of two ando soils, Kyushu. *Geoderma 14*:47-62.

Tokuda, T. 1960: The X-ray powder patterns and the natural lattice constants of natural cristobalite. *Mineralogical journal 3*:1-8.

Tonkin, P.J. 1970: The soils of the southeastern sector of Egmont National Park. *Earth science journal 4*:36-59.

Tonkin, P.J.; Runge, E.C.A.; Goh, K.M.; Walker, T.W. 1973: A study of Late Pleistocene loess deposits and associated paleosols, South Canterbury, New Zealand. *Abstracts of the 9th INQUA Congress, 1973, Christchurch*. p 371.

Tonkin, P.J.; Runge, E.C.A.; Ives, D.W. 1974: A study of Late Pleistocene loess deposits, South Canterbury, New Zealand. Pt. II Paleosols and their stratigraphic implications. *Quaternary research 4*:217-231.

Topping, W.W. 1973: Tephrostratigraphy and chronology of late Quaternary eruptives from the Tongariro Volcanic Centre, New Zealand. *New Zealand journal of geology and geophysics 16*:397-424.

Topping, W.W.; Kohn, B.P. 1973: Rhyolitic tephra marker beds in the Tongariro area, North Island, New Zealand. *New Zealand journal of geology and geophysics 16 (3)*:375-423.

Turner, M.A. 1944: Geology of northern Wellington and southern Hawkes Bay. Unpublished Ph.D. thesis, held in the Geology Department, Victoria University of Wellington.

Twiss, P.C; Suess, E.; Smith, R.M. 1969: Morphological classification of grass phytoliths. *Soil Science Society of America proceedings 33*:109-115.

Urey, H.C. 1947: The thermodynamic properties of the isotopic substances. *Journal of the Chemistry Society 98*:562-581.

Urey, H.C.; Lowenstam, H.A.; Epstein, S.; M^{c}Kinney, C.R. 1951: Measurement of paleotemperatures and temperatures of the Upper Cretaceous of England, Denmark, and the southeastern United States. *Geological society of America bulletin 62*:399-416.

Van Der Linden, W.J.M. 1969: Off-shore sediments, north west Nelson, South Island, New Zealand. *New Zealand journal of geology and geophysics 12*:87-103.

Van Der Linden, W.J.M.; Norris, R.M. 1974: Structure and Quaternary history of Karamea Bight, South Island, New Zealand. *New Zealand journal of geology and geophysics 17*:375-388.

Vella, P. 1983: Upper Pleistocene succession in inland Wairarapa Valley. *Transactions of the Royal Society of New Zealand, Geology 2*:63-78.

Veneman, P.L.M.; Lidbo, D.L. 1986: Fragipan formation. *Abstracts of the 13th International Society of Soil Science Congress, 1986, Hamburg III*:1310-1311.

Verhoogen, J. 1937: Mount St. Helens, a recent Cascade volcano. *California University, Department of Geological Sciences bulletin 24*:263-302.

Vucetich, C.G.; Birrell, K.S. 1977: Pre 40,000 year rhyolitic tephras in "Hamilton Ash Formation". *New Zealand soil news 25*: 84-87.

Vucetich, C.G.; Birrell, K.S.; Pullar, W.A. 1978: Ohinewai Tephra Formation: a c. 150 000-year-old tephra marker in New Zealand. *New Zealand journal of geology and geophysics 21*:71-73.

Vucetich, C.G.; Howorth, R. 1976: Proposed definition of the Kawakawa Tephra, the c. 20 000 years B.P. marker horizon in the New Zealand region. *New Zealand journal of geology and geophysics 19*:43-50.

Vucetich, C.G.; Kohn, B.P. 1973: The stratigraphic significance of a dated late Pleistocene ash bed near Amberley, South Island, New Zealand. *Abstract of the 9th INQUA conference, 1973, Christchurch*. p 390.

Vucetich, C.G.; Kohn, B.P.; Pullar, W.A. 1981: Correlation of Arotora Tephra, Ahuroa coverbed type section, Te Kuiti. Pp. 116-130. *In* Howorth, R.; Froggatt, P.; Vucetich, C.G.; Collen, J.D. *ed*.

Proceedings of the tephras workshop, June 30th-July 1st, 1980, Victoria University of Wellington. *Victoria University of Wellington, Geology Department publication 20.*

Vucetich, C.G.; Pullar, W.A. 1969: Stratigraphy and chronology of Late Pleistocene ashbeds in central North Island, New Zealand. *New Zealand journal of geology and geophysics 12*:784-837.

Wada, K. 1980: Mineralogical characteristics of andisols. Pp 87-107. *In* Theng, B.K.G. *ed.* Soils with variable charge. Lower Hutt, New Zealand Soil Science Society.

Wada, K.; Kakuto, Y. 1984: Summary of clay minerals analyses of Chile soil samples for the Sixth International Soils Classification Workshop. Anonymous *Classification and management of andisols, 1984: Sixth International Soil Classification Workshop, Chile and Equador. Tour guide part 1, Chile.*

Walker, P.H.; Costin, A.B. 1970: Atmospheric dust accessions in south-eastern Australia. *Australian journal of soil science 9*:1-6.

Walker, T.W. 1965: The significance of phosphorus in pedogenesis. *In* Experimental Pedology. *Proceedings of the 11th Easter School of Agricultural Science, University of Nottingham*:295-316.

Walker, T.W.; Adams, A.F.R. 1958: Studies on soil organic matter. I. Influence of phosphorus content of parent materials on accumulation of carbon, nitrogen, sulphur, and organic phosphorus in grassland soils. *Soil Science 85*:307-318.

Wallace, R.C.; Alloway, B.V.; Stewart, R.; Neall, V.E. 1986: The mineral chemistry as an indicator of petrogenesis at Egmont Volcano. *Abstracts of the International Volcanologic Congress, 1986 New Zealand*: 23.

Wallace, R.C.; Neall, V.E. 1984: The sand mineralogy of Tokomaru silt loam as an indicator of parent material provenance. Pp. 86-92. *In* Bruce, J.G. *ed.* Soil Groups of New Zealand. Part 7, Yellow-grey earths. New Zealand Society of Soil Science, Lower Hutt, New Zealand. 123 p.

Wallace, R.C.; Stewart, R.B.; Neall, V.E. 1985: Volcanic glass field laboratory test and procedure to prepare thin sections of the sand fraction of soils. *Massey University Department of Soil Science occasional report, number 7.*

Wang, C.; Nowlands, J.L.; Kodama, H. 1974: Properties of two fragipan soils in Nova Scotia including scanning electron micrographs. *Canadian journal of soil science 54*:159-170.

Ward W.T.1967: Volcanic ash beds of the lower Waikato Basin, North Island New Zealand. *New Zealand journal of geology and geophysics 10*:1109-1135.

Ward, W.T. 1967: Volcanic ash beds in the lower Waikato basin, North Island, New Zealand. *New Zealand journal of geology and geophysics 10*:1109-1135.

Wardle, P. 1963: Evolution and distribution of the New Zealand flora as effected by Quaternary climate. *New Zealand journal of botany 1*:3-17.

Weaver, F.M.; Wise, S.W. 1972: Ultramorphology of deep sea cristobalite chert. *Nature, physical sciences 237*:56-57.

Weaver, F.M.; Wise, S.W. 1974: Opaline sediments of the southeast coastal plain and horizon A: biogenic origin. *Science 184*:899-901.

Wellman H.W. 1972: Rate of horizontal fault displacement in New Zealand. *Nature 237*:275-277.

Wenk, H.R.; Champness, P.E.; Christie, J.M.; Cowley, J.M., Cowley, A.H.; Thomas, G.; Tighe N.J. 1976: Electron microscopy in mineralogy. New York. Springer-Verlag.

Westgate, J.A.; Fulton, R.J. 1975: Tephrastratigraphy of Olympia interglacial sediments in south-central British Columbia, Canada. *Canadian journal of earth science 12*:489-502.

Westgate, J.A.; Gorton, M.P. 1981: Correlation techniques in tephra studies. *In* Self, S.; Sparks, R.S.T. *eds*. Tephra studies as a tool in Quaternary research. *Proceedings of the NATO Advanced Studies Institute, 1980, Iceland*. Pp 73-94.

Westgate, J.A.; Smith, D.G.W.; Tomlinson, M. 1970: Late Quaternary tephra layers in southwest Canada. Pp 13-34. *Proceedings of the Second Annual Paleoenvironmental Workshop*. Calgary, Students Press.

Whalley, W.B. 1979: SEM examination of loess - a progress report. *Loess letter 2*:16-18.

Whalley, W.B.; Marshall, J.R.; Smith, B.J. 1982: Origin of desert loess from some experimental observations. *Nature 300*:433-435.

White, A.F.; Claasen, H.C. 1980: Short term dissolution of rhyolitic glass. *Chemical geology 28*:91-109.

White, D.E; Brannock, W.W.; Murata, K.J. 1956: Silica in hot-spring waters. *Geochimica et cosmochimica acta 10*:27.

Wilding, L.P.; Drees, L.R. 1971: Biogenic opal in Ohio soils. *Soil Science Society of America Proceedings 35*:1004-1010.

Wilding, L.P.; Drees, L.R. 1974: Contributions of forest opal and associated crystalline phases to fine silt and clay fractions of soils. *Clays and clay minerals 22*:295-306.

Wilding, L.P.; Smeck, N.E.; Drees, L.R. 1977: Silica in soils: quartz, cristobalite, tridymite and opal. Pp 471-552. *In* Dixon, J.B.; Weeds, S.B. *eds*. Minerals in Soil Environments. Madison, Soil Science Society of America.

Willet R.W. 1950: The Pleistocene snowline, climatic conditions and suggested biological effects. *New Zealand journal of science and technology 32B*: 18-48.

Wilson, C.J.N. 1985: The Taupo eruption, New Zealand. II. The Taupo ignimbrite. *Philosophical transactions of the Royal Society of London A314*:229-310.

Wilson, C.J.N.; Walker, G.P.L. 1985: The Taupo eruption, New Zealand. I. General aspects. *Philosophical Transactions of the Royal Society of London A314*:199-228.

Wilson, M.J.; Russell, J.D.; Tait, J.M. 1974: A new interpretation of the structure of disordered alpha-cristobalite. *Contributions to mineralogy and petrology 47*:1-6.

Windom, H.L. 1975: Eolian contributions to marine sediments. *Journal of sedimentary petrology 45*:520-529.

Wintle, A.G. 1981: Thermoluminescence dating of loess. *Loess letter 6*:5-9.

Wintle, A.G. 1982: Thermoluminescence properties of fine grained minerals in loess. *Soil science 134*:164-170.

Wise, S.W.; Hsu, K.J. 1971: Genesis and lithification of a deep sea chalk. *Eclogae Geologica Helvetica 64*:273.

Wise, S.W.; Kelts, K.M. 1972: Inferred diagenetic history of a weakly silicified deep sea chalk. *Transactions of the Gulf Coast Geological Associations 22*:117.

Wise, S.W.; Weaver, F.M. 1972: Origin of deep sea cristobalite chert. *Geological society of America abstract 4*:116.

Worthington, T.J. 1985: Geology and petrology of the Tauhara Volcanic Complex, Taupo, New Zealand. Unpublished M.Sc. thesis, held in the Library, Victoria University.

Yaalon, D.H. 1962: Mineral composition of the average shale. *Clay minerals bulletin* 5:31-36.

Yamada, I.; Shoji, S. 1977: Crystalline silica minerals in air-borne pyroclastic materials. *Soil science and plant nutrition 23*:541-544.

Yoshida, S.; Onishi, Y.; Kitagishi, K. 1959: The chemical nature of silicon in rice plant. *Soil and Plant Food 5:* 23-27.

Yoshida, S.; Onishi, Y.; Kitagishi, K. 1962a: Histochemistry of silicon in rice plant. II. Localisation of silicon within rice tissue. *Soil Science and Plant Nutrition 8 (1)*:36-41.

Yoshida, S.; Onishi, Y.; Kitagishi, K. 1962b: Histochemistry of silicon in rice plant. III. The presence of cuticle-silica double layer in epidermal tissue. *Soil Science and Plant Nutrition 8 (2)*:1-5.

Young, D.J. 1964: Stratigraphy and petrology of northeast Otago loess. *New Zealand journal of geology and geophysics* 7:839-863.